Theoretical Study of the Atomic Structure and the Radiative Parameters of Lowly and Moderately Ionized Heavy Elements

Applications to Cosmochronology and to the Spectral Analysis of Compact Astrophysical Objects

Sébastien Gamrath

Thesis supervisors
Pascal Quinet and Patrick Palmeri

University of Mons
Faculty of Sciences
Atomic Physics and Astrophysics Group

Academic year
2022-2023

Contents

Aknowledgements

First of all, this section will be the only one to be translated in French.

Je voudrais d'abord remercier mes deux promoteurs, Pascal Quinet et Patrick Palmeri, pour leur encadrement, leur temps et leurs conseils durant toute la durée de cette thèse. Les nombreuses discussions que nous avons pu avoir ont toujours été fructueuses scientifiquement. Je remercie aussi les professeurs Lydia Tchang-Brillet et Haikel Jelassi d'avoir acceptés d'être membre du jury de cette thèse pour leur lecture attentive de ce manuscrit. Je remercie aussi Claude Semay et Evelyne Daubie d'avoir accepté de faire partie du comité d'accompagnement ainsi que du jury de cette thèse.

D'un point de vue plus personnel, j'aimerais remercier mon épouse, Floriane, pour son amour et son soutien indéfectible qui me furent on ne peut plus précieux durant toutes ces années ainsi que pour sa relecture de ce manuscrit. La liste de ce pour quoi je devrais la remercier ne pourrait être exhaustive mais je la remercierai aussi en particulier pour la famille que nous formons avec notre fils Léo qui a contribué lui aussi, à sa manière (i.e. en dormant sur moi), à la rédaction de cette thèse.

Je tiens aussi à remercier mes parents qui m'ont permis de faire des études supérieures et qui m'ont toujours encouragé dans mes choix pour leur amour, leur soutien à toute épreuve et leur aide en toutes circonstances. Je remercie aussi mes deux frères, Laurent et Antoine, témoins de mon mariage, pour leur soutien au fil des années. Je remercie donc l'intégralité de ma famille pour m'avoir permis d'en arriver là.

J'aimerais aussi remercier mes amis les plus proches, Jérôme, Antoine et Ludovic mais aussi tant d'autres qui ont contribué à m'offrir des moments de détente plus que nécessaire durant le travail de longue haleine que représentait cette thèse. Je pense notamment à Anaïs, Eléonore, Marion, Valentine, Marie-Aurore et à tant d'autres.

J'ai aussi beaucoup de collègues à remercier, notamment l'équipe des travaux pratiques (Sabrina, Gilles, Thomas, Evelyne), avec laquelle, de part la forme de ce travail de chercheur à mi-temps et d'enseignant l'autre mi-temps, j'ai été amené a collaborer beaucoup et à partager de nombreux moments (certains festifs, d'autres moins). Je dois aussi aussi remercier tous les collègues avec qui nous partagions d'innombrables discussions scientifiques, notamment durant les temps de midi (Helena, Cyrille, Lorenzo et Alice par exemple) ainsi que Michel Voué et Bjorn Maes pour qui j'ai donné beaucoup de cours et qui m'ont toujours laissé une grande liberté pédagogique sur la manière de le faire, ce qui est très appréciable et qui a été très apprécié.

La dernière catégorie de personnes que je dois remercier sont mes étudiants. En effet, ces derniers m'ont permis d'en apprendre énormément sur moi-même tout en, je l'espère, apprenant de ma part. Ces remerciements sont d'autant plus importants que certains d'entre eux (qui ont fini par devenir d'anciens étudiants avec les années) sont devenus mes amis, certains même très proches. Je tiens donc à remercier tout particulièrement Ilènia et Alix qui, elles aussi, m'ont apporté énormément de soutien durant la réalisation de cette thèse, surtout dans la phase finale de rédaction. Parmi les étudiants que je souhaite remercier, je pourrais également citer Kélian, Pauline, Mariano, Maud, Thomas, Nicolas, Florian, Émilie, Dariane, Trisha, Ugo, Solène, Clara, Arnaud et tellement d'autres que je ne peux qu'en oublier en les listant. Je dois aussi remercier Lea et William qui, lors de la réalisation d'un stage sous ma supervision ont produit une (petite) partie des données exposées dans cette thèse ainsi que mes camarades de classe avec qui j'ai fait un petit bout de chemin dans le cadre de l'agrégation réalisée pendant la dernière année cette thèse; Nils, Mohammed, Anne et Aline.

Je me dois de clore ces remerciements en m'excusant auprès de toutes les personnes qui m'ont aidé ou soutenu que j'aurais oublié de nommer explicitement dans les listes précédentes. Le soutien de tout le monde m'a été précieux.

General Introduction

For a little more than a century, some of the most important developments in astrophysics have been possible thanks to a better interpretation of the observed stellar spectra. In this context, atomic physics has always played an essential role insofar as this discipline is able to provide all the necessary tools for the detailed analysis of astrophysical spectra. From the latter, it is indeed possible to deduce the presence and abundance of the different chemical elements in celestial objects only through the accurate knowledge of the atomic structures and the radiative parameters characterizing these elements.

In recent years, astronomical observing instruments have improved dramatically with new space and ground-based telescopes providing spectra with unprecedented resolution and signal-to-noise ratio across the whole range of wavelengths, from X-rays to the far infrared, for a very large number of various cosmic sources. Consequently, the astrophysical spectra currently recorded are getting richer and richer and include many spectral lines that can be identified only by a sufficient knowledge of the atomic parameters, both in quality and quantity, of all the elements in their different ionization stages.

The work presented in this thesis is part of this context since it aims to make an original contribution to the determination of fundamental atomic parameters essential to the development of current astrophysical hot topics, in particular for studies related to cosmochronology, hot white dwarfs, and stellar nucleosynthesis.

In cosmochronology, heavy elements such as uranium and thorium are of paramount importance. More precisely, the abundance ratios of the long-lived isotopes ^{232}Th and ^{238}U can be used to determine the age of stars. To date, some spectral lines of singly ionized thorium and uranium have been identified on some stellar spectra. Unfortunately, the atomic data characterizing these two ions are still too incomplete and too unreliable to perform a sufficiently precise stellar dating. This motivated us to perform a detailed investigation of these two ions whose complex atomic structures make theoretical modeling very complicated. Both thorium and uranium belong to the actinide group of the periodic table, with atomic numbers Z = 90 and Z = 92, respectively.

We started this study with singly ionized uranium (U II). Before our work, we looked for previously available data in U II. We found that, Blaise and Wyart [1] listed some preliminary energy levels in U II for both parities in 1992. These data were preceded in the literature by the publications about emission lines by Steinhaus *et al.* [2] and Palmer [3] in 1971 and 1980, respectively and it provided an update to the previous estimations made by Brewer [4] en 1971. This database was later extended by Blaise *et al.* [5] in 1994. More recently, in 2017, the latest energy levels of U II were construed by Meftah [6] using the Racah-Slater parametric method with the Cowan codes [7]. Meftah *et al.* parametric study [6] allowed them to re-investigate the high resolution UV spectrum of uranium which was recorded in the late eighties at the Meudon Observatory and of which the analysis was unfinished. Unfortunately, Meftah *et al.* [6] were not able to put all the interacting configurations in a single calculation. In our work, we used as a basis, the same kind of configurations but we put them all in one calculation and we added the effects of the core-polarization. This will be discussed in Chapter 3.1.

As regards the radiative decay rates, the first measurements of relative line intensities in U II were obtained from emission arc spectra by Meggers *et al.* [8], Corliss and Bozman [9], Voigt [10] and Corliss [11] more than 40 years ago. In the atlas of uranium lines published by Palmer [3] in 1980, relative intensities measured from uranium hollow-cathode spectra were listed for 4928 U I and 431 U II emission spectral lines. The oscillator strengths of the lines at $\lambda = 3859.571$ Å and $\lambda = 4050.041$ Å were later determined by Chen and Borzileri [12] who combined experimental lifetime measurements of the upper levels with unpublished branching fractions. Oscillator strengths were also reported for about 100 U II lines by Henrion *et al.* [13] in 1987. In his database, Kurucz [14] listed transition probabilities and oscillator strengths for many U II lines based on the experimental data reported by Meggers *et al.* [8], Corliss and Bosmann [9], and Chen [12]. Finally, about 20 years ago, accurate radiative lifetimes were measured by Lundberg *et al.* [15], using laser-induced fluorescence technique.Experimental oscillator strengths for 57 U II lines in the region 3500 – 6700 Å were then obtained by combining these radiative lifetimes with new branching fractions derived from the measured line intensities in the spectra emitted by a hollow cathode and analyzed using a Fourier transform spectrometer by Nilsson *et al.* [16].

Just after the calculation in U II, we started the calculations in Th II for those cosmochronological applications. The first investigation of the Th II spectrum was carried out by McNally *et al.* [17] in 1942. They identified 1091 lines of singly ionized thorium in a wavelength range from 2150 to 8140 Åallowing the classification of 219 levels.In order to link these two groups of energy levels, McNally [18] recorded the infrared spectrum of thorium in the region 8665 to 11230 Å in 1945. The separation between the ground leveland the first excited one was found to be only 4490.29 cm^{-1}. At the same period, independent experimental studies undertaken at the Zeeman laboratory of Amsterdam led to similar conclusions and the determination of additional levels [19, 20, 21]. All these published data, together with yet unpublished energy levels, were compiled in 1958 by Charles [22] in a list of 2850 classified lines of Th II from 165 odd and 191 even levels. McNally [18] pointed out that many of the strong transitions between low-lying Th II levels appear in the IR region and, although he observed some of them in the photographic infrared, the remaining lines were outside his region of observation. The majority of these lines were observed in the emission spectrum of thorium in the 1 – 2.5 μ region recorded by Steers [23]. In this study, about 60 lines were attributed to Th II transitions.A few years later, Minski [24] discovered 28 energy levels through the first extensive parametric study of the Th II.The analysis of Th II was then extended with improved observations of the spectrum between 2000 and 25000 Å by Zalubas and Corliss [25]. They classified 6500 lines as transitions between 199 odd levels and 271 even levels. The emission spectrum of thorium from 2777 to 13500 Å in 1974.

Most of the Th II data obtained in the works mentioned hereabove were listed in three compilations: those of Blaise and Wyart [1], Sansonetti and Martin [26] and Redman *et al.* [27]. In the latter, the previously published thorium line lists were combined with new precise observations of a thorium-argon hollow cathode lamp emission spectrum in the region between 3500 and 11750 Å with a high-resolution Fourier transform spectrometer to refine the energy levels in Th I, Th II, and Th III. Using these refined level values, accurate Ritz wavelengths were also calculated for 19874 thorium lines between 2500 and 55000 Å while 102 new thorium energy levels, among which 9 belonging to Th II, were found. The list of Th II energy level values reported in the NIST database [28] is entirely based on the Redman *et al.* compilation [27].

Regarding the study of hot white dwarfs spectra, for about 15 years, the Atomic Physics and Astrophysics group of University of Mons has undertaken a systematic study of trans-iron elements in their ionization stages between 3+ and 6+ [1] at the request of astrophysicists of University of Tübingen in Germany, the latter having identified numerous spectral lines of these heavy ions in the ultraviolet spectra of certain of those hot white dwarfs and deduced large overabundances of several orders of magnitude higher than the solar abundances. In order to best interpret the observed spectra, it is necessary to build non-local-thermodynamic-equilibrium (NLTE) synthetic models which requires to include the radiative parameters not only for the identified lines but also for all the transitions populating and depopulating the levels involved in the observed lines. The contribution we made in the framework of our thesis concerns the copper, indium, caesium and silver ions for which new semi-empirical calculations of radiative decay rates were determined, in their large majority for the first time.

The main source of atomic data related to the copper spectra is the paper published by Sugar & Musgrove [29] in which the available experimental energy levels of the copper atom, in all stages of ionization, have been compiled with ionization energies, either experimental or theoretical, experimental Landé g-factors, and leading components of calculated eigenvectors. This compilation is still being used as the standard reference database for the copper ions of interest at the National Institute of Standards and Technology [28]. For the fourth and fifth ionization stages of copper (Cu V and Cu VI), more recent data from Van Kleef *et al.* [30], and from Raassen and Van Kleef [31] have been used to perform the semi-empirical optimization of our HFR calculation. It is worth mentioning that our work is the first publication of radiative data in Cu IV,V and VII.

Using the most recent experimental data of Swapnil and Tauheed [32] and Ryabtsev and kononov [33], the radial parameters (average energies, Slater integrals, spin-orbit parameters and effective interaction parameters) were optimized during our fitting procedure included in the calculation for the third ionization stage of indium (In IV). We then compared our calculation including different configurations and core-polarization effects to theirs. When it came to the fourth ionization stage (In V), the fitting procedure aimed to minimize the differences between the calculated Hamiltonian eigenvalues and the experimental energy levels taken from Swapnil and Tauheed [34] and Ryabtsev [35]. Once again, we compared our calculation including different configurations and core-polarization effects to theirs. In the case of In VI, the experimental data from [36] and [37] were used for the fitting procedure. Finally, pertaining to In VII, we used experimental data of Ryabtsev *et al.* [38]. For all those ions, the goal was to consider the most complete and most recent set of experimental atomic data in order to have a more precise fit.

To perform our calculations in the caesium ions, we used the experimental energy levels from the compilation Sansonetti [39] and from Husain *et al.* [40]. Once again, those data are the most recent measured and compiled to our knowledge. Our work is the first one about radiative data in Cs IV, V and VI.

The last element studied in this framework of extreme overabundances in white dwarfs is silver. The experimental data used for the semi-empirical fits found in the literature, for the ions Ag IV, V, VI and VII ions are, respectively, Ankita and Tauheed [41] in Ag IV, Kildiyarova *et al.* [42] and Van Kleef *et al.* [43] in Ag V, Joshi *et al.* [44] in Ag VI and Ryabtsev and Kononov [45] in Ag VII.

Finally, it is important to mention that most of the studies published so far for the heavy elements were mainly focused on the lowest energy atomic states. However, highly excited states are of undeniable interest in astrophysics as they not only contribute to the construction of NLTE models, as mentioned above, but also involve radiative transitions that are increasingly observed in the spectra of celestial objects, in particular in the infrared range which is currently undergoing a considerable expansion with the recent launch

[1] Noted IV to VII in our conventions.

of the James Webb Telescope. As a consequence, the radiative parameters characterizing the transitions between highly excited states are in great demand by the astrophysical community, particularly for neutral and singly ionized atoms heavier than iron for which the identification on the astrophysical spectra makes it possible to establish constraints on nucleosynthesis models worked out for the determination of abundances in chemically peculiar stars. In order to help fill these gaps, we have performed semi-empirical studies leading to the determination of radiative rates in some selected elements, namely neutral and singly ionized iridium, neutral rhenium, neutral lanthanum, neutral barium and neutral rhodium. In these cases, the methodology was to combine experimental radiative data measured by time-resolved laser-induced-fluorescence spectroscopy at University of Jilin in China with theoretical branching fractions to obtain the relevant transition probabilities.

The present thesis is written as follows. The first chapter is devoted to the astrophysical context in which our work was carried out, beginning with a general introduction about the life of stars and some reminders about the Hertzprung-Russel diagram. Next, the nucleosynthesis theory which explains how the heavy elements are created in the Universe, is described, as well as the uranium-thorium cosmochronology and the study of white dwarfs. In the second chapter we make some fundamental reminders of atomic physics by particularly insisting on the parameters considered in this thesis. The theoretical methods used in our different studies, namely the pseudo-relativistic Hartree-Fock (HFR) and the fully relativistic Multiconfiguration Dirac-Hartree-Fock (MCDHF) approaches, are presented in Chapter 2 while the results we have obtained are detailed in Chapters 3 to 5. These last three chapters are divided in such a way that they bring to the light the astrophysical applications of the atomic parameters determined in our work in three specific topics, namely cosmochronological investigations (Chapter 3), the study of hot white dwarfs (Chapter 4) and the analysis of chemically peculiar stars (Chapter 5). In addition, in Chapter 5, we briefly describe the experimental technique used in collaboration with University of Jilin in China, i.e. the time-resolved laser-induced-fluorescence technique.

Chapter 1

Astrophysical Context

1.1 The Life of a Star

1.1.1 The Hertzprung-Russel Diagram

The Hertzsprung-Russell (HR) diagram is a fundamental tool in astrophysics in which the intrinsic luminosity of a star is plotted as a function of its effective temperature[1](and therefore its spectral type).

This allows to highlight that the stars are grouped according to certain regions of the graph, thus creating specific branches and sequences. The most important one is the main sequence, extending from the lower right corner (cold and faint stars) to the upper left corner of the diagram (the hot and highly luminous stars), which is the most important because this is the part of the diagram where stars spend most of their life. On the HR diagram shown in Figure 1.1, the region where the white dwarfs are located is also indicated. Since they are located in the lower left part of the diagram, we can deduce that they are hot and not very luminous. At the beginning of their life, most of stars are on the main sequence of the HR-Diagram once the nuclear fusion in them has been ignited. At that moment, the star has a stable core temperature and luminosity. Those stars are therefore called *main-sequence stars*. The exact position of the star on the main sequence depends on its mass [47]:

- the stars with the lowest masses and low surface temperatures and luminosities are situated in the right-bottom of the main-sequence;
- the massive stars with high temperatures and luminosities are located in the upper-left part of the sequence.

The latest continue their evolution further up in the diagram than the lower-mass stars. The time on the main sequence is the longest stage in the life of a star and depends of the mass of the star as shown in Table 1.1 using the data from Woosley *et al.* [48]. During

Table 1.1: Different stars' lifetimes on the main sequence compared to their total lifetimes depending on their mass - Source: [48]

Approximative initial mass $M_\odot$	Time on the main sequence Millions of years	Total lifetime Millions of years	Percentage of life spent on the main sequence %
0.8	2.0×10^4	3.2×10^4	62.5
1	9.2×10^3	1.2×10^4	76.7
2	8.7×10^2	1.2×10^3	72.5
5	78	102	76.5
15	11	13	84.6
25	6.7	7.5	89.3

[1]Defined as the surface temperature of a spherical black body with its luminosity and radius

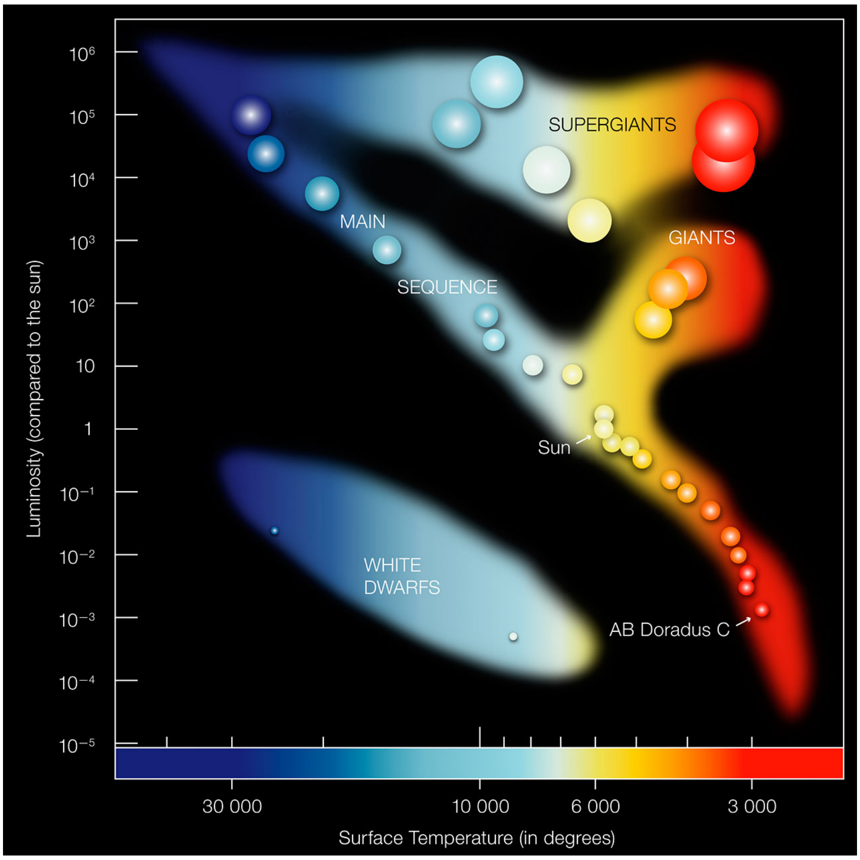

Figure 1.1: Hertzprung-Russel Diagram - Credit: ESO [46]

their time on this main sequence, stars fuse hydrogen to helium in their core:

$$4\ {}^{1}H + 2e^{-} \rightarrow\ {}^{4}He + 6\gamma. \tag{1.1}$$

This is called the *proton-proton cycle*. It allows the transformation of hydrogen into ^{4}He[2]. This cycle is more complex than the simplified equation here above. It is actually divided into several reactions. The first reaction of this cycle allows the transformation of a proton and a neutron into deuterium. Then, depending on what is available in the core of the star (i.e. depending on the time of its evolution at which this reaction occurs), through the intermediary of tritium or helium 3 with which the deuterium atoms will fuse, the star generates helium 4. This proton-proton cycle occurs mainly in low-mass stars. The heavier stars can also perform what is called the CNO (Carbon-Nitrogen-Oxygen) cycle whose principal cycle[3] is:

$$^{12}_{6}C +\ ^{1}_{1}H \rightarrow\ ^{13}_{7}N + \gamma + E \tag{1.2}$$

$$^{13}_{7}N \rightarrow\ ^{13}_{6}C + e^{+} + \nu_e + E \tag{1.3}$$

$$^{13}_{6}C +\ ^{1}_{1}H \rightarrow\ ^{14}_{7}N + \gamma + E \tag{1.4}$$

$$^{14}_{7}N +\ ^{1}_{1}H \rightarrow\ ^{15}_{8}O + \gamma + E \tag{1.5}$$

$$^{15}_{8}O \rightarrow\ ^{15}_{7}N + e^{+} + \nu_e + E \tag{1.6}$$

$$^{15}_{7}N +\ ^{1}_{1}H \rightarrow\ ^{12}_{6}C +^{4}_{2} He + E \tag{1.7}$$

In the course of these reactions, carbon is used as a catalyst, it is regenerated at the end of the cycle. A mix of proton-proton and CNO cycles can occur in stars. For example,

[2]Where γ represents photon emission.

[3]One should notice that secondary CNO cycles exist but are way less likely to happen.

in the case of the sun, it is estimated that the balance between those two phenomena is 99% (proton-proton) - 1% (CNO cycle)[4] [49].

The stars that are less massive than the Sun (or around its mass) spend a substantially longer time on the main sequence because they live a lot longer, as highlighted in Table 1.1. Because of their much lower luminosities, they burn their core hydrogen very slowly. More massive and more luminous stars, in contrast, burn their hydrogen fuel much more rapidly and that is why they live much less time.

After that main-sequence life, stars begin to go through the red giant branch phase as shown in Figure 1.1. That time as a red giant is also quite long, for example one star with a mass around $1M_{\odot}$ will be a red giant for about 1 billion years and a star of a mass around $10M_{\odot}$ will spend only about 1 million years in that phase.

What will happen to the star after that red giant phase only depends on its initial mass and is explained in the two following subsections.

1.1.2 Evolution of a Low-Mass Star

In this section we will consider stars with a mass lower than 8 $M_{\odot}$. Once such a star has reached the main sequence, it sustains the fusion of hydrogen into helium in its core during around 75% of its (long) life, as mentioned in the previous section.

The temperatures are much higher in the stellar core, which implies that the fusion of hydrogen occurs first. This also means that hydrogen is consumed first. It all forms a burning layer above the core where hydrogen continues to fuse into helium. This phase is called *shell burning* [47]. Afterwards, the newly formed core region underneath the hydrogen-burning shell begins to contract (in the absence of thermonuclear reactions) and slowly heats up in the process (the pressure rises resulting in a rise in temperature). This heating process eventually causes the hydrogen burning in the shell to flare up. The layers above the burning shell then expand very rapidly and begin to cool down in such a way that the star moves to the lower end of the red giant zone in the HR Diagram.

Once there, the (still) inert helium core of the star slowly continues to contract itself and therefore heats up. At the same time, the hydrogen-burning shell becomes thinner and thinner as the expansion goes on. As a result, the surface area increases and therefore the luminosity of the star increases too. As for the surface temperature, it undergoes a huge decrease at this point.

At the red giant phase peaks, the helium in the center of the star becomes so dense and so hot that its fusion can be ignited. Helium then fuses into carbon and oxygen (see section 1.2 for more details). In low-mass stars that ignition of helium fusion is called *The Helium Flash.* The star therefore enters a new phase of its life: the helium burning phase. It lasts much less time than the hydrogen-burning phase (around 100 times less) but helium burning provides a new source of energy. This leads to a fast decrease in the luminosity of the star, the star contracts itself, leading to a much higher surface temperature. At that point the star fuses helium into carbon and oxygen in its hot core while hydrogen is still fusing into helium in the burning shell above it.

When the star has (almost) fused all the helium in its core, a change similar to what happened at the end of core hydrogen fusing takes place: an helium- burning shell forms at the outer edge of the newly created carbon-oxygen core.

The helium-burning shell gets thinner and thinner with time. That thinning leads to thermal instabilities: it reacts very quickly and violently to any change (addition or diminution) of heat. Therefore, any tiny rise in temperature caused by the core below, immediately leads to an uncontrolled rise in temperature in the helium-burning shell.

[4] This was discovered thanks to the observation of solar neutrino in 2020 by the Borexino collaboration.

Those thermal instabilities lead to a temperature increase in the helium-burning shell around the core despite its expansion. At the same time, the surface temperature goes down because of the expansion of the layers above the helium- burning shell. This also includes regions where the hydrogen burning-shell is still present. As a result, the luminosity of the hydrogen-burning shell drops drastically. After a very short time (several years), the helium-burning shell has expanded enough for it to regain thermal stability. At this point of the process, any further expansion leads, once again, to cooling and not to additional heating.

The overall contraction of the stellar envelope causes the temperature in the hydrogen-burning shell to rise, therefore increasing the fusion rate in that shell. "Thermal pulses" originating from the bottom of the helium-burning shell occur at fairly regular intervals (around a few thousand years) in all stars with both helium and hydrogen burning shells (if the initial mass of the star is really too small, for example lower than 0.8 $M_\odot$, the process is stopped earlier as the fusion of the helium can never be ignited).

The helium-burning shell fuses ^{4}He into ^{12}C and ^{16}O and the hydrogen-burning shell then converts ^{12}C into ^{14}N. That nitrogen remains under the hydrogen-burning shell even as the shell is bigger and bigger because of the pulses. In the pulse that follows its creation, the nitrogen is mixed down into the helium-burning shell (by a convection zone operating between the shells).

For the low- and intermediate-mass stars that are of interest in this section, this is the very last step before the end of their evolution. Indeed, the stars with an initial mass lower than 8 $M_\odot$ do not have enough mass to cause a contraction and sufficient heating of the carbon-oxygen core to ignite carbon fusion. The remaining sources of energy are the helium- and hydrogen- burning shells. The smaller these two burning shells become, the closer they get to the stellar surface and the stronger the consequences of the thermal pulses become. The star will eject its outermost layers, layer by layer until the end. At this point, the entire material above the helium-burning shell has been blasted into the interstellar space. What is left of the initial star is its extremely hot and dense carbon-oxygen core a white dwarf surrounded by a gaseous cloud called a planetary nebula [47].

This final state is of particular interest to us since the study of the spectrum of these white dwarfs constitutes an entire chapter of this thesis. We will discuss those peculiarly hot and very dense astrophysical objects in more detail in Section 1.4 and Chapter 4.

1.1.3 Evolution of a High-Mass Star

Even if in the context of this thesis the evolution of high-mass stars is less relevant, it is still worth briefly explain how this kind of star evolves.

Massive stars also spend most of their life on the main sequence (around 90%). This time is just much shorter than less massive stars because of their much shorter lifetime. Exactly as low- and intermediate-mass stars, during their time on the main sequence, massive stars fuse their hydrogen into helium. And, exactly as explained in the previous subsection, this newly formed helium core contracts while hydrogen-burning shell moves outward, layer by layer. Massive stars also go on the red giant branch just after helium fusion has begun. But the end of the story from now on is a little bit different for massive stars than what is was for lighter stars. Indeed, in this case, every step, even if quite similar, happens much more quickly and much more intensively. The conditions are extreme and additional thermonuclear fusion reactions can occur. Massive stars are able to form a carbon core which is large enough to reach temperatures of over 1 billion K during the contraction phase subsequent to helium burning.

At such intense temperatures and high densities, large numbers of neutrinos are created (due to the reactions) in the stellar interior. Those neutrinos, which have practically no interaction with matter, will leave the star without contributing any counteracting pressure to gravity in the way photons would do[5]. The stellar core therefore continues to contract itself and to heat up, causing the nuclear reactions to occur more and more rapidly. This creates an iterative cyclical phenomenon: the hotter the core region, the more neutrinos are generated, the more neutrinos are generated, the more the star will contract itself, and the more it does, the more the temperature increases. As a result, nuclear burning in the star accelerates.

The final stage occurs at about 3 billion K, where the fusion of silicon can be ignited. This process of conversion of silicon into iron and nickel is very quick.

During those very advanced and intense phenomena within the core of a massive star, the outer envelope of the star is not affected much by the processes because the envelope cannot react so quickly to any changes. The star just continues to move along the asymptotic giant branch in the Hertzsprung-Russell diagram.

When the final stage of fusion has occurred, the conditions are too extreme and the star explodes as a gigantic supernova.

In the end, the remnant of a low- (or intermediate-)mass star is a white dwarf as mentioned in the previous section. A massive star leaves behind a neutron-star or black hole [47]. Those three kinds of dead stars are called compact bodies.

1.2 Stellar Nucleosynthesis

The theory of nucleosynthesis describes the distribution of the abundances of the different elements found in our current Universe and aims to explain how they were formed. One of the channels of element formation is the nucleosynthesis in the core of stars during a long period of their quiet evolution as described in sections 1.1.2 and 1.1.3. As mentioned in those sections, when the temperature in the core of the star is sufficient, the fusion of helium can ignite itself. Afterwards, the higher the temperature can rise, the heavier elements the fusion process will be able to create.

However, this stellar channel is unable to explain the formation of elements much heavier than iron (which are exactly the ones we are interested in for this thesis). As a result, the concept of explosive nucleosynthesis was introduced. The latter implies that matter is irradiated under a flux of neutrons from highly energetic phenomena. Even if exposures to neutron fluxes are of limited duration, neutron-capture reactions are a very plausible explanation for the creation of heavy elements.

In neutron capture, a nucleus (for example, a carbon or iron nucleus) is bombarded with neutrons. Since the number of protons does not change, the nucleus remains of the same species as before the bombardment, but becomes unstable due to the additional neutrons. In order to reach stability, the nucleus realizes a beta decay, and is then transformed into an element with an higher atomic number.

This process repeated in an iterative way can lead to the creation of heavy elements. The heaviest one reachable is lead which is, as iron, very stable.

In order to create elements heavier than lead and bismuth, the neutronic irradiation must be more intense and the time scale must be shorter, leading to a more rapid process explained in section 1.2.2.

[5]With radiation pressure as explained in section 1.4.2

1.2.1 S-process

1.2.1.1 Neutron Sources

As mentioned in section 1.1.2, at the very end of its life, a star of a mass lower than $8M_{\odot}$ ejects all its gaseous layers planetary nebula to form a planetary nebula.

Spectroscopic analyses of those nebulae have shown that they contain many heavy s-process elements.

At some point, the low mass star will (generally) reach a state where a very hot dense carbon core is surrounded by two burning shells, one burning helium and the other one burning hydrogen, with a convection zone between them.

Located underneath the stellar envelope is the hydrogen-burning shell, and below that the helium- burning shell. The s-process takes place in the pulsating intershell between those two burning shells. A neutron source arises if carbon isotopes (^{13}C) or neon isotopes (^{22}Ne) capture a helium nucleus. A neutron is released at each capture. It generates quite a low but long-lasting neutron density, depending on the stellar mass. The neutrons are mainly available at the bottom of the convection zone, where they are repeatedly incorporated into the available seed nuclei. The total abundance of new elements not only depends on the neutron flux but also on the number of available seed nuclei inside a star which partly depends on the stellar environment in which it was first created[6]. The star can enrich the stellar environment in heavy elements through stellar winds or, in the end, through the expulsion of its outer layers.

1.2.1.2 S-Process Basic Principle

Under weak neutron irradiation, an unstable nuclide is formed from a stable nuclide that has captured a neutron. This unstable nuclide will undergo a β decay in order to stabilize itself (as much as possible) before absorbing another neutron. We are thus talking about a fairly slow process. In this regime, matter that undergoes neutron irradiation is enriched, by successive steps of one atomic mass at a time, to create heavy elements. Neutron capture immediately followed by a β decay (or several successive β decays) can only follow one path in the nuclide map. This way is shown on figure 1.2.

About half of all the isotopes heavier than iron are produced by this s-process [47] capable of synthesizing elements up to lead. For larger atomic masses, the neutron absorption is not followed by a β decay but by a α decay that moves the element back 4 atomic masses. That's why lead is a difficult boundary to cross for the s-process. Elements with a magic number of neutrons generate points of partial limitation of the process. Because these elements only have complete layers of neutrons, they have a small effective absorption cross section of a new neutron. The $^{208}_{82}Pb$ is doubly magic (82 protons and 126 neutrons).

1.2.2 R-process

1.2.2.1 Neutron sources

Unlike the s-process, the r-process needs much more intense neutron irradiation. The required conditions to provide that kind of neutronic irradiation can only be achieved in a supernova or during neutron star mergers [47]. For a long time, the first one was the preferred candidate by astrophysicists but in the last few years, the tendency has been reversed, launching many studies on the kilonovae, supposed to be the biggest source of intense neutron irradiation.

[6] It also depends on whether the star had a companion star from which it could have drawn neutrons and s-process elements.

1.2.2.2 R-Process Basic Principle

Under intense neutron irradiation, unstable nuclides do not have time to undergo the β decay before absorbing a new neutron. Unstable, neutron-rich nuclides, far enough away from the valley of nuclear stability, can then be temporarily created under neutron irradiation. Under a given neutron flux and for a given γ irradiation (influenced by temperature), there is, for each Z, a boundary nuclide that the r-process can create and maintain. After neutron irradiation (which can come from a supernova for example), these boundary nuclides, which are unstable when the neutron flux is no longer there to maintain them, tend to return to the valley of nuclear stability through successive β disintegrations. Once again, nuclides with a magic number of neutrons are favored to play the role of boundary nuclides (because of their small effective absorption cross section for a new neutron). This process explains the natural abundance of heavy elements.

As for the synthesis of super-heavy elements (whose mass amounts to about 300 a.m.u.), it is made possible by a 2-step r-process, the second operating on a gas that has already undergone a first r-episode.

An example of s-r-processes' path through the Mendeleev Table is shown in Figure 1.2.

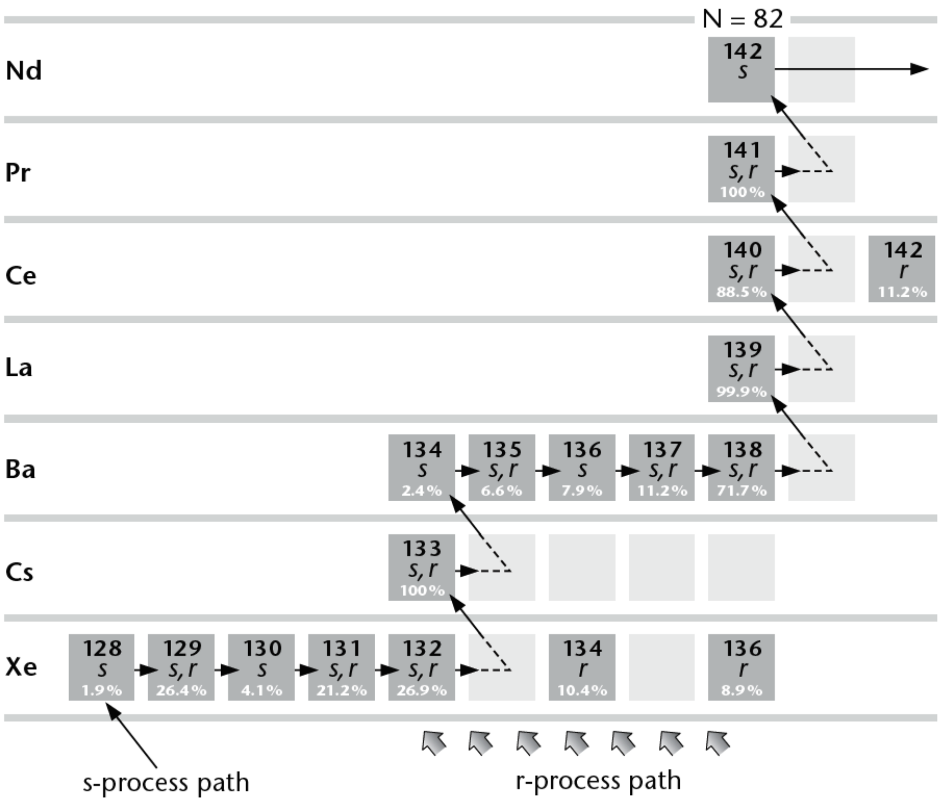

Figure 1.2: Example of s-r-nucleosynthesis processes in the Mendeleev Table. Credit: [47] data from [50]

.

1.3 Cosmochronology

In principle, radioactive decay can lead to a very precise age-dating technique for a specific star if the half-lives of the decaying isotopes are known[7] if the current isotopic abundance[8], can be measured and if the production of that isotope is well understood (see section 1.3.1 for more details on the technique).

In the case of stars where elemental abundances can be measured, the element involved must be free of any stable isotope with a more important abundance than the radioactive isotope.

The most suitable isotopes identified for this purpose are all (super-)heavy r-process nuclei. These elements can only be made by neutron capture. They all lie beyond the last stable elements, lead and bismuth, and cannot be reached via the s-process of neutron capture as mentioned in section 1.2. Their production mechanisms and rates are therefore known and it is also understood that they decay to lead or bismuth. The isotopes matching that description are:

- ^{187}Re (half life: 45 Gyr)
- ^{232}Th (half life: 14 Gyr)
- ^{235}U (half life: 0.7 Gyr)
- ^{238}U (half life: 4.5 Gyr)

After about a Gyr, one can ignore the lighter U isotope assuming it entirely decayed. This leads to the conclusion that ^{232}Th and ^{238}U are very suitable candidates to perform stellar datation.

Since the initial abundances has to be known, and each star has a different initial metallicity, the technique generally used by the astrophysicists is to compare the abundance ratios of the unstable isotope (element) that they are interested in to either another unstable isotope or to a stable one. The most often used ratios are Rhenium/Osmium (Re/Os), Thorium/Europium (Th/Eu), and Uranium/Thorium (U/Th) [51, 52]. Europium has two stable isotopes (^{151}Eu and ^{153}Eu) which are produced almost exclusively through the r-process neutron capture. The Th/Eu ratio cosmochronological study is the most used up to now but it is not ideal because of the high different atomic weight (151 or 153 versus 232 and atomic number Z = 63 versus 93). That means that there is a greater risk of error/uncertainty due to our current understanding of the r-process mechanisms. When it comes to predict the initial production ratios, the uncertainty is generally smaller when the two elements are as close in mass number as possible [52]. This is why U/Th ration seems a particularly good candidate.

1.3.1 Uranium-Thorium Cosmochronology

The U/Th (^{238}U/ ^{232}Th) ratio is, as mentioned above, of great significance in cosmochronology [53]:

$$R^{U/Th} = P^{U/Th} e^{\frac{T}{\tau_{Th}} - \frac{T}{\tau_U}} \tag{1.8}$$

where T is the age of the star studied, $R^{U/Th}$ is the Uranium/Thorium abundance ratio, $P^{U/Th}$ is the production rates ratio (supposedly known) and τ_U and τ_{Th} are the radioactive half-lives of the most abundant isotopes of Uranium (^{238}U) and Thorium (^{232}Th). For

[7]They are usually known based on experimental measurements.

[8]Or at least the abundance of the product of the decay.

example, in 2001, Cayrel *et al.* [54] dated the CS31082-001 star (also known as Cayrel's star) at

$$12.5 \pm 3.0 \text{ Gyr}$$

According to the latter authors, the main sources of uncertainty were:

- the nuclear models;
- the lack of atomic data;
- the fact that only few lines were identified.

Within the scope of this thesis, we will act on the last two sources of uncertainties. Indeed, in the particular case of CS31082-001, only one U II line was identified (for the first time ever!) and its relatively weak intensity made the identification very difficult (see figure 1.3). The numerical value of the age of CS31082-001 was later refined (see e.g. [55])

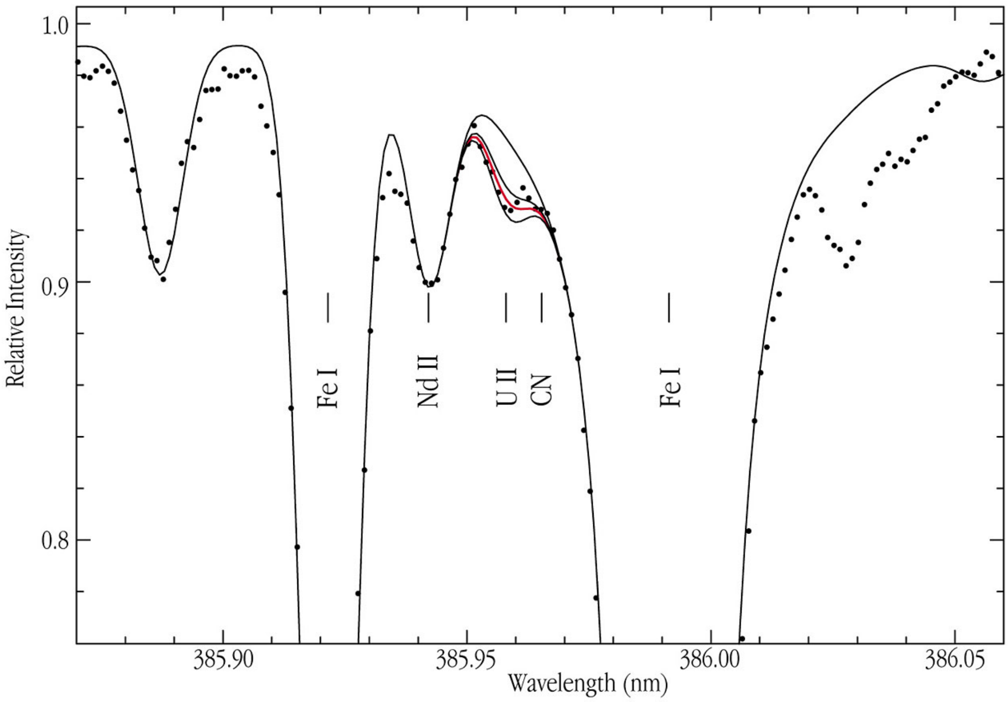

Figure 1.3: CS31082-001 spectrum around the U II line at 385.959 nm. The U II line is shown in red. Source: [54]

but the uncertainties are still important with similar causes. This maintains and even reinforces our motivation to perform calculations in U II and Th II.

1.3.1.1 U II

Oscillator strengths for electric dipole (E1) radiative transitions in U II are supposed to be of a great interest in cosmochronology. Indeed, as mentioned above, the age of a star can be determined using a radioactive isotope of a sufficiently long lifetime. Up until a few years ago, the radioisotope ^{232}Th, with a half-life of $\approx$ 14 Gyr, was used to date galactic stars (see e.g.[56]). As shown in [57], new accurate observations of heavy radioactive elements could improve the accuracy of those cosmochronometrical analyses. More particularly, the ^{238}U isotope, which has a half-life of 4.5 Gyr, should represent a more precise age indicator. Furthermore, the U/Th ratio might be a much better cosmochronometer than both previously used Th/Eu and Th/Dy ratios because of the fact that the mass difference between Th and U is much smaller than between either one of these two actinides and the lighter lanthanides.

Unfortunately, uranium is very hard to detect in stars. In 2001, Cayrel ([54]) reported the first detection of a spectral line at a wavelength of 3859.57 Å, from singly ionized uranium, in the very metal-poor star BPS CS31082-001. This star, also called Cayrel's star, is more metal deficient than the globular clusters, and was thus probably born in the Galaxy's very early times. This measurement was made with the ESO/VLT telescope, and the UVES spectrograph. It was therefore possible to use the U/Th ratio in order to determine the age of formation of these elements in the early Galaxy for the very first time. The derived uranium abundance yielded an age of 12.5 $\pm$ 3 Gyr, which led to the best estimate of the age of the Galaxy and consequently provided a lower limit to the age of the Universe. However, as mentioned in [54], the accuracy of this uranium dating technique is still largely limited by the uncertainty of the abundance ratio which is derived from observation, and by the uncertainty of the theoretical estimation of the U/Th production ratio. The improvement of this situation not only depends on a better estimation of the U/Th production ratio, on refinements of the models in nuclear physics and on the possible discovery of other metal-deficient r-process-enhanced stars in which U and Th abundances can be measured, but also on a comprehensive knowledge of the radiative properties for the potentially observable spectral lines, notably for the strongest U II electric dipole transitions.

1.3.1.2 Th II

While uranium is extremely hard to detect in stars, making the U II line at 3859.57 Å the only one that could be used as a cosmochronometer so far, thorium is often detectable in r-process stars. For example, in the star CS31082-001, 14 individual Th II lines were identified, 10 of which being sufficiently unblended to allow for a precise determination of its abundance [54]. In CS22892-052, there were only three Th II lines at 3539.59, 4019.13, and 4086.52 Å that might be used for abundance measurements as mentioned by Sneden & Cowan [58]. Roederer *et al.* [59] observed the four Th II lines at 3539.59, 4019.13, 4086.52, and 4094.75 Å in 14 metal-poor stars whose very heavy element enrichment was only produced by the r-process. A detailed analysis of the blending features was performed in this work, confirming or supplementing the discussion previously started by Lawler *et al.* [60], Morell *et al.* [61], Sneden *et al.* [62] , Norris *et al.* [63], and Johnson & Bolte [64] for different stars. Several Th II lines were detected by Frebel *et al.* [65] in the spectrum of the strongly r-process-enhanced metal-poor star HD1523-0901. However, most of them were severely blended with lines from other elements so that only the line at 4019.13 Å was selected to determine the age of the star. Based on this single line, Ren *et al.* [66] estimated thorium abundances for 17 stars, and upper limits for another 60 stars. Th II lines were also detected in several other stellar spectra, but it would be too tedious to list them all here. However, in all these studies, the number of observed thorium lines was very small, most of them being often blended with lines of other ions. It is therefore of paramount importance that astrophysicists have a list of strong transitions in Th II and U II ions at their disposal with radiative parameters sufficiently reliable to be used in uranium and thorium stellar abundance studies and, even more so, in cosmochronological analyses.

1.4 Study of White Dwarfs Spectra

1.4.1 White Dwarfs

White dwarfs (often referred to as WD) are objects of high density which are the result of the evolution of a low to moderate mass star ($M_{star} < 10M_{\odot}$). They are very small in size (hence the name dwarf) and have a high surface temperature (hence the term white). Typically, for a mass of about $1M_{\odot}$, they have a volume of about V_{Earth}. Upon their formation, they populate the lower left part of the Hertzprung-Russel diagram and drift to the right as they cool down. Their T_{eff} is generally between around 10 000K and 150 000K and, unless there is an accretion of surrounding matter, their radiation only comes from stored (unrenewed) heat. For that kind of astrophysical objects, the cooling process is very slow [67].

1.4.1.1 Formation Process

As already mentioned in section 1.1.2, white dwarfs are the residual end-of-life form of low-mass main sequence stars with masses ranging between 0.13 and 10 $M_{\odot}$.

As a quick reminder of what has already been explained in section 1.1.2, at the end of their lives, these low-mass stars have burnt most of their hydrogen into helium. Deprived of their primary fuel, these stars collapse due to their own mass. At this point, the pressure and temperature of the core increases, causing the helium to fuse and produce heavier elements such as carbon. At this stage of the process, there is an increase in energy, the star has become a red giant. Once the helium is consumed, the contraction resumes. The low mass does not provide the required conditions for the carbon fusion to occur: the core collapses into a white dwarf and the outer layers are expelled in the form of a nebula. The final result is a very hot white dwarf (composed mainly of a hydrogen and helium, which were not consumed during the fusion, atmosphere and an inert carbon and oxygen core) surrounded by a cloud of gas. The final composition of the white dwarf depends on the composition of the initial star.

1.4.1.2 Chandrasekhar Limit

White dwarf masses range from $0.13M_{\odot}$ to $1.33M_{\odot}$. There is a mass limit of $1.44M_{\odot}$ above which white dwarfs would no longer be able to withstand their own gravitational collapse. This also set an upper mass limit for a star to become a white dwarf (8-10$M_{\odot}$). The mass distribution of white dwarfs has a peak around $0.6M_{\odot}$ and therefore, the majority of white dwarfs are such that they have a mass around $0.5M_{\odot}$. However, for the most part, their radius is between 0.008 and $0.02R_{\odot}$. That means that white dwarfs are among the densest bodies in the Universe.

Those very high densities lead to the degeneration of internal matter. Such densities are indeed possible because we are in the plasma state. But, given that the star undergoes a cooling process, we could intuitively think that the energy will also decrease strongly. If, at some point we'd reach 0K, by Pauli's principle of exclusion, not all electrons can be in the fundamental state. We would then have a state called the Fermi Sea and even when the temperature decreases, we can have a quite high energy. To have a better idea of what degeneration pressure is, we can also use Heisenberg's uncertainty principle. Indeed, if the density is very high, the uncertainty of the position of the electrons is very low, which implies a large variation of the possible momenta or, in other words, a lot of kinetic energy. The degenerative pressure prevents gravitational collapse. It only depends on density and not on temperature, i.e. the star can cool down without collapsing on itself. That means that there is a balance between degenerative pressure and gravitational forces. There is therefore a limit mass. If the limit is exceeded and new fusion reactions do not start, then the star collapses on itself. It should be noted that, since degenerated matter is relatively compressible, the density of a high-mass white dwarf is higher than that of a low-mass white dwarf. Therefore, the radius of the white dwarf decreases as its mass increases.

1.4.1.3 Spectral Classification

White dwarfs are objects with a very high surface gravity, they are thus almost opaque to radiation. Nevertheless, some absorption lines have been observed and they led to the spectroscopic classification of white dwarfs. For each white dwarf, the first letter of the denomination is a D (for *Degenerate*). The second letter is given according to the spectral lines that could be observed. White dwarfs are classified as follows [68]:

Table 1.2: Spectral Classification of WD

Spectral Type	Main Absorption Lines
DA	Hydrogen
DB	He I
DO	He II
DQ	Atomic or Molecular Carbon
DZ	Other Element
DC	No marked line (i.e. optical depth $\leq 5\%$ of radiation)

If there are marked lines for more than one element, then the denomination will be D + the other appropriate letters. The general shape of the spectrum gives the effective surface temperature (in our case $T \neq T_{eff}$ because the star is not quite a black body). Consequently, a number is associated with the temperature in the spectral classification: $\frac{50400K}{T_{eff}}$. Other letters can be added such as E if we see emission lines or a letter associated with another parameter: the variability. For a given characteristic, if it is followed by an interrogation mark or two dots, it means that the characteristic is not yet certified. Most (75%) of the white dwarfs observed are of type DA.

1.4.2 Radiative Levitation

With a given mass and composition, the internal dynamics and structure of a star is determined by the balance between the gravitational and radiative forces within it. Radiative forces are caused by photon-atom interactions. Let us consider these photon-atom interactions for individual elements. Quite intuitively, we will say that the gravitational forces pull the particles *down* (i.e. towards the center of the star). If gravity dominates the kinetic forces, then the heaviest particles will be more attracted towards the center of the star and a segregation between heavy and light elements will be observed. However, when we add the radiation pressure to the gravitational forces (in addition to the gas pressures in the stellar interiors), we find that these radiation forces combined with the internal gas pressure are greater than the gravitational force. As a result, the elements are in *levitation* and rise to the surface [69]. Intuitively, one would tend to think that despite everything, the heavier elements will remain more attracted by the force of gravity, but if we add atomic physics into the mix, other conclusions can be drawn. Indeed, the radiative force depends on the absorption of the radiation by the element, which in turn depends strongly on the ionization state of the element (the ionization state itself depending on the local temperature and density conditions). As a matter of facts, some states of ionization have a much higher absorption cross section than others. As a result, the balance between radiative and gravitational forces in a star fluctuates according to the local conditions of the star. Therefore, the closer one gets to the center of the star, the more likely one is to have high temperatures and densities, and thus higher ionization states and the higher the radiative levitation phenomenon will be. That said, the phenomenon of radiative levitation can also (quite intuitively) explain why quite heavy elements (in a certain state of ionization) can be seen in the photosphere of some stars.

1.4.3 RE0503-289

The white dwarf RE0503-289 is located in an interstellar region of very low H I density and is itself of low hydrogen density. Its estimated temperature is situated between 60000 and 80000K [70]. It has been noticed that the abundance of carbon is in the order of a few %. Balmer's lines in absorption that we see for most white dwarfs are not to be seen but we have a large absorption for the 468.6 nm line of He II. RE0503-289 is thus a white dwarf of type DO or a star PG1159[9]. Moreover, RE0503-289 is located at the limit of the wind limit[10] (see Figure 1.4) which corroborates the hypothesis that it could be a transient state between a star of type PG1159 and a white dwarf.

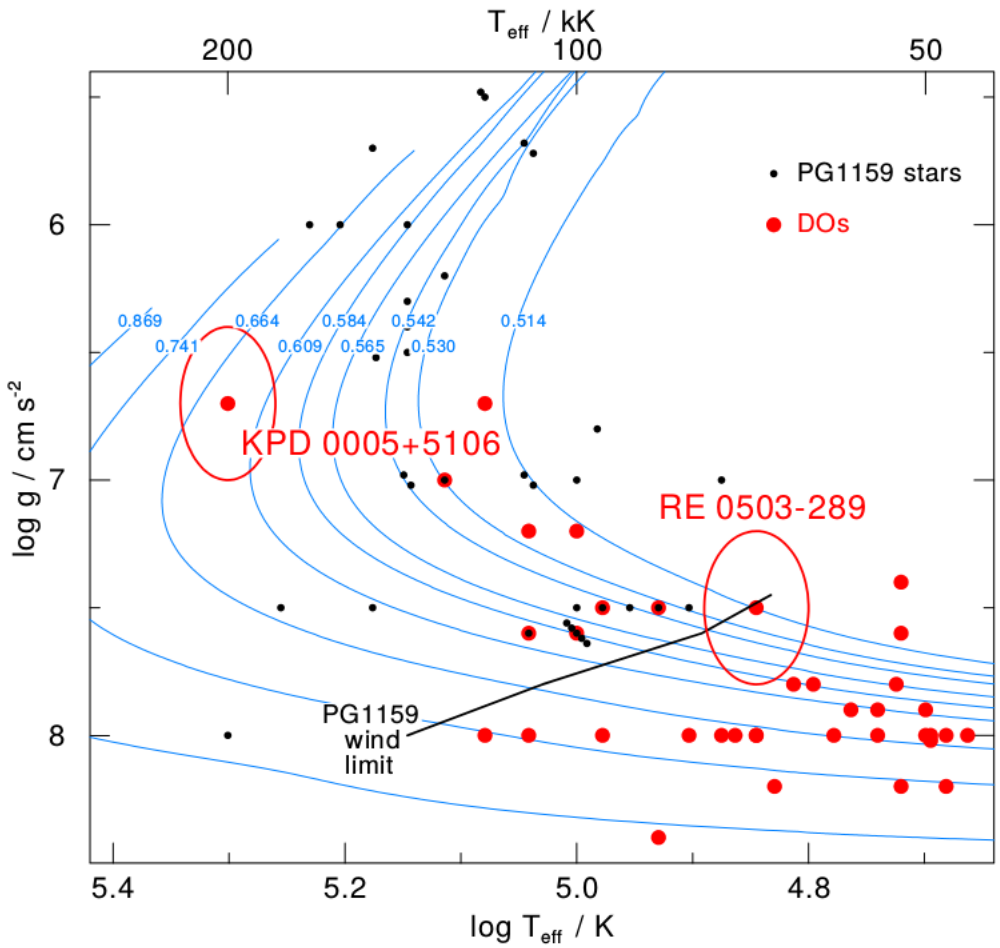

Figure 1.4: Position of RE0503-289 towards the wind limit. Source: [71]

[9] Transient state between a star and a white dwarf, i.e. a predegenerated star.

[10] The wind limit is a semi-empirical limit beyond which there can be no more stars of type PG1159 and therefore there can only be white dwarfs.

1.4.3.1 Peculiarities

RE0503-289 raises many interrogations due to its peculiarities:

1. *A priori* it looks like a DO type WD (see section 1.4.1.3) but its opacity model looks more like a DA type containing more heavy elements.

2. It is very close to another DA type WD: RE0457-281. This gives us a very rare occasion to study an interstellar space much smaller than usual. In addition, some interactions could occur between those two stars and can therefore be studied.

3. RE0503-289 has an overabundance (up to 4 orders of magnitude greater than solar abundances) of heavy elements as highlighted in Figure 1.5 [72, 73, 74, 75, 76]. Given the nature of these elements, their production is surely the result of a s-process nucleosynthesis (see section 1.2). However, their overabundance is a mystery. It could be partly explained by radiative levitation, but this is not sufficient. Also note that RE0503-289 has a carbon abundance of about 3-4% rather than the 1% expected.

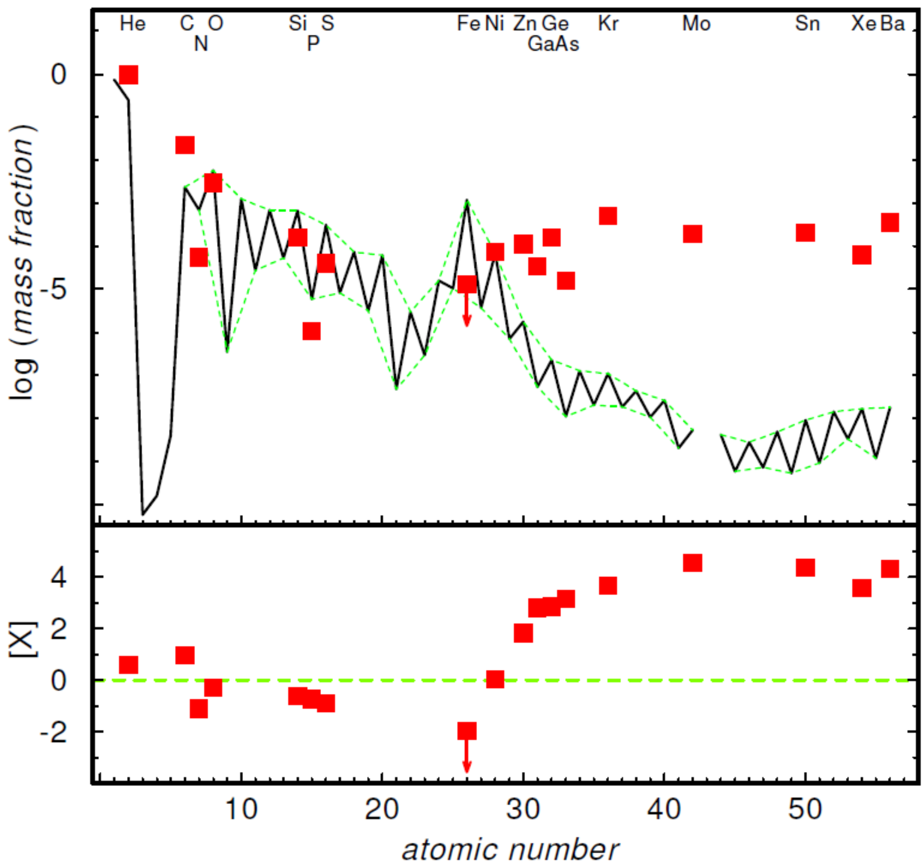

Figure 1.5: Extreme overabundances of Trans-Iron Elements (TIEs) in the spectrum of RE0503-289 - Source: [77]

One can wonder if this kind of phenomenon is a unique or common one. Rauch *et al.* [74] performed diffusion calculations to demonstrate that the extreme TIEs overabundances in RE 0503-289 are the result of efficient radiative levitation. They also observed three related objects close to the location of R0503-289, namely PG0109+111, PG1707+427, and WD0111+002. While RE 0503-289 is located directly on the PG1159 wind limit as shown in Figure 1.4, PG1707+427 lies towards higher T_{eff} and PG0109+111 and

WD0111+002 towards higher log g[11] even right of the full line that indicates where the photospheric carbon abundance is reduced by gravitational settling. The detailed spectral analysis presented by Hoyer *et al.* [78] showed equally high TIE abundance enhancements in PG0109+111 and WD0111+002 as in RE0503-289 and, thus, the TIE abundance enhancement due to radiative levitation. In contrast, no TIE line has been identified in the spectrum of PG1707+427. Their hypothesis was that in that star the stellar wind is too strong and prevents efficient diffusion of the TIEs. Later on, Löbling *et al.* [79] identified many TIEs lines in a DAO-type white dwarf (namely BD-22^{o}3467). This research topic is therefore still ongoing and new observations could be added to the models and lead to a better understanding of those overabundances, of radiative levitation and of white dwarfs.

1.4.3.2 Need of Atomic Data

The discovery of TIE lines in the spectrum of RE0503-289 [80] and the lack of reliable atomic data in the literature initiated a campaign to calculate transition probabilities and oscillator strengths at the University of Tübingen through The Tübingen Oscillator Strengths Service (TOSS). The Atomic Physics and Astrophysics group at the University of Mons later joined this project to perform precise atomic calculations. With those newly calculated data, abundance determinations for all TIEs with heretofore identified lines became possible. The ultimate goal of this collaboration is to produce reliable atomic data in all the TIEs elements up to cerium in their third to sixth ionization states in order to be able to have an exhaustive analysis of the spectrum of RE0503-289. This analysis could lead to a better understanding of the phenomenon mentioned in the previous subsections.

In the context of this thesis, we participated in that effort by calculating atomic data for four of those TIE elements: Cu, In, Cs and Ag.

[11] where g is the surface gravity

Chapter 2

Theoretical Methods

2.1 Atomic Physics Reminders

2.1.1 Einstein Coefficients

When an atom (or an ion) in a certain state $|i\rangle$ of energy E_i is put into an electromagnetic radiation with a spectral energy density $\omega_\nu(\nu)$, that atom (or ion) can absorb a photon hν such that it finds itself in a higher energy state $E_k = E_i + h\nu$. The variation in the population of the level E_i is given by the following relation:

$$\frac{dN_i(t)}{dt} = -B_{ik}N_i(t)\omega_\nu(\nu_{ik}) \tag{2.1}$$

where B_{ik} is the Einstein coefficient for absorption.

The radiation field can also cause atoms in an excited state E_k to de-excite to a lower state E_i by emitting a photon of energy E_k - E_i. In this case B_{ki} is the Einstein coefficient for induced emission (or stimulated emission). It is also possible that an atom in an excited state E_k spontaneously de-excites to an E_i state without a radiation field (or without the intervention of a field). In this case,

$$\frac{dN_k(t)}{dt} = -A_{ki}N_k(t) \tag{2.2}$$

where A_{ki} is the Einstein coefficient for spontaneous emission.

Quite intuitively, we can link these three processes. Indeed, at thermodynamic equilibrium (for a certain temperature T), the radiation density is given by:

$$\omega_\nu(\nu_{ik}) = \frac{8\pi h\nu_{ik}^3}{c^3}\frac{1}{e^{h\nu_{ik}/kT}-1} \tag{2.3}$$

which is equivalent to

$$\omega_\sigma(\sigma_{ik}) = 8\pi hc\sigma_{ik}^3\frac{1}{e^{h\sigma_{ik}/kT}-1} \tag{2.4}$$

where $\sigma_{ik} = \frac{1}{\lambda_{ik}}$ is the wavenumber. By the assumption of thermodynamic equilibrium, the populations of the levels verify the Boltzmann law:

$$\frac{N_i}{N_k} = \frac{g_i}{g_k}e^{-\frac{E_i-E_k}{kT}} = \frac{g_i}{g_k}e^{-\frac{h\sigma_{ik}}{kT}} \tag{2.5}$$

with $g_j = 2J_j + 1$. If we suppose in addition that we are in the conditions of a stationary regime we can then write:

$$B_{ik}N_i\omega_\sigma(\sigma_{ik}) = A_{ki}N_k + B_{ki}N_k\omega_\sigma(\sigma_{ik}) \tag{2.6}$$

From there, we can obtain:

$$g_i B_{ik} = g_k B_{ki} \tag{2.7}$$

and

$$A_{ki} = 8\pi hc\sigma_{ik}^3 B_{ki} \tag{2.8}$$

2.1.2 Radiative Transitions

For an electric dipole transition (E1) between a $|\gamma_k J_k M_k\rangle$ state of degeneracy[1] $g_k = 2J_k + 1$ and a $|\gamma_i J_i M_i\rangle$ state of degeneracy $g_i = 2J_i + 1$, making the analogy with the classical approach of the oscillating electric dipole, a spontaneous emission probability can be obtained (see e.g. [7]):

$$a(E1) = \frac{64\pi^4 e^2 a_0^2 \sigma^3}{3h} \sum_q |\langle \gamma_i J_i M_i| \ P_q^{(1)} |\gamma_k J_k M_k\rangle \ |^2 \tag{2.9}$$

where $P_q^{(1)} = \sum_j r_q^{(1)}(j)$ is the q^{th} component of the dipole momentum. For the transition probability from a state $|\gamma_k J_k\rangle$ to a state $|\gamma_i J_i\rangle$, A_{ki} we have:

$$A_{ki}(E1) = \frac{64\pi^4 e^2 a_0^2 \sigma^3}{3hg_k} \sum_{M_i} \sum_{M_k} \sum_q |\langle \gamma_i J_i M_i| \ P_q^{(1)} |\gamma_k J_k M_k\rangle \ |^2 \tag{2.10}$$

We will also use the notation gA(E1) such that $gA(E1) = g_k A_{ki}(E1)$. Associated to each type of transitions, there are selection rules, in particular for the electric dipole transitions, due to the fact that the multipole transition operators are irreducible tensor operators and that they obey the Wigner-Eckart theorem. For E1 transitions, we find:

$$\Delta J = J_i - J_k = 0, 1, -1 \tag{2.11}$$

with $J_i = J_k = 0$ not allowed and

$$\Delta M = M_i - M_k = 0, 1, -1 \tag{2.12}$$

$$\Delta S = 0 \tag{2.13}$$

and

$$\Delta L = 0, \pm 1 (0 \leftrightarrow 0 \text{ not allowed}) \tag{2.14}$$

with a mandatory change of parity.

Remark

It is important to note that the selection rules mentioned above are only valid for pure LS coupling, which is rarely the case in practice (especially for the heaviest elements). It is nevertheless important to know them because the deviation from the pure LS coupling is treated using the configuration interaction methods as explained in sections 2.2.4 and 2.3.5.

[1] i.e. its statistical weight.

2.1.3 Line Strength

It is usual in atomic physics to introduce a quantity that is symmetric[2], namely the line strength $S_{ik} = S_{ki}$ by writing

$$gA(E1) = \frac{64\pi^4 e^2 a_0^2 \sigma^3}{3h} S_{ik}(E1) \tag{2.15}$$

with

$$S_{ik} = |\langle\gamma_i J_i|\ ||P^{(1)}||\gamma_k J_k\rangle\ |^2 = |\sum_{M_i}\sum_{M_k}\sum_{q}\langle\gamma_i J_i M_i|\ |P_q^{(1)}||\gamma_k J_k M_k\rangle\ |^2 \tag{2.16}$$

where $P^{(1)}$ is the dipole transition operator.

2.1.4 Oscillator Strength

The oscillator strength f_{ik} is a dimensionless quantity that is defined as the number of oscillators[3] that it is necessary to associate with an atom in state i in order for the classical absorption coefficient to be equal to the Einstein coefficient B_{ik}. For an electric dipole transition,

$$f_{ik}(E1) = \frac{8\pi^2 mca_0^2\sigma}{3hg_i} S_{ik}(E1) \tag{2.17}$$

The notation $gf(E1) = g_i f_{ik}(E1)$ is often used.

The transition probability, can therefore be written as:

$$gA(E1) = \frac{8\pi^2 e^2 \sigma^2}{mc} gf(E1) \tag{2.18}$$

These two quantities are directly proportional and that is why we will treat them almost indifferently in this manuscript.

2.1.5 Branching Fraction

The branching fraction, BF, is defined as:

$$BF_{ki} = \frac{A_{ki}}{\sum_i A_{ki}} \tag{2.19}$$

2.1.6 Radiative Lifetime

Let's suppose that a level k is only depopulated by spontaneous emissions to lower energy levels, we can then write:

$$\frac{dN_k(t)}{dt} = -\sum_{i<k} A_{ki} N_k(t) \tag{2.20}$$

which gives

$$N_k(t) = N_k(0)e^{-\sum_{i<k} A_{ki} t} = N_k(0)e^{-\frac{t}{\tau_k}} \tag{2.21}$$

where, for the level k, we define the radiative lifetime:

$$\tau_k = \frac{1}{\sum_{i<k} A_{ki}} \tag{2.22}$$

[2] The symmetry concerns the two levels considered: k and i.

[3] By analogy with the classical theory of an oscillating dipole that absorbs part of the energy when subjected to continuous radiation.

2.2 Pseudo-Relativistic Hartree-Fock Method

The first method used to calculate atomic parameters in the present work is the HFR method (HFR stands for Hartree-Fock + Relativistic corrections). Developed by Cowan [7], the relativistic Hartree-Fock method is based on an iterative resolution of the Hartree-Fock equations (using the self-consistent field method) which themselves are obtained by the application of a variational principle minimizing the average energy of an electronic configuration. Single-electron relativistic corrections (spin-orbit, mass-velocity and Darwin term) are perturbatively added to the model (HFR is therefore a pseudo-relativistic method). The solutions of these equations are the radial parts of the wave functions, which are eigenfunctions of the Hamiltonian describing an atomic or ionic system. The HFR method was improved about twenty years ago by the Atomic Physics and Astrophysics Department at UMONS ([81, 82]) to incorporate the effects of core polarization (CPOL), which are particularly important to model heavy atoms and ions. In this thesis we will use atomic units:

$$\hbar = m_e = \frac{e^2}{4\pi\epsilon_0} = 1 \tag{2.23}$$

Our goal is to determine the energy levels of a given atomic or ionic system and the parameters associated with the possible transitions, i.e. the wavelengths corresponding to these transitions, the transition probabilities and the oscillator strengths. To that end, we must solve the Schrödinger's equation for stationary states, i.e. the eigenvalue equation

$$H\psi_k = E_k\psi_k \tag{2.24}$$

in order to obtain the eigen energies E_k associated with the eigen wavefunctions ψ_k. The (still non-relativistic) Hamiltonian is given by:

$$H = \sum_{i=1}^{N}(-\frac{1}{2}\Delta_i - \frac{Z}{r_i}) + \sum_{i>j}\frac{1}{r_{ij}} \tag{2.25}$$

where N is the number of electrons considered, r_i is the distance between the i^{th} electron and the nucleus (considered here as a point charge), r_{ij} is the distance between the i^{th} and the j^{th} electron and Δ_i is the Laplacian operator acting on r_i.

Given that the problem is not analytically solvable for $N > 1$, we will use the central field approximation in which we suppose that each electron moves independently of the others in a potential with a spherical symmetry which is generated by the nucleus and the $N-1$ other electrons. The Hamiltonian is therefore written:

$$H = \sum_{i=1}^{N}(-\frac{1}{2}\Delta_i - \frac{Z}{r_i} + V(r_i)) \tag{2.26}$$

where V(r_i) is the spherically symmetrical potential where the electron i finds itself. In this case, the problem is reduced to the case of a single electron in a spherically symmetrical system, which is quite similar to the hydrogen atom (it differs from the latter only in the shape of the potential). Therefore, for each electron, we can write, the single-electron wave function by separating the radial variables from the angular variables, which gives for the i^{th} electron:

$$\phi_i(r_i, \theta_i, \Phi_i, s_i) = \frac{1}{r_i}P_{n_il_i}(r_i)Y_{l_i}^{m_i}(\theta_i, \Phi_i)\sigma_{m_{s_i}}(s_i) \tag{2.27}$$

where (r_i, θ_i, Φ_i) are the spherical coordinates (whose origin is the nucleus), $P_{nl}(r)$ is the radial part of the single electron wave function, Y_l^m is a spherical harmonic (cf hydrogenoïd atom) and σ_{m_s}(s) the spin wave function. From these single-electron wave functions, an antisymmetric atomic wave function can be constructed by using a Slater determinant:

$$\psi(q_1, ..., q_N) = \frac{1}{\sqrt{N!}} \begin{vmatrix} \phi_1(q_1) & ... & \phi_1(q_N) \\ ... & ... & ... \\ \phi_N(q_1) & ... & \phi_N(q_N) \end{vmatrix} \tag{2.28}$$

where $q_i = (r_i, \theta_i, \Phi_i, s_i)$. The wave function obtained is an eigenfunction of the Hamiltonian (and satisfies Pauli's principle by its antisymmetry). It is therefore necessary to determine the monoelectronic radial parts (which depend on the shape of the potential) in order to obtain the atomic wave functions giving the (stationary) states of the system. The method used is the self-consistent field method described in the following section.

2.2.1 Self-consistent Field Method and Hartree-Fock Equations

In order to determine the radial parts of the single-electronic wave functions $P_{nl}(r)$, the Hartree-Fock (HF) equations are used. The latter are obtained by applying a variational principle of minimization of the mean energy of a configuration E_{av} to the radial parts $P_{nl}(r)$ to form a system of coupled integro-differential equations (i.e. the equation determining the radial part of the wave function for the electron i, $P_{n_il_i}$ implies all the other radial functions $P_{n_jl_j} \forall j \neq i$). The mean energy of an electronic configuration is given by

$$E_{av} = \frac{\sum_i (2J_i + 1) E_i}{\sum_i (2J_i + 1)} \tag{2.29}$$

where all the energy levels of the configuration are summed. It can also be written as the sum over all the energy states of the Hamiltonian operator's (H) average in each state belonging to an electronic configuration $|i\rangle$

$$E_{av} = \sum_i \langle i| \, H |i\rangle \tag{2.30}$$

By developing this expression, Cowan [7] showed that the terms of electronic interactions that can be expressed from Slater integrals appear in this expression. The generalized Slater integral R^k, representing the electrostatic interaction between 2 electrons belonging to different configurations, is given[4] as follows:

$$R^k(ij; tu) = \int_0^\infty \int_0^\infty \frac{2r_{min}^k}{r_{max}^{k+1}} P_i^*(r_1) P_j^*(r_2) P_t(r_1) P_u(r_2) dr_1 dr_2 \tag{2.31}$$

where r_{min} and r_{max} are respectively the smallest and largest values of r_1 and r_2. The direct electrostatic interaction $F^k(ij) = R^k(ij; ij)$ and the exchange electrostatic interaction[5] $G^k = R^k(ij; ji)$, which describe the interactions of electrons of a same configuration, are particular cases of the generalized Slater integrals. It can be shown that the latter only exist for given values of k: $F^k(ij)$ for k = 0,2,4,...,min($2l_i$,$2l_j$) and $G^k(ij)$ for k = $|l_i - l_j|, |l_i - l_j| + 2, ..., l_i + l_j$. The HF equations are therefore obtained by minimizing E_{av} for a given configuration

$$(n_1 l_1)^{w_1} (n_2 l_2)^{w_2} ... (n_q l_q)^{w_q} \text{ where } \sum_{i=1}^{q} w_i = N \tag{2.32}$$

[4]Using the notation i = $n_i l_i$.

[5]Due to the indiscernabilty of the electrons.

written as:

$$[-\frac{d^2}{dr^2}+\frac{l_i(l_i+1)}{r^2}-\frac{2Z}{r}+\sum_{j=1}^{q}(g_j-\delta_{ij})\int_0^\infty\frac{2}{r_{max}}P_j^2(r')dr'-(g_i-1)A_i(r)]P_i(r)=$$
$$\epsilon_iP_i(r)+\sum_{j=i,j\neq i}^{q}g_j[\delta_{ij}\epsilon_{ij}+B_{ij}(r)]P_j(r) \tag{2.33}$$

where

$$A_i(r)=\frac{2l_i+1}{4l_i+1}\sum_{k=1}^{\infty}\begin{pmatrix} l_i & k & l_i\\ 0 & 0 & 0\end{pmatrix}^2\int_0^\infty\frac{2r_{min}^k}{r_{max}^{k+1}}P_i^2(r')dr' \tag{2.34}$$

and

$$B_{ij}(r)=\frac{1}{2}\sum_{k=1}^{\infty}\begin{pmatrix} l_i & k & l_i\\ 0 & 0 & 0\end{pmatrix}^2\int_0^\infty\frac{2r_{min}^k}{r_{max}^{k+1}}P_i^2(r')P_j^2(r')dr' \tag{2.35}$$

where the symbols in brackets are Wigner's 3-j symbols[6] and r_{min} and r_{max} are respectively the smallest and the largest value of r. g_j is the statistical weight (*i.e.* degeneracy) of the subshell (n_j, l_j) and ϵ_i, ϵ_{ij} are Lagrange multipliers introduced into the variational problem to impose orthonormality constraints on P_i:

$$\int_0^\infty P_i^2(r)dr=1 \text{ and } \int_0^\infty P_i^*(r)P_j(r)dr=\delta_{n_in_j} \tag{2.36}$$

Since the HF equations are coupled equations, they can only be solved by an iterative procedure, called the Self Consistent Field Method. This method consists in choosing a certain set of starting radial wave functions and then calculating all terms appearing in each HF equation with this set of radial wave functions. The HF equations then have to be solved one by one to obtain a new set of radial wave functions and this process has to be repeated until a certain convergence criterion, set on radial wave functions and energies, has been reached.

2.2.2 Relativistic Corrections

To take into account relativistic effects, single-electronic corrections are added to the non-relativistic HF equations in a perturbative way. The resulting equations are then called relativistic Hartree-Fock equations (HFR).

1. Spin-orbit:

   The first correction made is the spin-orbit correction. It represents the interaction between the orbital angular momentum of an electron, $\vec{l_i}$, and its spin, $\vec{s_i}$. This interaction induces, firstly, a displacement of the sublevels and secondly a separation of these into several energy levels. This is called the fine structure. This correction is introduced in the Hamiltonian of the system through the addition of a term proportional to $\vec{l_i}.\vec{s_i}$ (which translates the coupling between $\vec{l_i}$ and $\vec{s_i}$). The proportionality factor is noted $\zeta_{n_il_i}$.

2. Mass-velocity:

   The second correction is the so-called *mass-velocity* correction, which is due to the relativistic dependence of the electron's mass on its speed. To obtain this correction, the difference between the relativistic expression of the energy of an electron (which

[6] Linked with Clebsch-Gordan coefficients.

is developed in series at the second order in $\frac{p^2}{m_0^2c^2}$) and the non-relativistic energy must be calculated. That is to say $E_r - E_{nr}$ where

$$E_r = c\sqrt{m_0^2c^2 + p^2} - m_0c^2 + E_{pot} \tag{2.37}$$

and

$$E_{nr} = \frac{p^2}{2m_0} + E_{pot} \tag{2.38}$$

The correction is obtained by applying the substitution $\vec{p} \to -i\hbar\vec{\nabla}$ and taking the average value of $E_r - E_{nr}$ (in which the Laplacian squared then intervenes) in a state characterized by the quantum numbers (n, l, m).

3. Darwin Term:

   The third and final correction takes into account the fact that, as a result of Heisenberg's uncertainty principle, the charge of the electron is delocalized, *spread* over a certain volume, which induces modifications in its potential energy.

   Indeed, the instantaneous position of an electron can only be precisely defined in a volume corresponding to λ_C^3 where $\lambda_C = \frac{\hbar}{m_e c}$ is the Compton wavelength. The potential energy of the electron in the Coulomb field of the nucleus can therefore be written:

$$E_{pot}(r) = \int f(\rho)E_{pot}(r+\rho)d^3\rho \tag{2.39}$$

   where the integral relates to the volume λ_C^3 around the point r. If we develop in Taylor series around the point $\rho = 0$ we have:

$$E_{pot}(r+\rho) = E_{pot}(r) + (\frac{dE_{pot}}{d\rho})_{\rho\to 0}\rho + \frac{1}{2}\frac{d^2E_{pot}}{d\rho^2}\rho^2 \tag{2.40}$$

   The first term corresponds to the non-perturbed energy, the second is zero because of the spherical symmetry of the potential and the third one is the Darwin term. This term will be equal to around $\lambda_C^2 \Delta E_{pot}$ (where Δ is the Laplacian operator).

   For $E_{pot} = \frac{-Ze^2}{4\pi\varepsilon_0 r}$,

$$\Delta E_{pot} = \frac{Ze^2}{\varepsilon_0}\delta(r). \tag{2.41}$$

   The Darwin correction is therefore given by:

$$\Delta E_D = \frac{Ze^2\hbar^2}{\varepsilon_0 m_e^2 c^2}\delta(r) \tag{2.42}$$

   and the Darwin term is the average value of this Darwin correction:

$$< \Delta E_D >= \frac{Ze^2\hbar^2}{\varepsilon_0 m_e^2 c^2}|\Psi(r=0)|^2 \tag{2.43}$$

   where $\Psi(r=0)$ is the wave function at the origin. This is non-zero only for the s-subshells (i.e. $l = 0$). This implies that the Darwin term only affects the s-electrons.

2.2.3 Core-Polarization Corrections (HFR + CPOL)

The spectroscopic properties of an atom (or an ion) are largely influenced by the valence electrons. The problem can therefore be simplified by replacing the HF Hamiltonian with a Hamiltonian that includes an approximate potential describing the core electrons. However, we must ensure that this simplification preserves the effects of the ionic core on the wave functions of the valence electrons (i.e. the screening effects and the orthogonality of the wave function of a valence electron to that of a core electron). Correlation effects can be separated into three types of interactions:

1. valence-valence;
2. core-valence;
3. core-core.

For heavy ions, Migdalek and Baylis [83] developed an approach according to which the correlation between valence electrons is represented by the interaction of configurations explicitly introduced in the model while the core-valence correlation is described by a core polarization model potential. For an ion with N valence electrons, the one-body part of the polarization potential is written [81, 82]:

$$V_{P1} = -\frac{1}{2}\alpha_d \sum_{i=1}^{N} \frac{r_i^2}{(r_i^2 + r_c^2)^3} \tag{2.44}$$

where α_d is the dipole polarizability of the ionic core and r_c is an adapted cut-off radius which is arbitrarily chosen to be a measure of the ionic core's size.

Additionally, the interaction between the modified electric fields undergone by the valence electrons generates a two-body contribution given by

$$V_{P2} = -\alpha_d \sum_{k>l} \frac{\vec{r_k}.\vec{r_l}}{[(r_k^2 + r_c^2)(r_l^2 + r_c^2)]^{3/2}} \tag{2.45}$$

There is a corresponding change to the radial matrix element of the length form of the oscillator strength: the radial integral $<P_{nl} \mid r \mid P_{n'l'}>$ has to be substituted by

$$< P_{nl}|r(1 - \frac{\alpha_d}{(r^2 + r_c^2)^{3/2}})|P_{n'l'} > \tag{2.46}$$

Moreover, in order to allow for a more accurate treatment of the penetration of the core by the valence electrons, a further correction has been included in our model. With this correction [84, 85], the penetration of the ionic core by the valence electrons[7] can be taken into account in a more realistic way. When we introduce the polarization of the core and the effects of penetration in the Hamiltonian, the operator of the dipole momentum[8] appearing in the transition matrix must be adjusted. Therefore, the dipole radial integral becomes:

$$\int_0^{\infty} P_{nl}(r) r \left(1 - \frac{\alpha_d}{(r^2 + r_c^2)^{\frac{3}{2}}}\right) P_{n'l'}(r) - \frac{\alpha_d}{r_c^3} \int_0^{r_c} P_{nl}(r) r P_{n'l'}(r) dr. \tag{2.47}$$

An accurate knowledge of the static dipole polarizability of the core α_d and the value of the cut-off radius are therefore required for this model. The values of α_d can be obtained

[7]Indeed, their wave function, and thus their probability of presence is non-zero in the core.

[8]Without all these effects in a spherically symmetric potential, the operator of dipole transition between a state ψ_1 and a state ψ_2 is simply given by r and we have the transition which can be written $\langle\psi_1| r|\psi_2\rangle$.

from theoretical calculations or experimental measurements. By contrast, the values of r_c cannot be inferred from the experiment. It is therefore common to take the mean value $< r >$ of the core's outermost orbital as value for r_c. Biémont *et al.* [86] showed that relativistic Hartree-Fock calculations with core polarization corrections (HFR + CPOL) gave results comparable to a fully relativistic calculation taking explicitly into account valence interactions as well as core-valence interactions.

2.2.4 Solving the Hamiltonian Eigenvalue Equation: Slater-Condon Method

The Slater-Condon method is a method used to solve the Schrödinger equation. To do so, we develop the atomic wave functions ψ_k, which are eigenfunctions of the Hamiltonian H on a set of basis wave functions ψ_b generally characterized by a pure electronic coupling scheme (LS or jj for example).

$$\Psi_k = \sum_b x_k^b \psi_b \qquad \text{with} \qquad \sum_b (x_k^b)^2 = 1 \tag{2.48}$$

They describe the so-called configuration interaction, i.e. the interaction between basis states belonging to different configurations where the atomic wave function does not correspond to a pure state but to a superposition of states (similar to interference effects). Generally, atomic wave functions are not pure (each atomic state is a superposition of basis states). The series corresponding to Ψ_k is generally an infinite series (in other words, the base consists of an infinity of basis functions) but, in practice, we truncate this series by cleverly choosing the electronic configurations that we will then explicitly introduce in the model and that will thus give a finite number of basic wave functions ψ_b. This truncature of the series introduces undesirable effects in the calculation of the transition probabilities. These effects are called cancellation effects and are comparable to destructive interference effects (but they do not correspond to any physical reality, they are only due to errors introduced in the calculations by truncating the series). These cancellation effects can result in a transition being calculated with a much lower intensity than its actual value. To evaluate the significance of these cancellation effects for a calculated transition (between a $|\psi_i\rangle$ state and a $|\psi_j\rangle$ state), the cancellation factor (CF) is used. It is defined from the line strength of the transition. The line strength (for an E1 dipole transition) is the square of the electric dipole transition matrix element of the operator $P^{(1)}$ between the states considered:

$$S_{ij} = |\langle\psi_i|\ P^{(1)}|\psi_j\rangle\ |^2 \tag{2.49}$$

We have shown in the previous chapter that the transition probabilities A_{ij} and the oscillator strenghts f_{ij} are commensurated to line strenght S_{ij}. We write:

$$\sqrt{S_{ij}} = \sum_b \sum_c x_j^b x_i^c \langle\psi_c|\ P^{(1)}|\psi_b\rangle \tag{2.50}$$

from which we can define:

$$CF_{ij} := \left(\frac{\sum_b \sum_c x_j^b x_i^c \langle\psi_c|\ P^{(1)}|\psi_b\rangle}{\sum_b \sum_c |x_j^b x_i^c \langle\psi_c|\ P^{(1)}|\psi_b\rangle\ |} \right)^2 \tag{2.51}$$

The smaller the CF value is, the less reliable the corresponding values for transition probability and oscillator strength[9] are. Using the serial development of Ψ_k (which has

[9] Which can be subject to a large error.

been truncated by only keeping n terms), the eigenvalue equation can be written as a matrix ($\forall k = 1, ..., n$):

$$\begin{pmatrix} H_{11} & ... & H_{1n} \\ ... & ... & ... \\ H_{n1} & ... & H_{nn} \end{pmatrix} \begin{pmatrix} x_k^1 \\ ... \\ x_k^n \end{pmatrix} = E_k \begin{pmatrix} x_k^1 \\ ... \\ x_k^n \end{pmatrix} \quad (2.52)$$

The Hamiltonian diagonalization will provide us with the eigen energies and the mixing coefficients x_k^b. The latter will give us the expression of the atomic wave function Ψ_k.

2.2.5 Semi-Empirical Process

Thanks to Cowan's code [7], it is possible to model atomic structures and to obtain the parameters associated with them. Those parameters are: the energy levels E_k, the eigenfunctions Ψ_k, as well as the various radiative parameters which are associated with the possible transitions between the various states, namely the transition probabilities between two levels i and j, A_{ij}, and the associated oscillator strength, f_{ij}, as well as the radiative lifetime of each level, τ_i[10]. This procedure is based on the HFR method to obtain the radial parts of mono-electronic wave function, and determines the energy levels and wave functions of the atomic system by diagonalizing the Hamiltonian using the method outlined in section 2.2.4. Knowing the eigenstates, the radiative parameters are then calculated through the calculation of the line strengths. Cowan's radiative parameter calculation procedure consists of four programs, called RCN, RCN2, RCG and RCE. These can be run in two different sequences:

1. an *ab initio* sequence: RCN, RCN2 and RCG, allowing the calculation of atomic parameters without any introduction of the experimental values;

2. an adjustment sequence of the energy levels by a least-squares method, in order to optimize the radial energy parameters. The latter consists in reducing the difference between the calculated energy levels and the known experimental levels and thus gives energy levels, wave functions and radiative parameters that are *a priori* more precise than in an *ab initio* calculation. It is performed by executing the *ab initio* sequence and then calling the RCE (which performs the optimization) and RCG programs in series.

2.2.5.1 *Ab initio* Sequence

The first program to be run is the RCN program. It needs the input, in the file named *in36*, of the configurations explicitly taken into account in the model. Then, it calculates, via the HFR method, the $P_{nl}(r)$ radial parts of the mono-electronic wave functions by solving the HF equations by the self-consistent field method. It gives the single-configuration parameters, i.e. the average energy of each configuration E_{av}, the single configuration Slater electrostatic interaction parameters $F^k(ij)$ and $G^k(ij)$ and the spin-orbit parameters ζ_{nl} . Afterwards, the RCN2 program requests the introduction of the scaling factors via the *in2* file. These factors are necessary because it was found that the values of the parameters F^k, G^k and R^k calculated *ab initio* were generally too high compared to their optimal values. This systematic error is due to the finite and limited number of configurations that are chosen to be explicitly introduced into the model, which do not allow the entire set of configuration interactions to be modeled. Scaling factors are therefore introduced in order to reduce these values to have a better agreement between the calculated and

[10]The radiative lifetime of a level p being defined as $\frac{1}{A(p\rightarrow)}$ corresponds to the inverse of the sum of the transition probabilities of all possible radiative decay channels from the upper level p.

experimentally observed energy levels. In general, according to Cowan [7], scaling factors between 0.8 and 0.9 should be introduced (but they can be lower, down to 0.7 or 0.6 for very heavy elements). The RCN2 program then calculates, from the single-electronic radial wave functions, the Slater R^k interaction parameters that reflect the interactions between configurations and the transition radial integrals $< P_{nl}/P^{(1)}/P_{nl} >$ for transitions between configurations.

Finally, the RCG program is executed. First, the code solves the angular part and builds the Hamiltonian H of the system thanks to the different radial parameters provided by RCN and RCN2 ($E_{av}, F^k, G^k, R^k, \zeta_{nl}$). Then, the eigen values and the eigen vectors of the atomic system are calculated by diagonalizing this Hamiltonian H. The wavelengths corresponding to the different possible transitions are then obtained by calculating the differences between the energy levels that may involve transitions. Finally, the radiative parameters (transition probabilities, oscillator strengths and radiative lifetimes) relative to these transitions are calculated using the line strengths. Cancellation factors are also calculated by RCG. RCN and RCN2 have been modified to take the CPOL effects into account. They now also read a new input, a file called *polpar*, that contains the α_d and r_c core-polarization parameters values.

2.2.5.2 Least-Square Adjustment Method - Fitting Procedure

Firstly, an *ab initio* procedure is initiated as explained in the previous section. Next, the RCE program is run, whose input file is the *ine20* file. In this file, experimental levels (classified by values of J and increasing energies) are introduced parity by parity. By minimizing the difference between the energy levels calculated by RCG and the experimental energy levels by a least-squares method, it then performs an optimization of the parameters E_{av}, F^k,G^k,R^k and ζ_{nl}. This program also adjusts the so-called effective interaction parameters (α, β, γ), which were previously set to zero. These parameters are there to correct some of the errors made by only including a limited number of configurations in the model (therefore not modeling all the configuration interactions). They adjust the electrostatic interaction parameters for the p, d and f subshells that are filled by more than one electron. Indeed, the "space" between the energy levels for these subshells is so small that it is comparable with the standard deviation of the fit. Thus, the effective interaction parameters α, β andγ correct respectively the electrostatic interaction parameters between the equivalent electrons of the subshells p, d and f. The RCE program then relaunches the first step of the RCG to obtain the new clean energies and eigenfunctions of the Hamiltonian built this time using the adjusted parameters (but, unlike the RCG program, the diagonalization of the Hamiltonian is done parity by parity). The procedure ends with a new execution of the RCG program, which calculates the optimized atomic and radiative parameters ($E_i, \Psi_i, \lambda_{ij}, A_{ij}, f_{ji}, \tau_i$), as well as the CF associated with each calculated transition by diagonalizing the constructed Hamiltonian with the adjusted parameters obtained from RCE.

2.3 Fully Relativistic Multiconfiguration Dirac-Hartree-Fock Method

The second theoretical method we used was the Multiconfiguration Dirac-Hartree-Fock (MCDF or MCDHF), which is the purely relativistic equivalent of the Hartree-Fock method. Here, the Dirac equation must be solved in an approximate way for each electron of the atom under consideration and this in the approximation of the central field (independent electrons in an effective potential with spherical symmetry taking into account the shielding). In this *multiconfiguration* method [87], each atomic state is described as a linear combination of well-chosen basis states. Then, by forcing an energy functional to be stationary with respect to small variations of the radial parts of the spin-orbitals, we obtain a system of coupled integro-differential equations (called Dirac-Fock equations) that we will solve iteratively using the method of the self-consistent field. At each iteration, the Hamiltonian diagonalization, constructed from the different interaction operators, provides us with an evaluation of the energy levels and atomic states. It is worth noting that quantum electrodynamics (QED)-related corrections are perturbatively added to the Hamiltonian of the system, allowing these effects to be taken into account in the final energy levels and atomic states.

2.3.1 Method's Basic Principle

In relativistic quantum mechanics, the wave equation governing the behavior of a free electron is the Dirac equation:

$$(i\gamma^{\mu}\partial_{\mu} - c)\psi = 0, \tag{2.53}$$

where γ^{μ} are given in the Dirac representation by:

$$\gamma^0 = \begin{pmatrix} \mathbb{1} & 0 \\ 0 & -\mathbb{1} \end{pmatrix}, \gamma^i = \begin{pmatrix} 0 & \sigma_i \\ -\sigma_i & 0 \end{pmatrix}, \tag{2.54}$$

$i = 1, 2, 3$ and σ_i are Pauli matrices. The problem of the hydrogen atom (i.e. the search for the bound stationary states of an electron in a Coulomb potential (potential with spherical symmetry) generated by the nucleus), is to search for the eigenstates of Dirac Hamiltonian [11].

$$h_D = c\vec{\alpha}.\vec{p} + (\beta - 1)c^2 + V_{nucl}(r), \tag{2.55}$$

where α^i, $i = 1, 2, 3$, and β are defined, from Dirac matrices, as:

$$\alpha^i = \gamma^0\gamma^i, \qquad \beta = \gamma^0. \tag{2.56}$$

Assuming that the nucleus is punctual of infinite mass and of charge Z, we take, for the nuclear potential, a Coulomb potential $V_{nucl}(r) = -\frac{Z}{r}$.

The eigenvectors of the Hamiltonian h_D (2.55), which we will call later *spin-orbitals* (or *relativistic orbitals*), can then be written, in spherical coordinates:

$$\psi(r, \theta, \phi) = \frac{1}{r} \begin{pmatrix} cP_{nk}(r)\chi_{\kappa,m}(\theta, \phi) \\ -iQ_{n\kappa}(r)\chi_{-\kappa,m}(\theta, \phi) \end{pmatrix}, \tag{2.57}$$

where $P_{n\kappa}(r)$ et $Q_{n\kappa}(r)$ are respectively the large and the small radial component which are solutions of the radial equations system:

$$\begin{pmatrix} (c^2 - \frac{Z}{r} - E_{n,\kappa}) & c(-\frac{d}{dr} + \frac{\kappa}{r}) \\ c(\frac{d}{dr} + \frac{\kappa}{r}) & (-c^2 - \frac{Z}{r} - E_{n,\kappa}) \end{pmatrix} \begin{pmatrix} P_{n\kappa}(r) \\ Q_{n\kappa}(r) \end{pmatrix} = \begin{pmatrix} 0 \\ 0 \end{pmatrix}, \tag{2.58}$$

where n is the principal quantum number and κ is a quantum number that will be defined later. The two-component spinors $\chi_{\kappa,m}$ are eigenvectors of the operators $\vec{j}^2$, j_3, $\vec{l}^2$ and $\vec{s}^2$ ($\vec{l}$, $\vec{s}$ and $\vec{j}$ being respectively the operators of orbital angular momentum, of spin and of total angular momentum acting on a two-dimensional spinner space with $\vec{j} = \vec{l} + \vec{s}$) having as eigenvalues $j(j+1)$, m, $l(l+1)$ and $s(s+1)$ where j is an half-integer. We

[11] The electron's rest energy c^2 is subtracted to shift the state of zero energy and thus coincide with the usual non-relativistic conventions used in atomic physics.

have in addition: $-j \leq \mathrm{m} \leq j$, $l = j + 1/2, j - 1/2$ and $s = 1/2$. The spinors $\chi_{\kappa,m}$ are also eigenvectors of the operator

$$K = -(1 + \vec{\sigma}.\vec{l}), \tag{2.59}$$

with eigenvalues

$$\kappa = (j + \frac{1}{2})\eta \text{ when } l = j + \frac{1}{2}\eta \text{ with } \eta = \pm 1, \tag{2.60}$$

The spinnors $\chi_{k,m}$ can be developped as

$$\chi_{k,m}(\theta, \phi) = \sum_{\sigma = ^{+}_{-}\frac{1}{2}} (l, m, -\sigma, 1/2, \sigma | l, 1/2, j, m) Y_l^{m-\sigma}(\theta, \phi) \Phi_\sigma, \tag{2.61}$$

where Φ_σ are two basis two-components spinnors.

$$\Phi_{\frac{1}{2}} = \begin{pmatrix} 1 \\ 0 \end{pmatrix} \text{ et } \Phi_{-\frac{1}{2}} = \begin{pmatrix} 0 \\ 1 \end{pmatrix}. \tag{2.62}$$

2.3.2 Dirac-Coulomb Hamiltonian and Atomic Wave Functions

The relativistic Hamiltonian for an N-electron atom is given by the Dirac-Coulomb Hamiltonian:

$$H_{DC} = \sum_{i=1}^{N} h_{D_i} + \sum_{i>j} \frac{1}{r_{ij}}, \tag{2.63}$$

where h_{D_i} is the mono-electronic Dirac Hamiltonian for the ith electron.

In the central field approximation, the hypothesis is that each electron moves independently from the other in a (spherical symmetry) effective potential V(r). This potential is generated by the nucleus and the N-1 other electrons as already explained in section 2.2. This allows us to write (2.55) as

$$h_D = c\vec{\alpha}.\vec{p} + (\beta - 1)c^2 + V(r), \tag{2.64}$$

where

$$V(r) = \frac{-Z}{r} + U(r), \tag{2.65}$$

and thus to approximate (2.63) by

$$H = \sum_{i=1}^{N} h_{D_i}. \tag{2.66}$$

Given the spherical symmetry, this allows the spin-orbitals to be expressed as (2.57). Therefore, only the radial parts $P(r)$ and $Q(r)$ remain to be determined in order to fully know the electronic spin-orbitals.

The starting point of the MCDHF method is the development of each atomic state wave function (ASF) $\Psi(P, J, M)$ describing an atomic state of parity P, characterized by the quantum number of total angular momentum J of projection M, as a combination of configuration state functions (CSF) with the same parity and the same angular momentum $\Phi(\gamma, P, J, M)$ where γ contains all the information to define the CSF in a unique way (the coupling scheme, the orbital occupancy numbers, ...):

$$\Psi(P, J, M) = \sum_{r=1}^{n_c} c_r \Phi(\gamma_r, P, J, M), \tag{2.67}$$

where the c_r are the mixing coefficients and where n_c is the number of CSF introduced in the model. The mixing coefficients obviously have to be normalized:

$$\sum_{r=1}^{n_c} |c_r|^2 = 1. \tag{2.68}$$

Each CSF is expressed as a linear combination of Slater determinants[12] constructed from spin-orbitals (2.57) whose radial parts are self-consistently optimized by solving the MCDHF equations (see section 2.3.4).

2.3.3 Hamiltonian Matrix in the Chosen CSF Basis

The first step is to build the Hamiltonian to be implemented in the method. The elements of the Hamiltonian matrix can be expressed [87] from angular coefficients that only depend on the angular parts of the selected CSFs and single and bielectronic radial integrals. The expression of the single-electron radial integral for an electron initially on an orbital a[13], is given by:

$$\begin{aligned} I(ab) = \delta_{\kappa_a\kappa_b} \int_0^\infty \Big[& cQ_a^*(r)\big(\frac{d}{dr} + \frac{\kappa_b}{r}\big)P_b(r) - cP_a^*(r)\big(\frac{d}{dr} + \frac{\kappa_b}{r}\big)Q(r)) \\ & -2c^2Q_a^*(r)Q_b(r) + V_{nucl}(r)\big[P_a^*(r)P_b(r) + Q_a^*(r)Q_b(r)\big]\Big] dr. \end{aligned} \tag{2.69}$$

The radial bi-electronic integral is given under the form of a generalized relativistic Slater-Integral,$R^k(abcd)$,

$$R^k(abcd) = \int_0^\infty \Big[\big(P_a^*(r)P_c(r) + Q_a^*(r)Q_c(r)\big)\frac{1}{r}Y^k(bd,r)\Big] dr, \tag{2.70}$$

with Y Hartree-function defined as:

$$Y^k(bd,r) = r\int_0^\infty U^k(r,s)\big(P_b^*(s)P_d(s) + Q_b^*(s)Q_d(s)\big)ds, \tag{2.71}$$

with

$$U^k(r,s) = \begin{cases} \dfrac{r^k}{s^k+1} & \text{if } r \le s \\ \dfrac{s^k}{r^k+1} & \text{if } s < r \end{cases} \tag{2.72}$$

This bielectronic integral describes the electrostatic interaction between two electrons that may belong to different configurations (which reflects the configuration interaction). The direct radial integral, $F^k(ab)$, and the exchange integral, $G^k(ab)$, are two special cases of Slater integral in a monoconfigurational case. They respectively reflect the direct electrostatic and exchange interaction (due to the indistinguishability of the particles) between two electrons of the same configuration. Their expressions are given by:

$$\begin{aligned} F^k(ab) &= R^k(abab), \\ G^k(ab) &= R^k(abba). \end{aligned} \tag{2.73}$$

[12]A Slater determinant allows the wave function of an atomic state to be written as an antisymmetric product of single-electron spin-orbitals, thus ensuring the antisymmetry of the wave function with respect to the exchange of two electrons as imposed by Pauli's exclusion principle.

[13]Characterized by quantum numbers (n_a, κ_a).

The diagonal matrix elements in the chosen CSF basis can be written as [87]:

$$H_{rr} = \sum_{a=1}^{n_0} \left(\; q_r(a)I(aa) + \sum_{b\leq a}^{n_0} \left[\; \sum_{k=0,2,...}^{k_0} f_r^k(ab)F^k(ab) + \sum_{k=k_1,k_1+2,...}^{k_2} g_r^k(ab)G^k(ab) \right] \; \right) , \tag{2.74}$$

where n_0 is the number of orbitals, $q_r(a)$ is the number of occupancy of orbital a (i.e. the number of electrons in the quantum number subshell (n_a,κ_a)) of the CSFr and where $f_r^k(ab)$ and $g_r^k(ab)$ are angular coefficients whose general expressions have been defined by [87]. These depend on the coupling scheme between equivalent (on the same subshell) and non-equivalent (on different subshells) electrons and, therefore, depend on the number of occupancy of each subshell. The standard coupling scheme used in the MCDHF method to construct CSFs is a jj coupling defined as follows:

1. the electrons from the same subshell a, with an occupation number $q(a) \leq 2j_a+1$ are coupled following a jj-coupling and thus give to each subshell an angular momentum J_a ;

2. T-the angular momenta J_a and J_b from successive subshell a and b are also jj-coupled in order to give an intermediate angular momentum X_1 which is itself coupled with the angular momentum of the subshell c, J_c, to get a new intermediate angular momentum X_2. And so on until all the angular momenta from all the subshells have been coupled to give a total angular momentum J. This can be schematized as:
$$(...(J_aJ_b)X_1J_c)X_2...)J. \tag{2.75}$$

The summation limits appearing in (2.74) are given by:

$$k_0 = (2j_a - 1)\delta_a b, \tag{2.76}$$

$$k_1 = \begin{cases} |j_a - j_b| \text{ if } \kappa_a\kappa_b > 0 \\ |j_a - j_b| + 1 \text{ if } \kappa_a\kappa_b < 0, \end{cases} \tag{2.77}$$

$$k_2 = \begin{cases} j_a + j_b \text{ if } j_a + j_b + \kappa \text{ is even} \\ j_a + j_b - 1 \text{ otherwise .} \end{cases} \tag{2.78}$$

The off-diagonal elements ($r \neq s$) of the Hamiltonian matrix in the chosen CSF basis, reflecting the configuration interactions between the different CSFs, can be expressed in the general form [87].

$$H_{rs} = \sum_{a,b} t_{rs}(ab)I(ab)\delta_{\kappa_a\kappa_b} + \sum_k \sum_{a,b,c,d} v_{rs}^k(abcd)R^k(abcd), \tag{2.79}$$

where $t_{rs}(ab)$ and $v_{rs}^k(abcd)$ are angular coupling coefficients of the same type as those appearing in (2.74), also depending on the coupling scheme and the subshells a, b, c and d contributing to H_{rs}. The expressions of these coefficients in the different cases[14] are given by [87].

2.3.4 Getting the Spin-Orbitals through the MCDHF Equations

In order to optimize the radial parts *P(r)* and *Q(r)* of the spin-orbitals (2.57), a system of integro-differential equations obtained by applying a variational principle to an energy functional is solved to make it stationary with respect to the variations of the radial

[14]Sub-layer complete or not, electrons equivalent or not, etc.

parts of the spin-orbitals. The method of Lagrange multipliers is used to account for orthogonality constraints on spin-orbitals. Let us consider the energy functional as:

$$\mathcal{E} = \sum_{r=1}^{n_C}\sum_{s=1}^{n_C} d_{rs}H_{rs} + \sum_{a}\sum_{b}(1-\delta_{ab})\overline{q}(a)\epsilon_{ab}(a|b), \tag{2.80}$$

where ϵ_{ab} are Lagrange multipliers in order to guarantee the orthonormality of radial parts of the spin-orbitals , where $\overline{q}(a)$ is the generalized occupation number and is defined as:

$$\overline{q}(a) = \sum_{r=1}^{n_C} d_{rr}q_r(a), \tag{2.81}$$

and where

$$(a|b) = \int_0^\infty \Big(P_a^*(r)P_b(r) + Q_a^*(r)Q_b(r)\Big)dr. \tag{2.82}$$

The coefficients d_{rs} are generalized weights that can be expressed in different ways leading to several variants of the energy functional:

- OL Mode (*Optimal Level*): In this mode, optimization is done on only one ASF at a time, so each ASF is optimized independently of the others. For an atomic state i, the generalized weights are then given by

  $$d_{rs} = c_{ri}c_{si}. \tag{2.83}$$

  The spin-orbitals obtained with this method may vary from one ASF to another.

- EOL Mode (*Extended Optimal Level*): This option allows optimization to be performed on a set of energy levels. The generalized weights are then written as:

  $$d_{rs} = \frac{1}{n_L}\sum_{i=1}^{n_L} c_{ri}c_{si}, \tag{2.84}$$

  where n_L is the number of levels chosen ($n_L \leq n_C$). In this case, the same set of spin-orbitals is used to describe the set of ASFs corresponding to the energy levels chosen to construct $\mathcal{E}$.

- AL Mode (*Average Level*): In this option, we optimize the trace of the Hamiltonian matrix. The generalized weights are then independent of the mixing coefficients and each CSF is weighted by its statistical weight:

  $$d_{rs} = \delta_{rs}\frac{2J_r+1}{\sum_{t=1}^{n_C}(2J_t+1)}. \tag{2.85}$$

  Unlike the OL and EOL modes, this option allows a global optimization on all energy levels.

- EAL Mode (*Extended Average Level*): This option optimizes a weighted trace of the Hamiltonian matrix. The weights, independent of the mixing coefficients, can then be chosen by the user.

Applying the variational principle to the energy functional for a relativistic orbital, we obtain a system of coupled interdifferential equations called the MCDHF equations. They are given by:

$$\begin{cases} -\dfrac{Z-Y(a;r)}{r}P_a(r) + c\Big(-\dfrac{d}{dr}+\dfrac{\kappa_a}{r}\Big)Q_a(r) - \epsilon_{aa}P_a(r) = -X_{+1}(a;r) \\ c\Big(\dfrac{d}{dr}+\dfrac{\kappa_a}{r}\Big)P_a(r) + \Big(-2c^2 - \dfrac{Z-Y(a;r)}{r}\Big)Q_a(r) - \epsilon_{aa}Q_a(r) = -X_{-1}(a;r), \end{cases} \tag{2.86}$$

with the normalization condition:

$$\int_0^\infty \Big(P_a^*(r)P_a(r) + Q_a^*(r)Q_a(r)\Big)dr = 1, \tag{2.87}$$

where $Y(a;r)$ is the direct interaction potential and $X_\beta(a;r)$, with $\beta = \pm 1$, is the exchange interaction potential. They can be written as:

$$Y(a;r) = \sum_k \sum_{b=1}^{n_0} \Big[y^k(ab)Y^k(bb;r) - \sum_{c=1}^{n_0} y^k(abac)Y^k(bc;r)\Big], \tag{2.88}$$

for $Y(a;r)$ where Y^k is the Hartree function (see 2.71)

$$y^k(ab) = \frac{1+\delta_{ab}}{\overline{q}(a)} \sum_{r=1}^{n_C} d_{rr} f_r^k(ab), \tag{2.89}$$

$$y^k(abac) = \frac{1}{\overline{q}(a)} \sum_{r=1}^{n_C} \sum_{s=1}^{n_C} d_{rs} v_{rs}^k(abac), \tag{2.90}$$

and as

$$\begin{aligned} X_\beta(a;r) = &- \sum_{b\neq a} \delta_{\kappa_a\kappa_b}\epsilon_{ab} R_{\gamma_b\beta_{\kappa_b}}(r) \\ &+ \sum_k \Big[\sum_{b\neq a} x^k(ab)\frac{Y^k(ba;r)}{r} R_{\gamma_b\beta_{\kappa_b}}(r) - \\ &\sum_{bcd}\Big(1 - \delta_{ac} x^k(abcd)\frac{Y^k(bd;r)}{r} R_{\gamma_b\beta_{\kappa_b}}(r)\Big)\Big], \end{aligned} \tag{2.91}$$

for $X_\beta(a;r)$

$$R_{\gamma_b\beta_{\kappa_b}}(r) = \begin{cases} P_{\gamma,\kappa}(r) \text{ if } \beta = +1 \\ Q_{\gamma,\kappa}(r) \text{ if } \beta = -1, \end{cases} \tag{2.92}$$

and where

$$x^k(ab) = \frac{1}{\overline{q}(a)} \sum_{r=1}^{n_C} d_{rr} g_r^k(ab), \tag{2.93}$$

$$x^k(abcd) = \frac{1}{\overline{q}(a)} \sum_{r=1}^{n_C} \sum_{s=1}^{n_C} d_{rs} v_{rs}^k(abcd). \tag{2.94}$$

Solving this system of coupled equations can only be done iteratively. It is thus the method of the self-consistent field which is used to obtain the radial parts $P(r)$ and $Q(r)$ of each spin-orbital (2.57). This method entails:

1. the selection of a set of starting radial functions $P(r)$ and $Q(r)$ (e.g. the radial parts of screened hydrogenic spin-orbitals);
2. the calculation of all the terms appearing in the MCDHF equations with the starting radial parts;
3. the resolution of the MCDHF equations to obtain new radial functions.

Steps 1, 2 and 3 are then repeated iteratively until a certain convergence criterion is reached. It should be noted, however, that the increase in the number of radial parts of relativistic orbitals relative to non-relativistic radial wave functions makes the optimization process much longer and more complex than in the non-relativistic (Hartree-Fock) case.

2.3.5 Solving the Eigenvalues Equation Using the Configuration Interaction Method

Once the orbitals are optimized, the mixing coefficients can be obtained with the interaction configuration method. An atom's energy in a state Γ described by an ASF is given by:

$$E_\Gamma = \vec{c_\Gamma}^\dagger H \vec{c_\Gamma}, \tag{2.95}$$

Where H is the Hamiltonian matrix in the chosen CSF basis and where $\vec{c_\Gamma}$ is a column vector with, as components, the mixing coefficients of the ASF describing the atomic state Γ : $\begin{pmatrix} c_{\Gamma,1} \\ ... \\ c_{\Gamma,n_C} \end{pmatrix}$ with the normalizing condition (2.67) which can be written $\vec{c_\Gamma}^\dagger \vec{c_\Gamma} = 1$.
Looking for stationary states of the system, i.e. eigenstates of the Hamiltonian, entails the resolution of the secular equation

$$H\vec{c_\Gamma} = E_\Gamma \vec{c_\Gamma}. \tag{2.96}$$

Eigenvalues and eigenvectors obtained by diagonalizing the Hamiltonian correspond to the atomic energy levels and to the mixing coefficient of the ASF. This allows us to write and describe the atomic states.

2.3.6 Quantum Electrodynamics Corrections

To describe the interactions between the bound electrons in an atom, the Coulomb interaction term is no longer sufficient. Indeed, it is necessary, in a relativistic context, to add some corrections coming from quantum electrodynamics (QED). The most important corrections are the electron-electron scattering, also called transverse interaction and corresponding to a first-order correction, as well as the vacuum polarization and the electron self-energy correction, both corresponding to second-order corrections. All these corrections are perturbatively added to the Hamiltonian when solving the secular equation by the configuration interaction method in order to correct energy levels and ASF.

2.3.6.1 Transverse interaction

In QED, electron-electron scattering is described by the exchange of a virtual photon[15]. The correction to the instantaneous Coulomb interaction term between two bound electrons of the atom that is due to this virtual photon exchange is called the transverse interaction. It is described by a Hamiltonian operator that is added to the Dirac-Coulomb Hamiltonian describing the system. Its expression is obtained by assuming that the energy of the photon exchanged between an electron of an orbital i and an electron of an orbital j is equal to the difference of the binding energies of the two orbitals. The expression of this transverse interaction operator is given by [87]:

$$B_{ij}^T = -\vec{\alpha_i}.\vec{\alpha_j}\frac{e^{i\omega_{ij}r_{ij}/c}}{r_{ij}} - (\vec{\alpha_i}.\vec{\nabla}_i)(\vec{\alpha_j}.\vec{\nabla}_j)\frac{e^{i\omega_{ij}r_{ij}/c}-1}{\omega_{ij}^2 r_{ij}/c^2}, \tag{2.97}$$

where $\vec{\alpha_i} = (\alpha_i^1, \alpha_i^2, \alpha_i^3)$ is a vector with the three Dirac matrices as components α^k acting on an electron from orbital i, $r_{ij} = |\vec{r_i} - \vec{r_j}|$, and where ω_{ij} is the emitted photon frequency i.e. $\hbar\omega_{ij} = |E_i - E_j|$ where E_i et E_j are the binding energies of electrons from orbitals i and j. The Feynman diagram of this interaction is given in Figure 2.1.

[15]Electromagnetic Interaction Gauge Boson

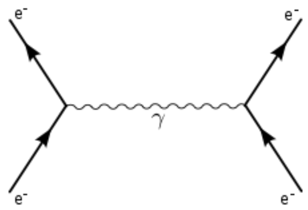

Figure 2.1: Feynman Diagram of the Transverse Interaction

2.3.6.2 Vacuum Polarization

The QED theory predicts that a fluctuation in vacuum energy ΔE can result in the creation of an electron-positron pair that annihilates after a time Δt so that Heisenberg's uncertainty principle $\Delta E.\Delta t \geq \hbar$ is satisfied. That way, dipoles spontaneously emerge from the vacuum for very short periods of time, changing the surrounding electromagnetic field. Indeed, an electron interacting with these dipoles modifies the spatial distribution of the latter, which gives rise to a polarization of the vacuum as well as a modification of the electromagnetic field generated by the electron (shielding of its charge). The electronic structure of the atoms is therefore also affected. The correction due to vacuum polarization is taken into account in the MCDHF method via an effective vacuum polarization potential in the vicinity of a point charge. This potential, called the Uehling potential [88], is perturbatively added to the Hamiltonian of the system. The vacuum polarization's Feynman diagram is given in Figure 2.2

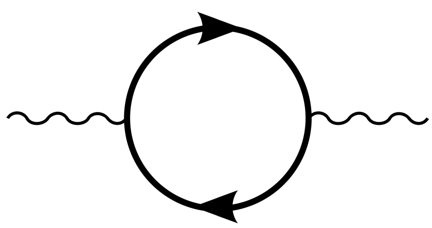

Figure 2.2: Feynman Diagram of the Vacuum Polarization

2.3.6.3 Self-Energy

The electron self-energy is another correction from the QED theory which is taken into account in the MCDHF method. It is the phenomenon by which an electron spontaneously emits a virtual photon of energy ΔE and reabsorbs it after a time Δt such that $\Delta E.\Delta t \geq \hbar$. This phenomenon contributes in particular to the mass-energy of the electrons (hence its name) because the electron interacts with its own electromagnetic field, thus also modifying the electronic structure of the atoms. The electron's self-energy can be calculated as part of the renormalization of quantum electrodynamics. Figure 2.3.6.3 shows the Feynman diagram of this interaction.

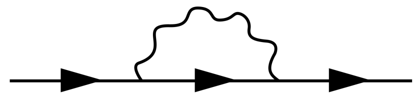

Figure 2.3: Feynman Diagram of the Self Energy

2.3.7 GRASP2K - GRASP2018 Programs

In our work, the MCDHF method was implemented using two recent versions of GRASP (General Relativistic Atomic Structure Package) namely GRASP2K [89] and GRASP2018 [90]. In these codes, a sequence of routines is executed as follows:

1. *rnucleus*: defines the nuclear data and generates the radial coordinates grid;
2. *rcsfgenerate*: generates the CSF list on the basis of excitation rules from the reference configurations;
3. *rangular*: generates the angular parts of the wavefunctions ;
4. *rwfnestimate*: generates the radial parts of the initial radial wavefunctions;
5. *rmcdhf*: solves the MCDHF equations using the self-consistent field method;
6. *rci*: solves the secular equation by diagonalizing the Hamiltonian matrix while taking into acount the QED corrections;
7. *rtransition*: determines all the possible transitions between the previously calculated levels.

Chapter 3

Atomic Data Calculations in U II and Th II for Cosmochronological Applications

In view of their potential use in cosmochronological investigations as mentioned in section 1.3.1, only the strongest spectral lines in singly ionized thorium and singly ionized uranium were considered in the present study. More precisely, we limited our study to the Th II and U II electric dipole transitions for which the HFR+CPOL log gf-values were found to be larger than -1. Such strong transitions are among the only ones likely to be observed in astrophysical spectra and they could therefore be of primary importance in cosmochronology. They also have the great advantage of not being too much affected by significant cancellation effects when calculating the line strengths, which suggests that the corresponding oscillator strengths can be expected to be fairly reliable (see [7]).

3.1 U II

Uranium is the heaviest natural element (Z = 92). Among uranium isotopes, ^{238}U is the most stable with a half-life of 4.5 billion years. This element was discovered in 1789 by the Prussian chemist Martin Heinrich Klaproth when he analyzed a piece of rock brought to him from the Saint Joachimstal mine [91]. He suggested the name *uran* or *uranite* for the compound he had just identified, in reference to the discovery of the planet Uranus made by William Herschel in 1781. This oxide, renamed uranium in 1790, had the property of giving a fine fluorescence to glass and a greenish yellow color to glasses. Henri Becquerel actually discovered the radioactivity of uranium much later, in 1896. He noticed that photographic plates placed next to uranium salts had been printed without having been exposed to light. The plates had been blackened by the radiation emitted by the salts; this was the manifestation of natural radioactivity [92, 93].

We started this study with singly ionized uranium (U II). Before our work, we looked for previously available data in U II. We found that, in their compilation of the energy levels and the spectra of actinides, Blaise and Wyart [1] listed, some preliminary energy levels in U II for both parities. These data were preceded in the literature by the publications about emission lines by Steinhaus *et al.* [2] and Palmer *et al.* [3]. Energy values of the lowest levels of configurations including 5f, 6d, 7s, 7p electrons were the main ones reported. It thus provided an update to the previous estimations made by Brewer [4]. This database was later extended by Blaise *et al.* [5] who measured uranium hollow-cathode Fourier-transform spectra between 1800 and 42000 cm^{-1} which, when combined with earlier visible and UV spectra, led to the determination of numerical values for 354 and 809 energy levels belonging to the four odd configurations 5f^{3}7s^2, 5f^{3}6d7s, 5f^{3}6d^2,

$5f^47p$, and to the six even configurations $5f^47s$, $5f^46d$, $5f^26d^27s$, $5f^26d7s^2$, $5f^37s7p$, $5f^36d7p$, respectively.

More recently, the latest energy levels of U II were construed by Meftah *et al.* [6] using the Racah-Slater parametric method with the Cowan codes [7]. In this work, 253 levels of the interacting odd-parity configurations $5f^37s^2 + 5f^36d7s + 5f^36d^2 + 5f^47p + 5f^5$ were represented by 24 free radial parameters and 64 constrained ones. The root mean square (rms) deviation found was 60 cm^{-1}. In the even parity, 125 levels were classified using a multiconfiguration basis including $5f^47s + 5f^46d + 5f^26d^27s + 5f^26d7s^2 + 5f^26d^3$ by 22 free parameters with a rms deviation of 84 cm^{-1}. Moreover, a separate semi-empirical model, including only the higher even configurations $5f^37s7p$ and $5f^36d7p$, led to the tentative classification of 12 energy levels within these configurations.

Unfortunately, for these two configurations, the semi-empirical method of parametric fitting was limited by the optimization of average energies and spin-orbit ζ_{5f} integrals, the quantitative evaluation of configuration interaction effects within the whole group $5f^4(7s + 6d) + 5f^2(6d + 7s)^3 + 5f^37s7p + 5f^36d7p$ having been tried unsuccessfully. Finally, Meftah *et al.* parametric study [6] allowed them to re-investigate the high resolution UV spectrum of uranium which was recorded in the late eighties at the Meudon Observatory and of which the analysis was unfinished. In the context of this study, 451 lines of U II were classified in the region 2344 – 2955 Å and a new level belonging to $5f^36d7p$ was established at 39115.98 cm^{-1} with $J = 11/2$.

As regards the radiative decay rates, the first measurements of relative line intensities in U II were obtained from emission arc spectra by Meggers *et al.* [8], Corliss and Bozman [9], Voigt [10] and Corliss [11]. In the atlas of uranium lines published by Palmer [3], relative intensities measured from uranium hollow-cathode spectra recorded with a Fourier transform spectrometer (FTS) were listed for 4928 U I and 431 U II emission spectral lines between 11000 and 26000 cm^{-1}. The oscillator strengths of the lines at λ = 3859.571 Å and λ = 4050.041 Å were later determined by Chen and Borzileri [12] who combined experimental lifetime measurements of the upper levels with unpublished branching fractions. Oscillator strengths were also reported for about 100 U II lines by Henrion *et al.* [13] from relative intensities measured on a hollow-cathode lamp spectrum. In his database, Kurucz [14] listed transition probabilities and oscillator strengths for many U II lines based on the experimental data reported by Meggers *et al.* [8], Corliss and Bosmann [9], and Chen [12]. Finally, about 20 years ago, accurate radiative lifetimes were measured by Lundberg *et al.* [15], using laser-induced fluorescence technique, for six even-parity energy levels of singly ionized uranium located at 23315.090 cm^{-1} ($J = 9/2$), 24684.132 cm^{-1} ($J = 9/2$), 25714.049 cm^{-1} ($J = 13/2$), 26191.309 cm^{-1} ($J = 13/2$), 28154.450 cm^{-1} ($J = 11/2$) and 30341.675 cm^{-1} ($J = 15/2$). Experimental oscillator strengths for 57 U II lines in the region 3500 – 6700 Å were then obtained by combining these latter radiative lifetimes with new branching fractions derived from the measured line intensities in the spectra emitted by a hollow cathode and analyzed using a Fourier transform spectrometer by Nilsson *et al.* [16].

3.1.1 HFR+CPOL Calculations

In the present study, the configurations retained in the calculations were those presented by Meftah *et al.* [6] as being the most interacting ones in the lowest part of the energy level spectrum, namely $5f^37s^2$, $5f^36d7s$, $5f^36d^2$, $5f^47p$, $5f^5$ for the odd parity, and $5f^47s$, $5f^46d$, $5f^26d^27s$, $5f^26d7s^2$, $5f^26d^3$, $5f^37s7p$, $5f^36d7p$ for the even parity. This represents a total of 3237 and 6039 energy levels in each parity, respectively.

Since the configurations mentioned hereabove explicitly include part of the correlation effects out of the $5f^2$ ionic core, core-polarization effects were considered using the dipole polarizability, α_d, equal to 9.79 a_0^3 as tabulated by Fraga *et al.* [94] for the U V ion. In the present work, we used r_c = 0.75 a_0, which depicts the distance at which the total probability density of the ionic core orbitals equates to 10% of its maximum value, as suggested by Hameed [84].

This is illustrated in Figure 3.1. This Figure shows the calculated probability density of the core in the ground configuration, together with the r_c value that we considered in our computations. We noticed that, when using these core-polarization parameters, electric dipole transition radial integrals were reduced by around 20-25%.

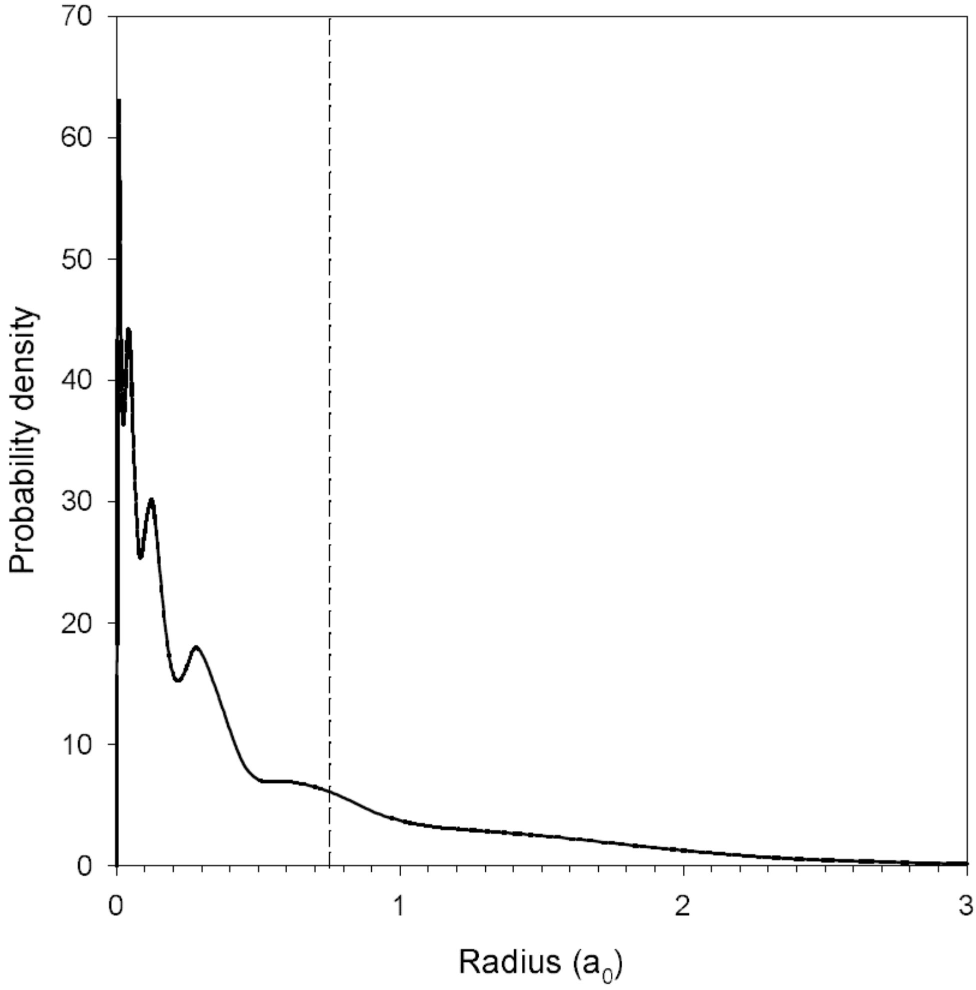

Figure 3.1: Electron probability density of the ionic core in the ground configuration ($5f^37s^2$) of U II. The cut-off radius is marked by a dash vertical line where the probability density fall to 10% of its maximum value.

However, for singly ionized uranium, the analytical core-polarization correction to the dipole operator introduced in section 2.2 is no longer valid for transitions involving 5f electrons. The latter are indeed too deeply interlocked inside the $6s^26p^6$ closed subshells as highlighted in Figure 3.2.

In order to take polarization effects more realistically into account for the 5f-6d transitions , the corresponding radial integrals were scaled down by a factor 0.80, in a similar way to that used for computing the 4f-5d transitions in lowly ionized lanthanides (Biemont *et al.* [86]).

In order to reduce as much as possible the differences between calculated and available experimental energy levels, we adopted the fitted radial parameters reported by Meftah *et al.* [6] for the five odd- and the seven even-parity configurations that we included in our physical model. As a reminder, for the odd configurations, they were able to fit up

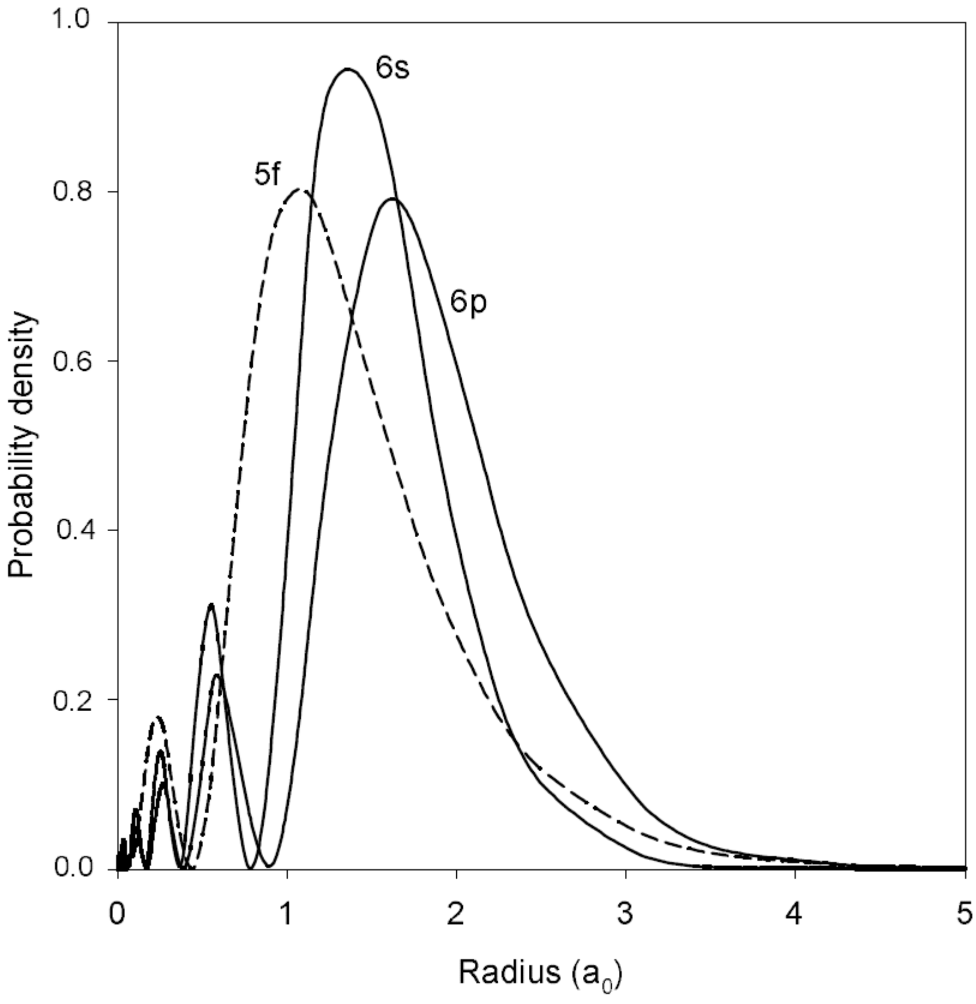

Figure 3.2: Electron probability densities of the outermost ionic core orbitals in U II, showing the overlap between 5f subshell and $6s^2 6p^6$ closed subshells

to 253 experimental energy levels with a final rms deviation of 60 cm^{-1} using 22 free and 64 constrained parameters among which the average energies (E_{av}), the electrostatic Slater integrals (F^k, G^k, R^k), the spin-orbit parameters (ζ_{nl}) and the effective interaction operators (α, β, γ). Their semi-empirical fitting procedure was less satisfactory in the even parity. Indeed, they were forced to separate their parametric analysis into two groups of configurations, i.e. $5f^4 7s$ + $5f^4 6d$ + $5f^2 6d^2 7s$ + $5f^2 6d 7s^2$ + $5f^2 6d^3$, on the one hand, and $5f^3 7s 7p$ + $5f^3 6d 7p$, on the other hand. For the first group of configurations, they found a rms deviation of 84 cm^{-1} for 125 energy levels which were fitted with 22 radial parameters. However, the interpretation of the second group's energy level structure with the same parametric method could only be carried out by only adjusting the average energies E_{av} and spin-orbit ζ_{5f} integrals. This led to a rms deviation of 441 cm^{-1} for 12 energy levels. In our work, we gathered all these 7 even configurations together in the same model with the fitted parameters taken from Meftah *et al.* [6] as a starting point. After a rather similar fitting procedure but with all the configuration interactions explicitly taken into account, we found a rather good average energy deviation of 280 cm^{-1} for the levels of interest, i.e. those involved in the strongest transitions reported in Table 3.1.

3.1.2 Results

In view of their potential future use in cosmochronological studies, only the strongest spectral lines (log gf > -1) were considered in our study. These transitions, involving energy levels up to 30342 cm^{-1}, are reported in Table 3.1. This corresponds to 38 U II spectral lines appearing in the wavelength range from 3337 to 4627 Å. For these lines, log gf-values obtained by our calculations are compared with the older data deduced from emission line intensity measurements by Corliss [11], Chen and Borzileri [12], Henrion *et al.* [13] and Kurucz [14], as well as with the more recent and more accurate experimental values obtained by Nilsson *et al.* [16]. It can be observed, from Table 3.1, that our calculated oscillator strengths are in reasonable agreement with the latter measurements, the mean relative difference between both sets of gf-values being found to be equal to 25% if we exclude four lines at 3670.068, 3865.916, 4155.409 and 4241.664 Å, for which our HFR+CPOL results are around twice as small as the experimental oscillator strengths of Nilsson *et al.* [16]. It is worth noting, however, that three of these transitions are characterized by the same upper even-parity level at 28154.451 cm^{-1}, which was found to be extremely mixed, and thus very sensitive to small changes in the eigenvector composition. Indeed, for this level, our calculations led to a main LS component, i.e. $5f^3(^4I)6d7p$ $^6L_{11/2}$, as weak as 7%, to be compared with the 18% obtained by Meftah *et al.* [6] using a more limited physical model.

For four other spectral lines, at $\lambda = 3337.785$, 3623.057, 4172.973 and 4178.995 Å, our computed log gf-values are given between square brackets in Table 3.1 to indicate that the corresponding results are more likely to be affected by larger uncertainties. This is because of the fact that, for the two upper even-parity levels involved in these transitions, it was extremely difficult to establish a trustworthy correspondence between the experimental values, i.e. $E = 28507.894$ and 30240.416 cm^{-1}, and the calculated ones, the retained theoretical levels being, moreover, very strongly mixed, with main LS components not exceeding 5% according to our calculations. For that matter, these two levels were not classified in the recent parametric analysis of the U II spectrum by Meftah *et al.*

Figure 3.3 shows the density of the energy levels distribution in U II and seen that proximity between the different levels, very high mixing effects due to very important configuration interaction are to be suspected.

Those effects have indeed been observed in our results as highlighted in Table 3.2 where the main LS-components of the most important levels (from our work) involved in the intense transitions displayed in Table 3.1 are given in percentages.

This also illustrates the strong intermediate coupling and configuration interaction characterizing heavy ions like U II. It is clear, as mentioned above, that the majority of levels appears to be extremely mixed, preventing any reliable spectroscopic designation. This is even more obvious in the even parity in which many levels were found to be the mixture of numerous (sometimes up to 20) significant contributions of comparable amplitudes and with the main component being often smaller than 10%.

Fortunately, the most intense transitions, more likely to be of use for the astrophysicists, are less affected by those cancellation effects. This can be seen in Table 3.1, because none of the most intense transitions is marked as affected by a high uncertainty. This is shown in Figure 3.4, where it is clear that the transitions with log $gf >$ -1 are much less likely to be affected by those cancellation effects[1].

The line 3859.571 Å is also of high interest because it was used as cosmochronometer by Cayrel *et al.* [54], as mentioned in section 1.3. For this transition, our gf-value of 0.875 is in excellent agreement with the accurate experimental result reported by Nilsson *et al.*, i.e. $gf = 0.857$, whereas all the previous data were very scattered between gf-values so different as 0.240 ([11]), 0.625 ([12]), 0.190 ([13] and 0.785 ([14]).

Finally, it appeared that the core-polarization effects that we included in our physical model have a major influence on the final oscillator strengths, the mean ratio $< gf_{HFR+CPOL}/gf_{HFR} >$ being found to be equal to 0.57. These effects, which are

[1]The bigger the CF is, the most reliable the log gf obtained is.

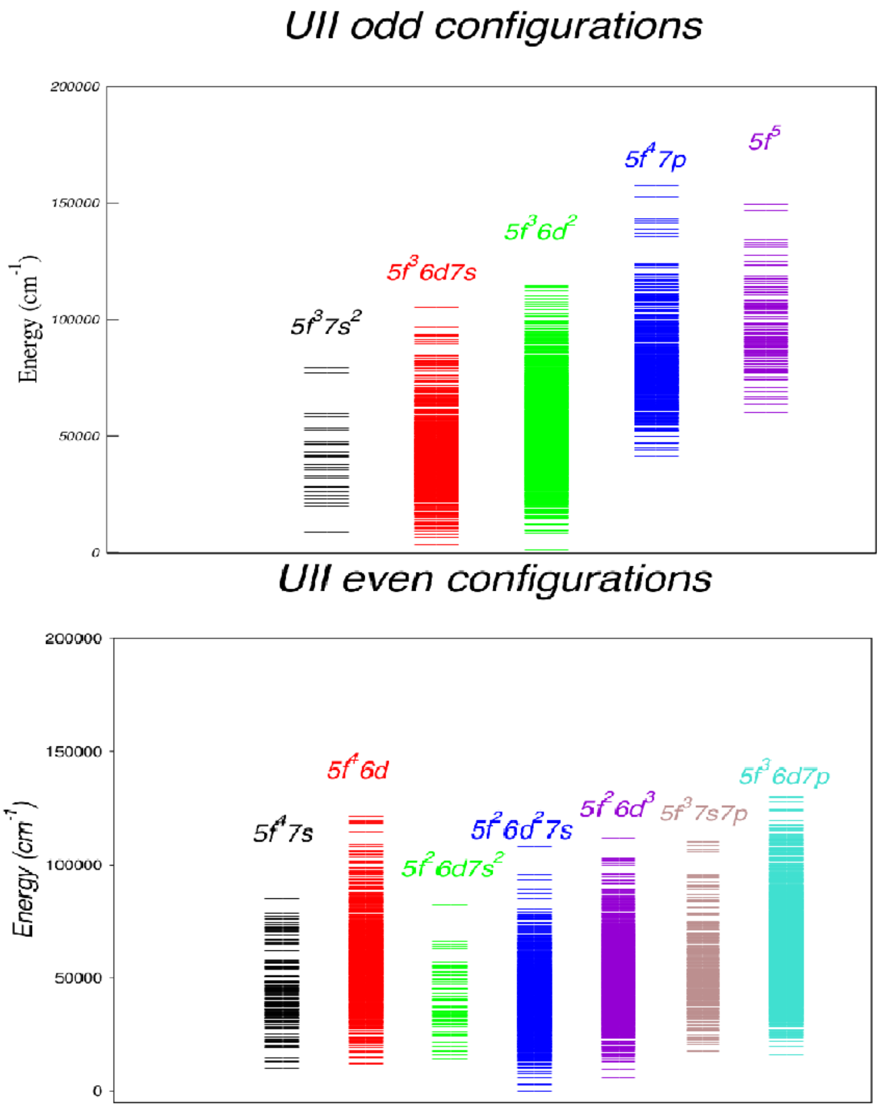

Figure 3.3: Energy Levels in U II - Original picture from Meftah *et al.* [6]

assumed to take into account the most important core-valence and core-core correlations, are expected to be much larger than those of intravalence correlations not explicitly considered in our multiconfiguration expansions. Furthermore, we observed that additional valence configurations have a rather negligible influence on the transition rates we computed. More exactly, as a first step, the configurations $5f^27s^27p$, $5f^26d7s7p$, $5f^26d^27p$, $5f^27s7p^2$ and $5f^26d7p^2$ were investigated. By comparing a nine-configuration *ab initio* HFR calculation (including $5f^37s^2$, $5f^36d7s$, $5f^36d^2$, $5f^47s$, $5f^46d$, $5f^26d7s^2$, $5f^26d^27s$, $5f^37s7p$ and $5f^36d7p$) with a fourteen-configuration calculation (adding $5f^27s^27p$, $5f^26d7s7p$, $5f^26d^27p$, $5f^27s7p^2$ and $5f^26d7p^2$), the effect of the latter five configurations was appraised and found rather small. As a matter of fact, the mean difference for the strongest lines (log gf > -1) was 0.09 dex[2], which corresponds to a relative discrepancy of a few percent. When adding $5f^37s7d$, $5f^36d7d$, $5f^47d$, $5f^27s^27d$ and $5f^26d^27d$ to the nine-configuration expansion, the mean difference was then 0.05 dex. Finally, the inclusion of the $5f^37s8s$, $5f^36d8s$, $5f^48s$, $5f^26d^28s$, $5f^27s^28s$, $5f^37s8p$ and $5f^36d8p$ was found to affect the log gf-values by less than 0.04 dex.

[2]Contraction of decimal exponent: N dex = 10^N.

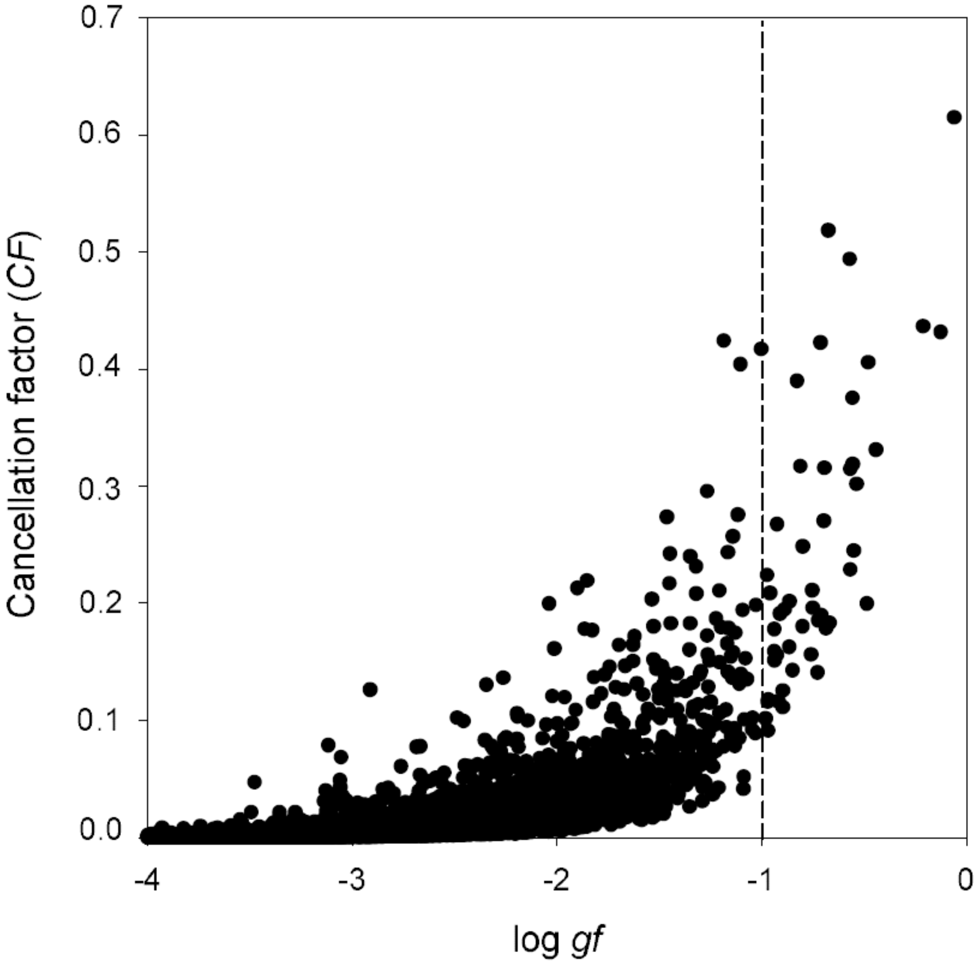

Figure 3.4: Cancellation factors plotted as a function of log gf-values for U II spectral lines. CF-values smaller than typically 0.05 indicate that the corresponding f-values may be affected by larger percentage errors.

Table 3.1: Strongest visible spectral lines in U II. The transitions listed are limited to those for which the log gf-values, computed in the present work, are greater than -1.0.

λ_{air} [a]	Lower odd level [b]		Upper even level [b]					log gf		
(Å)	E (cm^{-1})	J	E (cm^{-1})	J	C [c]	CB [d]	H [e]	K [f]	N [g]	This work [h]
3337.785	289.041	11/2	30240.416	11/2	-1.28			-0.897		[-0.794]
3357.930	289.041	11/2	30060.727	11/2	-1.39			-1.071		-0.703
3372.004	289.041	11/2	29936.466	11/2	-1.46			-1.170		-0.351
3406.269	914.765	9/2	30263.978	9/2	-1.42			-1.116		-0.892
3496.414	1749.123	13/2	30341.673	15/2	-1.12			-0.691	-0.821	-0.595
3546.677	1749.123	13/2	29936.466	11/2	-1.37			-1.066	-0.785	-0.549
3623.057	914.765	9/2	28507.894	11/2	-1.29			-1.002		[-0.925]
3640.945	1749.123	13/2	29206.703	11/2	-1.38			-1.121		-0.887
3670.068	914.765	9/2	28154.447	11/2	-0.72			-0.173	-0.192	-0.556
3700.571	914.765	9/2	27929.924	11/2	-1.21			-0.904		-0.909
3724.983	1749.123	13/2	28587.261	11/2	-1.45			-1.003		-0.896
3782.841	289.041	11/2	26716.697	13/2	-0.89			-0.478		-0.674
3826.507	289.041	11/2	26415.115	13/2	-1.17		-1.125	-0.904		-0.569
3859.571	289.041	11/2	26191.312	13/2	-0.62	-0.204	-0.721	-0.105	-0.067	-0.058
3865.916	2294.696	11/2	28154.447	11/2	-0.77			-0.273	-0.421	-0.800
3881.454	4585.434	13/2	30341.673	15/2	-0.80			-0.279	-0.509	-0.465
3932.021	289.041	11/2	25714.049	13/2	-0.89		-0.824	-0.528	-0.317	-0.478
3944.130	4585.434	13/2	29932.395	15/2	-1.23			-0.928		-0.959
3985.793	5259.653	15/2	30341.673	15/2	-0.71			-0.165	-0.278	-0.307
3990.420	914.765	9/2	25967.697	7/2	-1.29		-1.745	-1.116		-0.925
4004.064	1749.123	13/2	26716.697	13/2	-1.31			-1.138		-0.936
4044.412	5259.653	15/2	29978.143	13/2	-0.97			-0.554	-0.706	-0.810
4051.912	5259.653	15/2	29932.395	15/2	-0.95			-0.541		-0.692
4053.020	1749.123	13/2	26415.115	13/2	-1.51			-1.448		-0.752
4090.133	1749.123	13/2	26191.312	13/2	-0.78			-0.377	-0.184	-0.125
4116.097	0.000	9/2	24288.004	11/2	-1.19		-1.194	-1.036		-0.712
4155.409	6283.431	13/2	30341.673	15/2	-1.10			-0.759	-0.606	-0.948
4171.589	1749.123	13/2	25714.049	13/2	-0.92			-0.606	-0.474	-0.567
4172.973	6283.431	13/2	30240.416	11/2	-1.29			-1.051		[-0.917]
4174.189	5526.750	13/2	29476.743	13/2	-1.21			-0.948		-0.865
4178.995	4585.434	13/2	28507.894	11/2	-1.41			-1.261		[-0.667]
4211.658	4585.434	13/2	28322.361	11/2	-1.25			-1.040	-0.811	-0.709
4241.664	4585.434	13/2	28154.447	11/2	-0.83			-0.431	-0.103	-0.566
4282.460	4585.434	13/2	27929.924	11/2	-1.37			-1.242		-0.684
4341.686	289.041	11/2	23315.092	9/2	-1.24		-1.337	-1.161	-0.700	-0.536
4472.330	289.041	11/2	22642.478	9/2	-1.28		-1.398	-1.260		-0.863
4555.091	8394.362	15/2	30341.673	15/2	-1.34			-1.167	-0.650	-0.771
4627.075	4585.434	13/2	26191.312	13/2	-1.27			-1.178	-0.593	-0.486

[a] Experimental wavelengths from Kurucz (1995) [14]

[b] Experimental energy levels from Blaise *et al.* (1994) and Meftah *et al.* (2017) [6]

[c] Values from Corliss (1976) [11]

[d] Values from Chen and Borzileri (1981) [12]

[e] Values from Henrion *et al.* (1987) [13]

[f] Values from Kurucz (1995) [14]

[g] Values from Nilsson *et al.* (2002) [16]

[h] Values between square brackets correspond to uncertain line identifications in the calculations (see text)

Table 3.2: Main LS-coupling components of energy levels involved in the transitions in U II listed in Table 3.1

Energy^a (cm^{-1})	J	First component (%)	Second component (%)	Third component (%)
Even parity				
0	9/2	77 5f^{3}7s^2 (^{4}I)^{4}I	12.6 5f^{3}7s^2 (^{2}H)^{2}H	3.6 5f^{3}6d2 (^{4}I)^{4}I
289.041	11/2	76.8 5f^{3}6d7s (^{4}I)^{6}L	12.9 5f^{3}6d7s (^{2}H)^{4}K	4.9 5f^{3}6d7s (^{4}I)^{4}K
914.765	9/2	71.3 5f^{3}6d7s (^{4}I)^{6}K	10.5 5f^{3}6d7s (^{2}H)^{4}I	10.2 5f^{3}6d7s (^{4}I)^{4}I
1749.123	13/2	44.5 5f^{3}6d7s (^{4}I)^{6}L	26.1 5f^{3}6d7s (^{4}I)^{4}L	8.3 5f^{3}6d7s (^{2}H)^{4}K
2294.696	11/2	48.3 5f^{3}6d7s (^{4}I)^{6}K	17.6 5f^{3}6d7s (^{4}I)^{4}K	7.8 5f^{3}6d7s (^{4}I)^{4}I
4585.434	13/2	28.2 5f^{3}6d2 (^{4}I)^{6}M	27.3 5f^{3}6d7s (^{4}I)^{6}L	14.3 5f^{3}6d7s (^{4}I)^{4}L
5259.653	15/2	67.5 5f^{3}6d7s (^{4}I)^{6}L	17.8 5f^{3}6d7s (^{4}I)^{4}L	6.4 5f^{3}6d7s (^{2}H)^{4}K
5526.75	13/2	71 5f^{3}6d7s (^{4}I)^{6}K	12.3 5f^{3}6d7s (^{4}I)^{4}K	5.5 5f^{3}6d7s (^{2}H)^{4}I
6283.431	13/2	38.4 5f^{3}6d2 (^{4}I)^{6}M	21.6 5f^{3}6d7s (^{4}I)^{4}L	16.3 5f^{3}6d7s (^{4}I)^{6}L
8394.362	15/2	60.4 5f^{3}6d7s (^{4}I)^{6}K	14.2 5f^{3}6d2 (^{4}I)^{6}M	4.8 5f^{3}6d7s (^{4}I)^{4}K
Odd parity				
22642.478	9/2	10.4 5f^{3}7s7p (^{4}I)^{6}K	4.8 5f^{2}6d27s (^{3}F)^{4}I	3.9 5f^{2}6d27s (^{3}H)^{4}I
23315.092	9/2	23.7 5f^{3}7s7p (^{4}I)^{6}K	6 5f^{4}6d (^{5}I)^{6}G	5 5f^{3}7s7p (^{4}I)^{4}I
24288.004	11/2	7.9 5f^{3}7s7p (^{4}I)^{6}K	5.5 5f^{3}7s7p (^{4}I)^{4}K	3.6 5f^{4}6d (^{5}I)^{6}G
25714.049	13/2	9.1 5f^{3}6d7p (^{4}I)^{6}M	4.5 5f^{2}6d27s (^{3}H)^{4}K	4 5f^{2}6d27s (^{3}H)^{4}L
25967.697	7/2	19.7 5f^{3}7s7p (^{4}I)^{6}I	5.3 5f^{2}6d7s^2 (^{3}F)^{4}H	3.7 5f^{3}7s7p (^{4}I)^{4}H
26191.312	13/2	21.7 5f^{3}6d7p (^{4}I)^{6}M	8.9 5f^{2}6d27s (^{3}H)^{4}K	8 5f^{3}6d7p (^{4}I)^{4}L
26415.115	13/2	8.1 5f^{2}6d27s (^{3}H)^{6}H	7.1 5f^{3}6d7p (^{4}I)^{6}M	5.5 5f^{2}6d27s (^{3}H)^{4}K
26716.697	13/2	7.2 5f^{4}6d (^{5}F)^{6}H	5.6 5f^{2}6d27s (^{3}H)^{4}K	5.3 5f^{2}6d27s (^{1}G)^{4}K
27929.924	11/2	5.6 5f^{2}6d7s^2 (^{3}H)^{4}H	5.3 5f^{3}7s7p (^{4}I)^{6}K	4.5 5f^{3}6d7p (^{4}I)^{6}L
28154.447	11/2	7 5f^{3}6d7p (^{4}I)^{6}L	6.5 5f^{4}7s (^{3}H)^{4}H	3.5 5f^{4}7s (^{3}H)^{2}H
28322.361	11/2	8.1 5f^{3}6d7p (^{4}I)^{6}L	4.7 5f^{2}6d27s (^{3}F)^{6}H	3.6 5f^{2}6d27s (^{1}G)^{4}K
28507.894	11/2	5 5f^{4}6d (^{5}G)^{6}I	4 5f^{4}7s (^{3}H)^{4}H	3.7 5f^{2}6d7s^2 (^{3}H)^{4}H
28587.261	11/2	7.3 5f^{3}6d7p (^{4}I)^{6}L	5.3 5f^{2}6d27s (^{3}F)^{6}H	3.6 5f^{4}7s (^{1}H)^{2}H
29206.703	11/2	6.6 5f^{2}6d^3 (^{3}H)^{6}K	3.1 5f^{2}6d^3 (^{3}H)^{4}I	2.6 5f^{2}6d27s (^{3}F)^{6}G
29476.743	13/2	12.4 5f^{3}7s7p (^{4}I)^{6}K	5.1 5f^{2}6d27s (^{3}H)^{6}I	2.9 5f^{3}7s7p (^{4}I)^{4}K
29932.395	15/2	9.7 5f^{2}6d7s^2 (^{3}H)^{4}I	5.1 5f^{4}6d (^{5}F)^{6}H	5 5f^{3}6d7p (^{4}I)^{6}M
29936.466	11/2	11.9 5f^{3}6d7p (^{4}I)^{6}L	7.6 5f^{2}6d27s (^{3}F)^{6}G	4.7 5f^{2}6d27s (^{3}H)4G
29978.143	13/2	13.9 5f^{2}6d^3 (^{3}H)^{6}K	5.1 5f^{2}6d27s (^{3}H)^{6}I	3.7 5f^{3}7s7p (^{4}I)^{6}K
30060.727	11/2	5 5f^{3}6d7p (^{4}I)^{6}L	4.4 5f^{2}6d27s (^{3}H)^{6}G	2.7 5f^{4}6d (^{5}F)^{4}G
30240.416	11/2	3 5f^{4}7s (^{3}H)^{2}H	2.8 5f^{3}6d7p (^{4}I)^{6}L	2.2 5f^{2}6d7s^2 (^{3}H)^{4}H
30263.978	9/2	11.6 5f^{3}7s7p (^{4}I)^{6}I	3.4 5f^{2}6d^3 (^{3}H)^{6}I	3.4 5f^{3}6d7p (^{4}I)^{6}K
30341.673	15/2	18.4 5f^{3}6d7p (^{4}I)^{6}M	12.4 5f^{4}7s (^{1}K)^{2}K	5.2 5f^{2}6d27s (^{3}H)^{2}L

a: From Meftah *et al.* [6]

3.2 Th II

Thorium (Z = 90) was discovered on the island of Lovoy in Norway by Morten Thrane Esmark who sent a sample to his father, Prof. Jens Esmark, a distinguished mineralogist, who was unable to identify it and thus transferred the sample to the Swedish chemist Jöns Jakob Berzelius for examination in 1829 [95]. After analysis, Berzelius concluded it was a new element and named it thorium, after Thor, the Scandinavian God of thunder. The radioactivity of thorium was independently discovered in 1898 by the physicist Marie Curie and the chemist Gerhard Carl Schmidt. Between 1900 and 1903, Ernest Rutherford and Frederick Soddy demonstrated that thorium decays following an exponential decay law into a series of other elements. This led to the determination of its half-life as one of the important characteristics associated with a particles and to the establishment of the radioactivity theory [96]. Each isotope of thorium is radioactive, the most stable one being ^{232}Th, which has a very long half-life of 14 billion years.

The first investigation of the Th II spectrum was carried out by McNally *et al.* [17] in 1942. They used five sets of exposures to the thorium arc in silver, burning in a Bitter electromagnet at high fields, to identify 1091 lines of singly ionized thorium in a wavelength range from 2150 to 8140 Å. This allowed the classification of 219 levels belonging to two groups of configurations between which no combinations were found, namely $6d^27s$, $6d^3$, $6d7s^2$, $6d^27p$, 6d7s7p and 5f6d7s (with $6d^27s$ $^4F_{3/2}$ lying lowest), on the one hand, and $5f7s^2$, 5f6d7s, 5f7s7p and 5f6d7p (with $5f7s^2$ $^2F_{5/2}$ lying lowest), on the other hand. In order to link these two groups of energy levels, McNally [18] recorded the infrared spectrum of thorium in the region 8665 to 11230 Å using IR plates exposed in a Wadsworth stigmatic grating spectrograph in 1945. The separation between the ground level $^2D_{3/2}$ (from $6d7s^2$) and the excited level $^2F_{5/2}$ (from $5f7s^2$) was found to be only 4490.29 cm^{-1}. At the same period, independent experimental studies undertaken at the Zeeman laboratory of Amsterdam led to similar conclusions and the determination of additional levels [19, 20, 21]. All these published data, together with yet unpublished energy levels, were compiled by Charles [22] in a list of 2850 classified lines of Th II from 165 odd and 191 even levels.

McNally [18] pointed out that many of the strong transitions between low-lying Th II levels appear in the IR region and, although he observed some of them in the photographic infrared, the remaining lines were outside his region of observation. The majority of these lines were observed in the emission spectrum of thorium in the $1 - 2.5$ μ region recorded by Steers [23]. In this study, about 60 lines were attributed to Th II transitions but no new levels could be established. However, some values of Th II levels were revised by considering interferometric measurements from the visible and ultraviolet regions. In particular, a value of 4490.26 cm^{-1} was suggested for $5f7s^2$ $^2F_{5/2}$ and the interferometric measurements were used to revise other levels on this basis. A few years later, Minski [24] discovered 28 energy levels through the first extensive parametric study of the Th II configurations in three mixed groups in intermediate coupling with configuration interaction, i.e. the low even group $(6d + 7s)^3$, the high even group $5f^27s + 5f7s7p + 5f6d7p + 5f^26d$, and the six odd configurations $5f7s^2 + 5f6d7s + 5f6d^2 + 6d7s7p + 7s^27p + 6d^27p$. Brewer [97] predicted the position of the lowest terms of $5f^27p$ at 48000 ± 2000 cm^{-1}, $5f7p^2$ at $54\,000 \pm 4000$ cm^{-1}, and $5f^3$ at 55000 ± 5000 cm^{-1}. The analysis of Th II was then extended with improved observations of the spectrum between 2000 and 25000 Å by Zalubas and Corliss [25]. They classified 6500 lines as transitions between 199 odd levels and 271 even levels. The emission spectrum of thorium from 2777 to 13500 Å was remeasured from a hollow cathode discharge by means of a Fourier transform spectrometer, giving rise to wave numbers accurate to about 0.002 cm^{-1}, relative intensities accurate to about 8%, and energy levels accurate to about 0.003 cm^{-1}.

Most of the Th II data obtained in the works mentioned hereabove were listed in three compilations: those of Blaise and Wyart [1], Sansonetti and Martin [26] and Redman *et al.* [27]. In the latter, the previously published thorium line lists were combined with new precise observations of a thorium-argon hollow cathode lamp emission spectrum in the region between 3500 and 11750 Å with a high-resolution Fourier transform spectrometer to refine the energy levels in Th I, Th II, and Th III. Using these refined level values, accurate Ritz wavelengths were also calculated for 19874 thorium lines between 2500 and 55000 Å while 102 new thorium energy levels, among which 9 belonging to Th II, were found. The list of Th II energy level values reported in the NIST database [28] is entirely based on the Redman *et al.* compilation [27]. It contains 517 energy levels belonging to the 6d7s^2, 6d^{2}7s, 6d^3, 5f^{2}7s, 5f7s7p, 5f6d7p, 5f^{2}6d even-, and 5f7s^2, 5f6d7s, 5f6d^2, 6d7s7p, 6d^{2}7p, 7s^{2}7p, 5f^{2}7p, 5f7p^2 odd-parity configurations up to 66427.1381 cm^{-1}.

Finally, it is worth mentioning that resonant two-step laser excitation of trapped Th$^+$ ions led two different groups (see [98, 99]) to the measurement of 43 previously unknown levels from 7.3 to 8.3 eV (58875 – 66940 cm^{-1}), and 166 previously unknown levels from 7.8 to 9.8 eV (62907 – 79037 cm^{-1}), respectively. These new experimental results are not included in the current version of the NIST database.

3.2.1 HFR+CPOL Calculations

The configurations explicitly retained in our calculations were 6d7s^2, 6d7p^2, 6d^3, 5f^{2}7s, 5f^{2}8s, 5f^{2}6d, 5f^{2}7d, 5f^{2}8d, 5f6d7p, 5f6d8p, 5f7s7p, 5f7s8p, 6d^{2}7s, 6d^{2}8s, 6d^{2}7d, 6d^{2}8d, 7s7p^2, 5f6d7f for the even parity, and 5f6d^2, 5f6d7s, 5f6d8s, 5f7s^2, 5f7p^2, 5f7d^2, 5f8s^2, 5f^{2}7p, 5f^{2}8p, 5f^3, 5f6d7d, 5f6d8d, 5f7s8s, 5f7p8p, 5f^{2}6f, 5f7s7d, 6d7s7p, 6d7s8p, 6d^{2}7p, 6d^{2}8p, 7s^{2}7p, 7s^{2}8p, 7p^3 for the odd parity.

As we can see, this list of configurations includes a large amount of valence correlation outside of the Rn-like Th V ionic core, consisting of 86 electrons completely filling all subshells up to 6p, i.e. 1s^{2}2s^{2}2p^{6}3s^{2}3p^{6}3d^{10}4s^{2}4p^{6}4d^{10}4f^{14}5s^{2}5p^{6}5d^{10}6s^{2}6p^6. Therefore, we estimated the core-valence interactions by considering core-polarization contributions with the dipole polarizability, α_d, equal to 10.26 a_0^3 as tabulated in [94] for the Th V ion, and the cut-off radius, r_c, equal to 1.90 a_0, which corresponds to the HFR average value $<r>$ for the outermost core orbital (6p) of the investigated configurations. However, as already mentioned in the U II calculations (see section 3.1), with 5f electrons deeply embedded inside the closed 6s^{2}6p^6 subshells, the analytical core-polarization corrections to the dipole operator, as incorporated in our model [81, 82], are no longer valid for transitions involving these electrons. Instead, in order to take polarization effects into account for the 5f–nd (n = 6,7,8) transitions, the uncorrected $<5f||r||nd>$ radial integrals were reduced by 20%, in a similar way to the procedure used for U II.

In order to minimize the discrepancies between calculated energy levels and available experimental values, some radial integrals were adjusted focusing only on low-lying levels located below 33000 cm^{-1}. More precisely, the average energies (E_{av}), the Slater electrostatic integrals (F^k, G^k), the spin-orbit parameters (ζ_{nl}), and the effective interaction parameters (α, β) belonging to the 6d7s^2, 6d^3, 6d^{2}7s even-parity configurations and to the 5f7s^2, 5f6d^2, 5f6d7s, 6d7s7p odd-parity configurations were fitted using the experimental energy levels taken from the NIST compilation [28]. The Slater configuration interaction integrals (R^k) connecting 5f6d^2 and 5f6d7s were also adjusted with the constraint that the ratios of their values were held fixed. For higher configurations, namely 5f^{2}7s, 5f^{2}6d, 5f6d7p, 5f7s7p in the even parity, and 6d^{2}7p, 7s^{2}7p in the odd parity, only the average energies were adjusted using the lowest level experimentally known for each of these configurations. Moreover, a scaling factor of 0.75 was applied to the *ab initio* values of all the F^k, G^k and R^k integrals not fitted in the semi-empirical process to make a rough allowance for the cumulative effect of the infinity of small perturbations not explicitly included in the physical model, as recommended by Cowan [7]. At the end of the fitting procedure, the mean deviations between calculated and experimental energy levels were found to be equal to 226 and 264 cm^{-1} for even and odd parities, respectively. Finally, let us also note that this semi-empirical adjustment enabled us to unambiguously attribute the value of the total angular momentum, i.e. $J = 1/2$, to the even-parity level at 23346.8901 cm^{-1}, for which a doubt between $J = 1/2$ and $J = 3/2$ still remained in the most recent databases i.e. [27, 28].

3.2.2 Results

From our computations, we identified 91 Th II transitions with log gf > -1, involving energy levels up to 33000 cm^{-1}. These lines, appearing in the visible wavelength range from 3180 and 7526 Å, are listed in Table 3.4. In this table, our oscillator strengths are compared with the older data deduced from intensity measurements from Corliss and Bosman [9], subsequently renormalized by Corliss [100] using the experimental lifetimes, with the values listed in the database of Kurucz [14], and with the more accurate experimental results published by Nilsson *et al.* [101]. As mentioned above, it was indeed well verified that our calculated gf-values given in Table 3.4 were not subject to important cancellation effects, the cancellation factor (CF), as defined in section 2.2, being greater than 0.10 for each transition with the exception of the lines at 3863.405, 4432.963, 4844.165, 5183.989, 5415.433, and 6577.656 Å, for which the CF-values were found to be equal to 0.05, 0.08, 0.06, 0.06, 0.07, and 0.04, respectively. As a reminder, according to Cowan [7] , computed line strengths may be expected to show large percent errors when the CF is smaller than about 0.05.

When one looks at Table 3.4, it can be noticed that there are large disagreements between the oscillator strengths computed in the present work and the early data published by Corliss and Bosman [9], Corliss [100] and Kurucz [14], the corresponding discrepancies being reflected by the mean ratios $< gf_{This\ work} \ / \ gf_{CB} > = 4.97 \pm 3.16$ (57 common transitions), $< gf_{This\ work} \ / \ gf_{C} > = 1.70 \pm 1.05$ (35 common transitions), and $< gf_{This\ work} \ / \ gf_{K} > = 4.65 \pm 3.23$ (76 common transitions, excluding the two-order discrepancy observed for the line at 7393.438 Å), where the mean deviations represent the uncertainties. However, a much better agreement was found when comparing our results with the recent (and more accurate) experimental gf-values reported by Nilsson [101]. In this case, the mean ratio $< gf_{This\ work} \ / \ gf_{N} >$ was actually found to be equal to 1.25 ± 0.46. All these comparisons are illustrated in Figure 3.5.

It is also interesting to note that our investigations highlighted the fact that, as expected, core-valence interactions have a large influence on the final oscillator strengths, the latter being indeed systematically reduced by about 25% when including core-polarization contributions in the calculations. This is shown in Figure 3.6, where the log gf-values deduced from our HFR and HFR+CPOL models are compared.

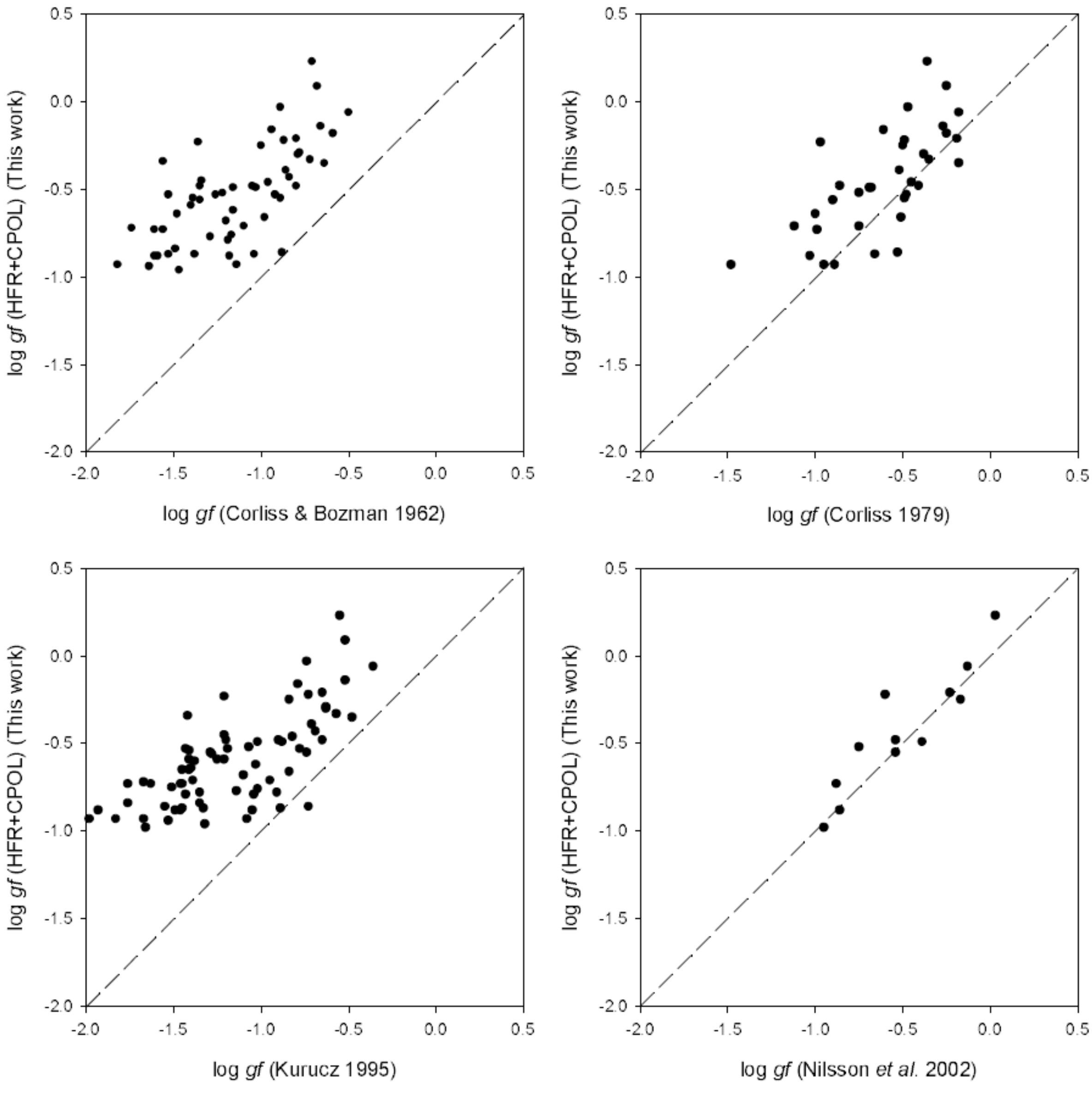

Figure 3.5: Comparison between the log gf for the strongest Th II calculated from this work with those reported by Corliss & Boltzman [9], Corliss [100], Kurucz [14] and Nilsson [101]

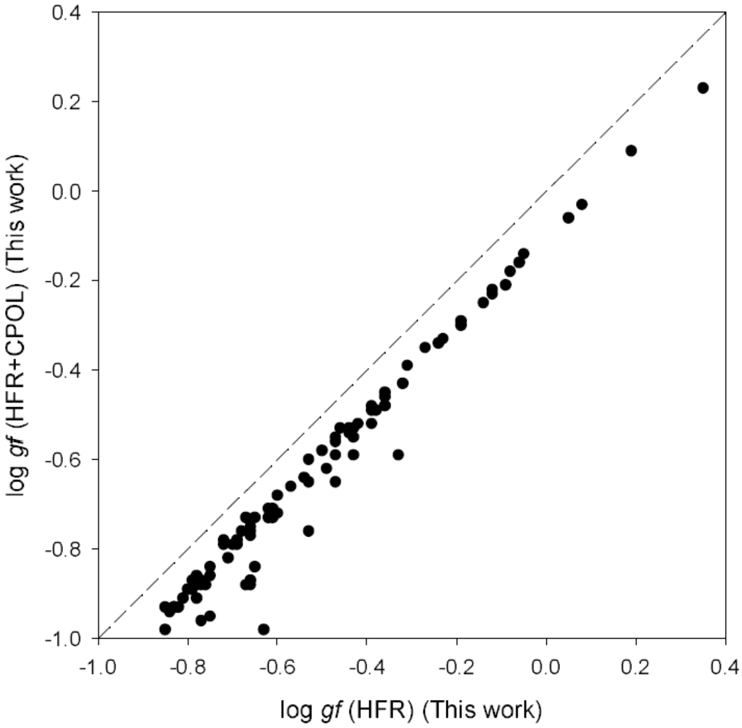

Figure 3.6: Comparison between the oscillator strengths obtained for the strongest Th II lines calculated in the present work without (HFR) and with (HFR+CPOL) the core-polarization effects

Finally, it is worth mentioning that the line at 4086.52 Å does not appear in Table 3.4, although it was detected in various astrophysical spectra (see e.g. [54, 59]). This is due to the fact that, for this particular line, our calculations gave a log gf-value equal to -1.42, i.e. well below the limit (log gf > -1.0) we imposed to the results listed in the table. Moreover, we must admit that little confidence could be given to our calculated value because the corresponding line strength was found to be affected by severe destructive interference effects, which are well known to erroneously make a weak transition even weaker [7]. This was confirmed by the poor agreement (about a factor of 3) that we observed when comparing our oscillator strength ($gf = 0.038$) with the experimental result ($gf = 0.118 \pm 0.007$) reported by Nilsson *et al.* [101] for this transition. It was also verified that the calculated oscillator strength was extremely sensitive to the configuration interaction, small variations in the eigenvector compositions of the levels involved in the transition (in particular for the upper odd level at 24463.790 cm^{-1}) giving rise to rather large changes of the final gf-value, as shown in Table 3.3. This can be explained by the fact that, due to strong level mixing, the final computed line strength for this transition is the result of the superposition of six main contributions, i.e. $6d^27s \rightarrow 6d^27p$, $6d^27s \rightarrow 5f6d7s$, $6d^27s \rightarrow 6d7s7p$, $6d7s^2 \rightarrow 6d7s7p$, $6d^3 \rightarrow 5f6d^2$, and $6d^3 \rightarrow 6d^27p$, which are characterized by electric dipole radial matrix elements (7s → 7p, 6d → 5f, and 6d → 7p) of the same order of magnitude.

Table 3.3: Influence of configuration mixing on the calculated oscillator strength corresponding to the line at 4086.52 Å

	Level	E (cm^{-1})	1^{st} (%)	2^{nd} (%)	3^{rd} (%)	4^{th} (%)	gf	log gf
Calculation A[a]	Lower	0.000	62.1 $6d^27s$	26.4 $6d7s^2$	6.9 $6d^3$	1.7 $5f^27s$	0.038	-1.42
	Upper	24463.790	76.6 $5f6d^2$	9.3 $6d^27p$	8.7 5f6d7s	4.2 6d7s7p		
Calculation B[b]	Lower	0.000	59.0 $6d^27s$	29.0 $6d7s^2$	7.5 $6d^3$	1.7 $5f^27s$	0.039	-1.41
	Upper	24463.790	76.6 $5f6d^2$	9.3 $6d^27p$	8.7 5f6d7s	4.2 6d7s7p		
Calculation C[c]	Lower	0.000	55.7 $6d^27s$	31.6 $6d7s^2$	8.0 $6d^3$	1.6 $5f^27s$	0.040	-1.40
	Upper	24463.790	76.6 $5f6d^2$	9.3 $6d^27p$	8.7 5f6d7s	4.2 6d7s7p		
Calculation D[d]	Lower	0.000	62.1 $6d^27s$	26.4 $6d7s^2$	6.9 $6d^3$	1.7 $5f^27s$	0.071	-1.15
	Upper	24463.790	72.0 $5f6d^2$	11.3 $6d^27p$	8.5 5f6d7s	6.8 6d7s7p		
Calculation E[e]	Lower	0.000	62.1 $6d^27s$	26.4 $6d7s^2$	6.9 $6d^3$	1.7 $5f^27s$	0.130	-0.89
	Upper	24463.790	64.9 $5f6d^2$	14.1 $6d^27p$	8.3 5f6d7s	11.4 6d7s7p		
Experiment[f]							0.118	-0.93

[a] HFR+CPOL calculation carried out in the present work and used as reference

[b] HFR+CPOL calculation with modified lower level composition, upper level mixing of calculation A unchanged

[c] HFR+CPOL calculation with modified lower level composition, upper level mixing of calculation A unchanged

[d] HFR+CPOL calculation with modified upper level composition, lower level mixing of calculation A unchanged

[e] HFR+CPOL calculation with modified upper level composition, lower level mixing of calculation A unchanged

[f] Experimental values from Nilsson *et al.* [101]

This highlights once again the difficulty to obtain reliable transition rates in lowly ionized heavy atoms, such as Th II. Exactly as for U II as discussed in section 3.1, the overlapping between the different configurations is tremendously high due to the orbitals close binding energies (of the 5f, 6d, 7s and 6p subshells). This is illustrated in Figure 3.7. Those very high mixing effects are also highlighted in Table 3.5, where the three main LS components (taken from our calculations) are given for the energy levels involved in the transitions listed in Table 3.4.

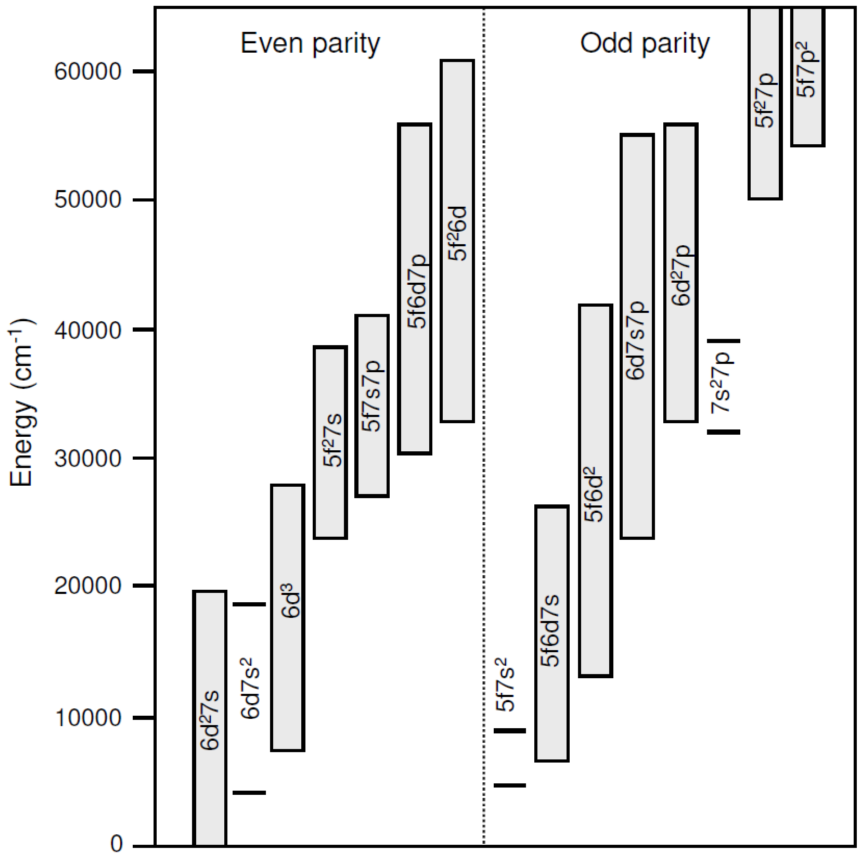

Figure 3.7: Energy levels in Th II

Table 3.4: Strongest visible spectral lines in Th II. The transitions listed are limited to those for which the log gf-values, computed in the present work, are greater than -1.0.

λ_{air}[a]	Lower odd level[b]			Upper even level[b]					log gf		
(Å)	E (cm^{-1})	P	J	E (cm^{-1})	P	J	CB[c]	C[d]	K[e]	N[f]	This work[g]
3180.193	1521.896	(e)	5/2	32957.431	(o)	7/2	-0.71	-0.36	-0.55	0.03	0.23
3351.228	1521.896	(e)	5/2	31353.127	(o)	3/2	-0.87	-0.49	-0.73	-0.60	-0.22
3358.602	1859.938	(e)	3/2	31625.680	(o)	1/2	-1.04	-0.66	-0.89		-0.87
3389.640	1859.938	(e)	3/2	31353.127	(o)	3/2	-1.36	-0.97	-1.21		-0.23
3392.035	1521.896	(e)	5/2	30994.267	(o)	7/2	-0.79	-0.38	-0.63		-0.30
3433.998	1859.938	(e)	3/2	30972.164	(o)	5/2	-0.89	-0.49	-0.74	-0.54	-0.55
3456.441	0.000	(e)	3/2	28923.204	(o)	5/2					-0.91
3469.920	4146.577	(e)	7/2	32957.431	(o)	7/2	-0.50	-0.18	-0.36	-0.13	-0.06
3478.874	4113.359	(e)	5/2	32850.065	(o)	5/2					-0.82
3497.049	0.000	(e)	3/2	28587.360	(o)	5/2					-0.52
3511.562	4490.262	(o)	5/2	32959.478	(e)	3/2	-0.78		-0.63		-0.29
3539.322	4490.262	(o)	5/2	32736.189	(e)	7/2	-1.10	-0.75	-0.95		-0.71
3539.587	0.000	(e)	3/2	28243.813	(o)	5/2	-1.35	-0.86	-1.20	-0.54	-0.48
3559.414	4490.262	(o)	5/2	32576.749	(e)	7/2					-0.89
3609.445	4113.359	(e)	5/2	31810.550	(o)	5/2	-0.72	-0.35	-0.57		-0.33
3613.779	4146.577	(e)	7/2	31810.550	(o)	5/2	-1.56		-1.42		-0.34
3648.421	1521.896	(e)	5/2	28923.204	(o)	5/2			-1.76		-0.73
3675.567	1521.896	(e)	5/2	28720.836	(o)	3/2	-1.22	-0.75	-1.07	-0.75	-0.52
3721.825	1859.938	(e)	3/2	28720.836	(o)	3/2	-1.16	-0.69	-1.02	-0.39	-0.49
3741.183	1521.896	(e)	5/2	28243.813	(o)	5/2	-1.00	-0.50	-0.84	-0.17	-0.25
3762.881	6168.356	(o)	7/2	32736.189	(e)	7/2	-0.84		-0.69		-0.43
3785.600	6168.356	(o)	7/2	32576.749	(e)	7/2	-1.03	-0.68	-0.88		-0.49
3839.746	6700.186	(o)	9/2	32736.189	(e)	7/2	-0.59	-0.25			-0.18
3863.405	6700.186	(o)	9/2	32576.749	(e)	7/2	-0.88	-0.53	-0.73		-0.86
3900.878	7331.485	(o)	5/2	32959.478	(e)	3/2	-0.94	-0.61	-0.79		-0.16
3929.669	0.000	(e)	3/2	25440.232	(o)	5/2	-1.61	-1.03	-1.46	-0.86	-0.88
3938.780	6244.295	(e)	1/2	31625.680	(o)	1/2			-1.43		-0.79
4019.129	0.000	(e)	3/2	24873.984	(o)	5/2	-0.80	-0.19	-0.65	-0.23	-0.21
4036.565	1859.938	(e)	3/2	26626.479	(o)	1/2	-1.82		-1.67		-0.93
4045.627	6168.356	(o)	7/2	30879.420	(e)	7/2			-1.83		-0.93
4059.889	7001.421	(e)	3/2	31625.680	(o)	1/2					-0.91
4069.201	6691.387	(o)	3/2	31259.297	(e)	5/2	-0.66	-0.27	-0.52		-0.14
4094.747	0.000	(e)	3/2	24414.643	(o)	3/2	-1.61	-0.99	-1.46	-0.88	-0.73
4105.330	7001.421	(e)	3/2	31353.127	(o)	3/2	-1.17		-1.02		-0.76
4105.350	8605.842	(e)	5/2	32957.431	(o)	7/2				-0.95	-0.98
4108.420	4490.262	(o)	5/2	28823.654	(e)	5/2	-0.98	-0.51	-0.84		-0.66
4116.714	6168.356	(o)	7/2	30452.725	(e)	9/2	-0.68	-0.25	-0.52		0.09
4148.181	7828.561	(e)	1/2	31928.714	(o)	3/2	-1.16		-1.03		-0.62
4178.059	7331.485	(o)	5/2	31259.297	(e)	5/2	-0.80	-0.41	-0.65		-0.48
4201.846	8018.193	(e)	3/2	31810.550	(o)	5/2	-1.29		-1.14		-0.77
4208.890	6700.186	(o)	9/2	30452.725	(e)	9/2	-0.89	-0.47	-0.74		-0.03
4254.453	9238.020	(o)	9/2	32736.189	(e)	7/2					-0.76
4273.357	8378.859	(o)	7/2	31773.080	(e)	9/2	-1.05		-0.90		-0.48
4282.041	6168.356	(o)	7/2	29515.135	(e)	9/2	-0.92	-0.48	-0.78		-0.53
4283.518	9238.020	(o)	9/2	32576.749	(e)	7/2	-1.34		-1.21		-0.45
4381.860	6700.186	(o)	9/2	29515.135	(e)	9/2	-0.64	-0.18	-0.48		-0.35
4391.111	4490.262	(o)	5/2	27257.148	(e)	7/2	-0.96	-0.45	-0.82		-0.46
4412.739	6168.356	(o)	7/2	28823.654	(e)	5/2	-1.49		-1.35		-0.84
4432.963	9202.265	(o)	7/2	31754.210	(e)	5/2			-0.91		-0.78
4440.866	8460.353	(e)	3/2	30972.164	(o)	5/2	-1.40		-1.25		-0.59
4465.341	8605.842	(e)	5/2	30994.267	(o)	7/2	-1.18		-1.05		-0.88
4510.526	10572.041	(o)	9/2	32736.189	(e)	7/2	-0.86	-0.52	-0.71		-0.39
4533.304	9720.298	(o)	7/2	31773.080	(e)	9/2	-1.19		-1.04		-0.79
4534.119	10572.041	(o)	9/2	32620.857	(e)	11/2	-1.47		-1.32		-0.96
4631.761	10189.067	(o)	11/2	31773.080	(e)	9/2	-1.20		-1.10		-0.68
4640.046	10379.123	(e)	9/2	31924.600	(o)	11/2			-1.41		-0.65
4651.555	7331.485	(o)	5/2	28823.654	(e)	5/2	-1.56		-1.45		-0.73

Table 3.4: Continued

λ_{air}[a]	Lower odd level[b]			Upper even level[b]			log gf				
(Å)	E (cm^{-1})	P	J	E (cm^{-1})	P	J	CB[c]	C[d]	K[e]	N[f]	This work[h]
4705.760	9711.962	(e)	7/2	30956.568	(o)	9/2			-1.21		-0.59
4724.772	9720.298	(o)	7/2	30879.420	(e)	7/2			-1.63		-0.73
4740.529	6168.356	(o)	7/2	27257.148	(e)	7/2	-1.59		-1.49		-0.88
4817.833	6213.490	(e)	9/2	26963.912	(o)	7/2					-0.79
4844.165	11116.585	(o)	7/2	31754.210	(e)	5/2	-1.64		-1.53		-0.94
4863.164	6213.490	(e)	9/2	26770.492	(o)	11/2		-0.95			-0.93
4863.173	6700.186	(o)	9/2	27257.148	(e)	7/2	-1.39		-1.29		-0.55
4919.816	6168.356	(o)	7/2	26488.647	(e)	5/2	-1.53		-1.43		-0.53
5017.254	7331.485	(o)	5/2	27257.148	(e)	7/2	-1.35	-0.90	-1.28		-0.56
5028.606	10572.041	(o)	9/2	30452.725	(e)	9/2	-1.26		-1.19		-0.53
5049.796	6691.387	(o)	3/2	26488.647	(e)	5/2	-1.48	-1.00	-1.40		-0.64
5183.989	12488.288	(o)	9/2	31773.080	(e)	9/2			-1.55		-0.86
5188.717	13468.968	(o)	9/2	32736.189	(e)	7/2					-0.58
5219.964	13468.968	(o)	9/2	32620.857	(e)	11/2					-0.95
5301.404	14101.799	(o)	1/2	32959.478	(e)	3/2			-1.38		-0.60
5325.144	12485.684	(o)	7/2	31259.297	(e)	5/2			-1.35		-0.78
5415.433	14275.577	(o)	9/2	32736.189	(e)	7/2	-1.14	-0.89	-1.08		-0.93
5435.892	12488.288	(o)	9/2	30879.420	(e)	7/2			-1.45		-0.65
5437.388	12570.494	(e)	7/2	30956.568	(o)	9/2			-1.76		-0.84
5449.479	14275.577	(o)	9/2	32620.857	(e)	11/2	-1.38		-1.33		-0.87
5462.613	14275.577	(o)	9/2	32576.749	(e)	7/2	-1.53		-1.45		-0.87
5539.910	9585.404	(o)	5/2	27631.225	(e)	3/2	-1.74		-1.67		-0.72
5564.201	12485.684	(o)	7/2	30452.725	(e)	9/2		-1.12	-1.39		-0.71
5568.013	13818.338	(o)	7/2	31773.080	(e)	9/2					-0.89
5707.103	6213.490	(e)	9/2	23730.654	(o)	9/2	-2.05	-1.48	-1.98		-0.93
6015.421	15305.264	(e)	9/2	31924.600	(o)	11/2			-1.41		-0.59
6021.034	14275.577	(o)	9/2	30879.420	(e)	7/2					-0.87
6087.262	15349.880	(o)	11/2	31773.080	(e)	9/2			-1.41		-0.54
6099.083	10379.123	(e)	9/2	26770.492	(o)	11/2			-2.12		-0.88
6120.556	14545.557	(o)	5/2	30879.420	(e)	7/2			-1.51		-0.75
6577.656	15349.880	(o)	11/2	30548.665	(e)	13/2			-1.66		-0.98
7191.133	10855.324	(e)	7/2	24757.507	(o)	9/2			-1.93		-0.88
7393.438	13248.709	(e)	9/2	26770.492	(o)	11/2			-2.77		-0.76
7525.508	9400.965	(e)	5/2	22685.447	(o)	7/2			-2.03		-0.87

[a] Wavelengths deduced from experimental energy levels

[b] Experimental energy levels from the NIST database (Kramida *et al.* 2019 [28]). The values rounded to the first three decimal places are given. (e) and (o) stand for even and odd parity, respectively.

[c] Values from Corliss & Bozman (1962) [9]

[d] Values from Corliss (1979) [100] - Renormalization using the experimental lifetimes

[e] Values from Kurucz (1995) [14]

[f] Values from Nilsson *et al.* (2002) [101]

[g] HFR+CPOL calculations (see text)

Table 3.5: Main *LS*-coupling components of energy levels involved in the transitions in Th II listed in Table 3.4. The energies are the experimental ones from the NIST compilation [28].

Energy (cm^{-1})	J	First component (%)	Second component (%)	Third component (%)
0.0	1.5	0.3 5f7s7p (^{3}F) ^{2}D	44.4 6d^{2}7s (^{3}F) ^{4}F	26.3 6d7s^2 (^{1}S) ^{2}D
1521.9	2.5	65.4 6d^{2}7s (^{3}F) ^{4}F	13.8 6d^{2}7s (^{1}D) ^{2}D	7.3 6d7s^2 (^{1}S) ^{2}D
1859.9	1.5	46.9 6d^{2}7s (^{3}F) ^{4}F	38.3 6d7s^2 (^{1}S) ^{2}D	3.9 6d^3 (^{2}D) ^{2}D
4113.4	2.5	39.2 6d7s^2 (^{1}S) ^{2}D	25.2 6d^{2}7s (^{3}F) ^{4}F	19.3 6d^{2}7s (^{1}D) ^{2}D
4146.6	3.5	92.1 6d^{2}7s (^{3}F) ^{4}F	2.3 5f^{2}7s (^{3}F) ^{4}F	2 6d^{2}7s (^{3}F) ^{2}F
4490.3	2.5	86.5 5f7s^2 (^{2}F) ^{2}F	3.7 5f6d7s (^{3}F) ^{2}F	3.4 5f6d^2 (^{1}S) ^{2}F
6168.4	3.5	82.1 5f6d7s (^{3}H) ^{4}H	13.2 5f6d7s (^{1}G) ^{2}G	2.8 5f6d^2 (^{3}F) ^{4}H
6213.5	4.5	86.1 6d^{2}7s (^{3}F) ^{4}F	7.5 6d^{2}7s (^{1}G) ^{2}G	2.3 5f^{2}7s (^{3}F) ^{4}F
6244.3	0.5	69.3 6d^{2}7s (^{3}P) ^{4}P	9.6 6d^{2}7s (^{3}P) ^{2}P	6.7 6d^3 (^{2}P) ^{2}P
6691.4	1.5	79.7 5f6d7s (^{3}F) ^{4}F	16 5f6d7s (^{1}D) ^{2}D	0.9 6d7s7p (^{3}D) ^{4}F
6700.2	4.5	45 5f6d7s (^{3}H) ^{4}H	22.4 5f6d7s (^{3}H) ^{2}H	21.5 5f6d7s (^{1}G) ^{2}G
7001.4	1.5	43.4 6d^3 (^{4}F) ^{4}F	13.4 6d7s^2 (^{1}S) ^{2}D	12.7 6d^3 (^{2}P) ^{2}P
7331.5	2.5	61 5f6d7s (^{3}F) ^{4}F	19.4 5f6d7s (^{1}D) ^{2}D	10 5f6d7s (^{3}F) ^{2}F
7828.6	0.5	36.6 6d^3 (^{2}P) ^{2}P	35.3 6d^{2}7s (^{3}P) ^{2}P	17.7 6d^{2}7s (^{3}P) ^{4}P
8018.2	1.5	85.2 6d^{2}7s (^{3}P) ^{4}P	5 5f^{2}7s (^{3}P) ^{4}P	1.8 6d^3 (^{4}F) ^{4}F
8378.9	3.5	78.4 5f7s^2 (^{2}F) ^{2}F	6.5 5f6d7s (^{3}F) ^{2}F	3.3 5f6d7s (^{1}G) ^{2}G
8460.4	1.5	20.4 6d^{2}7s (^{3}P) ^{2}P	37.1 6d^3 (^{4}F) ^{4}F	20.6 6d^3 (^{2}P) ^{2}P
8605.8	2.5	44.7 6d^{2}7s (^{3}F) ^{2}F	15.4 6d^{2}7s (^{3}P) ^{4}P	13.5 6d7s^2 (^{1}S) ^{2}D
9061.1	2.5	54.1 6d^{2}7s (^{3}P) ^{4}P	19.2 6d^{2}7s (^{3}F) ^{2}F	7 6d7s^2 (^{1}S) ^{2}D
9202.3	3.5	45.8 5f6d7s (^{1}G) ^{2}G	15.8 5f6d7s (^{3}G) ^{4}G	9.9 5f6d7s (^{3}F) ^{4}F
9238.0	4.5	44.8 5f6d7s (^{1}G) ^{2}G	30.1 5f6d7s (^{3}H) ^{4}H	16.9 5f6d7s (^{3}F) ^{4}F
9401.0	2.5	72.2 6d^3 (^{4}F) ^{4}F	10.1 6d^{2}7s (^{3}F) ^{2}F	4.3 6d7s^2 (^{1}S) ^{2}D
9585.4	2.5	82.5 5f6d7s (^{3}G) ^{4}G	6.1 6d^{2}7p (^{3}F) ^{4}G	5.6 5f6d7s (^{1}F) ^{2}F
9712.0	3.5	47.1 6d^{2}7s (^{1}G) ^{2}G	25.5 6d^3 (^{2}G) ^{2}G	12.5 6d^3 (^{4}F) ^{4}F
9720.3	3.5	66.3 5f6d7s (^{3}F) ^{4}F	11.4 5f6d7s (^{3}G) ^{4}G	7.7 5f6d7s (^{1}F) ^{2}F
10189.1	5.5	82.2 5f6d7s (^{3}H) ^{4}H	11.5 5f6d7s (^{3}H) ^{2}H	3.3 5f6d^2 (^{3}F) ^{4}H
10379.1	4.5	36.4 6d^{2}7s (^{1}G) ^{2}G	28.9 6d^3 (^{2}G) ^{2}G	16.1 6d^3 (^{4}F) ^{4}F
10572	4.5	45 5f6d7s (^{3}H) ^{2}H	19.7 5f6d7s (^{3}H) ^{4}H	15.3 5f6d^2 (^{1}D) ^{2}H
10673.1	2.5	29.8 5f6d7s (^{1}D) ^{2}D	34.3 5f6d7s (^{3}F) ^{4}F	19.1 5f6d7s (^{3}F) ^{2}F
10855.3	3.5	46.4 6d^3 (^{4}F) ^{4}F	28 6d^{2}7s (^{3}F) ^{2}F	8.7 6d^3 (^{2}F) ^{2}F
11116.6	3.5	38.1 5f6d7s (^{3}G) ^{4}G	16.4 5f6d7s (^{1}G) ^{2}G	9.7 5f6d7s (^{3}F) ^{4}F
11576.4	1.5	40.9 5f6d7s (^{3}D) ^{4}D	31 5f6d7s (^{1}D) ^{2}D	10.7 5f6d7s (^{3}F) ^{4}F
11725.4	0.5	57.6 5f6d7s (^{3}D) ^{4}D	9.5 5f6d^2 (^{1}D) ^{2}P	8 5f6d7s (^{1}P) ^{2}P
12220.0	1.5	49.7 6d^{2}7s (^{1}D) ^{2}D	10.1 6d^3 (^{4}P) ^{4}P	9 6d7s^2 (^{1}S) ^{2}D
12472.2	2.5	47.6 5f6d7s (^{3}F) ^{2}F	16.7 5f6d7s (^{3}D) ^{4}D	15.4 5f6d7s (^{1}D) ^{2}D
12485.7	3.5	36.9 5f6d^2 (^{3}F) ^{4}H	16.1 5f6d^2 (^{3}F) ^{2}G	13.2 5f6d7s (^{3}G) ^{4}G
12488.3	4.5	45.2 5f6d7s (^{3}F) ^{4}F	41.6 5f6d7s (^{3}G) ^{4}G	4.5 5f6d7s (^{3}G) ^{2}G
12570.5	3.5	34.6 6d^{2}7s (^{3}F) ^{2}F	30.9 6d^3 (^{4}F) ^{4}F	9 6d^3 (^{2}G) ^{2}G
12902.4	1.5	28.7 5f6d7s (^{1}D) ^{2}D	21.7 5f6d7s (^{3}D) ^{4}D	11.3 5f6d7s (^{3}P) ^{4}P
13248.7	4.5	52.5 6d^3 (^{4}F) ^{4}F	32.6 6d^{2}7s (^{1}G) ^{2}G	2.6 5f^{2}7s (^{1}G) ^{2}G
13250.5	2.5	39.6 6d^{2}7s (^{1}D) ^{2}D	16.9 6d7s^2 (^{1}S) ^{2}D	14.7 6d^{2}7s (^{3}P) ^{4}P
13406.4	6.5	95.4 5f6d7s (^{3}H) ^{4}H	4.1 5f6d^2 (^{3}F) ^{4}H	0.3 5f^{2}7p (^{3}H) ^{4}H
13469.0	4.5	29 5f6d7s (^{3}G) ^{4}G	31.8 5f6d^2 (^{3}F) ^{4}I	18.1 5f6d7s (^{3}F) ^{4}F
13818.3	3.5	13.9 5f6d7s (^{3}F) ^{2}F	19.3 5f6d7s (^{3}D) ^{4}D	18.2 5f6d7s (^{1}F) ^{2}F
14101.8	0.5	29.7 5f6d^2 (^{1}D) ^{2}P	27.8 5f6d7s (^{3}D) ^{4}D	24 5f6d7s (^{3}P) ^{2}P
14275.6	4.5	47.8 5f6d^2 (^{3}F) ^{4}I	15.5 5f6d7s (^{3}G) ^{4}G	11.3 5f6d7s (^{3}F) ^{4}F
14349.4	0.5	85 6d^3 (^{4}P) ^{4}P	5.7 5f^{2}6d (^{3}P) ^{4}P	5.3 6d^{2}7s (^{3}P) ^{2}P
14484.3	5.5	55.2 5f6d7s (^{3}H) ^{2}H	16.5 5f6d^2 (^{1}D) ^{2}H	13.1 5f6d7s (^{3}H) ^{4}H
14545.6	2.5	54.5 5f6d7s (^{3}D) ^{4}D	10.4 5f6d7s (^{1}D) ^{2}D	8.9 5f6d7s (^{3}P) ^{4}P
14791.0	3.5	41.8 5f6d7s (^{3}G) ^{2}G	24.6 5f6d^2 (^{3}F) ^{4}H	10.4 5f6d7s (^{3}F) ^{2}F
15144.7	1.5	48.5 5f6d7s (^{3}P) ^{4}P	13.8 5f6d7s (^{3}D) ^{4}D	12.5 5f6d7s (^{3}P) ^{2}P
15236.6	1.5	64.6 6d^3 (^{4}P) ^{4}P	17.8 6d^{2}7s (^{3}P) ^{2}P	4.3 5f^{2}6d (^{3}P) ^{4}P
15242.9	4.5	67.7 5f6d^2 (^{3}F) ^{4}H	16.1 5f6d^2 (^{3}F) ^{2}G	4.3 5f6d^2 (^{3}F) ^{4}I
15305.3	4.5	60.6 6d^3 (^{2}H) ^{2}H	16.2 6d^3 (^{4}F) ^{4}F	6.8 6d^3 (^{2}G) ^{2}G
15324.2	0.5	88.7 5f6d7s (^{3}P) ^{4}P	3.9 6d7s7p (^{3}D) ^{4}P	1.4 5f6d7s (^{3}P) ^{2}P
15349.9	5.5	88.8 5f6d7s (^{3}G) ^{4}G	3.9 6d^{2}7p (^{3}F) ^{4}G	3.8 5f6d7s (^{1}H) ^{2}H
15453.0	3.5	47.5 5f6d7s (^{3}D) ^{4}D	28.6 5f6d7s (^{3}F) ^{2}F	3.6 5f6d^2 (^{1}D) ^{2}F
15710.8	1.5	52.2 5f6d7s (^{3}D) ^{2}D	14.8 5f6d7s (^{3}P) ^{4}P	14.5 5f6d^2 (^{1}D) ^{2}D
15787.0	2.5	84.3 6d^3 (^{4}P) ^{4}P	5.7 5f^{2}6d (^{3}P) ^{4}P	3.9 6d^3 (^{2}D) ^{2}D

Table 3.5: Continued

Energy (cm^{-1})	J	First component (%)	Second component (%)	Third component (%)
16033.1	2.5	30 5f6d7s (^{3}D) ^{2}D	31.1 5f6d7s (^{1}F) ^{2}F	8.2 5f6d^2 (^{1}D) ^{2}D
16564.6	5.5	83.9 5f6d^2 (^{3}F) ^{4}I	8.8 5f6d7s (^{3}H) ^{2}H	2.1 5f6d^2 (^{1}G) ^{2}I
16818.1	3.5	51.2 6d^3 (^{2}G) ^{2}G	25.9 6d^{2}7s (^{1}G) ^{2}G	5.9 6d^{2}7s (^{3}F) ^{2}F
16906.6	3.5	28.1 5f6d^2 (^{3}F) ^{2}G	18 5f6d^2 (^{3}F) ^{4}H	10 5f6d^2 (^{3}F) ^{2}F
17121.6	1.5	29.8 5f6d7s (^{3}P) ^{2}P	25.7 5f6d^2 (^{1}D) ^{2}P	9 5f6d7s (^{1}D) ^{2}D
17272.3	4.5	54.5 5f6d7s (^{3}G) ^{2}G	10.7 5f6d^2 (^{1}D) ^{2}G	7.8 5f6d7s (^{1}H) ^{2}H
17460.6	2.5	71 5f6d7s (^{3}P) ^{4}P	12.6 5f6d7s (^{1}D) ^{2}D	4.2 5f6d7s (^{3}D) ^{4}D
17723.0	4.5	47 5f6d^2 (^{3}F) ^{2}G	23.2 5f6d^2 (^{3}F) ^{4}H	9.5 5f6d^2 (^{3}P) ^{2}G
17727.2	5.5	90.3 6d^3 (^{2}H) ^{2}H	3.8 5f^{2}6d (^{1}G) ^{2}H	2.2 5f6d7p (^{3}G) ^{2}H
17771.1	5.5	73.9 5f6d^2 (^{3}F) ^{4}H	11.6 5f6d^2 (^{1}G) ^{2}I	7.7 5f6d^2 (^{3}F) ^{2}I
17837.8	0.5	28.2 5f6d7s (^{3}P) ^{2}P	31.2 5f6d^2 (^{3}F) ^{4}D	14.3 5f6d^2 (^{3}F) ^{2}S
17983.4	2.5	23.8 5f6d^2 (^{3}F) ^{2}F	15.3 5f6d^2 (^{3}F) ^{4}D	9.8 5f6d^2 (^{1}D) ^{2}F
18118.7	1.5	39.3 6d^3 (^{2}D) ^{2}D	17.7 6d^3 (^{2}D) ^{2}D	9.5 6d^{2}7s (^{1}D) ^{2}D
18214.4	1.5	49.6 5f6d^2 (^{3}F) ^{4}F	6.6 5f6d^2 (^{3}F) ^{2}D	6.1 6d^{2}7p (^{3}F) ^{4}F
18568.3	0.5	46.2 5f6d^2 (^{3}F) ^{2}S	24.8 5f6d^2 (^{3}F) ^{4}D	15 5f6d^2 (^{3}F) ^{4}P
18816.9	6.5	87.5 5f6d^2 (^{3}F) ^{4}I	4 5f6d^2 (^{1}G) ^{2}I	3.7 5f6d^2 (^{3}F) ^{2}I
18973.8	3.5	39.5 5f6d7s (^{1}F) ^{2}F	11.2 5f6d^2 (^{3}F) ^{2}G	8.9 5f6d^2 (^{3}F) ^{4}D
19050.8	1.5	37.7 5f6d^2 (^{3}F) ^{4}D	13.4 5f6d7s (^{3}P) ^{2}P	12.3 5f6d^2 (^{3}F) ^{4}F
19248.3	2.5	31.4 5f6d^2 (^{3}F) ^{4}F	12.8 5f6d7s (^{3}D) ^{2}D	10.7 5f6d^2 (^{3}F) ^{4}G
19594.4	0.5	64.5 6d^{2}7s (^{1}S) ^{2}S	10.9 6d^3 (^{2}P) ^{2}P	10.5 5f^{2}7s (^{1}S) ^{2}S
19880.1	4.5	51.4 6d^3 (^{2}G) ^{2}G	22.8 6d^3 (^{2}H) ^{2}H	8.1 6d^3 (^{4}F) ^{4}F
19912.3	6.5	64.3 5f6d^2 (^{3}F) ^{4}H	13.1 5f6d^2 (^{1}G) ^{2}I	10 5f6d^2 (^{3}F) ^{2}I
20080.7	3.5	13.8 5f6d^2 (^{3}F) ^{2}F	15.6 5f6d^2 (^{3}F) ^{4}F	12.5 5f6d^2 (^{3}F) ^{2}G
20120.2	2.5	41.4 5f6d^2 (^{3}P) ^{4}G	17 5f6d^2 (^{3}F) ^{4}G	12.4 5f6d^2 (^{3}F) ^{4}F
20158.7	2.5	58.8 6d^3 (^{2}D) ^{2}D	11.5 6d^{2}7s (^{1}D) ^{2}D	7.7 6d^3 (^{2}D) ^{2}D
20288.6	5.5	44.1 5f6d^2 (^{1}G) ^{2}I	27.9 5f6d^2 (^{3}F) ^{2}I	21.4 5f6d^2 (^{3}F) ^{4}H
20310.9	2.5	13.1 5f6d7s (^{1}F) ^{2}F	15.9 5f6d^2 (^{3}P) ^{4}G	11.9 5f6d^2 (^{3}F) ^{4}F
20686.1	2.5	29.3 5f6d^2 (^{3}F) ^{4}G	19.6 5f6d^2 (^{3}P) ^{4}G	16.7 5f6d^2 (^{3}F) ^{4}F
20969.0	3.5	45.8 5f6d^2 (^{3}P) ^{4}G	17.7 5f6d^2 (^{3}F) ^{4}G	7.9 5f6d^2 (^{3}P) ^{2}G
20989.8	4.5	25.5 5f6d^2 (^{1}D) ^{2}H	21 5f6d7s (^{1}H) ^{2}H	13.7 5f6d7s (^{3}G) ^{2}G
21131.8	1.5	26.1 5f6d7s (^{1}P) ^{2}P	16.1 5f6d^2 (^{3}F) ^{2}P	12.3 5f6d^2 (^{3}P) ^{4}D
21297.4	2.5	13.7 5f6d^2 (^{1}D) ^{2}F	18.9 5f6d^2 (^{3}F) ^{4}D	13.4 5f6d^2 (^{3}F) ^{4}G
21682.7	3.5	42.1 5f6d^2 (^{3}F) ^{4}F	16.2 5f6d^2 (^{3}F) ^{4}D	7.1 5f6d^2 (^{3}P) ^{4}F
22014.9	5.5	59.9 5f6d7s (^{1}H) ^{2}H	17.5 5f6d^2 (^{1}D) ^{2}H	4 6d^{2}7p (^{1}G) ^{2}H
22028.0	7.5	96.8 5f6d^2 (^{3}F) ^{4}I	2.7 5f6d^2 (^{1}G) ^{2}K	0.4 5f3 (^{4}I) ^{4}I
22106.4	2.5	62.6 6d^3 (^{2}F) ^{2}F	6.9 6d^{2}7s (^{3}F) ^{2}F	6.7 6d^3 (^{2}D) ^{2}D
22139.7	4.5	25.6 5f6d^2 (^{3}P) ^{4}G	19 5f6d^2 (^{1}G) ^{2}G	18 5f6d^2 (^{3}F) ^{4}G
22355.2	0.5	40.5 5f6d7s (^{1}P) ^{2}P	13.7 5f6d7s (^{3}P) ^{2}P	13 5f6d^2 (^{3}F) ^{2}P
22513.3	2.5	39.9 5f6d^2 (^{3}P) ^{2}D	24.1 5f6d^2 (^{3}F) ^{4}D	8.3 5f6d^2 (^{3}P) ^{4}F
22642.1	4.5	33.1 5f6d7s (^{1}H) ^{2}H	11.1 5f6d^2 (^{1}G) ^{2}H	10 5f6d^2 (^{1}G) ^{2}G
22685.4	3.5	60.2 5f6d^2 (^{3}F) ^{4}G	18.3 5f6d^2 (^{3}P) ^{4}G	5.3 5f6d^2 (^{1}D) ^{2}G
22834.1	3.5	72.6 6d^3 (^{2}F) ^{2}F	13 6d^{2}7s (^{3}F) ^{2}F	3.3 5f^{2}6d (^{3}P) ^{2}F
23012.1	1.5	20.5 5f6d^2 (^{3}F) 4s	15 5f6d7s (^{1}P) ^{2}P	7.1 5f6d^2 (^{3}P) ^{4}D
23187.0	6.5	31.5 5f6d^2 (^{1}G) ^{2}I	28.2 5f6d^2 (^{3}F) ^{4}H	22.8 5f6d^2 (^{3}F) ^{2}I
23346.9	0.5	34.9 6d^{2}7s (^{3}P) ^{2}P	34.9 6d^3 (^{2}P) ^{2}P	11.6 6d^{2}7s (^{1}S) ^{2}S
23372.6	1.5	26.4 5f6d^2 (^{3}P) ^{4}F	16.2 6d7s7p (^{3}D) ^{4}F	14 5f6d^2 (^{3}P) ^{2}D
23518.4	3.5	14.9 5f6d^2 (^{1}D) ^{2}G	24.8 5f6d^2 (^{1}G) ^{2}G	20 5f6d^2 (^{3}P) ^{2}G
23697.7	3.5	18.9 5f6d^2 (^{3}F) ^{4}D	19.4 5f6d^2 (^{3}F) ^{4}F	11.1 5f6d^2 (^{3}P) ^{4}D
23730.7	4.5	45.2 5f6d^2 (^{3}F) ^{4}F	12.9 5f6d^2 (^{1}G) ^{2}H	11.7 5f6d7s (^{1}H) ^{2}H
24132.0	1.5	42.8 5f6d^2 (^{3}F) ^{4}P	15.6 6d7s7p (^{3}D) ^{4}F	13.2 5f6d^2 (^{3}F) 4s
24309.2	5.5	27 5f6d^2 (^{1}G) ^{2}H	24.1 5f6d^2 (^{3}F) ^{2}H	18.2 5f6d7s (^{1}H) ^{2}H
24381.8	3.5	70.8 5f^{2}7s (^{3}H) ^{4}H	10.9 5f6d7p (^{3}G) ^{4}H	7.6 5f6d7p (^{3}H) ^{4}H
24414.6	1.5	20.6 6d7s7p (^{3}D) ^{4}F	22.2 5f6d^2 (^{3}F) ^{4}P	11.8 5f6d^2 (^{3}P) ^{4}D
24463.8	2.5	46.3 5f6d^2 (^{3}F) ^{4}P	9.8 5f6d^2 (^{3}F) ^{2}D	7.3 5f6d7s (^{3}D) ^{2}D
24757.5	4.5	46.9 5f6d^2 (^{3}F) ^{4}G	38.2 5f6d^2 (^{3}P) ^{4}G	6.2 5f6d^2 (^{3}F) ^{2}H
24874.0	2.5	8 6d7s7p (^{3}D) ^{2}D	23.9 6d7s7p (^{3}D) ^{4}F	7.9 5f6d^2 (^{3}P) ^{4}F
24982.4	3.5	30.6 5f6d^2 (^{1}G) ^{2}G	20.7 5f6d^2 (^{1}D) ^{2}G	13.7 5f6d^2 (^{3}F) ^{2}F
25027.0	0.5	52.2 5f6d^2 (^{3}P) ^{4}D	9.4 6d^{2}7p (^{3}F) ^{4}D	8.6 5f6d^2 (^{3}F) ^{4}D
25188.1	1.5	11.5 5f6d^2 (^{3}P) ^{4}D	25.7 5f6d^2 (^{3}P) ^{4}F	18 5f6d^2 (^{3}F) ^{4}P
25246.3	4.5	40 5f^{2}7s (^{3}H) ^{4}H	30.7 5f^{2}7s (^{3}H) ^{2}H	5.9 5f^{2}7s (^{1}G) ^{2}G
25266.5	0.5	56.2 5f6d^2 (^{3}F) ^{4}P	13.5 5f6d^2 (^{3}F) ^{2}S	11 5f6d7s (^{1}P) ^{2}P

Table 3.5: Continued

Energy (cm^{-1})	J	First component (%)	Second component (%)	Third component (%)
25381.9	1.5	39.1 6d^3 (^{2}P) ^{2}P	28.8 6d^{2}7s (^{3}P) ^{2}P	10.8 6d^3 (^{2}D) ^{2}D
25414.9	5.5	47.5 5f6d^2 (^{3}F) ^{4}G	24.8 5f6d^2 (^{3}P) ^{4}G	23.8 5f6d^2 (^{1}G) ^{2}H
25440.2	2.5	1.2 6d^{2}7p (^{1}D) ^{2}D	32.3 5f6d^2 (^{3}F) ^{4}P	25.5 5f6d^2 (^{3}P) ^{4}F
25594.9	0.5	12 5f6d^2 (^{3}F) ^{2}P	23.3 6d7s7p (^{3}D) ^{4}D	17.1 5f6d7s (^{1}P) ^{2}P
25607.1	4.5	0 5f^{2}6f (^{1}I) ^{2}G	16.2 5f6d^2 (^{3}F) ^{4}G	16 5f6d^2 (^{3}P) ^{4}G
26424.5	2.5	32 5f6d^2 (^{3}P) ^{4}F	19.7 5f6d^2 (^{3}P) ^{2}D	17.9 5f6d^2 (^{3}P) ^{4}D
26488.6	2.5	30.2 5f7s7p (^{3}F) ^{4}G	22.7 5f7s7p (^{3}F) ^{4}F	10.1 5f7s7p (^{1}F) ^{2}F
26586.3	1.5	0.9 6d^{2}7p (^{1}D) ^{2}P	19.2 5f6d^2 (^{3}F) ^{4}S	16.1 5f6d^2 (^{3}F) ^{2}D
26626.5	0.5	27.5 6d7s7p (^{3}D) ^{4}D	11.6 5f6d^2 (^{3}F) ^{2}P	9.4 6d7s7p (^{3}D) ^{2}P
26647.8	6.5	83.3 5f6d^2 (^{1}G) ^{2}K	8.8 5f6d^2 (^{1}G) ^{2}I	5.3 5f6d^2 (^{3}F) ^{2}I
26762.3	1.5	35.6 5f^{2}7s (^{3}F) ^{4}F	22.8 5f7s7p (^{3}F) ^{4}F	21.3 5f6d7p (^{3}F) ^{4}F
26770.5	5.5	50.4 5f6d^2 (^{3}P) ^{4}G	33.6 5f6d^2 (^{3}F) ^{4}G	10.4 5f6d^2 (^{3}F) ^{2}H
26963.9	3.5	53.2 5f6d^2 (^{3}P) ^{4}D	21 5f6d^2 (^{3}F) ^{4}D	11.1 6d^{2}7p (^{3}F) ^{4}D
26965.2	1.5	32.5 5f6d^2 (^{3}P) ^{2}D	20.3 5f6d^2 (^{1}D) ^{2}D	18.5 5f6d^2 (^{3}P) ^{4}F
27249.5	3.5	70.9 5f6d^2 (^{3}P) ^{4}F	8.8 5f6d^2 (^{3}F) ^{4}F	5.1 5f6d^2 (^{3}F) ^{2}F
27257.1	3.5	10.9 5f7s7p (^{3}F) ^{2}F	26.2 5f7s7p (^{3}F) ^{4}G	19.1 5f7s7p (^{1}F) ^{2}F
27357.4	4.5	19.5 5f6d^2 (^{1}G) ^{2}H	17.6 5f6d^2 (^{3}P) ^{4}F	11.3 5f6d^2 (^{1}D) ^{2}G
27403.2	1.5	16.7 5f6d^2 (^{3}F) ^{2}P	18.5 5f6d^2 (^{3}P) ^{2}D	11.8 5f6d^2 (^{3}P) ^{4}D
27527.0	4.5	35 5f^{2}7s (^{3}H) ^{2}H	39.6 5f^{2}7s (^{3}H) ^{4}H	7.4 5f6d7p (^{3}H) ^{2}H
27594.0	2.5	33.9 5f^{2}7s (^{3}F) ^{4}F	19.8 5f^{2}7s (^{3}F) ^{2}F	9.3 5f7s7p (^{3}F) ^{4}G
27631.2	1.5	38.3 5f7s7p (^{3}F) ^{4}F	21.6 5f^{2}7s (^{3}F) ^{4}F	9.6 6d^3 (^{2}D) ^{2}D
27787.8	4.5	34.9 5f6d^2 (^{1}G) ^{2}G	25.7 5f6d^2 (^{1}G) ^{2}H	13.2 5f6d^2 (^{1}D) ^{2}G
27937.1	5.5	69.8 5f^{2}7s (^{3}H) ^{4}H	13.6 5f^{2}7s (^{3}H) ^{2}H	6.8 5f6d7p (^{3}G) ^{4}H
28011.2	1.5	35.8 6d^3 (^{2}D) ^{2}D	25 6d^3 (^{2}D) ^{2}D	12.7 5f7s7p (^{3}F) ^{4}F
28026.3	2.5	55.6 6d^3 (^{2}D) ^{2}D	12.1 6d^3 (^{2}F) ^{2}F	5.1 5f^{2}6d (^{1}S) ^{2}D
28243.8	2.5	24.8 6d7s7p (^{3}D) ^{4}F	15.6 6d^{2}7p (^{3}F) ^{4}G	11.4 6d^{2}7p (^{3}F) ^{2}F
28587.4	2.5	24.8 5f6d^2 (^{3}F) ^{2}D	22.3 5f6d^2 (^{1}G) ^{2}D	8 6d^{2}7p (^{3}F) ^{4}G
28720.8	1.5	44.6 6d7s7p (^{3}D) ^{4}D	8.4 5f6d^2 (^{3}P) ^{4}D	8.1 6d^{2}7p (^{3}F) ^{2}D
28823.7	2.5	24.9 5f7s7p (^{3}F) ^{4}F	28.4 5f7s7p (^{3}F) ^{4}G	10 5f7s7p (^{3}F) ^{4}D
28923.2	2.5	1.9 6d^{2}7p (^{1}D) ^{2}F	17 5f6d^2 (^{1}D) ^{2}F	13.9 6d7s7p (^{3}D) ^{4}F
29095.5	2.5	44.4 5f6d^2 (^{1}G) ^{2}F	17.4 5f6d^2 (^{3}F) ^{2}F	7.5 5f6d^2 (^{3}F) ^{2}D
29345.9	2.5	30.7 5f^{2}7s (^{3}F) ^{2}F	26.3 5f^{2}7s (^{3}F) ^{4}F	13.3 5f6d7p (^{3}F) ^{2}F
29431.8	3.5	30.7 5f^{2}7s (^{3}F) ^{4}F	21.1 5f^{2}7s (^{1}G) ^{2}G	12.7 5f6d7p (^{1}G) ^{2}G
29515.1	4.5	16.4 5f^{2}7s (^{1}G) ^{2}G	18.7 5f^{2}7s (^{3}F) ^{4}F	15.7 5f6d7p (^{1}G) ^{2}G
29720.3	1.5	15.5 5f6d^2 (^{1}D) ^{2}D	10.4 6d^{2}7p (^{1}D) ^{2}D	10.3 5f6d^2 (^{3}F) ^{2}D
29788.5	4.5	59.3 5f6d^2 (^{3}P) ^{4}F	15.1 5f6d^2 (^{1}D) ^{2}G	9 5f6d^2 (^{3}P) ^{2}G
29874.0	3.5	27.3 5f^{2}7s (^{3}F) ^{2}F	28.5 5f^{2}7s (^{3}F) ^{4}F	9 5f^{2}7s (^{1}G) ^{2}G
30101.4	3.5	57.6 5f6d^2 (^{1}G) ^{2}F	7.7 6d7s7p (^{3}D) ^{4}F	6.7 5f6d^2 (^{3}F) ^{2}F
30223.1	7.5	96 5f6d^2 (^{1}G) ^{2}K	2.7 5f6d^2 (^{3}F) ^{4}I	0.5 5f3 (^{2}K) ^{2}K
30310.2	5.5	20.9 5f6d^2 (^{1}D) ^{2}H	38.3 5f6d^2 (^{1}G) ^{2}H	10.5 5f6d7s (^{3}H) ^{2}H
30452.7	4.5	41.2 5f6d7p (^{3}H) ^{4}I	13.3 5f6d7p (^{3}H) ^{2}H	11.7 5f^{2}7s (^{3}F) ^{4}F
30484.7	5.5	63.9 5f^{2}7s (^{3}H) ^{2}H	13.1 5f^{2}7s (^{3}H) ^{4}H	7.3 5f6d7p (^{3}H) ^{2}H
30548.7	6.5	83.4 5f^{2}7s (^{3}H) ^{4}H	7.4 5f6d7p (^{3}G) ^{4}H	5.4 5f6d7p (^{3}H) ^{4}H
30564.6	0.5	5 6d^{2}7p (^{1}D) ^{2}P	28.6 5f6d^2 (^{1}D) ^{2}P	23.5 5f6d^2 (^{3}F) ^{2}P
30879.4	3.5	56.1 5f7s7p (^{3}F) ^{4}F	13.3 5f7s7p (^{3}F) ^{4}D	7 5f7s7p (^{1}F) ^{2}G
30956.6	4.5	48.4 5f6d^2 (^{3}F) ^{2}H	26 5f6d^2 (^{1}D) ^{2}H	5.9 6d^{2}7p (^{1}G) ^{2}H
30972.2	2.5	17.1 6d7s7p (^{1}D) ^{2}D	19.6 6d7s7p (^{3}D) ^{4}F	13.7 6d^{2}7p (^{3}F) ^{4}G
30994.3	3.5	58.1 6d7s7p (^{3}D) ^{4}F	5.4 6d^{2}7p (^{3}F) ^{2}F	5.2 6d^{2}7p (^{3}F) ^{4}G
31259.3	2.5	36.6 5f6d7p (^{3}F) ^{4}G	12 5f^{2}6d (^{3}F) ^{4}G	11.8 5f6d7p (^{1}D) ^{2}F
31353.1	1.5	17.8 6d^{2}7p (^{3}F) ^{2}D	16.2 6d7s7p (^{3}D) ^{4}F	10.2 6d^{2}7p (^{3}F) ^{4}F
31625.7	0.5	16.9 7s^{2}7p (^{1}S) ^{2}P	25.9 6d7s7p (^{3}D) ^{4}D	11.3 6d^{2}7p (^{1}S) ^{2}P
31754.2	2.5	37.1 5f7s7p (^{1}F) ^{2}F	18.2 5f7s7p (^{3}F) ^{4}F	16.6 5f7s7p (^{1}F) ^{2}D
31773.1	4.5	39.9 5f7s7p (^{3}F) ^{4}F	33.2 5f7s7p (^{3}F) ^{4}G	7.6 5f7s7p (^{3}F) ^{2}G
31800.2	3.5	32.2 5f6d^2 (^{1}D) ^{2}F	14.4 5f6d^2 (^{3}F) ^{2}F	8.2 5f6d^2 (^{1}G) ^{2}F
31810.6	2.5	63.9 6d7s7p (^{3}D) ^{4}D	11.5 6d7s7p (^{3}D) ^{4}P	5.2 6d7s7p (^{3}D) ^{2}D
31924.6	5.5	21.9 5f6d^2 (^{3}F) ^{2}H	23.1 5f6d^2 (^{3}F) ^{2}I	21.5 5f6d^2 (^{1}D) ^{2}H
31928.7	1.5	23.9 5f6d^2 (^{3}F) ^{2}D	13.5 6d7s7p (^{1}D) ^{2}D	8.5 6d^{2}7p (^{3}F) ^{2}D
32576.7	3.5	26.2 5f7s7p (^{1}F) ^{2}F	18.3 5f7s7p (^{3}F) ^{4}G	9.9 5f7s7p (^{3}F) ^{4}D
32620.9	5.5	69.1 5f^{2}6d (^{3}H) ^{4}K	13.2 5f^{2}6d (^{1}G) ^{2}I	11.2 5f^{2}6d (^{3}H) ^{2}I
32736.2	3.5	39.3 5f7s7p (^{3}F) ^{4}G	19.2 5f6d7p (^{3}H) ^{4}H	6.6 5f6d7p (^{3}H) ^{2}G
32850.1	2.5	25 5f6d^2 (^{1}D) ^{2}D	9.9 5f6d^2 (^{3}P) ^{2}D	8.3 5f6d^2 (^{3}F) ^{2}F
32957.4	3.5	60.1 6d^{2}7p (^{3}F) ^{4}G	9.6 6d7s7p (^{3}D) ^{4}F	5.9 5f6d^2 (^{1}D) ^{2}F
32959.5	1.5	33.4 5f6d7p (^{3}F) ^{2}D	10.3 5f6d7p (^{1}D) ^{2}P	10 5f7s7p (^{3}F) ^{4}F

3.3 Summary

As shown in the two previous subsections, we performed extensive HFR+CPOL calculations in singly ionized uranium and thorium and have obtained very conclusive results. Indeed, in the case of U II, 38 intense spectral lines with potential astrophysical interest were identified and designated among tenth of thousands. Among those 38 transitions, there are 8 experimental comparison points and our results reproduce well this data which reinforces the predictive character of our calculations. Unfortunately, the only spectral line identified so far (to our knowledge) in astrophysical spectra is by far the most intense one in our calculations.

For Th II, 91 intense spectral lines with astrophysical interest were identified and designated among thousands (12 experimental comparison points very well reproduced). Therefore, this work provided many intense lines of Th II that will hopefully be observable in astrophysical spectra.

These two calculations also allowed us to push the methods of atomic calculations to their limits by treating lowly ionized super-heavy elements where the configuration interaction plays a very crucial role and where consequently, the mixing effects are tremendously important.

Those results have been published respectively in Gamrath *et al.* [102, 103] in 2018 and 2020.

Chapter 4

Radiative Parameter Computations in Moderately Charged Trans-Iron Ions for the Study of Hot White Dwarfs Spectra

This section is related to the study of white dwarfs spectra. Indeed, as we mentioned in chapter 1, in collaboration with the Karl Ebenard Universität of Tübingen in Germany, an extensive study of the spectra of peculiar white dwarf has been undertaken. Those white dwarfs have the particularity of containing significantly more heavy elements than expected. In order to identify those trans-iron elements, reliable atomic data is mandatory. That is why, during this thesis, we performed atomic calculations in several heavy ions, namely copper, indium, caesium and silver. We considered the third to sixth ionization states and those were chosen because of the very high temperature of the considered white dwarfs.

All those calculations have been performed using the HFR+CPOL method described in section 2.2. The calculations of each ions mentioned here above are described in details in the section in the section especially dedicated to each one of them (respectively 4.1 for the copper ions, 4.2 for the indium ions, 4.3 for the caesium ions and 4.4 for the silver ions). Exactly as we did in the previous chapter, in order to take polarization effects more realistically into account, the radial integrals were scaled down by a factor 0.80 for all the ions considered in this chapter.

4.1 Cu IV - VII

The atomic number of copper is 29. Its name comes from old English *copor* (related to the Dutch word *koper* and the German word *Kupfer*), based on the late Latin word *cuprum* that comes from the Latin word *cyprium aes*: the Cyprus metal (so called because Cyprus was the first main source of copper). The atomic structure of copper is rather similar to silver and gold, because they all have an s orbital occupied by a single electron with completely filled p and d subshells, in their fundamental configurations which allows the formation of metallic bonds. The three metals of this copper group are increasingly noble and rare, from semi-noble copper to truly noble gold, their nobility being explained by their small atomic radius and their compact atomic stacking, their higher ionization potential because of the filled d subshells, their relatively high melting point and their low reactivity or relative chemical inertia [104]. Pure copper is one of the only colored metals with gold and caesium.

4.1.1 Models Used

The main source of atomic data related to the Cu IV-VII spectra is the paper published by Sugar & Musgrove [29] in which the available experimental energy levels of the copper atom, in all stages of ionization, have been compiled with ionization energies, either experimental or theoretical, experimental Landé g-factors, and leading components of calculated eigenvectors. This compilation is still being used as the standard reference database for the copper ions of interest at the National Institute of Standards and Technology [28].

More precisely, for Cu IV, experimental values are reported for 187 levels of the $3d^8$, $3d^74s$, $3d^75s$, $3d^74d$, and $3d^64s^2$ even-parity configurations and 110 levels of the $3d^74p$ odd-parity configuration. In the case of Cu V, many $3d^7$ - $3d^64p$ and $3d^64s$ - $3d^64p$ lines were identifed by Van Kleef *et al.* [30], allowing them to classify all the levels of the $3d^7$ configuration, as well as 53 of the 63 levels of $3d^64s$ and 175 of the 180 levels of $3d^64p$. The Cu VI experimental spectrum is taken from Raassen and Van Kleef [31], who used new exposures of a sliding spark discharge to analyze the $3d^6$ - $3d^54p$ and $3d^54s$ - $3d^54p$ transition arrays. This analysis led to the identification of all levels in the $3d^6$ configuration, except the highest $^1S_0$, as well as 208 of the 214 levels in $3d^54p$ and 13 of the 74 levels in $3d^54s$. Finally, the analysis of the Cu VII spectrum by Van Het Hof *et al.* [105] appeared too late to be included in the compilation of Sugar and Musgrove [29] . They determined all 37 levels of the $3d^5$ ground configuration and 129 of the 180 possible levels of the $3d^44p$ configuration.

The method adopted in our work to model the atomic structures and compute the radiative parameters in the Cu IV-VII ions was the HFR + CPOL (see section 2.2). For Cu IV, configuration interaction was considered among the configurations $3d^8$, $3d^74s$, $3d^75s$, $3d^74d$, $3d^75d$, $3d^64s^2$, $3d^64p^2$, $3d^64d^2$, $3d^64s5s$, and $3d^64s4d$ for the even parity, and $3d^74p$, $3d^75p$, $3d^74f$, $3d^75f$, $3d^64s4p$, $3d^64s5p$, $3d^64s4f$, and $3d^64p4d$ for the odd parity. The core-polarization parameters were the dipole polarizability of a Cu VI ionic core, as reported by Fraga *et al.* [94], i.e., α_d = 0.67 a.u., and the cut-off radius, r_c = 0.80 a.u, corresponding to the HFR mean value of the outermost core orbital (3d) radius ($<3d||r||3d>$). Using the experimental energy levels compiled at NIST [28], some radial integrals (average energy, Slater Integrals[1], spin-orbit, and effective interaction parameters) of $3d^8$, $3d^74s$, $3d^75s$, $3d^74d$, $3d^64s^2$, and $3d^74p$ configurations were optimized by a well-established least-squares fitting procedure in which the mean deviations[2] were found to be equal to 206 cm^{-1} for the even parity and 183 cm^{-1} for the odd parity.

It is worth noting that, when performing the fit, we found that the experimental energy level at 306941.8 cm^{-1} was incorrectly classified as J = 1 in the NIST tables, while according to our calculations, this level should be designated as J = 2. The energy levels we obtained and their good agreement with the experimental ones are to be found in Tables A1 and A2 for the even and the odd parity respectively. Those (long) tables are in appendix in order not to alter the readability of this thesis. As one can see in those tables, the experimental levels are very well reproduced by our calculations. We also give the main LS components of those levels according to our computations.

For Cu V, the configurations included in the HFR model were $3d^7$, $3d^64s$, $3d^65s$, $3d^64d$, $3d^54s^2$, $3d^54p^2$, $3d^54d^2$, and $3d^54s4d$ for the even parity, and $3d^64p$, $3d^65p$, $3d^64f$, $3d^54s4p$, $3d^54s5p$, and $3d^54s4f$ for the odd parity. In this ion the semi-empirical process was carried out to optimize the radial integrals corresponding to $3d^7$, $3d^64s$, and $3d^64p$ configurations using the experimental levels reported in the NIST database [28]. The mean deviations between calculated and experimental energy levels were 325 cm^{-1} and 259 cm^{-1} for even and odd parities, respectively. Core-polarization effects were estimated

[1]See eq. 2.31.

[2]The mean deviation is defined as the mean value of $|E_{exp} - E_{HFR}|$ for all the fitted energy levels.

using a dipole polarizability and a cut-off radius corresponding to a Cu VII ionic core, i.e., $\alpha_d = 0.47$ a.u. [94], and $r_c = 0.75$ a.u. (<3d||r||3d>). The comparison between the calculated energy levels and the experimental ones is shown in Tables A4 and A5 (given in appendix) for the even and odd parity respectively.

In the case of Cu VI, the configuration interaction was considered among the following configurations: $3d^6$, $3d^54s$, $3d^55s$, $3d^54d$, $3d^55d$, $3d^44s^2$, $3d^44p^2$, $3d^44d^2$, $3d^44s4d$, $3d^44s5d$ (even parity) and $3d^54p$, $3d^55p$, $3d^54f$, $3d^44s4p$, $3d^44s5p$, $3d^44s4f$ (odd parity). The core-polarization parameters were those corresponding to a Cu VIII ionic core, i.e., $\alpha_d = 0.40$ a.u. ([94]), and $r_c = 0.72$ a.u. (<3d||r||3d>). The radial parameters of the $3d^6$, $3d^54s$, and $3d^54p$ configurations were optimized in order to minimize the differences between the computed Hamiltonian eigenvalues and the experimental energy levels listed at NIST [28], giving rise to average deviations of 442 cm^{-1} (even parity) and 429 cm^{-1} (odd parity). The results that we obtained for those energy levels are displayed as a comparison between the calculated energy levels and the experimental ones in Tables A7 and A8 (in appendix) for respectively the even and odd parity. Finally, for Cu VII, ten even- and eight odd-parity configurations were included in the HFR model in order to compute the radiative parameters, i.e., $3d^5$, $3d^44s$, $3d^45s$, $3d^44d$, $3d^45d$, $3d^34s^2$, $3d^34p^2$, $3d^34d^2$, $3d^34s5s$, $3d^34s4d$, and $3d^44p$, $3d^45p$, $3d^44f$, $3d^45f$, $3d^34s4p$, $3d^34s5p$, $3d^34s4f$, and $3d^34p4d$, respectively. An ionic core of the type Cu IX was considered to estimate the core-polarization effects with the parameters $\alpha_d = 0.34$ a.u. [94] and $r_c = 0.70$ a.u. The semi-empirical fitting procedure was carried out to adjust the radial parameters in $3d^5$ and $3d^44p$ with the experimental energy levels taken from [105], leading to average energy deviations of 78 cm^{-1} and 365 cm^{-1} for even and odd parities, respectively. The comparison between the calculated energy levels and the experimental ones in Cu VII is to be found in Tables A10 and A11 (in the appendixes) for the even and odd parity, respectively.

4.1.2 Atomic Radial Parameters

The radial parameters adopted in our calculations are given in Tables 4.1, 4.2, 4.3, 4.4 for Cu IV, V, V, VII ions, respectively. As can be seen in those tables, some parameters had to be fixed (F) or linked together by their ratio (R) due to the fact that not all possible levels were experimentally known for some configurations. The fitted parameters are the mean energy, the spin-orbit and the Slater Integrals as defined in eq. 2.31.

Table 4.1: Final radial parameters (in cm^{-1}) adopted in our HFR+CPOL calculations in Cu IV

Configuration	Parameter	HFR	Fitted	Ratio
Even Parity				
$3d^8$	E_{av}	17190	16729	
	$F^2(3d,3d)$	112092	98330	0.877
	$F^4(3d,3d)$	69989	60209	0.860
	α	0	91	
	β	0	-237	
	ζ_{3d}	903	910	1.007
$3d^74s$	E_{av}	147324	152124	
	$F^2(3d,3d)$	118491	103197	0.871
	$F^4(3d,3d)$	74277	65197	0.878
	α	0	99	
	β	0	-350	
	ζ_{3d}	978	979	1.001
	$G^2(3d,4s)$	12035	10802	0.898
$3d^75s$	E_{av}	325664	330393	
	$F^2(3d,3d)$	119486	102897	0.861
	$F^4(3d,3d)$	74953	65472	0.874
	α	0	100	
	β	0	-350	
	ζ_{3d}	986	Fixed	
	$G^2(3d,4s)$	2897	2608	
$3d^74d$	E_{av}	312783	320069	
	$F^2(3d,3d)$	119438	103540	0.867
	$F^4(3d,3d)$	74922	64201	0.857
	α	0	73	
	β	0	361	
	ζ_{3d}	985	1021	1.037
	ζ_{4d}	68	Fixed	
	$F^2(3d,4d)$	13224	12461	0.942
	$F^4(3d,4d)$	5529	5503	0.995
	$G^0(3d,4d)$	5169	3754	0.726^R
	$G^2(3d,4d)$	5040	3660	0.726^R
	$G^4(3d,4d)$	3651	2651	0.726^R
$3d^64s^2$	E_{av}	334825	345297	
	$F^2(3d,3d)$	124695	112225	0.900
	$F^4(3d,3d)$	78447	70603	0.900
	α	0	Fixed	
	β	0	Fixed	
	ζ_{3d}	1056	Fixed	
Odd Parity				
$3d^74p$	E_{av}	218061	224378	
	$F^2(3d,3d)$	118845	103882	0.874
	$F^4(3d,3d)$	74519	64989	0.872
	α	0	101	
	β	0	-313	
	ζ_{3d}	980	1005	1.026
	ζ_{4p}	1185	1383	1.168
	$F^2(3d,4p)$	23861	22879	0.959
	$G^1(3d,4p)$	8425	7395	0.878
	$G^3(3d,4p)$	7571	7132	0.942

R: Fixed ratio.

Even Parity: 187 levels (mean deviation: 206 cm^{-1})

Odd Parity: 110 levels (mean deviation: 183 cm^{-1})

Table 4.2: Final radial parameters (in cm^{-1}) adopted in our HFR + CPOL calculations in Cu V

Configuration	Parameter	HFR	Fitted	Ratio
Even parity				
$3d^7$	E_{av}	30899	30322	
	$F^2(3d,3d)$	119816	105551	0.881
	$F^4(3d,3d)$	75176	65503	0.871
	α	0	109	
	β	0	-587	
	ζ_{3d}	989	1002	1.013
$3d^64s$	E_{av}	234957	237924	
	$F^2(3d,3d)$	125814	110315	0.877
	$F^4(3d,3d)$	79209	67072	0.847
	α	0	117	
	β	0	-154	
	ζ_{3d}	1066	1154	1.082
	$G^2(3d,4s)$	12797	11794	0.922
Odd parity				
$3d^64p$	E_{av}	316597	319750	
	$F^2(3d,3d)$	126094	109170	0.866
	$F^4(3d,3d)$	79402	66055	0.832
	α	0	114	
	β	0	213	
	ζ_{3d}	1069	1180	1.104
	ζ_{4p}	1596	1816	1.137
	$F^2(3d,4p)$	28011	26960	0.962
	$G^1(3d,4p)$	9612	9190	0.956
	$G^3(3d,4p)$	8916	7838	0.879

Even Parity: 72 levels (mean deviation: 325 cm^{-1})
Odd Parity: 175 levels (mean deviation: 259 cm^{-1})

Table 4.3: Final radial parameters (in cm^{-1}) adopted in our HFR+CPOL calculations in Cu VI

Configuration	Parameter	HFR	Fitted	Ratio
Even Parity				
$3d^6$	E_{av}	47058	46817	
	$F^2(3d,3d)$	127114	112843	0.888
	$F^4(3d,3d)$	80096	69557	0.868
	α	0	103	
	β	0	-264	
	ζ_{3d}	1080	1142	1.057
$3d^5 4s$	E_{av}	332771	334360	
	$F^2(3d,3d)$	132805	116707	0.879
	$F^4(3d,3d)$	83932	74133	0.883
	α	0	100	
	β	0	-250	
	ζ_{3d}	1161	Fixed	
	$G^2(3d,4s)$	13493	12647	0.937
Odd Parity				
$3d^5 4p$	E_{av}	424263	425870	
	$F^2(3d,3d)$	133032	116189	0.873
	$F^4(3d,3d)$	84088	72010	0.856
	α	0	127	
	β	0	-286	
	ζ_{3d}	1163	1247	1.073
	ζ_{4p}	2028	2320	1.144
	$F^2(3d,4p)$	31832	30768	0.967
	$G^1(3d,4p)$	10697	10190	0.953
	$G^3(3d,4p)$	10151	9203	0.907

F: Fixed Parameter.
Even Parity: 74 levels (mean deviation: 442 cm^{-1})
Odd Parity: 208 levels (mean deviation: 429 cm^{-1})

Table 4.4: Final radial parameters (in cm^{-1}) adopted in our HFR+CPOL calculations in Cu VII

Configuration	Parameter	HFR	Fitted	Ratio
Even Parity				
$3d^5$	E_{av}	78756	78522	
	$F^2(3d,3d)$	134086	119456	0.891
	$F^4(3d,3d)$	84807	74397	0.877
	α	0	118	
	β	0	-512	
	ζ_{3d}	1176	1202	1.022
Odd Parity				
$3d^4 4p$	E_{av}	553653	554223	
	$F^2(3d,3d)$	139722	123787	0.886
	$F^4(3d,3d)$	88617	78219	0.883
	α	0	123	
	β	0	-380	
	ζ_{3d}	1263	1121	0.888
	ζ_{4p}	2481	2647	1.067
	$F^2(3d,4p)$	35417	34983	0.988
	$G^1(3d,4p)$	11725	11199	0.955
	$G^3(3d,4p)$	11316	11458	1.013

Even Parity: 37 levels (mean deviation: 78 cm^{-1})
Odd Parity: 129 levels (mean deviation: 375 cm^{-1})

4.1.3 Radiative Transition Rates

The radiative transition rates obtained in the present work are listed in Tables A3, A6, A9 and A12 for the Cu IV, V, VI and VII spectral lines, respectively. It should be noted that, for Cu IV,V and VII, we are, to our knowledge, the first ones to provide data on transition probabilities and oscillator strengths. We initially the transitions for which log gf was $\geq$ -6, which consisted in thousands of E1 transitions, and we sent them to the astrophysicists at the University of Tübingen. In this work, we decided to restrict ourselves and impose the condition log gf $\geq$ -1, corresponding to the most intense and reliable transitions ($CF > 0.05$).

In the case of the Cu IV, imposing the criterion log gf $\geq$ -6 gives rise to 8725 transitions. With the more restrictive criterion log gf $\geq$ -1, we obtain 1024 intense transitions. Some of these transitions have been measured and reported in the literature (see e.g. the NIST database [28] or Sugar and Musgrove [29]) but our transition probabilities and oscillator strengths are the first to be published, which potentially makes 1024 new intense lines useful for astrophysicists in the framework of our collaboration with the University of Tübingen or for other astrophysicists. Some of them have actually been used to identify new lines of Cu IV in the spectrum of RE0503-289 (see section 4.1.3.1). Those 1024 transitions are listed in Table A3, where the energies are the experimental ones given in cm^{-1}.

When it came to Cu V, the criterion log gf $\geq$ -6 led to 5456 transitions and we obtained 695 transitions with log gf $\geq$ -1, which are listed in table A6 in which the energies are the experimental ones given in cm^{-1}. Some of these transitions have been measured and reported in [30] but no comparison point exists to our knowledge in the literature when it comes to gA and log gf. Once again some of those intense lines were used to identify spectral lines of Cu V in RE0503-289, as shown in section 4.1.3.1. Those data could therefore also be used to identify Cu V lines in other stellar spectra.

The case of Cu VI is particularly interesting because it is the only ion for which we found gA values in the literature. In our calculations, we once again imposed the log gf $\geq$ -6 and log gf $\geq$ -1 criteria and it led to respectively 3797 and 421 transitions. Those 421 most intense transitions are listed in Table A9 where the energies given are the experimental ones in cm^{-1}. Exactly as for the two previous ions, those intense lines have been used to identify lines of Cu VI in the spectrum of RE0503-289.

In their paper, Aggarwal *et al.* [106] performed a calculation using the quasi-relativistic (QR) approximation. This QR approximation is an Hartree-Fock calculation with the relativistic effects included using the Breit-Pauli approximation. To include the correlation, all one- and two-electron promotions of interest are considered in a large CI wavefunction expansion. If we compare these latter results with ours, we find an overall good agreement in particular for the strongest lines (log $gf > -1$), for which the mean deviation between the two sets of data was found to be about 20%, with a general tendency such that our log gf values appear systematically slightly higher than those of Aggarwal *et al.*, as shown in Figure 4.1. This could be explained by the fact that core-core correlations have been taken into account in their calculation thanks to the very large configuration interaction expansion. Nevertheless, the overall good agreement between the two calculations, especially for the strongest transitions, reinforces our results within a margin of error of about twenty percent.

Finally, for the last copper ion we treated in this work, namely Cu VII, the log gf $\geq$ -6 and log gf $\geq$ -1 criteria gave rise to 2253 and 284 transitions, respectively. Those 284 most intense transitions in Cu VII are given in Table A12 where, once again, the energies are the experimental ones given in cm^{-1}. Exactly as for the other copper ions, those transitions were used to identify spectral lines in RE0503-289 and could be used to identify copper lines in other stars.

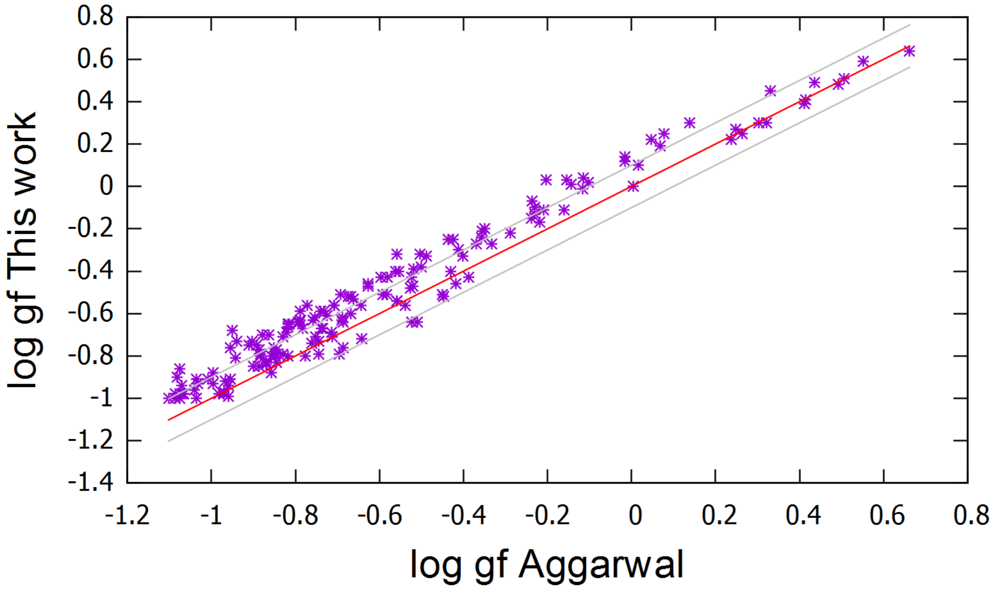

Figure 4.1: Comparison between the log gf values obtained in this work and the ones of [106] for the Cu VI ion, The red line represents the equality between the gf-values obtained in this work and the ones of [106].

4.1.3.1 Application of Our New Atomic Data to the Spectral Analysis of Hot White Dwarfs

Our calculation led to the detection of many Cu IV-VII lines in the spectrum of RE0503-289 (see [77]). As shown in Figure 4.2. 54 Cu lines were identified (1 of Cu IV, 51 of

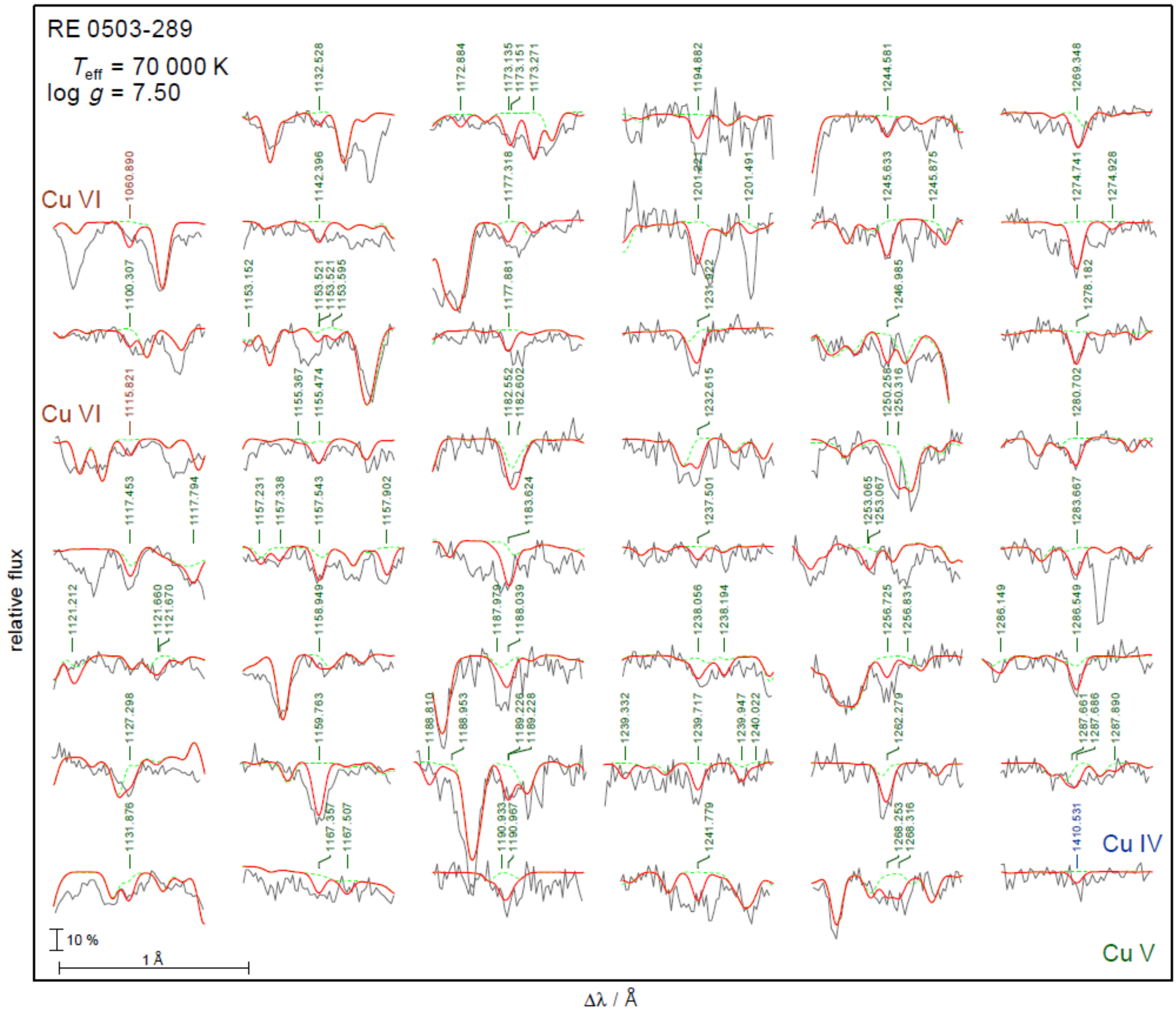

Figure 4.2: Prominent Cu lines in the observation (gray line) of RE 0503-289. Synthetic Spectra are given in red.

Cu V, and 2 of Cu VI). Detailed line-profile comparison of the Tübingen NLTE stellar atmosphere model (i.e. an effective temperature of T_{eff} =70 000K and a surface gravity[3] log g =7.5 in this case) with the UV observations[4] from the FUSE (Far Ultraviolet Spectroscopic Explorer) and the HST (Hubble Space Telescope), led to the determination of Cu abundance of $9.3^{+3.0}_{-2.0} \times 10^{-5}$ mass fraction (132 times the solar one!).

The uncertainty is determined through the T_{eff} error propagation by the evaluation from two models at the error limits with the highest and the lowest degree of ionization, (i.e. T_{eff} =72 000K and log g =7.4 and T_{eff} =68 000K and log g =7.6), respectively.

The abundance error is found smaller than 0.1 dex and the final mass fraction is adopted with uncertainties of 0.2 dex.

[3] g is the surface gravity.

[4] The spectra are described in Rauch *et al.* [107] and Hoyer *et al.* [108].

A similar analysis has been performed in the case of the spectrum of another white dwarf: G191-B2B. The four strongest Cu V lines in the synthetic spectrum are identified as highlighted in Figure 4.3.

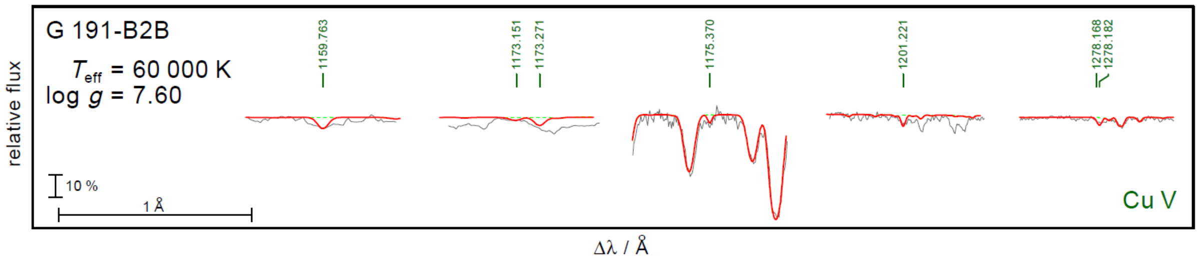

Figure 4.3: Prominent Cu lines in the observation (gray line) of G191-B2B. Synthetic Spectra are given in red.

They are well reproduced by a model (T_{eff} =60 000K, log g =7.6) with a Cu mass fraction of $6.3^{+3.0}_{-2.0} \times 10^{-6}$ (nine times the solar one). The error estimation is performed analogously to the one of RE 0503-289 and the same uncertainty of 0.2 dex was found.

4.2 In IV - VII

Indium has an atomic number of Z = 49 and is a very rare element on Earth. It is named after its supposed indigo-like color (*indicum* in classical Latin and *indium* in medieval Latin) when put through a flame. This color is actually explained by an intense dark blue line and a weaker violet line in its atomic visible spectrum. It was discovered by Ferdinand Reich and Hieronimus Theodor Richter in 1863 [109].

4.2.1 Models Used

In this work, we obtained new sets of oscillator strengths and transition probabilities using the pseudo-relativistic Hartree-Fock (HFR + CPOL) approach combined with a semi-empirical least-squares fitting procedure of radial energy parameters. Many electron correlations were considered by means of extended multiconfiguration expansions which were included in the physical models. Those expansions were chosen in order to include low-lying configurations, for which energy levels are experimentally known, together with some higher configurations with larger configuration interactions.The core-polarization effects were modeled using a core-polarization potential (see section 2.2).

More precisely, in In IV, the configuration interaction was explicitly considered among the configurations $4d^{10}$, $4d^95s$, $4d^96s$, $4d^97s$, $4d^98s$, $4d^95d$, $4d^96d$, $4d^97d$, $4d^85s^2$, $4d^85p^2$, $4d^85s5d$ in the even parity and $4d^95p$, $4d^96p$, $4d^97p$, $4d^94f$, $4d^95f$, $4d^96f$, $4d^97f$, $4d^85s5p$, $4d^85s6p$, $4d^85s5f$ in the odd one. Using the experimental data of Swapnil and Tauheed [32] and Ryabtsev and kononov [33], the radial parameters (average energies, Slater integrals, spin-orbit parameters and effective interaction parameters) of $4d^{10}$, $4d^95s$, $4d^96s$, $4d^97s$, $4d^98s$, $4d^95d$, $4d^96d$, $4d^97d$, $4d^85s^2$ in the even parity and $4d^95p$, $4d^96p$, $4d^97p$, $4d^94f$, $4d^95f$, $4d^85s5p$ in the odd parity were optimized during the fitting procedure. The mean deviations between calculated and experimental energy levels were 68 cm^{-1} (66 levels) in the even parity and 194 cm^{-1} (222 levels) in the odd parity. Concerning the latter, only 103 of 135 known levels were included in the calculation due to an energy cut-off at 395 000 cm^{-1} made because unambiguous identification was not possible for higher energy levels. α_d was chosen to be 2.02 a.u., as tabulated by Fraga *et al.* [94] for an In VI core and r_c was considered to be 1.11 a.u., which corresponds to the mean radius of the 4d orbital. The theoretical energy levels were compared to the experimental ones and the good agreement between the two sets can be seen in Tables A13 and A14 for the even and the odd parity respectively.

When it came to In V, the interacting configurations were $4d^9$, $4d^85s$, $4d^86s$, $4d^85d$, $4d^86d$, $4d^75s^2$, $4d^75p^2$, $4d^75d^2$, $4d^75s5d$ in the even parity and $4d^85p$, $4d^86p$, $4d^87p$, $4d^84f$, $4d^85f$, $4d^86f$, $4d^87f$, $4d^75s5p$, $4d^75s6p$, $4d^7$ in the odd one. In the even parity, the radial integrals corresponding to $4d^9$, $4d^85s$, $4d^86s$, $4d^85d$ and $4d^75s^2$ were adjusted to minimize the differences between the calculated Hamiltonian eigenvalues and the experimental energy levels taken from Swapnil and Tauheed [34] and Ryabtsev [35]. In this process, we found a mean deviation equal to 451 cm^{-1} (90 levels). The same procedure for $4d^85p$, $4d^86p$, $4d^87p$, $4d^84f$, $4d^85f$ and $4d^75s5p$ (158 levels) led to a mean deviation of 373 cm^{-1} in the odd parity. We chose α_d equals to 1.62 a.u. as tabulated in [94] for an In VII core and the value of r_c was 1.07 a.u., which corresponds to the HFR mean radius of the 4d orbital. The energy levels of In V are displayed in Tables A16 and A17 (for the even and the odd parity, respectively).

In the case of In VI, the configurations included in our HFR model were $4d^8$, $4d^75s$, $4d^76s$, $4d^75d$, $4d^76d$, $4d^65s^2$,$4d^65p^2$, $4d^65d^2$, $4d^65s5d$ and $4d^75p$, 4d76p, $4d^74f$, $4d^75f$, $4d^65s5p$, $4d^65ps6p$, $4d^65s5f$ for respectively the even and odd parity. The experimental data from [36] and [37] were used for the fitting procedure in order to optimize the radial parameters for the $4d^8$, $4d^7 5s$,$4d^6 5s^2$ and $4d^7 5p$, $4d^7 6p$, $4d^7 4f$ configurations. The mean deviations were found to be 88 cm^{-1} (46 levels) in the even parity and 435 cm^{-1} (194 levels) in the odd parity. For In IV, α_d was considered to be equal to 1.28 a.u. as tabulated by Fraga *et al.* [94] for an In VIII core and r_c taken as 1.04 a.u. which equates to the HFR mean radius of the 4d orbital. The comparison between the calculated and experimental In VI even energy levels is shown in Table A19 and the same comparison for the odd levels is in Table A20.

Finally, pertaining to In VII, we included the $4d^7$, $4d^6 5s$, $4d^6 6s$, $4d^6 5d$, $4d^6 6d$, $4d^5 5s^2$, $4d^5 5p^2$, $4d^5 5d^2$ and $4d^8 5s5d$ configurations for the even parity and $4d^6 5p$, $4d^6 6p$, $4d^6 4f$, $4d^6 5f$, $4d^5 5s5p$,$4d^5 5p6p$ and $4d^5 5s5f$ for the odd one. The radial parameters were respectively fitted for $4d^7$ and $4d^6 5p$. We respectively obtained a mean deviation of 87 cm^{-1} (17 levels) and of 202 cm^{-1} (131 levels) from experimental data of Ryabtsev *et al.* [38]. Finally, the polarization parameters were taken as $\alpha_d = 1.01$ a.u. (from Fraga [94] for an In IX core) and $r_c = 1.02$ a.u. (HFR mean radius of the 4d orbital). Those very good agreements between experimental and calculated energy levels are shown in Tables A22 and A23 for the even and the odd parity levels of In VII.

4.2.2 Atomic Radial Parameters

The values of the *ab initio* and fitted parameters for the even parity of In IV are given in Table 4.5. As one can see, many parameters for all the configurations with known experimental levels were fitted. The values of the *ab initio* and fitted parameters for the odd parity of In IV are given in Table 4.6.

In Table 4.7, the letter means that the variation of the parameters with the same letter (a,b or c) has been linked and thus forced to undergo a proportional modification during the fitting procedure. The α and β parameters of $4d^8 6s$ have been given as initial values identical to those obtained for the $4d^8 5s$ after a first use of the fitting procedure for the latter configuration. As one can see in that table, the fitting procedure in $4d^8 6s$ barely changes those values.

In Table 4.8, the letter code is the same as in the previous one. The α and β parameters are fixed alongside a Rydberg serie. Thus, the α,β were fitted for $4d^8 5p$ and $4d^8 4f$ and the same values were considered for $4d^8 np$ and $4d^8 nf$.

The values of the *ab initio* and fitted parameters for the even parity of In VI can be found in Table 4.9. In Table 4.10, the letter code is the same as in the previous tables. The α and β parameters of $4d^7 6p$ are considered as the same as in $4d^7 5p$. In table 4.11 the letter code is the same as in the previous tables. In the case of In VII, because there is only one configuration for each parity, both parities are depicted in the same table.

Table 4.5: Radial parameters for the even parity in In IV

Configuration	Parameter	HFR (cm^{-1})	Fitted (cm^{-1})	Ratio
$4d^{10}$	E_{av}	2984.1	2998.0	
$4d^9 5s$	E_{av}	136239.9	134625.6	
	ζ_{4d}	2740.5	2842.8	1.037
	$G^2(4d,5s)$	13512.6	13361.6	0.989
$4d^9 6s$	E_{av}	301143.3	301922.5	
	ζ_{4d}	2771.5	2855.6	1.029
	$G^2(4d,6s)$	2859.5	2846.2	0.995
$4d^9 7s$	E_{av}	362597.5	364033.8	
	ζ_{4d}	2777.5	2869.4	1.033
	$G^2(4d,7s)$	1156.1	1083.8	0.937
$4d^9 8s$	E_{av}	392667.1	394167.1	
	ζ_{4d}	2779.6	Fixed	
	$G^2(4d,8s)$	594.7	Fixed	
$4d^9 5d$	E_{av}	291735.9	294717.2	
	ζ_{4d}	2772.3	2834.3	1.022
	ζ_{5d}	216.6	277.0	1.278
	$F^2(4d,5d)$	12313.7	12228.3	0.993
	$F^4(4d,5d)$	5086.8	4947.1	0.972
	$G^0(4d,5d)$	2881.4	2613.9	0.907
	$G^2(4d,5d)$	3430.0	2785.0	0.811
	$G^4(4d,5d)$	2760.4	2687.9	0.973
$4d^9 6d$	E_{av}	359682.9	361295.1	
	ζ_{4d}	2777.8	2865.9	1.031
	ζ_{6d}	96.2	118.8	1.234
	$F^2(4d,6d)$	4734.7	4911.8	1.037
	$F^4(4d,6d)$	1989.9	1898.4	0.954
	$G^0(4d,6d)$	1126.8	907.4	0.805
	$G^2(4d,6d)$	1398.3	1516.1	1.084
	$G^4(4d,6d)$	1148.1	1391.2	1.212
$4d^9 7d$	E_{av}	391322.6	394322.6	
	ζ_{4d}	2779.8	Fixed	
	ζ_{7d}	51.8	Fixed	
	$F^2(4d,7d)$	2384.1	Fixed	
	$F^4(4d,7d)$	1025.4	Fixed	
	$G^0(4d,7d)$	574.3	Fixed	
	$G^2(4d,7d)$	725.6	Fixed	
	$G^4(4d,7d)$	601.0	Fixed	
$4d^8 5s^2$	E_{av}	300454.6	296791.9	
	$F^2(4d,4d)$	83410.2	69061.7	0.827
	$F^4(4d,4d)$	55223.9	42410.2	0.768
	α	0.0	-16.8	
	β	0.0	2667.6	
	ζ_{4d}	2876.5	Fixed	

66 levels included - mean deviation: 68 cm^{-1}

Table 4.6: Radial parameters for the odd parity in In IV

Configuration	Parameter	HFR (cm^{-1})	Fitted (cm^{-1})	Ratio
$4d^95p$	E_{av}	205646.4	204851.6	
	ζ_{4d}	2753.9	2853.7	1.036
	ζ_{5p}	3529.9	4140.1	1.172
	$F^2(4d,5p)$	24098.2	22577.7	0.937
	$G^1(4d,5p)$	8139.8	8059.9	0.990
	$G^3(4d,5p)$	7311.2	7694.3	1.052
$4d^96p$	E_{av}	325981.6	326545.3	
	ζ_{4d}	2773.5	2833.0	1.021
	ζ_{6p}	1244.5	1346.3	1.082
	$F^2(4d,6p)$	7524.1	6969.1	0.925
	$G^1(4d,6p)$	2132.2	1864.8	0.874
	$G^3(4d,6p)$	2085.2	1852.1	0.888
$4d^97p$	E_{av}	374562.0	375429.4	
	ζ_{4d}	2778.1	Fixed	
	ζ_{7p}	593.6	Fixed	
	$F^2(4d,7p)$	3354.6	Fixed	
	$G^1(4d,7p)$	928.2	Fixed	
	$G^3(4d,7p)$	930.6	Fixed	
$4d^94f$	E_{av}	333884.8	335095.5	
	ζ_{4d}	2772.5	2799.8	1.010
	ζ_{4f}	5.7	5.7	1.000
	$F^2(4d,4f)$	12411.5	12074.1	0.972
	$F^4(4d,4f)$	5486.3	5979.1	1.089
	$G^1(4d,4f)$	8503.7	7354.2	0.865^a
	$G^3(4d,4f)$	4886.9	4226.2	0.865^a
	$G^5(4d,4f)$	3341.3	2889.6	0.865^a
$4d^95f$	E_{av}	376284.5	377106.6	1.002
	ζ_{4d}	2774.8	Fixed	
	ζ_{5f}	4.7	Fixed	
	$F^2(4d,5f)$	7149.7	Fixed	
	$F^4(4d,5f)$	3614.7	Fixed	
	$G^1(4d,5f)$	6282.8	Fixed	
	$G^3(4d,5f)$	3675.0	Fixed	
	$G^5(4d,5f)$	2528.9	Fixed	
$4d^85s5p$	E_{av}	364119.1	363264.0	
	$F^2(4d,4d)$	83659.1	72948.5	0.871^b
	$F^4(4d,4d)$	55410.8	48316.8	0.871^b
	α	0.0	64.6	
	β	0.0	592.8	
	ζ_{4d}	2888.6	3126.2	1.08^c
	ζ_{5p}	4041.1	4373.5	1.08^c
	$F^2(4d,5p)$	25645.5	26182.0	1.020
	$G^1(4d,5s)$	13640.8	14018.3	1.027
	$G^1(4d,5p)$	8465.5	7213.6	0.851^d
	$G^3(4d,5p)$	7736.4	6592.3	0.851^d
	$G^1(5s,5p)$	51330.7	43739.7	0.851^d

a,b,c,d: Ratio linked during the fitting procedure.
103 levels included - mean deviation: 194 cm^{-1}

Table 4.7: Radial parameters for the even parity in In V

Configuration	Parameter	HFR (cm^{-1})	Fitted (cm^{-1})	Ratio
$4d^9$	E_{av}	4962.9	5065.0	
	ζ_{4d}	2782.0	2870.5	1.031
$4d^85s$	E_{av}	180844.6	178887.0	
	$F^2(4d,4d)$	84257.3	78258.7	0.928
	$F^4(4d,4d)$	55857.6	54905.9	0.983
	α	0.0	49.0	
	β	0.0	-596.0	
	ζ_{4d}	2916.2	3014.8	1.034
	$G^1(4d,5s)$	14296.8	14299.2	1.000
$4d^86s$	E_{av}	388421.1	395010.5	0.983
	$F^2(4d,4d)$	84965.4	85965.4	1.012
	$F^4(4d,4d)$	56388.7	57388.7	1.017
	α	0.0	49.2	
	β	0.0	-599.2	
	ζ_{4d}	2949.6	Fixed	
	$G^1(4d,6s)$	3268.8	Fixed	
$4d^85d$	E_{av}	365891.7	368052.0	
	$F^2(4d,4d)$	84939.0	75125.7	0.884[a]
	$F^4(4d,4d)$	56370.1	49857.4	0.884[a]
	α	0.0	-36.5	
	β	0.0	1938.1	
	ζ_{4d}	2948.7	3076.1	1.042[b]
	ζ_{5d}	326.6	340.6	1.042[b]
	$F^2(4d,5d)$	16071.9	15919.6	0.990[c]
	$F^4(4d,5d)$	7026.1	6959.6	0.990[c]
	$G^0(4d,5d)$	3892.0	3104.4	0.797[d]
	$G^2(4d,5d)$	4697.5	3746.8	0.797[d]
	$G^4(4d,5d)$	3832.3	3056.8	0.797[d]
$4d^75s^2$	E_{av}	388424.2	384730.4	1.010
	$F^2(4d,4d)$	86191.9	85051.1	0.987
	$F^4(4d,4d)$	57284.0	58881.3	1.027
	α	0.0	150.3	
	β	0.0	1813.3	
	ζ_{4d}	3052.5	Fixed	

a,b,c,d: Ratio linked during the fitting procedure

95 levels included - mean deviation: 451 cm^{-1}

Table 4.8: Radial parameters for the odd parity in In V

Configuration	Parameter	HFR (cm^{-1})	Fitted (cm^{-1})	Ratio
$4d^8 5p$	E_{av}	260182.2	259468.6	
	$F^2(4d,4d)$	84506.5	77843.3	0.920
	$F^4(4d,4d)$	56044.9	55024.1	0.981
	α	0.0	41.2	
	β	0.0	-353.0	
	ζ_{4d}	2929.0	3020.0	1.030
	ζ_{5p}	4567.6	5185.4	1.135
	$F^2(4d,5p)$	27605.4	26629.3	0.964
	$G^1(4d,5p)$	9111.4	8957.3	0.964
	$G^3(4d,5p)$	8422.0	8495.4	1.009
$4d^8 6p$	E_{av}	418587.4	418740.1	
	$F^2(4d,4d)$	84995.9	76037.8	0.894
	$F^4(4d,4d)$	56411.3	65434.5	1.160
	α	0.0	41.2	
	β	0.0	-353.0	
	ζ_{4d}	2951.6	3468.7	1.175
	ζ_{6p}	1721.7	1392.8	0.809
	$F^2(4d,6p)$	9275.0	9861.3	1.062
	$G^1(4d,6p)$	2503.4	2100.6	0.836^a
	$G^3(4d,6p)$	2529.2	2111.9	0.836^a
$4d^8 7p$	E_{av}	485669.6	485141.6	
	$F^2(4d,4d)$	85100.5	77100.5	0.905
	$F^4(4d,4d)$	56485.9	56489.5	1.001
	α	0.0	41.2	
	β	0.0	-353.0	
	ζ_{4d}	2957.3	Fixed	
	ζ_{7p}	847.6	Fixed	
	$F^2(4d,7p)$	4267.5	Fixed	
	$G^1(4d,7p)$	1113.5	Fixed	
	$G^3(4d,7p)$	1155.6	Fixed	
$4d^8 4f$	E_{av}	403399.5	403653.3	
	$F^2(4d,4d)$	84561.4	77610.9	0.934^b
	$F^4(4d,4d)$	56084.0	53436.0	0.934^b
	α	0.0	83.2	
	β	0.0	-1092.4	
	ζ_{4d}	2932.2	3113.5	1.061^c
	ζ_{4f}	22.6	24.0	1.061^c
	$F^2(4d,4f)$	27339.6	26902.1	0.984
	$F^4(4d,4f)$	14698.4	14631.3	0.995
	$G^1(4d,4f)$	25856.8	26067.0	1.008^d
	$G^3(4d,4f)$	15175.8	15299.1	1.008^d
	$G^5(4d,4f)$	10456.9	10541.9	1.008^d

Table 4.8: continued

Configuration	Parameter	HFR (cm^{-1})	Fitted (cm^{-1})	Ratio
$4d^85f$	E_{av}	473161.3	473548.4	
	$F^2(4d,4d)$	84857.1	80173.9	0.945
	$F^4(4d,4d)$	56306.8	56423.1	1.002
	α	0.0	83.2	
	β	0.0	-1092.4	
	ζ_{4d}	2944.4	3220.8	1 1.091^e
	ζ_{5f}	16.7	18.2	1.091^e
	$F^2(4d,5f)$	13617.8	12319.0	0.904^f
	$F^4(4d,5f)$	7751.0	7011.7	0.904^f
	$G^1(4d,5f)$	14324.3	14050.5	0.981^g
	$G^3(4d,5f)$	8688.7	8522.6	0.981^g
	$G^5(4d,5f)$	6061.7	Fixed	
$4d^86f$	E_{av}	512579.0	504639.6	

a,b,c,d,e,f,g: Linked parameters during the fitting procedure.
158 levels included - mean deviation: 373 cm^{-1}

Table 4.9: Radial parameters for the even parity in In VI

Configuration	Parameter	HFR (cm^{-1})	Fitted (cm^{-1})	Ratio
$4d^8$	E_{av}	16986.4	16293.8	
	$F^2(4d,4d)$	85189.9	79824.0	0.937
	$F^4(4d,4d)$	56556.2	55741.1	0.985
	α	0.0	45.8	
	β	0.0	-598.2	
	ζ_{4d}	2962.4	3060.2	1.033
$4d^75s$	E_{av}	237263.3	233884.7	
	$F^2(4d,4d)$	87035.9	81079.2	0.931
	$F^4(4d,4d)$	57917.7	57825.6	0.998
	α	0.0	47.4	
	β	0.0	-596.7	
	ζ_{4d}	3097.0	3197.5	1.031
	$G^2(4d,5s)$	14928.8	14805.3	0.992

47 levels included - mean deviation: 88 cm^{-1}

Table 4.10: Radial parameters for the odd parity in In VI

Configuration	Parameter	HFR (cm^{-1})	Fitted (cm^{-1})	Ratio
$4d^7 5p$	E_{av}	324553.5	323877.8	
	$F^2(4d,4d)$	87251.0	80920.0	0.927
	$F^4(4d,4d)$	58079.8	57202.2	0.985
	α	0.0	49.0	
	β	0.0	-481.1	
	ζ_{4d}	3109.2	3208.7	1.031
	ζ_{5p}	5618.2	6348.8	1.129
	$F^2(4d,5p)$	30715.7	29801.4	0.969
	$G^1(4d,5p)$	9918.4	9805.9	0.989
	$G^3(4d,5p)$	9380.9	8905.1	0.949
$4d^7 6p$	E_{av}	522135.4	523284.2	
	$F^2(4d,4d)$	87739.1	83428.5	0.950
	$F^4(4d,4d)$	58446.7	42408.0	0.725
	α	0.0	49.0	
	β	0.0	-481.1	
	ζ_{4d}	3134.5	Fixed	
	ζ_{6p}	2232.5	Fixed	
	$F^2(4d,6p)$	10945.7	10421.8	0.952
	$G^1(4d,6p)$	2836.4	Fixed	
	$G^3(4d,6p)$	2937.7	Fixed	
$4d^7 4f$	E_{av}	466128.9	465755.9	
	$F^2(4d,4d)$	86905.1	82713.4	0.951
	$F^4(4d,4d)$	57818.7	51789.0	0.896
	α	0.0	-64.2	
	β	0.0	2273.2	
	ζ_{4d}	3088.5	3597.2	1.164
	ζ_{4f}	54.7	51.5	0.941
	$F^2(4d,4f)$	44008.9	48334.9	1.098
	$F^4(4d,4f)$	25924.5	26185.5	1.010
	$G^1(4d,4f)$	47857.7	43367.9	0.905^a
	$G^3(4d,4f)$	28615.0	25930.5	0.905^a
	$G^5(4d,4f)$	19858.5	17995.5	0.905^a

a: Linked parameters during the fitting procedure

185 levels included - mean deviation: 435 cm^{-1}

Table 4.11: Radial parameters for the even and odd parities in In VII

Configuration	Parameter	HFR (cm^{-1})	Fitted (cm^{-1})	Ratio
Even Parity				
$4d^7$	E_{av}	25640.4	28484.5	
	$F^2(4d,4d)$	73289.7	87947.6	1.200^a
	$F^4(4d,4d)$	48835.5	58602.7	1.200^a
	α	0.0	39.3	
	β	0.0	-476.1	
	ζ_{4d}	3147.5	3242.7	1.029
Odd Parity				
$4d^65p$	E_{av}	384640.4	390251.0	
	$F^2(4d,4d)$	74866.5	83466.0	1.114
	$F^4(4d,4d)$	50001.8	59330.9	1.186
	α	0.0	44.9	
	β	0.0	-376.9	
	ζ_{4d}	3294.4	3410.8	1.035
	ζ_{5p}	6677.4	7457.0	1.117
	$F^2(4d,5p)$	27943.4	32758.3	1.172^b
	$G^1(4d,5p)$	8844.5	10363.8	1.172^b
	$G^3(4d,5p)$	8523.4	10285.3	1.172^b

a,b: Linked parameters during the fitting procedure.
Even Parity: 17 levels (mean deviation: 87 cm^{-1})
Odd Parity: 131 levels (mean deviation: 202 cm^{-1})

4.2.3 Radiative Transition Rates

Once again, for a better readability of the manuscript, the tables showing the radiative transition rates for the indium ions will be placed in the appendices. Indeed, we initially selected the transitions for which log gf was $\geq$ -4, which lead to (tenth of) thousands of transitions. We therefore decided to restrict ourselves and impose the condition log $gf \geq$ -1 corresponding to the most intense and reliable transitions ($CF > 0.05$). The energy levels given in those tables are taken from the NIST database [28].

The Table A15 shows those most intense transitions in In IV. With the log $gf \geq$ -1 condition this led to 458 intense transitions (shown in Table A15) that could be used by the astrophysicists to identify new In IV lines in stellar spectra. We also sent the astrophysicists a list with the transitions with a log $gf \geq$ -4 (2710 transitions) but obviously these less intense transitions ($-4 <$ log $gf < -1$) are much less likely to be observed in astrophysical spectra. However, they are used to flesh out the NLTE models built to identify new spectral lines.

When it comes to In V, once again, even though some transitions have been measured experimentally, there is no experimental comparison point in the literature for gf and gA values. If we apply the same criteria as for In IV on the log gf, the condition log $gf \geq$ -1 gives rise to 840 transitions listed in Table A18. Once again, the energy levels mentioned in this table are taken from the NIST data base. Exactly as for In IV, we provided the astrophysicists with a list even bigger with the transitions having a log $gf \geq$ -4, which represents 5895 transitions in this case.

If we look through the literature, it turns out that other HFR calculations have already been carried out in In IV. The first one by Swapnil and Tauheed [32] and the second one by Ryabtsev and Kononov [33]. In the former calculation [32], they included fewer configurations (21) than we did (22) and they did not include core-polarization effects. Regarding the calculations of [33], they included a few more configurations (29) but did not include the core polarization corrections either. In both cases, our calculation is the only one to include the core polarization corrections. If we compare the reproduction of the energy levels, with regard to the odd parity, the three calculations give quite similar results with a mean deviation around 150 cm^{-1} (respectively 194, 177 and 140 cm^{-1}) but in the even parity, our calculation is much closer with 68 cm^{-1} in comparison with 133 cm^{-1} for Swapnil ad Tauheed and 97 cm^{-1} for Ryabtsev and Kononov. Therefore, even if the mean deviation is slightly worse for odd parity, the fact that it is much better for even parity and that we added the core polarization corrections brings a real added value. Especially since the higher deviation in the odd parity comes from very high energy levels.

If we compare the gA for the most intense transitions in our calculation and in the one of Swapnil and Tauheed, we realize, as shown in Figure 4.4, that our values are systematically slightly lower than theirs. This effect is due to the addition of the core polarization corrections, which generally lower the gA as shown in many works before (e.g. [82]). The figure shows that in a [32] against our work graph, the vast majority of the data is, as expected, above the red line representing the equality between our calculations and the one of Swapnil and Tauheed.

If we make the same kind of comparison between our data and those of [33], we notice that the systematics is not as obvious as it was when we compared it to [32]. This is shown in Figure 4.5. We can even see on that figure that in fact, the values are quite close to each other. This comes from the fact that in their calculations, they have introduced configurations with incomplete 4p subshells (4p^5) which is indeed considered in our calculation as core-valence interaction and which is therefore also included, but via the core polarization potential. This also explains why they have included more configurations in their model than we have. Their calculation takes into account a part of the core-valence interactions, probably the most important ones, and this is why their results are closer to ours than the calculation of [32] without the core-valence interactions. Nevertheless, the values are slightly different because, contrary to them who only consider some interactions, we model all of them with our core polarization potential.

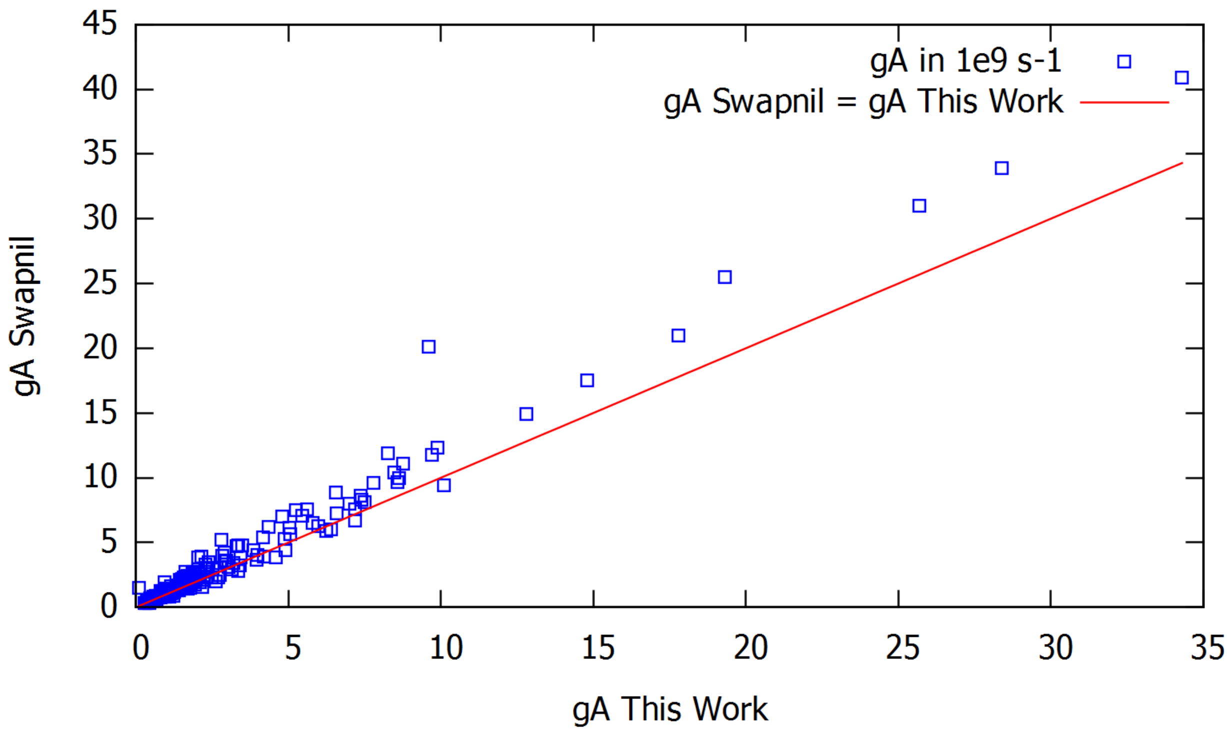

Figure 4.4: Comparison between the gA (in 10^9 s^{-1}) obtained in this work for In IV most intense transitions and the ones of [32]. The straight line of equality is drawn in red.

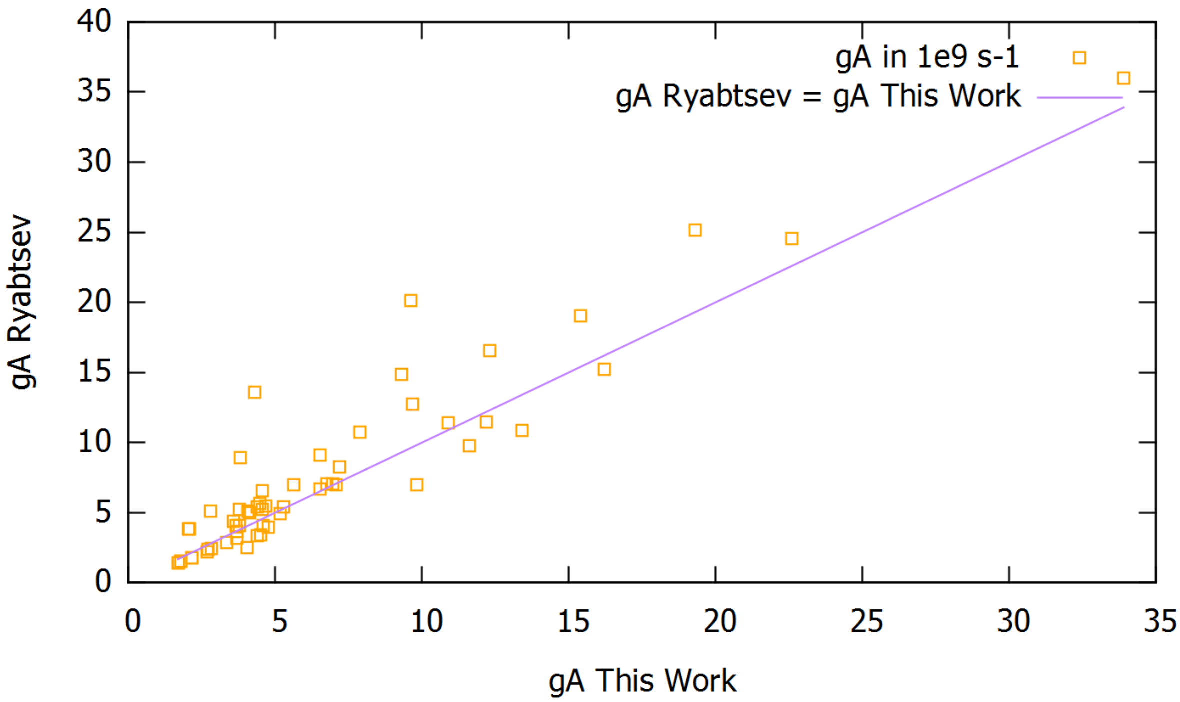

Figure 4.5: Comparison between the gA (in 10^9 s^{-1}) obtained in this work for In IV most intense transitions and the ones of [33]. The straight line of equality is drawn in purple.

The second ion we worked on is In V. For this ion, we obtained 5895 transitions with log $gf \geq$ -4 and 840 with log $gf \geq$ -1, which can be found in Table A18. The only comparison that we found in the literature for those intense transitions was with the atomic data from Swapnil and Tauheed [34]. Exactly as for In IV, they considered a bit less configurations (20) than we did (22) and they did not include core-polarization effects. The comparison between our calculations and theirs is shown in Figure 4.6. Exactly as for In IV, the gA values from our calculations with the core-polarization effects taken into account are systematically lower than theirs without it. This effect is all but surprising as it was already discussed for In IV and in section 3.2.

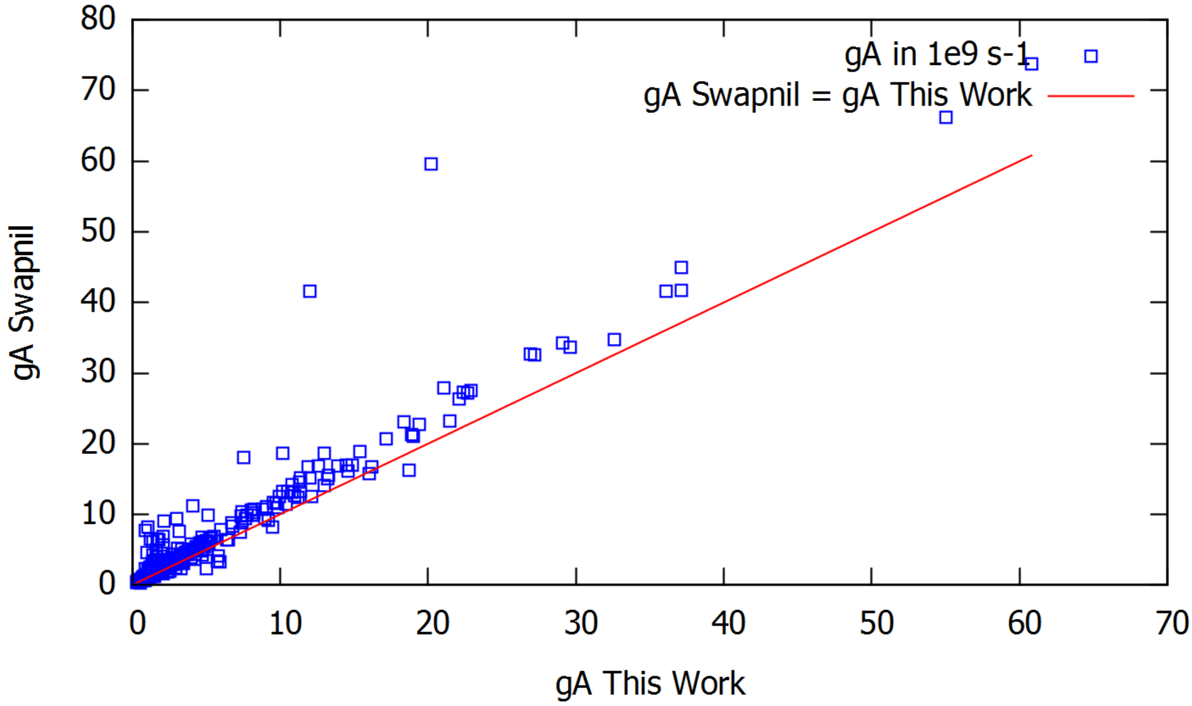

Figure 4.6: Comparison between the gA (in 10^9 s^{-1}) obtained in this work for In V most intense transitions and the ones of [34]. The straight line of equality is drawn in red.

The third ion treated in this section is In VI. The log $gf \geq$ -4 criterion produced 2265 transitions and the selection of the most intense ones with log $gf \geq$ -1 restricted this list to the 458 transitions that can be found in Table A21. There are few data concerning the transition rates of In VI in the literature. In their study, Ryabtsev *et al.* [37] produced some but there are too few comparison points between their rates and ours to draw a conclusion. The two data sets can thus be seen as complementary for astrophysicists to hope to identify lines of In VI in stellar spectra.

The fourth and last ion treated was In VII. We obtained 1072 transitions with log $gf \geq$ -4 and 255 more intense ones with log $gf \geq$ -1. Those transitions are listed in Table A24. There is, to our knowledge, no existing data in the literature about In VII transitions probabilities and oscillator strength. Our atomic data is therefore the first one produced in that ion. However, the method of calculation having proved itself reliable and the model being similar to that used for the other indium ions for which there were points of comparison allow us to be confident about the quality of this data.

4.2.3.1 Application of the new atomic data in Indium ions to the spectral analysis of hot white dwarfs

Using the less complete existing literature (see the previous subsection), our colleagues at the University of Tübingen already highlighted five In V lines in the spectrum of RE0503-289 as shown in Figure 4.7 while no In line could be identified in the UV observation of G191-B2B using the previously existing data.

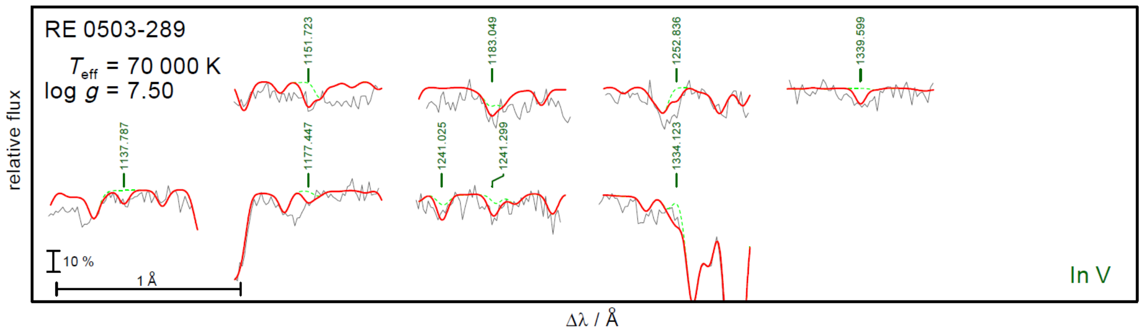

Figure 4.7: In V lines in the spectrum of RE0503-289

This led to the determination (using the same method as the one described in section 4.1.3.1) of an In mass fraction of $3.0 \pm 0.5 \times 10^{-6}$ (56 600 times the In solar mass fraction) with an uncertainty of 0.2 dex.

This strongly fueled the motivation to undertake calculations in the Indium ions as lines of at least one of them had already been observed.

The data presented above are currently being analyzed in Tübingen and we hope that they will lead soon to the identification of many other indium lines in RE0503-289 and in G191-B2B as was the case for copper. Those new identifications could hopefully lead to a refinement of the mass fraction given here above.

4.3 Cs IV-VII

Caesium, Z = 55, was named after the Latin word *caesius* (sky blue), due to the blue color light of the two characteristic lines of its visible emission spectrum. This element was first detected in 1860 by Robert Wilhelm Bunsen and Gustav Robert Kirchhoff from the spectroscopy of Dürkheim's mineral water, made with the spectroscope they had developed in 1859 (a few months later, they discovered rubidium in the same way) [109].

4.3.1 Models Used

We started with the case of Cs IV for which we considered the configuration interaction explicitly among the following configurations: $5s^2\,5p^4$, $5s^2\,5p^3\,6p$, $5s^2\,5p^3\,7p$, $5s^2\,5p^3\,8p$, $5s^2\,5p^3\,4f$, $5s^2\,5p^3\,5f$, $5s^2\,5p^3\,6f$, $5s^2\,5p^2\,5d\,6s$, $5s^2\,5p^2\,5d\,6d$, $5s^2\,5p^2\,6s^2$, $5s^2\,5p^2\,5d^2$, $5s^2\,5p^2\,6d^2$, $5s^2\,5p^2\,4f^2$, $5s\,5p^4\,6s$, $5s\,5p^4\,5d$, $5s\,5p^4\,6d$, $5s\,5p^4\,7d$, $5s\,5p^3\,5d\,4f$ and $5p^6$ for the even parity and $5s\,5p^5$, $5s^2\,5p^3\,5d$, $5s^2\,5p^3\,6d$, $5s^2\,5p^3\,7d$, $5s^2\,5p^3\,6s$, $5s^2\,5p^3\,7s$, $5s^2\,5p^3\,8s$, $5s^2\,5p^3\,9s$, $5s^2\,5p^3\,5g$, $5s^2\,5p^3\,6g$, $5s^2\,5p^2\,5d\,4f$, $5s^2\,5p^2\,5d\,5f$, $5s^2\,5p^2\,5d\,6f$, $5s\,5p^4\,6p$, $5s\,5p^4\,4f$, $5s\,5p^4\,5f$, $5s\,5p^4\,6f$, $5s\,5p^3\,5d^2$ and $5s\,5p^3\,6d^2$ for the odd one. The radial integrals (the average energy, Slater integrals, spin-orbit parameters and effective interaction parameters) corresponding to $5s^2\,5p^4$ in the even parity and $5s\,5p^5$, $5s^2\,5p^3\,5d$, $5s^2\,5p^3\,6d$, $5s^2\,5p^3\,7d$, $5s^2\,5p^3\,6s$ and $5s^2\,5p^3\,7s$ in the odd one were optimized during the fitting procedure using the experimental energy levels of Sansonetti [39]. That lead to a mean deviation between experimental and calculated levels of 67 cm^{-1} in the even parity (5 levels) and 409 cm^{-1} in the odd one (87 levels) as shown in Table A25 where the main *LS* coupling components (i.e. all those $\geq 5\%$) are given for the fitted levels. The core polarizability, α_d, was chosen to be 0.67 a.u. as tabulated in Fraga *et al.* ([94]) for a Cs X core and r_c was considered to be 0.83 a.u. which is to the HFR mean radius of the outermost core orbital (4d).

When it came to Cs V, the interacting configurations were $5s^2\,5p^3$, $5s^2\,5p^2\,6p$, $5s^2\,5p^2\,4f$, $5s^2\,5p^2\,5f$, $5s^2\,5p^2\,6f$, $5s^2\,5p\,5d\,6s$, $5s^2\,5p\,5d\,6d$, $5s^2\,5p\,6s^2$, $5s^2\,5p\,5d^2$, $5s^2\,5p\,4f^2$, $5s\,5p^3\,6s$, $5s\,5p^3\,5d$, $5s\,5p^3\,6d$, $5s\,5p^2\,4f\,5d$ and $5p^5$ in the odd parity and $5s\,5p^4$, $5s^2\,5p^2\,5d$, $5s^2\,5p^2\,6d$, $5s^2\,5p^2\,6s$, $5s^2\,5p^2\,5g$, $5s^2\,5p^2\,6g$, $5s^2\,5p\,5d\,6p$, $5s^2\,5p\,5d\,4f$, $5s^2\,5p\,5d\,5f$, $5s^2\,5p\,5d\,6f$, $5s\,5p^3\,6p$, $5s\,5p^3\,4f$, $5s\,5p^3\,5f$, $5s\,5p^3\,6f$ and $5s\,5p^2\,5d^2$ in the even one. In the odd parity, the radial integrals corresponding to $5s^2\,5p^3$ were adjusted to minimize the differences between the calculated Hamiltonian eigenvalues and the experimental energy levels taken from [39]. In this process, we found a mean deviations of 274 cm^{-1} (5 levels). The same procedure for $5s\,5p^4$, $5s^2\,5p^2\,5d$ and $5s^2\,5p^2\,6s$ (42 levels) led to a mean deviation of 475 cm^{-1} in the even parity. The comparison between the experimental and calculated energy levels is in Table A27. The core considered was the same as the one for Cs IV with therefore the same α_d. The r_c was considered as the HFR mean radius of the 4d orbitals: 0.83 a.u.

The third ion considered was Cs VI. The configurations included in our HFR model were $5s^2\,5p^2$, $5s^2\,5p\,6p$, $5s^2\,5p\,4f$, $5s^2\,5p\,5f$, $5s^2\,5p\,6f$, $5s^2\,5d\,6s$, $5s^2\,5d\,6d$, $5s^2\,6s^2$, $5s^2\,5d^2$, $5s^2\,4f^2$, $5s^2\,5f^2$, $5s\,5p^2\,6s$, $5s\,5p^2\,5d$, $5s\,5p^2\,6d$, $5s\,5p\,6s\,6p$, $5s\,5p\,6p\,5d$, $5s\,5p\,6p\,6d$, $5s\,5p\,4f\,5d$, $5s\,5p\,4f\,6d$, $5p^4$, $5p^3\,6p$, $5p^3\,4f$, $5p^3\,5f$ and $5p^3\,6f$ in the even parity and $5s\,5p^3$, $5s^2\,5p\,5d$, $5s^2\,5p\,6d$, $5s^2\,5p\,6s$, $5s^2\,5p\,7s$, $5s^2\,5p\,5g$, $5s^2\,5p\,6g$, $5s^2\,5d\,6p$, $5s^2\,5d\,4f$, $5s^2\,5d\,5f$, $5s^2\,5d\,6f$, $5s\,5p^2\,6p$, $5s\,5p^2\,4f$, $5s\,5p^2\,5f$, $5s\,5p^2\,6f$, $5s\,5p\,6s\,5d$, $5s\,5p\,6s\,6d$, $5s\,5p\,5d\,6d$, $5s\,5p\,6s^2$, $5s\,5p\,5d^2$, $5p^3\,6s$, $5p^3\,5d$ and $5p^3\,6d$ in the odd one. Once again, the [39] experimental data were used for the fitting procedure in order to optimize the radial parameters for the $5s^2\,5p^2$,$5s\,5p^3$,$5s^2\,5p\,5d$, and $5s^2\,5p\,6s$ configurations. The mean deviation were found to be 97 cm^{-1} (5 levels) in the even parity and 166 cm^{-1} (25 levels) in the odd one. This very good agreement between the experimental and the calculated energy levels is highlighted in Table A29. The core polarisability was considered equals to 0.67 a.u. (see [94]) and the r_c taken as 0.82 a.u. which is equal to the HFR mean radius of the 4d orbital.

Finally, pertaining to Cs VII, we included in our model the $5s^2\,5p$, $5s^2\,6p$, $5s^2\,7p$, $5s^2\,4f$, $5s^2\,5f$, $5s^2\,6f$, 5s 5p 6s, 5s 5p 7s, 5s 5p 5d, 5s 5p 6d, $5p^3$, $5p^2\,6p$, 5s 5p 5g, 5s 5d 6p, 5s 5d 4f, 5s 5d 5f, 5p 6s 5d, 5p 6s 6d, 5p 5d 6d, $5p\,6s^2$ and $5p\,5d^2$ configurations in the odd parity and $5s\,5p^2$, $5s^2\,5d$, 5s 5p 4f, $5s^2\,6s$, 5s 5p 6p, 5s 5p 5f, 5s 5d 6s, 5s 5d 6d, $5s\,6s^2$, $5s\,5d^2$, $5s\,4f^2$, $5s\,5f^2$, $5p^2\,6s$, $5s^2\,7s$, $5s^2\,6d$, $5s^2\,5g$, $5p^2\,5d$, $5p^2\,6d$ and 5p 6s 6p in the even one. The radial parameters were respectively fitted for $5s^2\,5p$, $5s^2\,6p$, $5s^2\,4f$, $5s^2\,5f$, 5s 5p 6s, 5s 5p 5d, $5p^3$ (in the odd parity) and $5s\,5p^2$, $5s^2\,5d$, 5s 5p 4f, $5s^2\,6s$ (in the even one). We obtained respectively a mean deviation of 306 cm^{-1} (42 levels) and 172 cm^{-1} (30 levels) in our fit using the recent (2020) experimental data from Husain *et al.* [40] as shown in Table A31. For this final caesium ion treated in this work, the polarization parameters were taken as: $\alpha_d = 0.67$ a.u. (Fraga *et al.* [94] for a Cs X core) and $r_c = 0.82$ a.u. (mean radius of the 4d orbital from our calculations).

4.3.2 Atomic Radial Parameters

In the case of Cs IV, the fit in the even parity was limited by the small number of experimentally known levels.

In the odd parity on the other hand, the fit was much more complex due to the strong mixing effects between the configurations. The final fitted parameters for Cs IV are shown in Tables 4.12 and 4.13 respectively.

When it came to Cs V, as one can see, the mean deviation between experimental and calculated levels is quite high. In the odd parity we were once again limited by the small number of known experimental levels and therefore the small number of parameters that could be adjusted. In the even parity, the high mixing effects between the configurations created some struggle in the calculations and that explains the relatively high mean deviation.

The final fitted parameters for Cs V, Cs VI and Cs VII are shown in Tables 4.14, 4.15, 4.16, 4.17, 4.18 and 4.19 respectively.

Table 4.12: Fitted parameters for the even parity of Cs IV

Configuration	Parameter	HFR (cm^{-1})	Fitted (cm^{-1})	Ratio
$5s^2\,5p^4$	E_{av}	27 106.0	28 994.6	
	F^2(5p,5p)	50 541.5	48 940.5	0.968
	ζ_{5p}	9 793.1	10 440.4	1.066

5 levels included - mean deviation: 67 cm^{-1}

Table 4.13: Fitted parameters for the odd parity of Cs IV

Configuration	Parameter	HFR (cm^{-1})	Fitted (cm^{-1})	Ratio
5s 5p^5	E_{av}	157 106.0	153 312.8	
	ζ_{5p}	9 784.9	Fixed	
	G^1(5s,5p)	66 532.5	54 918.8	0.825
5s^2 5p^3 5d	E_{av}	176 122.0	174 803.3	0.992
	F^2(5p,5p)	51 147.8	38 545.1	0.753
	α	0.0	574.0	
	ζ_{5p}	10 106.3	10 663.4	1.054
	ζ_{5d}	591.3	805.8	0.734
	F^2(5p,5d)	38 220.1	36 281.2	0.949
	G^1(5p,5d)	43 827.0	36 368.3	0.829
	G^3(5p,5d)	27 526.0	24 627.6	0.894
5s^2 5p^3 6d	E_{av}	277 426.6	269 750.8	
	F^2(5p,5p)	52 122.3	44 124.4	0.846
	α	0.0	−114.4	
	ζ_{5p}	10 528.8	10 723.0	1.018
	ζ_{6d}	184.4	246.8	0.747
	F^2(5p,6d)	10 788.6	8 503.1	0.788
	G^1(5p,6d)	6 966.7	6 202.2	0.890
	G^3(5p,6d)	4 911.8	2 879.9	0.586
5s^2 5p^3 7d	E_{av}	317 821.9	314 584.5	
	F^2(5p,5p)	52 227.3	Fixed	
	ζ_{5p}	10 586.0	Fixed	
	ζ_{7d}	89.0	Fixed	
	F^2(5p,7d)	4 756.9	Fixed	
	G^1(5p,7d)	2 740.9	Fixed	
	G^3(5p,7d)	2 008.0	Fixed	
5s^2 5p^3 6s	E_{av}	197 178.3	188 404.4	
	F^2(5p,5p)	51 687.8	44 584.1	0.862
	α	0.0	−95.6	
	ζ_{5p}	10 401.4	10 723.5	1.030
	G^1(5p,6s)	5 468.4	3 773.5	0.690
5s^2 5p^3 7s	E_{av}	281 879.2	272 894.4	
	F^2(5p,5p)	52 137.7	45 064.9	0.864
	α	0.0	−95.6	
	ζ_{5p}	10 554.9	10 870.9	1.029
	G^1(5p,7s)	1 635.2	1 518.9	0.928

87 levels included - mean deviation: 409 cm^{-1}

Table 4.14: Fitted parameters for the odd parity of Cs V

Configuration	Parameter	HFR (cm^{-1})	Fitted (cm^{-1})	Ratio
5s^2 5p^3	E_{av}	33 234.4	33 490.0	0.992
	F^2(5s,5p)	52 316.7	51 895.3	0.992
	ζ_{5p}	10 631.9	11 387.2	1.070

5 levels included - mean deviation: 274 cm^{-1}

Table 4.15: Fitted parameters for the even parity of Cs V

Configuration	Parameter	HFR (cm^{-1})	Fitted (cm^{-1})	Ratio
5s 5p^4	E_{av}	164 234.4	158 905.5	
	F^2(5p,5p)	52 355.0	56 316.5	1.075
	ζ_{5p}	10 611.1	11 100.8	1.046
	G^1(5s,5p)	68 543.9	52 750.7	0.769
5s^2 5p^2 5d	E_{av}	200 130.9	195 640.4	
	F^2(5p,5p)	52 802.0	37 229.6	0.705
	α	0.0	331.2	
	ζ_{5p}	10 906.1	11 897.8	1.090
	ζ_{5d}	725.1	509.0	0.701
	F^2(5p,5d)	41 456.6	40 013.2	0.965
	G^1(5p,5d)	48 122.3	41 047.3	0.853
	G^3(5p,5d)	30 427.6	29 968.1	0.985
5s^2 5p^2 6s	E_{av}	236 198.1	227 079.2	
	F^2(5p,5p)	53 308.0	47 021.1	0.881
	ζ_{5p}	11 225.0	11 372.4	1.013
	G^1(5p,6s)	6 097.3	5 705.9	0.935

42 levels included - mean deviation: 475 cm^{-1}

Table 4.16: Fitted parameters for the even parity of Cs VI

Configuration	Parameter	HFR (cm^{-1})	Fitted (cm^{-1})	Ratio
5s^2 5p^2	E_{av}	33 287.9	34 432.9	
	F^2(5p,5p)	53 954.4	55 236.4	1.023
	ζ_{5p}	11 491.6	12 070.5	1.050

5 levels included - mean deviation: 97 cm^{-1}

Table 4.17: Fitted Parameters for the odd parity of Cs VI

Configuration	Parameter	HFR (cm^{-1})	Fitted (cm^{-1})	Ratio
5s 5p^3	E_{av}	166 287.9	161 841.7	0.973
	F^2(5p,5p)	53 984.8	51 510.7	0.954
	α	0.0	104.6	
	ζ_{5p}	11 460.6	12 307.5	1.074
	G^1(5s,5p)	70 428.1	59 776.0	0.848
5s^2 5p 5d	E_{av}	218 802.6	213 327.8	0.974
	ζ_{5p}	11 734.3	12 536.3	1.068
	ζ_{5d}	854.3	1 155.5	1.353
	F^2(5p,5d)	44 134.6	43 073.4	0.975
	G^1(5p,5d)	51 670.0	45 009.0	0.871
	G^3(5p,5d)	32 836.8	30 719.1	0.935
5s^2 5p 6s	E_{av}	270 396.1	266 502.0	0.985
	ζ_{5p}	12 070.8	12 878.7	1.067
	G^1(5p,6s)	6 635.0	6 876.8	1.036

25 levels included - mean deviation: 166 cm^{-1}

Table 4.18: Fitted parameters for the odd parity of Cs VII

Configuration	Parameter	HFR (cm^{-1})	Fitted (cm^{-1})	Ratio
$5s^2\,5p$	E_{av}	21 045.0	20 859.7	
	ζ_{5p}	12 371.8	13 182.6	1.066
$5s^2\,6p$	E_{av}	335 205.9	334 894.6	
	ζ_{6p}	4 336.2	4 446.6	1.025
$5s^2\,4f$	E_{av}	180 777.2	168 202.0	
	ζ_{4f}	353.5	220.4	0.623
$5s^2\,5f$	E_{av}	391 701.1	383 546.6	
	ζ_{5f}	99.6	101.6	1.020
5s 5p 6s	E_{av}	404 544.0	408 648.9	
	ζ_{5p}	12 893.6	14 098.4	1.092
	G^1(5s,5p)	73 122.9	66 332.8	0.907
	G^0(5s,6s)	4 781.7	4 513.3	0.944
	G^1(5p,6s)	7 132.7	5 137.6	0.720
5s 5p 5d	E_{av}	332 951.8	332 683.1	
	ζ_{5p}	12 538.8	13 643.9	1.088
	ζ_{5d}	1 000.0	1 363.4	1.364
	F^2(5p,5d)	46 726.3	49 685.0	1.063
	G^1(5s,5p)	72 585.4	52 929.9	0.729
	G^2(5s,5d)	37 394.9	31 017.9	0.826
	G^1(5p,5d)	55 232.6	52 126.4	0.943
	G^3(5p,5d)	35 239.0	31 453.0	0.892
$5p^3$	E_{av}	295 010.2	294 366.0	
	F^2(5p,5p)	55 527.7	52 485.8	0.945
	α	0.0	459.4	
	ζ_{5p}	12 293.5	13 531.6	1.100

42 levels included - mean deviation: 306 cm^{-1}

Table 4.19: Fitted parameters for the even parity of Cs VII

Configuration	Parameter	HFR (cm^{-1})	Fitted (cm^{-1})	LSF [40]	Ratio
$5s\,5p^2$	E_{av}	150 045.0	149 023.4	146 889.7	
	F^2(5p,5p)	55 500.2	55 132.9	51 993.7	0.992
	α	0.0	436.6		
	ζ_{5p}	12 329.4	13 283.5	13 363.9	1.077
	G^1(5s,5p)	72 201.2	61 700.6	59 525.3	0.854
$5s^2\,5d$	E_{av}	219 126.0	211 269.8	210 015.6	
	ζ_{5d}	983.6	1 359.7	1 283.6	1.383
5s 5d 4f	E_{av}	298 318.2	290 549.4	290 781.0	
	ζ_{5d}	360.1	277.9	352.0	0.771
	ζ_{4f}	11 804.2	13 875.7	12 803.6	1.175
	F^2(5s,5d)	46 897.9	39 457.6	43 120.1	0.841
	G^3(5s,5d)	31 298.4	30 502.4	32 055.9	0.974
	G^2(5s,5d)	29 570.9	27 491.3	32 095.5	0.929
	G^4(5s,5d)	22 348.0	19 673.0	17 079.0	0.880
	G^1(5d,4f)	71 157.5	51 314.3	52 195.7	0.721
$5s^2\,6s$	E_{av}	286 721.3	282 484.0	279 901.7	

30 levels included - mean deviation: 172 cm^{-1}

4.3.3 Radiative Transition Rates

Exactly as for the indium ions, once the semi-empirical fit of the radial parameters performed, we calculated the transition probabilities and the oscillator strengths in the caesium ions. We calculated those with a cut-off at log $gf \geq$ -4 which led to respectively 251, 163, 83 and 138 transitions in Cs IV, V, VI and VII. The log $gf \geq$ -1 led to respectively 63, 73, 52 and 35 transitions listed in Tables A26 (for Cs IV), A28 (for Cs V), A30 (for Cs VI) and A32 (for Cs VII). The small number of transitions[5] comes from the small number of known experimental levels to perform the fit. Indeed, to be able to give a precise wavelength[6], the upper and the lower level have to be known experimentally. Therefore the real number of transitions with log $gf \geq$ -4 in our calculations is 8778 but among them, a lot include at least one theoretical (i.e. calculated) level which is not known experimentally. Indeed, as highlighted in Tables 4.12, 4.14 and 4.16 in the case of Cs IV and VI only one configuration has experimentally known levels in the even parity and only one in the odd parity in the case of Cs V. Those four tables are nevertheless given in the appendices (as all the 16 transition tables of this section 4).

To our knowledge, those new radiative data are the first ones in the literature concerning gA and log gf when it comes to Cs IV, V and VI. In Cs VII, Wajid *et al.* [110] performed a MCDHF calculation. However, the points of comparison are too few (only 7 transitions) to draw a conclusion. On these 7 transitions the agreement between the two calculations is about thirty percent which is rather satisfactory. In their work, Wajid *et al.* [110] present only 19 E1 transitions. Our work therefore represents a substantial and consistent contribution of new reliable intense transitions in Cs VII.

For these four ions, what has been achieved in the framework of this thesis is therefore very innovative since it has been carried out for the first time and provides numerous reliable radiative data that were previously non-existent (to our knowledge) in the literature. We therefore hope that these new data will allow the identification of caesium spectral lines in the spectrum of RE0503-289.

[5]In comparison with Cu IV-VII or In IV-VII for example.

[6]We chose to give the Ritz wavelength for all the transitions given in this section.

4.4 Ag IV-VII

The last element we studied in this chapter is silver (Z = 47). Its symbol, Ag, comes from the Latin word *argentum* meaning shiny [111]. The exact origin of the name silver in English is quite blurred. It appears in Old English with different spelling: *seofor* or *siolfor*. Similar words are found in Old High German, Gothic and the Celtic languages. The Balto-Slavic words for silver are very similar to these Germanic ones suggesting a very old origin. This would seem logical as silver has been known by Humanity since the neolithic age. This precious malleable metal is white and shiny. Dedicated to the Moon or to the lunar goddess Artemis/Diane, it has been among the seven sacred metals since Antiquity, well known and even overvalued by medieval alchemy. It is known for the multi-millennial manufacture of jewels, coins, as well as for its increasing industrial applications in the 20th century.

The experimental data used for the semi-empirical fits found in the literature, for the ions Ag IV, V, VI and VII ions are, respectively, Ankita and Tauheed [41] in Ag IV, Kildiyarova *et al.* [42] and Van Kleef *et al.* [43] in Ag V, Joshi *et al.* [44] in Ag VI and Ryabtsev and Kononov [45] in Ag VII. The configuration models built are based on the models we made for indium (In) ions. This choice comes from the fact that, as it turns out , In VI is isoelectronic with Ag IV. The model that we have built for Ag IV has been constructed in a similar way to the one existing for In VI, and those for Ag V, VI and VII have been built by gradually removing a 4d electron to the model of the previous ion.

4.4.1 Models Used

The model for each silver ion consists of the configurations necessary to describe it (the set of these configurations is also called configuration interaction model), the dipole polarizability of the core and the cut-off radius describing the core-polarization. These parameters are introduced in the *ab initio* procedure, and the radial parts of the single-electron wave functions are then calculated following the self-consistent field procedure.

Ag IV being isoelectronic with In VI, we have taken the model describing the latter ion, but we added the configurations $4d^7 7s$, $4d^7 7d$ and $4d^7 7p$, in order to further improve our representation of the configuration interaction. The configurations we introduced in the model are namely: $4d^8$, $4d^7 5s$, $4d^7 5d$, $4d^6 5s^2$, $4d^7 6s$, $4d^7 6d$, $4d^6 5p^2$, $4d^7 7s$, $4d^7 7d$ and $4d^6 5s5d$ for the even parity and $4d^7 5p$, $4d^7 4f$, $4d^6 5s5p$, $4d^7 6p$, $4d^7 5f$, $4d^6 5s6p$, $4d^7 7p$ and $4d^6 5s5f$ for the odd one.

To describe the core-valence interactions, we considered that the last orbital of the ionic core is the 4d. We therefore took the average radius of the 4d subshell (from our HFR calculations) as the cut-off radius, which is equal to 1.2 a_0. The polarization parameters of the core are those corresponding to an Ag VI ($4d^6$)-type ionic core (chosen to represent at best double excitations of electrons from the core to the valence electrons), which for the dipolar polarizability (from [94]) corresponds to α_d equal to 2.23 a_0^3. The methodology explained above was the same for the following ions, and the values of r_c and α_d is modified each time to best represent the problem. The configurations of Ag IV for which there are experimentally known energy levels are $4d^8$, $4d^7 5s$, $4d^7 5d$ and $4d^7 6s$ for even parity, and $4d^7 5p$ for odd parity. The fundamental is a $4d^8$ $^3F_4$ state.

This led to mean deviations between the experimental and calculated energy levels of respectively 103 cm^{-1} and 159 cm^{-1} for the even and the odd parity as shown in Tables A33 and A34.

The configuration model used for Ag V is realized by removing an electron from the $4d$ layer of the Ag IV model. That means that the configurations introduced in the model are: $4d^7$, $4d^6 5s$, $4d^6 5d$, $4d^5 5s^2$, $4d^6 6s$, $4d^6 6d$, $4d^5 5p^2$,$4d^6 7s$, $4d^4 7d$ and $4d^5 5s5d$ for the even parity and $4d^65p$, $4d^64f$, $4d^55s5p$, $4d^66p$, $4d^65f$, $4d^55s6p$, $4d^67p$ and $4d^55s5f$ for the odd one.

In the case of Ag V, the value of r_c from our calculations is 1.16 a_0. α_d is equal to 1.69 a_0^3 ([94]) and corresponds to an Ag VII core ($4d^5$). The configurations of this model whose energy levels are known experimentally are $4d^7$ and $4d^65s$ for the even parity, and $4d^65p$ for the odd parity. The fundamental of the atomic system is $^4F_{9/2}$.

Those fits led to average deviations between the experimental and calculated set of energy levels of respectively 138 cm^{-1} and 134 cm^{-1} for the even and the odd parity as shown in Tables A36 and A37.

The configurations we introduced in our model for Ag VI are: $4d^6$, $4d^55s$, $4d^55d$, $4d^45s^2$, $4d^56s$, $4d^56d$, $4d^45p^2$, $4d^57s$, $4d^37d$ and $4d^45s5d$ for the even parity and $4d^55p$, $4d^54f$, $4d^45s5p$, $4d^56p$, $4d^55f$, $4d^45s6p$, $4d^57p$ and $4d^45s5f$ for the odd one.

This time, core-polarization effects are considered using a polarizability α_d equal to 1.35 a_0^3 (Ag VIII core - $4d^4$) and a cut-off radius equal to 1.12 a_0. The configurations of this model whose energy levels are known experimentally are $4d^6$ for the even parity, and $4d^55p$ for the odd parity. The fundamental of the atomic system is an energy level of configuration $4d^6\ ^4D_4$.

The mean deviations between the experimental and calculated energy levels were found to be 198 cm^{-1} and 116 cm^{-1} for the even and the odd parity respectively, as one can see in Tables A39 and A40.

The configurations that we considered in our calculations for Ag VII are respectively $4d^5$, $4d^45s$, $4d^4\ 5d$, $4d^35s^2$, $4d^46s$, $4d^46d$, $4d^35p^2$, $4d^47s$, $4d^47d$, $4d^35s5d$ for the even parity and $4d^45p$, $4d^44f$, $4d^35s5p$, $4d^46p$, $4d^45f$, $4d^35s6p$, $4d^47p$, $4d^35s5f$ for the odd one.

Core-polarization was here taken into account by using a dipole polarizability α_d equal to 1.08 a_0^3 (Ag IX core - $4d^3$) and r_c equal to 1.09 a_0. The configurations of this model whose energy levels are known experimentally are $4d^5$ for even parity, and $4d^45p$ for odd parity. The fundamental is $4d^5\ ^6S_{5/2}$.

The average deviations between the experimental and calculated energy levels resulting from our calculations were 144 cm^{-1} and 129 cm^{-1} for the even and the odd parity respectively, as highlighted in TablesA42 and A43.

4.4.2 Atomic Radial Parameters

The radial parameters obtained by our calculations are listed in Tables 4.20 and 4.21 for Ag IV, 4.22 for Ag V, 4.23 for Ag VI and 4.24 for Ag VII.

Table 4.20: Radial parameters for the even configurations of Ag IV

Configuration	Parameter	HFR (cm^{-1})	Fit (cm^{-1})	Ratio
$4d^8$	E_{av}	14214.0	13526.6	
	F^2(4d,4d)	72568.5	67253.0	0.935
	F^4(4d,4d)	47717.9	46369.9	0.975
	α	0	348	
	β	0	0	
	ζ_{4d}	1927.3	2 001.6	1.039
$4d^7 5s$	E_{av}	124858.5	122845.5	
	F^2(4d,4d)	74813.2	68754.2	0.912
	F^4(4d,4d)	49362.3	48558.9	0.982
	α	0	400	
	β	0	-4138	
	ζ_{4d}	2 039.6	21.253	1.040
	G^2(4d,5s)	14051.3	133.459	0.946
$4d^7 6s$	E_{av}	279447.7	280303.2	
	F^2(4d,4d)	75658.5	70768.2	0.932
	F^4(4d,4d)	49992.1	47935.9	0.966
	α	0	0	
	β	0	0	
$4d^7 5d$	E_{av}	269921.8	272607.1	
	F^2(4d,4d)	75653.5	70923.1	0.946
	F^4(4d,4d)	49 989.4	49354.2	0.986
	α	0	0	
	β	0	0	
	ζ_{4d}	2069.9	2124.4	1.026
	ζ_{5d}	203.9	196.8	0.962
	F^2(4d,5d)	12863.3	11236.8	0.875
	F^4(4d,5d)	5537.7	3960.8	0.715
	G^0(4d,5d)	3351.5	3586.6	1.076
	G^2(4d,5d)	3872.7	4144.3	1.076
	G^4(4d,5d)	3112.6	3330.8	1.072

74 levels included - mean deviation: 103 cm^{-1}

Table 4.21: Radial parameters for the odd parity of Ag IV

Configuration	Parameter	HFR (cm^{-1})	Fit (cm^{-1})	Ratio
$4d^7 5p$	E_{av}	189157.3	187829.3	
	F^2(4d,4d)	75113.2	68520.9	0.912
	F^4(4d,4d)	49586.1	48204.8	0.972
	α	0	415	
	β	0	-3254	
	ζ_{4d}	2051.3	2140.5	1.043
	ζ_{5p}	306.6	346.2	1.129
	F^2(4d,5p)	24280.9	22900.3	0.943
	G^1(4d,5p)	8661.5	8180.2	0.944
	G^3(4d,5p)	7731.3	6542.4	0.846

110 levels included - mean deviation: 159 cm^{-1}

Table 4.22: Radial Parameters for Ag V

Configuration	Parameter	HFR	Fit	Ratio
Even				
$4d^7$	E_{av}	24627.7	23504.8	
	F^2(4d,4d)	75959.1	70981.6	0.934
	F^4(4d,4d)	50214.7	49726.6	0.990
	α	0	386	
	β	0	-5672	
	ζ_{4d}	20836	21404	1.027
$4d^6 5s$	E_{av}	174254.6	171195.4	0.983
	F^2(4d,4d)	77964.4	72471.0	0.930
	F^4(4d,4d)	51688.2	49686.9	0.866
	α	0	484	
	β	0	-4412	
	ζ_{4d}	2196.1	2310.0	1.051
Odd				
$4d^6 5p$	E_{av}	247668.7	245697.6	
	F^2(4d,4d)	78211.5	72095.5	0.921
	F^4(4d,4d)	51873.5	49443.3	0.953
	α	0	48	
	β	0	-2957	
	ζ_{4d}	2207.0	2309.6	1.046
	ζ_{5p}	3919.2	44732	1.141
	F^2(4d,5p)	27492.3	25970.9	0.945
	G^1(4d,5p)	9451.7	9142.1	0.968
	G^3(4d,5p)	8704.3	7632.6	0.876

Even Parity: 78 levels (mean deviation: 138 cm^{-1})
Odd Parity: 175 levels (mean deviation: 134 cm^{-1})

Table 4.23: Radial parameters for Ag VI

Configuration	Parameters	HFR	Fit	Ratio
Even				
$4d^6$	E_{av}	35313.2	33808.8	
	F^2(4d,4d)	79035.2	74116.7	0.938
	F^4(4d,4d)	52488.9	50919.7	0.971
	α	0	41.2	
	β	0	-438.3	
	ζ_{4d}	2242.5	2363.3	1.054
Odd				
$4d^45p$	E_{av}	300000	305117.7	
	F^2(4d,4d)	81063	74779.5	0.922
	F^4(4d,4d)	53984.8	53334.7	0.988
	α	0	0	
	β	0	0	
	ζ_{4d}	2365.8	2470.1	1.044
	ζ_{5p}	4788.2	5348.4	1.117
	F^2(4d,5p)	30380.2	29089.3	0.957
	G^1(4d,5p)	10124.2	9432.6	0.931
	G^3(4d,5p)	9557.5	9085.4	0.951

Even Parity: 30 levels (mean deviation: 198 cm^{-1})
Odd Parity: 110 levels (mean deviation: 116 cm^{-1})

Table 4.24: Radial parameters for Ag VII

Configuration	Parameter	HFR	Fit	Ratio
Even				
$4d^5$	E_{av}	55219	52621	0.953
	F^2(4d,4d)	81891.4	76836.8	0.938
	F^4(4d,4d)	55166.7	54120.5	0.981
	α	0	40.9	
	β	0	-535.7	
	ζ_{4d}	2406	2474	1.028
Odd				
$4d^45p$	E_{av}	375533.1	374230.7	
	F^2((4d,4d)	83678	77934.9	0.931
	F^4(4d,4d)	55924.1	55160.7	0.986
	α	0	46.4	
	β	0	-636.6	
	ζ_{4d}	2524.4	2630.3	1.042
	ζ_{5p}	5681.5	6303.9	1.109
	F^2(4d,5p)	33076.5	31370.5	0.948
	G^1(4d,5p)	10756.1	10368.3	0.964
	G^3(4d,5p)	10356	9336.2	0.901

Even Parity :34 levels (mean deviation: 144 cm^{-1})
Odd Parity : 143 levels (mean deviation: 183 cm^{-1})

4.4.3 Radiative Transition Rates

Exactly as for the previous elements, the tables containing the radiative transition rates of Ag IV, V, VI and VII are in the appendices. Once again, the calculations were performed in order to obtain all the transitions with log $gf \geq$ -4 (2989 transitions for Ag IV, 5319 for Ag V, 2168 for Ag VI and 2232 for Ag VII), but only the most intense ones with log $gf \geq$ -1 are given in Tables A35 (615 transitions), A38 (915 transitions), A41 (362 transitions) and A44 (441 transitions) for Ag IV,V, VI and VII respectively.

One should note that for Ag V and Ag VI, even if the transitions have been measured (with their transition rates), no transition probability is available in the literature. For Ag IV, Ankita and Tauheed [41] performed a HFR calculation to obtain gA but with a more restricted model without core polarization. Figure 4.4.3 shows the comparison between our data for the most intense Ag IV lines and the ones of [41]. As expected, our values are systematically lower than theirs due to the addition of the core-polarization effects.

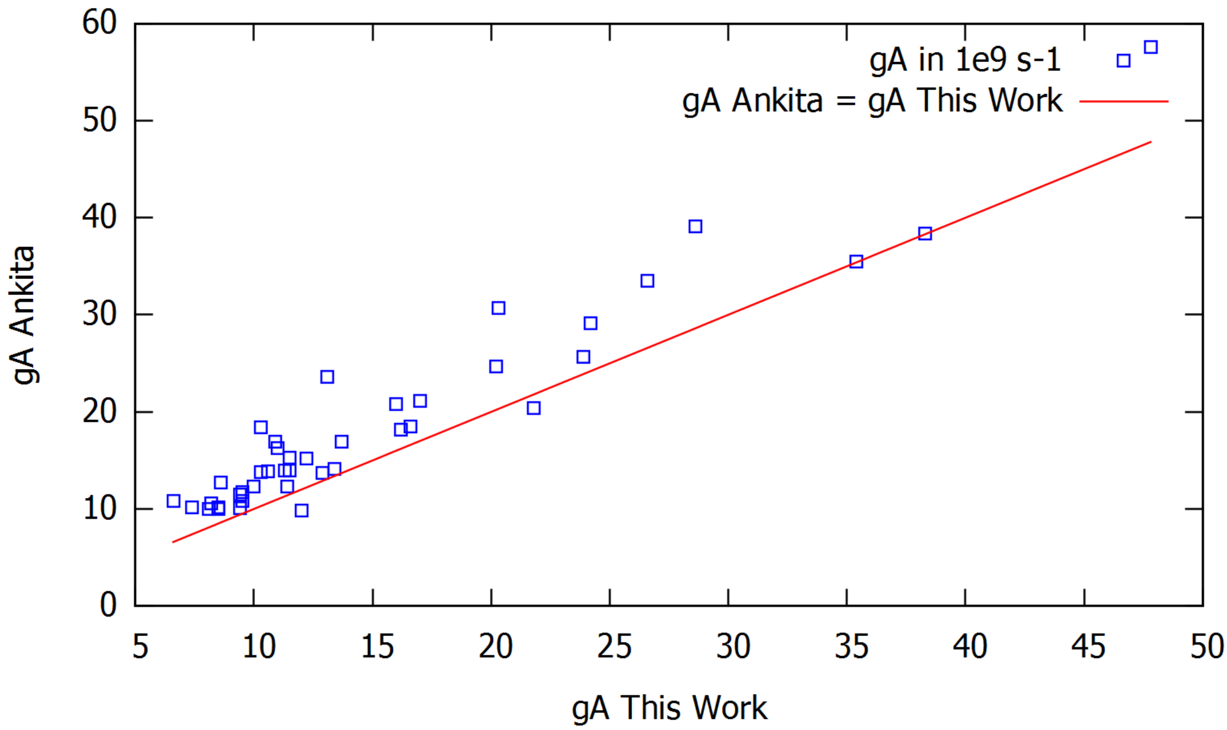

Figure 4.8: Comparison between the gA (in $10^9 s^{-1}$)obtained by our HFR+CPOL calculations and the former calculation of Ankita and Tauheed [41] for the Ag IV ion. The straight line of equality is drawn in red.

For Ag VII, our theoretical gA are compared to gA obtained by Ryabtsev and Kononov [45] in figure 4.9. This figure shows the good agreement between the values. Again, as discussed for example for copper ions, in their calculations they introduced some core-valence interactions (e.g. considering configurations like $4d^3 5s^2$) that are actually included in our core polarization potential. It would seem that this time, given the good agreement between our data, these interactions that they explicitly consider are clearly the most important ones. However, we see a tendency for our values to be slightly lower than theirs suggesting that there are indeed core-valence interactions that have not been included in their model, making ours more complete.

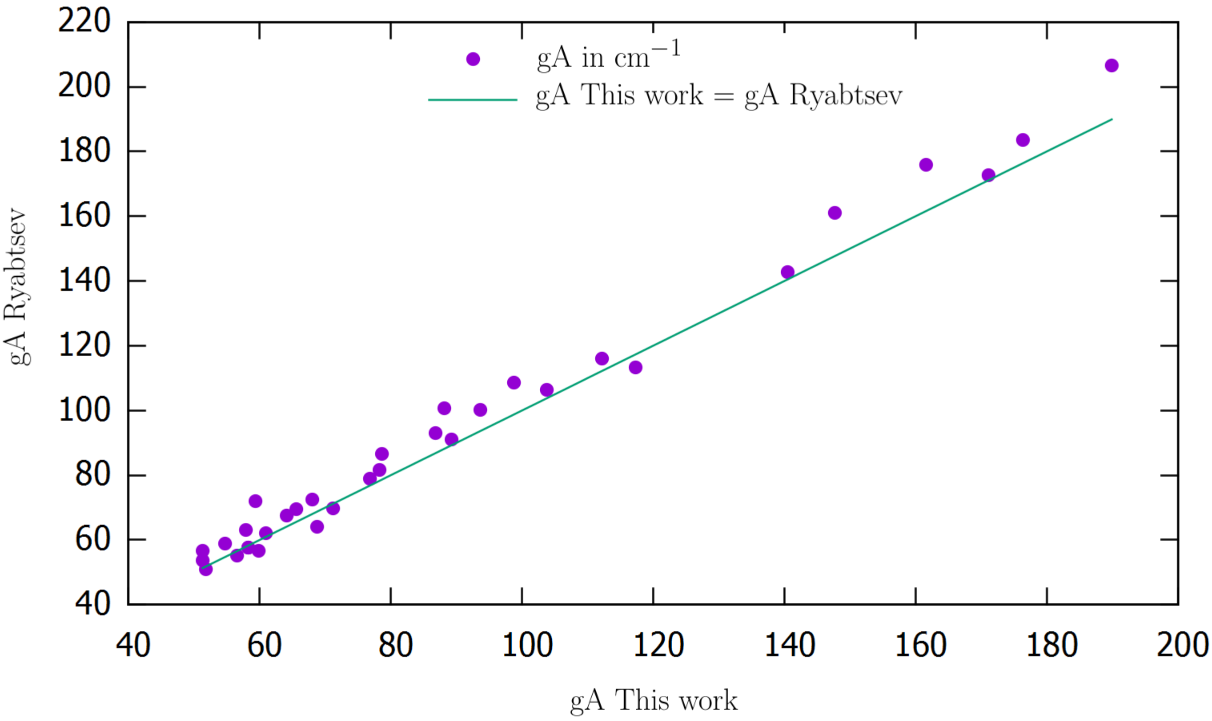

Figure 4.9: Comparison between HFR intense gA (in $10^9 s^{-1}$)and experimental ones from [45] for the Ag VII ion. The straight line of equality is drawn in green

4.5 Conclusion - Applications

In the context of the collaboration with astrophysicists from the University of Tübingen, our new results were sent to them so that they could incorporate them in their NLTE models of synthetic spectra in order to identify new lines in the spectra of white dwarfs, and in particular of RE0503-289. These analyses led to the identification of Cu IV-VII lines as mentioned in Section 4.1.3.1 and were published in [77]. The other ions shown in this section are currently being analyzed by our colleagues and we hope that this will also lead to the new identifications of spectral lines in white dwarfs spectra.

The collaboration between the University of Tübingen and the University of Mons had begun before the start of this thesis and had already been performed calculations and line identifications in the spectrum of RE0503-289 in several TIE (in their third to sixth ionization stages) represented by the green boxes in the Mendeleev table shown in Figure 4.10. The elements for which we have done the full atomic calculations, and for which we presented the detailed results in the previous subsections, are represented by the red frames. The blue boxes represent elements for which the calculations are in progress and in direct collaboration between the two universities. The calculations and the semi-empirical adjustments are carried out in Tübingen and the addition of the corrections of polarization of the ionic core are made by ourselves in Mons. Those elements are a work in progress and we do not have the results with the synthetic spectra yet. We do not present the detailed results for those ions (Sn IV-VII, Sb IV-VII, I IV-VII, Rb IV-VII and Y IV-VII) in this thesis since, as mentioned earlier, we have only performed a small part of the calculations.

However, we hope that these outgoing calculations, which are still in progress, are an open door to continue this collaboration between the two universities.

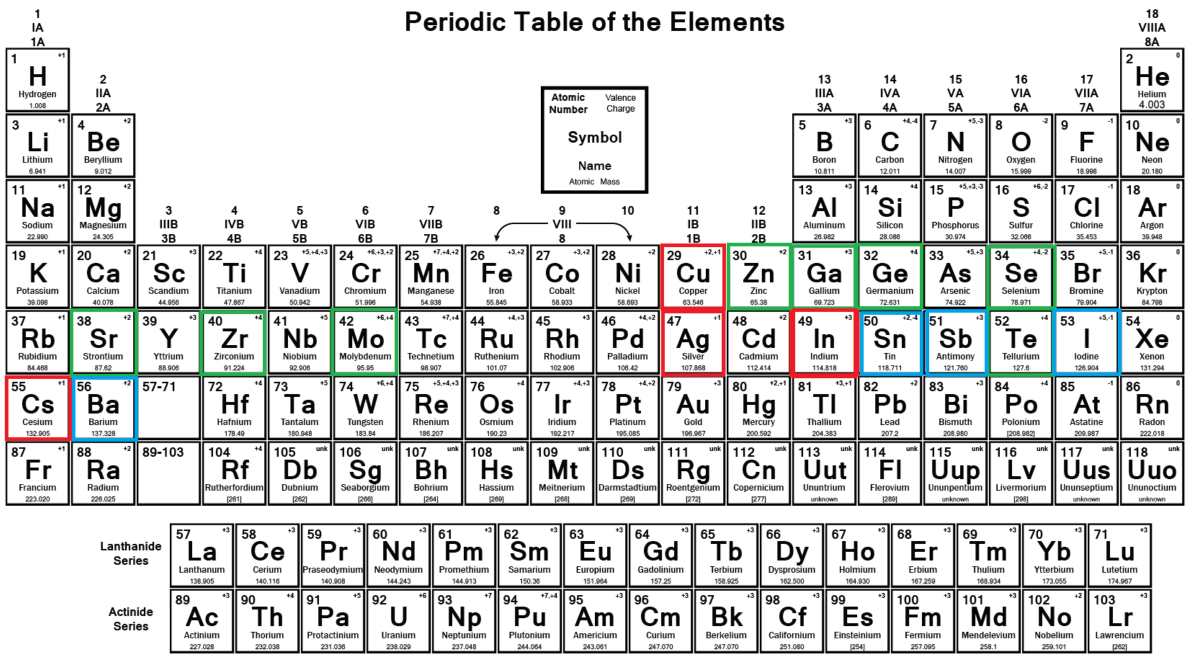

Figure 4.10: TIEs treated in collaboration with the University of Tübingen for the purpose of white dwarfs analysis - Original picture from: sciencesnote.org (©Todd Helmenstine)

Chapter 5

Radiative Decay Rates in Neutral and Singly Ionized Atoms for Stellar Nucleosynthesis Analyses

As we already mentioned in the previous chapters, abundances of heavy elements can provide crucial information about the conditions required for the formation of such elements. Those informations can be used to corroborate the theory of the nucleosynthesis described in Section 1.2. Precise radiative parameters such as transition probabilities and oscillator strengths of these heavy elements are, of course, mandatory for line identifications from which elemental abundances in stellar spectra can be determined.

This is what motivated us to undertake calculations in these elements exactly as for the two previous chapters. But, in this chapter, under the impulse of an experimental group looking for a theoretical backup to their measurements, these calculations have been combined with their experimental measurements in order to produce semi-empirical atomic data. This experimental group with whom we produced new semi-empirical data is located in the Jilin University in China. In collaboration with them, we produced data in neutral rhodium, barium, rhenium, iridium and singly ionized iridium. The astrophysical applications of each of those elements will be described in the associated sections.

In this chapter, we will therefore first describe the technique used by our collaborators for the experimental measurements. This technique is the time-resolved laser-induced fluorescence (TR-LIF) technique. We will then, as we did in the previous chapters, present our theoretical models and the results we obtained for the various ions treated in this collaboration with the University of Jilin. Those ions will be presented in a decreasing atomic number (Z) order starting with neutral and once ionized iridium[1] (Z = 77), then rhenium (Z = 75), lanthanum (Z = 57), barium (Z = 56) and finishing with rhodium (Z = 45).

The goal of this analysis was to produce a new set of semi-empirical gA- and gf-values in collaboration with the experimental group of the University of Jilin in China. Indeed, they performed some precise radiative lifetime measurements that we combined to our theoretical branching fractions (BFs) B_{ki} to get gA-values using the formula:

$$A_{ki} = \frac{B_{ki}}{\tau_k} \tag{5.1}$$

where k and i represent the upper and lower levels. The gf are obtained with:

$$gf = g_{ik}f = 1.4992 \times 10^{-16} \lambda^2 g_k A_{ki} \tag{5.2}$$

This technique can be seen as a normalization of HFR+CPOL gA-values using the experimental lifetimes. This method is effective when branching fractions cannot be

[1]For which both neutral an singly ionized stages have been treated during this thesis.

measured for all depopulating transitions of the same upper level because the available experimental spectra do not cover the whole range of wavelengths where all lines involving the concerned level are supposed to appear. If the sum of all the intensities of all these lines is not negligible, its omission introduces a systematic error in the experimentally deduced transition probabilities. It is worth noting that the sum of the missing intensities is often estimated by experimentalists using theoretical methods, such as the HFR approach (see e.g. Sikström *et al.* [112]). Let us add that, in our work, we were mainly interested in highly excited levels for each of the elements considered. As these levels are depopulated by numerous transitions appearing in different regions of the electromagnetic spectrum, it was impossible to measure all the branching fractions because of the (partial or even total) lack of experimental spectra. The only way to obtain a reliable and consistent set of transition probabilities was therefore to combine the measured TR-LIF lifetimes with the theoretical HFR+CPOL branching fractions.

5.1 Lifetime Measurements

The lifetime, τ_i of an excited level i can be measured by studying the population decay of its population N_i,

$$N_i(t) = N_i(0)e^{-t/\tau_i}. \quad (5.3)$$

Another way to investigate the lifetime of an excited level is by observing its fluorescent decay:

$$I(t) = -c\frac{dN_i}{dt} = I(0)e^{-t/\tau_i} \quad (5.4)$$

where c is a positive constant. By observing the time-resolved fluorescence signal $I(t)$ from an excited level, its lifetime can simply be obtained by fitting an exponential to the measured decay curve.

5.1.1 TR-LIF Spectroscopy Technique

In order to investigate atomic lifetimes, a short-pulse excitation is used, shortly followed by a fast time-resolved detection of the fluorescence de-excitation.

During the excitation with the laser pulse, the population of the upper level (for a two-level system) is given by:

$$\frac{dN_2(t)}{dt} = B_{12}\rho(\nu,t).N_1(t) - [B_{21}.\rho(\nu,t) + A_{21}].N_2(t) \quad (5.5)$$

where B_{12} and B_{21} are the Einstein coefficients for absorption and stimulated emission and A_{21} is the spontaneous emission transition probability. $\rho(\nu,t)$ is the spectral energy density of the excitation laser and N_1 is the population of the lower level.

If $N_1(t) >> N_2(t)$, N_1 can be considered as a constant and Eq. 5.5 becomes:

$$\frac{dN_2(t)}{dt} = B_{12}\rho(\nu,t).N_1 - [B_{21}.\rho(\nu,t) + A_{21}].N_2(t) \quad (5.6)$$

If the lifetime of the upper level is much longer than the excitation laser pulse duration and the response of the detection system, as the example shown in Figure 5.1.1, then, after the pulse has disappeared (i.e. $\rho \approx 0$), Eq. 5.6 finally becomes

$$\frac{dN_2(t)}{dt} = -A_{21}N_2(t) \quad (5.7)$$

which can easily be integrated to an equation similar to Eq. 5.4 and the lifetime can therefore be obtained by a pure exponential fit of the measured fluorescence decay curve.

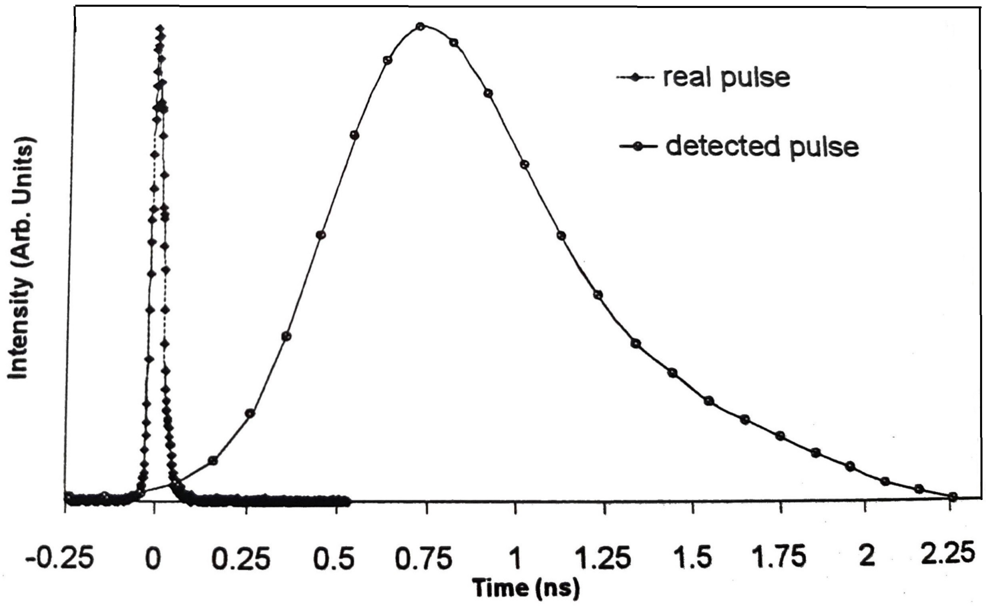

Figure 5.1: Example of a measurement with a laser pulse duration much shorter than the radiative lifetime.

If the lifetime is comparable to the laser pulse duration or to the response of the detection system, it becomes a bit more tricky. In that case, Eq. 5.6 becomes something like:

$$I(t) = C \int_{-\infty}^{t} P(t')E(t-t').dt' \tag{5.8}$$

where $I(t)$ is the fluorescence intensity (as in equation 5.4), C a constant $P(t)$ is the laser pulse shape and is proportional to $\rho(\nu, t)$. $E(t)$ is the fluorescence decay curve for an instantaneous excitation and is equal to $e^{-t/\tau}$ if t ≥ 0 or to 0 otherwise. This leads to

$$I(t) = C.P(t) \otimes E(t) \tag{5.9}$$

which means that the fluorescence curve of interest is the convolution between the laser pulse shape and an exponential decay with instantaneous excitation. In order to take every parameter into account, the instrumental response must be taken into account through $R(t)$ (i.e. the experimental response function):

$$I(t) = C.[P(t) \otimes E(t)] \otimes R(t) \tag{5.10}$$

Since the excitation laser pulse is detected with the same detection system we can actually define

$$P_{PR}(t) = P(t) \otimes R(t) \tag{5.11}$$

and therefore equation 5.10 becomes:

$$I'(t) = C.E(t) \otimes P_{PR}(t) \tag{5.12}$$

This means that the recorded fluorescence signal can be expressed as a convolution between the recorded excitation laser pulse and a pure exponential. In practical conditions, the exciting laser pulse is recorded at the same time as the fluorescence decay curve. Therefore, by fitting this fluorescence signal to the convolution of the detected laser pulse and a pure exponential decay, the effects of the duration of the excitation laser pulse and the response time of the detector are taken into account.

5.1.2 Experimental Setup

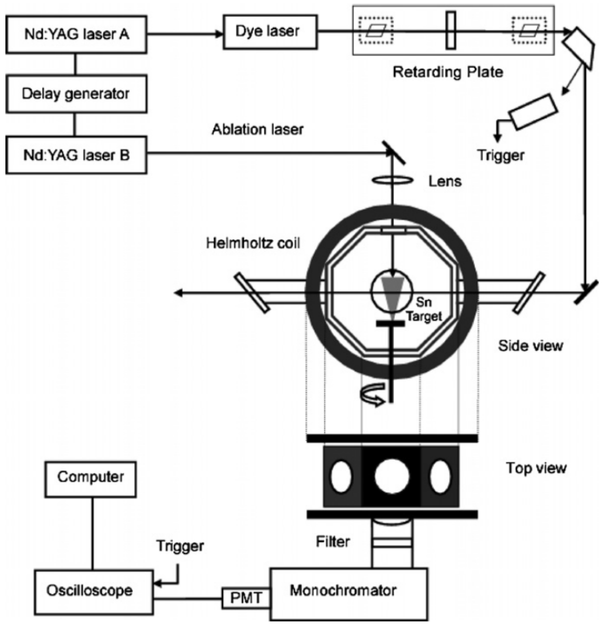

Figure 5.2: Typical TR-LIF experimental setup used for lifetime measurements.

A typical experimental setup used for lifetime measurements is shown in Figure 5.2. In order to produce a sufficient density of atoms in metastable states in order to take precise measurements, a laser-produced plasma obtained with a laser ablation on a pure sample (a 99.8% pure tin (Sn) sample is used in the figure) is employed as an atomic source.

As shown in [113, 114], this technique is suitable, efficient and reliable for lifetime measurements. A 5 mJ 532 nm pulse, with approximately 8 ns duration, emitted by a Q-switched Nd:YAG laser working at a 10 Hz repetition rate, is focused on a thin target, fixed on a rotating platform with a rotation speed appropriate to ensure an ablation position different for each laser pulse. A dye laser with linear polarization is used for the excitation. The linewidth of this dye laser is around 0.08 cm^{-1}.

The light emitted by the excitation laser ($\approx$ 5–7 ns pulse duration) is sent horizontally throughout the vacuum chamber, where it interacts with a vertical atomic beam about 10 mm above the target. The interval between the excitation and ablation pulses can be adjusted by a digital delay generator. Following that excitation, the fluorescence signal is focused into a grating monochromator by a convex silica lens in a perpendicular direction to the laser and to the atomic beam. It is afterwards detected by a photomultiplier tube (PMT). In the experiments performed at University of Jilin, the monochromator was placed by rotating it 90 degrees, so that its entrance slit was horizontal and parallel to the excitation beam in order to enhance the fluorescence collection efficiency. A spectral filter, which cuts the light with a tunable wavelength limit (e.g. 300 nm), is used between the lens and the monochromator to prevent the cascade fluorescence at about the chosen limit (in our example 320 nm). Since the levels are selectively excited by the laser, there are no cascade emissions from higher excitation levels [115].

The time-resolved fluorescence photo-current signal from the PMT is registered by a 500 MHz digital oscilloscope which is triggered by the excitation laser with a photoelectric diode. This oscilloscope is connected to a computer in which the experimental data can be stored and analyzed as shown in Figure 5.2.

The data we obtained using HFR + CPOL concerning Ir I and II (Sections 5.2.1 and 5.2.2), Re I (Section 5.3), Ba I (Section 5.5), and Rh I (Section 5.6) have been combined to the experimental data obtained using the technique described here above by our collaborators at the University of Jilin in China.

5.2 Ir I-II

Iridium (Z = 77) was discovered in 1803 by Smithson Tennant in London. Its name comes from the Latin *iris* meaning rainbow, because of its compounds which are very colorful [109, 116].

In astrophysics, the accuracy of stellar chemical abundances largely depends on the adequacy and accuracy of the atomic radiative and structure data. In the case of iridium ($Z = 57$), there are two stable isotopes, ^{191}Ir and ^{193}Ir, with relative abundances of 37.3% and 62.7% on the Earth. Ir abundances in stars are of great significance not only in radioactive cosmochronology, but also in the structure and nucleosynthetic evolution of supernovae originating from the first stellar generation (see Ivarsson *et al.* [117]).

Indeed, during the last decades, high-resolution near-ultraviolet spectra from the Hubble Space Telescope were used to detect the rapid neutron-capture (r-process) elements (like osmium, iridium and platinum) in r-process enriched stars such as some metal-poor halo stars and chemically peculiar (CP) stars (see e.g. [118, 119, 120]). The abundances of these heavy elements provide valuable information about the conditions required for the formation of these elements in the supernovae, merging neutron stars, and about the atmospheric processes that lead to anomalies in spectra of CP stars, and these elements are more appropriate for the age dating of the oldest stars than the lighter elements [119, 121, 122]. Once again, as we mentioned in Section 1, the radiative parameters such as transition probabilities or oscillator strengths of atoms and ions of these heavy elements are, of course, crucial for the determination of elemental abundances.

Until now in the previous sections, we have only presented purely theoretical data. Another reliable and convenient method to obtain oscillator strengths is through the combination of measured radiative lifetimes with reliable branching fractions (BFs). I ridium ($Z = 77$) is a heavy element only produced in the r-process and its neutral and once ionized spectra are detected in many stars, for example the CP star χ Lupi [122], or for the MP halo star HD 160617 [119] and many others.

5.2.1 Ir I

Twelve even- and nine odd-parity configurations were explicitly included in our theoretical calculations, namely 5d^{7}6s^2, 5d^{7}6p^2, 5d^{7}6d^2, 5d^{7}6s7s, 5d^{7}6s6d, 5d^{6}6s^{2}7s, 5d^{6}6s^{2}6d, 5d^{6}6s6p^2, 5d^{8}6s, 5d^{8}7s, 5d^{8}6d and 5d^9 in the even parity and 5d^{7}6s6p, 5d^{7}6s7p, 5d^{7}6s5f, 5d^{7}6s6f, 5d^{6}6s^{2}6p, 5d^{8}6p, 5d^{8}7p, 5d^{8}5f and 5d^{8}6f in the odd one. The core-polarization effects were estimated using the dipole polarizability reported by Fraga [94] for an Ir IV ionic core, i.e. $\alpha_d = 6.48\ a_0^3$, and a cut-off radius $r_c = 1.60\ a_0$, corresponding to the expected value of $< r >$ for the outermost core orbital (5d), as obtained with the HFR method. Moreover, a semi-empirical fitting procedure was applied to the radial parameters related to the 5d^{7}6s^2, 5d^{8}6s, 5d^9, 5d^{7}6s6p, 5d^{6}6s^{2}6p and 5d^{8}6p configurations. It is important to note that the energy levels above 50000 cm^{-1} were not included in the fit because many of them were found to be strongly mixed with unknown levels which made very doubtful the correspondence between the calculated energies and the available experimental values. For this reason, our HFR+CPOL calculations of the atomic structure and radiative parameters in Ir I were limited to the energy levels situated below 50000 cm^{-1}.

The goal of this analysis was to produce a new set of semi-empirical gA- and gf-values in collaboration with the experimental group of the University of Jilin in China. Indeed, they performed some precise radiative lifetime measurements that we combined to our theoretical branching fractions (BFs).

Using the theoretical branching fractions and the experimental lifetimes, we deduced the transition probabilities and oscillator strengths for all the lines depopulating the odd-parity levels below 50000 cm^{-1}. The results obtained are reported in Table 5.1. In that table 134 Ir I spectral lines are to be found in a wavelength range going from 205 to 418 nm. As far as we know, transition probabilities were experimentally measured by Gough *et al.* [123] for only two transitions among those considered in the present work. These are found to be in good agreement (within 20%) with our values.

Table 5.1: Branching fractions, transition probabilities, oscillator strengths for highly excited levels of Ir I and comparison with previous results

Upper Level[a] E (cm^{-1}	Lower Level[a] E (cm^{-1}	λ_{air} (nm)	BF	gA (10^6 s^{-1}) This work	Previous[b]	log gf This work	Previous[c]
32513.43	0	307.476	0.1	2.89 (E)		-2.38 (E)	-2.34
τ (ns) = 345(11)	2834.98	336.848	0.21	6.09 (D+)		-1.98 (D+)	-1.98
	6323.91	381.724	0.17	4.93 (E)		-1.97 (E)	-1.96
	7106.61	393.484	0.51	14.7 (D+)		-1.47 (D+)	-1.45
33874.43	2834.98	322.078	0.8	225 (B)	192.9	-0.46 (B)	-0.47
τ (ns) = 28.4(6)	6323.91	362.867	0.06	16.9 (E)	22.7	-1.48 (E)	-1.51
35540.34	4078.94	317.758	0.6	12.8 (D+)		-1.71 (D+)	
τ (ns) = 281(15)	7106.61	351.594	0.23	4.91 (D+)		-2.05 (D+)	
37446.13	4078.94	299.609	0.44	13.6 (D+)		-1.74 (D+)	-1.7
τ (ns) = 194(15)	5784.62	315.75	0.11	3.40 (E)		-2.29 (E)	-2.28
	6323.91	321.221	0.11	3.40 (E)		-2.28 (E)	-2.36
	9877.54	362.629	0.22	6.80 (D+)		-1.87 (D+)	-1.85
	11831.09	390.285	0.09	2.78 (E)		-2.20 (E)	-2.16
40524.73	5784.62	287.768	0.3	58.8 (D+)		-1.14 (D+)	
τ (ns) = 20.4(14)	9877.54	326.2	0.15	29.4 (E)		-1.33 (E)	
	10578.68	333.838	0.19	37.3 (E)		-1.21 (E)	
	12505.68	356.798	0.07	13.7 (E)		-1.58 (E)	
	12951.67	362.57	0.1	19.6 (E)		-1.41 (E)	
	16565.35	417.255	0.14	27.4 (E)		-1.14 (E)	
41522.22	4078.94	266.992	0.16	57.1 (E)		-1.21 (E)	
τ (ns) = 16.8(5)	5784.62	279.735	0.24	85.7 (D+)		-1.00 (D+)	
	6324.91	284.021	0.25	89.3 (D+)		-0.97 (D+)	
	7106.61	290.481	0.14	50.0 (E)		-1.20 (E)	
	9877.54	315.918	0.06	21.4 (E)		-1.49 (E)	
	10578.68	323.076	0.11	39.3 (E)		-1.21 (E)	
42267.86	4078.94	261.778	0.5	129 (D+)		-0.88 (D+)	
τ (ns) = 23.3(13)	6323.91	278.129	0.33	85.0 (D+)		-1.01 (D+)	
	9877.54	308.644	0.09	23.2 (E)		-1.48 (E)	
42279.28	2834.98	253.446	0.89	120 (C+)		-0.94 (C+)	
τ (ns) = 74.0(27)							
43176.15	0	231.538	0.09	36.5 (E)		-1.53 (E)	
τ (ns) = 19.7(9)	5784.62	267.361	0.15	60.9 (E)		-1.19 (E)	
	6323.91	271.274	0.14	56.8 (E)		-1.20 (E)	
	9877.54	300.225	0.14	56.8 (E)		-1.11 (E)	
	12218.47	322.929	0.18	73.1 (E)		-0.94 (E)	
	13087.9	332.26	0.2	81.2 (D+)		-0.87 (D+)	
43529.21	2834.98	245.281	0.07	9.96 (E)		-2.04 (E)	
τ (ns) = 56.2(56)	5784.62	264.418	0.1	14.2 (E)		-1.82 (E)	
	7106.61	274	0.07	9.96 (E)		-1.95 (E)	
	9877.54	296.52	0.05	7.12 (E)		-2.02 (E)	
	13087.9	327.729	0.17	24.2 (E)		-1.41 (E)	
	13939.8	337.144	0.09	12.8 (E)		-1.66 (E)	
44596.77	4078.94	246.73	0.31	106 (D+)		-1.01 (D+)	
τ (ns) = 17.5(14)	9877.54	287.941	0.36	123 (D+)		-0.82 (D+)	
	12951.67	315.914	0.09	30.9 (E)		-1.34 (E)	
	13087.9	317.279	0.06	20.6 (E)		-1.51 (E)	
44642.67	2834.98	239.117	0.51	530 (D+)		-0.34 (D+)	
τ (ns) = 7.7(5)	12218.47	308.322	0.11	114 (E)		-0.79 (E)	
	12951.67	315.456	0.07	72.7 (E)		-0.97 (E)	
	13087.9	316.817	0.14	145 (E)		-0.66 (E)	
44652.43	0	223.882	0.15	123 (E)		-1.03 (E)	
τ (ns) = 12.2(8)	2834.98	239.062	0.31	254 (D+)		-0.66 (D+)	
	6323.91	260.824	0.11	90.2 (E)		-1.04 (E)	
	7106.61	266.262	0.34	279 (D+)		-0.53 (D+)	
	13087.9	316.719	0.07	57.4 (E)		-1.06 (E)	
44785.44	9877.54	286.384	0.17	95.8 (E)		-0.93 (E)	
τ (ns) = 7.1(4)	12218.47	306.971	0.27	152 (D+)		-0.67 (D+)	
	12951.67	314.041	0.1	56.3 (E)		-1.08 (E)	
	16103.32	348.549	0.14	78.9 (E)		-0.84 (E)	
	16681.2	355.716	0.15	84.5 (E)		-0.79 (E)	

Table 5.1: Continued

Upper Level[a] E (cm^{-1}	Lower Level[a] E (cm^{-1}	λ_{air} (nm)	BF	gA (10^6s^{-1}) This work	Previous([b]	log gf This work	Previous[c]
45111.68	5784.62	254.202	0.07	31.3 (E)		-1.51 (E)	
τ (ns) = 17.9(8)	7106.61	263.051	0.08	35.8 (E)		-1.43 (E)	
	9877.54	283.739	0.25	112 (D+)		-0.87 (D+)	
	12218.47	303.932	0.42	188 (D+)		-0.58 (D+)	
	13087.9	312.18	0.07	31.3 (E)		-1.34 (E)	
45185.95	7106.61	262.532	0.51	294 (D+)		-0.52 (D+)	
τ (ns) = 10.4(3)	11831.09	299.719	0.07	40.4 (E)		-1.26 (E)	
	12218.47	303.241	0.16	92.3 (E)		-0.89 (E)	
	13087.9	311.455	0.07	40.4 (E)		-1.23 (E)	
45259.14	4078.94	242.761	0.16	38.1 (E)		-1.47 (E)	
τ (ns) = 16.8(5)	5784.62	253.252	0.23	54.8 (D+)		-1.28 (D+)	
	9877.54	282.55	0.08	19.0 (E)		-1.64 (E)	
	11831.09	299.063	0.34	80.9 (D+)		-0.96 (D+)	
45570.89	4078.94	240.938	0.63	289 (C)		-0.61 (C)	
τ (ns) = 13.1(4)	5784.62	251.267	0.06	27.5 (E)		-1.59 (E)	
	9877.54	280.081	0.15	68.7 (E)		-1.10 (E)	
45895.85	0	217.817	0.23	242 (D+)		-0.76 (D+)	
τ (ns) = 7.6(2)	7106.61	257.726	0.27	284 (D+)		-0.55 (D+)	
	13087.9	304.715	0.28	295 (D+)		-0.39 (D+)	
	13939.8	312.839	0.11	116 (E)		-0.77 (E)	
46220.32	0	216.287	0.36	316 (D+)		-0.65 (D+)	
τ (ns) = 11.4(6)	2834.98	230.422	0.28	246 (D+)		-0.71 (D+)	
	6323.91	250.574	0.05	43.9 (E)		-1.38 (E)	
	13087.9	301.731	0.26	228 (D+)		-0.51 (D+)	
46371.64	0	215.581	0.45	199 (D+)		-0.86 (D+)	
τ (ns) = 22.6(8)	2834.98	229.62	0.08	35.4 (E)		-1.55 (E)	
	6323.91	249.627	0.14	61.9 (E)		-1.24 (E)	
	7106.61	254.604	0.2	88.5 (D+)		-1.06 (D+)	
	13087.9	300.359	0.09	39.8 (E)		-1.27 (E)	
47165.12	5784.62	241.587	0.06	33.6 (E)		-1.53 (E)	
τ (ns) = 14.3(8)	6323.91	244.777	0.24	134 (D+)		-0.92 (D+)	
	7106.61	249.56	0.11	61.5 (E)		-1.24 (E)	
	12218.47	286.066	0.36	201 (D+)		-0.61 (D+)	
	13087.9	293.365	0.07	39.2 (E)		-1.30 (E)	
47205.57	0	211.772	0.09	28.4 (E)		-1.72 (E)	
τ (ns) = 31.7(11)	2834.98	225.305	0.05	15.8 (E)		-1.92 (E)	
	6323.91	244.534	0.12	37.9 (E)		-1.47 (E)	
	7106.61	249.308	0.64	202 (E)		-0.73 (E)	
	13939.8	300.521	0.06	18.9 (E)		-1.59 (E)	
47548.69	0	210.244	0.17	62.7 (E)		-1.38 (E)	
τ (ns) = 21.7(7)	2834.98	223.576	0.23	84.8 (D+)		-1.20 (D+)	
	9877.54	265.376	0.07	25.8 (E)		-1.56 (E)	
	12218.47	282.961	0.13	47.9 (E)		-1.24 (E)	
	16103.32	317.92	0.19	70.0 (E)		-0.97 (E)	
47858.47	0	208.883	0.89	2886 (C+)		0.28 (C+)	
τ (ns) = 3.7(3)	2834.98	222.037	0.11	357 (E)		-0.58 (E)	
48206.57	4078.94	226.545	0.16	116 (E)		-1.05 (E)	
τ (ns) = 8.3(7)	6323.91	238.689	0.3	217 (D+)		-0.73 (D+)	
	9877.54	260.821	0.15	108 (E)		-0.96 (E)	
	10578.68	265.681	0.16	116 (E)		-0.91 (E)	
	12951.67	283.566	0.09	65.1 (E)		-1.11 (E)	
	18547.04	337.063	0.05	36.1 (E)		-1.21 (E)	
48440.83	10578.68	264.037	0.07	45.2 (E)		-1.32 (E)	
τ (ns) = 6.2(2)	11831.09	273.07	0.62	400 (C)		-0.35 (C)	
	12505.68	278.197	0.1	64.5 (D)		-1.13 (D)	
48448.65	5784.62	234.317	0.09	84.7 (E)		-1.16 (E)	
τ (ns) = 8.5(3)	6323.91	237.318	0.55	517 (D+)		-0.36 (D+)	
	7106.61	241.812	0.14	132 (E)		-0.94 (E)	
	12218.47	275.931	0.1	94.1 (E)		-0.97 (E)	
48629.22	0	205.572	0.06	76.2 (E)		-1.32 (E)	
τ (ns) = 6.3(3)	2834.98	218.3	0.45	571 (D+)		-0.39 (D+)	
	5784.62	233.33	0.24	305 (D+)		-0.60 (D+)	
	7106.61	240.76	0.09	114 (E)		-1.00 (E)	
	9877.54	257.976	0.05	63.5 (E)		-1.20 (E)	
49779.37	4078.94	218.748	0.15	81.8 (E)		-1.23 (E)	
τ (ns) = 11.0(6)	6323.91	230.05	0.1	54.5 (E)		-1.36 (E)	
	7106.61	234.27	0.18	98.2 (E)		-1.09 (E)	
	10578.68	255.021	0.12	65.5 (E)		-1.20 (E)	
	13087.9	272.462	0.16	87.3 (E)		-1.01 (E)	
	16565.35	300.99	0.08	43.6 (E)		-1.23 (E)	
	18547.04	320.089	0.08	43.6 (E)		-1.17 (E)	
49823.54	5784.62	227.002	0.29	143 (D+)		-0.96 (D+)	
τ (ns) = 16.2(5)	6323.91	229.816	0.31	153 (D+)		-0.92 (D+)	
	9877.54	250.263	0.15	74.1 (E)		-1.16 (E)	
	19060.62	324.973	0.09	44.4 (E)		-1.15 (E)	

a: From the NIST database [28].
b: From Gough *et al.* [123].
c: From Xu *et al.* [124].

The estimated uncertainties of the transition probabilities and oscillator strengths obtained in our work are also reported in Table 5.1. We used the same code letter as the one usually employed in the NIST database (see [28]). To determine them, we assigned an uncertainty to all our calculated HFR+CPOL BF-values by comparing them to those deduced from experimental measurements by Gough *et al.* [123] and Ivarsson *et al.* [117] for some transitions depopulating Ir I levels (up to 40710 cm^{-1}). This is illustrated in Figure 5.3 where the relative differences $\frac{BF_{calc}-BF_{exp}}{BF_{calc}}$ are reported against BF_{calc}. This figure clearly shows a regular pattern of increasingly deviating weak branches, the average uncertainties on calculated BF-values being found to be about 10%, for $0.8 < BF_{calc} < 1.0$, 20% for $0.6 < BF_{calc} < 0.8$, 30% for $0.4 < BF_{calc} < 0.6$, 40% for $0.2 < BF_{calc} < 0.4$ and 100% for $0.0 < BF_{calc} < 0.2$.

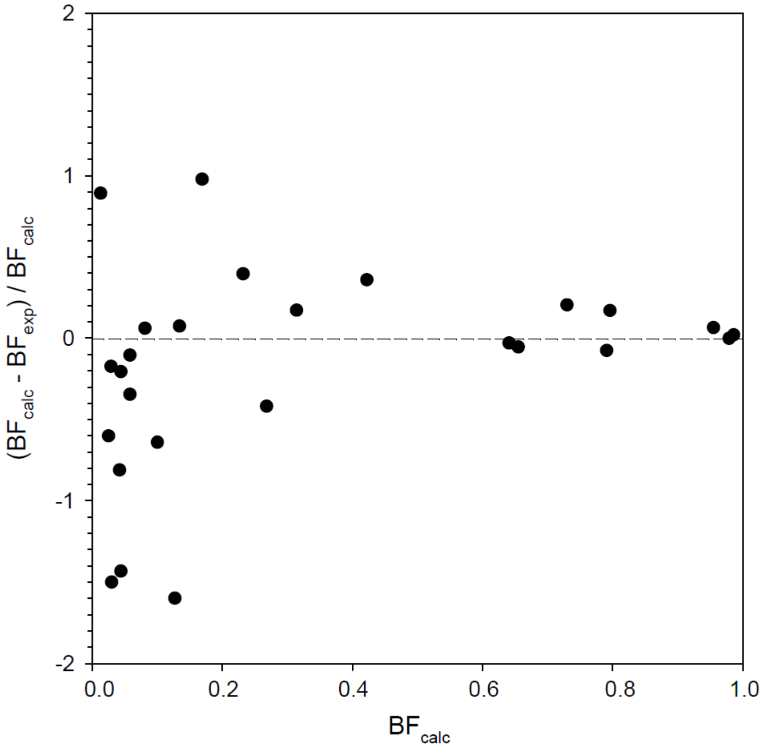

Figure 5.3: Comparison between calculated and experimental BFs in order to determine an uncertainty on the chosen value for BF

All that data represents new reliable semi-empirical atomic data that can be of use for the astrophysicists in Ir I.

5.2.2 Ir II

Ivarsson *et al.* [122] used the time-resolved laser-induced fluorescence (TR-LIF) technique to measure the radiative lifetimes for nine odd-parity levels of Ir II, and combined them with BFs determined by Fourier's transform spectroscopic measurements to obtain the oscillator strengths and transition probabilities of 23 transitions of Ir II. Based on that data, they determined the abundance of iridium in the CP star χ Lupi.

Among the 76 energy levels of Ir II included in the NIST Atomic Spectroscopy Database [28], the experimental lifetimes of a total of 10 levels in the energy range 44575.66–52510.1 cm^{-1} have been published so far. Our experimental collaborators from the University of Jilin in China measured the radiative lifetimes of 15 highly excited levels falling between 47003 and 61475 cm^{-1} by TR-LIF technique. Among those 15 levels, only four of them have their experimental lifetimes reported in the literature. The new radiative lifetime data that they obtained was combined with branching fractions deduced from a HFR+CPOL calculation that we performed to determine semi-empirical transition probabilities and oscillator strengths for 124 Ir II spectral lines.

More precisely, the physical model we considered in our HFR+CPOL calculation was represented by the $5d^76s$, $5d^77s$, $5d^76d$, $5d^66s^2$, $5d^66p^2$, $5d^66s7s$, $5d^66s6d$, $5d^56s^27s$, $5d^56s^26d$ and $5d^8$ even-parity configurations, and $5d^76p$, $5d^77p$, $5d^75f$, $5d^66s6p$, $5d^66s7p$, $5d^66s5f$ and $5d^56s26p$ odd-parity configurations. The core-polarization effects corresponding to a Ta-like ionic core were considered using the dipole polarizabilty of Ir V [94], i.e. α_d = 4.59 a.u., and a cut-off radius, r_c = 1.61 a.u., which corresponds to the expected value of $< r >$ for the outermost core orbital, i.e. 5d, as obtained with Cowan code.

The BFs, gA and log gf for highly excited levels of Ir II are listed in Table 5.2 with the previous available reported results in order to compare them. The lifetimes shown in that table are the experimental ones but one should note that for the 15 levels considered, the agreement between the experimental and theoretical values for the lifetimes was excellent. To be precise the ratio (between the experimental and theoretical values) was found to be equal to 1.05 ± 0.14 with, as expected a clear core polarization effect lengthening the HFR radiative rates, making them therefore closer to the experimental values.

The results of BFs determined by our HFR+CPOL calculation were combined with the experimental lifetimes obtained by our colleagues of the University of Jilin to deduce the gA and log gf for all transitions with $BF > 0.01$ by the Eq. 5.1 and 5.2. Ivarsson *et al.* [122] measured BFs and transition probabilities for eight transitions which were also investigated in the present work, and our results are in agreement within 40%. The uncertainties affecting our gA- and gf-values were estimated by combining experimental lifetime uncertainties with those evaluated for theoretical branching fraction calculations exactly as we did for Ir I.

Once again (exactly as for Ir I), the average uncertainties on computed BF-values were systematically found to be around 10-20% for $0.8 < BF < 1.0$, 20-30% for $0.6 < BF < 0.8$, 30-40% for $0.4 < BF < 0.6$, 40-50% for $0.2 < BF < 0.4$, and 50-100 % for $0.0 < BF < 0.2$. The uncertainties affected the results presented in Table 5.2 are given using the same letter convention as the one used for Ir I which is the one usually employed in the NIST database [28], i.e. B ($\leq$ 10 %), C ($\leq$25%), D+ ($\leq$40 %), D ($\leq$50 %), and E (>50 %).

The radiative data that we presented in this section largely supplements the laconic literature of radiative data of the Ir II ion especially for high-excited states, which are of great significance in order to understand the radiative properties and could have an importance on the astronomical spectral analyses of stellar spectra.

Table 5.2: Branching fractions, transition probabilities, oscillator strengths for highly excited levels of Ir II, and comparison with available data in the literature

Upper level[a] E (cm^{-1}) Lifetime (ns)	Lower level[a] E (cm-1)	λ^b (nm)	BFs This work	BFs Previous Exp[c]	BFs Cal.[d]	gA ($10^7 s^{-1}$) This work	gA Previous Exp.[c]	gA Cal.[d]	Log(gf) This work	Log(gf) Previous Exp.[c]
47003.95	0	212.681	0.736	0.688	0.738	197.44(C+)	172.07	189.74*	0.13 (C+)	0.07
τ =4.1(3)	4787.92	236.805	0.181	0.26	0.181	48.65 (E)	64.91	46.67*	-0.39 (E)	-0.26
	11719.11	283.325	0.064		0.064	17.10 (E)		16.40*	-0.69 (E)	
	19279.04	360.584	0.011		0.011	2.88 (E)		2.76*	-1.25 (E)	
50302.01	0	198.799	0.487	0.637	0.491	12.90 (C)	16.87	12.83*	-1.12 (C)	-1
τ = 34(3)	2262.84	208.097	0.014		0.014	0.38 (E)		0.38*	-2.60 (E)	
	4787.92	219.643	0.253	0.3	0.253	6.71 (D+)	7.93	6.63*	-1.31 (D+)	–1.24
	8186.89	237.373	0.019		0.019	0.50 (E)		0.50*	-2.37 (E)	
	11719.11	259.105	0.053		0.053	1.40 (E)		1.39*	-1.85 (E)	
	12714.66	265.968	0.016		0.016	0.43 (E)		0.42*	-2.34 (E)	
	17210.16	302.101	0.052		0.052	1.37 (E)		1.35*	-1.73 (E)	
	17477.99	304.565	0.038		0.038	1.01 (E)		1.01*	-1.85 (E)	
	19279.04	322.249	0.047		0.047	1.23 (E)		1.22*	-1.72 (E)	
51333	0	194.806	0.606	0.845	0.606	12.57 (C+)	17.87	12.82*	-1.15 (C+)	-0.99
τ =53(3)	4787.92	214.778	0.021		0.021	0.43 (E)		0.45*	-2.52 (E)	
	17210.16	292.973	0.214		0.215	4.45 (D+)		4.54*	-1.24 (D+)	
	19279.04	311.884	0.133		0.133	2.75 (E)		2.81*	-1.40 (E)	
51371.97	3090.16	207.051	0.154		0.154	11.63 (E)		11.71*	-1.13 (E)	
τ =6.6(4)	8186.89	231.491	0.288	0.25	0.288	21.78 (D+)	18.96	21.88*	-0.76 (D+)	-0.82
	8974.95	235.794	0.161	0.146	0.161	12.16 (E)	11.07	12.23*	-0.99 (E)	-1.03
	12714.66	258.606	0.291	0.469	0.291	22.04 (D+)	35.54	22.14*	-0.66 (D+)	-0.45
	15676.25	280.063	0.069		0.069	5.25 (E)		5.27*	-1.21 (E)	
	18944.91	308.295	0.013		0.013	0.95 (E)		0.95*	-1.87 (E)	
53678.68	3090.16	197.673	0.017		0.017	1.37 (E)		1.24	-2.10 (E)	
τ =6.3(10)	8186.89	219.751	0.501		0.502	39.79 (C)		36.13	-0.54 (C)	
	8974.95	223.626	0.08		0.08	6.32 (E)		5.73	-1.32 (E)	
	9062.22	224.062	0.041		0.041	3.28 (E)		2.98	-1.61 (E)	
	11307.53	235.936	0.083		0.083	6.61 (E)		5.99	-1.26 (E)	
	11957.83	239.615	0.017		0.017	1.38 (E)		1.25	-1.93 (E)	
	12714.66	244.043	0.059		0.059	4.70 (E)		4.26	-1.38 (E)	
	17499.26	276.318	0.134		0.134	10.63 (E)		9.64	-0.91 (E)	
	18944.91	287.82	0.013		0.013	1.01 (E)		0.91	-1.90 (E)	
	20440.64	300.772	0.02		0.02	1.58 (E)		1.43	-1.67 (E)	
53691.38	0	186.25	0.314		0.315	101.55 (D+)		133.3	-0.28 (D+)	
τ =3.4(3)	2262.84	194.444	0.056		0.056	18.24 (E)		20.25	-0.99 (E)	
	4787.92	204.419	0.494		0.495	159.97 (C)		178.1	0.00 (C)	
	11719.11	238.179	0.111		0.111	35.86 (E)		39.93	-0.52 (E)	
	17210.16	274.032	0.013		0.013	4.30 (E)		4.78	-1.32 (E)	
	22266.92	318.132	0.005		0.005	1.63 (E)		1.81	-1.61 (E)	
55852.5	2262.84	186.603	0.015		0.015	1.86 (E)		1.49	-2.01 (E)	
τ =5.8(3)	4787.92	195.83	0.034		0.034	4.15 (E)		3.32	-1.62 (E)	
	8186.89	209.728	0.062		0.062	7.47 (E)		5.98	-1.31 (E)	
	8974.95	213.255	0.207		0.207	24.99 (D+)		20.04	-0.77 (D+)	
	9927.84	217.68	0.026		0.026	3.19 (E)		2.55	-1.64 (E)	
	11307.53.	224.421	0.045		0.045	5.47 (E)		4.38	-1.38 (E)	
	11719.11	226.516	0.14		0.14	16.87 (E)		13.52	-0.89 (E)	
	12714.66	231.744	0.133		0.132	15.99 (E)		12.77	-0.89 (E)	
	15676.25	248.829	0.094		0.094	11.36 (E)		9.09	-0.98 (E)	
	17499.26	260.656	0.093		0.093	11.24 (E)		9	-0.94 (E)	
	18944.91	270.867	0.095		0.095	11.43 (E)		9.15	-0.90 (E)	
	25563.67	330.06	0.014		0.014	1.65 (E)		1.32	-1.57 (E)	
56233.93	0	177.829	0.127		0.127	34.70 (E)		28.45	-0.78 (E)	
τ =3.3(2)	2262.84	185.284	0.06		0.06	16.31 (E)		13.37	-1.08 (E)	
	4787.92	194.379	0.111		0.111	30.32 (E)		24.93	-0.77 (E)	
	8186.89	208.064	0.084		0.084	23.01 (E)		18.93	-0.83 (E)	
	11719.11	224.574	0.26		0.26	70.98 (D+)		58.29	-0.27 (D+)	
	12714.66	229.712	0.063		0.063	17.05 (E)		14.01	-0.87 (E)	
	17210.16	256.177	0.027		0.026	7.23 (E)		5.94	-1.15 (E)	
	17477.99	257.947	0.215		0.215	58.69 (D+)		48.15	-0.23 (D+)	
	19279.04	270.52	0.018		0.018	4.91 (E)		4.03	-1.27 (E)	
56241.53	3090.16	188.142	0.039		0.039	1.36 (E)		1.75	-2.14 (E)	
τ =8.5(4)	8974.95	211.499	0.011		0.011	0.40 (E)		0.51	-2.57 (E)	
	9062.22	211.89	0.058		0.058	2.06 (E)		2.65	-1.86 (E)	
	11307.53	222.479	0.193		0.193	6.83 (D+)		8.75	-1.30 (D+)	
	11957.83	225.746	0.417		0.417	14.73 (C)		18.9	-0.95 (C)	
	15676.25	246.442	0.11		0.11	3.89 (E)		4.99	-1.45 (E)	
	17413.25	257.467	0.038		0.038	1.33 (E)		1.71	-1.88 (E)	
	18676.49	266.126	0.051		0.051	1.82 (E)		2.32	-1.71 (E)	
	18944.91	268.041	0.02		0.02	0.69 (E)		0.89	-2.13 (E)	
	22467.78	296.002	0.035		0.035	1.23 (E)		1.58	-1.79 (E)	
56354.21	8186.89	207.544	0.19			10.2 (D+)			-1.18 (D+)	
τ =9.3(3)	9927.84	215.327	0.021			1.12 (E)			-2.11 (E)	
	11957.83	225.173	0.049			2.63 (E)			-1.70 (E)	
	12714.66	229.079	0.57			30.66 (C)			-0.62 (C)	
	17499.26	257.291	0.049			2.63 (E)			-1.58 (E)	
	18676.49	265.33	0.044			2.36 (E)			-1.60 (E)	
	23727.67	306.41	0.021			1.16 (E)			-1.79 (E)	
	25563.67	324.682	0.015			0.80 (E)			-1.90 (E)	
56644.46	8186.89	206.3	0.018			1.92 (E)			-1.91 (E)	
τ =4.6(4)	8974.95	209.711	0.103			11.16 (E)			-1.13 (E)	
	9062.22	210.095	0.116			12.60 (E)			-1.08 (E)	
	11307.53	220.501	0.419			45.59 (C)			-0.48 (C)	
	11957.83	223.711	0.186			20.20 (D+)			-0.82 (D+)	
	15676.25	244.018	0.058			6.33 (E)			-1.25 (E)	
	17499.26	255.382	0.019			2.10 (E)			-1.69 (E)	
	18944.91	265.176	0.021			2.33 (E)			-1.61 (E)	
	22467.78	292.511	0.033			3.56 (E)			-1.34 (E)	
56875.79	9062.22	209.079	0.728		0.728	13.23 (C+)		14.68	-1.06 (C+)	
τ =5.5(3)	18676.49	261.707	0.197		0.197	3.58 (D+)		3.98	-1.43 (D+)	
	20440.64	274.379	0.06		0.06	1.09 (E)		1.2	-1.91 (E)	
59132.98	3090.16	178.435	0.022		0.022	1.85 (E)		1.74	-2.06 (E)	

Table 5.2: Continued

Upper level[a] E (cm^{-1}) Lifetime (ns)	Lower level[a] E (cm-1)	λ^b (nm)	BFs This work	BFs Previous Exp[c]	BFs Cal.[d]	gA ($10^7 s^{-1}$) This work	gA Previous Exp.[c]	gA Cal.[d]	Log(gf) This work	Log(gf) Previous Exp.[c]
τ =5.9(3)	8186.89	196.286	0.146		0.146	12.41 (E)		11.68	-1.14 (E)	
	8974.95	199.37	0.185		0.186	15.7 (D+)		14.81	-1.03 (D+)	
	9062.22	199.717	0.303		0.303	25.67 (D+)		24.2	-0.81 (D+)	
	9927.84	203.166	0.056		0.056	4.74 (E)		4.47	-1.53 (E)	
	11307.53	209.027	0.045		0.046	3.85 (E)		3.63	-1.60 (E)	
	11957.83	211.908	0.047		0.047	3.99 (E)		3.75	-1.57 (E)	
	17499.26	240.117	0.06		0.06	5.08 (E)		4.79	-1.36 (E)	
	17413.25	239.622	0.014		0.014	1.21 (E)		1.14	-1.98 (E)	
	18944.91	248.755	0.02		0.02	1.69 (E)		1.59	-1.81 (E)	
	22467.78	272.657	0.012		0.012	1.00 (E)		0.94	-1.95 (E)	
	28600.34	327.424	0.01		0.01	0.85 (E)		0.8	-1.86 (E)	
60313.63	2262.84	172.263	0.055			11.32 (E)			-1.30 (E)	
τ =3.4(3)	4787.92	180.097	0.013			2.68 (E)			-1.89 (E)	
	8186.89	191.84	0.302			62.18 (D+)			-0.46 (D+)	
	8974.95	194.785	0.125			25.74 (E)			-0.83 (E)	
	11719.11	205.719	0.244			50.24 (D+)			-0.50 (D+)	
	15676.25	223.958	0.027			5.56 (E)			-1.38 (E)	
	17499.26	233.495	0.062			12.76 (E)			-0.98 (E)	
	18944.91	241.655	0.02			4.12 (E)			-1.44 (E)	
	20294.25	249.804	0.062			12.76 (E)			-0.92 (E)	
	23727.61	273.248	0.028			5.76 (E)			-1.19 (E)	
61474.19	2262.84	168.886	0.032			5.73 (E)			-1.61 (E)	
τ =3.9(3)	3090.16	171.28	0.262			47.06 (D+)			-0.68 (D+)	
	8186.89	187.662	0.03			5.41 (E)			-1.54 (E)	
	11307.53	199.335	0.092			16.59 (E)			-1.01 (E)	
	11719.11	200.919	0.022			3.99 (E)			-1.62 (E)	
	12714.66	205.022	0.142			25.46 (E)			-0.79 (E)	
	15676.25	218.283	0.122			21.81 (E)			-0.81 (E)	
	17210.16	225.847	0.104			18.68 (E)			-0.84 (E)	
	17413.25	226.888	0.077			13.77 (E)			-0.97 (E)	
	18944.91	235.06	0.033			5.91 (E)			-1.31 (E)	
	19279.04	236.922	0.013			2.34 (E)			-1.71 (E)	
	22467.78	256.291	0.026			4.74 (E)			-1.33 (E)	

a: Energy levels from the NIST database [28].
b: λ above 200 nm given in air and inn vacuum below.
c: From Ivarsson *et al.* [122].
d: From Xu *et al.* [124].

5.3 Re I

The framework for this section is exactly the same as for the previous ones: in collaboration with the University of Jilin in China, we combined their TR-LIF experimental radiative lifetimes with our theoretical branching fractions in order to obtain reliable semi-empirical transition probabilities and oscillator strengths in neutral rhenium. Exactly as for Ir I, Ir II, we did not participate to the experimental part of this work.

Rhenium (Z = 75) was discovered in 1925 in Germany and was named after the river Rhine (in latin *Rhenus*). Rhenium was actually the last stable element to be discovered. It is even one of the very last natural elements to be discovered, before francium, technetium and astatine, which are short-lived radioactive and exist only in trace amounts on Earth [125].

In this section, we will focus on the determination of radiative parameters in neutral rhenium (Re I, $Z = 75$) which has already been observed in peculiar stars (see e.g. Guthrie *et al.* [126]) and on which too few works have focused, resulting in a relatively incomplete set of atomic data in the literature.

The first extended experimental analysis of neutral rhenium's spectrum is the one of Klinkenberg *et al.* [127]. They classified 2764 lines between 171 and 1162 nm with transitions observed among 282 atomic energy levels. However, they only considered the configurations $5d^56s^2$ and $5d^66s$ in their least-squares fit of the energy levels and these two-configuration calculations resulted in a rather high average deviation of 371 cm^{-1}. More than 20 years later, the inclusion of the $5d^7$ configuration by Wyart [128] significantly reduced this deviation to 89 cm^{-1}.

In our calculation, we introduced the following configurations: $5d^6ns$, $5d^56sns$, $5d^7$, $5d^66d$, $5d^56s6d$, $5d^46s^26d$, $5d^56p^2$ and $5d^46s6p^2$ (n = 6–8) in the even parity and $5d^6np$, $5d^56snp$, 5d^{4}6s26p and $5d^46p^3$ (n = 6–8) in the odd parity exactly as in Palmeri *et al.* [129]. We considered a $5d^4$ (Re IV) ionic core surrounded by three valence electrons. The dipole polarizability was adopted from tabulated values from Fraga *et al.* [94], i.e. 6.81 au. The cut-off radius used was the HFR mean radius of the 5d orbital in the Re I ground configuration, i.e. 1.87 a.u.

The HFR + CPOL method was then combined with a least-squares optimization fitting procedure minimizing the discrepancies between calculated and experimental energy levels published by Klinkenberg *et al.* [127] and Wyart [128] . The average mean deviations of those fits were found to be 88 and 176 cm^{-1} for the even and odd parity respectively.

As one can see, this calculation is exactly the same as the one performed by Palmeri *et al.* [129]. This previous calculation was very accurate and no new experimental level would have justified a different analysis. However, thanks to the new radiative lifetimes measured at the University of Jilin, we were able to extract new branching fractions from that calculation that have been combined with the new radiative lifetimes to produce brand new reliable transition probabilities and oscillator strengths using the method explained in Section 5.2 and the Eq. 5.1 and 5.2. Palmeri *et al.* [129] already did something similar in their paper but with a smaller number of measured radiative lifetimes and therefore a smaller number of gA and gf given. Our values and the comparison between them and what already existed in the literature is given in Table 5.3. The uncertainty for our values is given using the NIST code [28] as in Ir I, II in the previous sections.

It is worth remembering that carrying out accurate calculations in such a complex heavy neutral atom as Re I with a large number of overlapping configurations is a very challenging task. In Re I, a strong configuration interaction is also present for the low-lying levels [129] and even more so for the high-lying ones measured in this study as highlighted in Table 5.4. The major LS components are to be found equal to 20 % or even less. This has consequences on the calculation of the line strengths of depopulating channels and

Table 5.3: New reliable BF, gA and log gf obtained for Re I

Upper level[a]		Lower level[a]		λ (air)	BF	gA ($10^6 s^{-1}$)		log gf	
E (cm^{-1})	J	E(cm^{-1})	J	(nm)		This work	Previous[b]	This work	Previous[b]
32592	1.5	0	2.5	306.738	0.804	24.4 (C)	24.0	-1.47	-1.47
τ = 132(8) ns									
41557	1.5	0	2.5	240.56	0.669	84.1 (D+)	74.2	-1.12	- 1.19
τ = 31.6(15) ns		17238	0.5	441.089	0.150	18.9(E)	16.7	-1.29	-1.37
41844	3.5	11755	4.5	332.2481	0.664	68.7(D+)	-	-0.95	-
τ= 77.3 ns		15770	2.5	383.4234	0.149	15.4(E)	-	-1.47	-
42254	1.5	0	2.5	332.248	0.441	90.1 (D+)	-	-0.95	-
τ = 19.6(8)		11584	2.5	325.955	0.236	48.1 (D)	-	-1.12	-
		13826	1.5	351.664	0.148	30.3(E)	-	-1.25	-
43044	2.5	14217	3.5	346.796	0.198	42.0(E)	-	-1.12	-
τ = 28.3(8) ns									
43342	1.5	14621	2.5	348.085	0.551	56.6(D+)	-	-0.98	-
τ= 38.9(15) ns		17238	0.5	382.981	0.21	21.6(D+)	-	-1.32	-
43815	3.5	0	2.5	228.1619	0.648	274(C)	-	-0.67	-
τ= 18.9(7) ns		11755	4.5	311.82	0.234	98.9(D+)	-	-0.85	-
49350	2.5	14217	3.5	336.2287	0.373	226(D)	-	-0.42	-
τ= 9.9(7) ns		14621	2.5	340.8672	0.159	96.3(E)	-	-0.77	-
		0	2.5	227.4611	0.18	109(E)	-	-1.07	-
45876	1.5	0	2.5	217.909	0.753	78.9(C)	-	-1.25	-
τ= 38.2(16) ns									
45937	3.5	0	2.5	217.6204	0.724	460(C)	-	-0.49	-
τ = 12.6(10) ns									
46112	2.5	0	2.5	216.7941	0.526	304(D+)	-	-0.67	-
τ= 10.4(6) ns		14621	2.5	317.4614	0.21	121(D+)	-	-0.74	-
46353	3.5	14217	3.5	311.086	0.411	154(D+)	-	-0.65	-
τ= 21.4(9) ns		0	2.5	215.668	0.275	103(D+)	-	-1.14	-
		15770	2.5	326.8894	0.116	43.3(E)	-	-1.16	-
46509	2.5	17331	3.5	342.6189	0.205	60.1(D+)	-	-0.97	-
τ= 20.5(10) ns		0	2.5	214.9426	0.455	133(D+)	-	-1.03	-
		15058	3.5	317.8608	0.123	35.9(E)	-	-1.26	-
46649	2.5	14217	3.5	308.2426	0.476	182(D+)	-	-0.58	-
τ= 15.7(9) ns		0	2.5	214.2974	0.326	124(D)	-	-1.06	-
46733	1.5	0	2.5	213.9124	0.611	136(C)	-	-1.03	-
τ= 18.0(6) ns		16328	1.5	328.7891	0.165	36.6(E)	-	-1.23	-
47102	2.5	14217	3.5	304.0039	0.161	59.6(E)	-	-1.08	-
τ= 16.2(6) ns		16328	1.5	324.8549	0.115	42.6(E)	-	-1.17	-
		17331	3.5	335.8032	0.122	45.4(E)	-	-1.11	-
		11584	2.5	281.4673	0.183	67.7(E)	-	-1.09	-
		15770	2.5	319.0785	0.128	47.4(E)	-	-1.14	-
47358	3.5	0	2.5	211.0891	0.493	94.9(D+)	-	-1.20	-
τ= 41.6(17) ns		15058	3.5	309.506	0.15	28.8(E)	-	-1.38	-
47971	2.5	14621	2.5	299.7684	0.387	94.8(E)	-	-0.89	-
τ= 24.5(25) ns		16328	1.5	315.9311	0.163	39.9(E)	-	-1.22	-
		15770	2.5	310.4651	0.171	42(E)		-1.22	-

a: From NIST database [28]
b: Palmeri *et al.* [129]

therefore on the corresponding theoretical lifetimes, hence the interest in producing semi-empirical data by combining them with experimental measurements. It allowed us to deduce the semi-empirical transition probabilities gA and oscillator strengths for 47 lines from 18 upper levels in the wavelength range between 204 and 441 nm as shown in Table 5.3. One should note that only the transitions with $BF \geq 0.1$ are given in that table (the other ones being not reliable enough due to cancellation effects).

Table 5.4: LS composition and comparison between experimental and calculated level energies and Landé g-factors, for the Re I odd-parity energy levels involved in the transitions mentioned in Table 5.3

E_{exp}[a]	E_{calc}	J	g^a_{exp}	g_{calc}	LS Composition[b]
32 591.63	32 817	3/2	1.762	1.781	21 B (^{4}D)^{6}D^o + 18 C (^{5}D)^{6}D^o + 9 C (^{5}D)^{4}P^o
41 557.08	40 752	3/2	1.655	1.496	20 B (^{4}P)^{6}D^o + 12 B (^{6}S)6P^o + 8 C (^{5}D)^{6}F^o
41 843.85	41 743	7/2	1.19	1.302	18 B (4 G)6H^o + 8 B (^{6}D)6P^o + 7 B (^{4}D)^{4}F^o
42 254.19	42 499	3/2	1.578	1.489	14 B (^{6}S)^{4}P^o + 11 B (^{4}P)6P^o + 7 C (^{5}D)^{4}P^o
43 44.02	42 997	5/2	1.449	1.446	8 B (^{4}D)^{4}D^o + 7 B (^{4}P)^{6}D^o + 7 B (^{4}D)^{4}D^o
43 341.85	43 340	3/2	0.975	1.032	17 B (^{4}P)^{6}D^o + 9 B (^{2}D)^{4}F^o + 9 B (4 G)^{4}F^o
43 815.01	43 937	7/2	1.348	1.388	14 B (^{6}S)6P^o + 14 B (^{4}G)6G^o + 8 A (^{5}D)6P^o
43 949.98	43 852	5/2	1.385	1.567	19 B (^{4}P)^{6}S^o + 13 B (^{4}D)6P^o + 5 A (^{5}D)^{4}P^o
45 876.34	45 974	3/2	1.384	1.555	14 B (^{4}P)^{6}D^o + 9 C (^{5}D)^{6}F^o + 8 B (^{4}D)^{6}F^o
45 937.18	46 49	7/2	1.298	1.282	11 B (^{6}S)6P^o + 8 B (^{4}G)^{6}F^o + 6 C (^{3}G)^{4}G^o
46 112.24	46 223	5/2	1.405	1.345	20 B (^{4}D)^{6}F^o + 12 B (^{4}P)^{6}D^o + 11 B (^{4}G)^{6}F^o
46 352.99	46 392	7/2	1.271	1.274	15 B (^{4}G)^{6}F^o + 13 B (^{4}D)^{6}F^o + 7 B (^{4}G)6G^o
46 509.4	46 476	5/2	1.371	1.528	17 B (^{6}S)^{4}P^o + 8 B (^{4}P)^{6}S^o + 7 B (^{6}S)6P^o
46 649.42	46 573	5/2	1.334	1.304	15 B (^{4}G)^{6}F^o + 8 C (^{5}D)^{6}F^o + 7 B (^{4}F)^{6}F^o
46 733.38	46 680	3/2	1.858	1.796	18 B (^{4}D)6P^o + 16 B (4 G)^{6}F^o + 14 B (^{4}P)6P^o
47 101.61	46 984	5/2	0.893	0.864	14 B (^{2}F)^{4}G^o + 13 B (^{4}G)^{4}G^o + 10 C (^{3}F)^{4}G^o
47 358.36	47 365	7/2	1.151	1.076	14 B (^{2}F)^{4}G^o + 14 B (^{4}G)^{4}G^o + 8 C (^{3}F)^{4}G^o
47 970.82	47 875	5/2	1.169	1.287	11 B (^{4}G)^{6}F^o + 9 C (^{5}D)^{6}F^o + 7 B (^{4}P)^{6}D^o

a: From [127].
b: First three major components given in %. A, B, and C mean respectively the $5d^66p$, $5d^56s6p$ and $5d^46s^26p$ configurations.

5.4 La I

Lanthanum is a chemical element with an atomic number of Z = 57. Lanthanum gave its name to the family of lanthanides which are part of the rare earths. This element usually occurs together with cerium (as an oxyde) and was first found by the Swedish researcher Carl Gustaf Mosander in 1839 as an impurity in cerium nitrate. The name lanthanum comes from the Ancient Greek *lanthanein*, which means to lie hidden. Even though it is chemically classified as a rare earth element, lanthanum is actually the 28th most abundant element in the Earth's crust, almost three times as abundant as lead. But its etymology comes from the fact that pure lanthanum metal was only first isolated in 1923 [109].

Lanthanides represent a very hot topic in atomic astrophysics since the observation of gravitational waves by the LIGO-VIRGO interferometer in 2017 [130]. Indeed, the radiative parameters can be used for the calculation of the corresponding opacities in the astrophysical context of kilonovae. Those kilonovae result from the coalescence of neutron stars, such as the GW170817 event detected in 2017 [130]. They indeed have a spectrum characterized by many lines belonging to heavy elements among which the lanthanides seem to play an important role. Because of the huge amount of spectral lines in their spectra, their contribution to the observed opacities is high as highlighted by Kasen *et al.* [131]. In order to estimate these opacities, it is therefore essential to have a precise knowledge of the radiative data relating to the very numerous lines belonging to the lanthanide atoms.

Since this work is about low ionization states, we focused on neutral lanthanum, which is described by the 5d6s^2 ^{2}D$_{3/2}$ ground level, while the lowest excited levels belong to many different configurations such as 5d6s^2, 5d^{2}6s, 5d^3, 4f6s6p, 5d^{2}7s and 5d6s7s in the even parity, and 5d6s6p, 5d^{2}6p, 4f5d6s, 6s^{2}6p and 4f6s^2 in the odd one (see [28]). The overlap of these configurations is responsible for the strong mixing of most energy levels, which makes both experimental and theoretical analyses very tricky.

5.4.1 HFR+CPOL Calculations

The first computational procedures that we used in order to model the atomic structure and to calculate the radiative parameters in La I were the HFR [7] and HFR+CPOL [81, 82] ones. Three different physical models were developed in our calculations. For the first model (HFR-NOPOL), only intravalence correlations were considered by explicitly including the following 37 even- and 37 odd-parity configurations, namely 5d6s^2, 5d^{2}6s, 5d^{2}7s, 5d^{2}6d, 5d^3, 5d6p^2, 5d6d^2, 5d7s^2, 5d6s6d, 5d6s7s, 5d6p7p, 5d6d7s, 4f^{2}5d, 4f^{2}6d, 4f^{2}6s, 4f^{2}7s, 4f5d6p, 4f5d7p, 4f6s6p, 4f6s7p, 4f6p6d, 4f6p7s, 4f6d7p, 4f7s7p, 6s^{2}6d, 6s^{2}7s, 6s6p^2, 6s6d^2, 6s7s^2, 6s6p7p, 6s6d7s, 6p^{2}6d, 6p^{2}7s, 6p6d7p, 6p7s7p, 6d7s^2, 7s6d^2, and 5d^{2}6p, 5d^{2}7p, 5d6s6p, 5d6s7p, 5d6p6d, 5d6p7s, 5d6d7p, 5d7s7p, 4f^3, 4f^{2}6p, 4f^{2}7p, 4f5d^2, 4f6s^2, 4f6p^2, 4f6d^2, 4f7s^2, 4f5d6s, 4f5d7s, 4f5d6d, 4f6s6d, 4f6s7s, 4f6p7p, 4f6d7s, 6s^{2}6p, 6s^{2}7p, 6s6p6d, 6s6p7s, 6s6d7p, 6s7s7p, 6p^3, 6p^{2}7p, 6p6d^2, 6p7s^2, 6p6d7s, 6d^{2}7p, 6d7s7p, 7s^{2}7p, respectively. One should note that those multiconfiguration expansions are considerably more extensive than the ones included in a previous HFR calculation performed by the UMONS Atomic Physics and Astrophysics group which was published nearly 20 years ago [132].

In the second model (HFR+CPOL1), the same set of configurations as the one given hereabove was explicitly considered in the computations. In addition, core-polarization effects were estimated by assuming a Xe-like La IV ionic core with the dipole polarizability value reported by Fraga [94] i.e. $\alpha_d = 9.50\ a_0^3$, and a cut-off radius equal to the HFR average value of the outermost core orbital (5p), i.e. $r_c = 1.80\ a_0$.

However, as mentioned, for example, by Hibbert *et al.* [133], the cut-off radius is not an unambiguously defined parameter. Therefore, we differently took into account the core-polarization effects in a third model (HFR+CPOL2), in which we used the same dipole polarizability as the one used in HFR+CPOL1, but with a different value of the cut-off radius, namely $r_c = 1.20\ a_0$, representing the distance at which the total density of probability of the ionic core orbitals falls to 10 % of its maximum value, as suggested by Hameed [84]. This is illustrated in Figure 5.4, which shows the calculated probability density of the La IV ionic core in the ground configuration of the lanthanum atom.

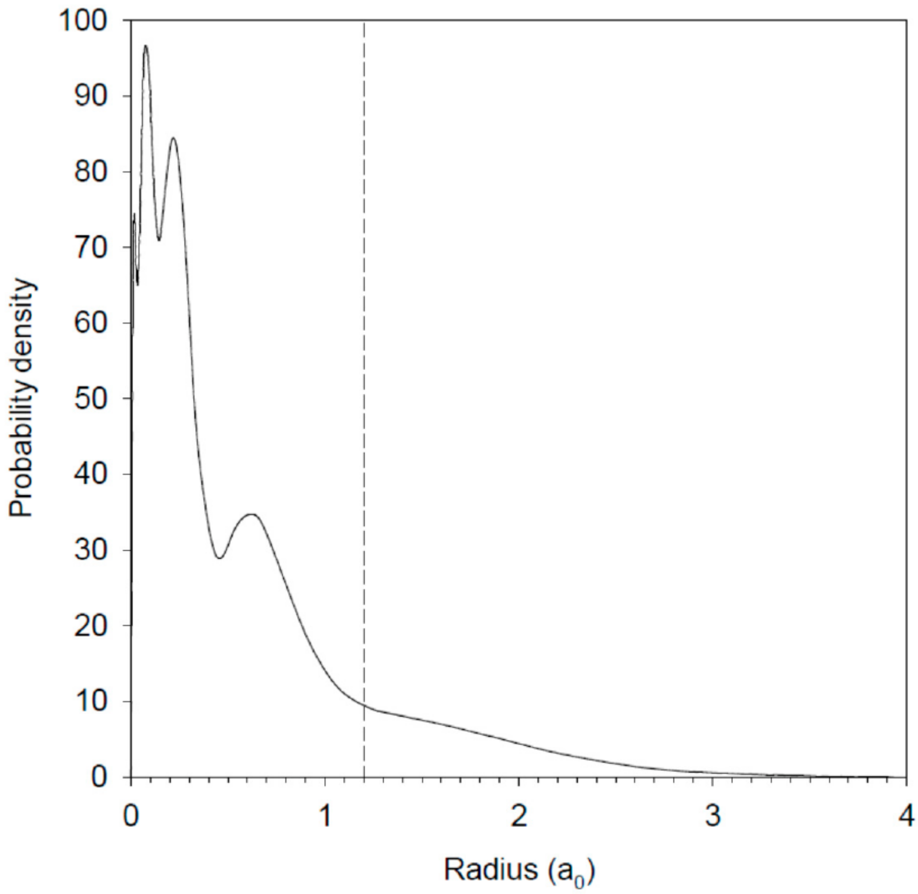

Figure 5.4: Electron probability density of the La IV ionic core in the ground configuration of neutral Lanthanum (5d6s^2). Dashed vertical line marks a radius of $r_c = 1.20\ a_0$.

In each of these three models, the calculated eigenvalues of the Hamiltonian were optimized using the observed energy levels via a least-squares fitting procedure in which all the experimentally known levels included in the NIST compilation [28] up to 32 140 cm^{-1} were included, most of the level values above that limit being dubious or having unknown assignments. One should note that the newly identified even-parity level at 25 558.774 cm^{-1} ($J = 3/2$) from Basar *et al.* [134] was also incorporated in our fitting process. For this particular level, the leading component (52%) was found to be $5d^3$ $^2D_{3/2}$, according to our calculations. In this semi-empirical procedure, some radial energy parameters describing the $5d6s^2$, $5d^26s$, $5d^27s$, $5d^26d$, $5d^3$, 5d6s7s and 4f6s6p even-parity configurations and the $5d^26p$, 5d6s6p, $4f6s^2$, 4f5d6s and $6s^26p$ odd-parity configurations were adjusted, giving rise to standard deviations of 129 cm^{-1} and 173 cm^{-1} for even and odd parities, respectively, in all three models.

5.4.2 MCDHF Calculations

In order to assess the reliability of our pseudo-relativistic Hartree–Fock computations described above, the other theoretical method that we described in section 2.3 was used for neutral lanthanum. The version we used is the one implemented in the GRASP2K computer package [89].

In a first step, the $5d6s^2$, $5d^26s$, $5d^27s$, $5d^26d$, $5d^3$, 5d6s7s and 4f6s6p even-parity configurations and the $5d^26p$, $5d^27p$, 5d6s6p, 5d6s7p, 6s26p, 6s27p, $4f5d^2$ and $4f6s^2$ odd-parity configurations were chosen as a multireference (MR) to optimize all the involved orbitals using the extended average level (EAL) option (see [89]). The valence-valence correlations were then taken into account by allowing single and double excitations from the multireference to 5d, 5f, 5g, 6s, 6p, 6d, 7s, 7p, 7d, 8s, 8p and 8d orbitals, giving rise to 20 265 CSFs. In this step, the additional 5f, 5g, 7d, 8s, 8p and 8d orbitals were first obtained by an EOL variational procedure, keeping all the other orbitals frozen, before re-optimizing all the orbitals together. Finally, the most important core-valence correlations were considered by including the 5p → 4f, 5s → 5d single excitations, and the $5p^2 \rightarrow 5d^2$, $5s^2 \rightarrow 4f^2$ and 5s5p → 4f5d double excitations within the relativistic configuration interaction (RCI) approximation.

5.4.3 Results

5.4.3.1 Radiative Lifetimes

In Table 5.5, the calculated lifetime values that we obtained using the three different HFR models described in section 5.4.1 are compared with the available measurements in the literature[2] for 96 odd-parity levels in La I.

This table shows that the theoretical results are in very good agreement with the most recent and the most accurate experimental data of Den Hartog *et al.* [135],with the exception of the three levels at 17 947.13, 23 221.10 and 24 173.83 cm^{-1} for which large discrepancies are observed. This can be explained by the uncertain representation of these levels in our theoretical models. This effect is highlighted by the rather bad agreement we found when comparing the calculated HFR Landé g-factors, i.e. g = 1.06, 1.08, and 0.72, with the experimental values from the NIST database [28], namely g = 1.516, 0.781, and 0.806,. It is, however, interesting to notice that, for the level at 24 173.83 cm^{-1}, the lifetime computed by Karaçoban and Özdemir [136], i.e. τ = 6.04 ns, is in better agreement with our values (ranging from 9.6 to 12.0 ns) than with the experimental one (35.9 ns).

[2]Most of them performed by time-resolved laser-induced fluorescence spectroscopy (TR-LIF).

When we looked at those results in more details (with the exception of the three levels mentioned above), we found that, by comparing our data to the experimental values of Den Hartog [135] (noted EXP[135]), the mean ratios between them are found to be:

- $< \tau(\text{HFR-NOPOL})/\tau(\text{EXP}[135])> = 0.77 \pm 0.18$;
- $< \tau(\text{HFR+CPOL1})/\tau(\text{EXP}[135])> = 0.90 \pm 0.23$;
- $< \tau(\text{HFR+CPOL2})/\tau(\text{EXP}[135])> = 0.94 \pm 0.22$;

where the uncertainty corresponds to the standard deviation from the average.

As expected, it is clear from those comparisons that the core-valence correlations play a non-negligible role, the calculated lifetimes increasing by about 15% when including core-polarization contributions[3]. It then appears that the HFR+CPOL2 model gives the best overall agreement with the experimental radiative lifetimes from [135]. This agreement is also better than the one obtained between the previously calculated theoretical lifetimes from Biémont *et al.* [137] (for 17 levels) and from Karaçoban and Özdemir [136](for 37 levels) and the experimental measurements. Indeed, in these two cases, the mean ratios $< \tau(\text{THEORY})/\tau(\text{EXP}[135])>$ are found to be equal to 0.98 ± 0.33 and 0.89 ± 0.47. As one can see, the standard deviations (and therefore the scattering of results) are larger than the value that we obtained with our HFR+CPOL2 model which can therefore be considered as the most reliable one.

The agreement between our radiative lifetimes computed with the latter model and the TR-LIF experimental data of [135] is illustrated in Figure 5.5.

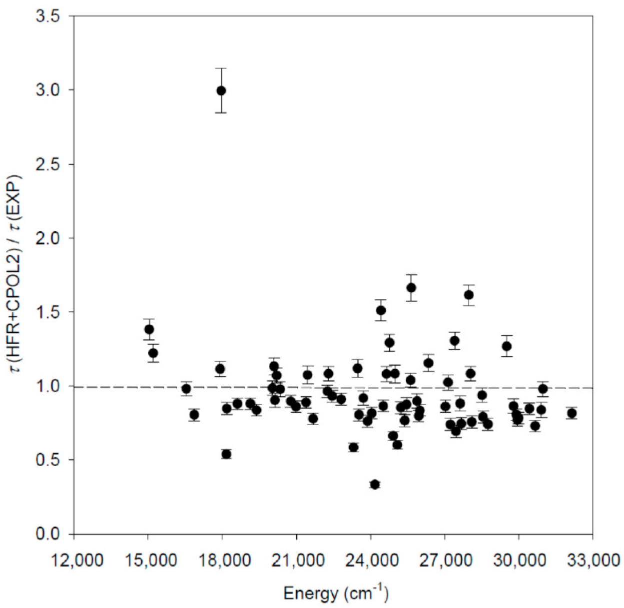

Figure 5.5: Comparison between the radiative lifetimes computed in La I using the HFR+CPOL2 model and the most recent laser-induced fluorescence experimental measurements from [135], where the dashed line indicates equality between them.

[3]Which would seem logical because the addition of the CPOL effects tends to lower the transitions probabilities.

Some other TR-LIF lifetime measurements were published before those of Den Hartog *et al.* [135]. This data [137, 138, 139, 140] is also reported in Table 5.5. The comparison between our HFR+CPOL2 calculated values and those older experimental measurements gives the mean ratios:

- $< \tau(\text{HFR+CPOL2})/\tau(\text{EXP[137]})> = 0.81 \pm 0.20$;
- $< \tau(\text{HFR+CPOL2})/\tau(\text{EXP[138]})> = 0.93 \pm 0.24$;
- $< \tau(\text{HFR+CPOL2})/\tau(\text{EXP[139]})> = 0.88 \pm 0.20$;
- $< \tau(\text{HFR+CPOL2})/\tau(\text{EXP[140]})> = 0.91 \pm 0.43$.

As one can see from those comparisons, the larger scattering observed between theoretical and experimental data is with the data of Yarlagadda *et al.* [140], which is mainly due to the fact that many of the levels considered in their analysis have quite long lifetimes ($\tau > 100$ ns), which are more difficult to precisely determine both experimentally and theoretically[4].

The MCDHF lifetimes calculated in the present work are not listed in Table 5.5 because, for many levels (about 50%), either the identifications are rather difficult due to unambiguously identification of the energy levels in the calculations (in particular for E > 26 000 cm^{-1}), or most of the computed radiative decay rates are strongly affected by severe cancellation effects leading to very uncertain lifetimes (in particular for $\tau > 100$ ns).

Nevertheless, for unambiguous identified levels in our MCDHF calculations, it is interesting to point out that the theoretical lifetimes are generally slightly shorter than the experimental data of Den Hartog *et al.*[135] exactly like the HFR+CPOL2 ones. If we compare the mean ratios between MCDHF and the experimental data and between MCDHF andd HFR+CPOL2, we find $< \tau(\text{MCDHF})/\tau(\text{EXP [22]})> = 0.85 \pm 0.46$ and $< \tau(\text{MCDHF})/\tau(\text{HFR+CPOL2})>= 0.81 \pm 0.43$, respectively. This can be explained by the fact that core-valence interactions are taken into account more effectively by using the core-polarization corrections in the HFR method than by explicitly incorporating a limited set of core-excited configurations in the MCDHF model. That all means that our HFR+CPOL2 calculations would tend to be a better representation of the atomic structure of La I.

[4]It is due to the fact that they involve less intense transitions which are generally much more affected by the cancellation effects.

Table 5.5: Comparison of the radiative lifetimes computed in the present work using three different HFR models with the available experimental values for odd-parity levels in neutral lanthanum.

			This work[b] (ns)			Experiments (ns)
E[a] (cm^{-1})	J	HFR+NOPOL	HFR+CPOL1	HFR+CPOL2	DH[c]	
13,260.38	1.5	232	287	335		256.9 ± 12.3 [f]
13,631.04	2.5	213	260	295		224.5 ± 13.8 [f]
14,095.69	0.5	119	149	179		220.9 ± 14.3 [f]
14,708.92	1.5	158	198	239		166.3 ± 9.3 [f]
14,804.08	2.5	194	236	270		257.9 ± 21.5 [f]
15,019.51	3.5	247	305	357		313 ± 17.8 [f]
15,031.64	1.5	155	192	224	162 ± 8	183.7 ± 12.8 [f]
15,196.83	2.5	106	123	132	108 ± 5	127 ± 7 [f]
15,219.89	0.5	355	459	585		205.4 ± 16.9 [f]
15,503.64	2.5	106	132	158		131.8 ± 6.8 [f]
16,099.29	3.5	102	127	153		156.7 ± 14.2 [f]
16,280.26	1.5	211	269	337		271.6 ± 19.2 [f]
16,538.39	3.5	68.1	78.8	83.7	85.3 ± 4.3	112.9 ± 9.5 [f]
16,856.80	2.5	34.6	40.6	42.2	52.4 ± 2.6	68.4 ± 5.1 [f]
17,797.29	1.5	236	287	341		130.2 ± 11.5 [f]
17,910.17	3.5	44.4	52	54.5	48.9 ± 2.4	64.6 ± 2.7 [f]
17,947.13	2.5	115	138	154	51.4 ± 2.6	68.3 ± 3.1 [f]
18,156.97	2.5	28.4	33.1	34.5	64 ± 3.2	68.4 ± 3.1 [f]
18,172.35	1.5	10.7	12.7	13.3	15.7 ± 0.8	17.7 ± 1.4 [d]
18,603.92	3.5	27.5	31.8	33.1	37.6 ± 1.9	54.8 ± 3.5 [f]
19,129.31	4.5	21.7	25	25.9	29.4 ± 1.5	46 ± 2.6 [f]
19,379.40	2.5	10.3	12.2	12.8	15.3 ± 0.8	17.2 ± 1 [d]
						15.9 ± 1 [d]
20,018.99	1.5	11.2	13.2	13.9	14.1 ± 0.7	17 ± 0.8 [f]
20,082.98	1.5	14.2	16.4	17.1	15.1 ± 0.8	17.5 ± 1.6 [f]
20,117.38	5.5	20.6	23.7	24.6	27.2 ± 1.4	32 ± 2.2 [f]
20,197.34	0.5	8.4	9.9	10.5	9.8 ± 0.5	17.2 ± 0.8 [f]
20,338.25	2.5	15.1	17.5	18.3	18.7 ± 0.9	20 ± 0.9 [f]
20,763.21	3.5	15.2	17.6	18.3	20.4 ± 1	25.8 ± 1.4 [f]
20,972.17	2.5	17.9	21	22.1	25.7 ± 1.3	35 ± 3.5 [f]
21,384.00	4.5	14.6	17	17.7	19.9 ± 1	23 ± 2.1 [f]
21,447.86	3.5	26	30	31.4	29.2 ± 1.5	34.1 ± 3.3 [f]
21,662.51	3.5	20.4	23.8	25	32.1 ± 1.6	39.8 ± 2.1 [f]
22,246.64	0.5	6.7	7.9	8.3	8.6 ± 0.4	10.1 ± 0.9 [d]
						9.6 ± 0.6 [f]
22,285.77	4.5	47	53.5	56.1	51.8 ± 2.6	73.4 ± 6.1 [f]
22,439.36	1.5	6.6	7.7	8.2	8.8 ± 0.4	10.2 ± 0.5 [d]
						9.5 ± 0.7 [f]
22,804.25	2.5	6.6	7.7	8.1	8.9 ± 0.4	10.7 ± 1 [d]
						10.4 ± 0.3 [f]
23,221.10	3.5	109	127	134	21.1 ± 1.1	22 ± 1.4 [d]
						27.5 ± 2.7 [f]
23,260.92	0.5	13.6	16	17		18.1 ± 1.5 [f]
23,303.26	3.5	6.9	8.1	8.6	14.7 ± 0.7	16.1 ± 1 [d]
						16.5 ± 1.1 [f]
23,466.84	4.5	56	64.7	67.8	60.6 ± 3	67.9 ± 3.8 [f]
23,528.45	0.5	16.6	19.3	20.3	25.2 ± 1.3	27.8 ± 1.8 [f]
23,704.81	1.5	20.4	23.7	24.8	27 ± 1.4	31.2 ± 2.5 [f]
23,874.95	2.5	9.2	10.8	11.2	14.7 ± 0.7	16.2 ± 1 [d]
						14.7 ± 1.1 [e]
24,046.10	2.5	21.6	25.1	26.2	32.1 ± 1.6	16.1 ± 1 [f]
24,088.54	3.5	81.9	95.6	100		247 ± 12 [e]
						207.5 ± 14.5 [f]
24,173.83	1.5	9.6	11.4	12	35.9 ± 1.8	37.7 ± 1.4 [f]
24,409.68	3.5	17.9	20.7	21.6	14.3 ± 0.7	15.7 ± 0.7 [d]
						14.6 ± 1.2 [e]
24,507.87	2.5	13.5	15.9	16.7	19.3 ± 1	21.9 ± 1 [d]
						19.2 ± 1.5 [e]
						22.2 ± 1.9 [f]
						20 ± 0.8 [g]
24,639.26	1.5	13.9	16.4	17.3	16 ± 0.8	14.9 ± 0.9 [e]
24,762.60	1.5	11.3	13.2	13.7	10.6 ± 0.5	12.4 ± 1.1 [e]
24,910.38	1.5	16.8	19.4	20.3	30.6 ± 1.5	32.4 ± 1.8 [f]
24,984.29	2.5	19.1	22.3	23.4	21.6 ± 1.1	27.2 ± 1.9 [f]

Table 5.5: Continued

Level		This work[b] (ns)				Experiments (ns)
E^a (cm^{-1})	J	HFR+NOPOL	HFR+CPOL1	HFR+CPOL2	DH[c]	
25,083.36	3.5	9.5	11	11.5	19.1 ± 1	21.1 ± 0.9 [f]
25,218.27	2.5	9.8	11.6	12.3	14.4 ± 0.7	15.7 ± 1.1 [d]
25,380.27	3.5	13.2	15.6	16.4	21.4 ± 1.1	23.2 ± 1.3 [f]
25,453.95	0.5	6.6	7.8	8.4	9.6 ± 0.5	19.4 ± 0.8 [d]
25,616.95	0.5	15.3	17.7	18.5	17.8 ± 0.9	17.6 ± 1.1 [f]
25,643.00	1.5	18.7	21.7	22.8	13.7 ± 0.7	16.2 ± 0.8 [e]
25,874.52	5.5	46.4	53	55.4		61.7 ± 3.1 [f]
25,950.32	1.5	7.6	8.9	9.5	11.9 ± 0.6	11.8 ± 0.9 [e]
25,997.17	4.5	14.1	16.8	17.7	21.2 ± 1.1	23.3 ± 1.5 [d]
						21.8 ± 0.9 [f]
						21.6 ± 0.6 [g]
26,338.93	2.5	15.9	18.5	19.3	16.7 ± 0.8	16.5 ± 1.2 [e]
27,022.62	2.5	13.7	16.3	16.8	19.5 ± 1	18.9 ± 1.4 [e]
						20.9 ± 1.3 [f]
27,054.96	4.5	56.5	64.3	67.1		89.7 ± 4.4 [g]
27,132.44	3.5	13.5	15.9	16.8	16.4 ± 0.8	16.6 ± 1.2 [e]
27,225.26	1.5	9.3	10.8	11.4	15.4 ± 0.8	17.1 ± 0.9 [d]
27,393.04	2.5	13.1	15.6	16.2	12.4 ± 0.6	14.1 ± 0.6 [d]
						12.6 ± 0.8 [e]
						12.6 ± 0.6 [g]
27,455.31	3.5	11.1	13.2	13.6	19.6 ± 1	21.6 ± 1.6 [d]
						19.8 ± 1.4 [e]
27,619.54	4.5	10.9	12.7	13.4	12.7 ± 0.6	14.3 ± 1.1 [e]
27,669.37	2.5	9.6	11.1	11.7	15.7 ± 0.8	17.8 ± 0.9 [d]
						15.6 ± 0.7 [g]
27,748.97	0.5	10.7	12.6	13.3		27 ± 2.6 [f]
27,968.54	1.5	8.6	9.6	10.5	6.5 ± 0.3	9.5 ± 0.9 [f]
28,039.45	3.5	10.4	12.4	12.9	11.9 ± 0.6	13 ± 0.9 [d]
						11.9 ± 0.8 [e]
28,089.17	4.5	11.5	13.8	14	18.5 ± 0.9	21.8 ± 1.8 [f]
28,506.41	2.5	6.2	7.1	7.5	8 ± 0.4	7.9 ± 0.3 [d]
						7.9 ± 0.4 [e]
28,543.08	3.5	13.1	15.2	15.9	20.1 ± 1	21.7 ± 1.2 [d]
						19.7 ± 1.1 [e]
28,743.24	5.5	10.9	13.1	13.2	17.8 ± 0.9	23.8 ± 1.6 [f]
28,893.51	0.5	10.3	12.2	12.8		20 ± 1.7 [f]
28,971.84	1.5	9.9	11.5	12		17.2 ± 1.2 [f]
29,199.57	1.5	8.6	10.1	10.5		15.4 ± 0.8 [e]
29,466.67	3.5	12.2	14.2	14.7		28.3 ± 0.9 [f]
29,502.18	2.5	11.6	13.4	14.2	11.2 ± 0.6	10.4 ± 0.9 [e]
29,564.70	0.5	10.1	11.8	12.6		16.9 ± 0.8 [g]
29,775.58	2.5	9.3	11	11.5	13.3 ± 0.7	12.3 ± 1.1 [e]
29,894.91	3.5	10.3	12.2	12.6	15.6 ± 0.8	14.9 ± 0.8 [e]
29,936.74	1.5	8	9.4	10	13 ± 0.7	12.5 ± 0.8 [e]
29,985.46	0.5	9.9	11.7	12.3	15.7 ± 0.8	
30,417.46	1.5	9.3	10.9	11.6	13.7 ± 0.7	13.6 ± 0.9 [e]
30,650.28	4.5	13.2	15.3	15.7	21.5 ± 1.1	20.8 ± 1.5 [e]
30,788.45	2.5	9.4	10.9	11.4		14.4 ± 1.2 [f]
30,896.84	2.5	8.8	10.4	10.9	13 ± 0.7	18.6 ± 1.7 [f]
30,964.71	3.5	8.2	9.5	9.9	10.1 ± 0.5	11.9 ± 0.6 [f]
31,477.22	2.5	5.9	6.7	7		8.7 ± 0.4 [g]
31,751.48	1.5	11.1	12.9	13.3		12.3 ± 0.8 [g]
32,140.55	3.5	5.2	5.9	6.2	7.6 ± 0.4	7.3 ± 0.5 [e]

a: Energy levels taken from the NIST compilation [28].
b: As explained in 5.4.1.
c: From Den Hartog *et al.* [135].
d: From Biémont *et al.* [137].
e: From Feng *et al.*[138].
f: From Yagaladda *et al.*[140].
g: From Shang *et al.*[139].

5.4.3.2 Oscillator Strengths and Transitions Probabilities

In Table 5.6, we give the oscillator strengths and transition probabilities that we computed using the HFR+CPOL2 model[5] for a set of 392 La I transitions with log gf-values > -1.

These lines appears from 317 nm (near UV) to 7843 nm (mid-infared). The experimental data recently published by Den Hartog *et al.* [135] is also reported for comparison in the table. There are 165 transitions that can be compared between this latter work and ours. It appears that for around more than a half of the lines, the discrepancies between both sets of results do not exceed 25%. Furthermore, for about three-quarter of the transitions, we can note an agreement better than a factor of two between our calculated oscillator strengths and the experimental values. This is illustrated in Figure 5.6 where the HFR+CPOL2 and experimental log gf values are compared. It also appears that the

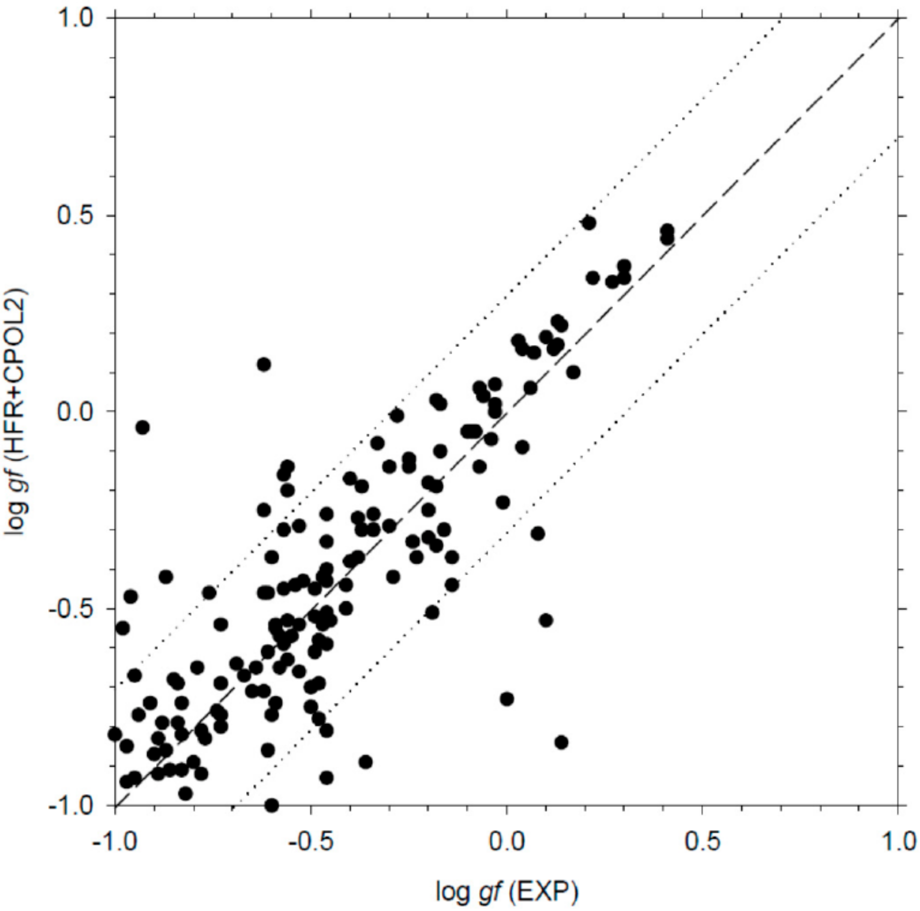

Figure 5.6: Comparison between the gf obtained in La I with our HFR+CPOL2 model and the experimental ones from [135]. The dashed line corresponds to a perfect agreement and the dotted ones to a discrepancy of a factor of two on the gf-value.

calculated transition rates obtained in the present work can be considered as much more reliable than the theoretical data reported by Karaçoban and Özdemir [136] and Kurucz [14], these two latter data being found to deviate by more than a factor of two from the experimental oscillator strengths, as highlighted by Den Hartog *et al.* [135]. Another interesting comparison is the one that we made between the results obtained with the HFR+CPOL2 model and those deduced from our MCDHF calculation, as described in Section 5.4.2. This comparison is displayed in Figure 5.7.

[5] Chosen because of its better agreement with the experimental data for the atomic structure, as shown in the previous section.

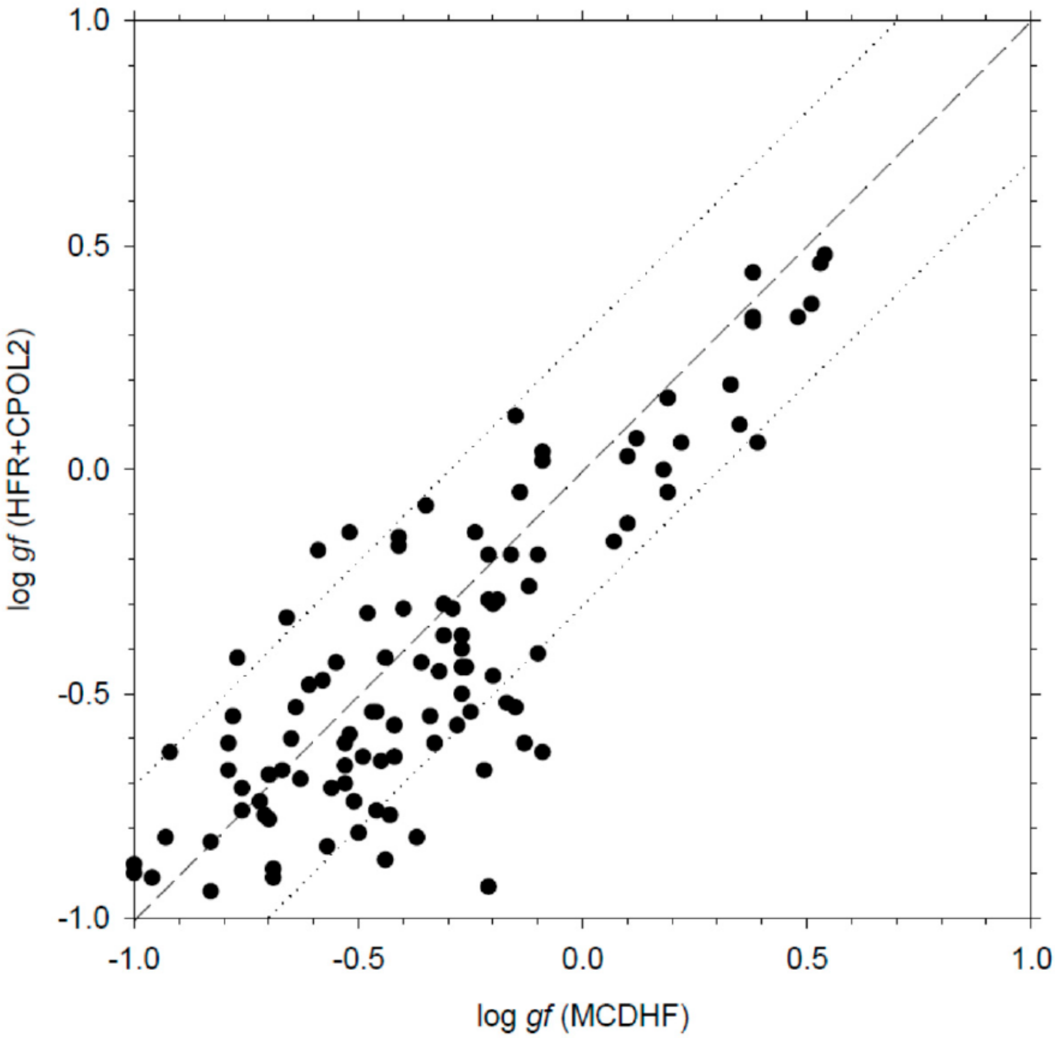

Figure 5.7: Comparison between the gf obtained in La I with our HFR+CPOL2 model and the ones from our MCDHF calculation. The dashed line corresponds to a perfect agreement and the dotted ones to a discrepancy of a factor of two on the gf-value.

As one can see on that figure, the agreement between both theoretical sets of oscillator strengths is found to be rather good especially knowing the complexity of the La I atomic structure. As Figure 5.7 shows, the discrepancies do not exceed 30% for more than half of the transitions (within the limit log $gf > -1$) and are anyway not larger than a factor of two for 95% of the entire set of common lines. A comparable agreement is observed when comparing our MCDHF calculations to the experimental gf -values of Den Hartog *et al.* [135], as illustrated in Figure 5.8.

5.4.3.3 Conclusion

In summary, the oscillator strengths and transition probabilities computed here using the HFR+CPOL2 model are expected to be accurate for the vast majority of the La I spectral lines listed in Table 5.6 within at maximum an uncertainty of a factor of two and even better than 30% for many of them. These new atomic and radiative parameters therefore represent the most reliable set of theoretical radiative rates produced up to now in lanthanum atom and can be considered as a valuable complement to the available experimental data from Den Hartog *et al.* [135].

As mentioned before, we computed new reliable oscillator strengths and transition probabilities for 392 spectral lines of neutral lanthanum. This was firstly assessed from

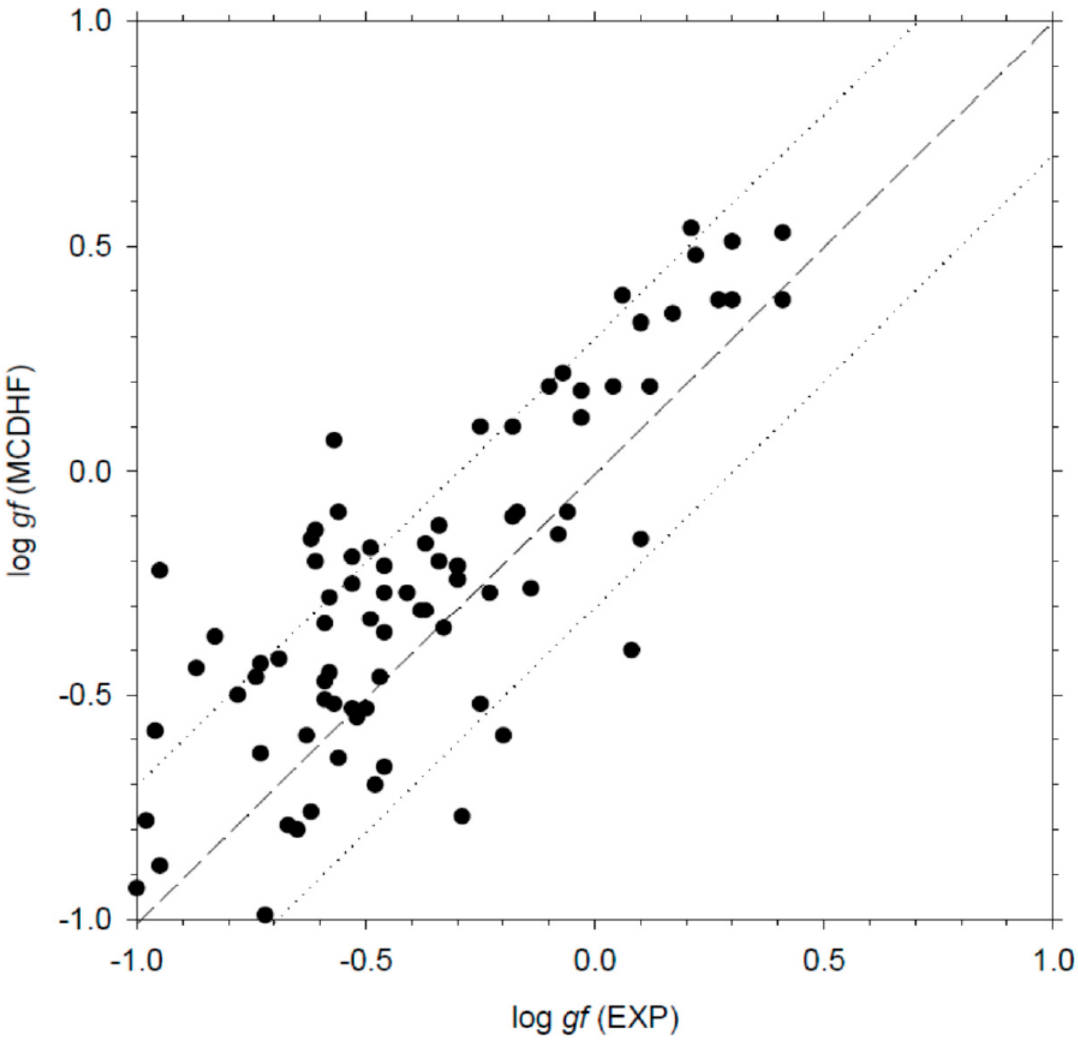

Figure 5.8: Comparison between the gf in La I obtained with our MCDHF calculation and the experimental ones from [135]. The dashed line corresponds to a perfect agreement and the dotted ones to a discrepancy of a factor of two on the gf-value

our detailed comparisons between different theoretical models based on the HFR+CPOL and the MCDHF methods, and secondly between the theoretical results and the available experimental data. Among the La I lines listed in the present work, approximately 60% have gf- and gA-values determined for the first time and that can be of use to the astrophysicists especially knowing that lanthanides have a very hot topic application in astrophysics in the study of kilonovae, as mentioned in Just *et al.* [141].

Table 5.6: Calculated oscillator strengths (log gf) and transition probabilities (gA) for spectral lines in La I

	Lower level[b]		Upper level[b]		This work[c]		Experiment[d]	
λ^a	E (cm^{-1})	J	E (cm^{-1})	J	log gf	gA (s^{-1})	log gf	gA (s^{-1})
317.5982	0	1.5	31477	2.5	-0.74	1.21E+08		
321.581	1053	2.5	32141	3.5	-0.45	2.32E+08	-0.49	2.08E+08
324.7034	0	1.5	30788	2.5	-0.99	6.34E+07		
334.223	1053	2.5	30965	3.5	-0.37	2.53E+08	-0.14	4.32E+08
336.2042	1053	2.5	30788	2.5	-0.89	7.32E+07		
340.4519	1053	2.5	30417	1.5	-0.94	6.62E+07	-1.01	5.60E+07
342.3726	0	1.5	29200	1.5	-0.73	1.07E+08		
346.1184	1053	2.5	29937	1.5	-0.68	1.16E+08	-0.85	7.84E+07
348.0605	1053	2.5	29776	2.5	-0.96	6.09E+07		
350.698	0	1.5	28506	2.5	-0.87	7.48E+07		
357.4425	0	1.5	27969	1.5	-0.44	1.90E+08	-0.14	3.80E+08
361.3074	0	1.5	27669	2.5	-0.54	1.47E+08	-0.73	9.42E+07
363.6661	1053	2.5	28543	3.5	-0.77	8.52E+07	-0.94	5.76E+07
364.1519	1053	2.5	28506	2.5	-0.09	4.20E+08	0.04	5.46E+08
370.4532	1053	2.5	28039	3.5	-0.81	7.28E+07	-0.46	1.66E+08
378.6495	1053	2.5	27455	3.5	-0.7	9.16E+07		
385.2424	0	1.5	25950	1.5	-0.91	5.71E+07	-1.57	1.20E+07
387.8879	4122	4.5	29895	3.5	-0.91	5.41E+07	-0.83	6.56E+07
392.7551	0	1.5	25454	0.5	-0.3	2.21E+08	-0.37	1.86E+08
399.4164	3010	2.5	28039	3.5	-0.36	1.79E+08	-1.19	2.72E+07
401.5388	1053	2.5	25950	1.5	-0.18	2.78E+08	-0.2	2.60E+08
404.3371	2668	1.5	27393	2.5	-0.41	1.55E+08		
406.0316	4122	4.5	28743	5.5	0.34	9.03E+08	0.22	6.72E+08
406.4778	3495	3.5	28089	4.5	0.18	6.15E+08	0.03	4.32E+08
407.917	0	1.5	24508	2.5	-0.63	9.56E+07	-0.56	1.11E+08
408.961	3010	2.5	27455	3.5	-0.14	2.84E+08	-0.07	3.36E+08
410.487	2668	1.5	27023	2.5	-0.32	1.89E+08	-0.2	2.47E+08
410.9481	1053	2.5	25380	3.5	-0.68	8.32E+07	-1.11	3.04E+07
413.5538	0	1.5	24174	1.5	-0.6	9.84E+07		
413.7031	1053	2.5	25218	2.5	-0.54	1.08E+08	-0.53	1.15E+08
414.3907	3495	3.5	27620	4.5	-0.83	5.83E+07	-0.77	6.60E+07
416.0258	1053	2.5	25083	3.5	0.12	5.04E+08	-0.62	9.20E+07
416.3303	3010	2.5	27023	2.5	-0.94	4.39E+07	-0.97	4.08E+07
417.1124	4122	4.5	28089	4.5	-0.82	5.78E+07	-1	3.79E+07
417.231	3495	3.5	27455	3.5	-0.79	6.11E+07	-0.84	5.52E+07
417.7481	1053	2.5	24984	2.5	-0.69	8.03E+07	-0.73	7.08E+07
418.731	0	1.5	23875	2.5	0.04	4.27E+08	-0.06	3.31E+08
421.6542	1053	2.5	24763	1.5	-0.93	4.47E+07	-1.47	1.28E+07
427.1148	7491	1.5	30897	2.5	-0.53	1.09E+08	-0.45	1.30E+08
428.0256	1053	2.5	24410	3.5	-0.53	1.09E+08	0.1	4.55E+08
429.3445	7680	2.5	30965	3.5	-0.79	5.80E+07	-1.41	1.44E+07
430.5996	7680	2.5	30897	2.5	-0.27	1.97E+08	-0.38	1.51E+08
431.1725	7231	0.5	30417	1.5	-0.74	6.58E+07	-0.91	4.40E+07
434.072	8446	1.5	31477	2.5	-0.03	3.33E+08		
435.4793	9184	2.5	32141	3.5	0.23	6.01E+08	0.13	4.72E+08
440.264	9044	0.5	31751	1.5	-0.39	1.43E+08		
440.3015	7231	0.5	29937	1.5	-0.87	4.64E+07	-0.9	4.36E+07
442.3905	8052	3.5	30650	4.5	0.22	5.69E+08	0.14	4.65E+08
444.2675	3495	3.5	25997	4.5	-0.93	4.01E+07	-0.95	3.76E+07
444.4197	7491	1.5	29985	0.5	-0.43	1.25E+08	-0.52	1.00E+08
445.2149	7012	2.5	29467	3.5	0.02	3.50E+08		
446.8965	3010	2.5	25380	3.5	-0.92	4.10E+07	-0.89	4.24E+07
447.4538	8446	1.5	30788	2.5	-0.39	1.30E+08		
448.6053	7491	1.5	29776	2.5	-0.17	2.29E+08	-0.4	1.31E+08
449.1748	7680	2.5	29937	1.5	-0.44	1.20E+08	-0.54	9.44E+07
449.904	9920	4.5	32141	3.5	-0.01	3.23E+08	-0.28	1.71E+08
450.0206	7680	2.5	29895	3.5	0.15	4.70E+08	0.07	3.83E+08
450.1565	3010	2.5	25218	2.5	-0.67	6.78E+07	-1.21	2.04E+07
454.1773	7491	1.5	29502	2.5	-0.59	8.06E+07	-0.46	1.12E+08
454.9498	3010	2.5	24984	2.5	-0.93	3.90E+07	-0.46	1.11E+08
455.0164	2668	1.5	24639	1.5	-0.4	1.27E+08	-1.57	8.68E+06
455.0766	7231	0.5	29200	1.5	-0.64	7.57E+07		
456.7904	3495	3.5	25380	3.5	-0.05	2.86E+08	-0.09	2.62E+08
457.0023	4122	4.5	25997	4.5	0.17	4.86E+08	0.13	4.34E+08
458.1197	7680	2.5	29502	2.5	-0.2	1.95E+08	-0.56	8.76E+07
458.989	9184	2.5	30965	3.5	-0.38	1.30E+08		
459.8436	7231	0.5	28972	1.5	-0.8	5.01E+07		
460.4237	9184	2.5	30897	2.5	-0.26	1.76E+08	-0.46	1.08E+08
461.5064	7231	0.5	28894	0.5	-0.49	1.02E+08		
462.2072	3010	2.5	24639	1.5	-0.97	3.27E+07		
464.3129	7012	2.5	28543	3.5	-0.9	3.92E+07	-1.01	3.05E+07
464.6335	9961	3.5	31477	2.5	-0.03	2.94E+08		
465.0322	3010	2.5	24508	2.5	-0.55	8.90E+07	-0.98	3.24E+07
465.1874	8446	1.5	29937	1.5	-0.86	4.24E+07	-1.15	2.16E+07
465.3905	7491	1.5	28972	1.5	-0.42	1.16E+08		
470.2641	4122	4.5	25380	3.5	-0.83	4.50E+07	-0.89	3.92E+07
470.8186	9184	2.5	30417	1.5	-0.3	1.51E+08	-0.57	8.12E+07
473.3826	8446	1.5	29565	0.5	-0.67	6.21E+07		
475.0419	9920	4.5	30965	3.5	-0.23	1.71E+08	-0.01	2.88E+08
475.9711	9961	3.5	30965	3.5	-0.97	3.13E+07	-0.82	4.48E+07
476.6891	0	1.5	20972	2.5	-0.46	1.02E+08	-0.62	7.08E+07
477.0425	7012	2.5	27969	1.5	-0.51	9.08E+07	-0.46	1.02E+08
479.9992	9961	3.5	30788	2.5	-0.34	1.27E+08		
481.7112	8446	1.5	29200	1.5	-0.51	9.09E+07		
481.7247	9184	2.5	29937	1.5	-0.86	3.98E+07	-0.61	7.00E+07
483.9514	7012	2.5	27669	2.5	0.02	2.92E+08	-0.03	2.63E+08
485.0812	1053	2.5	21663	3.5	-0.46	9.95E+07	-0.76	4.96E+07
485.495	9184	2.5	29776	2.5	-0.33	1.36E+08	-0.24	1.62E+08
487.0558	8446	1.5	28972	1.5	-0.73	5.28E+07		
487.8848	8052	3.5	28543	3.5	-0.1	2.26E+08	-0.17	1.90E+08
488.7595	8052	3.5	28506	2.5	-0.14	2.12E+08	-0.56	7.68E+07
490.1867	1053	2.5	21448	3.5	-0.86	3.95E+07	-0.87	3.76E+07
492.0278	9184	2.5	29502	2.5	-0.75	4.83E+07		
494.5845	7012	2.5	27225	1.5	-0.79	4.39E+07	-0.88	3.64E+07
494.9765	0	1.5	20197	0.5	-0.19	1.72E+08	-0.18	1.80E+08
497.7952	0	1.5	20083	1.5	-0.95	2.91E+07	-1.35	1.20E+07
500.1785	8052	3.5	28039	3.5	-0.51	7.93E+07	-0.19	1.70E+08
504.6871	3495	3.5	23303	3.5	-0.4	1.05E+08	-0.46	9.04E+07
505.0564	3010	2.5	22804	2.5	-0.29	1.34E+08	-0.3	1.30E+08
505.6459	2668	1.5	22439	1.5	-0.43	9.59E+07	-0.46	9.04E+07

Table 5.6: Continued

	Lower level[b]		Upper level[b]		This work[c]		Experiment[d]	
λ^a	E (cm^{-1})	J	E (cm^{-1})	J	log gf	gA (s^{-1})	log gf	gA (s^{-1})
510.6233	2668	1.5	22247	0.5	-0.05	2.23E+08	-0.08	2.10E+08
511.4489	9920	4.5	29467	3.5	-0.76	4.35E+07		
514.5417	3010	2.5	22439	1.5	0.16	3.57E+08	0.12	3.28E+08
515.2367	8052	3.5	27455	3.5	-0.77	4.23E+07		
515.8681	0	1.5	19379	2.5	-0.57	6.72E+07	-0.58	6.60E+07
516.7783	4122	4.5	23467	4.5	-0.8	3.98E+07	-0.73	4.60E+07
517.7296	3495	3.5	22804	2.5	0.34	5.40E+08	0.3	4.92E+08
517.9119	8446	1.5	27749	0.5	-0.76	4.23E+07		
518.391	1053	2.5	20338	2.5	-0.91	2.97E+07	-0.86	3.42E+07
521.1854	4122	4.5	23303	3.5	0.48	7.43E+08	0.21	3.98E+08
523.4274	4122	4.5	23221	3.5	-0.84	3.52E+07	0.14	3.38E+08
527.1174	1053	2.5	20019	1.5	0.03	2.59E+08	-0.18	1.60E+08
527.6413	8446	1.5	27393	2.5	-0.58	6.17E+07	-0.48	7.98E+07
530.1974	9184	2.5	28039	3.5	-0.44	8.34E+07		
530.4012	7491	1.5	26339	2.5	-0.69	4.71E+07	-0.48	7.80E+07
532.3555	8446	1.5	27225	1.5	-0.67	5.02E+07	-0.95	2.64E+07
534.0705	7231	0.5	25950	1.5	-0.95	2.72E+07		
535.7856	7680	2.5	26339	2.5	-0.25	1.28E+08	-0.2	1.48E+08
536.8136	9920	4.5	28543	3.5	-0.61	5.69E+07		
538.0005	9961	3.5	28543	3.5	-0.71	4.57E+07	-0.65	5.20E+07
545.5142	1053	2.5	19379	2.5	0.16	3.26E+08	0.04	2.44E+08
547.5155	9920	4.5	28179	5.5	-0.32	1.06E+08		
549.106	7012	2.5	25218	2.5	-0.69	4.32E+07	-0.84	3.24E+07
550.1337	0	1.5	18172	1.5	0.07	2.55E+08	-0.03	2.05E+08
550.2246	9920	4.5	28089	4.5	-0.77	3.73E+07	-0.6	5.60E+07
551.5274	7491	1.5	25617	0.5	-0.46	7.24E+07	-0.61	5.32E+07
551.7344	9920	4.5	28039	3.5	-0.73	3.88E+07	0	2.21E+08
552.9882	9961	3.5	28039	3.5	-0.25	1.17E+08	-0.62	5.20E+07
554.1249	9184	2.5	27225	1.5	-0.14	1.57E+08	-0.25	1.22E+08
554.4916	9719	1.5	27749	0.5	-0.43	8.03E+07		
556.5434	7680	2.5	25643	1.5	-0.33	9.81E+07	-0.46	7.44E+07
556.9905	9184	2.5	27132	3.5	-0.49	7.05E+07		
558.5518	7012	2.5	24910	1.5	-0.93	2.62E+07		
558.8328	3495	3.5	21384	4.5	-0.61	5.19E+07	-0.49	6.90E+07
563.1222	3010	2.5	20763	3.5	-0.5	6.52E+07	-0.41	8.16E+07
564.5449	9961	3.5	27669	2.5	-0.71	4.06E+07		
564.8239	9920	4.5	27620	4.5	0.44	5.81E+08	0.41	5.33E+08
565.4868	7231	0.5	24910	1.5	-0.47	7.41E+07	-0.96	2.28E+07
565.6586	9719	1.5	27393	2.5	-0.65	4.53E+07	-0.64	4.80E+07
565.7719	2668	1.5	20338	2.5	-0.65	4.54E+07	-0.58	5.52E+07
567.1428	7012	2.5	24639	1.5	-0.89	2.62E+07		
570.2536	7231	0.5	24763	1.5	-0.84	3.00E+07		
571.4527	9961	3.5	27455	3.5	-0.55	5.69E+07		
571.4735	7491	1.5	24984	2.5	-0.77	3.58E+07		
573.4941	9961	3.5	27393	2.5	-0.89	2.55E+07	-0.36	8.94E+07
574.0652	2668	1.5	20083	1.5	-0.08	1.63E+08	-0.33	9.52E+07
574.4403	7680	2.5	25083	3.5	-0.31	9.86E+07	0.08	2.44E+08
576.9324	3010	2.5	20338	2.5	0	1.95E+08	-0.03	1.87E+08
577.7682	9719	1.5	27023	2.5	-0.96	2.14E+07		
578.8086	7491	1.5	24763	1.5	-0.32	9.78E+07		
578.9224	3495	3.5	20763	3.5	0.19	3.07E+08	0.1	2.48E+08
579.1322	4122	4.5	21384	4.5	0.37	4.67E+08	0.3	3.93E+08
580.8081	9920	4.5	27132	3.5	-0.4	7.96E+07		
582.1977	9961	3.5	27132	3.5	0.1	2.51E+08	0.17	2.94E+08
582.3818	8052	3.5	25218	2.5	-0.38	7.79E+07	-0.4	7.86E+07
582.5238	7012	2.5	24174	1.5	-0.48	6.48E+07		
582.7543	9184	2.5	26339	2.5	-0.37	8.19E+07	-0.6	4.92E+07
584.8365	9961	3.5	27055	4.5	-0.17	1.30E+08		
585.2267	7680	2.5	24763	1.5	-0.42	7.62E+07	-0.87	2.64E+07
585.5586	3010	2.5	20083	1.5	-0.81	2.89E+07	-0.78	3.24E+07
586.995	8052	3.5	25083	3.5	-0.89	2.46E+07	-1.16	1.33E+07
587.4728	7491	1.5	24508	2.5	-0.52	5.97E+07	-0.49	6.18E+07
590.4296	8052	3.5	24984	2.5	-0.88	2.59E+07	-1.01	1.86E+07
593.0608	1053	2.5	17910	3.5	-0.57	5.15E+07	-0.55	5.36E+07
593.0681	0	1.5	16857	2.5	-0.65	4.46E+07	-0.79	3.10E+07
593.5285	3495	3.5	20338	2.5	-0.77	3.13E+07	-0.73	3.54E+07
596.0586	8446	1.5	25218	2.5	-0.74	3.29E+07	-0.83	2.76E+07
597.5723	7680	2.5	24410	3.5	-0.04	1.71E+08	-0.93	2.19E+07
599.5495	13631	2.5	30306	2.5	-0.73	3.51E+07		
600.736	4122	4.5	20763	3.5	-0.82	2.74E+07	-0.83	2.80E+07
601.714	13260	1.5	29875	1.5	-0.36	7.69E+07		
603.8588	7491	1.5	24046	2.5	-0.29	9.19E+07	-0.53	5.40E+07
606.8711	7231	0.5	23705	1.5	-0.54	5.13E+07	-0.59	4.68E+07
607.0418	15220	0.5	31689	1.5	-0.99	1.84E+07		
607.5237	8052	3.5	24508	2.5	-0.9	2.36E+07		
610.8477	7680	2.5	24046	2.5	-0.3	8.84E+07	-0.34	8.16E+07
612.1221	15020	3.5	31352	2.5	-0.66	3.68E+07		
612.577	15032	1.5	31352	2.5	-0.93	2.09E+07		
613.4384	7231	0.5	23528	0.5	-0.55	4.82E+07	-0.59	4.60E+07
614.2961	13631	2.5	29905	2.5	-0.13	1.29E+08		
614.5306	15020	3.5	31288	3.5	-0.62	4.07E+07		
616.4989	15032	1.5	31248	1.5	-0.42	6.69E+07		
616.5693	7491	1.5	23705	1.5	-0.44	6.18E+07	-0.41	6.80E+07
621.821	9920	4.5	25997	4.5	-0.94	2.04E+07		
621.9456	14096	0.5	30170	1.5	-0.62	4.16E+07		
623.4838	9184	2.5	25218	2.5	-0.81	2.53E+07		
624.9909	4122	4.5	20117	5.5	0.46	4.86E+08	0.41	4.42E+08
626.6013	9920	4.5	25875	5.5	0.06	1.96E+08	0.06	1.94E+08
627.827	14096	0.5	30019	0.5	-0.84	2.42E+07		
629.3556	3495	3.5	19379	2.5	-0.92	2.02E+07	-0.78	2.76E+07
630.8216	15504	2.5	31352	2.5	-0.19	1.10E+08		
631.75	16099	3.5	31924	4.5	-0.51	5.46E+07		
632.5908	1053	2.5	16857	2.5	-0.89	2.27E+07	-0.8	2.62E+07
633.3798	15504	2.5	31288	3.5	-0.58	4.56E+07		
635.6416	8446	1.5	24174	1.5	-0.45	5.93E+07		
637.5467	16243	4.5	31924	4.5	-0.85	2.32E+07		
639.4227	3495	3.5	19129	4.5	0.33	3.56E+08	0.27	3.01E+08
640.9845	14709	1.5	30306	2.5	-0.82	2.54E+07		
641.0984	3010	2.5	18604	3.5	0.06	1.88E+08	-0.07	1.37E+08
642.6591	15504	2.5	31060	3.5	-0.98	1.74E+07		
645.0317	9719	1.5	25218	2.5	-0.7	3.06E+07		
645.4502	2668	1.5	18157	2.5	-0.16	1.14E+08	-0.57	4.32E+07
645.5984	1053	2.5	16538	3.5	-0.26	8.89E+07	-0.34	7.36E+07
648.5531	8052	3.5	23467	4.5	-0.64	3.67E+07	-0.69	3.30E+07

Table 5.6: Continued

	Lower level[b]		Upper level[b]		This work[c]		Experiment[d]	
λ[a]	E (cm^{-1})	J	E (cm^{-1})	J	log gf	gA (s^{-1})	log gf	gA (s^{-1})
650.6187	14804	2.5	30170	1.5	-0.38	6.50E+07		
652.3878	9184	2.5	24508	2.5	-0.84	2.32E+07		
652.9738	14709	1.5	30019	0.5	-0.28	8.42E+07		
654.0084	15020	3.5	30306	2.5	-0.24	8.60E+07		
656.595	9184	2.5	24410	3.5	-0.87	2.13E+07		
657.8502	0	1.5	15197	2.5	-0.61	3.72E+07	-0.61	3.84E+07
658.2197	16099	3.5	31288	3.5	0.09	2.01E+08		
660.0158	3010	2.5	18157	2.5	-0.92	1.89E+07	-1.02	1.47E+07
660.7728	9044	0.5	24174	1.5	-0.68	3.26E+07		
660.8239	9961	3.5	25089	4.5	-0.15	1.12E+08		
661.6572	3495	3.5	18604	3.5	-0.76	2.69E+07	-0.74	2.78E+07
663.3476	14804	2.5	29875	1.5	-0.47	5.07E+07		
664.5148	16243	4.5	31288	3.5	0.18	2.26E+08		
666.139	4122	4.5	19129	4.5	-0.74	2.79E+07	-0.59	3.90E+07
667.6849	15197	2.5	30170	1.5	-0.79	2.49E+07		
670.9481	3010	2.5	17910	3.5	-0.37	6.43E+07	-0.23	8.72E+07
671.5948	15020	3.5	29905	2.5	-0.68	2.91E+07		
674.8109	8446	1.5	23261	0.5	-0.83	2.26E+07		
682.3775	7012	2.5	21663	3.5	-0.78	2.41E+07	-0.48	4.72E+07
691.6659	17023	3.5	31477	2.5	-0.98	1.47E+07		
692.524	7012	2.5	21448	3.5	-0.14	1.03E+08	-0.3	6.96E+07
697.6842	9920	4.5	24249	4.5	-0.63	3.13E+07		
702.3688	8052	3.5	22286	4.5	-0.05	1.25E+08	-0.1	1.07E+08
703.2039	9044	0.5	23261	0.5	-0.61	3.45E+07		
704.5963	2668	1.5	16857	2.5	-0.42	5.38E+07	-0.47	4.50E+07
705.9527	17947	2.5	32108	3.5	-0.75	2.31E+07		
707.6374	9961	3.5	24089	3.5	-0.71	2.56E+07		
712.7473	15020	3.5	29046	3.5	-0.83	1.84E+07		
716.1216	7012	2.5	20972	2.5	-0.12	9.78E+07	-0.25	7.32E+07
716.6031	14804	2.5	28755	2.5	-0.97	1.39E+07		
723.1903	17141	4.5	30965	3.5	-0.61	3.02E+07		
726.2753	17023	3.5	30788	2.5	-0.26	6.51E+07		
734.5327	8052	3.5	21663	3.5	0.02	1.31E+08	-0.17	8.24E+07
737.9665	9920	4.5	23467	4.5	-0.3	6.19E+07	-0.16	8.60E+07
738.2683	9719	1.5	23261	0.5	-0.57	3.45E+07		
739.6431	18172	1.5	31689	1.5	-0.35	5.56E+07		
743.7636	17910	3.5	31352	2.5	-0.67	2.54E+07		
745.8144	17947	2.5	31352	2.5	-0.95	1.33E+07		
746.3028	8052	3.5	21448	3.5	-0.7	2.46E+07	-0.5	3.76E+07
749.393	17947	2.5	31288	3.5	-0.39	4.84E+07		
750.9376	16857	2.5	30170	1.5	-0.86	1.53E+07		
756.8598	17910	3.5	31119	2.5	-0.84	1.63E+07		
763.6844	18157	2.5	31248	1.5	-0.32	5.36E+07		
767.9457	16857	2.5	29875	1.5	-0.46	3.63E+07		
781.2982	19129	4.5	31925	3.5	-0.71	2.07E+07		
784.2407	18604	3.5	31352	2.5	-0.37	4.50E+07		
790.3695	18316	4.5	30965	3.5	-0.35	4.63E+07		
796.1502	17797	1.5	30354	2.5	-0.9	1.41E+07		
796.873	19379	2.5	31925	3.5	-0.65	2.35E+07		
798.815	18604	3.5	31119	2.5	-0.57	2.74E+07		
800.1873	3010	2.5	15504	2.5	-0.96	1.11E+07		
802.8791	17567	0.5	30019	0.5	-0.99	1.10E+07		
808.4499	9920	4.5	22286	4.5	-0.45	3.73E+07	-0.57	2.70E+07
810.192	18311	5.5	30650	4.5	-0.33	4.83E+07		
811.0853	17141	4.5	29467	3.5	-0.37	4.31E+07		
816.1092	13747	4.5	25997	4.5	-0.97	1.11E+07		
824.747	4122	4.5	16243	4.5	-0.74	1.84E+07		
832.4721	3495	3.5	15504	2.5	-0.64	2.14E+07		
833.4405	17910	3.5	29905	2.5	-0.35	4.08E+07		
834.6542	4122	4.5	16099	3.5	-0.31	4.42E+07		
837.966	19129	4.5	31060	3.5	-0.09	7.70E+07		
846.7526	20117	5.5	31924	4.5	0.13	1.29E+08		
851.3598	9920	4.5	21663	3.5	-0.75	1.69E+07		
852.0643	18172	1.5	29905	2.5	-0.78	1.50E+07		
854.3427	18604	3.5	30306	2.5	-0.99	9.37E+06		
854.3488	9961	3.5	21663	3.5	-0.66	2.09E+07	-0.53	2.72E+07
854.5451	3010	2.5	14709	1.5	-0.76	1.52E+07		
855.908	19379	2.5	31060	3.5	-0.66	2.03E+07		
863.393	18316	4.5	29895	3.5	-0.66	1.95E+07		
867.212	9920	4.5	21448	3.5	-0.75	1.64E+07	-0.5	2.80E+07
867.4419	3495	3.5	15020	3.5	-0.94	1.08E+07		
870.3136	9961	3.5	21448	3.5	-0.74	1.65E+07		
874.8416	2668	1.5	14096	0.5	-0.92	1.07E+07		
880.1268	20393	0.5	31751	1.5	-0.73	1.60E+07		
881.8966	13747	4.5	25083	3.5	-0.97	9.08E+06		
882.167	20019	1.5	31352	2.5	-0.7	1.68E+07		
882.5854	8052	3.5	19379	2.5	-0.53	2.50E+07	-0.56	2.34E+07
895.6565	18038	1.5	29200	1.5	-0.85	1.21E+07		
895.776	7012	2.5	18172	1.5	-0.67	1.75E+07	-0.67	1.80E+07
904.693	20197	0.5	31248	1.5	-0.81	1.28E+07		
907.9116	9961	3.5	20972	2.5	-0.42	3.13E+07	-0.29	4.14E+07
908.9274	18777	2.5	29776	2.5	-0.81	1.30E+07		
912.7555	20972	2.5	31925	3.5	-0.99	7.96E+06		
915.7172	12787	2.5	23705	1.5	-0.78	1.29E+07		
922.6653	9184	2.5	20019	1.5	-0.91	9.70E+06		
925.0058	13238	3.5	24046	2.5	-0.59	1.96E+07	-0.57	2.10E+07
932.8854	20972	2.5	31689	1.5	-0.68	1.60E+07		
937.6175	13747	4.5	24410	3.5	-0.59	1.97E+07		
948.51	21384	4.5	31924	4.5	0.06	8.76E+07		
954.1972	21448	3.5	31925	3.5	-0.71	1.36E+07		
957.0444	21663	3.5	32108	3.5	-0.95	7.73E+06		
964.0855	17023	3.5	27393	2.5	-0.34	3.16E+07	-0.18	4.74E+07
970.9394	20763	3.5	31060	3.5	-0.13	5.47E+07		
972.9114	20972	2.5	31248	1.5	-0.85	9.81E+06		
973.7092	7680	2.5	17947	2.5	-0.85	1.00E+07	-0.97	7.50E+06
974.1552	21663	3.5	31925	3.5	-0.48	2.21E+07		
977.5166	18316	4.5	28543	3.5	-0.74	1.27E+07		
980.4358	21944	3.5	32141	3.5	-0.74	1.30E+07		
985.2573	20972	2.5	31119	2.5	-0.34	3.03E+07		
991.119	20083	1.5	30170	1.5	-0.57	1.96E+07		
999.7999	17023	3.5	27023	2.5	-0.86	9.03E+06		
1000.5724	17141	4.5	27132	3.5	-0.07	5.72E+07	-0.04	6.08E+07
1002.9997	20338	2.5	30306	2.5	-0.58	1.86E+07		
1006.6821	18038	1.5	27969	1.5	-0.98	6.80E+06		

Table 5.6: Continued

	Lower level[b]		Upper level[b]		This work[c]		Experiment[d]	
λ[a]	E (cm^{-1})	J	E (cm^{-1})	J	log gf	gA (s^{-1})	log gf	gA (s^{-1})
1011.2194	20019	1.5	29905	2.5	-0.78	1.04E+07		
1013.0834	18311	5.5	28179	5.5	-0.85	9.04E+06		
1017.77	22286	4.5	32108	3.5	-0.75	1.07E+07		
1018.4625	12431	1.5	22247	0.5	-0.71	1.21E+07	-0.62	1.54E+07
1020.963	20083	1.5	29875	1.5	-0.89	8.57E+06		
1021.989	21969	2.5	31751	1.5	-0.34	2.96E+07		
1027.4898	18777	2.5	28506	2.5	-0.46	2.42E+07		
1028.147	18316	4.5	28039	3.5	-0.38	2.42E+07		
1029.4429	18038	1.5	27749	0.5	-0.99	6.14E+06		
1031.8059	21663	3.5	31352	2.5	-0.88	7.90E+06		
1033.0277	20197	0.5	29875	1.5	-0.85	8.93E+06		
1033.2348	21384	4.5	31060	3.5	-0.75	1.12E+07		
1033.7188	21448	3.5	31119	2.5	-0.34	2.67E+07		
1034.9172	9719	1.5	19379	2.5	-0.77	1.07E+07		
1035.7755	12787	2.5	22439	1.5	-0.54	1.76E+07	-0.47	2.12E+07
1037.143	22286	4.5	31925	3.5	-0.19	3.74E+07		
1044.9646	20338	2.5	29905	2.5	-0.9	7.82E+06		
1045.0906	13238	3.5	22804	2.5	-0.37	2.59E+07	-0.38	2.58E+07
1046.178	13747	4.5	23303	3.5	-0.19	3.95E+07	-0.37	2.64E+07
1048.2913	20338	2.5	29875	1.5	-0.93	7.41E+06		
1048.6541	21944	3.5	31477	2.5	-0.88	8.26E+06		
1051.4688	21969	2.5	31477	2.5	-0.97	6.64E+06		
1057.1829	21663	3.5	31119	2.5	-0.92	6.62E+06		
1063.8575	21663	3.5	31060	3.5	-0.94	6.62E+06		
1073.9789	18311	5.5	27620	4.5	0.1	7.40E+07		
1093.5386	20763	3.5	29905	2.5	-0.82	8.36E+06		
1093.8605	18316	4.5	27455	3.5	-0.62	1.29E+07		
1096.1008	22804	2.5	31925	3.5	-0.85	7.91E+06		
1110.6662	22247	0.5	31248	1.5	-0.85	7.92E+06		
1115.9028	16991	0.5	25950	1.5	-0.91	6.95E+06		
1121.7452	22439	1.5	31352	2.5	-0.82	8.18E+06		
1128.6458	21448	3.5	30306	2.5	-0.88	6.67E+06		
1139.4294	22286	4.5	31060	3.5	-0.83	7.33E+06		
1143.972	18316	4.5	27055	4.5	-0.79	8.00E+06		
1144.6872	17141	4.5	25875	5.5	-0.89	6.68E+06		
1145.6378	9184	2.5	17910	3.5	-0.85	7.44E+06		
1151.2147	9920	4.5	18604	3.5	-0.96	5.62E+06		
1151.8035	22439	1.5	31119	2.5	-0.67	1.08E+07		
1154.5037	20083	1.5	28742	1.5	-0.95	5.79E+06		
1159.6811	23303	3.5	31924	4.5	-0.08	4.23E+07		
1182.0631	21448	3.5	29905	2.5	-0.71	8.50E+06		
1183.2985	18777	2.5	27225	1.5	-0.93	5.66E+06		
1187.7876	20338	2.5	28755	2.5	-0.86	6.76E+06		
1202.35	22804	2.5	31119	2.5	-0.95	5.13E+06		
1207.0127	20763	3.5	29046	3.5	-0.88	6.14E+06		
1210.991	22804	2.5	31060	3.5	-0.38	1.95E+07		
1245.3833	16735	1.5	24763	1.5	-0.83	6.67E+06		
1251.1674	9920	4.5	17910	3.5	-0.69	8.88E+06		
1252.1106	23303	3.5	31288	3.5	-0.61	1.07E+07		
1279.4518	23875	2.5	31689	1.5	-0.48	1.27E+07		
1293.2303	22439	1.5	30170	1.5	-0.88	5.52E+06		
1300.6688	18311	5.5	25997	4.5	-0.95	4.63E+06		
1304.5776	17099	2.5	24763	1.5	-0.67	8.81E+06		
1306.4272	12431	1.5	20083	1.5	-0.67	7.76E+06		
1309.1039	13747	4.5	21384	4.5	-0.19	2.50E+07		
1310.5444	22247	0.5	29875	1.5	-0.91	4.97E+06		
1321.7602	18311	5.5	25875	5.5	-0.53	1.14E+07		
1322.6731	21944	3.5	29502	2.5	-0.92	4.37E+06		
1323.9928	12787	2.5	20338	2.5	-0.61	8.80E+06		
1328.5602	13238	3.5	20763	3.5	-0.41	1.42E+07		
1465.8062	24089	3.5	30909	2.5	-0.6	7.60E+06		
1475.9447	18316	4.5	25089	4.5	-0.79	5.26E+06		
1486.3792	25415	2.5	32141	3.5	-0.84	4.43E+06		
1517.4482	23467	4.5	30055	3.5	-0.9	3.66E+06		
1572.4612	23221	3.5	29579	2.5	-0.61	7.64E+06		
1611.4542	17099	2.5	23303	3.5	-0.7	5.09E+06		
1624.8588	24249	4.5	30402	3.5	-0.46	1.07E+07		
1640.6878	24841	5.5	30935	4.5	-0.32	1.45E+07		
1647.238	16735	1.5	22804	2.5	-0.97	2.57E+06		
1666.4281	21969	2.5	27969	1.5	-0.96	2.65E+06		
1686.7932	25997	4.5	31924	4.5	-0.63	5.34E+06		
1689.1713	25559	1.5	31477	2.5	-0.82	3.66E+06		
1760.2624	25380	3.5	31060	3.5	-0.82	3.23E+06		
1889.6931	25997	4.5	31288	3.5	-0.9	2.26E+06		
2321.1898	17141	4.5	21448	3.5	-0.53	3.98E+06		
2515.1319	18311	5.5	22286	4.5	-0.39	4.83E+06		
2531.7177	17023	3.5	20972	2.5	-0.99	1.11E+06		
2906.0572	27620	4.5	31060	3.5	-0.95	8.68E+05		
2987.2656	18316	4.5	21663	3.5	-0.91	1.03E+06		
3143.0848	28743	5.5	31924	4.5	-0.54	1.91E+06		
3365.4959	28089	4.5	31060	3.5	-0.82	8.75E+05		
4080.4865	27455	3.5	29905	2.5	-0.95	4.30E+05		
4472.6128	29905	2.5	32141	3.5	-0.93	4.71E+05		
7842.7216	30650	4.5	31925	3.5	-0.9	1.16E+05		

a: Air wavelength calculated using the Edlen formula.
b: Energies from the NIST compilation.
c: Calculated with our HFR+CPOL2 model.
d: From [135].

5.5 Ba I

Barium (Z = 56) is a soft, silvery alkaline earth metal. The element barium was identified for the first time in 1774, but was only reduced to a metal 34 years later with the advent of electrolysis. The name barium comes from the Greek *barys*, meaning heavy.

Barium lines are present in abnormally large quantities in the spectrum of a distinct class of peculiar giant stars that were named Barium stars. The spectral data for the strong lines of s-process elements, such as Ba II at 455.4 nm, was very useful in order to determine the chemical abundances, which are very important to build and put to the test the theoretical stellar models (see e.g. [142]). The atomic radiative lifetimes, transition probabilities, and oscillator strengths are very important data especially for the study of isotopes, atomic structure calculations, and element abundance analyses. Thus, the transition probabilities and oscillator strengths of barium, which can be deduced by combining the measured radiative lifetimes with experimental or theoretical branching fractions, are of crucial importance.

Not having taken part in the experimental measurements since these were carried out by our collaborators at the University of Jilin in China, they will not be described in this manuscript as the method used is TR-LIF spectroscopy and is described in the section 5.2. We will focus in this chapter on the results that we obtained i.e. the semi-empirical gA and gf that we determined in a similar way as we did with Ir I and II (see Section 5.2).

The physical model we used was built to take into account the effects of high Rydberg states. Therefore, the CI model considered for the HFR+CPOL calculations was constituted of the following configurations: 6s^2, 6s(n=7-25)s, 6s(n=5-25)d, 6s(n=5-25)g, , 5d^2, 5d(n=6-8)d, 5d(n=7-8)s, 6p^2, 6p4f and 4f^2 for the even parity and 6s(n=6-25)p, 6s(n=4-25)f, 5d(n=6-9)p and 5d4f the odd one. In other words, we assumed that the Ba I atomic system is composed of a Ba III ionic core with 54 electrons surrounded by 2 valence electrons. The intravalence correlation was considered through the configuration interaction (CI) by explicitly including the CI expansions mentioned here above in the calculations.

The core-polarization effects were taken into account by considering the core polarizability of the Ba III ionic core as calculated by Johnson *et al.* [143]: $\alpha_d = 1.921$ a.u. The cut-off radius was chosen to be the average radius of the outermost core orbital (5p) obtained from our HFR calculations: r_c= 10.61 a.u. In addition, we applied a least-squares fitting procedure to the radial parts, as explained in Chapter 2.2 which was based upon the experimental energy levels obtained by Curry *et al.* [144]. The standard deviations of the fits were found to be respectively 150 and 134 cm^{-1} for the even and odd parities.

The transition probabilities and oscillator strengths were obtained by combining the experimental lifetimes measured by our collaborators at the University of Jilin in China and the theoretical BFs we obtained using the HFR+CPOL model describe above. Those results are reported in Table 5.7. These correspond to 46 Ba I spectral lines within the wavelength range from 240 to 3765 nm. Regarding the BFs, we only give the values larger than 0.1 in the table, most of the weaker decay channels are found to be affected by large cancellation effects in our calculations ($CF \leq 0.05$). The estimated uncertainties of the transition probabilities and oscillator strengths obtained are given using the same letter coding as the one usually used in the NIST database [28]. They were evaluated following a very similar procedure as the one used for Ir I and Ir II and explained in Section 5.2.

Firstly, an uncertainty was assigned to each of our calculated BF values by comparing them to those deduced from recent experimental measurements for some transitions by Wang *et al.* [145]. That comparison allowed us to point out some regular trends as far as the discrepancies between theoretical and experimental branching fractions were concerned. More precisely, the mean deviations $< \frac{BF_{calc-BF_{exp}}}{BF_{calc}} >$ were found to be equal to 18% for $0.8 < BF_{calc} < 1.0$, 28% for $0.6 < BF_{calc} < 0.8$, 34% for $0.4 < BF_{calc} < 0.6$, 39% for $0.2 < BF_{calc} <0.4$, and 53% for $0.1 < BF_{calc} < 0.2$, respectively. From that, we estimated the uncertainties affecting our branching fractions to be respectively of 20%, 30%, 35%, 40%, and 55% for BF = 0.8–1.0, 0.6–0.8, 0.4–0.6, 0.2–0.4, and 0.1–0.2. These uncertainties were then combined with the experimental lifetime uncertainties derived from the measurements performed at University of Jilin to obtain the final uncertainties affecting our gA- and gf-values given in Table 5.7. As a final result, due to the fact that many of the highly excited levels considered in the present work are depopulated by quite a number of weak lines, among the 46 transitions listed in Table 5.7, about half of them have an estimated decay rate accuracy that is equal or better than 50%.

These are nevertheless very satisfying results because those new radiative data in neutral barium can, as mentioned at the beginning of this section, be useful for the observation of Ba I lines in astrophysical spectra.

Table 5.7: Branching fractions, transition probabilities and oscillator strengths for highly excited levels of Ba I.

Upper Level E^a (cm^{-1})	J	Lower Level E^a (cm^{-1})	J	λ^b	BF	gA (s^{-1})	log gf	Uncertainty
26,816.27	3	9596.533	3	580.568	0.133	2.02(7)	-0.99	E
τ = 46(4) ns		11,395.35	2	648.291	0.863	1.31(8)	-0.08	C
39,311.95	1	0	0	254.299	0.296	8.30(6)	-2.09	D +
τ = 107(5) ns		11,395.35	2	358.108	0.395	1.11(7)	-1.67	D +
		26,757.30	0	796.299	0.115	3.22(6)	-1.51	E
40,662.86	1	23,062.05	2	567.998	0.148	9.06(6)	-1.36	E
τ = 49(4) ns		23,479.98	1	581.813	0.476	2.91(7)	-0.83	D +
		23,918.92	2	597.065	0.122	7.47(6)	-1.4	E
40,736.81	1	23,918.92	2	594.44	0.119	3.34(6)	-1.75	E
τ = 107(8) ns		26,757.30	0	715.136	0.194	5.44(6)	-1.38	E
		28,230.23	0	799.359	0.262	7.35(6)	-1.15	D
40,742.60	1	12,266.02	0	351.065	0.326	2.45(6)	-2.34	D
τ = 400(40) ns		12,636.62	1	355.695	0.211	1.58(6)	-2.52	D
41,159.83	1	30,750.67	2	960.429	0.259	1.24(6)	-1.77	D
τ = 628(60)ns		32,943.77	2	1216.796	0.154	7.36(5)	-1.79	E
41,295.93	0	30,695.62	1	943.11	0.483	9.11(5)	-1.92	D +
τ = 530(50) ns		32,805.17	1	1177.428	0.27	5.09(5)	-1.97	D
41,296.96	1	30,695.62	1	943.018	0.107	1.29(6)	-1.76	E
τ = 248(20) ns		30,750.67	2	947.941	0.312	3.77(6)	-1.29	D
		32,943.77	2	1196.82	0.182	2.20(6)	-1.33	E
41,299.33	2	30,818.12	3	953.826	0.414	3.91(6)	-1.27	D +
τ = 530(34) ns		33,526.60	3	1286.198	0.247	2.33(6)	-1.24	D
41,307.88	1	0	0	242.011	0.335	3.54(6)	-2.51	D
τ = 284(28) ns		11,395.35	2	334.212	0.104	1.10(6)	-2.74	E
		28,230.23	0	764.453	0.107	1.13(6)	-2	E
41,404.40	1	30,695.62	1	933.557	0.124	1.22(6)	-1.8	E
τ = 304(30) ns		30,750.67	2	938.381	0.357	3.52(6)	-1.33	D
		32,943.77	2	1181.622	0.189	1.87(6)	-1.41	E
41,406.53	2	30,818.12	3	944.169	0.432	5.26(6)	-1.15	D +
τ = 411(40) ns		33,526.60	3	1268.7	0.247	3.00(6)	-1.14	D
41,411.04	1	9215.501	2	310.512	0.145	1.06(6)	-2.81	E
τ = 410(40) ns		11,395.35	2	333.063	0.1	7.32(5)	-2.91	E
		30,236.83	2	894.672	0.252	1.84(6)	-1.65	D
		30,750.67	2	937.797	0.2	1.46(6)	-1.71	D
41,470.96	3	34,602.77	2	1455.589	0.233	2.40(7)	-0.12	D
τ = 68(5) ns		37,394.87	2	2452.661	0.198	2.04(7)	0.26	E
		38,815.70	2	3765.083	0.127	1.31(7)	0.44	E
41,490.09	1	30,695.62	1	926.146	0.136	9.49(5)	-1.91	E
τ = 430(30) ns		30,750.67	2	930.894	0.326	2.27(6)	-1.53	D
		32,943.77	2	1169.775	0.2	1.40(6)	-1.54	D
41,494.39	1	0	0	240.923	0.112	6.09(5)	-3.28	E
τ = 552(22) ns		30,236.83	2	888.048	0.395	2.15(6)	-1.6	D +
		30,750.67	2	930.521	0.103	5.60(5)	-2.14	E
41,559.45	1	26,160.29	1	649.207	0.284	3.16(6)	-1.7	D +
τ = 270(15) ns		30,750.67	2	924.92	0.254	2.82(6)	-1.44	D +
		32,943.77	2	1160.357	0.133	1.48(6)	-1.53	E

5.6 Rh I

Rhodium (Z = 45) belongs to the fifth row of the periodic table. Its name derives from the Greek word *rhodon* which means pink. This name was proposed by its discoverer (William Hyde Wollaston in 1803) because of the pink-red color of some of rhodium's lead compounds, especially the hydroxide. The first metal obtained also seems to have been slightly impure, harboring significant traces of copper or iron with a red glowing effect [109].

As mentioned in Section 1.2, reliable atomic data of heavy elements such as Rhodium ($Z = 45$) allows for a possible test of the nucleosynthesis models in which the s-and r-processes intervene (see [146]).

In addition, there is an important need of a large numbers of precise radiative parameters of neutral, singly, and doubly ionized heavy atoms with the aim of understanding the large overabundances of heavy elements in chemically peculiar stars (see Zhang *et al.* [147]).

Rhodium is a very important element for which lines have been observed in the solar photosphere and in meteorites for high-lying excited states (Cameron *et al.* [148]). As far as we know, there is very limited radiative data available in the literature about it. This data is unfortunately very insufficient (in number and in accuracy) to meet the needs of astrophysicists.

In 1962, the experimental transition probabilities of Rh I were first determined experimentally by Corliss and Bosman [9], but their measurements were affected by very significant errors. In 1982, radiative lifetimes of 13 levels in Rh I were measured using TR-LIF spectroscopy technique by Kwiatkowski *et al.* [149]. With their new experimental measurements, they deduced new oscillator strengths and used them to redetermine the photospheric abundances of Rh I. It appeared that the result was in excellent agreement with the meteoritic value. A year later, new experiments were made using the same method by Salih, Duquette and Lawler [150] to measure the lifetimes of 22 levels in Rh I.

Afterwards (in 1985), by combining their experimental BF with the previous lifetimes mentioned here above, Duquette and Lawler [151] obtained transition probabilities for 115 transitions in Rh I. The most recent data comes from Malcheva *et al.* [152] who measured radiative lifetimes of 17 levels in Rh I and compared them to a HFR+CPOL calculation. In summary, the lifetimes of 37 levels in Rh I have been reported in literature so far.

In the framework of the collaboration with the University of Jilin, radiative lifetime measurements were carried out for 20 odd-parity levels in Rh I in the region from 31 101.75 to 50 721.44 cm^{-1}. We then combined these lifetimes with our theoretical branching fractions obtained by the HFR+CPOL method to deduce semi-empirical transition probabilities and oscillator strengths (log gf) for 63 Rh I lines as shown in Table 5.8 (only the transitions with $BF \geq 0.1$ are given in that table, the smaller ones being affected by high cancellation effects). The uncertainty affecting those values is given using the NIST coding convention [28].

We adopted the same model for the HFR+CPOL calculations than the most recent one from [152]. The configurations explicitly included in the calculations were $4d^85s$, $4d^86s$, $4d^85d$, $4d^86d$, $4d^9$, $4d^75s^2$, $4d^75p^2$, $4d^75d^2$, $4d^75s6s$, $4d^75s5d$, and $4d^75s6d$ for the even parity, and $4d^85p$, $4d^86p$, $4d^84f$, $4d^85f$, $4d^75s5p$, $4d^75s6p$, $4d^75p5d$, and $4d^75p6s$ for the odd parity.

We took the core-polarization effects into account by considering a Rh III ionic core with a dipole polarizability taken from Fraga *et al.* [94]: $\alpha_d = 7.42\ a_0^3$, and a cut-off radius, as usual, corresponding to the HFR average value, $< r >$, of the outermost core orbital (4d in this case): $r_c = 1.50\ a_0$.

We also adjusted some of the radial integrals characterizing the $4d^85s$, $4d^9$, $4d^75s^2$ and

$4d^86s$ even configurations, and the $4d^85p$ and $4d^75s5p$ odd configurations using the fitting procedure described in Section 2.2. The experimental energy levels used to perform this fit were taken from the NIST compilation [28]. The final average energy deviations were found to be of 35 and 43 cm^{-1}, respectively (see [152]). However, it is worth mentioning that, despite the fact that the fit had been limited to levels below 47 000 cm^{-1} in Malcheva *et al.* [152] because of high mixing effects, we were able to identify two higher levels for which lifetimes were measured by our colleagues: 48797.74 cm^{-1} with $J = 5/2$ and 48811.47 cm^{-1} with $J = 7/2$. For these experimental levels, the values calculated with our HFR+CPOL model were found to be equal to 48523 and 48787 cm^{-1}. Their identification in the calculations were made possible by the good agreement obtained between the theoretical Landé g-factors (1.039 and 0.918) and the equivalent experimental values (1.066 and 0.928) given in the NIST tables [28].

Table 5.8: New reliable BF, gA and log gf obtained in Rh I and comparison with previously existing values in the literature.

Upper level[a]	Lower level[a]	λ (air)[a]	BF	gA ($10^6 s^{-1}$)		log gf	
E (cm^{-1})	E(cm^{-1})	(nm)		This work	Previous[b]	This work	Previous[c]
31101.75	2598.03	350.7311	0.311	273 (D+)	270	-0.30	- 0 .28
τ =9.1(9)ns	3309.86	359.7146	0.490	431 (D+)	470	-0.08	-0.06
	5690.97	393.4224	0.124	109 (E)	126	-0.60 (E)	-0.59
31613.78	1529.97	332.3091	0.507	624 (D+)	630	0.01	0.01
τ =8.1(5) ns	5690.97	385.6513	0.490	603 (D+)	590	0.13	0.12
36985.25	5657.97	319.1183	0.175	135 (E)	-	-1.15	-1.23
τ = 7.8(9) ns	10313	374.8207	0.569	438 (D+)	-	-0.04	-0.11
	11968.23	399.6149	0.101	78 (E)	-	-0.73	-0.81
37368.62	11006.05	379.2180	0.143	23 (E)	-	-1.30 (E)	-1.25
τ = 12.5(3) ns	11968.23	393.5833	0.739	118 (C)	-	-0.56	-0.50
38038.12	10313.41	360.5862	0.384	120 (D+)	-	-0.63	-0.57
τ = 12.8(4) ns	11006.05	369.8257	0.345	108 (D+)	-	-0.65	-0.60
38668.83	11968.23	374.4170	0.431	155 (D+)	-	-0.49	- 0.45
τ = 11.1 (4) ns	13520.69	397.5313	0.312	112 (D+)	-	-0.58	-0.54
38718.11	5657.97	302.3910	0.145	34 (D)	-	-1.33	-1.26
τ = 25.5(14)ns	11968.23	373.7272	0.668	157 (C)	-	-0.48	- 0.41
39126.76	10313.41	346.9620	0.136	52 (E)	-	-1.03	-1.02
τ = 15.6(4) ns	11968.23	368.1036	0.590	227 (D+)	-	-0.34	-0.33
39231.38	2598.03	272.8945	0.106	50 (E)	-	-1.25	-1.25
τ = 8.5 (4) ns	11006.05	354.1905	0.252	118 (D+)	-	-0.65	-0.65
	11968.23	366.6910	0.132	62 (E)	-	-0.90	- 0.90
	14382.19	402.3139	0.106	50 (E)	-	-0.92	-0.91
39788.09	13520.69	380.5920	0.811	383 (B)	-	-0.08	-0.09
τ = 12.7(7) ns							
40576.95	5657.97	286.2931	0.240	189 (D+)	-	-0.63	-0.67
τ =7.6(9) ns	14382.19	381.6474	0.659	520 (C)	-	0.06	0.02
40603.48	9221.22	318.5592	0.115	58 (E)	-	-1.05	-1.13
τ =8.0(7) ns	10313.41	330.0462	0.218	109 (D+)	-	-0.75	-0.82
	13974.73	375.4273	0.276	138 (D+)	-	-0.54	-0.60
45177.63	16120.72	3440.0536	0.865	753 (B)	-	0.13	0.20
τ =9.2(7) ns							
46511.10	5690.97	244.9030	0.527	137 (D+)	-	-0.91	-0.97
τ =38.4(20) ns	14787.87	295.8764	0.239	62 (D+)	-	-1.03	-1.09
	16120.72	328.9567	0.113	29 (E)	-	-1.33	-1.38
48797.74	5690.97	231.9109	0.174	127 (E)	-	-0.99	-
τ =8.2(3) ns	7791.23	243.7898	0.552	404 (D+)	-	-0.44	-
	11968.23	271.4409	0.109	80 (E)	-	-1.05	-
48811.47	5690.97	231.8370	0.330	78 (D+)	-	-1.20	-
τ =33.9(12) ns	7791.23	243.7082	0.243	57 (D+)	-	-1.29	-
	13520.69	283.2768	0.109	26 (E)	-	-1.50	-
	16118.69	305.7890	0.166	39 (E)	-	-1.26	-

a: From NIST database [28].
b: From Duquette *et al.* [151].
c: From Malcheva *et al.* [152].

We hope that these new reliable semi-empirical atomic data (shown in Table 5.8) are likely to be used for the analysis and interpretation of astrophysical spectra which could contain neutral rhodium lines in order to improve abundance determinations of this element in different astrophysical objects.

General Conclusion

As mentioned in our general introduction, developments in atomic physics have always played a major role in astrophysics. Conversely, the improvement of astronomical observing instruments, with more and more powerful ground-based and space telescopes, on the one hand, and the development of more and more sophisticated stellar models, on the other hand, implies that an increasing amount of accurate atomic data is required. Such demands are particularly acute for heavy atoms and ions (typically beyond the iron group) as these elements have been little studied in the past, mainly because of their complex electronic structures. However, the latter are of indisputable interest since they are more and more often identified in the spectra of many different astrophysical sources, so that a precise knowledge of the fundamental spectroscopic parameters that characterize them is urgently required for the development of many hot topics in astronomy. The investigations of atomic structures and radiative processes that we have carried out in the present thesis are part of this context insofar as they concern neutral, lowly- and moderately-ionized atoms, presenting a particular interest in different astrophysical areas such as cosmochronology, the study of hot white dwarfs, the analysis of chemically peculiar stars and the development of stellar nucleosynthesis models.

More precisely, a large amount of new data such as energy levels, wavelengths, radiative lifetimes, oscillator strengths, and transition probabilities have been determined in our work, most of them for the first time, in atomic systems as diverse as singly ionized thorium and uranium (of interest to cosmochronology), three- to six-times ionized copper, indium, caesium and silver (of interest to hot white dwarf studies), and neutral and/or singly ionized iridium, rhenium, lanthanum, barium and rhodium (of interest for the study of chemically peculiar stars). For this purpose, the most complete physical models possible have been developed on the basis of the pseudo-relativistic Hartree-Fock (HFR) theoretical method in which valence-valence electron correlations were explicitly included in multi-configuration expansions while core-valence interactions, which are extremely important in order to model the atomic structures of neutral and lowly ionized heavy elements, were considered using a core-polarization potential and a correction to the dipole operator depending on two parameters, i.e. a dipole polarizability and a cut off radius corresponding to the ionic core, giving rise to the so-called HFR+CPOL approach.

In the specific case of the lanthanum atom, another independent theoretical method was used in our calculations, namely the fully relativistic Multiconfiguration Dirac-Hartree-Fock (MCDHF) approach. It should be noted that this method is more complex to use and requires much longer computation times than the HFR+CPOL method. It also often presents convergence problems during the optimization of orbitals, especially for neutral and lowly ionized atoms. However, we have shown that the HFR+CPOL radiative rates were in good agreement with the MCDHF results for most of the spectral lines considered in neutral lanthanum, allowing to highlight the reliability of the HFR+CPOL method when a large number of radiative data must be determined for a specific heavy atomic system.

Part of our work has also involved experimental measurements of atomic parameters. In particular, we have obtained new transition probabilities for a large number of spectral lines involving highly excited states in neutral and/or singly ionized heavy atoms such as iridium, rhenium, barium and rhodium, thanks to the combination of theoretical branching fractions calculated with the HFR+CPOL method and accurate radiative lifetimes measured using time-resolved laser-induced-fluorescence (TR-LIF) spectroscopy. The latter measurements were carried out in collaboration with Chinese experimentalists who built a TR-LIF setup at the University of Jilin. This allowed us not only to estimate the accuracy of the HFR+CPOL calculations, but also to provide new semi-empirical spectroscopic parameters that are more accurate than if they had been obtained entirely using a purely theoretical model.

As already mentioned above, all the atomic physics studies carried out in the present thesis have been motivated by their potential applications in astrophysics. In particular, our work relating to the Th II and U II ions made it possible to establish, for the first time, a list of some tens of spectral lines belonging to these ions likely to be used as cosmochronometers, allowing astrophysicists to consider future studies aiming at determining the age of some stars using the ^{238}U/^{232}Th ratio.

Many atomic parameters obtained in our work have also been directly applied to the study of hot white dwarfs. Indeed, the new transition probabilities and oscillator strengths that we have calculated for the ions Cu IV-VII, In IV-VII, Cs IV-VII and Ag IV-VII have not only allowed the identification of lines of these ions in the spectra of the white dwarfs RE0503-289 and RE0457-281, but have also been incorporated in the NLTE models used to interpret these spectra and to deduce the chemical abundances. This work, performed in close collaboration with the Astronomy and Astrophysics Department of the University of Tübingen in Germany, has confirmed the large overabundances (of several orders of magnitude compared to solar abundances) already deduced in these white dwarfs for other elements heavier than iron, thus consolidating the hypothesis of radiative levitation. In addition, it is worth mentioning that the new semi-empirical radiative data obtained for the highly-excited states in Ir I, Ir II, Re I, La I, Ba I and Rh I are directly applicable to the detection of these elements in chemically peculiar stars and thus to the establishment of constraints on the nucleosynthesis models developed to explain the production of heavy atomic species in these celestial objects.

Finally, we would like to point out that the different works presented in this thesis have been the subject of 10 publications in peer-review scientific journals [77, 79, 102, 103, 153, 154, 155, 156, 157, 158].

Although the results reported in the present manuscript constitute a significant contribution to the knowledge of electronic structures and the spectroscopic parameters characterizing heavy atoms and ions, a very large effort must still be pursued in this field to fully meet the needs of the astrophysical community. These crucial needs for new investigations of atomic processes of astrophysical interest were recently reminded by the prestigious American Astronomical Society in its latest review of research in Astrophysics [159] in which the urgent priorities in this scientific field were presented in various White Papers. Among these, we will pinpoint two articles co-authored by about one hundred renowned astrophysicists entitled Atomic Data for Astrophysicists: Needs and Challenges [160] and State of the Profession Considerations for Laboratory Astrophysicists [161], in which the study of atomic processes in heavy atomic systems was clearly identified as one of the key priorities in order to explore the origin of trans-iron elements in the Universe. This necessity will be even more exacerbated with the launches of new space telescopes recording high-resolution astrophysical spectra, such as, for example, the James Webb Telescope in the infrared region. The recent first detection of gravitational waves from a neutron star merger has also opened the way to huge demands for new reliable atomic data in heavy elements which seem to be created in large quantities during those mergers [131]. It is therefore obvious that the atomic physicists still have a lot of work ahead of them in order to meet all the current and future requests made by astrophysicists.

As we already mentioned here above, within the framework of our study, many ions (25) of many elements (11 different elements) have been studied. To finish on a more visual note, Figure 5.9 shows in black on the Mendeleev table, all the elements for which at least one ion has been studied in the course of this thesis.

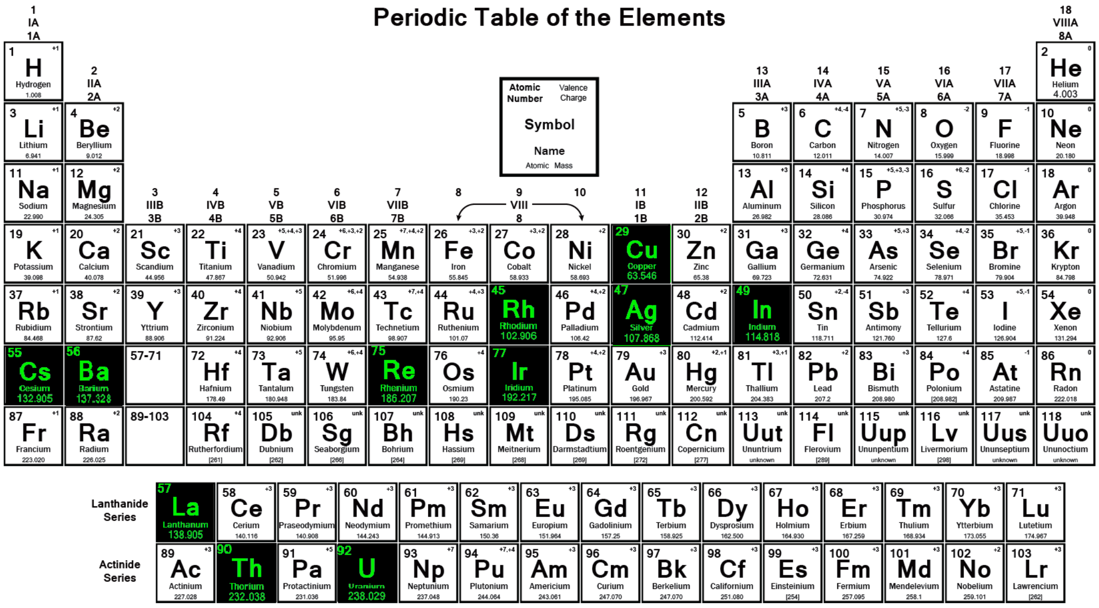

Figure 5.9: Heavy elements for which at least one ion have been studied during this thesis - Original picture from: sciencesnote.org (©Todd Helmenstine)

Bibliography

[1] J. Blaise and J.F. Wyart. Selected constants energy levels and atomic spectra of actinides. *Centre National de la Recherche Scientifique*, Vol 22, 1992.

[2] D.W. Steinhaus, L.J.Jr. Radziemski, R.D. Cowan, J. Blaise, G. Guelachvili, Z. Ben Osman, and J. Vergès. Lasl report la-4501. *Los Alamos Scientific Laboratory, NM, USA*, UC-34, 1971.

[3] B.A. Palmer, R.A. Keller, and Jr. R. Engleman. Lasl report la-4501. *Los Alamos Scientific Laboratory, NM, USA*, UC-34a, 1980.

[4] L. Brewer. Energies of the electronic configurations of the lanthanide and actinide neutral atoms. *Journal of the Optical Society of America*, 12, 1971.

[5] J. Blaise, J.-F. Wyart, J. Vergès, Jr. R. Engleman, B.A. Palmer, and L.J. Radziemski. Energy levels and isotope shifts for singly ionized uranium (U II). *Journal of the Optical Society of America B*, 11, 1994.

[6] A. Meftah, M. Sabri, J.-F. Wyart, and W Tchang-Brillet. Spectrum of singly charged uranium (U II) : Theoretical interpretation of energy levels, partition function and classified ultraviolet lines. *Atoms*, 5, 2017.

[7] R.D. Cowan. *The Theory of Atomic Structure and spectra*. California Press, 1981.

[8] W.F. Meggers, C.H. Corliss, and B.F. Schribner. Tables of spectral-line intensities. *US Government Printing Office, Washington DC*, NBS Monograph 32, 1961.

[9] C.H. Corliss and W.R. Bosman. Experimental transition probabilities for spectral lines of severnty elements. *US Government Printing Office, Washington DC*, NBS Monograph 53, 1962.

[10] P.A. Voigt. Measurement of U I and U textscII relative oscillator strengths. *Physical Review A*, 11, 1975.

[11] C.H. Corliss. *Journal of Research of the National Bureau of Standards*, 80A, 1976.

[12] H.L. Chen and C. Borzileri. Laser induced fluorescence studies of U II produced by photoionization of uranium. *Journal of Chemical Physics*, 74, 1981.

[13] G. Henrion, M. Fabry, and M. Remy. Determination of oscillator strengths for **U** I and U II lines. *Journal of Quantitative Spectroscopy and Radiative Transfer*, 37, 1987.

[14] R.L. Kurucz. *Atomic Spectral line Database from CD-ROM 23*, 1995.

[15] H. Lundberg, S. Johansson, H. Nilsson, and Z. Zhang. New laboratory lifetime measurements of U II for the uranium cosmochronometer. *Astronomy and Astrophysics*, 372(L50-L52), 2001.

[16] H. Nilsson, S. Ivarsson, S. Johansson, and H. Lundberg. Experimental oscillator strengths in U II of cosmochronological interest. *Astronomy and Astrophysics*, 381, 2002.

[17] J.R.Jr. McNally, G.R. Harrison, and Park H.B. General properties of the thorium atom and thorium ions. *Journal of the Optical Society of America*, 32, 1942.

[18] J.R. McNally. First spark spectrum of thorium—infra-red spectrum and further classification of th II∗. *Journal of the Optical Society of America*, 35(6):390–398, 1945.

[19] T.L. De Bruin, Klinkenberg P.F.A., and Schuurmans Ph. Die struktur des ThII-spektrums. II. *Zeitschrift für Physik*, 122, 1944.

[20] T.L. De Bruin, Schuurmans Ph., and Klinkenberg P.F.A. Die struktur des ThII-spektrums. I. *Zetschrift für Physik*, 121, 1943.

[21] Ph. Schuurmans. *PhD Thesis.* Zeeman Laboratory, Amsterdam, The Netherlands, 1946.

[22] G. W. Charles. A compilation of data on some spectra of thorium. 1958.

[23] E.B.M. Steers. The emission spectrum of thorium in the 1–2.5 μ region. *Spectrochimica Acta B*, 23(135), 1967.

[24] N. Minski. *PhD Thesis.* Hebrew Univ. of Jerusalem, Israel, 1969.

[25] R. Zalubas and C.H. Corliss. Energy levels and classified lines in the second spectrum of thorium. *Journal of Research of the National Bureau of Standards A*, 78(163), 1974.

[26] J.E. Sansonetti and W.C. Martin. Handbook of basic atomic spectroscopic data. *Journal of Physical and Chemical Reference Data*, 34, 2005.

[27] S.L. Redman, G. Nave, and C.J. Sansonetti. The spectrum of thorium from 250 nm to 5500 nm : Ritz wavelengths and optimized energy levels. *Astrophysical Journal Supplement Series*, 211(4), 2014.

[28] A. Kramida, Y. Ralchenko, J. Reader, and NIST ASD Team. Nist atomic spectra database (ver.5.7.1.), 2019.

[29] J. Sugar and A. Musgrove. Energy levels of copper, cu I through cu XXIX. *Journal of Physical and Chemical Reference Data*, 19(527), 1990.

[30] T. A. M. Van Kleef, A. J. J. Raassen, and Y. N. Joshi. Analysis of the fifth spectrum of copper (cu V). *Physica B+C*, 84(401), 1976.

[31] A. J. J. Raassen and T. A. M. Van Kleef. Analysis of the sixth spectrum of copper (Cu VI). *Physica B+C*, 103(412), 1981.

[32] Swapnil and A. Tauheed. Revised and extended analysis of the fourth spectrum of indium: In IV. *Journal of Quantitative Spectroscopy*, 129:31–47, 2013.

[33] A.N. Ryabtsev and Y.A. Kononov. High lying configurations in the spectrum of three times ionized indium (In IV). *Journal of Quantitative Spectroscopy and Radiative Transfer*, 168, 2015.

[34] Swapnil and A. Tauheed. Spectral analysis of the fifth spectrum of indium : In V. *Journal of Quantitative Spectroscopy*, 168:102–141, 2016.

[35] A.N. Ryabtsev. The $4d^8$ nf (n = 5 and 6) and $4d^8$ 7p configurations in the spectrum of four times ionized indium (In V). *Journal of Quantitative Spectroscopy and Radiative Transfer*, 220:102–141, 2018.

[36] J.F. Wyart, A.J.J. Raassen, P.H.M. Huylings, and Y.N. Joshi. Spectra of high-z ions of stellar interest. a theoretical study of (d + s) m ix ed configurations in 5d- and 4d-elements. *Phys. Scr.*, T47:59–64, 1993.

[37] A.N. Ryabtsev, A. Tauheed, Swapnil, R.R. Kildiyarova, and Y.A Kononov. The 4d 8 –($4d^7$ 4f + $4d^7$ 6p + $4p^5$ $4d^9$) transitions in the spectrum of five times ionized indium (In VI). *Journal of Quantitative Spectroscopy*, 212:50–58, 2018.

[38] A.N. Ryabtsev, V.I. Azarov, and Y.N. Joshi. Analysis of the $4d^7$ and $4d^6$ 5p configurations of six times ionized indium (In VII). *Physica Scripta*, 45:598–606, 1992.

[39] J.E. Sansonetti. Wavelengths, transition probabilities, and energy levels for the spectra of cesium (Cs I – Cs LV). *Journal Of Physical and Chemical Reference Data*, 38(761), 2009.

[40] A. Husain, K. Haris, S. Jabeen, and A. Tauheed. Critically evaluated energy levels, wavelengths, transition probabilities, and intensities of six-times ionized cesium : Cs VII. *Journal of Quantitative Spectroscopy and Radiative Transfer (JQSRT*, 247(106956), 2020.

[41] S. Ankita and Tauheed A. Spectral analysis of triply ionized silver (Ag IV). *Journal of Quantitative Spectroscopy and Radiative Transfer*, 254, 2020.

[42] R.R Kildiyarova, A.A. Valk, and Y.N. Joshi. The analysis of the $4d^65s$ - $4d^65p$ tansitions of four-times ionized silver : Ag V. *Physica Scripta*, 52(5), 1995.

[43] T. Kleef, A.J.J. Raassen, and Y.N. Joshi. The analysis of the 4d565s - $4d^55p$ tansitions in the fifth spectrum of silver (Ag V). *Physica Scripta*, 36(1), 1987.

[44] Y.N. Joshi, A.J.J. Raassen, T.A.M. Van Kleef, and A.A. Valk. The sitxh spectrum of silver : Ag VI and a study of the parameter valuer in 4d-spectra. *Physica Scripta*, 38(5), 1988.

[45] A. Ryabtsev and E. Kononov. Resonance transitions in the spectra of the Ag^{6+} - Ag^{8+} ions. *Atoms*, 5(4):11, 2017.

[46] `https://www.eso.org/public/`. The european southern observatory.

[47] A. Frebel. *Searching for the Oldest Stars : Ancient Relics from Early Universe*. Princeton University Press, 2019.

[48] S. E. Woosley, A. Heger, and T. A. Weaver. The evolution and explosion of massive stars. *Reviews of Modern Physics*, 74:1015–1071, 2002.

[49] Borexino Collaboration. Experimental evidence of neutrinos produced in cno fusion cycle in the sun. *Nature*, 587:577–582, 2020.

[50] C. Sneden, J.J. Cowan, and R. Gallino. Neutron-capture elements in the early galaxy. *Annual Review of Astronomy and Astrophysics*, 46(1):241–288, 2008.

[51] K-L Kratz, K. Farouqi, B. Pfeiffer, J.W. Truran, C. Sneden, and J.J. Cowan. Explorations of the r-processes: comparisons between calculations and observations of low-metallicity stars. *The Astrophysical Journal*, 662(1):39–52, 2007.

[52] J.J. Truran, S.M. Burles, J.J. Cowan, and C. Sneden. Nucleosynthesis clocks and the age of the galaxy. *arXiv: Astrophysics*, 2001.

[53] N. Dauphas. Uranium-thorium cosmochronology. *Lunar and Planetary Science*, XXXVI, 2005.

[54] R. Cayrel, V. Hill, T.C. Beers, B. Barbuy, M. Spite, F. Spite, B. Flez, J. Andersen, P. Bonifacio, P. François, P. Molaro, B. Nordström, and F. Primas. Measurement of stellar age from uranium decay. *Nature*, 469:691–692, 2001.

[55] Barbuy, B., Spite, M., Hill, V., Primas, F., Plez, B., Cayrel, R., Spite, F., Wanajo, S., Siqueira Mello, C., Andersen, J., Nordström, B., Beers, T. C., Bonifacio, P., François, P., and Molaro, P. First stars - xv. third-peak r-process element and actinide abundances in the uranium-rich star cs31082-001. *Astronomy and Astrophysics*, 534:A60, 2011.

[56] H.R. Butcher. Thorium in g-dwarf stars as a chronometer for the galaxy. *Nature*, 328(127), 1987.

[57] S. Goriely and B. Clerbaux. Uncertainties in the Th cosmochronometry. *Astronomy and Astrophysics*, 346(798), 1999.

[58] C. Sneden and J. J. Cowan. The age of the galaxy from thorium cosmochronometry. *Rev. Mex. Astron. Astrof. Ser. Conf.*, 10:221, 2001.

[59] I.U. Roederer, K.L. Kratz, A. Frebel, N. Christlieb, B. Pfeiffer, J.J. Cowan, and C. Sneden. The end of nucleosynthesis : Production of lead and thorium in the early galaxy. *Astrophysical Journal*, 698(1963), 2009.

[60] J.E. Lawler, W. Whaling, and Grevesse N. Contamination of the Th II line and the age of the galaxy. *Nature*, 346:635–637, 1990.

[61] O. Morell, D. Kallander, and H. R. Butcher. The age of the galaxy from thorium in g dwarfs, a re-analysis. *Astronomy and Astrophysics*, 259:543–548, 1992.

[62] C. Sneden, G. W. McWilliam, A.and Preston, J. J. Cowan, D. L. Burris, and B. J. Armosky. The ultra–metal-poor, neutron-capture–rich giant star cs 22892-052. *Astrophysical Journal*, 467:819, 1996.

[63] J.E. Norris, S.G. Ryan, and T.C. Beers. Extremely metal-poor stars. the carbon-rich, neutron capture element poor object CS 22957-027. *The Astrophysical Journal*, 489(2):L169–L172, 1997.

[64] J.A. Johnson and M. Bolte. Th ages for metal-poor stars. *The Astrophysical Journal*, 554(2):888–902, 2001.

[65] A. Frebel, N. Christlieb, J.E. Norris, C. Thom, T.C Beers, and J. Rhee. Discovery of HE 1523-0901, a strongly r-process-enhanced metal-poor star with detected uranium. *Astrophysical Journal Letters*, 660:117, 2007.

[66] Ren, J., Christlieb, N., and Zhao, G. The hamburg/eso r-process enhanced star survey (heres) - vii. thorium abundances in metal-poor stars. *Astronomy and Astrophysics*, 537:A118, 2012.

[67] C. Keeton. *Principle of Astrophysics*. Springer, 2014.

[68] H.M. Van Horn. *Unlocking the Secrets of White Dwarf Stars*. Springer, 2015.

[69] S.D. Kawaler. *White dwarf Stars*. Springer, 1997.

[70] T. Rauch, K. Werner, P. Quinet, and J.W.A. Kruk. Stellar laboratories II : New Zn IV and Zn V oscillator strenght and their validation in hot white dwarfs g191-2b2 and RE0503-289. *Astronomy and Astrophysics*, 564, 2014.

[71] K. Werner, T. Rauch, E. Ringat, and J. Kruk. 2013.

[72] T. Rauch, D. Hoyer, P. Quinet, M. Gallardo, and M. Raineri. Stellar laboratories - v. the xeultraviolet spectrum and the xenon abundance in the hot do-type white dwarf re3-289. *Astronomy and Astrophysics*, 577:A88, 2015.

[73] T. Rauch, P. Quinet, D. Hoyer, K. Werner, M. Demleitner, and J. W. Kruk. Stellar laboratories - VI. new Mo IV-VII oscillator strengths and the molybdenum abundance in the hot white dwarfs g191-b2b and re3-289. *Astronomy and Astrophyics*, 587:A39, 2016.

[74] T. Rauch, P. Quinet, D. Hoyer, K. Werner, P. Richter, J. W. Kruk, and M. Demleitner. Stellar laboratories - VII. new Kr IV-VII oscillator strengths and an improved spectral analysis of the hot, hydrogen-deficient do-type white dwarf re3-289+. *Astronomy and Astrophysics*, 590:A128, 2016.

[75] T. Rauch, K. Werner, É. Biémont, P. Quinet, and J. W. Kruk. Stellar laboratories: new Ge V and Ge VI oscillator strengths and their validation in the hot white dwarf RE3-289. *Astronomy and Astrophysics*, 546:A55, 2012.

[76] T. Rauch, K. Werner, P. Quinet, and J. W. Kruk. Stellar laboratories - iv. new ga IV and ga V and ga VI oscillator strengths and the gallium abundance in the hot white dwarfs g191-b2b and RE3-289. *Astronomy and Astrophysics*, 577:A6, 2015.

[77] T. Rauch, S. Gamrath, P. Quinet, M. Demleitner, M. Knörzer, K. Werner, and J.W. Kruk. New cu iv – vii oscillator strengths and the first detection of copper and indium in hot white dwarfs. *Astronomy and Astrophysics*, 637(A4), 2020.

[78] D. Hoyer, T. Rauch, K. Werner, and J. W. Kruk. Search for trans-iron elements in hot, helium-rich white dwarfs with the hst cosmic origins spectrograph. *Astronomy and Astrophysics*, 612(A62), 2018.

[79] L. Löbling, M. A. Maney, T. Rauch, P. Quinet, S. Gamrath, J. W. Kruk, and K. Werner. First discovery of trans-iron elements in a dao-type white dwarf (BD-22^o3467). *Monthly Notices of the Royal Astronomical Society*, 492(1):528–548, 2019.

[80] K. Werner, T. Rauch, E. Ringat, and J.W. Kruk. First detection of krypton and xenon in white dwarfs. *The Astrophysical Journal*, 753(1):L7, 2012.

[81] P. Quinet, P. Palmeri, E. Biémont, M.M. Mc Curdy, G. Rieger, E.H Pinnington, M.E. Wickliffe, and J.E. Lawler. Experimental and theoretical radiative lifetimes, branching fractions and oscillator strengths in Lu II. *Monthly Notices of the Royal Astronomical Society*, 307(934), 1999.

[82] P. Quinet, P. Palmeri, E. Biémont, Z.S. Li, Z.G. Zhang, and S. Svanberg. Radiative lifetime measurements and transition probability calculations in lanthanide ions. *Journal of Alloys and Compounds*, 344(255), 2002.

[83] J. Migdalek and M.K. Baylis. Implicit and explicit treatment of valence-core electron exchange and core polarization in model potentials. *Journal of Quantitative Spectroscory and Radiative Transfer*, 22(2), 1979.

[84] S. Hameed. Core polarization corrections to oscillator strengths and singlet-triplet splittings in alkaline earth atoms. *Journal of Physics B*, 4(746), 1972.

[85] S. Hameed, A. Herzenberg, and M.G. James. Core polarization corrections to oscillator strengths in the alkali atoms. *Journal of Physics B*, 1(822), 1968.

[86] E. Biémont, H.P. Garnir, P. Palmeri, P. Quinet, Z.S. Li, Z.G. Zhang, and S. Svansberg. Core-polarization effects and radiative lifetime measurements in Pr III. *Physical Review A*, 64(022503), 2001.

[87] I.P. Grant. *Relativistic Quantum Theory of Atoms and Molecules*. Springer, 2007.

[88] W. Greiner and J. Reinhardt. *Quantum Electrodynamics*. Springer, 2002.

[89] P. Jönsson, G. Gaigalas, C. Froese Fischer, and I.P. Grant. New version: Grasp2k relativistic atomic structure package. *Computer Physics Communication*, 184, 2013.

[90] C. Froese Fischer, G. Gaigalas, P. Jönsson, and J. Biéron. Grasp2018—a fortran 95 version of the general relativistic atomic structure package. *Computer Physics Communication*, 237, 2019.

[91] E.E. Koch. *Uran Gebundene Ausgabe*. Andre Bonne, 1957.

[92] H. Becquerel. *Compte-rendu de l'Académie des sciences, séance du 1er mars 1896; Sur les radiations invisibles émises par les corps phosphorescent*. Académie des Sciences de Paris, 1896.

[93] H. Becquerel. *Compte-rendu de l'Académie des sciences, séance du 24 février 1896, Sur les radiations émises par phosphorescence*. Académie des Sciences de Paris, 1896.

[94] S. Fraga, J. Karkowski, and K.M.S Saxena. *Handbook of Atomic Data*. Elsevier, 1979.

[95] A.P. Jones, F. Wall, and C.T. Williams. *Rare Earth Minerals : Chemistry, Origin and Ore Deposits*. Springer, 1996.

[96] B. Fernandez. *De l'atome au noyau. Une approche historique de la physique atomique et de la physique nucléaire*. ellipses, 2006.

[97] L. Brewer. Energies of the electronic configurations of the singly, doubly, and triply ionized lanthanides and actinides. *Journal of the Optical Society of America*, 61(12):1666–1682, 1971.

[98] O.A. Herrera-Sancho, N. Nemitz, M.V. Okhapkin, and Peik E. Energy levels of Th^+between 7.3 and 8.3 eV. *Physical Review A*, 88(012512), 2013.

[99] D.-M. Meier, J. Thielking, P. Głowacki, M. V. Okhapkin, R. A. Müller, A. Surzhykov, and E. Peik. Electronic level structure of Th^+ in the range of the ^{229m}Th isomer energy. *Physical Review A*, 99:052514, 2019.

[100] C. H. Corliss. Oscillator strengths for lines of ionized thorium (Th II). *Monthly Notices of the Royal Astronomical Society*, 189(3):607–610, 1979.

[101] H. Nilsson, Z.G. Zhang, H. Lundberg, S. Johansson, and B. Nordström. Experimental oscillator strengths in Th II. *Astronomy and Astrophysics*, 382(368), 2002.

[102] S. Gamrath, P. Palmeri, and P. Quinet. Calculated oscillator strengths for the strongest lines of cosmochronological interest in the visible spectrum of singly ionized uranium. *Monthly Notices of the Royal Astronomical Society*, 480(4):4754–4760, 2018.

[103] S. Gamrath, M.R. Godefroid, P. Palmeri, P. Quinet, and K. Wang. Spectral line list of potential cosmochronological interest deduced from new calculations of radiative transition rates in singly ionized thorium (Th II). *Monthly Notices of the Royal Astronomical Society*, 496:4507–4516, 2020.

[104] T.R. Dulski. *Manual for the Chemical Analysis of Metals*. ASTM, 1996.

[105] G. J. Van het Hof, A. J. J. Raassen, P. H. M. Uylings, Y.N Yoshi, L.I Podobedova, and A.N. Ryabstev. Analysis of the seventh spectrum of copper using orthogonal operators for the ground configuration. *Physica Scripta*, 41(240), 1990.

[106] K.M. Aggarwal, P. Bogdanovich, F.P. Keenan, and R. Kisielius. Energy levels and radiative rates for cr-like cu VI and zn VII. *Atomic Data and Nuclear Data Tables*, 111-112:280–345, 2016.

[107] T. Rauch, K. Werner, R. Bohlin, and J. W. Kruk. The virtual observatory service theossa: Establishing a database of synthetic stellar flux standards - i. nlte spectral analysis of the da-type white dwarf g191-b2b. *Astronomy and Astrophysics*, 560:A106, 2013.

[108] D. Hoyer, T. Rauch, K. Werner, J. W. Kruk, and P. Quinet. Complete spectral energy distribution of the hot, helium-rich white dwarf rx03.9-2854. *Astronomy and Astrophysics*, 598:A135, 2017.

[109] D.R. Lide. *Handbook of Chemistry and Physics*. CRC Press Inc, 2009.

[110] A. Wajid, A. Husain, S. Jabeen, and A. Tauheed. The multi-configuration dirac-hartree-fock calculations for cs vii. *Journal of Atomic, Molecular, Condensed Matter and Nano Physics*, 7(1):35–40, 2020.

[111] A. Ernout and A. Meillet. *Dictionnaire étymologique de la langue latine. Histoire des mots*. Librairie C. Klicksieck, Paris, 1939.

[112] C.M. Sikström, H. Nilsson, U. Litzén, A. Blom, and H. Lundberg. Uncertainty of oscillator strengths derived from lifetimes and branching fractions. *Journal of Quantitative Spectroscopy and Radiative Transfer*, 74:355, 2002.

[113] U. Berzinsh, L. Caiyan, R. Zerne, S. Svanberg, and E. Biémont. Determination of radiative lifetimes of neutral sulfur by time-resolved vacuum-ultraviolet laser spectroscopy. *Physical Review A*, 55:1836–1841, 1997.

[114] Z. Dai, J. Zhankui, H. Xu, Z. Zhiguo, S. Svanberg, E. Biemont, P.H. Lefebvre, and P. Quinet. Time-resolved laser-induced fluorescence measurements of rydberg states in Lu I and comparison with theory. *Journal of Physics B: Atomic, Molecular and Optical Physics*, 36(3):479–487, 2003.

[115] J.E Lawler, Bonvallet G., and C. Sneden. Experimental radiative lifetimes, branching fractions, and oscillator strengths for La II : a new determination of the solar lanthanum abundance. *The Astrophysical Journal*, 556(1):452–460, 2001.

[116] P. Pascal. *Nouveau traité de chimie minérale.* Masson, Paris, 1956.

[117] S. Ivarsson, J. Andersen, B. Nordström, X. Dai, S. Johansson, H. Lundberg, H. Nilsson, V. Hill, M. Lundqvist, and J.F. Wyart. Improved oscillator strengths and wavelengths for Os I and Ir I, and new results on earlyr-process nucleosynthesis. *Astronomy and Astrophysics*, 409:1141–1149, 2003.

[118] J.J. Cowan, . Sneden, J.W. Truran, and D.L. Burris. First detection of platinum, osmium, and lead in a metal-poor halo star: HD 126238. *The Astrophysical Journal*, 460(2), 2006.

[119] I.U. Roederer and J.. Lawler. Detection of elements at all thee r-process peaks in the metal pool star hd16017. *The Astrophysical Journal*, 750(1):76, 2012.

[120] C. Sneden, J.J Cowan, D.L. Burris, and J.W. Truran. Hubble space telescope observations of neutron-capture elements in very metal poor stars. *The Astrophysical Journal*, 496(1):235–245, 1998.

[121] A. Frebel. From nuclei to the cosmos: Tracing heavy-element production with the oldest stars. *Annual Review of Nuclear and Particle Science*, 68(1):237–269, 2018.

[122] S. Ivarsson, G.M. Wahlgren, Z. Dai, H. Lundberg, and D. Leckrone. Constraining the very heavy elemental abundance peak in the chemically peculiar star lupi, with new atomic data for Os II and Ir II. *Astronomy and Astrophysics*, 425:353, 2004.

[123] D.S. Gough, P. Hannaford, and R.M. Lowe. Radiative lifetimes and oscillator strengths in neutral iridium. *Journal of Physics B: Atomic and Molecular Physics*, 16(5):785–791, 1983.

[124] H.L. Xu, S. Svanberg, P. Quinet, P. Palmeri, and E. Biémont. Improved atomic data for iridium atom (Ir I) and ion (Ir II) and the solar content of iridium. *Journal of Quantitative Spectroscopy and Radiative Transfer*, 104(1):52–70, 2007.

[125] M. Fontani, M. Costa, and M.V. Orna. *The Lost Elements : The Periodic Table's Shadow side.* Oxford University Press, 2014.

[126] B.N.G. Guthrie. The Os-**P**t-**H**g abundance peak ik ap stars and the problem of very heavy cosmic rays. *Astrophysics and Space Science*, 15:214–228, 1972.

[127] P.F.A. Klinkenberg, W.F Meggers, R. Velasco, and M.A. Catalan. Term analysis of the first spectrum of rhenium (Re I). *Journal of Research of the Natural Bureau of Standards*, 59(5), 1957.

[128] J.F. Wyart. A systematic study of even configurations in the neutral atoms of the platinum group. *Physica Scripta*, 18(2):87–95, 1978.

[129] P. Palmeri, P. Quinet, E. Biémont, S. Svanberg, and H.L. Xu. Radiative lifetime measurements and semi-empirical transition probability calculations in neutral rhenium. *Physica Scripta*, 74(3):297–303, 2006.

[130] B. P. Abbott, R. Abbott, T. D. Abbott, F. Acernese, K. Ackley, C. Adams, T. Adams, P. Addesso, R. X. Adhikari, V. B. Adya, C. Affeldt, M. Afrough, B. Agarwal, M. Agathos, K. Agatsuma, N. Aggarwal, O. D. Aguiar, L. Aiello, A. Ain, P. Ajith, B. Allen, G. Allen, A. Allocca, P. A. Altin, A. Amato, A. Ananyeva, S. B. Anderson, W. G. Anderson, S. V. Angelova, S. Antier, S. Appert, K. Arai, M. C. Araya, J. S. Areeda, N. Arnaud, K. G. Arun, S. Ascenzi, G. Ashton, M. Ast, S. M.

Aston, P. Astone, D. V. Atallah, P. Aufmuth, C. Aulbert, K. AultONeal, C. Austin, A. Avila-Alvarez, S. Babak, P. Bacon, M. K. M. Bader, S. Bae, M. Bailes, P. T. Baker, F. Baldaccini, G. Ballardin, S. W. Ballmer, S. Banagiri, J. C. Barayoga, S. E. Barclay, B. C. Barish, D. Barker, K. Barkett, F. Barone, B. Barr, L. Barsotti, M. Barsuglia, D. Barta, S. D. Barthelmy, J. Bartlett, I. Bartos, R. Bassiri, A. Basti, J. C. Batch, M. Bawaj, J. C. Bayley, M. Bazzan, B. Bécsy, C. Beer, M. Bejger, I. Belahcene, A. S. Bell, B. K. Berger, G. Bergmann, S. Bernuzzi, J. J. Bero, C. P. L. Berry, D. Bersanetti, A. Bertolini, J. Betzwieser, S. Bhagwat, R. Bhandare, I. A. Bilenko, G. Billingsley, C. R. Billman, J. Birch, R. Birney, O. Birnholtz, S. Biscans, S. Biscoveanu, A. Bisht, M. Bitossi, C. Biwer, M. A. Bizouard, J. K. Blackburn, J. Blackman, C. D. Blair, D. G. Blair, R. M. Blair, S. Bloemen, O. Bock, N. Bode, M. Boer, G. Bogaert, A. Bohe, F. Bondu, E. Bonilla, R. Bonnand, B. A. Boom, R. Bork, V. Boschi, S. Bose, K. Bossie, Y. Bouffanais, A. Bozzi, C. Bradaschia, P. R. Brady, M. Branchesi, J. E. Brau, T. Briant, A. Brillet, M. Brinkmann, V. Brisson, P. Brockill, J. E. Broida, A. F. Brooks, D. A. Brown, D. D. Brown, S. Brunett, C. C. Buchanan, A. Buikema, T. Bulik, H. J. Bulten, A. Buonanno, D. Buskulic, C. Buy, R. L. Byer, M. Cabero, L. Cadonati, G. Cagnoli, C. Cahillane, J. Calderón Bustillo, T. A. Callister, E. Calloni, J. B. Camp, M. Canepa, P. Canizares, K. C. Cannon, H. Cao, J. Cao, C. D. Capano, E. Capocasa, F. Carbognani, S. Caride, M. F. Carney, G. Carullo, J. Casanueva Diaz, C. Casentini, S. Caudill, M. Cavaglià, F. Cavalier, R. Cavalieri, G. Cella, C. B. Cepeda, P. Cerdá-Durán, G. Cerretani, E. Cesarini, S. J. Chamberlin, M. Chan, S. Chao, P. Charlton, E. Chase, E. Chassande-Mottin, D. Chatterjee, K. Chatziioannou, B. D. Cheeseboro, H. Y. Chen, X. Chen, Y. Chen, H.-P. Cheng, H. Chia, A. Chincarini, A. Chiummo, T. Chmiel, H. S. Cho, M. Cho, J. H. Chow, N. Christensen, Q. Chu, A. J. K. Chua, S. Chua, A. K. W. Chung, S. Chung, G. Ciani, R. Ciolfi, C. E. Cirelli, A. Cirone, F. Clara, J. A. Clark, P. Clearwater, F. Cleva, C. Cocchieri, E. Coccia, P.-F. Cohadon, D. Cohen, A. Colla, C. G. Collette, L. R. Cominsky, M. Constancio, L. Conti, S. J. Cooper, P. Corban, T. R. Corbitt, I. Cordero-Carrión, K. R. Corley, N. Cornish, A. Corsi, S. Cortese, C. A. Costa, M. W. Coughlin, S. B. Coughlin, J.-P. Coulon, S. T. Countryman, P. Couvares, P. B. Covas, E. E. Cowan, D. M. Coward, M. J. Cowart, D. C. Coyne, R. Coyne, J. D. E. Creighton, T. D. Creighton, J. Cripe, S. G. Crowder, T. J. Cullen, A. Cumming, L. Cunningham, E. Cuoco, T. Dal Canton, G. Dálya, S. L. Danilishin, S. D'Antonio, K. Danzmann, A. Dasgupta, C. F. Da Silva Costa, V. Dattilo, I. Dave, M. Davier, D. Davis, E. J. Daw, B. Day, S. De, D. DeBra, J. Degallaix, M. De Laurentis, S. Deléglise, W. Del Pozzo, N. Demos, T. Denker, T. Dent, R. De Pietri, V. Dergachev, R. De Rosa, R. T. DeRosa, C. De Rossi, R. DeSalvo, O. de Varona, J. Devenson, S. Dhurandhar, M. C. Díaz, T. Dietrich, L. Di Fiore, M. Di Giovanni, T. Di Girolamo, A. Di Lieto, S. Di Pace, I. Di Palma, F. Di Renzo, Z. Doctor, V. Dolique, F. Donovan, K. L. Dooley, S. Doravari, I. Dorrington, R. Douglas, M. Dovale Álvarez, T. P. Downes, M. Drago, C. Dreissigacker, J. C. Driggers, Z. Du, M. Ducrot, R. Dudi, P. Dupej, S. E. Dwyer, T. B. Edo, M. C. Edwards, A. Effler, H.-B. Eggenstein, P. Ehrens, J. Eichholz, S. S. Eikenberry, R. A. Eisenstein, R. C. Essick, D. Estevez, Z. B. Etienne, T. Etzel, M. Evans, T. M. Evans, M. Factourovich, V. Fafone, H. Fair, S. Fairhurst, X. Fan, S. Farinon, B. Farr, W. M. Farr, E. J. Fauchon-Jones, M. Favata, M. Fays, C. Fee, H. Fehrmann, J. Feicht, M. M. Fejer, A. Fernandez-Galiana, I. Ferrante, E. C. Ferreira, F. Ferrini, F. Fidecaro, D. Finstad, I. Fiori, D. Fiorucci, M. Fishbach, R. P. Fisher, M. Fitz-Axen, R. Flaminio, M. Fletcher, H. Fong, J. A. Font, P. W. F. Forsyth, S. S. Forsyth, J.-D. Fournier, S. Frasca, F. Frasconi, Z. Frei, A. Freise, R. Frey, V. Frey, E. M. Fries, P. Fritschel, V. V. Frolov, P. Fulda, M. Fyffe, H. Gabbard, B. U. Gadre, S. M.

Gaebel, J. R. Gair, L. Gammaitoni, M. R. Ganija, S. G. Gaonkar, C. Garcia-Quiros, F. Garufi, B. Gateley, S. Gaudio, G. Gaur, V. Gayathri, N. Gehrels, G. Gemme, E. Genin, A. Gennai, D. George, J. George, L. Gergely, V. Germain, S. Ghonge, Abhirup Ghosh, Archisman Ghosh, S. Ghosh, J. A. Giaime, K. D. Giardina, A. Giazotto, K. Gill, L. Glover, E. Goe. Gw170817: Observation of gravitational waves from a binary neutron star inspiral. *Phys. Rev. Lett.*, 119:161101, 2017.

[131] D. Kasen, B. Metzger, J. Barnes, E. Quataert, and E. Ramirez-Ruiz. Origin of the heavy elements in binary neutron-star mergers from a gravitational-wave event. *Nature*, 551:80–84, 2017.

[132] E. Biémont, P. Quinet, and H.L. Xu. *The European Physical Journal D - Atomic, Molecular, Optical and Plasma Physics*, 30:157–162, 2004.

[133] A. Hibbert, E. Biémont, M. Godefroid, and N. Vaeck. El transitions of astrophysical interest in neutral oxygen. *Journal of Physics B*, 24:3943–3958, 1991.

[134] G. Başar, B. Gamper, I.K Güzelçimen, F.and Öztürk, T. Binder, G. Başar, S. Kröger, and L. Windholz. New even and odd parity fine structure levels of la i discovered by means of laser-induced fluorescence spectroscopy. *Journal of Quantitative Spectroscopy and Radiative Transfer*, 187:505–510, 2017.

[135] E.A Den Hartog, A.J Palmer, and J.E. Lawler. Radiative lifetimes and transition probabilities of neutral lanthanum. *Journal of Physics B: Atomic, Molecular and Optical Physics*, 48(15):155001, 2015.

[136] B. Karaçoban and L. Özdemir. Electric dipole transitions for la I (Z = 57). *Journal of Quantitative Spectroscopy and Radiative Transfer*, 113(6):1968–1985, 2008.

[137] E. Biémont, P. Quinet, S. Svanberg, and H. L. Xu. Lifetime measurements and calculations in la I. *The European Physical Journal D - Atomic, Molecular, Optical and Plasma Physics*, 30(2):157–162, 2004.

[138] Y. Feng, W. Zhang, Bo. Kuang, L. Ning, Z. Jiang, and Z. Dai. Radiative lifetime measurements on odd-parity levels of la I by time-resolved laser spectroscopy. *Journal of the Optical Society of America B*, 28(3):543–546, 2011.

[139] X. Shang, Y. Tian, Q. Wang, S. Fan, W. Bai, and Z. Dai. Radiative lifetime measurements of some la i and la ii levels by time-resolved laser spectroscopy. *Monthly Notices of the Royal Astronomical Society*, 442(1):138–141, 06 2014.

[140] S. Yarlagadda, S. Mukund, and S.G. Nakhate. Radiative lifetime measurements in neutral lanthanum using time-resolved laser-induced fluorescence spectroscopy in supersonic free-jet. *Journal of the Optical Physical Society of America B*, 28(8):1928–1933, 2011.

[141] O. Just, I. Kullmann, S. Goriely, A. Bauswein, H-T. Janka, and C.E Collins. Dynamical ejecta of neutron star mergers with nucleonic weak processes II: kilonova emission. *Monthly Notices of the Royal Astronomical Society*, 510:2820–2840, 2022.

[142] G.C. Yang, Y.C. Liang, M. Spite, Y.Q. Chen, G. Zhao, B. Zhang, G.Q Liu, Y.J. Liu, N. Liu, and L.i Deng. Chemical abundance analysis of 19 barium stars. *Research in Astronomy and Astrophysics*, 16(1):019, 2016.

[143] W.R. Johnson, D. Kolb, and K.N. Huang. Electric-dipole, quadrupole, and magnetic-dipole susceptibilities and shielding factors for closed-shell ions of the he, ne, ar, ni (cu+), kr, pb, and xe isoelectronic sequences. *Atomic Data and Nuclear Data Tables*, 28(2):333–340, 1983.

[144] J. J. Curry. Compilation of wavelengths, energy levels, and transition probabilities for Ba I and Ba II. *Journal of Physical and Chemical Reference Data*, 33(3):725–746, 2004.

[145] Q. Wang, L.Y. Jiang, P. Quinet, P. Palmeri, W. Zhang, X. Shang, Y.S. Tian, and Z. Dai. Tr-lif lifetimes measurements and hfr+cpol calculations of radiative parameters in vanadium atom. *The Astrophysical Journal Supplement Series*, 211(2):31, 2014.

[146] L. Mashonkina. Atomic data necessary for the non-LTE analysis of stellar spectra. *Physica Scripta*, T134:014004, 2009.

[147] W. Zhang, P. Palmeri, and P. Quinet. Atomic data for radiative transitions in the third spectra of rhodium (Rh III), palladium (Pd III) and silver (Ag III). *Physica Scripta*, 88(6):065302, 2013.

[148] A.G.W. Cameron, C.A. Barnes, D.D. Clayton, and D.N. Schramm. Essays in nuclear astrophysics. *Cambridge, England*, 1982.

[149] Kwiatkowski M., P. Zimmerman, E. Biémont, and N. Grevesse. New lifetime measurements for Nb I and Rh I and the solar photospheric abundances of Nb and Rh. *Astronomy and Astrophysics*, 112:337–340, 1982.

[150] S. Salih, D. W. Duquette, and J. E. Lawler. Radiative lifetimes in Rh I and in Ta I. *Physical Review A*, 27:1193–1196, 1983.

[151] D.W. Duquette and J.E. Lawler. Branching ratios and transition probabilities in rhodium I. *Journal of the Optical Society of America B*, 2:1948–1952, 1985.

[152] G. Malcheva, L. Engström, H. Lundberg, H. Nilsson, H. Hartman, K. Blagoev, P. Palmeri, and P. Quinet. Radiative lifetimes and transition probabilities in Rh I. *Monthly Notices of the Royal Astronomical Society*, 450(1):223–228, 2015.

[153] L. Zhou, S. Gamrath, P. Palmeri, P. Quinet, M. Zhang, and Z.W. Dai. Experimental and theoretical radiative lifetimes, branching fractions, transition probabilities and oscillator strengths of some highly-excited odd-parity levels in Ir I. *Astrophysical Journal Supplement Series*, 238(3):1–12, 2018.

[154] H. Ma, M. Liu, Y. Geng, T. Wang, Y. Ziqing, H. Zheng, S. Gamrath, P. Quinet, and Z. Dai. Experimental and theoretical radiative parameters of highly excited odd-parity levels in Ir II. *The Astrophysical Journal Supplement Series*, 260:56, 2022.

[155] Y. Li, S. Gamrath, P. Palmeri, P. Quinet, Q. Li, Q. Yu, M. Zhang, L. Zhou, and Z.W. Dai. Radiative lifetimes, branching fractions, and oscillator strengths of high-lying levels in Re I. *Monthly Notices of the Royal Astronomical Society*, 491:2953–2958, 2020.

[156] S. Gamrath, P. Palmeri, and P. Quinet. Radiative transition parameters in atomic lanthanum from pseudo-relativistic hartree-fock and fully relativistic dirac-hartree-fock calculations. *Atoms*, 7(38):1–17, 2019.

[157] Q. Wang, S. Gamrath, P. Palmeri, P. Quinet, Q. Yu, M. Zhang, and Z.W. Dai. Radiative lifetime measurements and semi-empirical transition parameter calculations for high-lying levels in **B**a I. *Journal of Quantitative Spectroscopy and Radiative Transfer*, 225:35–38, 2019.

[158] Y. Li, Y. Geng, M. Liu, H. Ma, Y. Wu, L. Zhang, S. Gamrath, P. Quinet, and Z. Dai. Radiative parameters of high-lying levels in neutral rhodium. *Monthly Notices of the Royal Astronomical Society*, 503(4):5085–5090, 2021.

[159] `https://www.nationalacademies.org`. Decadal survey on astronomy and astrophysics, 2020.

[160] G. Nave, P. Barklem, M.T. Belmonte, N. Brickhouse, P. Butler, F. Cashman, M. Chatzikos, C.R. Cowley, E. Den Hartog, S. Federman, G. Ferland, M. Fogle, H. Hartman, F. Guzman, S. Heap, F. Kerber, A. Kramida, V.P. Kulkarni, J.E. Lawler, J. Marler, S. Nahar, J. Pickering, P. Quinet, Y. Ralchenko, D. Savin, C. Sneden, E. Takacs, G. Wahlgren, J. Webb, J. Wiseman, and M. Wood. Atomic data for astrophysics: Needs and challenges. *Bulletin of the American Astronomical Society*, 51(7), 2019.

[161] D. W. Savin, J.F. Babb, P. Barklem, P.M. Bellan, G. Betancourt-Martinez, J. Blum, C. Boersma, M.D. Boryta, J. Brisset, C. Brogan, J. Cami, P. Caselli, A. Chutjian, L. Corrales, K. Crabtree, G. Dominguez, S.R. Federman, C.J. Fontes, R. Freedman, L. Gavilan-Marin, B. Gibson, L. Golub, T.W. Gorczyca, M. Hahn, D. Hartmann, S.M. Hörst, R.L. Hudson, H. Ji, H. Kreckel, J. Kuhn, J.E. Lawler, T.J. Lee, M.A. Leutenegger, R. Mancini, J. P. Marler, L. I. Mashonkina, M. C. McCarthy, M. McCoustra, B.A. McGuire, S. N. Milam, N.A. Montgomery, M.and Murphy, G. Nave, R. M. Nelson, K.M. Nollett, A.A. Norton, O. Novotný, A. Papol, J.C. Raymond, F. Salama, E.M. Sciamma-O'Brien, R. Smith, C. Sosolik, C. Sousa-Silva, A. Spyrou, P.C. Stancil, K. Sung, . Tennyson, F. Timmes, V. L. Trimble, O. Venot, B. J. Wahlgren, G.and Wargelin, D. Winget, and M.P. Wood. State of the Profession Considerations for Laboratory Astrophysics. *Bulletin of the American Astronomical Society*, 51(7), 2019.

Appendix

Preliminary Remark

The experimental values of the energy levels given in the tables comparing experimental and theoretical energy levels are given with an accuracy of 0.1 cm^{-1} in order to be directly compared to the theoretical values. All the energies are given in 0.1 cm^{-1}.

All the wavelength given in the transition tables are the Ritz wavelength determined using the most accurate known value of the experimental energy levels (i.e. with a better accuracy than 0.1 cm^{-1}). The references from which these values are taken are cited at the bottom of each table.

Cu IV-VII

Cu IV

Energy levels

Table A1: Comparison between available experimental data and calculated even energy levels (in cm^{-1}) in Cu IV

E^a_{exp}	E^b_{calc}	ΔE	J	Leading components (in %) in LS coupling ^{c}
0	8	−8	4	99 $3d^8\ ^3F$
1861.4	1857	4	3	99 $3d^8\ ^3F$
3077.6	3074	4	2	98 $3d^8\ ^3F$
16248	16238	10	2	82 $3d^8\ ^1D$ + 17 $3d^8\ ^3P$
19696.6	19750	−53	2	82 $3d^8\ ^3P$ + 17 $3d^8\ ^1D$
20096.6	20072	25	1	99 $3d^8\ ^3P$
20422.6	20405	18	0	99 $3d^8\ ^3P$
26913	26912	1	4	99 $3d^8\ ^1G$
61456.4	61456	0	0	98 $3d^8\ ^1S$
119632.4	119747	−115	5	99 $3d^7(^4F)4s\ ^5F$
120918.7	120980	−61	4	99 $3d^7(^4F)4s\ ^5F$
121929.8	121955	−25	3	99 $3d^7(^4F)4s\ ^5F$
122663.8	122666	−2	2	99 $3d^7(^4F)4s\ ^5F$
123139.8	123128	12	1	99 $3d^7(^4F)4s\ ^5F$
128343.3	128356	−13	4	98 $3d^7(^4F)4s\ ^3F$
130060.3	130024	36	3	99 $3d^7(^4F)4s\ ^3F$
131218.6	131157	62	2	99 $3d^7(^4F)4s\ ^3F$
139695.3	139522	173	3	99 $3d^7(^4P)4s\ ^5P$
140065.7	139952	114	2	96 $3d^7(^4P)4s\ ^5P$
140715	140603	112	1	97 $3d^7(^4P)4s\ ^5P$
144065.9	143959	107	5	97 $3d^7(^2G)4s\ ^3G$
144749	144616	133	4	94 $3d^7(^2G)4s\ ^3G$
145579.9	145422	158	3	99 $3d^7(^2G)4s\ ^3G$
147736.6	147668	69	2	77 $3d^7(^4P)4s\ ^3P$ + 18 $3d^7(^2P)4s\ ^3P$
147929.8	148006	−76	1	71 $3d^7(^4P)4s\ ^3P$ + 15 $3d^7(^2P)4s\ ^3P$ + 11 $3d^7(^2P)4s\ ^1P$
148233.8	148438	−204	0	67 $3d^7(^4P)4s\ ^3P$ + 33 $3d^7(^2P)4s\ ^3P$
148860.7	148746	115	4	90 $3d^7(^2G)4s\ ^1G$ + 5 $3d^7(^2H)4s\ ^3H$
148903.6	149198	−294	2	65 $3d^7(^2P)4s\ ^3P$ + 22 $3d^7(^4P)4s\ ^3P$ + 7 $3d^7(^2D)4s$ 3D
149667.2	149962	−295	1	67 $3d^7(^2P)4s\ ^3P$ + 21 $3d^7(^4P)4s\ ^3P$ + 8 $3d^7(^2D)4s$ 3D
151622.7	151769	−146	6	100 $3d^7(^2H)4s\ ^3H$
152231.7	152012	220	3	77 $3d^7(^2D)4s\ ^3D$ + 22 $3d^7(^2D)4s\ ^3D$
152301.7	152407	−105	5	95 $3d^7(^2H)4s\ ^3H$
152400.2	152648	−248	1	38 $3d^7(^2D)4s\ ^3D$ + 35 $3d^7(^2P)4s\ ^1P$ + 14 $3d^7(^2P)4s\ ^3P$
153198.2	153260	−62	4	92 $3d^7(^2H)4s\ ^3H$ + 6 $3d^7(^2G)4s\ ^1G$
153375.7	153186	190	2	65 $3d^7(^2D)4s\ ^3D$ + 17 $3d^7(^2D)4s\ ^3D$ + 8 $3d^7(^2P)4s\ ^3P$
155476.7	155645	−168	1	54 $3d^7(^2P)4s\ ^1P$ + 33 $3d^7(^2D)4s\ ^3D$ + 7 $3d^7(^2D)4s\ ^3D$
156458.7	156584	−125	5	96 $3d^7(^2H)4s\ ^1H$
157536.1	157257	279	2	71 $3d^7(^2D)4s\ ^1D$ + 18 $3d^7(^2D)4s\ ^1D$ + 5 $3d^7(^2D)4s\ ^3D$
170066.5	169989	78	2	99 $3d^7(^2F)4s\ ^3F$
170277.7	170245	33	3	98 $3d^7(^2F)4s\ ^3F$
170619	170661	−42	4	99 $3d^7(^2F)4s\ ^3F$
174831.3	174625	206	3	98 $3d^7(^2F)4s\ ^1F$
196853.5	196964	−111	1	80 $3d^7(^2D)4s\ ^3D$ + 19 $3d^7(^2D)4s\ ^3D$
197138.5	197228	−90	2	78 $3d^7(^2D)4s\ ^3D$ + 20 $3d^7(^2D)4s\ ^3D$
197659.5	197695	−36	3	77 $3d^7(^2D)4s\ ^3D$ + 22 $3d^7(^2D)4s\ ^3D$
201771	201650	121	2	77 $3d^7(^2D)4s\ ^1D$ + 21 $3d^7(^2D)4s\ ^1D$
287319.5	287391	−72	5	90 $3d^7(^4F)4d\ ^5F$ + 8 $3d^7(^4F)4d\ ^5G$
287589.3	287966	−377	4	78 $3d^7(^4F)4d\ ^5F$ + 11 $3d^7(^4F)4d\ ^5D$ + 7 $3d^7(^4F)4d\ ^5G$
288566.4	288677	−111	3	70 $3d^7(^4F)4d\ ^5F$ + 14 $3d^7(^4F)4d\ ^5D$ + 6 $3d^7(^4F)4d\ ^5P$
288697.8	288687	11	6	94 $3d^7(^4F)4d\ ^5G$ + 6 $3d^7(^4F)4d\ ^5H$
289370.2	289474	−104	2	82 $3d^7(^4F)4d\ ^5F$ + 9 $3d^7(^4F)4d\ ^5D$
289529.7	289613	−83	3	74 $3d^7(^4F)4d\ ^5P$ + 12 $3d^7(^4F)4d\ ^5F$ + 9 $3d^7(^4F)4d\ ^5D$
289572.9	289542	31	5	66 $3d^7(^4F)4d\ ^5G$ + 20 $3d^7(^4F)4d\ ^3G$ + 7 $3d^7(^4F)4d\ ^5H$
289641.5	289963	−322	4	58 $3d^7(^4F)4d\ ^5D$ + 18 $3d^64s^2\ ^5D$ + 16 $3d^7(^4F)4d\ ^5G$
289688.2	289700	−12	7	99 $3d^7(^4F)4d\ ^5H$
289974	290076	−102	1	93 $3d^7(^4F)4d\ ^5F$
290445.4	290416	29	6	60 $3d^7(^4F)4d\ ^5H$ + 36 $3d^7(^4F)4d\ ^3H$
290552.8	290575	−22	4	60 $3d^7(^4F)4d\ ^5G$ + 13 $3d^7(^4F)4d\ ^5F$ + 10 $3d^7(^4F)4d\ ^3G$

Table A1: Continued

E^a_{exp}	E^b_{calc}	ΔE	J	Leading components (in %) in LS coupling ^{c}
290773.5	290933	−160	2	54 $3d^7(^4F)4d\ ^5P$ + 29 $3d^7(^4F)4d\ ^5D$ + 7 $3d^7(^4F)4d\ ^5F$
290885.1	291074	−189	3	48 $3d^7(^4F)4d\ ^5G$ + 24 $3d^7(^4F)4d\ ^5D$ + 9 $3d^7(^4F)4d\ ^5P$
291147.3	291004	143	5	70 $3d^7(^4F)4d\ ^3G$ + 20 $3d^7(^4F)4d\ ^5G$ + 6 $3d^7(^4F)4d\ ^3H$
291298.7	291394	−95	3	37 $3d^7(^4F)4d\ ^5G$ + 21 $3d^7(^4F)4d\ ^5D$ + 8 $3d^64s^2\ ^5D$
291561.6	291570	−8	5	79 $3d^7(^4F)4d\ ^5H$ + 12 $3d^7(^4F)4d\ ^3H$ + 5 $3d^7(^4F)4d\ ^3G$
291570.8	291841	−270	1	55 $3d^7(^4F)4d\ ^5D$ + 27 $3d^7(^4F)4d\ ^5P$ + 13 $3d^64s^2\ ^5D$
291730	291745	−15	2	92 $3d^7(^4F)4d\ ^5G$
291865	291764	101	6	63 $3d^7(^4F)4d\ ^3H$ + 34 $3d^7(^4F)4d\ ^5H$
291953.9	292147	−193	3	75 $3d^7(^4F)4d\ ^3D$ + 9 $3d^7(^4F)4d\ ^5D$ + 6 $3d^64s^2\ ^5D$
291997.1	292224	−227	2	39 $3d^7(^4F)4d\ ^5P$ + 36 $3d^7(^4F)4d\ ^5D$ + 14 $3d^64s^2\ ^5D$
292296.7	292187	110	4	65 $3d^7(^4F)4d\ ^3G$ + 16 $3d^7(^4F)4d\ ^5G$ + 8 $3d^7(^4F)4d\ ^5H$
292440	292414	26	4	79 $3d^7(^4F)4d\ ^5H$ + 16 $3d^7(^4F)4d\ ^3G$
292639.1	292782	−143	1	71 $3d^7(^4F)4d\ ^5P$ + 19 $3d^7(^4F)4d\ ^5D$ + 8 $3d^64s^2\ ^5D$
292913.3	292946	−33	3	89 $3d^7(^4F)4d\ ^5H$ + 6 $3d^7(^4F)4d\ ^5G$
293021.7	293176	−154	2	84 $3d^7(^4F)4d$ 3D + 6 $3d^7(^4F)4d\ ^3P$
293399.2	293267	132	5	80 $3d^7(^4F)4d\ ^3H$ + 14 $3d^7(^4F)4d\ ^5H$
293513.5	293352	162	3	88 $3d^7(^4F)4d\ ^3G$ + 6 $3d^7(^4F)4d\ ^5H$
294015.3	294184	−169	1	95 $3d^7(^4F)4d\ ^3D$
294152	294269	−117	4	72 $3d^64s^2\ ^5D$ + 21 $3d^7(^4F)4d\ ^5D$
294464.4	294316	148	4	89 $3d^7(^4F)4d\ ^3H$ + 5 $3d^7(^4F)4d\ ^5H$
295307.8	295383	−75	3	72 $3d^64s^2\ ^5D$ + 22 $3d^7(^4F)4d\ ^5D$
295910.4	295840	70	4	80 $3d^7(^4F)4d\ ^3F$ + 7 $3d^7(^2G)4d\ ^3F$
296040.3	296106	−66	2	71 $3d^64s^2\ ^5D$ + 21 $3d^7(^4F)4d\ ^5D$
296494.2	296559	−65	1	73 $3d^64s^2\ ^5D$ + 20 $3d^7(^4F)4d\ ^5D$
296573.4	296474	99	2	81 $3d^7(^4F)4d\ ^3P$ + 5 $3d^7(^4F)4d\ ^3D$ + 5 $3d^7(^4P)4d\ ^3P$
296912.3	296847	65	3	78 $3d^7(^4F)4d\ ^3F$ + 7 $3d^7(^2G)4d\ ^3F$
297554.4	297481	73	2	78 $3d^7(^4F)4d\ ^3F$ + 8 $3d^7(^2G)4d\ ^3F$
297931	297840	91	1	88 $3d^7(^4F)4d\ ^3P$ + 6 $3d^7(^4P)4d\ ^3P$
301632	301720	−88	5	99 $3d^7(^4F)5s\ ^5F$
302682.3	302741	−59	4	82 $3d^7(^4F)5s\ ^5F$ + 17 $3d^7(^4F)5s\ ^3F$
303798.4	303819	−21	3	91 $3d^7(^4F)5s\ ^5F$ + 7 $3d^7(^4F)5s\ ^3F$
304244.9	304274	−29	4	82 $3d^7(^4F)5s\ ^3F$ + 17 $3d^7(^4F)5s\ ^5F$
304599.7	304601	−1	2	96 $3d^7(^4F)5s\ ^5F$
305116	305106	10	1	98 $3d^7(^4F)5s\ ^5F$
305856	305842	14	3	91 $3d^7(^4F)5s\ ^3F$ + 7 $3d^7(^4F)5s\ ^5F$
306941.8	306904	38	2	96 $3d^7(^4F)5s\ ^3F$
306982.5	306884	99	1	98 $3d^7(^4P)4d\ ^5P$
307167	307089	78	2	97 $3d^7(^4P)4d\ ^5P$
307517.3	307459	58	3	95 $3d^7(^4P)4d\ ^5P$
309413.9	309295	119	5	97 $3d^7(^4P)4d\ ^5F$
309490.4	309427	63	4	91 $3d^7(^4P)4d\ ^5F$
309653.1	309630	23	3	88 $3d^7(^4P)4d\ ^5F$
309864.7	309874	−9	2	88 $3d^7(^4P)4d\ ^5F$
310057.1	310095	−38	1	89 $3d^7(^4P)4d\ ^5F$ + 5 $3d^7(^2P)4d\ ^3D$
310800.2	310865	−65	3	80 $3d^7(^2G)4d\ ^3D$ + 5 $3d^7(^4P)4d\ ^3F$
311010.7	311031	−20	3	51 $3d^7(^4P)4d\ ^3F$ + 23 $3d^7(^2G)4d\ ^1F$ + 5 $3d^7(^2P)4d\ ^1F$
311177	311018	159	4	81 $3d^7(^4P)4d\ ^3F$ + 9 $3d^7(^2G)4d\ ^3F$
311274	311367	−93	2	44 $3d^7(^2G)4d\ ^3D$ + 30 $3d^7(^4P)4d\ ^3F$ + 5 $3d^7(^2P)4d\ ^3D$
311628	311504	124	7	95 $3d^7(^2G)4d\ ^3I$
311726.7	311911	−184	1	37 $3d^7(^4P)4d\ ^3P$ + 24 $3d^7(^2G)4d\ ^3D$ + 11 $3d^7(^2P)4d\ ^3P$
311742.9	311630	113	6	67 $3d^7(^2G)4d\ ^3I$ + 24 $3d^7(^2G)4d\ ^1I$
311998.3	312124	−126	5	61 $3d^7(^2G)4d\ ^3G$ + 20 $3d^7(^2G)4d\ ^3H$ + 11 $3d^7(^2G)4d\ ^3I$
312061.4	312033	28	2	51 $3d^7(^4P)4d\ ^3F$ + 30 $3d^7(^2G)4d\ ^3D$ + 5 $3d^7(^4P)4d\ ^3P$
312082.5	312061	22	3	56 $3d^7(^2G)4d\ ^1F$ + 22 $3d^7(^4P)4d\ ^3F$ + 9 $3d^7(^2G)4d$ 3D
312415.5	312373	43	5	37 $3d^7(^2G)4d\ ^3I$ + 31 $3d^7(^2G)4d\ ^3G$ + 16 $3d^7(^2G)4d\ ^1H$
312466.7	312609	−142	4	65 $3d^7(^2G)4d\ ^3G$ + 18 $3d^7(^4P)4d\ ^5D$ + 6 $3d^7(^2G)4d\ ^3H$
312514.9	312454	61	6	75 $3d^7(^2G)4d\ ^3H$ + 20 $3d^7(^2G)4d\ ^1I$
312601.5	312713	−112	2	34 $3d^7(^4P)4d\ ^5D$ + 33 $3d^7(^4P)4d\ ^3P$ + 9 $3d^7(^2G)4d$ 3D
312629.9	312676	−46	4	74 $3d^7(^4P)4d\ ^5D$ + 15 $3d^7(^2G)4d\ ^3G$
312956.8	312990	−33	3	86 $3d^7(^4P)4d\ ^5D$
313253.3	313249	4	5	50 $3d^7(^2G)4d\ ^3I$ + 29 $3d^7(^2G)4d\ ^3H$ + 19 $3d^7(^2G)4d\ ^1H$
313257	313454	−197	3	93 $3d^7(^2G)4d\ ^3G$
313294.7	313245	50	2	56 $3d^7(^4P)4d\ ^5D$ + 20 $3d^7(^4P)4d\ ^3P$ + 7 $3d^7(^4P)4d$ 3D
313715.4	313602	113	6	53 $3d^7(^2G)4d\ ^1I$ + 28 $3d^7(^2G)4d\ ^3I$ + 18 $3d^7(^2G)4d\ ^3H$
313871.5	313936	−65	4	89 $3d^7(^2G)4d\ ^3H$ + 9 $3d^7(^2G)4d\ ^3G$
314262.2	314282	−20	5	59 $3d^7(^2G)4d\ ^1H$ + 36 $3d^7(^2G)4d\ ^3H$
314987.8	315132	−144	4	50 $3d^7(^2G)4d\ ^3F$ + 14 $3d^7(^2G)4d\ ^1G$ + 8 $3d^7(^2P)4d\ ^3F$
315450	314164	1286	3	84 $3d^7(^4P)4d\ ^3D$
315598.5	315602	−4	4	58 $3d^7(^2G)4d\ ^1G$ + 12 $3d^7(^2H)4d\ ^1G$ + 11 $3d^7(^2G)4d\ ^3F$
315846	315136	710	2	47 $3d^7(^2G)4d\ ^1D$ + 11 $3d^7(^2P)4d\ ^1D$ + 8 $3d^7(^2G)4d\ ^3F$
315912.2	315663	249	3	59 $3d^7(^2G)4d\ ^3F$ + 9 $3d^7(^2P)4d\ ^3F$ + 7 $3d^7(^2H)4d\ ^3F$
316191.7	316424	−232	2	59 $3d^7(^2G)4d\ ^3F$ + 10 $3d^7(^2H)4d\ ^3F$ + 9 $3d^7(^2P)4d\ ^3F$
316732.3	317512	−780	4	43 $3d^7(^2P)4d\ ^3F$ + 25 $3d^7(^2H)4d\ ^3F$ + 10 $3d^7(^2D)4d\ ^3F$
317017	316886	131	3	68 $3d^7(^2P)4d$ 3D + 7 $3d^7(^2D)4d\ ^3F$ + 5 $3d^7(^2D)4d$ 3D
317810.5	317611	200	3	26 $3d^7(^2P)4d\ ^1F$ + 22 $3d^7(^2H)4d\ ^3F$ + 10 $3d^7(^2P)4d\ ^3F$
318452.4	318293	159	8	100 $3d^7(^2H)4d\ ^3K$
318510	318355	155	7	60 $3d^7(^2H)4d\ ^3K$ + 39 $3d^74d\ (^2H)\ ^1K$
318746.1	318838	−92	5	94 $3d^7(^2H)4d\ ^3G$
319268.4	318617	651	3	37 $3d^7(^2H)4d\ ^1F$ + 28 $3d^74d\ (^2P)\ ^3F$ + 7 $3d^7(^2H)4d$
319586.7	319643	−56	4	43 $3d^7(^2H)4d\ ^3G$ + 19 $3d^74d\ (^2D)\ ^3F$ + 10 $3d^7(^2H)4d$
319703.7	319596	108	6	95 $3d^7(^2H)4d\ ^3K$
319896.1	320030	−134	4	41 $3d^7(^2H)4d\ ^3G$ + 20 $3d^74d\ (^2D)\ ^3F$ + 11 $3d^7(^2P)4d$
319992.7	319604	389	3	28 $3d^7(^2D)4d\ ^3D$ + 26 $3d^74d\ (^2H)\ ^1F$ + 14 $3d^7(^2P)4d$
320141.7	319962	180	7	59 $3d^7(^2H)4d\ ^1K$ + 37 $3d^74d\ (^2H)\ ^3K$
320601.1	320611	−10	6	58 $3d^7(^2H)4d\ ^3H$ + 39 $3d^64s^2\ ^3H$
320781.7	320746	36	5	73 $3d^7(^2D)4d\ ^3G$ + 21 $3d^74d\ (^2D)\ ^3G$
320952.7	320917	36	4	38 $3d^7(^2D)4d\ ^1G$ + 30 $3d^74d\ (^2D)\ ^3G$ + 11 $3d^7(^2D)4d$
321064	321082	−18	5	50 $3d^7(^2H)4d\ ^3H$ + 29 $3d^64s^2\ ^3H$ + 15 $3d^7(^2H)4d\ ^1H$
321135.1	321194	−59	7	99 $3d^7(^2H)4d\ ^3I$
321542.1	321586	−44	6	82 $3d^7(^2H)4d\ ^3I$ + 14 $3d^74d\ (^2H)\ ^1I$
322051.3	322028	23	3	35 $3d^7(^2D)4d\ ^1F$ + 16 $3d^74d\ (^2D)\ ^3F$ + 10 $3d^7(^2D)4d$
322317.4	322358	−41	5	47 $3d^7(^2H)4d\ ^3I$ + 33 $3d^74d\ (^2H)\ ^1H$ + 14 $3d^64s^2$
322338.2	322156	182	3	95 $3d^7(^4P)5s\ ^5P$
322524	322670	−146	5	46 $3d^7(^2H)4d\ ^3I$ + 45 $3d^74d\ (^2H)\ ^1H$

Table A1: Continued

E^a_{exp}	E^b_{calc}	ΔE	J	Leading components (in %) in LS coupling [c]
322608.1	322491	117	2	93 $3d^7(^4P)5s\ ^5P$ + 6 $3d^75s\ (^2P)\ ^3P$
323155.3	323377	−222	4	27 $3d^7(^2D)4d\ ^3G$ + 24 $3d^74d\ (^2D)\ ^1G$ + 16 $3d^7(^2P)4d$
323249	323131	118	1	79 $3d^7(^4P)5s\ ^5P$ + 5 $3d^74d\ (^2D)$ 3D
323754.8	323586	169	6	44 $3d^7(^2H)4d\ ^1I$ + 32 $3d^64s^2\ ^3H$ + 18 $3d^7(^2H)4d\ ^3H$
324118.1	323759	359	6	38 $3d^7(^2H)4d\ ^1I$ + 22 $3d^64s^2\ ^3H$ + 22 $3d^7(^2H)4d\ ^3H$
324418.7	324414	5	2	75 $3d^7(^4P)5s\ ^3P$ + 9 $3d^64s^2\ ^3P$ + 6 $3d^64s^2\ ^3P$
324619.3	324222	397	5	44 $3d^64s^2\ ^3H$ + 41 $3d^74d\ (^2H)\ ^3H$
324731.4	324455	276	4	45 $3d^64s^2\ ^3H$ + 42 $3d^74d\ (^2H)\ ^3H$
324759.9	324572	188	5	95 $3d^7(^2G)5s\ ^3G$
325225.9	325037	189	4	75 $3d^7(^2G)5s\ ^3G$ + 17 $3d^75s\ (^2G)\ ^1G$
326247.5	326050	198	3	99 $3d^7(^2G)5s\ ^3G$
326979.8	326764	216	4	69 $3d^7(^2G)5s\ ^1G$ + 21 $3d^75s\ (^2G)\ ^3G$
327356.7	327318	39	4	42 $3d^7(^2H)4d\ ^3F$ + 13 $3d^74d\ (^2D)\ ^3F$ + 9 $3d^7(^2G)4d$
328720	328760	−40	3	39 $3d^7(^2H)4d\ ^3F$ + 12 $3d^74d\ (^2D)\ ^3F$ + 11 $3d^7(^2G)4d$
329181.7	329441	−259	2	34 $3d^7(^2H)4d\ ^3F$ + 12 $3d^74d\ (^2G)\ ^3F$ + 11 $3d^7(^2D)4d$
329341.2	329712	−371	2	77 $3d^7(^2P)5s\ ^3P$ + 8 $3d^75s\ (^2D)$ 3D + 5 $3d^7(^4P)5s$
329632.8	330121	−488	1	51 $3d^7(^2P)5s\ ^3P$ + 24 $3d^75s\ (^2P)\ ^1P$ + 14 $3d^7(^2D)5s$
331041.9	331669	−627	1	53 $3d^7(^2P)5s\ ^1P$ + 39 $3d^75s\ (^2P)\ ^3P$
332035.9	332203	−167	4	61 $3d^7(^2H)4d\ ^1G$ + 13 $3d^74d\ (^2F)\ ^1G$ + 11 $3d^7(^2G)4d$
332436.4	332584	−148	6	99 $3d^7(^2H)5s\ ^3H$
332854.7	332986	−131	5	78 $3d^7(^2H)5s\ ^3H$ + 20 $3d^75s\ (^2H)\ ^1H$
333005.7	332799	207	3	77 $3d^7(^2D)5s\ ^3D$ + 22 $3d^75s\ (^2D)\ ^3D$
333736.7	333127	610	2	27 $3d^7(^2D)5s\ ^3D$ + 27 $3d^75s\ (^2D)\ ^1D$ + 8 $3d^7(^2D)5s$
333868.7	333962	−93	4	95 $3d^7(^2H)5s\ ^3H$
334564.8	334649	−84	5	78 $3d^7(^2H)5s\ ^1H$ + 19 $3d^7(^2H)5s\ ^3H$
335885.5	335708	178	2	44 $3d^7(^2D)5s\ ^1D$ + 22 $3d^7(^2D)5s$ 3D + 11 $3d^7(^2P)5s\ ^3P$
338974.8	339070	−95	5	88 $3d^7(^2F)4d\ ^3H$ + 8 $3d^7(^2F)4d\ ^1H$
339378.8	339547	−168	6	96 $3d^7(^2F)4d\ ^3H$
339392.7	339687	−294	3	86 $3d^7(^2F)4d\ ^3G$ + 6 $3d^7(^2F)4d\ ^1F$
339763.8	340079	−315	4	89 $3d^7(^2F)4d\ ^3G$
339808.5	339916	−108	5	90 $3d^7(^2F)4d\ ^1H$ + 8 $3d^7(^2F)4d\ ^3H$
340161.9	340554	−392	5	94 $3d^7(^2F)4d\ ^3G$
347248.7	347352	−103	4	81 $3d^7(^2F)4d\ ^1G$ + 7 $3d^7(^2H)4d\ ^1G$
351520.2	351425	95	3	93 $3d^7(^2F)5s\ ^3F$ + 6 $3d^7(^2F)5s\ ^1F$
351908.8	351901	8	4	99 $3d^7(^2F)5s\ ^3F$

a: From the NIST compilation [28]
b: This work
c: Only the components ≥ to 5% are given

Table A2: Comparison between available experimental data and calculated odd energy levels (in cm^{-1}) in Cu IV

E$^{a}_{exp}$	E$^{b}_{calc}$	ΔE	J	Leading components (in %) in LS coupling ^{c}
190527.7	190558	−30	5	91 3d^7(^{4}F)4p ^{5}F + 7 3d^7(^{4}F)4p ^{5}G
190553.6	190616	−62	4	54 3d^7(^{4}F)4p ^{5}F + 38 3d^7(^{4}F)4p ^{5}D
191761.8	191801	−39	3	70 3d^7(^{4}F)4p ^{5}F + 23 3d^7(^{4}F)4p ^{5}D
192741	192763	−22	2	83 3d^7(^{4}F)4p ^{5}F + 12 3d^7(^{4}F)4p ^{5}D
192752.8	192764	−11	4	51 3d^7(^{4}F)4p ^{5}D + 34 3d^7(^{4}F)4p ^{5}F + 9 3d^7(^{4}F)4p ^{5}G
193434.4	193443	−9	1	93 3d^7(^{4}F)4p ^{5}F + 5 3d^7(^{4}F)4p ^{5}D
193947.8	193923	25	6	99 3d^7(^{4}F)4p ^{5}G
194132.4	194149	−17	3	63 3d^7(^{4}F)4p ^{5}D + 18 3d^7(^{4}F)4p ^{5}F + 11 3d^7(^{4}F)4p ^{5}G
194339.1	194309	30	5	75 3d^7(^{4}F)4p ^{5}G + 16 3d^7(^{4}F)4p ^{3}G + 9 3d^7(^{4}F)4p ^{5}F
195054.9	195010	45	4	78 3d^7(^{4}F)4p ^{5}G + 10 3d^7(^{4}F)4p ^{5}F + 7 3d^7(^{4}F)4p ^{3}G
195085.9	195114	−28	2	71 3d^7(^{4}F)4p ^{5}D + 11 3d^7(^{4}F)4p ^{5}G + 9 3d^7(^{4}F)4p ^{5}F
195544.1	195496	48	3	80 3d^7(^{4}F)4p ^{5}G + 10 3d^7(^{4}F)4p ^{5}F
195684.3	195732	−48	1	84 3d^7(^{4}F)4p ^{5}D + 10 3d^7(4P)4p ^{5}D + 5 3d^7(^{4}F)4p ^{5}F
195827	195780	47	2	84 3d^7(^{4}F)4p ^{5}G + 6 3d^7(^{4}F)4p ^{5}F + 6 3d^7(^{4}F)4p ^{5}D
195932	195990	−58	0	88 3d^7(^{4}F)4p ^{5}D + 11 3d^7(4P)4p ^{5}D
197325	197340	−15	5	81 3d^7(^{4}F)4p ^{3}G + 18 3d^7(^{4}F)4p ^{5}G
198179.2	198209	−30	4	88 3d^7(^{4}F)4p ^{3}F
199202.3	199214	−12	4	86 3d^7(^{4}F)4p ^{3}G + 10 3d^7(^{4}F)4p ^{5}G
199598.8	199633	−34	3	84 3d^7(^{4}F)4p ^{3}F + 5 3d^7(^{4}F)4p ^{3}D
200482.6	200497	−14	3	92 3d^7(^{4}F)4p ^{3}G
200720	200734	−14	2	89 3d^7(^{4}F)4p ^{3}F + 5 3d^7(2G)4p ^{3}F
201210.9	201378	−167	3	87 3d^7(^{4}F)4p ^{3}D + 6 3d^7(^{4}F)4p ^{3}F
202360.6	202528	−167	2	88 3d^7(^{4}F)4p ^{3}D
203139.5	203306	−167	1	90 3d^7(^{4}F)4p ^{3}D
203868.9	203936	−67	2	97 3d^7(4P)4p 5S
213360.4	213346	14	1	57 3d^7(4P)4p ^{5}D + 11 3d^7(2P)4p ^{3}P + 10 3d^7(4P)4p ^{3}S
213534.5	213340	195	2	76 3d^7(4P)4p ^{5}D + 9 3d^7(^{4}F)4p ^{5}D
213664.9	213412	253	3	78 3d^7(4P)4p ^{5}D + 8 3d^7(^{4}F)4p ^{5}D + 7 3d^7(4P)4p 3D
213932.1	213784	148	0	82 3d^7(4P)4p ^{5}D + 11 3d^7(^{4}F)4p ^{5}D + 6 3d^7(2P)4p ^{3}P
214318.7	214025	294	4	89 3d^7(4P)4p ^{5}D + 6 3d^7(^{4}F)4p ^{5}D
214413.4	214464	−51	1	42 3d^7(4P)4p ^{3}S + 25 3d^7(4P)4p ^{5}D + 10 3d^7(2P)4p ^{3}S
214835.3	214638	197	5	67 3d^7(2G)4p ^{3}H + 17 3d^7(2G)4p ^{1}H + 10 3d^7(2G)4p ^{3}G
215132.8	214971	162	4	55 3d^7(2G)4p ^{3}F + 12 3d^7(2G)4p ^{3}G + 8 3d^7(2G)4p ^{3}H
215733.9	215533	201	4	82 3d^7(2G)4p ^{3}H + 8 3d^7(2G)4p ^{3}F
216071.3	215829	242	6	95 3d^7(2G)4p ^{3}H
216428.9	216928	−499	0	67 3d^7(2P)4p ^{3}P + 16 3d^7(2D)4p ^{3}P + 6 3d^7(2D)4p ^{3}P
216702.9	217017	−314	2	31 3d^7(2P)4p ^{3}P + 34 3d^7(4P)4p ^{5}P + 16 3d^7(4P)4p ^{3}D
217079.2	216916	163	3	73 3d^7(2G)4p ^{3}F + 16 3d^7(2G)4p ^{3}G
217109.3	217546	−437	1	48 3d^7(2P)4p ^{3}P + 18 3d^7(4P)4p ^{5}P + 9 3d^7(2D)4p ^{3}P
217444.6	217385	60	4	46 3d^7(2G)4p ^{1}G + 25 3d^7(2G)4p ^{3}F + 16 3d^7(2H)4p ^{1}G
217621.1	217294	327	3	54 3d^7(4P)4p ^{5}P + 29 3d^7(4P)4p ^{3}D + 8 3d^7(4P)4p ^{5}D
217649.6	217743	−93	2	48 3d^7(4P)4p ^{5}P + 26 3d^7(4P)4p ^{3}D + 5 3d^7(2D)4p ^{3}D
217999.5	217971	29	5	79 3d^7(2G)4p ^{3}G + 15 3d^7(2G)4p ^{1}H
218027.5	217915	113	2	13 3d^7(2P)4p ^{1}D + 28 3d^7(2P)4p ^{3}P + 16 3d^7(4P)4p ^{3}D
218137.6	217882	256	3	48 3d^7(4P)4p 3D + 34 3d^7(4P)4p ^{5}P
218170.7	217871	300	1	63 3d^7(4P)4p ^{5}P + 24 3d^7(4P)4p ^{3}S
218628	218499	129	3	45 3d^7(2G)4p ^{3}G + 31 3d^7(2G)4p ^{1}F + 9 3d^7(2G)4p ^{3}F
218631.1	218617	14	1	64 3d^7(4P)4p 3D + 18 3d^7(2P)4p ^{3}D
218726.2	218501	225	2	92 3d^7(2G)4p ^{3}F + 5 3d^7(^{4}F)4p ^{3}F
218814.5	218633	182	5	63 3d^7(2G)4p ^{1}H + 27 3d^7(2G)4p ^{3}H + 8 3d^7(2G)4p ^{3}G
218944.8	218965	−20	4	72 3d^7(2G)4p ^{3}G + 11 3d^7(2G)4p ^{1}G + 8 3d^7(2G)4p ^{3}H
219402.7	219383	20	3	36 3d^7(2G)4p ^{1}F + 34 3d^7(2G)4p ^{3}G + 8 3d^7(2G)4p ^{3}F
219867.4	220519	−652	0	49 3d^7(4P)4p ^{3}P + 39 3d^7(2P)4p ^{1}S + 9 3d^7(2P)4p ^{3}P
220315.6	220202	114	2	66 3d^7(4P)4p ^{3}P + 11 3d^7(2D)4p ^{3}P + 6 3d^7(4P)4p ^{5}P
220917	220971	−54	5	92 3d^7(2H)4p ^{3}G + 5 3d^7(2F)4p ^{3}G
221271.6	221206	66	1	67 3d^7(4P)4p ^{3}P + 16 3d^7(2P)4p ^{3}D
221601.6	221713	−111	6	69 3d^7(2H)4p 3I + 28 3d^7(2H)4p ^{1}I
221650	222030	−380	3	61 3d^7(2P)4p 3D + 14 3d^7(2D)4p ^{3}D + 6 3d^7(2D)4p ^{3}D
221738.5	221783	−45	2	22 3d^7(4P)4p 3D + 18 3d^7(4P)4p ^{3}P + 15 3d^7(2P)4p ^{1}D
222335.9	222349	−13	1	29 3d^7(2P)4p 3D + 24 3d^7(2D)4p ^{3}D + 20 3d^7(4P)4p ^{3}P
222397.7	222405	−7	4	87 3d^7(2H)4p ^{3}G + 6 3d^7(2F)4p ^{3}G
222527.4	222622	−95	5	93 3d^7(2H)4p 3I
222602.5	222746	−144	2	29 3d^7(2D)4p 3D + 24 3d^7(2P)4p ^{3}D + 10 3d^7(2P)4p ^{1}D
222665.8	222751	−85	7	100 3d^7(2H)4p 3I
223000	222545	455	3	47 3d^7(2D)4p 3D + 17 3d^7(2D)4p ^{3}F + 12 3d^7(2D)4p ^{3}D
223623	223580	43	3	79 3d^7(2H)4p ^{3}G + 6 3d^7(2F)4p ^{3}G
223764.1	223734	30	1	29 3d^7(2D)4p 3D + 27 3d^7(2P)4p ^{3}D + 18 3d^7(2P)4p ^{1}P
223847.4	224457	−610	0	56 3d^7(2P)4p ^{1}S + 43 3d^7(4P)4p ^{3}P
224070.6	224131	−60	2	34 3d^7(2P)4p 3D + 22 3d^7(2D)4p ^{3}D + 16 3d^7(2P)4p ^{1}D
224959.1	225045	−86	6	69 3d^7(2H)4p ^{1}I + 27 3d^7(2H)4p ^{3}I
225386.9	225131	256	4	77 3d^7(2D)4p ^{3}F + 20 3d^7(2D)4p ^{3}F
225858.9	225659	200	3	48 3d^7(2D)4p ^{3}F + 13 3d^7(2P)4p ^{3}D + 11 3d^7(2D)4p ^{3}F
226271.3	226057	214	2	51 3d^7(2D)4p ^{3}F + 11 3d^7(2D)4p ^{3}D + 10 3d^7(2D)4p ^{3}F
226558	227127	−569	1	39 3d^7(2P)4p ^{1}P + 24 3d^7(2P)4p ^{3}S + 11 3d^7(2D)4p ^{3}P
227159.6	227375	−215	1	53 3d^7(2P)4p ^{3}S + 20 3d^7(2P)4p ^{1}P + 9 3d^7(4P)4p ^{3}S

Table A2: Continued

E^{a}_{exp}	E^{b}_{calc}	ΔE	J	Leading components (in %) in LS coupling [c]
227959.5	227765	195	2	28 $3d^7$(2D)4p ^{1}D + 23 $3d^7$(2D)4p ^{3}P + 22 $3d^7$(2P)4p ^{1}D
227993.2	228180	−187	6	97 $3d^7$(2H)4p ^{3}H
228479.7	228640	−160	5	93 $3d^7$(2H)4p ^{3}H
229064	229213	−149	4	94 $3d^7$(2H)4p ^{3}H
229694.2	229500	194	2	34 $3d^7$(2D)4p ^{3}P + 19 $3d^7$(2D)4p ^{1}D + 13 $3d^7$(2P)4p ^{3}P
230235.9	230367	−131	4	67 $3d^7$(2H)4p ^{1}G + 29 $3d^7$(2G)4p ^{1}G
230331.1	230057	274	3	56 $3d^7$(2D)4p ^{1}F + 17 $3d^7$(2G)4p ^{1}F + 13 $3d^7$(2D)4p ^{1}F
231216.3	231151	65	1	49 $3d^7$(2D)4p ^{3}P + 14 $3d^7$(2P)4p ^{1}P + 11 $3d^7$(2P)4p ^{3}P
231825.2	231633	192	0	65 $3d^7$(2D)4p ^{3}P + 17 $3d^7$(2P)4p ^{3}P + 12 $3d^7$(2D)4p ^{3}P
232441.8	232271	171	1	72 $3d^7$(2D)4p ^{1}P + 12 $3d^7$(2D)4p ^{1}P + 5 $3d^7$(2P)4p ^{3}S
233298.6	233428	−129	5	94 $3d^7$(2H)4p ^{1}H
241854.9	241819	36	2	57 $3d^7$(2F)4p ^{1}D + 32 $3d^7$(2F)4p ^{3}F + 5 $3d^7$(2F)4p ^{3}D
242529.8	242488	42	3	74 $3d^7$(2F)4p ^{3}G + 15 $3d^7$(2F)4p ^{3}F + 7 $3d^7$(2H)4p ^{3}G
243028.9	243071	−42	4	60 $3d^7$(2F)4p ^{3}G + 21 $3d^7$(2F)4p ^{3}F + 11 $3d^7$(2F)4p ^{1}G
243725.3	243724	1	3	49 $3d^7$(2F)4p 3D + 34 $3d^7$(2F)4p ^{3}F + 7 $3d^7$(2F)4p ^{3}G
244071.6	244091	−19	2	62 $3d^7$(2F)4p ^{3}F + 28 $3d^7$(2F)4p ^{1}D + 5 $3d^7$(2F)4p ^{3}D
244417.1	244379	38	3	46 $3d^7$(2F)4p ^{3}F + 38 $3d^7$(2F)4p ^{3}D + 8 $3d^7$(2F)4p ^{3}G
244671.4	244680	−9	5	93 $3d^7$(2F)4p ^{3}G + 6 $3d^7$(2H)4p ^{3}G
244753.1	244733	20	4	40 $3d^7$(2F)4p ^{3}F + 31 $3d^7$(2F)4p ^{3}G + 24 $3d^7$(2F)4p ^{1}G
244812.8	244714	99	2	80 $3d^7$(2F)4p 3D + 10 $3d^7$(2F)4p ^{1}D
244943	244768	175	1	90 $3d^7$(2F)4p 3D + 5 $3d^7$(2D)4p ^{3}D
245204.3	245250	−46	4	63 $3d^7$(2F)4p ^{1}G + 33 $3d^7$(2F)4p ^{3}F
250622.8	250488	135	3	95 $3d^7$(2F)4p ^{1}F
266196.5	266194	3	2	77 $3d^7$(2D)4p ^{3}P + 20 $3d^7$(2D)4p ^{3}P
266460.9	266482	−21	1	78 $3d^7$(2D)4p ^{3}P + 18 $3d^7$(2D)4p ^{3}P
266775	266786	−11	0	81 $3d^7$(2D)4p ^{3}P + 17 $3d^7$(2D)4p ^{3}P
268006	268109	−103	2	76 $3d^7$(2D)4p ^{3}F + 18 $3d^7$(2D)4p ^{3}F
268956.3	269006	−50	3	74 $3d^7$(2D)4p ^{3}F + 19 $3d^7$(2D)4p ^{3}F
270239.5	270255	−16	4	75 $3d^7$(2D)4p ^{3}F + 21 $3d^7$(2D)4p ^{3}F
272352.4	272380	−28	1	79 $3d^7$(2D)4p ^{1}P + 12 $3d^7$(2D)4p ^{1}P
272943.7	272785	159	3	74 $3d^7$(2D)4p ^{1}F + 20 $3d^7$(2D)4p ^{1}F
275672.9	275697	−24	1	71 $3d^7$(2D)4p 3D + 21 $3d^7$(2D)4p ^{3}D
275970.3	276048	−78	2	61 $3d^7$(2D)4p 3D + 18 $3d^7$(2D)4p ^{3}D + 13 $3d^7$(2D)4p ^{1}D
276545.9	276677	−131	2	58 $3d^7$(2D)4p ^{1}D + 20 $3d^7$(2D)4p ^{1}D + 12 $3d^7$(2D)4p ^{3}D
277108.7	277111	−2	3	70 $3d^7$(2D)4p 3D + 24 $3d^7$(2D)4p ^{3}D

a: From the NIST compilation [28]
b: This work
c: Only the components ≥ to 5% are given

Transitions

Table A3: Computed oscillator strengths and transition probabilities in Cu IV.

Wavelength	Lower Level	J_{low}	Upper Level	J_{up}	log gf	gA	CF
405.68	19697	2	266197	2	-0.62	9.65E+09	-0.573
406.339	20097	1	266197	2	-0.92	4.92E+09	0.698
406.453	26913	4	272944	3	-0.23	2.39E+10	-0.63
443.249	16248	2	241855	2	-0.87	4.59E+09	0.371
443.682	0	4	225387	4	-0.86	4.64E+09	0.515
444.215	19697	2	244813	2	-0.83	5.05E+09	-0.63
444.748	20097	1	244943	1	-0.9	4.29E+09	-0.707
444.997	19697	2	244417	3	-0.57	9.01E+09	-0.696
445.006	20097	1	244813	2	-0.49	1.09E+10	-0.688
445.394	20423	0	244943	1	-0.8	5.27E+09	-0.654
446.371	19697	2	243725	3	-0.49	1.08E+10	-0.61
447.008	26913	4	250623	3	-0.03	3.09E+10	0.849
448.43	0	4	223000	3	-0.87	4.48E+09	0.174
450.026	1861	3	224071	2	-0.48	1.09E+10	0.599
451.162	0	4	221650	3	-0.16	2.26E+10	0.793
452.503	3078	2	224071	2	-0.87	4.43E+09	-0.738
452.659	0	4	220917	5	0.07	3.84E+10	0.846
453.131	3078	2	223764	1	-0.4	1.28E+10	0.782
453.421	3078	2	223623	3	-0.14	2.38E+10	0.77
453.44	1861	3	222398	4	0.01	3.28E+10	0.839
454.8	1861	3	221739	2	-0.52	9.79E+09	-0.863
458.103	26913	4	245204	4	-0.88	4.17E+09	0.21
458.426	0	4	218138	3	-1	3.16E+09	-0.116
458.717	0	4	218000	5	-0.65	7.09E+09	0.551
459.514	0	4	217621	3	-0.9	3.94E+09	0.237
459.887	0	4	217445	4	-0.59	8.08E+09	0.724
461.326	1861	3	218628	3	-0.73	5.87E+09	0.767
462.548	16248	2	232442	1	-0.45	1.11E+10	0.553
463.534	0	4	215734	4	-0.97	3.33E+09	-0.768
463.717	3078	2	218726	2	-0.27	1.65E+10	0.751
463.929	3078	2	218628	3	-0.92	3.71E+09	0.325
464.646	1861	3	217079	3	-0.25	1.75E+10	0.601
464.829	0	4	215133	4	-0.19	2.00E+10	0.652
467.108	16248	2	230331	3	-0.44	1.10E+10	0.693
468.502	16248	2	229694	2	-0.96	3.35E+09	0.158
470.046	19697	2	232442	1	-0.97	3.21E+09	-0.336
472.341	16248	2	227960	2	-0.22	1.80E+10	0.731
472.769	19697	2	231216	1	-0.89	3.88E+09	-0.334
474.167	61456	0	272352	1	-0.28	1.57E+10	0.786
475.489	16248	2	226558	1	-0.55	8.28E+09	-0.506
476.196	19697	2	229694	2	-0.39	1.19E+10	-0.53
482.014	19697	2	227160	1	-0.64	6.58E+09	-0.413
482.945	20097	1	227160	1	-1	2.84E+09	0.406
484.53	26913	4	233299	5	-0.01	2.81E+10	-0.734
491.598	26913	4	230331	3	-0.58	7.27E+09	-0.279
491.829	26913	4	230236	4	0.4	6.98E+10	-0.817
492.236	16248	2	219403	3	-0.57	7.42E+09	-0.431
494.12	16248	2	218628	3	-0.67	5.89E+09	-0.406
496.991	0	4	201211	3	-0.13	1.99E+10	0.552
498.755	1861	3	202361	2	-0.31	1.30E+10	0.509
499.845	3078	2	203140	1	-0.54	7.71E+09	0.481
504.594	0	4	198179	4	-0.05	2.32E+10	0.466
504.862	20097	1	218171	1	-1	2.58E+09	-0.517
505.721	1861	3	199599	3	-0.2	1.66E+10	0.426
505.964	3078	2	200720	2	-0.3	1.30E+10	0.442
506.778	0	4	197325	5	-0.92	3.14E+09	0.434
513.566	19697	2	214413	1	-0.96	2.76E+09	-0.225
521.101	26913	4	218815	5	-0.94	2.79E+09	0.762
547.295	20423	0	203140	1	-0.98	2.34E+09	-0.44
548.655	20097	1	202361	2	-0.64	5.04E+09	-0.443
550.921	19697	2	201211	3	-0.48	7.29E+09	-0.429
774.129	198179	4	327357	4	-0.92	1.33E+09	-0.129
837.661	203869	2	323249	1	-1	9.43E+08	-0.324
841.324	190554	4	309414	5	-0.74	1.72E+09	-0.261
842.182	203869	2	322608	2	-0.61	2.33E+09	0.487
844.101	203869	2	322338	3	-0.36	4.05E+09	-0.547
844.154	220917	5	339379	6	-0.49	3.03E+09	0.232
849.411	191762	3	309490	4	-0.91	1.15E+09	-0.28
853.824	217445	4	334565	5	-0.63	2.15E+09	-0.399
854.607	230236	4	347249	4	-0.25	5.17E+09	0.472
856.622	192753	4	309490	4	-0.98	9.49E+08	-0.27
857.184	192753	4	309414	5	-0.82	1.39E+09	0.16
857.801	222398	4	338975	5	-0.53	2.67E+09	0.247
865.646	194132	3	309653	3	-0.92	1.08E+09	-0.251
866.867	194132	3	309490	4	-0.77	1.50E+09	0.172
871.241	195086	2	309865	2	-0.93	1.03E+09	-0.27
872.85	195086	2	309653	3	-0.83	1.28E+09	0.188
875.807	195684	1	309865	2	-0.94	1.00E+09	0.208
877.577	233299	5	347249	4	-0.78	1.44E+09	0.441
878.913	201211	3	314988	4	-0.87	1.17E+09	-0.44
880.657	202361	2	315912	3	-0.99	8.75E+08	-0.381
883.225	218815	5	332036	4	-0.79	1.39E+09	0.491
883.362	216429	0	329633	1	-0.99	8.76E+08	0.522
887.797	216703	2	329341	2	-0.95	9.47E+08	0.219
887.934	198179	4	310800	3	-0.82	1.27E+09	0.495
889.022	191762	3	304245	4	-0.94	9.75E+08	-0.507
891.012	217109	1	329341	2	-0.69	1.70E+09	0.528
891.076	215133	4	327357	4	-0.45	3.00E+09	-0.391
891.527	222398	4	334565	5	-0.54	2.44E+09	0.638
891.832	190554	4	302682	4	-0.49	2.73E+09	0.246
892.565	191762	3	303798	3	-0.57	2.26E+09	0.235
893.985	192741	2	304600	2	-0.68	1.77E+09	0.275
894.335	224071	2	335886	2	-0.68	1.75E+09	-0.502
895.403	193434	1	305116	1	-0.72	1.57E+09	0.401
895.73	217079	3	328720	3	-0.57	2.23E+09	-0.29
896.705	220917	5	332436	6	0.17	1.23E+10	-0.698
896.925	192753	4	304245	4	-0.76	1.44E+09	-0.557

Table A3: Continued

Wavelength	Lower Level	J_{Low}	Upper level	J_{Up}	log gf	gA	CF
897.782	227993	6	339379	6	-0.94	9.60E+08	-0.371
898.023	221650	3	333006	3	-0.88	1.08E+09	0.325
898.139	222527	5	333869	4	0.19	1.27E+10	-0.752
898.362	218028	2	329341	2	-0.43	3.13E+09	0.524
898.851	221602	6	332855	5	0.25	1.48E+10	-0.752
898.91	215734	4	326980	4	-0.75	1.46E+09	0.659
899.561	193434	1	304600	2	-0.7	1.66E+09	0.649
899.813	222603	2	333737	2	-0.76	1.40E+09	0.185
900.055	190528	5	301632	5	0.18	1.25E+10	0.769
900.265	190554	4	301632	5	-0.07	7.03E+09	0.685
900.435	192741	2	303798	3	-0.41	3.19E+09	0.635
901.547	191762	3	302682	4	-0.28	4.36E+09	0.639
902.244	221602	6	332436	6	-0.85	1.16E+09	-0.744
904.538	218628	3	329182	2	-0.95	9.25E+08	-0.193
904.866	215734	4	326248	3	-0.03	7.69E+09	-0.701
905.018	228480	5	338975	5	-0.96	8.94E+08	-0.345
905.33	222398	4	332855	5	-0.06	7.04E+09	-0.613
905.342	218726	2	329182	2	-0.6	2.04E+09	-0.377
905.874	214835	5	325226	4	0.06	9.39E+09	-0.616
907.065	223623	3	333869	4	-0.09	6.55E+09	-0.619
908.322	215133	4	325226	4	-0.82	1.22E+09	-0.183
908.871	225859	3	335886	2	-0.75	1.44E+09	0.203
909.044	223000	3	333006	3	-0.12	6.22E+09	0.681
909.047	214413	1	324419	2	-0.97	8.66E+08	-0.272
909.674	192753	4	302682	4	-0.14	5.92E+09	0.66
909.714	214835	5	324760	5	-0.46	2.80E+09	-0.679
909.913	217079	3	326980	4	-0.64	1.83E+09	0.618
910.013	213360	1	323249	1	-0.9	1.02E+09	-0.233
910.991	222666	7	332436	6	0.35	1.78E+10	-0.804
911.457	213535	2	323249	1	-0.9	1.02E+09	-0.276
911.859	224071	2	333737	2	-0.95	8.83E+08	0.2
911.86	194132	3	303798	3	-0.23	4.74E+09	0.644
911.865	241855	2	351520	3	-0.59	2.07E+09	0.822
912.183	215133	4	324760	5	-0.01	7.86E+09	-0.821
912.361	224959	6	334565	5	0.28	1.54E+10	-0.837
912.949	217445	4	326980	4	-0.58	2.09E+09	0.229
913.127	195086	2	304600	2	-0.4	3.20E+09	0.621
913.812	195684	1	305116	1	-0.75	1.43E+09	0.576
914.435	218000	5	327357	4	-0.82	1.20E+09	-0.34
914.772	213932	0	323249	1	-0.97	8.46E+08	-0.527
915.005	195827	2	305116	1	-0.18	5.22E+09	-0.817
915.351	213360	1	322608	2	-0.74	1.44E+09	-0.614
915.591	218138	3	327357	4	-1	8.00E+08	0.105
915.885	195932	0	305116	1	-1	7.89E+08	-0.523
916.812	213535	2	322608	2	-0.39	3.23E+09	-0.743
916.963	195544	3	304600	2	-0.02	7.53E+09	-0.822
917.512	242530	3	351520	3	-0.43	2.92E+09	-0.796
917.91	213665	3	322608	2	-0.37	3.39E+09	-0.459
918.144	195684	1	304600	2	-0.9	9.90E+08	-0.267
918.443	243029	4	351909	4	-0.26	4.35E+09	-0.848
918.449	192753	4	301632	5	-0.68	1.65E+09	-0.151
919.595	195055	4	303798	3	0.1	9.95E+09	-0.833
919.857	195086	2	303798	3	-0.88	1.04E+09	-0.169
920.06	216071	6	324760	5	0.27	1.45E+10	-0.828
920.189	213665	3	322338	3	-0.37	3.34E+09	-0.682
921.235	194132	3	302682	4	-0.81	1.22E+09	-0.149
921.733	243029	4	351520	3	-0.44	2.82E+09	-0.275
922.174	222603	2	331042	1	-0.62	1.91E+09	-0.503
922.92	218628	3	326980	4	-0.58	2.04E+09	-0.28
922.993	194339	5	302682	4	0.2	1.24E+10	-0.845
924.355	243725	3	351909	4	-0.16	5.37E+09	-0.792
924.511	218815	5	326980	4	0.12	1.03E+10	-0.784
924.67	217079	3	325226	4	-0.16	5.43E+09	-0.666
925.626	218945	4	326980	4	-0.27	4.15E+09	-0.644
925.759	214319	4	322338	3	0.05	8.69E+09	-0.762
926.561	227960	2	335886	2	-0.38	3.21E+09	0.525
926.833	221739	2	329633	1	-0.31	3.80E+09	0.811
926.975	225859	3	333737	2	-0.25	4.38E+09	-0.599
927.805	217445	4	325226	4	-0.19	4.97E+09	0.72
928.581	221650	3	329341	2	-0.1	6.10E+09	-0.751
928.641	193948	6	301632	5	0.27	1.43E+10	-0.843
929.2	218628	3	326248	3	-0.27	4.11E+09	0.809
929.206	225387	4	333006	3	0.08	9.37E+09	-0.808
929.566	219403	3	326980	4	-0.32	3.67E+09	-0.452
930.048	218726	2	326248	3	-0.16	5.30E+09	-0.847
930.304	244417	3	351909	4	-0.79	1.26E+09	-0.215
931.834	217445	4	324760	5	-0.78	1.28E+09	-0.256
931.943	218945	4	326248	3	-0.56	2.09E+09	-0.771
932.159	223764	1	331042	1	-0.73	1.45E+09	0.591
932.51	244671	5	351909	4	0.16	1.11E+10	-0.848
932.606	218000	5	325226	4	-0.53	2.26E+09	-0.666
933.221	244753	4	351909	4	-0.52	2.30E+09	0.345
933.68	244417	3	351520	3	-0.28	3.98E+09	0.561
934.741	221739	2	328720	3	-0.49	2.45E+09	0.498
934.83	224071	2	331042	1	-0.6	1.95E+09	0.449
935.28	197325	5	304245	4	0.19	1.18E+10	-0.868
935.937	219403	3	326248	3	-0.4	3.02E+09	-0.764
936.351	217621	3	324419	2	-0.52	2.31E+09	0.694
936.601	217650	2	324419	2	-0.99	7.71E+08	0.325
936.618	244753	4	351520	3	-0.08	6.27E+09	-0.845
936.677	218000	5	324760	5	0.04	8.30E+09	0.702
937.142	244813	2	351520	3	-0.42	2.91E+09	-0.528
937.168	245204	4	351909	4	-0.39	3.09E+09	0.81
937.614	199202	4	305856	3	0.1	9.56E+09	-0.863
938.105	218628	3	325226	4	-0.73	1.41E+09	-0.236
938.561	216703	2	323249	1	-0.71	1.46E+09	-0.493
939.327	200483	3	306942	2	-0.03	7.06E+09	-0.845
939.499	220917	5	327357	4	0.34	1.64E+10	-0.675
940.536	222398	4	328720	3	0.21	1.21E+10	-0.648
940.901	218138	3	324419	2	-0.39	3.06E+09	-0.63
940.901	218945	4	325226	4	-0.5	2.38E+09	0.224
941.113	199599	3	305856	3	-0.18	4.94E+09	0.547
941.426	200720	2	306942	2	-0.3	3.81E+09	0.597
941.697	229694	2	335886	2	-0.77	1.27E+09	0.283
942.639	228480	5	334565	5	-1	7.52E+08	-0.13
942.812	198179	4	304245	4	0.03	8.10E+09	0.737

Table A3: Continued

Wavelength	Lower Level	J_{Low}	Upper level	J_{Up}	log gf	gA	CF
945.895	223000	3	328720	3	-0.89	9.68E+08	0.277
946.014	221650	3	327357	4	-0.09	5.97E+09	-0.577
946.653	216703	2	322338	3	-0.99	7.53E+08	0.306
946.975	217650	2	323249	1	-0.83	1.10E+09	-0.247
947.34	223623	3	329182	2	0	7.46E+09	-0.555
947.379	230331	3	335886	2	-0.31	3.66E+09	-0.424
948.608	223764	1	329182	2	-0.22	4.46E+09	-0.623
951.149	200720	2	305856	3	-0.8	1.16E+09	0.755
951.374	224071	2	329182	2	-0.82	1.12E+09	0.356
951.661	217445	4	322524	5	-0.98	7.74E+08	-0.12
951.962	227960	2	333006	3	-0.89	9.45E+08	0.441
952.499	217621	3	322608	2	-0.41	2.85E+09	-0.595
953.639	227993	6	332855	5	-0.87	9.80E+08	-0.695
954.156	229064	4	333869	4	0.04	8.02E+09	0.666
954.616	190554	4	295308	3	-0.91	8.98E+08	0.133
954.954	217621	3	322338	3	-0.76	1.26E+09	0.198
955.572	224071	2	328720	3	-0.27	3.95E+09	-0.491
955.602	199599	3	304245	4	-0.62	1.74E+09	0.759
955.611	201211	3	305856	3	-0.66	1.61E+09	0.63
956.195	202361	2	306942	2	-0.79	1.18E+09	0.726
956.909	198179	4	302682	4	-0.79	1.19E+09	0.332
957.458	227993	6	332436	6	0.19	1.12E+10	0.665
957.511	218171	1	322608	2	-0.73	1.35E+09	0.526
958.084	228480	5	332855	5	0.08	8.76E+09	0.658
958.252	223000	3	327357	4	-0.46	2.53E+09	-0.23
958.507	230236	4	334565	5	-0.09	5.84E+09	-0.711
958.97	191762	3	296040	2	-0.88	9.60E+08	0.2
959.511	243029	4	347249	4	-0.68	1.53E+09	-0.525
959.687	218138	3	322338	3	-0.59	1.86E+09	0.51
960.586	220316	2	324419	2	-0.3	3.64E+09	0.558
962.628	227160	1	331042	1	-0.82	1.09E+09	-0.47
963.37	203140	1	306942	2	-0.41	2.78E+09	-0.743
964.8	203869	2	307517	3	0.29	1.41E+10	-0.583
965.025	190528	5	294152	4	-0.8	1.14E+09	0.226
966.227	202361	2	305856	3	-0.32	3.39E+09	-0.584
966.709	232442	1	335886	2	-0.7	1.43E+09	-0.304
967.066	230331	3	333737	2	-0.37	3.03E+09	-0.345
967.946	229694	2	333006	3	-0.66	1.56E+09	-0.567
968.072	203869	2	307167	2	0.21	1.16E+10	0.707
968.982	220917	5	324118	6	-0.47	2.38E+09	0.281
969.489	221272	1	324419	2	-0.95	8.04E+08	0.327
969.804	203869	2	306983	1	0.03	7.54E+09	-0.717
970.169	226558	1	329633	1	-0.79	1.15E+09	0.352
970.553	201211	3	304245	4	-0.22	4.22E+09	-0.56
970.707	221602	6	324619	5	-0.97	7.52E+08	0.132
972.185	225859	3	328720	3	-0.84	1.03E+09	-0.26
972.405	220917	5	323755	6	-0.65	1.58E+09	-0.241
974.48	230236	4	332855	5	-0.68	1.47E+09	-0.612
975.152	217445	4	319993	3	-0.88	9.16E+08	0.237
975.416	231216	1	333737	2	-0.54	1.99E+09	-0.503
975.652	244753	4	347249	4	-0.52	2.14E+09	0.395
977.281	218628	3	320953	4	-0.74	1.28E+09	-0.258
978.267	222398	4	324619	5	-0.27	3.76E+09	0.356
978.435	222527	5	324731	4	-0.7	1.38E+09	0.31
978.65	227160	1	329341	2	-0.98	7.38E+08	-0.343
979.966	245204	4	347249	4	-0.04	6.31E+09	-0.521
980.683	225387	4	327357	4	-0.59	1.78E+09	-0.448
982.089	217445	4	319268	3	-0.84	9.96E+08	-0.144
982.318	230236	4	332036	4	0.29	1.34E+10	-0.466
983.238	230331	3	332036	4	-0.33	3.24E+09	-0.6
984.737	219403	3	320953	4	-0.5	2.20E+09	-0.352
985.499	201211	3	302682	4	-0.89	8.78E+08	-0.471
986.201	192753	4	294152	4	-0.4	2.74E+09	0.34
987.217	232442	1	333737	2	-0.31	3.29E+09	-0.522
987.496	233299	5	334565	5	0.1	8.66E+09	0.611
987.743	218028	2	319268	3	-0.97	7.23E+08	-0.088
988.383	194132	3	295308	3	-0.57	1.86E+09	0.332
989.038	223623	3	324731	4	-0.32	3.29E+09	0.434
989.227	222666	7	323755	6	-0.86	9.43E+08	-0.354
990.546	195086	2	296040	2	-0.92	8.19E+08	0.337
992.266	215133	4	315912	3	-0.7	1.36E+09	0.16
995.365	215133	4	315599	4	-0.32	3.24E+09	0.194
996.453	195684	1	296040	2	-0.8	1.07E+09	0.458
996.869	216703	2	317017	3	-0.15	4.67E+09	-0.342
997.786	195086	2	295308	3	-0.76	1.17E+09	0.45
998.739	222398	4	322524	5	-1	6.75E+08	0.581
999.804	194132	3	294152	4	-0.88	8.87E+08	0.414
1000.008	190554	4	290553	4	-0.86	9.20E+08	0.044
1000.034	222527	5	322524	5	0.19	1.04E+10	-0.744
1000.595	221602	6	321542	6	0.46	1.94E+10	-0.76
1000.657	213360	1	313295	2	-0.73	1.24E+09	-0.183
1000.824	190528	5	290445	6	-0.75	1.18E+09	0.111
1001.356	215734	4	315599	4	-0.38	2.81E+09	-0.504
1001.452	215133	4	314988	4	-0.3	3.32E+09	-0.173
1002.104	222527	5	322317	5	0.01	6.86E+09	-0.507
1002.175	218028	2	317811	3	-0.55	1.86E+09	0.175
1002.404	213535	2	313295	2	-0.92	7.92E+08	-0.185
1003.169	220917	5	320601	6	0.02	6.98E+09	-0.588
1003.41	224959	6	324619	5	-0.93	7.79E+08	-0.247
1003.476	222398	4	322051	3	-0.92	7.98E+08	-0.598
1003.716	213665	3	313295	2	-0.71	1.29E+09	0.378
1004.459	233299	5	332855	5	-0.84	9.62E+08	0.182
1005.405	221602	6	321064	5	-0.27	3.52E+09	-0.546
1005.811	213535	2	312957	3	-0.79	1.08E+09	-0.119
1006.366	217650	2	317017	3	-0.69	1.34E+09	0.229
1007.131	213665	3	312957	3	-0.26	3.61E+09	-0.387
1008.053	192753	4	291954	3	-0.91	8.11E+08	0.182
1008.481	224959	6	324118	6	0.25	1.16E+10	-0.735
1008.845	191762	3	290885	3	-0.65	1.49E+09	0.109
1008.941	190528	5	289642	4	-0.36	2.85E+09	-0.226
1008.954	217079	3	316192	2	-0.36	2.89E+09	0.442
1009.418	213535	2	312602	2	-0.96	7.25E+08	-0.2
1009.64	190528	5	289573	5	-0.51	2.00E+09	0.132
1009.904	190554	4	289573	5	0.16	9.52E+09	-0.386
1009.982	191762	3	290774	2	-0.17	4.44E+09	0.309
1010.208	218028	2	317017	3	0.03	6.98E+09	-0.461

Table A3: Continued

Wavelength	Lower Level	J_{Low}	Upper level	J_{Up}	log gf	gA	CF
1010.213	192741	2	291730	2	-0.66	1.44E+09	0.179
1010.314	220917	5	319896	4	-0.55	1.83E+09	0.658
1010.345	190554	4	289530	3	0.01	6.70E+09	0.315
1011.473	218945	4	317811	3	-0.94	7.42E+08	-0.305
1011.808	217079	3	315912	3	-0.09	5.27E+09	-0.315
1011.841	192741	2	291571	1	-0.34	3.01E+09	-0.417
1012.056	192753	4	291562	5	-0.54	1.89E+09	0.232
1012.19	224959	6	323755	6	0.06	7.42E+09	-0.56
1012.238	191762	3	290553	4	0.08	7.79E+09	-0.284
1012.788	233299	5	332036	4	0.11	8.36E+09	-0.641
1012.832	198179	4	296912	3	-0.99	6.59E+08	0.136
1013.517	222398	4	321064	5	-0.14	4.74E+09	-0.525
1013.807	214319	4	312957	3	-0.89	8.38E+08	0.344
1014.349	197325	5	295910	4	-0.54	1.86E+09	-0.445
1014.634	192741	2	291299	3	-0.16	4.49E+09	-0.244
1014.815	221602	6	320142	7	-0.98	6.77E+08	0.012
1014.937	215734	4	314262	5	-0.72	1.25E+09	-0.262
1015.03	217079	3	315599	4	-0.8	1.03E+09	0.316
1015.545	222666	7	321135	7	0.53	2.19E+10	-0.758
1016.074	214835	5	313253	5	-0.28	3.42E+09	-0.219
1016.317	192753	4	291147	5	-0.32	3.05E+09	0.438
1016.608	213360	1	311727	1	-0.83	9.60E+08	-0.249
1016.852	221650	3	319993	3	-0.29	3.25E+09	-0.565
1017.178	214319	4	312630	4	-0.1	5.20E+09	-0.578
1017.215	194132	3	292440	4	-0.43	2.39E+09	0.457
1017.34	193434	1	291730	2	0.17	9.47E+09	-0.749
1017.852	221650	3	319896	4	-0.84	9.28E+08	0.063
1018.453	214413	1	312602	2	0.02	6.70E+09	-0.634
1018.64	190528	5	288698	6	0.64	2.80E+10	-0.7
1018.808	217445	4	315599	4	-0.23	3.83E+09	-0.148
1018.91	192741	2	290885	3	0	6.42E+09	-0.5
1018.977	215734	4	313872	4	0.23	1.10E+10	-0.668
1018.99	193434	1	291571	1	-0.52	1.97E+09	-0.556
1019.117	215133	4	313257	3	-0.86	9.01E+08	-0.37
1019.346	221602	6	319704	6	-0.79	1.04E+09	0.824
1020.07	192741	2	290774	2	-0.21	3.95E+09	0.424
1020.275	190554	4	288566	3	0.32	1.33E+10	0.821
1020.871	199599	3	297554	2	-0.9	8.13E+08	0.181
1020.901	223000	3	320953	4	-0.64	1.48E+09	0.154
1021.082	222666	7	320601	6	-0.26	3.48E+09	-0.584
1021.61	218028	2	315912	3	-0.74	1.15E+09	-0.308
1021.662	191762	3	289642	4	-0.22	3.83E+09	0.3
1021.819	194132	3	291997	2	-0.91	7.81E+08	-0.046
1022.191	220917	5	318746	5	0.53	2.18E+10	-0.779
1022.193	217621	3	315450	3	-0.86	8.59E+08	0.172
1022.209	195086	2	292913	3	-0.66	1.41E+09	0.308
1022.27	194132	3	291954	3	-0.71	1.25E+09	0.342
1022.551	214835	5	312630	4	-0.91	7.85E+08	0.604
1022.831	191762	3	289530	3	-0.09	5.19E+09	0.402
1023.215	198179	4	295910	4	0.33	1.35E+10	-0.512
1023.437	199202	4	296912	3	-0.72	1.22E+09	-0.287
1023.683	195827	2	293514	3	-0.6	1.60E+09	-0.378
1024.127	216071	6	313715	6	-0.68	1.34E+09	0.183
1024.261	214835	5	312467	4	-0.22	3.83E+09	-0.742
1024.397	221650	3	319268	3	-0.75	1.12E+09	-0.338
1024.502	191762	3	289370	2	0.15	9.03E+09	0.811
1024.798	214835	5	312416	5	-0.25	3.57E+09	0.215
1024.959	224959	6	322524	5	-0.45	2.27E+09	-0.535
1024.971	218628	3	316192	2	-0.32	3.06E+09	-0.357
1025.187	217445	4	314988	4	0.19	9.87E+09	-0.665
1025.244	241855	2	339393	3	0.04	6.99E+09	-0.718
1025.369	194339	5	291865	6	-0.39	2.58E+09	0.063
1025.398	215734	4	313257	3	-0.34	2.93E+09	-0.635
1025.437	215734	4	313253	5	0.49	1.96E+10	-0.582
1025.658	222398	4	319896	4	0.1	7.97E+09	-0.629
1025.695	220316	2	317811	3	-0.97	6.79E+08	-0.156
1026.004	218726	2	316192	2	0.02	6.64E+09	-0.684
1026.457	218028	2	315450	3	-0.43	2.29E+09	0.468
1026.797	222603	2	319993	3	-0.16	4.30E+09	-0.502
1026.851	195055	4	292440	4	-0.63	1.49E+09	0.179
1027.019	195544	3	292913	3	-0.72	1.20E+09	0.171
1027.045	217621	3	314988	4	-0.76	1.11E+09	-0.278
1027.134	224959	6	322317	5	-0.92	7.60E+08	0.198
1027.391	215133	4	312467	4	0.11	8.17E+09	0.697
1027.436	223623	3	320953	4	-0.54	1.82E+09	0.571
1027.607	199599	3	296912	3	0.21	1.02E+10	-0.478
1027.609	214413	1	311727	1	-0.29	3.23E+09	0.537
1027.618	218138	3	315450	3	-0.3	3.09E+09	-0.48
1027.787	225859	3	323155	4	0.19	9.86E+09	-0.353
1027.916	218628	3	315912	3	-0.37	2.68E+09	-0.448
1027.932	215133	4	312416	5	-0.72	1.22E+09	-0.061
1028.447	242530	3	339764	4	-0.77	1.07E+09	0.13
1028.457	192741	2	289974	1	-0.16	4.42E+09	0.804
1028.568	194339	5	291562	5	-0.84	9.23E+08	0.093
1028.616	218628	3	315846	2	-0.76	1.08E+09	-0.111
1028.923	222398	4	319587	4	0.2	1.01E+10	-0.71
1028.955	218726	2	315912	3	-0.64	1.44E+09	-0.563
1029.057	222527	5	319704	6	0.87	4.70E+10	-0.887
1029.198	214835	5	311998	5	0.26	1.16E+10	0.649
1029.516	243029	4	340162	5	-0.44	2.30E+09	0.183
1029.656	218726	2	315846	2	-0.61	1.53E+09	0.572
1030.011	195827	2	292913	3	0.53	2.11E+10	-0.814
1030.165	200483	3	297554	2	-0.75	1.13E+09	-0.381
1030.274	190528	5	287589	4	0.14	8.70E+09	0.807
1030.549	190554	4	287589	4	0.48	1.90E+10	-0.602
1031.005	223000	3	319993	3	-0.68	1.30E+09	-0.159
1031.052	218000	5	314988	4	0.02	6.64E+09	-0.729
1031.241	218628	3	315599	4	-0.63	1.48E+09	-0.209
1031.274	218945	4	315912	3	-0.14	4.50E+09	-0.547
1031.408	195684	1	292639	1	-0.15	4.44E+09	-0.683
1031.872	195086	2	291997	2	-0.12	4.77E+09	-0.385
1031.902	221602	6	318510	7	0.93	5.35E+10	-0.9
1031.911	214835	5	311743	6	0.84	4.37E+10	-0.841
1032.033	223000	3	319896	4	0.17	9.40E+09	-0.586
1032.035	195544	3	292440	4	0.61	2.54E+10	-0.88
1032.112	192753	4	289642	4	0.43	1.71E+10	-0.656

Table A3: Continued

Wavelength	Lower Level	J_{Low}	Upper level	J_{Up}	log gf	gA	CF
1032.304	222398	4	319268	3	-0.64	1.40E+09	-0.483
1032.333	195086	2	291954	3	-0.96	6.82E+08	0.557
1032.359	215133	4	311998	5	0.25	1.13E+10	-0.559
1032.387	242530	3	339393	3	0.15	8.97E+09	-0.668
1032.412	214413	1	311274	2	-0.83	9.28E+08	-0.448
1032.522	218138	3	314988	4	-0.54	1.81E+09	0.313
1032.691	200720	2	297554	2	0.19	9.58E+09	-0.681
1032.843	192753	4	289573	5	0.21	1.00E+10	-0.519
1032.87	217445	4	314262	5	-0.56	1.71E+09	-0.094
1033.009	191762	3	288566	3	0.15	8.85E+09	-0.343
1033.14	217079	3	313872	4	-0.67	1.34E+09	0.167
1033.145	190528	5	287320	5	0.58	2.37E+10	-0.728
1033.229	218815	5	315599	4	-0.37	2.71E+09	-0.517
1033.276	243029	4	339809	5	0.29	1.21E+10	-0.833
1033.304	192753	4	289530	3	0.22	1.05E+10	-0.457
1033.422	190554	4	287320	5	-0.18	4.11E+09	0.182
1033.563	194132	3	290885	3	0.25	1.11E+10	0.79
1033.564	195544	3	292297	4	-0.14	4.48E+09	0.348
1033.657	230236	4	326980	4	-0.37	2.68E+09	-0.797
1033.753	243029	4	339764	4	0.07	7.35E+09	-0.441
1034.04	199202	4	295910	4	-0.36	2.70E+09	-0.614
1034.05	195932	0	292639	1	-0.22	3.75E+09	-0.813
1034.161	213360	1	310057	1	-0.18	4.15E+09	0.799
1034.323	215734	4	312416	5	0.35	1.40E+10	-0.476
1034.491	222603	2	319268	3	-0.23	3.64E+09	-0.468
1034.622	218945	4	315599	4	0.15	8.73E+09	0.708
1034.724	195086	2	291730	2	-0.25	3.48E+09	0.657
1034.756	194132	3	290774	2	0.07	7.26E+09	-0.398
1034.884	192741	2	289370	2	-0.02	5.98E+09	-0.387
1034.919	250623	3	347249	4	0.45	1.76E+10	-0.802
1035.285	216703	2	313295	2	-0.69	1.27E+09	0.204
1035.339	223000	3	319587	4	0.11	8.17E+09	0.597
1035.844	193434	1	289974	1	-0.16	4.35E+09	-0.553
1036.027	213535	2	310057	1	-0.85	8.74E+08	-0.737
1036.167	219403	3	315912	3	-0.43	2.30E+09	0.411
1036.197	195055	4	291562	5	0.77	3.67E+10	-0.896
1036.223	213360	1	309865	2	0.03	6.68E+09	-0.64
1036.432	195086	2	291571	1	-0.22	3.78E+09	0.393
1036.875	216071	6	312515	6	0.38	1.49E+10	-0.82
1036.879	219403	3	315846	2	0.04	6.77E+09	-0.647
1037.025	200483	3	296912	3	-0.62	1.50E+09	-0.587
1037.125	194132	3	290553	4	0.16	9.00E+09	-0.515
1037.777	218628	3	314988	4	-0.76	1.08E+09	-0.276
1037.945	216071	6	312416	5	-1	6.17E+08	0.217
1038.096	213535	2	309865	2	0.05	7.01E+09	0.798
1038.284	195684	1	291997	2	0	6.25E+09	-0.827
1038.297	199599	3	295910	4	-0.72	1.17E+09	-0.136
1038.806	215734	4	311998	5	-0.87	8.43E+08	-0.055
1038.919	216703	2	312957	3	-0.09	4.99E+09	-0.52
1039.334	217079	3	313295	2	-0.87	8.37E+08	-0.515
1039.363	195086	2	291299	3	0.08	7.50E+09	-0.596
1039.503	213665	3	309865	2	-0.85	8.75E+08	-0.695
1039.546	219403	3	315599	4	-0.16	4.27E+09	-0.572
1039.584	200720	2	296912	3	-0.65	1.39E+09	-0.262
1039.653	195544	3	291730	2	-0.94	7.10E+08	0.246
1039.741	217079	3	313257	3	-0.01	6.08E+09	0.741
1039.76	224959	6	321135	7	-0.88	8.19E+08	0.606
1039.824	195827	2	291997	2	-0.57	1.66E+09	-0.553
1040.154	228480	5	324619	5	0.1	7.61E+09	0.397
1040.312	213932	0	310057	1	-0.2	3.87E+09	-0.654
1040.313	227993	6	324118	6	-0.23	3.59E+09	0.23
1040.381	213535	2	309653	3	0.37	1.46E+10	-0.715
1040.515	194339	5	290445	6	0.85	4.36E+10	-0.899
1040.665	195055	4	291147	5	-0.73	1.14E+09	0.153
1040.886	221739	2	317811	3	0.29	1.19E+10	0.863
1041.187	215133	4	311177	4	-0.78	1.02E+09	-0.375
1041.249	243725	3	339764	4	-0.03	5.77E+09	0.429
1041.795	213665	3	309653	3	0.08	7.39E+09	0.798
1042.254	243029	4	338975	5	0.43	1.64E+10	-0.51
1042.459	216071	6	311998	5	-0.23	3.63E+09	-0.709
1042.513	224071	2	319993	3	-0.56	1.69E+09	0.178
1042.72	195827	2	291730	2	-0.32	2.92E+09	-0.294
1042.768	216703	2	312602	2	-0.67	1.30E+09	0.209
1042.993	215133	4	311011	3	-0.59	1.60E+09	0.56
1043.36	222666	7	318510	7	-0.86	8.33E+08	0.877
1043.512	195055	4	290885	3	-0.53	1.81E+09	0.439
1043.564	213665	3	309490	4	0.59	2.37E+10	-0.799
1043.675	220917	5	316732	4	0.14	8.59E+09	0.786
1043.747	217445	4	313253	5	0.02	6.38E+09	-0.828
1043.987	222666	7	318452	8	1	6.12E+10	-0.898
1044.059	226271	2	322051	3	0.25	1.10E+10	0.779
1044.26	227993	6	323755	6	0.03	6.48E+09	-0.536
1044.336	195544	3	291299	3	-0.02	5.93E+09	-0.414
1044.491	193948	6	289688	7	0.95	5.40E+10	-0.898
1045.182	225387	4	321064	5	-0.93	7.30E+08	0.748
1045.242	216071	6	311743	6	-0.29	3.16E+09	0.843
1045.288	215133	4	310800	3	0.38	1.49E+10	-0.853
1045.288	229064	4	324731	4	0.1	7.68E+09	0.549
1045.532	217650	2	313295	2	-0.24	3.48E+09	0.403
1045.605	228480	5	324118	6	-0.3	3.01E+09	0.295
1046.349	202361	2	297931	1	-0.02	5.86E+09	-0.59
1046.499	216071	6	311628	7	0.94	5.37E+10	-0.896
1046.514	229064	4	324619	5	-0.56	1.67E+09	0.632
1046.565	217079	3	312630	4	-0.82	9.23E+08	0.247
1046.876	217079	3	312602	2	-0.75	1.08E+09	0.462
1047.021	194132	3	289642	4	-0.51	1.90E+09	-0.171
1047.143	195055	4	290553	4	0.21	9.81E+09	-0.457
1047.206	217109	1	312602	2	-0.86	8.38E+08	0.159
1047.225	244671	5	340162	5	0.33	1.32E+10	-0.771
1047.431	195827	2	291299	3	-0.51	1.88E+09	-0.224
1047.655	214413	1	309865	2	-0.66	1.33E+09	-0.263
1047.694	218815	5	314262	5	0.37	1.42E+10	-0.721
1048.077	222398	4	317811	3	-0.1	4.83E+09	0.626
1048.121	244753	4	340162	5	0.3	1.22E+10	-0.696
1048.275	225387	4	320782	5	0.79	3.72E+10	-0.886
1048.355	217079	3	312467	4	-0.14	4.44E+09	-0.396

Table A3: Continued

Wavelength	Lower Level	J_{Low}	Upper level	J_{Up}	log gf	gA	CF
1048.442	216703	2	312083	3	-0.49	1.95E+09	0.706
1048.581	221650	3	317017	3	-0.53	1.79E+09	-0.185
1048.63	201211	3	296573	2	0.22	1.01E+10	-0.546
1048.804	244417	3	339764	4	0.34	1.35E+10	-0.83
1048.925	217621	3	312957	3	-0.39	2.52E+09	0.245
1049.086	244072	2	339393	3	0.08	7.24E+09	-0.523
1049.126	218945	4	314262	5	0.42	1.61E+10	0.839
1049.239	217650	2	312957	3	0.21	9.81E+09	-0.69
1049.292	194339	5	289642	4	-0.48	2.03E+09	-0.569
1049.555	221739	2	317017	3	-0.98	6.39E+08	0.107
1049.735	199202	4	294464	4	-0.97	6.46E+08	0.148
1049.827	218000	5	313253	5	-0.9	7.63E+08	-0.154
1049.94	218628	3	313872	4	0.24	1.04E+10	-0.852
1050.047	194339	5	289573	5	0.36	1.38E+10	-0.607
1050.444	224071	2	319268	3	-0.24	3.45E+09	0.4
1050.582	217445	4	312630	4	-0.73	1.13E+09	0.486
1050.612	224959	6	320142	7	0.94	5.17E+10	-0.902
1050.733	214319	4	309490	4	-0.06	5.25E+09	0.809
1051.144	220316	2	315450	3	0.32	1.23E+10	-0.648
1051.259	218171	1	313295	2	-0.11	4.76E+09	-0.575
1051.578	214319	4	309414	5	0.76	3.51E+10	-0.853
1051.593	225859	3	320953	4	0.47	1.79E+10	-0.867
1051.72	221650	3	316732	4	0.51	1.96E+10	-0.853
1051.897	215734	4	310800	3	-0.5	1.91E+09	0.675
1052.018	244753	4	339809	5	-0.08	5.01E+09	0.259
1052.387	217445	4	312467	4	-0.39	2.47E+09	-0.311
1052.513	244753	4	339764	4	-0.3	3.02E+09	-0.243
1052.534	217621	3	312630	4	0.37	1.43E+10	-0.805
1052.535	195544	3	290553	4	-0.42	2.27E+09	-0.129
1052.829	217079	3	312061	2	-0.08	5.07E+09	0.715
1052.945	197325	5	292297	4	-0.82	9.13E+08	0.562
1052.954	217445	4	312416	5	0.15	8.56E+09	0.77
1053.102	245204	4	340162	5	0.23	1.02E+10	-0.858
1053.444	218945	4	313872	4	-0.63	1.42E+09	-0.142
1053.731	218815	5	313715	6	0.87	4.41E+10	-0.914
1054.345	217621	3	312467	4	-0.27	3.24E+09	-0.704
1054.639	218138	3	312957	3	-0.84	8.78E+08	0.129
1054.947	203140	1	297931	1	-0.26	3.30E+09	-0.794
1055.409	193948	6	288698	6	0.49	1.86E+10	-0.879
1055.884	244671	5	339379	6	0.85	4.22E+10	-0.851
1055.972	201211	3	295910	4	0.23	1.02E+10	-0.802
1056.119	119632	5	214319	4	-0.87	8.00E+08	0.43
1056.173	220917	5	315599	4	-0.97	6.37E+08	-0.297
1056.659	217445	4	312083	3	0.06	6.92E+09	-0.685
1056.758	218628	3	313257	3	0.04	6.59E+09	-0.514
1057.036	245204	4	339809	5	0.55	2.14E+10	-0.782
1057.369	221272	1	315846	2	-0.65	1.31E+09	-0.461
1057.405	216703	2	311274	2	-0.88	7.82E+08	0.288
1057.455	192753	4	287320	5	0.04	6.57E+09	-0.311
1057.622	202361	2	296912	3	0.11	7.66E+09	-0.8
1057.753	197325	5	291865	6	0.85	4.24E+10	-0.9
1057.856	218726	2	313257	3	-0.11	4.68E+09	-0.668
1058	195055	4	289573	5	-0.57	1.62E+09	-0.078
1058.029	218000	5	312515	6	0.7	2.95E+10	-0.868
1058.098	225387	4	319896	4	-0.19	3.93E+09	-0.654
1058.287	218138	3	312630	4	0.02	6.28E+09	-0.506
1058.551	219403	3	313872	4	0.11	7.67E+09	0.807
1058.605	218138	3	312602	2	-0.73	1.11E+09	-0.495
1058.953	217650	2	312083	3	-0.82	8.94E+08	-0.239
1059.143	218000	5	312416	5	0.22	9.95E+09	0.611
1059.155	203140	1	297554	2	-0.09	4.80E+09	-0.797
1059.159	222603	2	317017	3	-0.76	1.02E+09	0.103
1059.786	194339	5	288698	6	-0.7	1.18E+09	-0.073
1060.118	218138	3	312467	4	-0.87	8.00E+08	-0.179
1060.308	218945	4	313257	3	-0.96	6.49E+08	0.18
1060.319	199202	4	293514	3	-0.85	8.35E+08	0.656
1060.35	218945	4	313253	5	0.17	8.67E+09	-0.41
1060.358	216703	2	311011	3	-0.19	3.79E+09	-0.697
1060.407	244671	5	338975	5	-0.67	1.28E+09	0.765
1060.561	195684	1	289974	1	-0.95	6.72E+08	0.166
1060.622	195086	2	289370	2	-0.93	7.06E+08	0.066
1060.658	215133	4	309414	5	-0.76	1.04E+09	0.606
1060.886	198179	4	292440	4	-0.88	7.87E+08	0.444
1061.159	197325	5	291562	5	-0.94	6.84E+08	-0.126
1061.327	244753	4	338975	5	0.44	1.64E+10	-0.832
1061.427	202361	2	296573	2	-0.12	4.43E+09	-0.685
1061.573	225387	4	319587	4	-0.13	4.39E+09	0.765
1061.606	199202	4	293399	5	0.8	3.71E+10	-0.907
1061.63	217079	3	311274	2	-0.03	5.54E+09	-0.707
1061.868	221739	2	315912	3	-0.36	2.54E+09	-0.576
1062.502	198179	4	292297	4	-0.11	4.62E+09	0.691
1062.792	227960	2	322051	3	-0.49	1.92E+09	-0.2
1063.029	220917	5	314988	4	-0.41	2.33E+09	0.471
1063.208	218028	2	312083	3	-0.84	8.63E+08	-0.292
1063.355	195932	0	289974	1	-0.8	9.43E+08	-0.364
1063.409	225859	3	319896	4	-0.99	6.03E+08	-0.043
1063.446	218028	2	312061	2	-0.74	1.08E+09	-0.472
1063.637	223000	3	317017	3	-0.12	4.49E+09	0.633
1063.843	218000	5	311998	5	0.28	1.14E+10	-0.484
1064.036	200483	3	294464	4	0.7	2.95E+10	-0.898
1064.413	221650	3	315599	4	-0.91	7.22E+08	-0.39
1064.796	199599	3	293514	3	-0.27	3.18E+09	0.586
1065.068	218171	1	312061	2	-0.72	1.12E+09	-0.557
1065.481	219403	3	313257	3	-0.38	2.46E+09	0.234
1065.658	218628	3	312467	4	-0.68	1.23E+09	-0.152
1065.845	197325	5	291147	5	0.39	1.44E+10	-0.88
1066.386	198179	4	291954	3	0.05	6.59E+09	-0.736
1066.433	245204	4	338975	5	-0.58	1.56E+09	0.568
1066.742	218000	5	311743	6	-0.6	1.48E+09	-0.147
1066.997	217079	3	310800	3	-0.9	7.38E+08	-0.241
1067.105	221739	2	315450	3	-0.45	2.04E+09	-0.204
1067.231	218815	5	312515	6	-0.69	1.20E+09	-0.059
1067.396	195684	1	289370	2	-0.57	1.58E+09	-0.194
1067.406	218945	4	312630	4	-0.57	1.56E+09	0.334
1068.098	217650	2	311274	2	-0.94	6.66E+08	-0.264
1068.763	217445	4	311011	3	-0.48	1.94E+09	-0.429

Table A3: Continued

Wavelength	Lower Level	J_{Low}	Upper level	J_{Up}	log gf	gA	CF
1068.88	217621	3	311177	4	0.13	7.97E+09	0.625
1068.937	224959	6	318510	7	-0.95	6.53E+08	-0.014
1069.268	218945	4	312467	4	0.03	6.21E+09	-0.331
1069.353	222398	4	315912	3	-0.8	9.14E+08	0.184
1069.495	213665	3	307167	2	-0.97	6.24E+08	-0.355
1069.742	195086	2	288566	3	-0.5	1.84E+09	-0.136
1069.976	229064	4	322524	5	0.12	7.60E+09	-0.518
1070.012	194132	3	287589	4	-0.25	3.28E+09	-0.179
1070.039	218628	3	312083	3	-0.38	2.43E+09	-0.305
1070.317	218631	1	312061	2	0.02	6.13E+09	-0.634
1070.401	199599	3	293022	2	0.08	7.01E+09	-0.852
1070.988	193948	6	287320	5	-0.16	4.06E+09	-0.799
1071.11	217650	2	311011	3	-0.17	3.93E+09	0.51
1071.132	225387	4	318746	5	-0.77	1.01E+09	-0.74
1071.173	217445	4	310800	3	-0.42	2.22E+09	-0.222
1071.377	221650	3	314988	4	-0.39	2.34E+09	0.363
1071.865	200720	2	294015	1	-0.16	4.05E+09	-0.881
1072.347	229064	4	322317	5	0.35	1.29E+10	-0.881
1072.384	194339	5	287589	4	-0.91	7.28E+08	-0.113
1072.528	199202	4	292440	4	-0.5	1.84E+09	-0.33
1073.148	218815	5	311998	5	-0.92	7.06E+08	0.065
1073.22	218000	5	311177	4	-0.85	8.10E+08	-0.642
1073.53	217650	2	310800	3	-0.98	6.07E+08	0.415
1073.631	227993	6	321135	7	0.72	3.01E+10	-0.916
1073.679	218945	4	312083	3	-0.79	9.42E+08	0.312
1073.879	197325	5	290445	6	-0.42	2.22E+09	-0.06
1073.889	198179	4	291299	3	-0.95	6.50E+08	-0.272
1074.178	199202	4	292297	4	0.06	6.64E+09	-0.447
1074.548	228480	5	321542	6	0.62	2.38E+10	-0.908
1074.706	151623	6	244671	5	-0.81	9.00E+08	0.439
1074.813	218138	3	311177	4	0.41	1.48E+10	-0.807
1074.912	200483	3	293514	3	0.07	6.78E+09	-0.639
1075.263	218726	2	311727	1	-0.43	2.19E+09	-0.671
1075.463	218028	2	311011	3	-0.14	4.16E+09	0.535
1075.495	194339	5	287320	5	-0.79	9.32E+08	-0.105
1075.511	220316	2	313295	2	-0.7	1.16E+09	0.186
1075.638	198179	4	291147	5	0.5	1.81E+10	-0.751
1076.202	230236	4	323155	4	-0.77	9.84E+08	-0.565
1076.738	218138	3	311011	3	-0.33	2.70E+09	0.735
1077.108	199599	3	292440	4	-0.89	7.43E+08	-0.113
1077.305	230331	3	323155	4	0.48	1.73E+10	0.862
1077.662	200720	2	293514	3	0.23	9.72E+09	-0.625
1078.211	120919	4	213665	3	-0.96	6.28E+08	0.441
1078.773	199599	3	292297	4	0.34	1.26E+10	-0.659
1078.984	219403	3	312083	3	-0.03	5.34E+09	-0.646
1079.377	218628	3	311274	2	-0.53	1.72E+09	-0.727
1079.414	218631	1	311274	2	-0.25	3.26E+09	-0.453
1079.821	227993	6	320601	6	0.51	1.84E+10	-0.799
1080.097	228480	5	321064	5	0.43	1.53E+10	-0.752
1080.279	223623	3	316192	2	-0.83	8.60E+08	0.179
1080.509	218628	3	311177	4	-0.74	1.04E+09	-0.55
1080.523	218726	2	311274	2	-0.68	1.21E+09	-0.697
1081.928	223764	1	316192	2	-0.71	1.11E+09	0.361
1082.454	218628	3	311011	3	-0.68	1.21E+09	-0.254
1082.754	229694	2	322051	3	-0.38	2.40E+09	-0.389
1082.777	199599	3	291954	3	-0.89	7.41E+08	0.125
1083.563	230236	4	322524	5	-0.06	4.98E+09	-0.709
1083.589	220316	2	312602	2	-0.22	3.44E+09	-0.589
1084.678	200720	2	292913	3	-0.51	1.77E+09	0.778
1085.99	223764	1	315846	2	-0.94	6.45E+08	0.276
1085.994	230236	4	322317	5	-0.93	6.65E+08	0.123
1086.564	227960	2	319993	3	-0.26	3.06E+09	0.47
1089.142	230236	4	322051	3	-0.83	8.31E+08	0.632
1089.196	201211	3	293022	2	-0.43	2.10E+09	0.271
1090.272	230331	3	322051	3	-0.17	3.80E+09	-0.611
1091.052	202361	2	294015	1	-0.54	1.63E+09	0.403
1091.608	219403	3	311011	3	-0.75	9.88E+08	-0.21
1093.896	228480	5	319896	4	-0.09	4.51E+09	-0.675
1093.959	220316	2	311727	1	-0.7	1.12E+09	0.584
1094.122	219403	3	310800	3	-0.9	7.06E+08	0.463
1094.167	198179	4	289573	5	-0.3	2.77E+09	-0.289
1094.746	225387	4	316732	4	-0.92	6.89E+08	-0.223
1094.824	242530	3	333869	4	-0.61	1.37E+09	-0.879
1095.042	233299	5	324619	5	-0.43	2.03E+09	-0.655
1096.995	225859	3	317017	3	-0.83	8.28E+08	0.141
1097.611	228480	5	319587	4	0	5.56E+09	-0.771
1099.404	220316	2	311274	2	-0.74	1.01E+09	-0.456
1099.457	199599	3	290553	4	-0.77	9.40E+08	-0.215
1099.763	229064	4	319993	3	-0.78	9.14E+08	-0.786
1100.403	203140	1	294015	1	-0.19	3.53E+09	-0.582
1100.981	230236	4	321064	5	-0.68	1.15E+09	-0.561
1101.085	233299	5	324118	6	0.33	1.15E+10	-0.838
1101.147	216703	2	307517	3	-0.49	1.76E+09	-0.509
1101.893	227993	6	318746	5	0.38	1.31E+10	-0.889
1102.013	201211	3	291954	3	0.28	1.04E+10	-0.733
1102.205	152302	5	243029	4	-0.94	6.32E+08	0.45
1102.332	230236	4	320953	4	-1	5.41E+08	0.33
1103.009	202361	2	293022	2	-0.04	5.06E+09	-0.469
1103.49	230331	3	320953	4	-0.02	5.28E+09	-0.239
1104.767	227993	6	318510	7	-0.87	7.36E+08	-0.536
1105.507	233299	5	323755	6	0.32	1.13E+10	-0.824
1105.521	221272	1	311727	1	-0.74	1.01E+09	-0.356
1106.88	221739	2	312083	3	-0.86	7.43E+08	0.31
1107.438	229694	2	319993	3	-0.86	7.45E+08	-0.151
1107.67	216703	2	306983	1	-0.75	9.69E+08	0.548
1107.832	228480	5	318746	5	-0.88	7.17E+08	-0.298
1107.863	213535	2	303798	3	-0.81	8.45E+08	-0.856
1107.91	220917	5	311177	4	-0.75	9.55E+08	-0.632
1108.593	229064	4	319268	3	-0.65	1.20E+09	0.585
1110.028	201211	3	291299	3	-0.79	8.71E+08	-0.296
1112.394	217621	3	307517	3	-0.05	4.82E+09	-0.759
1112.567	203140	1	293022	2	-0.95	6.08E+08	-0.24
1112.747	217650	2	307517	3	-0.59	1.39E+09	-0.28
1112.883	233299	5	323155	4	-0.97	5.78E+08	-0.702
1113.266	243029	4	332855	5	-0.81	8.41E+08	-0.756
1114.122	230236	4	319993	3	-0.1	4.25E+09	0.787

Table A3: Continued

Wavelength	Lower Level	J_{Low}	Upper level	J_{Up}	log gf	gA	CF
1115.148	201211	3	290885	3	-0.8	8.53E+08	0.377
1116.155	202361	2	291954	3	-0.98	5.64E+08	-0.195
1116.746	217621	3	307167	2	-0.5	1.70E+09	0.524
1116.981	221650	3	311177	4	-0.9	6.62E+08	0.276
1118.822	218138	3	307517	3	-0.31	2.61E+09	-0.69
1119.408	217650	2	306983	1	-0.66	1.17E+09	0.375
1119.425	153198	4	242530	3	-0.89	6.80E+08	0.5
1119.971	226558	1	315846	2	-0.96	5.62E+08	0.22
1120.757	233299	5	322524	5	0.29	1.05E+10	-0.682
1122.87	227960	2	317017	3	-0.77	8.96E+08	0.184
1123.185	230236	4	319268	3	0.14	7.19E+09	-0.809
1123.224	218138	3	307167	2	-0.6	1.33E+09	0.725
1123.358	233299	5	322317	5	0.24	9.24E+09	0.761
1123.376	213665	3	302682	4	-0.71	1.05E+09	-0.846
1123.642	218171	1	307167	2	-0.5	1.69E+09	-0.53
1124.388	230331	3	319268	3	-0.87	7.07E+08	-0.446
1125.977	218171	1	306983	1	-1	5.23E+08	0.478
1133.228	233299	5	321542	6	-0.72	9.93E+08	-0.14
1137.831	227960	2	315846	2	-0.79	8.20E+08	-0.386
1139.401	233299	5	321064	5	-0.53	1.51E+09	-0.215
1139.406	244671	5	332436	6	-0.55	1.46E+09	-0.889
1141.884	230236	4	317811	3	-0.82	7.64E+08	-0.631
1143.126	230331	3	317811	3	-0.79	8.35E+08	-0.313
1145.301	214319	4	301632	5	-0.6	1.28E+09	-0.887
1145.701	244753	4	332036	4	-0.92	6.17E+08	0.48
1151.654	245204	4	332036	4	-0.51	1.56E+09	-0.542
1154.043	242530	3	329182	2	-0.91	6.18E+08	-0.4
1159.775	225859	3	312083	3	-0.86	6.83E+08	0.351
1166.982	243029	4	328720	3	-0.92	5.93E+08	-0.396
1169.387	230331	3	315846	2	-0.76	8.31E+08	0.309
1190.104	230236	4	314262	5	-0.11	3.61E+09	0.781
1204.567	230236	4	313253	5	-0.81	7.13E+08	0.398
1209.405	244671	5	327357	4	-0.78	7.58E+08	-0.449
1215.068	233299	5	315599	4	-0.53	1.33E+09	-0.581
1216.847	230236	4	312416	5	-0.69	9.12E+08	-0.507
1223.221	230331	3	312083	3	-0.82	6.79E+08	0.306
1227.44	148861	4	230331	3	-0.56	1.20E+09	-0.574
1228.304	250623	3	332036	4	-0.42	1.68E+09	-0.502
1228.876	148861	4	230236	4	-0.19	2.85E+09	0.613
1237.768	148904	2	229694	2	-0.76	7.49E+08	-0.316
1250.466	197139	2	277109	3	-0.66	9.36E+08	0.642
1258.666	197660	3	277109	3	0.2	6.59E+09	-0.703
1258.97	243725	3	323155	4	-0.98	4.44E+08	0.353
1259.049	152400	1	231825	0	-0.88	5.43E+08	0.46
1259.328	197139	2	276546	2	-0.82	6.41E+08	-0.369
1263.954	196854	1	275970	2	-0.61	1.03E+09	0.762
1264.928	148904	2	227960	2	-0.7	8.13E+08	0.538
1268.524	197139	2	275970	2	-0.1	3.26E+09	-0.636
1268.723	196854	1	275673	1	-0.23	2.46E+09	-0.745
1271.808	147930	1	226558	1	-1	4.18E+08	-0.246
1273.327	197139	2	275673	1	-0.85	5.81E+08	-0.448
1274.493	213535	2	291997	2	-0.92	4.95E+08	-0.425
1274.822	139695	3	218138	3	-0.24	2.35E+09	-0.749
1276.963	197660	3	275970	2	-0.92	4.91E+08	-0.401
1277.857	148904	2	227160	1	-0.65	9.09E+08	0.403
1280.328	140066	2	218171	1	-0.44	1.46E+09	-0.607
1280.871	140066	2	218138	3	-0.85	5.77E+08	0.245
1282.803	139695	3	217650	2	-0.75	7.29E+08	-0.277
1283.272	139695	3	217621	3	-0.43	1.51E+09	-0.258
1283.517	218000	5	295910	4	-0.99	4.14E+08	0.523
1284.677	153376	2	231216	1	-0.4	1.63E+09	0.536
1289.401	140066	2	217621	3	-0.06	3.45E+09	0.757
1290.947	152232	3	229694	2	-0.32	1.93E+09	0.711
1291.061	140715	1	218171	1	-0.77	6.73E+08	0.667
1294.121	121930	3	199202	4	-0.89	5.09E+08	-0.356
1296.872	213665	3	290774	2	-0.76	6.97E+08	-0.51
1298.066	153198	4	230236	4	-0.87	5.30E+08	-0.74
1298.573	139695	3	216703	2	-0.74	7.36E+08	-0.548
1298.732	148861	4	225859	3	-0.98	4.16E+08	-0.436
1299.805	140715	1	217650	2	-0.3	1.99E+09	0.646
1300.546	149667	1	226558	1	-0.84	5.74E+08	-0.328
1301.407	156459	5	233299	5	0.46	1.14E+10	-0.76
1308.793	120919	4	197325	5	-0.49	1.26E+09	-0.408
1309.406	151623	6	227993	6	0.51	1.26E+10	-0.758
1309.783	155477	1	231825	0	-0.89	4.97E+08	-0.662
1310.298	153376	2	229694	2	-0.91	4.83E+08	-0.258
1312.715	152302	5	228480	5	0.44	1.07E+10	-0.759
1315.999	140715	1	216703	2	-0.49	1.27E+09	0.774
1318.117	153198	4	229064	4	0.35	8.62E+09	-0.808
1319.171	197139	2	272944	3	-0.87	5.15E+08	-0.825
1319.409	174831	3	250623	3	0.26	7.04E+09	-0.798
1320.313	155477	1	231216	1	-0.5	1.21E+09	0.736
1320.519	152232	3	227960	2	-0.6	9.68E+08	-0.499
1321.152	152302	5	227993	6	-0.61	9.50E+08	0.734
1327.619	214319	4	289642	4	-0.91	4.74E+08	-0.396
1328.348	153198	4	228480	5	-0.72	7.28E+08	0.739
1329.593	214319	4	289530	3	-0.61	9.44E+08	-0.631
1333.451	220917	5	295910	4	-0.75	6.62E+08	0.501
1335.012	157536	2	232442	1	-0.11	2.93E+09	0.842
1335.533	170067	2	244943	1	-0.12	2.82E+09	0.832
1337.125	218726	2	293514	3	-1	3.73E+08	-0.555
1337.347	201771	2	276546	2	0.05	4.25E+09	-0.798
1337.624	152400	1	227160	1	-0.96	4.06E+08	0.262
1340.062	139695	3	214319	4	0.35	8.22E+09	0.858
1340.747	170619	4	245204	4	-0.12	2.84E+09	-0.814
1341.65	170278	3	244813	2	-0.02	3.54E+09	0.741
1342.019	222398	4	296912	3	-0.84	5.36E+08	0.438
1342.725	170278	3	244753	4	0.12	4.92E+09	0.838
1344.025	149667	1	224071	2	-0.69	7.42E+08	0.239
1344.979	170067	2	244417	3	-0.33	1.71E+09	0.825
1345.616	119632	5	193948	6	0.56	1.32E+10	0.893
1347.391	155477	1	229694	2	-0.83	5.35E+08	-0.654
1347.722	201771	2	275970	2	-0.79	6.04E+08	0.435
1347.785	144749	4	218945	4	0.07	4.28E+09	-0.464
1348.81	170278	3	244417	3	0	3.68E+09	-0.568
1348.907	170619	4	244753	4	-0.26	2.03E+09	-0.336

Table A3: Continued

Wavelength	Lower Level	J_{Low}	Upper level	J_{Up}	log gf	gA	CF
1349.593	148904	2	223000	3	-0.57	9.69E+08	-0.385
1350.156	144749	4	218815	5	-0.31	1.81E+09	-0.29
1350.395	170619	4	244671	5	0.45	1.02E+10	0.852
1351.258	170067	2	244072	2	-0.04	3.34E+09	-0.844
1351.907	139695	3	213665	3	-0.08	3.00E+09	0.833
1352.565	144066	5	218000	5	0.34	7.99E+09	-0.749
1352.605	223623	3	297554	2	-0.98	3.83E+08	0.421
1352.935	147737	2	221650	3	-0.18	2.41E+09	-0.856
1353.565	144749	4	218628	3	-0.97	3.86E+08	0.151
1353.709	152400	1	226271	2	-0.45	1.29E+09	0.335
1354.294	139695	3	213535	2	-0.8	5.77E+08	0.807
1354.595	145580	3	219403	3	-0.11	2.83E+09	0.837
1355.048	170619	4	244417	3	-0.48	1.20E+09	0.231
1355.309	153376	2	227160	1	-0.99	3.80E+08	-0.574
1355.432	156459	5	230236	4	0.22	5.99E+09	0.815
1356.882	140715	1	214413	1	-0.6	9.20E+08	0.65
1357.611	170067	2	243725	3	-0.56	9.95E+08	-0.586
1358.71	140066	2	213665	3	-0.11	2.80E+09	0.49
1359.897	147737	2	221272	1	-0.72	6.93E+08	-0.436
1361.122	140066	2	213535	2	-0.12	2.70E+09	0.837
1361.515	170278	3	243725	3	-0.93	4.23E+08	0.077
1362.019	120919	4	194339	5	0.43	9.69E+09	0.895
1362.793	144066	5	217445	4	-0.42	1.37E+09	0.374
1363.05	145580	3	218945	4	-0.26	1.96E+09	0.863
1364.355	140066	2	213360	1	-0.47	1.21E+09	0.793
1365.178	144749	4	218000	5	-0.35	1.62E+09	0.853
1365.801	140715	1	213932	0	-0.63	8.33E+08	0.838
1365.865	120919	4	194132	3	-0.38	1.48E+09	0.214
1366.451	153376	2	226558	1	-0.88	4.78E+08	0.328
1366.94	121930	3	195086	2	-0.47	1.21E+09	0.262
1366.957	152232	3	225387	4	0.38	8.64E+09	0.889
1367.123	145580	3	218726	2	0.11	4.59E+09	0.879
1367.519	121930	3	195055	4	0.36	8.16E+09	0.894
1367.607	119632	5	192753	4	-0.32	1.71E+09	0.212
1367.871	170619	4	243725	3	0.12	4.65E+09	0.803
1368.961	145580	3	218628	3	0	3.60E+09	-0.853
1369.154	148234	0	221272	1	-0.73	6.63E+08	0.393
1369.478	122664	2	195684	1	-0.5	1.13E+09	0.43
1371.078	149667	1	222603	2	-0.67	7.65E+08	-0.287
1372.113	122664	2	195544	3	0.25	6.32E+09	0.894
1372.352	128343	4	201211	3	0.12	4.70E+09	0.627
1373.259	140715	1	213535	2	-0.63	8.23E+08	0.328
1373.721	157536	2	230331	3	0.18	5.30E+09	0.846
1373.774	123140	1	195932	0	-0.62	8.58E+08	0.86
1374.548	170278	3	243029	4	-0.05	3.18E+09	0.396
1374.638	148904	2	221650	3	-0.01	3.46E+09	0.587
1375.599	144749	4	217445	4	-0.15	2.49E+09	-0.85
1375.758	123140	1	195827	2	0.1	4.44E+09	0.893
1376.322	152302	5	224959	6	-0.24	2.04E+09	-0.323
1376.55	140715	1	213360	1	-0.6	8.81E+08	0.375
1377.79	197660	3	270240	4	0.37	8.31E+09	0.858
1377.809	147737	2	220316	2	-0.08	2.94E+09	-0.76
1378.464	123140	1	195684	1	-0.38	1.47E+09	-0.872
1379.63	153376	2	225859	3	0.21	5.70E+09	0.87
1379.638	155477	1	227960	2	-0.61	8.48E+08	-0.483
1380.009	170067	2	242530	3	-0.02	3.39E+09	0.498
1380.794	122664	2	195086	2	-0.04	3.16E+09	-0.87
1381.027	170619	4	243029	4	0	3.50E+09	0.851
1381.486	147930	1	220316	2	-0.87	4.67E+08	0.177
1382.548	144749	4	217079	3	0.21	5.70E+09	0.838
1383.12	130060	3	202361	2	-0.02	3.36E+09	0.671
1384.043	170278	3	242530	3	-0.17	2.34E+09	0.812
1384.992	121930	3	194132	3	0.13	4.68E+09	-0.872
1385.846	157536	2	229694	2	-0.48	1.15E+09	-0.524
1387.515	149667	1	221739	2	-0.08	2.85E+09	-0.857
1388.785	144066	5	216071	6	0.55	1.21E+10	0.906
1390.094	147930	1	219867	0	-0.9	4.47E+08	-0.447
1390.416	131219	2	203140	1	-0.13	2.59E+09	0.851
1392.003	152232	3	224071	2	-0.98	3.64E+08	-0.789
1392.097	120919	4	192753	4	0.26	6.23E+09	-0.88
1392.412	197139	2	268956	3	0.17	5.08E+09	0.767
1392.983	170067	2	241855	2	-0.54	9.83E+08	-0.478
1395.033	155477	1	227160	1	-0.83	5.04E+08	0.488
1395.276	152400	1	224071	2	-0.57	9.08E+08	-0.246
1395.323	144066	5	215734	4	-0.89	4.38E+08	-0.407
1396.562	149667	1	221272	1	-0.59	8.66E+08	0.672
1397.093	170278	3	241855	2	-0.55	9.54E+08	-0.826
1400.325	148904	2	220316	2	-0.95	3.77E+08	-0.218
1401.269	152400	1	223764	1	-0.33	1.59E+09	-0.71
1402.587	197660	3	268956	3	-0.6	8.58E+08	0.833
1403.4	128343	4	199599	3	-0.33	1.58E+09	-0.869
1405.033	201771	2	272944	3	0.24	5.82E+09	0.83
1405.432	196854	1	268006	2	0.01	3.49E+09	0.816
1405.47	130060	3	201211	3	-0.39	1.38E+09	-0.709
1405.639	131219	2	202361	2	-0.54	9.90E+08	-0.832
1406.84	155477	1	226558	1	-0.57	9.07E+08	-0.411
1407.125	144066	5	215133	4	0.23	5.72E+09	0.876
1407.596	151623	6	222666	7	0.61	1.38E+10	0.919
1408.75	144749	4	215734	4	-0.5	1.06E+09	0.584
1410.016	119632	5	190554	4	0.24	5.76E+09	-0.875
1410.531	119632	5	190528	5	0.47	9.76E+09	-0.909
1411.084	197139	2	268006	2	-0.64	7.61E+08	0.795
1411.57	120919	4	191762	3	0.11	4.35E+09	-0.874
1412.206	121930	3	192741	2	-0.06	2.91E+09	-0.874
1412.537	155477	1	226271	2	-0.11	2.56E+09	-0.878
1413.016	122664	2	193434	1	-0.36	1.45E+09	-0.879
1413.04	144066	5	214835	5	-0.17	2.25E+09	0.855
1413.062	152232	3	223000	3	0.17	4.86E+09	-0.858
1414.401	147930	1	218631	1	-0.58	8.75E+08	0.5
1414.529	153376	2	224071	2	-0.28	1.77E+09	-0.664
1415.234	130060	3	200720	2	-0.52	1.01E+09	-0.871
1416.804	201771	2	272352	1	-0.13	2.45E+09	0.822
1417.595	148861	4	219403	3	-0.09	2.68E+09	0.736
1419.767	147737	2	218171	1	-0.89	4.25E+08	-0.413
1419.954	153198	4	223623	3	0.21	5.33E+09	0.899
1419.983	157536	2	227960	2	-0.28	1.72E+09	-0.649

Table A3: Continued

Wavelength	Lower Level	J_{Low}	Upper level	J_{Up}	log gf	gA	CF
1420.434	147737	2	218138	3	-0.24	1.90E+09	0.491
1420.509	148234	0	218631	1	-0.52	9.87E+08	0.505
1420.781	144749	4	215133	4	-0.69	6.69E+08	0.189
1421	174831	3	245204	4	0.2	5.31E+09	0.9
1422.584	123140	1	193434	1	-0.44	1.20E+09	-0.483
1423.98	152302	5	222527	5	-0.75	5.92E+08	0.712
1424.455	152400	1	222603	2	-0.56	9.12E+08	0.355
1425.435	145580	3	215734	4	0.23	5.62E+09	0.761
1426.58	147930	1	218028	2	-0.5	1.02E+09	-0.374
1426.615	152302	5	222398	4	0.33	7.01E+09	0.873
1426.812	144749	4	214835	5	0.3	6.52E+09	0.684
1426.857	148861	4	218945	4	-0.26	1.79E+09	0.773
1426.998	122664	2	192741	2	-0.41	1.27E+09	-0.316
1428.949	174831	3	244813	2	-0.68	6.88E+08	0.876
1429.002	151623	6	221602	6	-0.6	8.12E+08	0.857
1429.515	148861	4	218815	5	0.37	7.64E+09	0.908
1430.169	174831	3	244753	4	-0.34	1.51E+09	-0.566
1430.175	196854	1	266775	0	-0.56	8.87E+08	0.891
1430.349	147737	2	217650	2	-0.53	9.71E+08	-0.722
1430.932	147737	2	217621	3	-0.31	1.59E+09	-0.594
1431.928	128343	4	198179	4	0.35	7.32E+09	-0.866
1432.008	121930	3	191762	3	-0.32	1.56E+09	-0.26
1433.336	148861	4	218628	3	-0.28	1.71E+09	0.585
1434.313	147930	1	217650	2	-0.56	8.85E+08	-0.464
1436.062	120919	4	190554	4	-0.25	1.83E+09	-0.259
1436.629	196854	1	266461	1	-0.82	4.92E+08	-0.532
1437.755	145580	3	215133	4	-0.91	3.96E+08	0.313
1438.052	130060	3	199599	3	0.11	4.15E+09	-0.652
1438.82	131219	2	200720	2	-0.02	3.07E+09	-0.696
1440.542	152232	3	221650	3	-0.68	6.88E+08	-0.342
1442.204	152400	1	221739	2	-0.62	7.73E+08	-0.27
1442.394	153198	4	222527	5	0.43	8.67E+09	0.86
1442.535	197139	2	266461	1	-0.18	2.10E+09	0.886
1443.004	152302	5	221602	6	0.43	8.58E+09	0.833
1443.12	151623	6	220917	5	0.44	8.78E+09	0.899
1443.751	131219	2	200483	3	0.23	5.44E+09	0.88
1444.246	174831	3	244072	2	-0.42	1.24E+09	-0.792
1444.377	148904	2	218138	3	-0.42	1.20E+09	0.506
1444.527	153376	2	222603	2	-0.28	1.70E+09	-0.555
1446.299	130060	3	199202	4	0.34	7.01E+09	0.897
1446.366	148861	4	218000	5	-0.49	1.04E+09	0.475
1446.678	148904	2	218028	2	-0.23	1.87E+09	-0.604
1448.058	197139	2	266197	2	-0.83	4.67E+08	-0.462
1449.66	128343	4	197325	5	0.4	7.98E+09	0.897
1454.057	147930	1	216703	2	-0.47	1.07E+09	0.633
1454.859	157536	2	226271	2	-0.81	4.88E+08	0.37
1458.068	148861	4	217445	4	-0.08	2.61E+09	-0.528
1459.066	197660	3	266197	2	0.08	3.72E+09	0.887
1459.845	156459	5	224959	6	0.46	9.07E+09	0.923
1459.873	147930	1	216429	0	-0.96	3.44E+08	-0.869
1462.615	155477	1	223847	0	-0.91	3.93E+08	0.766
1466.153	148904	2	217109	1	-0.48	1.03E+09	-0.645
1466.327	174831	3	243029	4	-0.49	1.02E+09	0.78
1468.776	152232	3	220316	2	-0.92	3.72E+08	-0.602
1474.941	148904	2	216703	2	-0.91	3.82E+08	-0.168
1482.753	149667	1	217109	1	-0.79	4.94E+08	-0.42
1492.012	174831	3	241855	2	-0.16	2.10E+09	0.769
1495.367	148861	4	215734	4	-0.78	4.98E+08	-0.67
1497.865	149667	1	216429	0	-0.82	4.50E+08	-0.563
1499.772	147737	2	214413	1	-0.52	8.92E+08	0.637
1502.98	157536	2	224071	2	-0.89	3.82E+08	0.73
1508.931	148861	4	215133	4	-0.85	4.09E+08	0.297
1515.248	128343	4	194339	5	-0.53	8.49E+08	0.431
1515.735	148861	4	214835	5	-0.66	6.28E+08	0.183
1535.087	156459	5	221602	6	-0.29	1.45E+09	0.329
1538.589	130060	3	195055	4	-0.92	3.39E+08	0.38
1551.08	152232	3	216703	2	-0.8	4.48E+08	-0.811
1557.574	157536	2	221739	2	-0.94	3.18E+08	0.36
1558.273	139695	3	203869	2	-0.14	2.01E+09	0.926
1567.32	140066	2	203869	2	-0.39	1.13E+09	-0.792
1583.433	140715	1	203869	2	-0.69	5.45E+08	0.566
1600.356	156459	5	218945	4	-0.89	3.34E+08	-0.617
1616.381	157536	2	219403	3	-0.81	3.98E+08	0.613
1636.878	157536	2	218628	3	-0.98	2.61E+08	0.63
1639.723	156459	5	217445	4	-0.38	1.03E+09	0.737
1867.187	170067	2	223623	3	-0.98	2.02E+08	-0.681
1884.748	139695	3	192753	4	-0.99	1.94E+08	-0.864
1918.649	170278	3	222398	4	-0.89	2.34E+08	-0.753
1988.151	170619	4	220917	5	-0.81	2.61E+08	-0.83

Cu V

Energy Levels

Table A4: Comparison between available experimental data and calculated even energy levels (in cm^{-1}) in Cu V

E$_{exp}^{a}$	E$_{calc}^{b}$	ΔE	J	Leading components (in %) in LS coupling ^{c}
0	136	−136	4.5	99 3d^{7} ^{4}F
1615.9	1715	−99	3.5	100 3d^{7} ^{4}F
2759.3	2840	−81	2.5	99 3d^{7} ^{4}F
3528.1	3596	−68	1.5	99 3d^{7} ^{4}F
20826.8	20622	205	2.5	99 3d^{7} ^{4}P
21065.9	20952	114	1.5	91 3d^{7} ^{4}P + 8 3d^{7} ^{2}P
21935.1	21818	117	0.5	96 3d^{7} ^{4}P
22575.3	22345	230	4.5	96 3d^{7} ^{2}G
24099.8	23858	242	3.5	99 3d^{7} ^{2}G
27015.9	27397	−381	1.5	76 3d^{7} ^{2}P + 13 3d^{7} ^{2}D + 8 3d^{7} ^{4}P
28366.6	28954	−587	0.5	96 3d^{7} ^{2}P
30401.7	30561	−159	5.5	100 3d^{7} ^{2}H
30966	30512	454	2.5	77 3d^{7} ^{2}D + 22 3d^{7} ^{2}D
31823.4	31946	−123	4.5	97 3d^{7} ^{2}H
33292.4	32954	338	1.5	67 3d^{7} ^{2}D + 16 3d^{7} ^{2}D + 16 3d^{7} ^{2}P
49490	49377	113	2.5	99 3d^{7} ^{2}F
50071.9	50070	2	3.5	99 3d^{7} ^{2}F
76838.2	76962	−124	1.5	80 3d^{7} ^{2}D + 19 3d^{7} ^{2}D
77668	77725	−57	2.5	77 3d^{7} ^{2}D + 22 3d^{7} ^{2}D
187779.4	187825	−46	4.5	99 3d^{6}(5D)4s ^{6}D
188832.7	188907	−74	3.5	99 3d^{6}(5D)4s ^{6}D
189586.9	189682	−95	2.5	99 3d^{6}(5D)4s ^{6}D
190100.3	190210	−110	1.5	99 3d^{6}(5D)4s ^{6}D
190400.3	190520	−120	0.5	99 3d^{6}(5D)4s ^{6}D
199441.3	199411	30	3.5	99 3d^{6}(5D)4s ^{4}D
200648.2	200665	−17	2.5	99 3d^{6}(5D)4s ^{4}D
201412.8	201459	−46	1.5	99 3d^{6}(5D)4s ^{4}D
201849.7	201913	−63	0.5	99 3d^{6}(5D)4s ^{4}D
219203.4	219228	−25	2.5	60 3d^{6}(3P)4s ^{4}P + 39 3d^{6}(3P)4s ^{4}P
220207.8	220486	−278	6.5	99 3d^{6}(3H)4s ^{4}H
220622.8	220820	−197	5.5	96 3d^{6}(3H)4s ^{4}H
220938.1	221022	−84	4.5	84 3d^{6}(3H)4s ^{4}H + 6 3d^{6}(3F)4s ^{4}F + 6 3d^{6}(3G)4s ^{4}G
221271.9	221321	−49	3.5	89 3d^{6}(3H)4s ^{4}H
221664.1	221818	−154	1.5	56 3d^{6}(3P)4s ^{4}P + 35 3d^{6}(3P)4s ^{4}P
222401.3	222321	80	4.5	64 3d^{6}(3F)4s ^{4}F + 19 3d^{6}(3F)4s ^{4}F + 12 3d^{6}(3H)4s ^{4}H
222885.7	222810	76	3.5	69 3d^{6}(3F)4s ^{4}F + 19 3d^{6}(3F)4s ^{4}F + 7 3d^{6}(3H)4s ^{4}H
223214.2	223136	78	2.5	76 3d^{6}(3F)4s ^{4}F + 19 3d^{6}(3F)4s ^{4}F
223375.5	223571	−196	0.5	60 3d^{6}(3P)4s ^{4}P + 37 3d^{6}(3P)4s ^{4}P
223476.5	223428	49	1.5	80 3d^{6}(3F)4s ^{4}F + 19 3d^{6}(3F)4s ^{4}F
226310.8	226324	−13	5.5	67 3d^{6}(3G)4s ^{4}G + 30 3d^{6}(3H)4s ^{2}H
226888.8	227030	−141	1.5	56 3d^{6}(3P)4s ^{2}P + 35 3d^{6}(3P)4s ^{2}P + 5 3d^{6}(3P)4s ^{4}P
227542.6	227577	−34	4.5	66 3d^{6}(3G)4s ^{4}G + 25 3d^{6}(3H)4s ^{2}H + 5 3d^{6}(3F)4s ^{4}F
227800.5	228027	−227	5.5	68 3d^{6}(3H)4s ^{2}H + 29 3d^{6}(3G)4s ^{4}G
228020.3	227952	68	3.5	76 3d^{6}(3G)4s ^{4}G + 10 3d^{6}(3F)4s ^{2}F + 5 3d^{6}(3F)4s ^{4}F
228047.5	228150	−103	4.5	68 3d^{6}(3H)4s ^{2}H + 24 3d^{6}(3G)4s ^{4}G + 5 3d^{6}(3G)4s ^{2}G
228105.3	227973	132	2.5	83 3d^{6}(3G)4s ^{4}G + 10 3d^{6}(3F)4s ^{2}F
229587.5	229420	168	3.5	60 3d^{6}(3F)4s ^{2}F + 17 3d^{6}(3F)4s ^{2}F + 15 3d^{6}(3G)4s ^{4}G
229773.6	229975	−201	0.5	58 3d^{6}(3P)4s ^{2}P + 36 3d^{6}(3P)4s ^{2}P
230531.7	230526	6	2.5	70 3d^{6}(3F)4s ^{2}F + 17 3d^{6}(3F)4s ^{2}F + 13 3d^{6}(3G)4s ^{4}G
234036.4	234037	−1	4.5	94 3d^{6}(3G)4s ^{2}G
235052.5	235044	9	3.5	93 3d^{6}(3G)4s ^{2}G + 5 3d^{6}(3F)4s ^{2}F
236039.8	235553	487	1.5	98 3d^{6}(3D)4s ^{4}D
236058.9	235609	450	2.5	98 3d^{6}(3D)4s ^{4}D
236108.8	235599	510	0.5	98 3d^{6}(3D)4s ^{4}D
236331.2	235900	431	3.5	99 3d^{6}(3D)4s ^{4}D
238233.6	238377	−143	6.5	99 3d^{6}(1I)4s ^{2}I
238305.2	238426	−121	5.5	98 3d^{6}(1I)4s ^{2}I
239540.9	238438	1103	4.5	63 3d^{6}(1G)4s ^{2}G + 32 3d^{6}(1G)4s ^{2}G
239614.5	238499	1116	3.5	63 3d^{6}(1G)4s ^{2}G + 32 3d^{6}(1G)4s ^{2}G
243140.4	242661	479	2.5	97 3d^{6}(3D)4s ^{2}D
246476.5	247554	−1078	2.5	75 3d^{6}(1D)4s ^{2}D + 21 3d^{6}(1D)4s ^{2}D
246624.3	247631	−1007	1.5	74 3d^{6}(1D)4s ^{2}D + 20 3d^{6}(1D)4s ^{2}D
256272.5	256475	−203	3.5	96 3d^{6}(1F)4s ^{2}F
256272.9	256496	−223	2.5	96 3d^{6}(1F)4s ^{2}F
265691.5	265657	35	1.5	80 3d^{6}(3F)4s ^{4}F + 19 3d^{6}(3F)4s ^{4}F
265752.4	265730	22	4.5	77 3d^{6}(3F)4s ^{4}F + 22 3d^{6}(3F)4s ^{4}F
265886	265881	5	2.5	78 3d^{6}(3F)4s ^{4}F + 19 3d^{6}(3F)4s ^{4}F
265975	265980	−5	3.5	76 3d^{6}(3F)4s ^{4}F + 20 3d^{6}(3F)4s ^{4}F
272755.1	272606	149	3.5	76 3d^{6}(3F)4s ^{2}F + 21 3d^{6}(3F)4s ^{2}F
272800.8	272670	131	2.5	79 3d^{6}(3F)4s ^{2}F + 20 3d^{6}(3F)4s ^{2}F
278281.8	278581	−299	4.5	65 3d^{6}(1G)4s ^{2}G + 34 3d^{6}(1G)4s ^{2}G
278380	278641	−261	3.5	64 3d^{6}(1G)4s ^{2}G + 33 3d^{6}(1G)4s ^{2}G

a: Experimental energies from [30]
b: This work
c: Only the components $\geq$ to 5% are given

Table A5: Comparison between available experimental data and calculated odd energy levels (in cm^{-1}) in Cu V

E^a_{exp}	E^b_{calc}	ΔE	J	Leading components (in %) in LS coupling ^{c}
266226.7	266263	−36	4.5	97 $3d^6$(5D)4p ^{6}D
266560	266652	−92	3.5	94 $3d^6$(5D)4p ^{6}D
267068.8	267218	−149	2.5	96 $3d^6$(5D)4p ^{6}D
267488.7	267680	−191	1.5	98 $3d^6$(5D)4p ^{6}D
267759	267975	−216	0.5	99 $3d^6$(5D)4p ^{6}D
274003.9	273786	218	5.5	99 $3d^6$(5D)4p ^{6}F
274064.5	273895	170	4.5	92 $3d^6$(5D)4p ^{6}F + 5 $3d^6$(5D)4p ^{4}F
274073.2	273952	121	3.5	89 $3d^6$(5D)4p ^{6}F
274146.2	274061	85	2.5	92 $3d^6$(5D)4p ^{6}F
274188.5	274127	62	1.5	94 $3d^6$(5D)4p ^{6}F
274209.7	274160	50	0.5	95 $3d^6$(5D)4p ^{6}F
276368	276236	132	3.5	77 $3d^6$(5D)4p ^{6}P + 15 $3d^6$(5D)4p ^{4}D
278294.6	278210	85	2.5	79 $3d^6$(5D)4p ^{6}P + 16 $3d^6$(5D)4p ^{4}D
278663.1	278601	62	3.5	77 $3d^6$(5D)4p ^{4}D + 18 $3d^6$(5D)4p ^{6}P
279421.1	279246	175	4.5	92 $3d^6$(5D)4p ^{4}F + 6 $3d^6$(5D)4p ^{6}F
279496.8	279479	18	2.5	75 $3d^6$(5D)4p ^{4}D + 19 $3d^6$(5D)4p ^{6}P
279589.5	279530	60	1.5	84 $3d^6$(5D)4p ^{6}P + 13 $3d^6$(5D)4p ^{4}D
280065.7	280080	−14	1.5	78 $3d^6$(5D)4p ^{4}D + 14 $3d^6$(5D)4p ^{6}P
280373.3	280427	−54	0.5	91 $3d^6$(5D)4p ^{4}D
280928.7	280810	119	3.5	93 $3d^6$(5D)4p ^{4}F + 5 $3d^6$(5D)4p ^{6}F
281942.4	281852	90	2.5	95 $3d^6$(5D)4p ^{4}F
282621.5	282550	72	1.5	96 $3d^6$(5D)4p ^{4}F
284520.9	284782	−261	2.5	96 $3d^6$(5D)4p ^{4}P
285546.4	285841	−295	1.5	97 $3d^6$(5D)4p ^{4}P
286068.7	286393	−324	0.5	97 $3d^6$(5D)4p ^{4}P
300401.2	300616	−215	5.5	65 $3d^6$(3H)4p ^{4}G + 22 $3d^6$(3F)4p ^{4}G + 8 $3d^6$(3G)4p ^{4}G
300837.1	300768	69	4.5	30 $3d^6$(3H)4p ^{4}G + 25 $3d^6$(3F)4p ^{4}G + 10 $3d^6$(3G)4p ^{4}G
301080.5	301048	33	2.5	24 $3d^6$(3P)4p ^{4}P + 22 $3d^6$(3P)4p 4P + 10 $3d^6$(3P)4p ^{4}D
301255.4	301141	114	3.5	27 $3d^6$(3F)4p ^{4}G + 21 $3d^6$(3H)4p ^{4}G + 11 $3d^6$(3G)4p ^{4}G
301286.4	301317	−31	5.5	50 $3d^6$(3H)4p ^{4}I + 32 $3d^6$(3H)4p ^{4}H + 11 $3d^6$(3G)4p ^{4}H
301336.1	301490	−154	6.5	49 $3d^6$(3H)4p ^{4}I + 34 $3d^6$(3H)4p ^{4}H + 10 $3d^6$(3H)4p ^{2}I
301385.6	301509	−123	4.5	35 $3d^6$(3H)4p ^{4}I + 29 $3d^6$(3H)4p ^{4}H + 18 $3d^6$(3H)4p ^{4}G
301533.4	301520	13	2.5	43 $3d^6$(3F)4p ^{4}G + 34 $3d^6$(3H)4p ^{4}G + 7 $3d^6$(3G)4p ^{4}G
301586.7	301667	−80	3.5	26 $3d^6$(3H)4p ^{4}H + 20 $3d^6$(3H)4p ^{4}G + 17 $3d^6$(3H)4p ^{2}G
302961.2	303061	−100	0.5	44 $3d^6$(3P)4p ^{4}P + 42 $3d^6$(3P)4p ^{4}P
302980.4	302984	−4	4.5	43 $3d^6$(3H)4p ^{4}I + 16 $3d^6$(3H)4p ^{2}G + 13 $3d^6$(3H)4p ^{4}H
303209.3	303251	−42	3.5	20 $3d^6$(3H)4p ^{4}H + 17 $3d^6$(3F)4p ^{4}F
303241.7	303153	89	2.5	28 $3d^6$(3P)4p ^{2}D + 19 $3d^6$(3P)4p ^{4}P + 19 $3d^6$(3P)4p ^{2}D
303456.4	303417	39	7.5	99 $3d^6$(3H)4p ^{4}I
303479.1	303505	−26	2.5	47 $3d^6$(3F)4p ^{4}F + 16 $3d^6$(3F)4p ^{4}F + 8 $3d^6$(3D)4p ^{4}F
303679.5	303754	−75	1.5	60 $3d^6$(3F)4p ^{4}F + 20 $3d^6$(3F)4p ^{4}F + 11 $3d^6$(3D)4p ^{4}F
303734.1	303801	−67	1.5	23 $3d^6$(3P)4p ^{4}S + 21 $3d^6$(3P)4p ^{4}D + 7 $3d^6$(3P)4p ^{2}D
303931.7	304054	−122	5.5	43 $3d^6$(3H)4p ^{4}H + 42 $3d^6$(3H)4p ^{4}I + 7 $3d^6$(3G)4p ^{4}H
304062.3	304286	−224	6.5	53 $3d^6$(3H)4p ^{4}H + 34 $3d^6$(3H)4p ^{4}I + 7 $3d^6$(3G)4p ^{4}H
304092.2	304129	−37	4.5	44 $3d^6$(3F)4p ^{4}F + 17 $3d^6$(3F)4p ^{4}F + 10 $3d^6$(3H)4p ^{4}G
304199	304174	25	3.5	46 $3d^6$(3P)4p ^{4}D + 27 $3d^6$(3P)4p ^{4}D + 7 $3d^6$(3H)4p ^{4}H
304456.1	304732	−276	4.5	38 $3d^6$(3H)4p ^{2}G + 21 $3d^6$(3H)4p ^{4}H + 12 $3d^6$(3G)4p ^{2}G
304655	304739	−84	3.5	20 $3d^6$(3H)4p ^{2}G + 19 $3d^6$(3F)4p ^{4}F + 10 $3d^6$(3H)4p ^{4}G
305453.3	305657	−204	3.5	41 $3d^6$(3F)4p ^{4}D + 13 $3d^6$(3H)4p ^{2}G + 9 $3d^6$(3F)4p ^{4}D
305844.4	306031	−187	1.5	16 $3d^6$(3P)4p ^{4}P + 16 $3d^6$(3P)4p ^{4}P + 14 $3d^6$(3P)4p ^{2}D
305882.7	305838	45	6.5	79 $3d^6$(3H)4p ^{2}I + 16 $3d^6$(3H)4p ^{4}I
306115.6	306249	−133	2.5	49 $3d^6$(3F)4p ^{4}D + 10 $3d^6$(3F)4p ^{4}D + 10 $3d^6$(3D)4p ^{4}D
306678.1	306886	−208	1.5	55 $3d^6$(3F)4p ^{4}D + 11 $3d^6$(3D)4p ^{4}D + 11 $3d^6$(3F)4p ^{4}D
306892.2	306715	177	5.5	74 $3d^6$(3H)4p ^{2}I + 5 $3d^6$(3F)4p ^{4}G + 5 $3d^6$(3H)4p ^{4}I
306905.8	307159	−253	2.5	37 $3d^6$(3P)4p ^{4}D + 18 $3d^6$(3P)4p ^{4}D + 8 $3d^6$(3F)4p ^{4}D
306989.1	307210	−221	0.5	63 $3d^6$(3F)4p ^{4}D + 14 $3d^6$(3D)4p ^{4}D + 11 $3d^6$(3F)4p ^{4}D
307138.8	307406	−267	1.5	24 $3d^6$(3P)4p ^{4}D + 14 $3d^6$(3P)4p ^{2}D + 10 $3d^6$(3P)4p ^{4}D
307824.5	307669	156	4.5	28 $3d^6$(3F)4p ^{4}G + 16 $3d^6$(3H)4p ^{4}G + 13 $3d^6$(3F)4p ^{2}G
307909.5	307805	105	2.5	24 $3d^6$(3F)4p ^{2}F + 14 $3d^6$(3G)4p ^{4}G + 14 $3d^6$(3H)4p ^{4}G
307990.7	307971	20	3.5	24 $3d^6$(3F)4p ^{4}G + 17 $3d^6$(3H)4p ^{4}G + 11 $3d^6$(3F)4p ^{2}F
308064.9	308024	41	5.5	47 $3d^6$(3F)4p ^{4}G + 14 $3d^6$(3F)4p ^{4}G + 13 $3d^6$(3H)4p ^{2}I
308817.8	308845	−27	4.5	53 $3d^6$(3G)4p ^{4}F + 23 $3d^6$(3G)4p ^{4}G + 7 $3d^6$(3D)4p ^{4}F
309269.1	309498	−229	5.5	31 $3d^6$(3G)4p ^{2}H + 25 $3d^6$(3G)4p ^{4}G + 13 $3d^6$(3H)4p ^{4}H
309294.1	309129	165	3.5	22 $3d^6$(3F)4p ^{2}F + 14 $3d^6$(3H)4p ^{4}G + 12 $3d^6$(3F)4p ^{2}F
309569.9	309249	321	2.5	33 $3d^6$(3H)4p ^{4}G + 16 $3d^6$(3F)4p ^{4}G + 10 $3d^6$(3F)4p ^{4}G
309702.9	309831	−128	0.5	28 $3d^6$(3P)4p ^{2}P + 25 $3d^6$(3P)4p ^{2}P + 18 $3d^6$(3P)4p ^{2}S
309772	309710	62	4.5	26 $3d^6$(3F)4p ^{2}G + 22 $3d^6$(3G)4p ^{2}H + 13 $3d^6$(3F)4p ^{4}G
309801.3	309738	63	3.5	40 $3d^6$(3G)4p ^{4}F + 36 $3d^6$(3G)4p ^{4}G + 5 $3d^6$(3F)4p ^{4}F
310450.4	310932	−482	1.5	42 $3d^6$(3P)4p ^{2}P + 30 $3d^6$(3P)4p ^{2}P + 5 $3d^6$(3G)4p ^{4}F
310483.1	310472	11	5.5	45 $3d^6$(3G)4p ^{4}G + 17 $3d^6$(3H)4p ^{2}H + 14 $3d^6$(3H)4p ^{4}G
310753.8	310708	46	2.5	32 $3d^6$(3G)4p ^{4}F + 31 $3d^6$(3G)4p ^{4}G + 8 $3d^6$(3F)4p ^{2}F
310874.9	310872	3	4.5	21 $3d^6$(3F)4p ^{2}G + 13 $3d^6$(3H)4p ^{2}H + 5 $3d^6$(3F)4p ^{2}G
311220.3	310952	268	3.5	55 $3d^6$(3F)4p ^{2}G + 13 $3d^6$(3F)4p ^{2}G + 8 $3d^6$(3F)4p ^{4}G
311232.9	311297	−64	4.5	39 $3d^6$(3G)4p ^{4}G + 16 $3d^6$(3H)4p ^{2}H + 10 $3d^6$(3H)4p ^{4}G
311582.4	311651	−69	3.5	39 $3d^6$(3G)4p ^{4}G + 24 $3d^6$(3G)4p ^{4}F + 9 $3d^6$(3D)4p ^{4}F
311706.3	311627	79	1.5	57 $3d^6$(3G)4p ^{4}F + 17 $3d^6$(3D)4p ^{4}F + 6 $3d^6$(3P)4p ^{2}D
311837.8	311765	73	2.5	37 $3d^6$(3G)4p ^{4}G + 29 $3d^6$(3G)4p ^{4}F + 11 $3d^6$(3D)4p ^{4}F
311888.8	311877	12	6.5	82 $3d^6$(3G)4p ^{4}H + 13 $3d^6$(3H)4p ^{4}H
311982	312209	−227	0.5	49 $3d^6$(3P)4p ^{2}S + 22 $3d^6$(3P)4p ^{2}S + 9 $3d^6$(3P)4p ^{2}P
312073.1	312087	−14	3.5	64 $3d^6$(3G)4p ^{4}H + 14 $3d^6$(3H)4p ^{4}H + 7 $3d^6$(3F)4p ^{2}G
312105.5	312128	−23	5.5	66 $3d^6$(3G)4p ^{4}H + 14 $3d^6$(3H)4p ^{2}H + 7 $3d^6$(3H)4p ^{4}H
312138	312122	16	4.5	65 $3d^6$(3G)4p ^{4}H + 10 $3d^6$(3H)4p ^{4}H + 8 $3d^6$(3H)4p ^{2}H
314237.9	314264	−26	2.5	59 $3d^6$(3F)4p ^{2}D + 10 $3d^6$(3P)4p ^{2}D + 8 $3d^6$(3F)4p ^{2}D
314988	315060	−72	1.5	61 $3d^6$(3F)4p ^{2}D + 16 $3d^6$(3P)4p ^{2}D + 6 $3d^6$(3P)4p ^{2}D
316134	316427	−293	2.5	39 $3d^6$(3G)4p ^{2}F + 22 $3d^6$(3D)4p ^{2}F + 10 $3d^6$(1D)4p ^{2}F
316149.4	316217	−68	5.5	51 $3d^6$(3H)4p ^{2}H + 37 $3d^6$(3G)4p ^{2}H
316642.6	316833	−190	3.5	45 $3d^6$(3G)4p ^{2}F + 21 $3d^6$(3D)4p ^{2}F + 9 $3d^6$(3F)4p ^{2}F
317201.1	317043	158	4.5	32 $3d^6$(3G)4p ^{2}H + 31 $3d^6$(3H)4p ^{2}H + 6 $3d^6$(3G)4p ^{2}G
317240.4	317272	−32	6.5	96 $3d^6$(1I)4p ^{2}K
318923.1	318699	224	2.5	84 $3d^6$(3D)4p ^{4}P
319304.2	319143	161	3.5	61 $3d^6$(3G)4p ^{2}G + 10 $3d^6$(1G)4p ^{2}F + 7 $3d^6$(3H)4p ^{2}G

Table A5: Continued

E^a_{exp}	E^b_{calc}	ΔE	J	Leading components (in %) in LS coupling ^{c}
319404.1	319180	224	1.5	67 3d^6(3D)4p ^{4}P + 11 3d^6(3D)4p ^{2}P + 8 3d^6(3D)4p ^{4}D
319407.6	319379	29	7.5	99 3d^6(1I)4p ^{2}K
319418.8	318815	604	4.5	42 3d^6(1G)4p ^{2}H + 19 3d^6(1G)4p ^{2}H + 13 3d^6(3G)4p ^{2}H
319689	319707	−18	4.5	64 3d^6(3G)4p ^{2}G + 16 3d^6(3H)4p ^{2}G + 10 3d^6(3H)4p ^{2}H
319951.5	319765	187	5.5	42 3d^6(1I)4p ^{2}H + 32 3d^6(1G)4p ^{2}H + 9 3d^6(1G)4p ^{2}H
320216.4	320024	192	0.5	43 3d^6(3D)4p ^{4}P + 24 3d^6(3D)4p ^{4}D + 17 3d^6(3D)4p ^{2}P
320935.3	320671	264	0.5	47 3d^6(3D)4p ^{4}P + 19 3d^6(3D)4p ^{4}D + 16 3d^6(3D)4p ^{2}P
321074	320755	319	1.5	51 3d^6(3D)4p ^{4}F + 24 3d^6(3G)4p ^{4}F + 7 3d^6(3D)4p ^{4}D
321364.9	321140	225	2.5	49 3d^6(3D)4p ^{4}F + 20 3d^6(3G)4p ^{4}F + 13 3d^6(3D)4p ^{4}D
321433	320982	451	3.5	36 3d^6(1G)4p ^{2}G + 17 3d^6(1G)4p ^{2}G + 11 3d^6(3D)4p ^{4}F
321443.1	321034	409	1.5	30 3d^6(3D)4p ^{2}P + 18 3d^6(3D)4p 4P + 18 3d^6(3D)4p ^{4}D
321795.8	321587	209	3.5	26 3d^6(3D)4p ^{4}D + 16 3d^6(1G)4p ^{2}G + 11 3d^6(3H)4p ^{2}G
322192.1	321878	314	2.5	64 3d^6(3D)4p ^{4}D + 16 3d^6(3D)4p ^{4}F + 7 3d^6(3F)4p ^{4}D
322375.9	321553	823	4.5	49 3d^6(1G)4p ^{2}G + 22 3d^6(1G)4p ^{2}G + 8 3d^6(1G)4p ^{2}H
322464.1	321921	543	3.5	55 3d^6(3D)4p ^{4}F + 12 3d^6(3G)4p ^{4}F + 11 3d^6(1G)4p ^{2}F
322470	322037	433	1.5	46 3d^6(3D)4p ^{4}D + 30 3d^6(3D)4p ^{2}P + 7 3d^6(1S)4p ^{2}P
322569	322293	276	0.5	35 3d^6(3D)4p ^{4}D + 30 3d^6(3D)4p ^{2}P + 12 3d^6(1S)4p ^{2}P
322744.4	322544	200	3.5	45 3d^6(3D)4p ^{4}D + 13 3d^6(1G)4p ^{2}F + 7 3d^6(3F)4p ^{4}D
322875.8	322434	442	4.5	77 3d^6(3D)4p ^{4}F + 14 3d^6(3G)4p ^{4}F
323222.4	322958	264	2.5	34 3d^6(1G)4p ^{2}F + 16 3d^6(3G)4p ^{2}F + 16 3d^6(1G)4p ^{2}F
323506.3	322768	738	5.5	29 3d^6(1G)4p ^{2}H + 28 3d^6(1I)4p ^{2}H + 26 3d^6(1G)4p ^{2}H
323616.8	323762	−145	4.5	70 3d^6(1I)4p ^{2}H + 10 3d^6(3G)4p ^{2}H + 9 3d^6(1G)4p ^{2}H
324623.5	324849	−226	6.5	97 3d^6(1I)4p ^{2}I
324668.3	324824	−156	5.5	87 3d^6(1I)4p ^{2}I + 9 3d^6(1I)4p ^{2}H
324908.8	324866	43	1.5	70 3d^6(3D)4p ^{2}D + 8 3d^6(1D)4p ^{2}P + 6 3d^6(1F)4p ^{2}D
325518.5	325443	76	2.5	84 3d^6(3D)4p ^{2}D
325923.4	325688	235	1.5	32 3d^6(1S)4p ^{2}P + 20 3d^6(1D)4p ^{2}P + 12 3d^6(3D)4p ^{2}D
326477.1	326236	241	3.5	64 3d^6(3D)4p ^{2}F + 11 3d^6(1D)4p ^{2}F + 7 3d^6(3G)4p ^{2}F
327268	327269	−1	2.5	57 3d^6(3D)4p ^{2}F + 14 3d^6(1D)4p ^{2}F + 7 3d^6(1G)4p ^{2}F
327379.7	326541	839	0.5	40 3d^6(1S)4p ^{2}P + 25 3d^6(3D)4p ^{2}P + 12 3d^6(1S)4p ^{2}P
329339.6	329710	−370	2.5	25 3d^6(1D)4p ^{2}D + 24 3d^6(1D)4p ^{2}F + 11 3d^6(1F)4p ^{2}D
329960.8	330412	−451	1.5	50 3d^6(1D)4p ^{2}D + 12 3d^6(1F)4p ^{2}D + 10 3d^6(1D)4p ^{2}D
330765.1	331371	−606	2.5	30 3d^6(1D)4p ^{2}D + 23 3d^6(1D)4p ^{2}F + 18 3d^6(1F)4p ^{2}D
331353.6	331611	−257	0.5	58 3d^6(1D)4p ^{2}P + 22 3d^6(1D)4p ^{2}P + 9 3d^6(1S)4p ^{2}P
331435	332108	−673	3.5	54 3d^6(1D)4p ^{2}F + 14 3d^6(1D)4p ^{2}F + 9 3d^6(3G)4p ^{2}F
332946.3	332577	369	1.5	32 3d^6(1D)4p ^{2}P + 17 3d^6(1S)4p ^{2}P + 14 3d^6(1D)4p ^{2}D
335935.2	336160	−225	3.5	87 3d^6(1F)4p ^{2}G
338015.8	338917	−901	2.5	48 3d^6(1F)4p ^{2}D + 20 3d^6(1D)4p ^{2}D + 6 3d^6(1D)4p ^{2}D
338059.3	338289	−230	4.5	92 3d^6(1F)4p ^{2}G
339377.8	339843	−465	1.5	28 3d^6(3F)4p ^{4}D + 22 3d^6(3P)4p ^{4}D + 22 3d^6(1F)4p ^{2}D
339845.5	339817	29	0.5	38 3d^6(3P)4p ^{4}D + 35 3d^6(3F)4p ^{4}D + 17 3d^6(3P)4p ^{4}D
340482.7	340952	−469	1.5	53 3d^6(1F)4p ^{2}D + 13 3d^6(3P)4p ^{4}D + 10 3d^6(3F)4p ^{4}D
340722.8	340846	−123	2.5	39 3d^6(3F)4p ^{4}D + 28 3d^6(3P)4p ^{4}D + 13 3d^6(3P)4p ^{4}D
340819.5	340897	−78	3.5	52 3d^6(3F)4p ^{4}D + 22 3d^6(3P)4p ^{4}D + 11 3d^6(3F)4p ^{4}D
343301.1	343466	−165	2.5	80 3d^6(1F)4p ^{2}F + 5 3d^6(1F)4p ^{2}D + 5 3d^6(1G)4p ^{2}F
343337.2	343465	−128	3.5	81 3d^6(1F)4p ^{2}F + 5 3d^6(1G)4p ^{2}F
347219	346993	226	2.5	76 3d^6(3F)4p ^{4}G + 17 3d^6(3F)4p ^{4}G
347793.1	347578	215	3.5	75 3d^6(3F)4p ^{4}G + 17 3d^6(3F)4p ^{4}G
348323.7	348098	226	4.5	71 3d^6(3F)4p ^{4}G + 17 3d^6(3F)4p ^{4}G
349167.6	348848	320	5.5	77 3d^6(3F)4p ^{4}G + 20 3d^6(3F)4p ^{4}G
349300.5	349038	263	1.5	72 3d^6(3P)4p ^{4}S + 25 3d^6(3P)4p ^{4}S
351430.8	351331	100	1.5	49 3d^6(3F)4p ^{2}D + 22 3d^6(3P)4p ^{2}D + 9 3d^6(3P)4p ^{2}D
351671.9	351981	−309	0.5	46 3d^6(3P)4p ^{4}P + 39 3d^6(3P)4p ^{4}P + 7 3d^6(3P)4p ^{2}S
352004.5	352402	−398	1.5	47 3d^6(3P)4p ^{4}P + 40 3d^6(3P)4p ^{4}P
352419.2	352501	−82	2.5	45 3d^6(3F)4p ^{2}D + 21 3d^6(3P)4p ^{2}D + 11 3d^6(3P)4p ^{2}D
352582.3	352325	257	4.5	63 3d^6(3F)4p ^{2}G + 16 3d^6(3F)4p ^{2}G
353485.7	353743	−257	2.5	24 3d^6(3P)4p ^{4}P + 20 3d^6(3P)4p ^{4}P + 12 3d^6(3P)4p ^{4}D
353590	353445	145	0.5	45 3d^6(3F)4p ^{4}D + 22 3d^6(3P)4p ^{4}D + 15 3d^6(3P)4p ^{4}D
353645.9	353464	182	3.5	65 3d^6(3F)4p ^{2}G + 15 3d^6(3F)4p ^{2}G + 8 3d^6(3F)4p ^{4}F
354039.3	353996	43	1.5	29 3d^6(3F)4p ^{4}D + 19 3d^6(3P)4p ^{4}D + 13 3d^6(3P)4p ^{4}D
354548	354714	−166	2.5	24 3d^6(3F)4p ^{4}F + 22 3d^6(3P)4p ^{4}P + 19 3d^6(3P)4p 4P
354796.7	354750	47	1.5	51 3d^6(3F)4p ^{4}F + 17 3d^6(3F)4p ^{4}F + 9 3d^6(3F)4p ^{4}D
354905.2	354857	48	3.5	39 3d^6(3F)4p ^{4}F + 15 3d^6(3F)4p ^{4}F + 15 3d^6(3P)4p ^{4}D
355606	355610	−4	2.5	34 3d^6(3F)4p ^{4}F + 20 3d^6(3F)4p ^{4}D + 14 3d^6(3P)4p ^{4}D
355875	355799	76	4.5	64 3d^6(3F)4p ^{4}F + 25 3d^6(3F)4p ^{4}F + 8 3d^6(3F)4p ^{2}G
356372.1	356428	−56	3.5	23 3d^6(3P)4p ^{4}D + 23 3d^6(3F)4p ^{4}F + 20 3d^6(3F)4p ^{4}D
356661.9	356858	−196	1.5	26 3d^6(3F)4p ^{2}D + 21 3d^6(3P)4p ^{2}D + 17 3d^6(3P)4p ^{2}D
357881	358177	−296	0.5	52 3d^6(3P)4p ^{2}P + 36 3d^6(3P)4p ^{2}P
357948.3	358385	−437	2.5	33 3d^6(3P)4p ^{2}D + 26 3d^6(3P)4p ^{2}D + 24 3d^6(3F)4p ^{2}D
358724.8	359025	−300	3.5	51 3d^6(3F)4p ^{2}F + 22 3d^6(3F)4p ^{2}F + 14 3d^6(1G)4p ^{2}F
359141.2	359648	−507	1.5	42 3d^6(3P)4p ^{2}P + 30 3d^6(3P)4p ^{2}P + 8 3d^6(3P)4p ^{2}D
359491.9	359658	−166	2.5	66 3d^6(3F)4p ^{2}F + 25 3d^6(3F)4p ^{2}F
360058.2	360296	−238	4.5	57 3d^6(1G)4p ^{2}H + 34 3d^6(1G)4p ^{2}H
362142.8	362451	−308	3.5	26 3d^6(1G)4p ^{2}G + 25 3d^6(1G)4p ^{2}F + 12 3d^6(1G)4p ^{2}F
362144.7	362340	−195	5.5	61 3d^6(1G)4p ^{2}H + 36 3d^6(1G)4p ^{2}H
363396.8	363765	−368	2.5	54 3d^6(1G)4p ^{2}F + 26 3d^6(1G)4p ^{2}F + 8 3d^6(1F)4p ^{2}F
364606.6	364872	−265	4.5	63 3d^6(1G)4p ^{2}G + 27 3d^6(1G)4p ^{2}G
365071.1	365357	−286	3.5	40 3d^6(1G)4p ^{2}G + 17 3d^6(1G)4p ^{2}G + 16 3d^6(1G)4p ^{2}F
386004.2	385757	247	1.5	78 3d^6(1D)4p ^{2}D + 17 3d^6(1D)4p ^{2}D
386705	386447	258	2.5	78 3d^6(1D)4p ^{2}D + 17 3d^6(1D)4p ^{2}D
392652.5	392333	320	2.5	69 3d^6(1D)4p ^{2}F + 22 3d^6(1D)4p ^{2}F
394248.5	393841	408	1.5	64 3d^6(1D)4p ^{2}P + 25 3d^6(1D)4p ^{2}P + 7 3d^6(1S)4p ^{2}P
394391	394030	361	3.5	72 3d^6(1D)4p ^{2}F + 23 3d^6(1D)4p ^{2}F
394912.4	394512	400	0.5	65 3d^6(1D)4p ^{2}P + 25 3d^6(1D)4p ^{2}P + 8 3d^6(1S)4p ^{2}P

a: Experimental energies from [30]
b: This work
c: Only the components ≥ to 5% are given

Transitions

Table A6: Computed oscillator strengths and transition probabilities in Cu V.

Wavelength	Lower Level	J_{low}	Upper Level	J_{up}	log gf	gA	CF
297.059	50072	3.5	386705	2.5	-0.57	2.03E+10	-0.58
297.164	49490	2.5	386004	1.5	-0.7	1.49E+10	-0.626
298.022	20827	2.5	356372	3.5	-1	7.48E+09	-0.284
299.218	30402	5.5	364607	4.5	-0.41	2.92E+10	0.483
300.077	31823	4.5	365071	3.5	-0.57	2.01E+10	0.408
300.824	21066	1.5	353486	2.5	-0.99	7.59E+09	0.312
302.737	31823	4.5	362143	3.5	-0.87	9.78E+09	0.308
304.438	20827	2.5	349301	1.5	-0.54	2.09E+10	-0.755
304.66	21066	1.5	349301	1.5	-0.77	1.21E+10	0.638
305.469	21935	0.5	349301	1.5	-0.99	7.34E+09	-0.723
307.245	30402	5.5	355875	4.5	-1	7.10E+09	-0.59
310.385	30402	5.5	352582	4.5	-0.26	3.80E+10	-0.383
310.73	31823	4.5	353646	3.5	-0.28	3.63E+10	-0.403
312.507	20827	2.5	340820	3.5	-0.28	3.57E+10	-0.804
312.835	21066	1.5	340723	2.5	-0.76	1.20E+10	-0.507
314.392	76838	1.5	394912	0.5	-0.68	1.42E+10	0.79
315.875	77668	2.5	394249	1.5	-0.39	2.70E+10	0.77
316.876	49490	2.5	365071	3.5	-0.92	8.01E+09	-0.287
317.93	50072	3.5	364607	4.5	-0.45	2.33E+10	-0.848
318.566	49490	2.5	363397	2.5	-0.66	1.46E+10	-0.244
319.844	49490	2.5	362143	3.5	-0.8	1.05E+10	-0.462
320.132	30966	2.5	343337	3.5	-0.82	9.99E+09	-0.291
322.572	33292	1.5	343301	2.5	-1	6.49E+09	-0.265
322.579	49490	2.5	359492	2.5	-0.64	1.46E+10	0.419
322.616	1616	3.5	311582	3.5	-0.58	1.68E+10	0.426
323.451	76838	1.5	386004	1.5	-0.53	1.90E+10	0.674
323.542	2759	2.5	311838	2.5	-0.57	1.73E+10	0.498
323.586	77668	2.5	386705	2.5	-0.39	2.57E+10	0.6
323.772	22575	4.5	331435	3.5	-0.99	6.54E+09	0.078
323.816	0	4.5	308818	4.5	-0.21	3.92E+10	0.521
323.989	50072	3.5	358725	3.5	-0.27	3.46E+10	0.586
324.19	2759	2.5	311220	3.5	-0.91	7.75E+09	0.809
324.48	1616	3.5	309801	3.5	-0.39	2.58E+10	0.464
324.488	3528	1.5	311706	1.5	-0.43	2.38E+10	0.842
324.511	1616	3.5	309772	4.5	-0.88	8.40E+09	0.567
324.607	0	4.5	308065	5.5	-0.21	3.93E+10	-0.865
324.681	2759	2.5	310754	2.5	-0.76	1.11E+10	0.339
324.806	50072	3.5	357948	2.5	-0.7	1.27E+10	0.185
324.86	0	4.5	307825	4.5	-0.4	2.51E+10	-0.873
325.037	30402	5.5	338059	4.5	-0.22	3.80E+10	-0.74
325.494	3528	1.5	310754	2.5	-0.53	1.85E+10	-0.784
325.519	1616	3.5	308818	4.5	-0.42	2.40E+10	-0.871
325.531	33292	1.5	340483	1.5	-0.7	1.27E+10	-0.36
325.68	30966	2.5	338016	2.5	-0.71	1.23E+10	-0.164
325.688	2759	2.5	309801	3.5	-0.53	1.84E+10	-0.583
325.847	0	4.5	306892	5.5	-0.86	8.66E+09	-0.85
325.934	2759	2.5	309570	2.5	-0.78	1.03E+10	0.538
326.227	2759	2.5	309294	3.5	-0.93	7.32E+09	0.427
326.398	1616	3.5	307991	3.5	-0.63	1.48E+10	-0.716
326.575	1616	3.5	307825	4.5	-0.53	1.85E+10	-0.413
326.872	27016	1.5	332946	1.5	-0.73	1.16E+10	-0.236
327.382	0	4.5	305453	3.5	-0.74	1.14E+10	-0.338
327.62	2759	2.5	307991	3.5	-0.59	1.59E+10	-0.432
328.408	1616	3.5	306116	2.5	-0.25	3.50E+10	-0.796
328.535	3528	1.5	307910	2.5	-0.58	1.62E+10	-0.638
328.732	0	4.5	304199	3.5	-0.4	2.44E+10	0.631
328.826	31823	4.5	335935	3.5	-0.33	2.87E+10	-0.507
329.035	2759	2.5	306678	1.5	-0.42	2.33E+10	-0.81
329.054	22575	4.5	326477	3.5	-0.09	5.04E+10	-0.542
329.219	27016	1.5	330765	2.5	-0.88	8.18E+09	-0.22
329.532	3528	1.5	306989	0.5	-0.68	1.29E+10	-0.842
329.805	0	4.5	303209	3.5	-0.37	2.64E+10	0.533
329.85	24100	3.5	327268	2.5	-0.08	5.06E+10	-0.613
330.047	28367	0.5	331354	0.5	-0.66	1.33E+10	-0.844
330.604	1616	3.5	304092	4.5	-0.7	1.21E+10	0.584
330.745	50072	3.5	352419	2.5	-0.12	4.68E+10	0.749
330.771	27016	1.5	329340	2.5	-0.61	1.49E+10	-0.499
331.191	49490	2.5	351431	1.5	-0.29	3.11E+10	0.78
331.216	20827	2.5	322744	3.5	-0.8	9.74E+09	-0.398
331.24	2759	2.5	304655	3.5	-0.95	6.75E+09	0.421
331.571	28367	0.5	329961	1.5	-0.59	1.56E+10	-0.681
331.823	20827	2.5	322192	2.5	-0.87	8.24E+09	-0.576
332.406	0	4.5	300837	4.5	-0.77	1.02E+10	0.558
332.813	30966	2.5	331435	3.5	-0.74	1.10E+10	0.265
332.888	0	4.5	300401	5.5	0.02	6.29E+10	0.627
332.915	21066	1.5	321443	1.5	-0.95	6.73E+09	-0.626
333.146	22575	4.5	322744	3.5	-0.46	2.10E+10	0.464
333.479	21066	1.5	320935	0.5	-0.79	9.64E+09	-0.692
333.555	22575	4.5	322376	4.5	-0.07	5.06E+10	-0.627
333.557	30966	2.5	330765	2.5	-0.69	1.22E+10	0.35
333.589	1616	3.5	301386	4.5	-0.89	7.80E+09	0.478
333.718	33292	1.5	332946	1.5	-0.58	1.59E+10	0.384
333.734	1616	3.5	301255	3.5	-0.84	8.57E+09	0.383
333.871	24100	3.5	323617	4.5	-0.59	1.56E+10	0.213
333.929	1616	3.5	301081	2.5	-0.8	9.50E+09	-0.656
334.201	1616	3.5	300837	4.5	-0.5	1.88E+10	0.337
334.311	24100	3.5	323222	2.5	-0.29	3.05E+10	-0.327
334.607	22575	4.5	321433	3.5	-0.99	6.11E+09	-0.166
334.641	2759	2.5	301587	3.5	-0.95	6.65E+09	-0.33
334.922	20827	2.5	319404	1.5	-0.76	1.03E+10	-0.566
335.013	2759	2.5	301255	3.5	-0.81	9.21E+09	0.226
335.462	20827	2.5	318923	2.5	-0.31	2.94E+10	-0.65
335.565	3528	1.5	301533	2.5	-0.77	1.01E+10	0.291
335.691	27016	1.5	324909	1.5	-0.78	9.86E+09	-0.298
335.731	21066	1.5	318923	2.5	-0.56	1.64E+10	0.658
335.913	24100	3.5	321796	3.5	-0.57	1.58E+10	0.221
336.07	28367	0.5	325923	1.5	-0.95	6.64E+09	0.565

Table A6: Continued

Wavelength	Lower Level	J_{Low}	Upper level	J_{Up}	log gf	gA	CF
336.165	33292	1.5	330765	2.5	-0.87	8.04E+09	0.215
336.169	21935	0.5	319404	1.5	-0.63	1.39E+10	0.64
336.274	22575	4.5	319952	5.5	-0.18	3.93E+10	0.527
336.323	24100	3.5	321433	3.5	-0.16	4.10E+10	-0.661
337.008	22575	4.5	319304	3.5	-0.83	8.66E+09	0.173
338.617	24100	3.5	319419	4.5	-0.26	3.18E+10	-0.754
338.748	24100	3.5	319304	3.5	-0.56	1.60E+10	-0.21
339.032	30966	2.5	325923	1.5	-0.24	3.32E+10	0.587
339.414	22575	4.5	317201	4.5	-0.36	2.52E+10	-0.368
339.498	30966	2.5	325519	2.5	-0.49	1.87E+10	-0.361
339.828	30402	5.5	324668	5.5	-0.69	1.18E+10	-0.467
339.88	30402	5.5	324624	6.5	-0.12	4.40E+10	-0.896
340.035	33292	1.5	327380	0.5	-0.37	2.46E+10	0.652
340.058	22575	4.5	316643	3.5	-0.18	3.85E+10	-0.311
340.164	33292	1.5	327268	2.5	-0.96	6.27E+09	0.174
340.355	49490	2.5	343301	2.5	-0.59	1.49E+10	-0.536
340.63	22575	4.5	316149	5.5	-0.55	1.63E+10	-0.353
340.988	50072	3.5	343337	3.5	-0.5	1.83E+10	-0.501
341.175	30402	5.5	323506	5.5	0.02	5.91E+10	-0.613
341.478	31823	4.5	324668	5.5	-0.23	3.36E+10	-0.666
342.426	24100	3.5	316134	2.5	-0.49	1.85E+10	-0.249
342.496	30402	5.5	322376	4.5	-0.94	6.54E+09	-0.2
342.708	31823	4.5	323617	4.5	0.29	1.10E+11	-0.8
342.838	31823	4.5	323506	5.5	-0.86	7.77E+09	0.373
343.055	30966	2.5	322464	3.5	-0.87	7.60E+09	0.705
343.736	31823	4.5	322744	3.5	-0.9	7.10E+09	-0.556
344.172	31823	4.5	322376	4.5	-0.95	6.26E+09	0.215
344.86	31823	4.5	321796	3.5	-0.4	2.23E+10	0.445
344.911	33292	1.5	323222	2.5	-1	5.65E+09	0.106
345.364	30402	5.5	319952	5.5	0	5.56E+10	-0.524
345.387	22575	4.5	312106	5.5	-0.83	8.29E+09	-0.59
345.677	30402	5.5	319689	4.5	0.03	5.90E+10	0.602
346	30402	5.5	319419	4.5	-0.84	7.96E+09	0.317
347.256	27016	1.5	314988	1.5	-0.87	7.45E+09	0.377
347.333	22575	4.5	310483	5.5	-0.98	5.83E+09	0.217
347.849	31823	4.5	319304	3.5	-0.37	2.37E+10	0.309
347.943	77668	2.5	365071	3.5	-0.41	2.17E+10	0.615
348.163	27016	1.5	314238	2.5	-0.48	1.80E+10	0.363
348.193	22575	4.5	309772	4.5	-0.36	2.39E+10	-0.496
348.286	24100	3.5	311220	3.5	-0.6	1.39E+10	-0.351
348.892	28367	0.5	314988	1.5	-0.81	8.46E+09	0.369
348.969	76838	1.5	363397	2.5	-0.32	2.61E+10	0.527
349.959	30402	5.5	316149	5.5	-0.29	2.78E+10	-0.195
350.046	30966	2.5	316643	3.5	-0.36	2.39E+10	-0.372
350.413	31823	4.5	317201	4.5	-0.65	1.20E+10	-0.086
350.571	22575	4.5	307825	4.5	-0.85	7.68E+09	-0.463
350.816	21066	1.5	306116	2.5	-0.89	6.96E+09	-0.202
350.919	27016	1.5	311982	0.5	-0.74	9.78E+09	-0.289
351.338	20827	2.5	305453	3.5	-0.81	8.49E+09	-0.193
351.525	77668	2.5	362143	3.5	-0.28	2.85E+10	-0.557
352.815	27016	1.5	310450	1.5	-0.79	8.72E+09	-0.253
353.018	30966	2.5	314238	2.5	-0.42	2.03E+10	0.521
353.555	33292	1.5	316134	2.5	-0.46	1.87E+10	-0.4
353.748	27016	1.5	309703	0.5	-0.87	7.24E+09	0.211
353.79	76838	1.5	359492	2.5	-0.61	1.32E+10	0.358
354.76	22575	4.5	304456	4.5	-0.6	1.34E+10	-0.213
354.983	30402	5.5	312106	5.5	-0.77	9.00E+09	-0.263
355.274	77668	2.5	359141	1.5	-0.66	1.17E+10	0.246
355.413	50072	3.5	331435	3.5	-0.26	2.92E+10	-0.441
355.524	49490	2.5	330765	2.5	-0.86	7.34E+09	-0.221
355.8	77668	2.5	358725	3.5	-0.97	5.65E+09	0.087
355.818	76838	1.5	357881	0.5	-0.88	7.01E+09	0.336
355.962	0	4.5	280929	3.5	-0.98	5.53E+09	0.554
356.436	24100	3.5	304655	3.5	-0.89	6.83E+09	-0.204
356.627	22575	4.5	302980	4.5	-0.93	6.14E+09	-0.221
356.786	77668	2.5	357948	2.5	-0.98	5.53E+09	-0.089
357.039	30402	5.5	310483	5.5	-0.46	1.82E+10	0.304
357.335	49490	2.5	329340	2.5	-0.57	1.43E+10	0.318
357.368	76838	1.5	356662	1.5	-0.87	7.10E+09	0.165
357.802	30966	2.5	310450	1.5	-0.54	1.52E+10	0.376
357.883	0	4.5	279421	4.5	-0.29	2.67E+10	0.543
357.898	31823	4.5	311233	4.5	-0.65	1.17E+10	0.23
358.022	1616	3.5	280929	3.5	-0.53	1.53E+10	0.407
358.188	2759	2.5	281942	2.5	-0.69	1.06E+10	0.4
358.303	3528	1.5	282622	1.5	-0.78	8.63E+09	0.432
358.357	31823	4.5	310875	4.5	-0.71	1.00E+10	0.165
358.593	30402	5.5	309269	5.5	-0.62	1.26E+10	0.185
358.822	33292	1.5	311982	0.5	-0.92	6.23E+09	0.3
358.856	0	4.5	278663	3.5	-0.04	4.75E+10	0.532
359.288	30966	2.5	309294	3.5	-0.95	5.82E+09	0.211
359.779	31823	4.5	309772	4.5	-0.99	5.29E+09	-0.085
359.866	1616	3.5	279497	2.5	-0.23	3.06E+10	0.501
360.612	2759	2.5	280066	1.5	-0.4	2.06E+10	0.502
360.949	1616	3.5	278663	3.5	-0.84	7.44E+09	-0.517
361.213	3528	1.5	280373	0.5	-0.53	1.52E+10	0.526
361.353	2759	2.5	279497	2.5	-0.82	7.79E+09	-0.502
361.43	1616	3.5	278295	2.5	-0.91	6.24E+09	-0.493
361.614	3528	1.5	280066	1.5	-0.95	5.75E+09	-0.504
361.788	50072	3.5	326477	3.5	-0.89	6.53E+09	-0.146
361.836	0	4.5	276368	3.5	-0.78	8.46E+09	-0.501
363.001	30402	5.5	305883	6.5	-0.64	1.16E+10	-0.671
363.047	50072	3.5	325519	2.5	-0.83	7.53E+09	-0.283
363.083	49490	2.5	324909	1.5	-0.95	5.67E+09	-0.332
363.545	31823	4.5	306892	5.5	-0.77	8.49E+09	-0.484
363.966	77668	2.5	352419	2.5	0.02	5.30E+10	0.643
364.176	76838	1.5	351431	1.5	-0.21	3.12E+10	0.606
365.32	49490	2.5	323222	2.5	-0.91	6.15E+09	0.087
367.234	49490	2.5	321796	3.5	-0.75	8.73E+09	0.237
367.237	50072	3.5	322376	4.5	-0.9	6.18E+09	-0.224
370.625	49490	2.5	319304	3.5	-0.48	1.61E+10	0.38
370.896	50072	3.5	319689	4.5	-0.23	2.88E+10	0.628
375.135	50072	3.5	316643	3.5	-0.69	9.77E+09	0.12
377.355	21066	1.5	286069	0.5	-0.63	1.10E+10	0.614
377.758	20827	2.5	285546	1.5	-0.59	1.19E+10	0.556
379.227	20827	2.5	284521	2.5	-0.22	2.78E+10	0.576
379.346	21935	0.5	285546	1.5	-0.65	1.04E+10	-0.532

Table A6: Continued

Wavelength	Lower Level	J_{Low}	Upper level	J_{Up}	log gf	gA	CF
379.571	21066	1.5	284521	2.5	-0.66	1.02E+10	-0.485
387.843	20827	2.5	278663	3.5	-0.77	7.61E+09	0.434
933.499	256273	2.5	363397	2.5	-0.89	9.99E+08	0.474
944.552	256272	3.5	362143	3.5	-1	7.49E+08	-0.265
996.581	222401	4.5	322744	3.5	-0.99	6.92E+08	0.238
1006.984	222886	3.5	322192	2.5	-0.78	1.09E+09	0.552
1026.709	234036	4.5	331435	3.5	-0.68	1.35E+09	-0.647
1035.572	226311	5.5	322876	4.5	-0.54	1.76E+09	-0.627
1053.502	227543	4.5	322464	3.5	-0.74	1.07E+09	-0.49
1057.357	227801	5.5	322376	4.5	-0.72	1.12E+09	0.703
1058.831	228020	3.5	322464	3.5	-1	5.87E+08	0.532
1060.59	235053	3.5	329340	2.5	-0.95	6.73E+08	0.488
1060.972	227543	4.5	321796	3.5	-0.91	7.18E+08	0.455
1070.83	228048	4.5	321433	3.5	-0.83	8.59E+08	0.505
1070.914	226311	5.5	319689	4.5	-0.83	8.70E+08	0.494
1071.299	228020	3.5	321365	2.5	-0.55	1.65E+09	-0.5
1075.631	228105	2.5	321074	1.5	-0.65	1.28E+09	-0.586
1078.857	230532	2.5	323222	2.5	-0.7	1.14E+09	-0.546
1081.775	234036	4.5	326477	3.5	-0.82	8.51E+08	-0.63
1083.236	272755	3.5	365071	3.5	-0.89	7.34E+08	-0.202
1088.209	239541	4.5	331435	3.5	-0.6	1.48E+09	0.607
1088.275	227801	5.5	319689	4.5	-0.67	1.20E+09	-0.365
1088.714	272755	3.5	364607	4.5	-0.92	6.90E+08	-0.707
1090.739	220208	6.5	311889	6.5	-0.27	3.03E+09	-0.799
1091.485	227801	5.5	319419	4.5	-1	5.49E+08	-0.739
1092.427	246477	2.5	338016	2.5	-0.41	2.17E+09	-0.555
1093.103	220623	5.5	312106	5.5	-0.57	1.51E+09	-0.471
1095.81	228048	4.5	319304	3.5	-0.58	1.45E+09	-0.616
1096.492	220938	4.5	312138	4.5	-0.72	1.06E+09	-0.267
1097.085	239615	3.5	330765	2.5	-0.79	9.36E+08	0.716
1099.259	265692	1.5	356662	1.5	-0.98	5.87E+08	0.741
1100.307	187779	4.5	278663	3.5	-0.52	1.66E+09	0.678
1101.307	221272	3.5	312073	3.5	-0.63	1.28E+09	-0.364
1102.972	188833	3.5	279497	2.5	-0.9	6.85E+08	0.425
1103.513	265752	4.5	356372	3.5	-0.74	9.95E+08	0.146
1103.63	220623	5.5	311233	4.5	-0.89	7.06E+08	-0.207
1105.142	265886	2.5	356372	3.5	-0.84	7.84E+08	0.617
1106.23	265975	3.5	356372	3.5	-0.05	4.90E+09	-0.728
1107.723	220208	6.5	310483	5.5	-0.45	1.94E+09	-0.526
1109.6	265752	4.5	355875	4.5	0.34	1.17E+10	-0.776
1111.079	189587	2.5	279590	1.5	-0.67	1.15E+09	0.438
1111.538	190100	1.5	280066	1.5	-0.81	8.43E+08	-0.755
1112.168	265692	1.5	355606	2.5	-0.75	9.67E+08	0.795
1112.225	189587	2.5	279497	2.5	-0.68	1.13E+09	-0.688
1112.347	265975	3.5	355875	4.5	-0.58	1.42E+09	0.804
1113.107	226311	5.5	316149	5.5	-0.71	1.06E+09	0.151
1113.209	188833	3.5	278663	3.5	-0.85	7.64E+08	-0.58
1114.515	239615	3.5	329340	2.5	-0.7	1.12E+09	-0.664
1114.579	265886	2.5	355606	2.5	-0.02	5.19E+09	-0.749
1114.62	229588	3.5	319304	3.5	-0.85	7.62E+08	0.357
1115.343	227543	4.5	317201	4.5	-0.89	6.93E+08	0.224
1117.453	190100	1.5	279590	1.5	-0.5	1.67E+09	-0.514
1117.694	234036	4.5	323506	5.5	-0.89	6.71E+08	-0.478
1117.794	188833	3.5	278295	2.5	-0.28	2.78E+09	0.436
1118.722	272755	3.5	362143	3.5	-0.45	1.92E+09	0.55
1121.212	190400	0.5	279590	1.5	-0.39	2.16E+09	0.811
1121.66	228048	4.5	317201	4.5	-0.06	4.58E+09	-0.617
1121.67	265752	4.5	354905	3.5	-0.22	3.19E+09	-0.742
1121.715	220623	5.5	309772	4.5	-0.86	7.25E+08	0.566
1122.269	265692	1.5	354797	1.5	-0.07	4.53E+09	-0.805
1123.353	265886	2.5	354905	3.5	-0.8	8.44E+08	0.52
1124.477	265975	3.5	354905	3.5	-0.22	3.19E+09	-0.4
1127.298	189587	2.5	278295	2.5	-0.36	2.26E+09	-0.457
1127.438	222886	3.5	311582	3.5	-0.95	5.89E+08	0.323
1127.879	265886	2.5	354548	2.5	-0.74	9.59E+08	-0.248
1128.079	220623	5.5	309269	5.5	-0.7	1.04E+09	-0.219
1128.813	187779	4.5	276368	3.5	0.01	5.35E+09	0.5
1129.012	265975	3.5	354548	2.5	-0.45	1.88E+09	-0.756
1129.123	235053	3.5	323617	4.5	-0.6	1.31E+09	-0.567
1130.281	222401	4.5	310875	4.5	-0.82	7.85E+08	-0.417
1131.785	220938	4.5	309294	3.5	-0.92	6.27E+08	0.205
1131.876	227801	5.5	316149	5.5	0.21	8.45E+09	-0.783
1132.528	221272	3.5	309570	2.5	-0.25	2.90E+09	0.586
1133.86	190100	1.5	278295	2.5	-0.42	1.98E+09	0.805
1134.174	235053	3.5	323222	2.5	-0.62	1.23E+09	0.524
1134.387	265886	2.5	354039	1.5	-0.27	2.75E+09	0.736
1137.676	265692	1.5	353590	0.5	-0.51	1.57E+09	0.801
1138.212	220208	6.5	308065	5.5	-0.47	1.73E+09	-0.559
1139.473	265886	2.5	353646	3.5	-0.89	6.54E+08	-0.579
1139.479	234036	4.5	321796	3.5	-0.94	5.89E+08	0.284
1140.356	235053	3.5	322744	3.5	-0.81	7.85E+08	0.747
1140.629	265975	3.5	353646	3.5	-0.95	5.68E+08	0.338
1140.856	239615	3.5	327268	2.5	-0.68	1.09E+09	0.738
1142.396	188833	3.5	276368	3.5	-0.41	1.99E+09	-0.356
1142.717	265975	3.5	353486	2.5	-0.4	2.05E+09	-0.728
1143.614	220623	5.5	308065	5.5	-0.67	1.08E+09	0.728
1144.831	226889	1.5	314238	2.5	-0.64	1.17E+09	0.673
1146.767	220623	5.5	307825	4.5	-0.42	1.91E+09	-0.438
1147.752	220938	4.5	308065	5.5	-0.78	8.44E+08	-0.289
1148.571	256272	3.5	343337	3.5	0.22	8.29E+09	-0.735
1148.576	256273	2.5	343337	3.5	-0.76	8.74E+08	0.722
1148.698	229588	3.5	316643	3.5	-0.91	6.26E+08	-0.265
1148.731	220938	4.5	307991	3.5	-0.46	1.73E+09	-0.451
1149.053	256273	2.5	343301	2.5	0.14	7.01E+09	-0.813
1150.269	239541	4.5	326477	3.5	-0.85	7.25E+08	0.621
1150.843	222401	4.5	309294	3.5	-0.7	9.96E+08	0.384
1150.928	220938	4.5	307825	4.5	-0.44	1.80E+09	0.47
1150.929	222886	3.5	309772	4.5	-0.49	1.62E+09	-0.457
1151.677	265752	4.5	352582	4.5	-0.9	6.27E+08	0.293
1152.216	278282	4.5	365071	3.5	-0.56	1.39E+09	0.284
1152.325	189587	2.5	276368	3.5	-0.43	1.88E+09	0.828
1152.827	235053	3.5	321796	3.5	-0.52	1.52E+09	-0.603
1153.152	221272	3.5	307991	3.5	-0.69	1.01E+09	0.456
1153.521	278380	3.5	365071	3.5	0.22	8.22E+09	-0.844
1153.521	272801	2.5	359492	2.5	0.14	6.93E+09	-0.768
1153.595	236059	2.5	322744	3.5	-0.3	2.51E+09	0.822

Table A6: Continued

Wavelength	Lower Level	J_{Low}	Upper level	J_{Up}	log gf	gA	CF
1154.233	221272	3.5	307910	2.5	-0.56	1.36E+09	-0.562
1154.637	265975	3.5	352582	4.5	-0.65	1.12E+09	-0.59
1155.367	221272	3.5	307825	4.5	-0.8	7.90E+08	-0.488
1155.474	236331	3.5	322876	4.5	0.32	1.04E+10	0.85
1156.473	246477	2.5	332946	1.5	-0.49	1.55E+09	0.386
1156.602	236109	0.5	322569	0.5	-0.89	6.49E+08	-0.799
1156.943	238234	6.5	324668	5.5	-0.85	6.98E+08	0.216
1157.003	236040	1.5	322470	1.5	-0.77	8.45E+08	-0.476
1157.231	236331	3.5	322744	3.5	-0.18	3.31E+09	-0.487
1157.259	236059	2.5	322470	1.5	-0.89	6.48E+08	-0.455
1157.338	236059	2.5	322464	3.5	0.03	5.28E+09	0.812
1157.543	238234	6.5	324624	6.5	0.55	1.77E+10	-0.816
1157.902	238305	5.5	324668	5.5	0.48	1.51E+10	-0.871
1157.927	236109	0.5	322470	1.5	-0.66	1.09E+09	0.814
1158.416	278282	4.5	364607	4.5	0.35	1.11E+10	-0.746
1158.453	246624	1.5	332946	1.5	-0.41	1.89E+09	-0.738
1158.503	238305	5.5	324624	6.5	-0.58	1.31E+09	0.887
1158.949	187779	4.5	274065	4.5	-0.74	9.07E+08	0.189
1159.735	278380	3.5	364607	4.5	-0.51	1.53E+09	0.693
1159.763	187779	4.5	274004	5.5	0.52	1.63E+10	0.9
1160.735	236040	1.5	322192	2.5	-0.03	4.66E+09	0.845
1160.993	236059	2.5	322192	2.5	-0.39	2.04E+09	-0.268
1160.997	236331	3.5	322464	3.5	-0.85	6.92E+08	0.464
1161.529	223477	1.5	309570	2.5	-0.33	2.31E+09	-0.771
1161.711	223214	2.5	309294	3.5	-0.47	1.69E+09	-0.692
1163.201	272755	3.5	358725	3.5	0.19	7.64E+09	-0.801
1163.412	220938	4.5	306892	5.5	-0.43	1.81E+09	-0.821
1163.94	234036	4.5	319952	5.5	-0.56	1.35E+09	-0.585
1165.573	226311	5.5	312106	5.5	-0.73	9.08E+08	0.152
1167.357	222401	4.5	308065	5.5	0.25	8.78E+09	0.726
1167.507	234036	4.5	319689	4.5	0.32	1.02E+10	-0.83
1168.193	230532	2.5	316134	2.5	-0.95	5.57E+08	-0.489
1168.525	226311	5.5	311889	6.5	0.21	7.86E+09	0.498
1170.075	236331	3.5	321796	3.5	-0.28	2.57E+09	-0.782
1170.915	236040	1.5	321443	1.5	-0.9	6.08E+08	-0.199
1171.862	236109	0.5	321443	1.5	-0.43	1.82E+09	0.795
1171.988	236040	1.5	321365	2.5	-0.54	1.42E+09	0.242
1172.174	238305	5.5	323617	4.5	0.3	9.72E+09	0.88
1172.25	236059	2.5	321365	2.5	-0.16	3.35E+09	0.831
1172.708	238234	6.5	323506	5.5	0.02	4.91E+09	0.816
1172.884	220623	5.5	305883	6.5	-0.21	2.97E+09	-0.691
1173.135	221664	1.5	306906	2.5	-0.11	3.78E+09	0.534
1173.151	188833	3.5	274073	3.5	-0.22	2.93E+09	0.505
1173.271	188833	3.5	274065	4.5	0.39	1.17E+10	0.903
1173.511	229774	0.5	314988	1.5	-0.66	1.07E+09	0.792
1173.694	238305	5.5	323506	5.5	-0.7	9.47E+08	0.384
1173.803	272755	3.5	357948	2.5	-0.35	2.21E+09	-0.74
1175.063	236331	3.5	321433	3.5	-0.5	1.51E+09	-0.745
1175.182	226889	1.5	311982	0.5	-1	4.84E+08	0.185
1175.37	199441	3.5	284521	2.5	0.09	6.02E+09	0.808
1175.997	236040	1.5	321074	1.5	-0.33	2.25E+09	0.833
1176.238	278380	3.5	363397	2.5	0.11	6.29E+09	0.825
1176.531	219203	2.5	304199	3.5	0.2	7.63E+09	0.9
1176.952	236109	0.5	321074	1.5	-0.71	9.39E+08	0.258
1177.045	246477	2.5	331435	3.5	0.21	7.64E+09	0.866
1177.318	222886	3.5	307825	4.5	0.08	5.82E+09	0.782
1177.881	200648	2.5	285546	1.5	-0.19	3.14E+09	0.807
1178.877	236109	0.5	320935	0.5	-0.48	1.62E+09	-0.823
1179.572	223214	2.5	307991	3.5	-0.15	3.41E+09	0.818
1180.229	246624	1.5	331354	0.5	-0.4	1.88E+09	0.748
1181.253	201413	1.5	286069	0.5	-0.58	1.26E+09	0.82
1181.329	229588	3.5	314238	2.5	0.07	5.69E+09	0.846
1182.097	227543	4.5	312138	4.5	-1	4.78E+08	0.089
1182.552	227543	4.5	312106	5.5	0.14	6.54E+09	0.551
1182.602	189587	2.5	274146	2.5	-0.18	3.16E+09	0.665
1183.559	222401	4.5	306892	5.5	-0.59	1.22E+09	0.368
1183.624	189587	2.5	274073	3.5	0.15	6.71E+09	0.796
1184.044	230532	2.5	314988	1.5	-0.14	3.41E+09	0.849
1184.112	221664	1.5	306116	2.5	-0.99	4.87E+08	-0.519
1184.371	223477	1.5	307910	2.5	-0.63	1.11E+09	0.708
1185.307	235053	3.5	319419	4.5	-0.43	1.74E+09	0.559
1186.169	227801	5.5	312106	5.5	-0.66	1.03E+09	-0.182
1186.4	246477	2.5	330765	2.5	-0.53	1.37E+09	-0.293
1186.92	235053	3.5	319304	3.5	0.04	5.11E+09	-0.631
1187.381	201850	0.5	286069	0.5	-0.57	1.27E+09	-0.851
1187.51	256273	2.5	340483	1.5	-0.29	2.42E+09	0.664
1187.979	236040	1.5	320216	0.5	-0.45	1.70E+09	0.839
1188.039	226311	5.5	310483	5.5	0.27	8.88E+09	-0.743
1188.484	246624	1.5	330765	2.5	-0.14	3.36E+09	0.858
1188.586	201413	1.5	285546	1.5	-0.46	1.65E+09	-0.841
1188.81	228020	3.5	312138	4.5	0.2	7.44E+09	0.741
1189.195	228048	4.5	312138	4.5	-0.95	5.25E+08	-0.123
1189.226	227801	5.5	311889	6.5	0.21	7.52E+09	0.862
1189.228	190100	1.5	274189	1.5	-0.23	2.75E+09	0.843
1189.655	228048	4.5	312106	5.5	-0.03	4.41E+09	0.743
1189.826	190100	1.5	274146	2.5	-0.07	3.97E+09	0.807
1189.934	219203	2.5	303242	2.5	-0.53	1.40E+09	-0.445
1190.191	222886	3.5	306906	2.5	-0.96	5.26E+08	0.714
1190.393	219203	2.5	303209	3.5	-0.35	2.11E+09	0.887
1190.444	239615	3.5	323617	4.5	-0.59	1.24E+09	0.622
1190.933	228105	2.5	312073	3.5	-0.01	4.66E+09	0.525
1190.967	239541	4.5	323506	5.5	0.25	8.48E+09	0.871
1191.546	223214	2.5	307139	1.5	-0.95	5.28E+08	0.77
1192.283	200648	2.5	284521	2.5	-0.51	1.47E+09	-0.833
1192.422	278282	4.5	362145	5.5	0.5	1.47E+10	0.897
1192.448	272801	2.5	356662	1.5	-0.48	1.55E+09	0.774
1192.449	278282	4.5	362143	3.5	0.03	5.01E+09	-0.822
1192.542	220208	6.5	304062	6.5	0.14	6.47E+09	-0.486
1192.843	220623	5.5	304456	4.5	-0.98	4.91E+08	0.482
1193.068	228020	3.5	311838	2.5	-0.59	1.21E+09	0.232
1193.184	190400	0.5	274210	0.5	-0.38	1.96E+09	0.895
1193.485	190400	0.5	274189	1.5	-0.43	1.73E+09	0.831
1193.84	223376	0.5	307139	1.5	-0.63	1.11E+09	0.623
1193.847	278380	3.5	362143	3.5	-0.37	2.02E+09	-0.309
1194.279	228105	2.5	311838	2.5	-0.23	2.73E+09	-0.469
1194.502	220938	4.5	304655	3.5	-0.57	1.27E+09	0.469

Table A6: Continued

Wavelength	Lower Level	J_{Low}	Upper level	J_{Up}	log gf	gA	CF
1194.882	227543	4.5	311233	4.5	0.24	8.04E+09	-0.859
1195.062	227543	4.5	311220	3.5	-1	4.67E+08	-0.704
1196.059	239615	3.5	323222	2.5	-0.05	4.23E+09	0.884
1196.158	228105	2.5	311706	1.5	-0.21	2.89E+09	0.879
1196.715	228020	3.5	311582	3.5	0	4.68E+09	-0.591
1196.722	226889	1.5	310450	1.5	-0.26	2.59E+09	-0.596
1197.104	228048	4.5	311582	3.5	-0.95	5.27E+08	0.183
1197.347	220938	4.5	304456	4.5	-0.65	1.05E+09	0.22
1197.424	223477	1.5	306989	0.5	-0.38	1.97E+09	0.891
1197.83	246477	2.5	329961	1.5	-0.54	1.31E+09	-0.775
1198.044	220623	5.5	304092	4.5	-0.7	9.26E+08	0.426
1198.123	223214	2.5	306678	1.5	-0.37	2.01E+09	0.529
1198.473	220623	5.5	304062	6.5	0.22	7.63E+09	0.69
1198.822	265752	4.5	349168	5.5	0.5	1.45E+10	0.9
1199.284	221272	3.5	304655	3.5	-0.91	5.71E+08	0.195
1199.829	236059	2.5	319404	1.5	-0.12	3.53E+09	0.864
1199.952	243140	2.5	326477	3.5	0.19	7.22E+09	0.871
1199.954	246624	1.5	329961	1.5	-0.29	2.34E+09	-0.568
1200.352	220623	5.5	303932	5.5	-0.1	3.66E+09	-0.33
1201.221	220208	6.5	303456	7.5	0.64	1.99E+10	0.935
1201.491	222886	3.5	306116	2.5	-0.3	2.34E+09	0.386
1201.873	239541	4.5	322744	3.5	-0.27	2.53E+09	-0.86
1201.9	223477	1.5	306678	1.5	-0.51	1.45E+09	-0.863
1202.151	221272	3.5	304456	4.5	-0.64	1.07E+09	-0.329
1203.081	272755	3.5	355875	4.5	-0.58	1.22E+09	0.836
1203.152	228105	2.5	311220	3.5	-0.26	2.51E+09	-0.797
1203.298	256273	2.5	339378	1.5	-0.51	1.45E+09	-0.813
1204.065	222401	4.5	305453	3.5	-0.28	2.46E+09	0.377
1204.912	220938	4.5	303932	5.5	0.13	6.15E+09	0.546
1205.425	226311	5.5	309269	5.5	-0.42	1.76E+09	0.214
1205.684	227543	4.5	310483	5.5	-0.46	1.60E+09	0.748
1205.935	239541	4.5	322464	3.5	-0.56	1.28E+09	0.534
1206.252	223214	2.5	306116	2.5	-0.24	2.65E+09	-0.813
1206.794	236059	2.5	318923	2.5	-0.92	5.59E+08	-0.219
1206.81	246477	2.5	329340	2.5	-0.13	3.35E+09	-0.856
1207.006	239615	3.5	322464	3.5	-0.7	9.30E+08	-0.71
1207.219	239541	4.5	322376	4.5	0.24	8.03E+09	-0.688
1207.33	228048	4.5	310875	4.5	-0.04	4.14E+09	0.822
1207.524	226889	1.5	309703	0.5	-0.4	1.82E+09	-0.824
1208.293	239615	3.5	322376	4.5	-0.21	2.81E+09	0.8
1208.7	228020	3.5	310754	2.5	-0.1	3.61E+09	0.744
1208.966	246624	1.5	329340	2.5	-0.69	9.16E+08	-0.219
1210.563	234036	4.5	316643	3.5	-0.02	4.35E+09	0.795
1210.772	236331	3.5	318923	2.5	0.12	6.01E+09	0.889
1211.075	265752	4.5	348324	4.5	-0.44	1.65E+09	0.861
1211.129	222886	3.5	305453	3.5	-0.29	2.37E+09	-0.665
1211.38	229588	3.5	312138	4.5	-0.38	1.89E+09	0.849
1212.018	226311	5.5	308818	4.5	-0.04	4.11E+09	0.468
1212.578	223376	0.5	305844	1.5	-0.13	3.34E+09	0.9
1213.915	243140	2.5	325519	2.5	0.16	6.55E+09	-0.884
1214.217	220623	5.5	302980	4.5	-0.86	6.27E+08	-0.534
1214.348	265975	3.5	348324	4.5	0.33	9.52E+09	0.789
1215.677	227543	4.5	309801	3.5	-0.04	4.15E+09	0.721
1215.733	239541	4.5	321796	3.5	-0.46	1.61E+09	0.697
1215.967	223214	2.5	305453	3.5	-0.88	5.99E+08	0.835
1216.421	229774	0.5	311982	0.5	-0.41	1.76E+09	-0.859
1216.438	221272	3.5	303479	2.5	-0.63	1.05E+09	0.77
1216.822	239615	3.5	321796	3.5	-0.35	2.06E+09	0.565
1217.306	235053	3.5	317201	4.5	0.01	4.60E+09	0.771
1217.834	234036	4.5	316149	5.5	0.08	5.39E+09	0.733
1217.962	272801	2.5	354905	3.5	-0.63	1.07E+09	0.895
1218.472	221664	1.5	303734	1.5	-0.04	4.05E+09	-0.891
1218.883	220938	4.5	302980	4.5	-0.64	1.02E+09	-0.179
1219.588	229588	3.5	311582	3.5	-0.4	1.81E+09	-0.652
1220.444	221272	3.5	303209	3.5	-0.46	1.55E+09	-0.414
1220.514	229774	0.5	311706	1.5	-0.96	4.88E+08	-0.524
1220.895	265886	2.5	347793	3.5	0.21	7.20E+09	0.789
1221.343	219203	2.5	301081	2.5	0.08	5.33E+09	-0.891
1222.217	239615	3.5	321433	3.5	0.08	5.50E+09	-0.834
1222.223	265975	3.5	347793	3.5	-0.43	1.66E+09	0.862
1222.6	272755	3.5	354548	2.5	-0.89	5.85E+08	-0.782
1222.691	256272	3.5	338059	4.5	0.4	1.13E+10	0.917
1222.778	228020	3.5	309801	3.5	-0.65	1.00E+09	0.152
1222.847	278282	4.5	360058	4.5	-0.55	1.27E+09	0.852
1222.953	222886	3.5	304655	3.5	-0.38	1.86E+09	-0.41
1222.966	243140	2.5	324909	1.5	-0.61	1.10E+09	-0.816
1223.18	226311	5.5	308065	5.5	-0.62	1.07E+09	0.476
1223.185	228048	4.5	309801	3.5	-0.39	1.80E+09	0.787
1223.216	228020	3.5	309772	4.5	-0.37	1.90E+09	-0.536
1223.342	256272	3.5	338016	2.5	-0.04	4.16E+09	0.851
1223.593	227543	4.5	309269	5.5	-0.97	4.81E+08	0.142
1223.623	228048	4.5	309772	4.5	-0.36	1.96E+09	-0.733
1223.722	238234	6.5	319952	5.5	0.16	6.44E+09	0.871
1223.863	221272	3.5	302980	4.5	0.12	5.79E+09	0.783
1224.05	228105	2.5	309801	3.5	-1	4.42E+08	-0.418
1224.127	222401	4.5	304092	4.5	0.2	7.04E+09	-0.722
1224.317	278380	3.5	360058	4.5	0.35	1.00E+10	0.794
1224.809	229588	3.5	311233	4.5	-0.7	8.89E+08	0.427
1225.827	221664	1.5	303242	2.5	-0.2	2.81E+09	0.897
1225.935	222886	3.5	304456	4.5	-0.81	6.92E+08	-0.743
1226.371	230532	2.5	312073	3.5	-0.16	3.06E+09	0.897
1226.536	222401	4.5	303932	5.5	-0.27	2.39E+09	0.824
1226.58	265692	1.5	347219	2.5	0.09	5.45E+09	0.856
1227.184	199441	3.5	280929	3.5	-0.73	8.15E+08	0.388
1227.467	227801	5.5	309269	5.5	0.06	5.08E+09	0.793
1227.527	228105	2.5	309570	2.5	-0.89	5.71E+08	0.268
1229.513	265886	2.5	347219	2.5	-0.6	1.11E+09	0.876
1229.811	222886	3.5	304199	3.5	-0.85	6.28E+08	0.375
1229.92	230532	2.5	311838	2.5	-0.43	1.65E+09	-0.72
1230.056	221664	1.5	302961	0.5	-0.31	2.14E+09	-0.902
1230.1	200648	2.5	281942	2.5	-0.49	1.42E+09	0.656
1230.203	229588	3.5	310875	4.5	-0.28	2.30E+09	0.371
1230.388	227543	4.5	308818	4.5	-0.65	9.83E+08	0.203
1230.409	228020	3.5	309294	3.5	-0.75	7.75E+08	0.392
1231.395	201413	1.5	282622	1.5	-0.56	1.20E+09	0.787
1231.429	222886	3.5	304092	4.5	-0.48	1.46E+09	0.752

Table A6: Continued

Wavelength	Lower Level	J_{Low}	Upper level	J_{Up}	log gf	gA	CF
1231.922	238234	6.5	319408	7.5	0.63	1.88E+10	0.945
1232.615	220208	6.5	301336	6.5	0.27	8.16E+09	0.925
1232.839	238305	5.5	319419	4.5	-0.73	8.09E+08	-0.578
1232.865	278380	3.5	359492	2.5	-0.96	4.86E+08	-0.771
1233.327	235053	3.5	316134	2.5	-0.14	3.21E+09	0.781
1233.371	220208	6.5	301286	5.5	-0.84	6.34E+08	0.875
1234.304	227801	5.5	308818	4.5	0.02	4.52E+09	0.899
1236.933	272801	2.5	353646	3.5	0.23	7.37E+09	0.891
1237.501	222401	4.5	303209	3.5	-0.2	2.76E+09	-0.672
1238.056	201850	0.5	282622	1.5	-0.13	3.25E+09	0.904
1238.194	220623	5.5	301386	4.5	-0.07	3.72E+09	0.883
1238.953	220623	5.5	301336	6.5	0.16	6.26E+09	0.505
1239.332	230532	2.5	311220	3.5	0.02	4.55E+09	0.618
1239.514	229774	0.5	310450	1.5	-0.63	1.03E+09	0.8
1239.717	220623	5.5	301286	5.5	0.22	7.12E+09	0.846
1239.947	220938	4.5	301587	3.5	-0.09	3.56E+09	-0.859
1240.022	246624	1.5	327268	2.5	-0.37	1.81E+09	-0.69
1240.796	222886	3.5	303479	2.5	-0.32	2.07E+09	-0.565
1241.017	222401	4.5	302980	4.5	-0.78	7.16E+08	0.186
1241.779	201413	1.5	281942	2.5	0.08	5.19E+09	0.902
1241.892	227543	4.5	308065	5.5	-0.76	7.55E+08	0.185
1242.772	223214	2.5	303680	1.5	-0.47	1.47E+09	-0.87
1243.047	220938	4.5	301386	4.5	-0.19	2.76E+09	0.392
1243.116	278282	4.5	358725	3.5	-0.32	2.07E+09	-0.797
1243.617	239541	4.5	319952	5.5	0.14	6.11E+09	-0.894
1244.581	220938	4.5	301286	5.5	0.05	4.87E+09	0.442
1244.964	222886	3.5	303209	3.5	-0.63	1.02E+09	-0.202
1245.062	220938	4.5	301255	3.5	-0.93	5.04E+08	0.138
1245.101	221272	3.5	301587	3.5	-0.51	1.34E+09	-0.27
1245.611	227543	4.5	307825	4.5	-1	4.23E+08	0.161
1245.633	200648	2.5	280929	3.5	0.26	7.80E+09	0.905
1245.875	223214	2.5	303479	2.5	-0.41	1.66E+09	-0.299
1245.927	221272	3.5	301533	2.5	-0.35	1.90E+09	0.636
1246.106	226889	1.5	307139	1.5	-0.54	1.24E+09	-0.705
1246.539	230532	2.5	310754	2.5	-0.45	1.52E+09	0.546
1246.661	220623	5.5	300837	4.5	-0.26	2.35E+09	0.514
1246.668	229588	3.5	309801	3.5	-0.88	5.74E+08	0.318
1246.836	223477	1.5	303680	1.5	-0.24	2.49E+09	-0.649
1246.985	220208	6.5	300401	5.5	0.32	8.96E+09	0.921
1247.124	229588	3.5	309772	4.5	-0.04	3.95E+09	0.627
1248.226	221272	3.5	301386	4.5	-0.26	2.37E+09	0.318
1249.133	199441	3.5	279497	2.5	-0.49	1.39E+09	-0.9
1249.728	228048	4.5	308065	5.5	-0.47	1.45E+09	-0.515
1249.734	226889	1.5	306906	2.5	-0.29	2.22E+09	-0.899
1249.959	223477	1.5	303479	2.5	-0.62	1.02E+09	0.663
1249.991	246477	2.5	326477	3.5	-0.81	6.46E+08	-0.272
1250.077	223214	2.5	303209	3.5	-0.86	5.96E+08	0.529
1250.258	221272	3.5	301255	3.5	-0.15	2.99E+09	-0.852
1250.316	199441	3.5	279421	4.5	0.39	1.05E+10	0.906
1250.463	228020	3.5	307991	3.5	-0.5	1.35E+09	0.383
1251.58	220938	4.5	300837	4.5	-0.03	3.99E+09	-0.916
1251.911	239541	4.5	319419	4.5	-0.47	1.45E+09	0.831
1252.706	272755	3.5	352582	4.5	0.32	8.95E+09	0.886
1253.065	239615	3.5	319419	4.5	0.18	6.57E+09	0.771
1253.067	228105	2.5	307910	2.5	-0.26	2.35E+09	0.793
1253.709	239541	4.5	319304	3.5	-0.56	1.19E+09	-0.573
1254.601	229588	3.5	309294	3.5	-0.22	2.57E+09	-0.637
1255.271	272755	3.5	352419	2.5	-0.11	3.33E+09	0.841
1255.293	256272	3.5	335935	3.5	-0.76	7.45E+08	0.849
1255.299	256273	2.5	335935	3.5	0.24	7.42E+09	0.843
1256.725	226311	5.5	305883	6.5	0.13	5.72E+09	-0.662
1256.831	221272	3.5	300837	4.5	-0.53	1.24E+09	-0.362
1258.702	246477	2.5	325923	1.5	-0.51	1.26E+09	0.717
1259.168	200648	2.5	280066	1.5	-0.46	1.47E+09	-0.906
1260.246	227543	4.5	306892	5.5	-0.17	2.85E+09	-0.453
1260.564	243140	2.5	322470	1.5	-0.52	1.26E+09	-0.809
1262.279	199441	3.5	278663	3.5	0.19	6.41E+09	-0.879
1265.211	230532	2.5	309570	2.5	-0.94	4.78E+08	-0.278
1265.714	238234	6.5	317240	6.5	-0.62	9.92E+08	0.898
1266.074	222401	4.5	301386	4.5	-0.81	6.44E+08	0.41
1266.456	201413	1.5	280373	0.5	-0.6	1.05E+09	-0.911
1266.862	238305	5.5	317240	6.5	0.53	1.42E+10	0.884
1267.493	238305	5.5	317201	4.5	-0.79	6.69E+08	0.753
1268.165	222401	4.5	301255	3.5	-0.47	1.41E+09	0.712
1268.253	200648	2.5	279497	2.5	-0.15	2.94E+09	-0.758
1268.316	228048	4.5	306892	5.5	0.22	6.88E+09	0.637
1269.348	187779	4.5	266560	3.5	-0.1	3.33E+09	-0.918
1271.409	201413	1.5	280066	1.5	-0.48	1.37E+09	-0.748
1271.493	222886	3.5	301533	2.5	-0.79	6.67E+08	0.858
1271.779	272801	2.5	351431	1.5	-0.26	2.25E+09	0.813
1273.502	201850	0.5	280373	0.5	-0.62	9.94E+08	-0.882
1273.887	222886	3.5	301386	4.5	-0.8	6.61E+08	0.299
1274.741	187779	4.5	266227	4.5	0.39	1.01E+10	-0.945
1274.928	222401	4.5	300837	4.5	-0.5	1.30E+09	0.29
1275.958	223214	2.5	301587	3.5	-0.73	7.69E+08	-0.524
1276.003	222886	3.5	301255	3.5	-0.39	1.68E+09	0.345
1276.826	223214	2.5	301533	2.5	-0.43	1.52E+09	0.862
1277.095	243140	2.5	321443	1.5	-0.62	9.91E+08	0.596
1278.168	229588	3.5	307825	4.5	-0.49	1.31E+09	0.441
1278.182	188833	3.5	267069	2.5	-0.04	3.76E+09	-0.925
1278.511	201850	0.5	280066	1.5	-0.77	6.89E+08	0.596
1279.667	226311	5.5	304456	4.5	-0.22	2.50E+09	-0.825
1280.672	201413	1.5	279497	2.5	-0.71	7.84E+08	0.447
1280.702	227801	5.5	305883	6.5	0.24	6.96E+09	0.541
1280.917	234036	4.5	312106	5.5	-0.94	4.69E+08	-0.811
1281.117	223477	1.5	301533	2.5	-0.29	2.09E+09	0.553
1281.374	223214	2.5	301255	3.5	-0.44	1.46E+09	0.309
1281.806	200648	2.5	278663	3.5	-0.94	4.66E+08	0.263
1282.053	222401	4.5	300401	5.5	-0.21	2.50E+09	0.693
1282.851	222886	3.5	300837	4.5	-0.41	1.57E+09	0.253
1283.521	227543	4.5	305453	3.5	-0.67	8.73E+08	0.53
1283.667	189587	2.5	267489	1.5	-0.12	3.06E+09	-0.933
1286.149	226311	5.5	304062	6.5	-0.11	3.13E+09	-0.917
1286.549	188833	3.5	266560	3.5	-0.01	3.94E+09	-0.66
1287.661	239541	4.5	317201	4.5	-0.77	7.01E+08	-0.314
1287.686	190100	1.5	267759	0.5	-0.36	1.77E+09	-0.942

Table A6: Continued

Wavelength	Lower Level	J_{Low}	Upper level	J_{Up}	log gf	gA	CF
1287.89	200648	2.5	278295	2.5	-0.71	7.77E+08	0.881
1288.882	239615	3.5	317201	4.5	-0.73	7.61E+08	-0.43
1290.624	189587	2.5	267069	2.5	-0.53	1.17E+09	-0.529
1291.893	228048	4.5	305453	3.5	-0.8	6.42E+08	-0.509
1292.09	188833	3.5	266227	4.5	-0.64	9.10E+08	0.258
1292.36	230532	2.5	307910	2.5	-0.6	1.00E+09	-0.296
1292.571	229774	0.5	307139	1.5	-0.76	6.94E+08	-0.388
1296.808	227543	4.5	304655	3.5	-1	3.98E+08	-0.207
1296.988	239541	4.5	316643	3.5	-0.77	6.99E+08	-0.747
1297.212	190400	0.5	267489	1.5	-0.53	1.18E+09	0.515
1299.155	189587	2.5	266560	3.5	-0.44	1.42E+09	0.327
1299.233	190100	1.5	267069	2.5	-0.41	1.55E+09	0.411
1299.939	199441	3.5	276368	3.5	-0.51	1.21E+09	0.876
1304.298	226311	5.5	302980	4.5	-0.53	1.17E+09	-0.601
1304.536	227801	5.5	304456	4.5	-0.32	1.88E+09	0.424
1304.892	228020	3.5	304655	3.5	-0.97	4.24E+08	-0.254
1305.355	228048	4.5	304655	3.5	-0.44	1.42E+09	0.548
1305.362	230532	2.5	307139	1.5	-0.99	4.01E+08	0.589
1306.341	228105	2.5	304655	3.5	-0.72	7.46E+08	0.799
1308.101	234036	4.5	310483	5.5	-0.39	1.57E+09	0.702
1308.287	228020	3.5	304456	4.5	-0.51	1.23E+09	0.636
1309.087	227543	4.5	303932	5.5	-0.43	1.46E+09	-0.496
1309.708	226889	1.5	303242	2.5	-0.34	1.78E+09	0.438
1310.759	227801	5.5	304092	4.5	-0.82	5.86E+08	0.43
1312.674	235053	3.5	311233	4.5	-0.6	9.67E+08	0.78
1314.565	229774	0.5	305844	1.5	-0.76	6.64E+08	0.503
1318.871	235053	3.5	310875	4.5	-0.33	1.79E+09	0.797
1319.296	236040	1.5	311838	2.5	-0.98	4.06E+08	0.521
1322.795	236109	0.5	311706	1.5	-0.89	5.01E+08	0.615
1324.091	236059	2.5	311582	3.5	-0.88	5.06E+08	0.576
1328.768	234036	4.5	309294	3.5	-0.53	1.10E+09	-0.81
1329.209	234036	4.5	309269	5.5	-0.01	3.70E+09	0.785
1330.143	227801	5.5	302980	4.5	-0.79	6.02E+08	0.258
1332.134	229588	3.5	304655	3.5	-0.77	6.41E+08	0.473
1332.142	265752	4.5	340820	3.5	0.09	4.68E+09	0.937
1336.241	265886	2.5	340723	2.5	-0.99	3.88E+08	-0.521
1337.832	265975	3.5	340723	2.5	-0.15	2.64E+09	0.93
1338.339	235053	3.5	309772	4.5	-0.72	7.13E+08	-0.176
1340.542	265886	2.5	340483	1.5	-0.77	6.35E+08	0.747
1341.968	235053	3.5	309570	2.5	-0.97	3.90E+08	-0.855
1342.415	256272	3.5	330765	2.5	-0.5	1.18E+09	-0.868
1347.86	226889	1.5	301081	2.5	-0.64	8.29E+08	-0.346
1348.545	265692	1.5	339846	0.5	-0.65	8.21E+08	0.922
1349.703	226311	5.5	300401	5.5	-0.61	9.02E+08	-0.625
1352.186	234036	4.5	307991	3.5	-0.83	5.44E+08	-0.603
1357.075	256273	2.5	329961	1.5	-0.9	4.57E+08	-0.736
1359.819	228048	4.5	301587	3.5	-0.5	1.13E+09	0.506
1359.886	227801	5.5	301336	6.5	-0.43	1.34E+09	0.375
1360.503	243140	2.5	316643	3.5	-0.42	1.40E+09	0.648
1360.696	265886	2.5	339378	1.5	-0.61	9.04E+08	0.572
1363.042	228020	3.5	301386	4.5	-0.99	3.67E+08	0.225
1365.395	228048	4.5	301286	5.5	-0.76	6.20E+08	0.28
1368.605	256272	3.5	329340	2.5	-0.79	5.86E+08	-0.744
1372.552	235053	3.5	307910	2.5	-0.78	5.86E+08	-0.651
1377.986	238305	5.5	310875	4.5	-1	3.54E+08	0.68
1379.565	236331	3.5	308818	4.5	-0.76	6.24E+08	0.744
1384.093	238234	6.5	310483	5.5	-0.81	5.35E+08	0.857
1388.904	229588	3.5	301587	3.5	-0.93	4.05E+08	0.477
1399.251	238305	5.5	309772	4.5	-0.93	4.00E+08	-0.829
1407.747	238234	6.5	309269	5.5	-0.62	8.12E+08	0.808
1420.057	234036	4.5	304456	4.5	-0.52	1.01E+09	-0.634
1425.19	246477	2.5	316643	3.5	-0.65	7.22E+08	0.748
1427.415	236059	2.5	306116	2.5	-0.91	4.15E+08	0.59
1436.73	235053	3.5	304655	3.5	-0.98	3.42E+08	-0.3
1446.715	236331	3.5	305453	3.5	-0.73	6.01E+08	0.702
1475.775	236331	3.5	304092	4.5	-0.91	3.85E+08	0.837
1482.815	236040	1.5	303479	2.5	-0.91	3.82E+08	0.819
1537.151	278282	4.5	343337	3.5	-0.79	4.51E+08	0.828

Cu VI

Energy Levels

Table A7: Comparison between available experimental data and calculated even energy levels (in cm^{-1}) in Cu VI

E^{a}_{exp}	E^{b}_{calc}	ΔE	J	Leading components (in %) in LS coupling ^{c}
0	−84	84	4	99 $3d^6\ ^5D$
1195.8	1124	72	3	100 $3d^6\ ^5D$
1986.8	1925	62	2	99 $3d^6\ ^5D$
2489.4	2435	54	1	99 $3d^6\ ^5D$
2733.4	2683	50	0	99 $3d^6\ ^5D$
29285	29833	−548	2	60 $3d^6\ ^3P$ + 38 $3d^6\ ^3P$
30417.6	30593	−175	6	99 $3d^6\ ^3H$
31009.2	31085	−76	5	95 $3d^6\ ^3H$ + 5 $3d^6\ ^3G$
31287.6	31238	50	4	78 $3d^6\ ^3H$ + 9 $3d^6\ ^3F$ + 7 $3d^6\ ^3G$
32684.9	33379	−694	1	61 $3d^6\ ^3P$ + 37 $3d^6\ ^3P$
32756	32863	−107	4	61 $3d^6\ ^3F$ + 18 $3d^6\ ^3F$ + 17 $3d^6\ ^3H$
33295.8	33384	−88	3	74 $3d^6\ ^3F$ + 20 $3d^6\ ^3F$ + 6 $3d^6\ ^3G$
33739.6	33871	−131	2	80 $3d^6\ ^3F$ + 19 $3d^6\ ^3F$
33867.8	34556	−688	0	59 $3d^6\ ^3P$ + 36 $3d^6\ ^3P$
37378.1	37313	65	5	95 $3d^6\ ^3G$ + 5 $3d^6\ ^3H$
38468.9	38428	41	4	90 $3d^6\ ^3G$ + 6 $3d^6\ ^3F$
38907.4	38799	108	3	93 $3d^6\ ^3G$ + 5 $3d^6\ ^3F$
46405.8	46390	16	6	99 $3d^6\ ^1I$
46714.2	46253	461	2	97 $3d^6\ ^3D$
46848.3	46295	553	1	99 $3d^6\ ^3D$
47119.1	46637	482	3	99 $3d^6\ ^3D$
47611.6	46790	822	4	64 $3d^6\ ^1G$ + 32 $3d^6\ ^1G$
53786.6	51951	1836	0	75 $3d^6\ ^1S$ + 21 $3d^6\ ^1S$
54747.1	56277	−1530	2	76 $3d^6\ ^1D$ + 21 $3d^6\ ^1D$
64967.6	65300	−332	3	97 $3d^6\ ^1F$
74712	74760	−48	0	63 $3d^6\ ^3P$ + 37 $3d^6\ ^3P$
75774.1	75865	−91	1	62 $3d^6\ ^3P$ + 38 $3d^6\ ^3P$
77145	77096	49	2	80 $3d^6\ ^3F$ + 19 $3d^6\ ^3F$
77223.8	77161	63	4	77 $3d^6\ ^3F$ + 22 $3d^6\ ^3F$
77467.9	77433	35	3	77 $3d^6\ ^3F$ + 20 $3d^6\ ^3F$
77908.8	78179	−270	2	60 $3d^6\ ^3P$ + 39 $3d^6\ ^3P$
87505.9	87861	−355	4	65 $3d^6\ ^1G$ + 34 $3d^6\ ^1G$
117084.3	116858	226	2	78 $3d^6\ ^1D$ + 22 $3d^6\ ^1D$
250876.6	250877	0	3	100 $3d^5(6S)4s\ ^7S$
265639.1	265603	36	2	100 $3d^5(6S)4s$ 5S
299143	299305	−162	6	100 $3d^5(4G)4s\ ^5G$
299250.6	299155	96	2	99 $3d^5(4G)4s\ ^5G$
299256	299330	−74	5	100 $3d^5(4G)4s\ ^5G$
299282.1	299226	56	3	99 $3d^5(4G)4s\ ^5G$
299292.9	299293	0	4	100 $3d^5(4G)4s\ ^5G$
308997.5	309110	−113	5	99 $3d^5(4G)4s\ ^3G$
309046.1	308936	110	3	49 $3d^5(4G)4s\ ^3G$ + 43 $3d^5(4D)4s\ ^5D$ + 7 $3d^5(4P)4s\ ^5P$
309110.8	309120	−9	4	98 $3d^5(4G)4s\ ^3G$
322791.9	322686	106	5	98 $3d^5(2I)4s\ ^3I$
322804.7	322780	25	6	98 $3d^5(2I)4s\ ^3I$
322877.3	322955	−78	7	100 $3d^5(2I)4s\ ^3I$

a: Experimental energies from [31]
b: This work
c: Only the components ≥ to 5% are given

Table A8: Comparison between available experimental data and calculated odd energy levels (in cm^{-1}) in Cu VI

E$^a_{exp}$	E$^b_{calc}$	ΔE	J	Leading components (in %) in LS coupling ^{c}
342225.2	342141	84	2	98 3d^5(6S)4p ^{7}P
343276.6	343180	97	3	97 3d^5(6S)4p ^{7}P
345137.1	345018	119	4	100 3d^5(6S)4p ^{7}P
355259.2	355237	22	3	95 3d^5(6S)4p ^{5}P
356137.2	356133	4	2	96 3d^5(6S)4p ^{5}P
356674	356681	−7	1	97 3d^5(6S)4p ^{5}P
388191.7	388311	−119	2	89 3d^5(4G)4p ^{5}G + 5 3d^5(4G)4p ^{3}F
388236.1	388349	−113	3	77 3d^5(4G)4p ^{5}G + 16 3d^5(4G)4p ^{5}H
388312.3	388472	−160	4	73 3d^5(4G)4p ^{5}G + 20 3d^5(4G)4p ^{5}H
388442.1	388673	−231	5	73 3d^5(4G)4p ^{5}G + 20 3d^5(4G)4p ^{5}H
388707.5	389019	−312	6	78 3d^5(4G)4p ^{5}G + 16 3d^5(4G)4p ^{5}H
390618.2	390155	463	3	81 3d^5(4G)4p ^{5}H + 13 3d^5(4G)4p ^{5}G
391198.1	390846	352	4	74 3d^5(4G)4p ^{5}H + 17 3d^5(4G)4p ^{5}G + 5 3d^5(4G)4p ^{5}F
391691.7	391484	208	5	63 3d^5(4G)4p ^{5}H + 19 3d^5(4G)4p ^{5}F + 12 3d^5(4G)4p ^{5}G
391986.5	391562	425	2	50 3d^5(4P)4p ^{5}D + 18 3d^5(4D)4p ^{5}D + 11 3d^5(4D)4p ^{5}F
392255.1	391888	367	3	35 3d^5(4P)4p ^{5}D + 20 3d^5(4G)4p ^{5}F + 14 3d^5(4D)4p ^{5}F
392516.7	392483	34	5	65 3d^5(4G)4p ^{5}F + 13 3d^5(4G)4p ^{5}H + 10 3d^5(4G)4p ^{5}G
392593.6	392347	247	6	80 3d^5(4G)4p ^{5}H + 18 3d^5(4G)4p ^{5}G
392712.6	392579	134	4	58 3d^5(4G)4p ^{5}F + 13 3d^5(4D)4p ^{5}F + 8 3d^5(4P)4p ^{5}D
393090.2	392801	289	7	100 3d^5(4G)4p ^{5}H
393425.4	393484	−59	2	63 3d^5(4P)4p ^{5}S + 10 3d^5(4P)4p ^{3}P + 8 3d^5(4G)4p ^{5}F
394014.7	393843	172	1	66 3d^5(4G)4p ^{5}F + 18 3d^5(4D)4p ^{5}F + 7 3d^5(4F)4p ^{5}F
394117.4	393985	132	3	53 3d^5(4G)4p ^{5}F + 16 3d^5(4P)4p ^{5}D + 12 3d^5(4P)4p ^{5}P
394133.8	394018	116	2	55 3d^5(4G)4p ^{5}F + 16 3d^5(4P)4p ^{5}D + 10 3d^5(4P)4p ^{5}S
395407.1	395136	271	4	58 3d^5(4P)4p ^{5}D + 19 3d^5(4G)4p ^{5}F + 17 3d^5(4D)4p ^{5}D
395601	395515	86	3	38 3d^5(4P)4p ^{5}P + 32 3d^5(4D)4p ^{5}P + 15 3d^5(4P)4p ^{5}D
396283.7	396337	−53	2	53 3d^5(4P)4p ^{5}P + 26 3d^5(4D)4p ^{5}P + 7 3d^5(4P)4p ^{5}S
396454.5	396408	47	2	78 3d^5(4G)4p ^{3}F + 5 3d^5(4G)4p ^{5}G
396523.6	396301	223	1	68 3d^5(4P)4p ^{5}P + 12 3d^5(4D)4p ^{5}P + 9 3d^5(4P)4p ^{3}P
396617.1	396817	−200	3	80 3d^5(4G)4p ^{3}F
396929.1	397233	−304	4	86 3d^5(4G)4p ^{3}F + 5 3d^5(4F)4p ^{3}F
397404.4	397291	113	6	91 3d^5(4G)4p ^{3}H
398022.8	397796	227	5	93 3d^5(4G)4p ^{3}H
398273.1	398215	58	2	44 3d^5(4P)4p ^{3}P + 16 3d^5(4D)4p ^{3}P + 14 3d^5(4P)4p ^{5}S
398376.6	398048	329	4	94 3d^5(4G)4p ^{3}H
398722.7	398594	129	1	44 3d^5(4P)4p ^{3}P + 16 3d^5(4D)4p ^{3}P + 9 3d^5(4P)4p ^{5}P
399112.8	399062	51	1	63 3d^5(4D)4p ^{5}F + 23 3d^5(4G)4p ^{5}F + 7 3d^5(4P)4p ^{3}P
399329	399161	168	0	61 3d^5(4P)4p ^{3}P + 20 3d^5(4D)4p ^{3}P + 12 3d^5(4D)4p ^{5}D
399434.6	399401	34	2	68 3d^5(4D)4p ^{5}F + 20 3d^5(4G)4p ^{5}F
399881.3	399835	46	3	69 3d^5(4D)4p ^{5}F + 13 3d^5(4G)4p ^{5}F
400562.7	400563	0	4	73 3d^5(4D)4p ^{5}F + 10 3d^5(4G)4p ^{5}F + 9 3d^5(4P)4p ^{5}D
401264.1	401233	31	5	89 3d^5(4D)4p ^{5}F + 7 3d^5(4G)4p ^{5}F
402134.1	401793	341	3	48 3d^5(4D)4p ^{5}D + 17 3d^5(4P)4p ^{5}D + 17 3d^5(4P)4p ^{3}D
402534.3	402164	370	4	67 3d^5(4D)4p ^{5}D + 20 3d^5(4P)4p ^{5}D + 5 3d^5(4F)4p ^{5}D
402766.8	402492	275	2	51 3d^5(4D)4p ^{5}D + 16 3d^5(4P)4p ^{3}D + 16 3d^5(4P)4p ^{5}D
402988.8	402994	−5	3	87 3d^5(4G)4p ^{3}G
403086.6	403204	−117	4	89 3d^5(4G)4p ^{3}G
403132.9	403356	−223	5	91 3d^5(4G)4p ^{3}G
403358	403166	192	1	46 3d^5(4D)4p ^{5}D + 15 3d^5(4P)4p ^{5}D + 13 3d^5(4P)4p ^{3}D
403366	403234	132	3	55 3d^5(4P)4p ^{3}D + 14 3d^5(4D)4p ^{5}P + 8 3d^5(4D)4p ^{3}F
403961.1	403895	66	2	51 3d^5(4P)4p ^{3}D + 17 3d^5(4D)4p ^{5}P + 6 3d^5(4P)4p ^{5}P
404096.2	404155	−59	1	38 3d^5(4P)4p ^{3}D + 34 3d^5(4D)4p ^{5}P + 11 3d^5(4D)4p ^{3}D
404184	403885	299	0	60 3d^5(4D)4p ^{5}D + 21 3d^5(4P)4p ^{5}D + 13 3d^5(4P)4p ^{3}P
404901.7	404853	49	1	37 3d^5(4D)4p ^{5}P + 18 3d^5(4P)4p ^{3}D + 17 3d^5(4D)4p ^{5}D
405213.5	404932	282	3	47 3d^5(4D)4p ^{3}D + 14 3d^5(4D)4p ^{5}D + 12 3d^5(4P)4p ^{5}P
405505.8	405583	−77	2	37 3d^5(4D)4p ^{5}P + 19 3d^5(4P)4p ^{5}P + 14 3d^5(4D)4p ^{5}D
406659.4	406340	319	2	68 3d^5(4D)4p 3D + 9 3d^5(4D)4p ^{5}P + 8 3d^5(4F)4p 3D
406752.6	406794	−41	3	35 3d^5(4D)4p ^{5}P + 29 3d^5(4D)4p 3D + 19 3d^5(4P)4p ^{5}P
407217.4	406829	388	1	58 3d^5(4D)4p 3D + 22 3d^5(4P)4p 3D + 11 3d^5(4F)4p 3D
407355.9	407418	−62	4	80 3d^5(4D)4p ^{3}F + 5 3d^5(2G)4p ^{3}F
408177.6	408244	−66	3	68 3d^5(4D)4p ^{3}F + 10 3d^5(4P)4p 3D + 5 3d^5(2G)4p ^{3}F
408281.7	408282	0	2	74 3d^5(4D)4p ^{3}F + 10 3d^5(4P)4p 3D + 5 3d^5(2G)4p ^{3}F
410288.7	410132	157	1	88 3d^5(4P)4p ^{3}S
411872.1	411571	301	6	72 3d^5(2I)4p ^{3}K + 22 3d^5(2I)4p ^{3}I
412326.4	412417	−91	5	60 3d^5(2I)4p ^{3}I + 20 3d^5(2I)4p ^{1}H + 8 3d^5(2I)4p ^{3}H
412439.9	412338	102	7	59 3d^5(2I)4p ^{3}K + 30 3d^5(2I)4p ^{3}I + 9 3d^5(2I)4p 1K
412469.3	412937	−468	0	73 3d^5(4D)4p ^{3}P + 21 3d^5(4P)4p ^{3}P
413072.5	413620	−548	1	64 3d^5(4D)4p ^{3}P + 20 3d^5(4P)4p ^{3}P + 6 3d^5(4P)4p ^{3}S
413692	413746	−54	2	30 3d^5(2F)4p ^{3}F + 27 3d^5(2D)4p ^{3}F + 9 3d^5(2D)4p ^{3}F
414203.7	414269	−65	6	52 3d^5(2I)4p ^{3}I + 22 3d^5(2I)4p ^{3}H + 21 3d^5(2I)4p ^{3}K
414298.5	414354	−56	2	61 3d^5(4D)4p ^{3}P + 23 3d^5(4P)4p ^{3}P + 6 3d^5(2D)4p ^{3}P
415258.3	414553	705	3	32 3d^5(2D)4p ^{3}F + 22 3d^5(2F)4p ^{3}F + 14 3d^5(2F)4p ^{3}G
415520	415237	283	8	100 3d^5(2I)4p ^{3}K
415694.4	415718	−24	7	65 3d^5(2I)4p ^{3}I + 35 3d^5(2I)4p ^{3}K
415851.8	415791	61	2	24 3d^5(2D)4p ^{1}D + 19 3d^5(2D)4p ^{3}F + 16 3d^5(2F)4p ^{1}D
416024.9	416303	−278	5	46 3d^5(2I)4p ^{1}H + 31 3d^5(2I)4p ^{3}I + 7 3d^5(2I)4p ^{3}H
416410.9	416685	−274	6	67 3d^5(2I)4p ^{3}H + 20 3d^5(2I)4p ^{3}I
417099.5	416822	278	4	34 3d^5(2D)4p ^{3}F + 26 3d^5(2F)4p ^{3}F + 20 3d^5(2F)4p ^{3}G
417221.3	417595	−374	5	73 3d^5(2I)4p ^{3}H + 14 3d^5(2I)4p ^{1}H
417267.3	416949	318	7	89 3d^5(2I)4p 1K + 5 3d^5(2I)4p ^{3}K
417511.5	417362	150	4	70 3d^5(2I)4p ^{3}H + 8 3d^5(2G)4p ^{3}H
419364.9	419479	−114	4	37 3d^5(2F)4p ^{1}G + 12 3d^5(2I)4p ^{3}H + 10 3d^5(2F)4p ^{3}G
419365.2	419002	363	2	37 3d^5(2D)4p ^{3}P + 12 3d^5(2D)4p ^{3}P + 11 3d^5(2F)4p ^{3}D
419605.8	419346	260	1	33 3d^5(2D)4p ^{3}P + 25 3d^5(2D)4p ^{3}D + 10 3d^5(2D)4p ^{3}P
419864.2	419166	698	3	36 3d^5(2F)4p ^{3}G + 25 3d^5(2F)4p ^{3}F + 17 3d^5(2D)4p ^{1}F
420151.2	419979	172	2	73 3d^5(4F)4p ^{5}G + 7 3d^5(2F)4p ^{3}F
420201.1	420068	133	3	75 3d^5(4F)4p ^{5}G + 7 3d^5(2F)4p ^{3}G
420355.8	420300	56	3	34 3d^5(2F)4p ^{3}D + 30 3d^5(2D)4p ^{3}D + 11 3d^5(2D)4p ^{3}D
420699.4	420569	130	4	64 3d^5(4F)4p ^{5}G + 5 3d^5(2F)4p ^{1}G + 5 3d^5(4F)4p ^{5}F
420914.7	420771	144	5	53 3d^5(4F)4p ^{5}G + 9 3d^5(4F)4p ^{5}F + 8 3d^5(2G)4p ^{3}H
421423.5	421052	372	0	64 3d^5(2D)4p ^{3}P + 20 3d^5(2D)4p ^{3}P + 9 3d^5(4F)4p ^{5}D
421467.7	421427	41	2	44 3d^5(2D)4p ^{3}D + 15 3d^5(2D)4p 3D + 14 3d^5(4F)4p ^{5}F

Table A8: Continued

E^a_{exp}	E^b_{calc}	ΔE	J	Leading components (in %) in LS coupling ^{c}
421516.1	421296	220	1	28 3d^5(2D)4p ^{3}D + 24 3d^5(2D)4p ^{3}P + 10 3d^5(2D)4p 3D
421622.9	421647	−24	3	33 3d^5(2F)4p ^{3}D + 12 3d^5(2D)4p ^{3}D + 11 3d^5(2D)4p ^{3}F
421924.7	421657	268	4	31 3d^5(2F)4p ^{3}F + 26 3d^5(2F)4p ^{3}G + 12 3d^5(4F)4p ^{5}F
422221.2	422297	−76	3	55 3d^5(4F)4p ^{5}F + 23 3d^5(4F)4p ^{5}D
422269.8	422079	191	6	62 3d^5(4F)4p ^{5}G + 15 3d^5(2I)4p ^{1}I + 12 3d^5(2G)4p ^{3}H
422425.6	422346	80	4	32 3d^5(4F)4p ^{5}F + 22 3d^5(4F)4p ^{5}D + 16 3d^5(2F)4p ^{3}F
422613.1	422699	−86	2	49 3d^5(4F)4p ^{5}F + 25 3d^5(4F)4p ^{5}D + 8 3d^5(2D)4p ^{3}D
422833.7	422345	489	5	53 3d^5(2F)4p ^{3}G + 23 3d^5(4F)4p ^{5}G + 8 3d^5(2H)4p ^{3}G
422841.4	422565	276	4	33 3d^5(2G)4p ^{3}H + 31 3d^5(2H)4p ^{3}H + 5 3d^5(4F)4p ^{5}F
422858.7	422845	14	6	63 3d^5(2I)4p ^{1}I + 26 3d^5(4F)4p ^{5}G + 5 3d^5(2H)4p ^{3}H
423078	422925	153	1	33 3d^5(2F)4p ^{3}D + 25 3d^5(2D)4p ^{1}P + 21 3d^5(4F)4p ^{5}F
423123.7	423192	−68	5	37 3d^5(4F)4p ^{5}F + 29 3d^5(2F)4p ^{3}G + 9 3d^5(4F)4p ^{5}G
423304.7	423326	−21	1	50 3d^5(4F)4p ^{5}F + 15 3d^5(4F)4p ^{5}D + 10 3d^5(2D)4p ^{3}D
423374.7	423293	82	2	29 3d^5(2F)4p ^{3}F + 19 3d^5(2F)4p ^{3}D + 16 3d^5(2D)4p ^{3}F
423403.4	422923	480	3	17 3d^5(2F)4p ^{3}G + 15 3d^5(2D)4p ^{3}F + 13 3d^5(2F)4p ^{3}F
423618.3	423551	67	5	29 3d^5(2G)4p ^{3}H + 28 3d^5(4F)4p ^{5}F + 24 3d^5(2H)4p ^{3}H
424332.5	424006	327	4	16 3d^5(2D)4p ^{3}F + 15 3d^5(2H)4p ^{3}G
424482.8	424558	−75	3	17 3d^5(2D)4p ^{1}F + 16 3d^5(2F)4p ^{3}G + 7 3d^5(2F)4p ^{3}G
424511.8	424603	−91	2	40 3d^5(2F)4p ^{3}D + 10 3d^5(2D)4p ^{3}P + 9 3d^5(4F)4p ^{5}F
424590.4	424758	−168	5	43 3d^5(2H)4p ^{3}G + 13 3d^5(2G)4p ^{3}G + 9 3d^5(2F)4p ^{3}G
424697.7	424804	−106	4	24 3d^5(2H)4p ^{3}G + 10 3d^5(2G)4p ^{3}G + 7 3d^5(2F)4p ^{3}G
425101.8	425296	−194	4	41 3d^5(4F)4p ^{5}D + 25 3d^5(4F)4p ^{5}F + 5 3d^5(4F)4p ^{5}G
425544.3	425465	79	6	30 3d^5(2H)4p ^{3}H + 29 3d^5(2G)4p ^{3}H + 17 3d^5(2I)4p ^{1}I
425599.1	425439	160	3	25 3d^5(2H)4p ^{3}G + 14 3d^5(2G)4p ^{3}G + 6 3d^5(2D)4p ^{1}F
425877	425993	−116	3	57 3d^5(4F)4p ^{5}D + 21 3d^5(4F)4p ^{5}F + 5 3d^5(4D)4p ^{5}D
425954.6	426044	−89	0	87 3d^5(4F)4p ^{5}D + 7 3d^5(2D)4p ^{3}P
426008.4	426107	−99	1	73 3d^5(4F)4p ^{5}D + 10 3d^5(4F)4p ^{5}F
426112.6	426272	−159	2	59 3d^5(4F)4p ^{5}D + 15 3d^5(4F)4p ^{5}F + 6 3d^5(2F)4p ^{3}D
427330.6	426943	388	5	80 3d^5(2H)4p ^{3}I + 9 3d^5(2H)4p ^{3}H + 5 3d^5(2G)4p ^{3}H
427367.3	427382	−15	4	19 3d^5(2F)4p ^{1}G + 17 3d^5(2G)4p ^{1}G + 16 3d^5(2G)4p ^{3}G
427940.9	427716	225	3	29 3d^5(2G)4p ^{3}G + 22 3d^5(4F)4p ^{3}G + 9 3d^5(2G)4p ^{3}F
428048.7	427903	146	1	34 3d^5(2F)4p 3D + 31 3d^5(2D)4p ^{1}P + 8 3d^5(2D)4p ^{1}P
428386	428190	196	5	63 3d^5(4F)4p ^{3}G + 11 3d^5(2G)4p ^{3}G + 11 3d^5(4F)4p ^{5}F
428430.6	428144	287	6	70 3d^5(2H)4p ^{3}I + 11 3d^5(2H)4p ^{1}I + 8 3d^5(2G)4p ^{3}H
428503.5	428561	−58	2	47 3d^5(2F)4p ^{1}D + 22 3d^5(2D)4p ^{1}D + 9 3d^5(2G)4p ^{3}F
428672.9	428362	311	4	55 3d^5(4F)4p ^{3}G + 13 3d^5(2G)4p ^{3}G + 6 3d^5(2F)4p ^{1}G
429135.6	429119	17	3	30 3d^5(4F)4p ^{3}G + 26 3d^5(2G)4p ^{3}F + 17 3d^5(2F)4p ^{1}F
429577.5	429705	−128	4	46 3d^5(2G)4p ^{3}F + 15 3d^5(2G)4p ^{1}G + 9 3d^5(2F)4p ^{1}G
429657.4	429915	−258	2	51 3d^5(2G)4p ^{3}F + 10 3d^5(4F)4p ^{3}F + 7 3d^5(4D)4p ^{3}F
429749.9	429487	263	7	94 3d^5(2H)4p ^{3}I
429873.4	429616	257	3	40 3d^5(2F)4p ^{1}F + 28 3d^5(2G)4p ^{3}F + 6 3d^5(4F)4p 3D
431218.3	430922	296	6	72 3d^5(2H)4p ^{1}I + 11 3d^5(2H)4p ^{3}H + 10 3d^5(2H)4p ^{3}I
431231.7	431470	−238	2	46 3d^5(4F)4p ^{3}D + 14 3d^5(2F)4p ^{1}D + 10 3d^5(2F)4p ^{3}F
431530.7	431645	−114	3	39 3d^5(4F)4p ^{3}D + 12 3d^5(2F)4p ^{3}D + 12 3d^5(2F)4p ^{3}F
431766.6	432093	−326	4	56 3d^5(4F)4p ^{3}F + 25 3d^5(2F)4p ^{3}F
432272.4	432478	−206	1	76 3d^5(4F)4p ^{3}D + 7 3d^5(4D)4p ^{3}D + 6 3d^5(2F)4p ^{3}D
432839.7	433122	−282	3	57 3d^5(4F)4p ^{3}F + 17 3d^5(4F)4p ^{3}D + 11 3d^5(2F)4p ^{3}F
432840.8	432637	204	5	31 3d^5(2G)4p ^{3}H + 25 3d^5(2G)4p ^{3}G + 21 3d^5(2H)4p ^{3}H
432939.3	432771	168	4	38 3d^5(2H)4p ^{3}H + 28 3d^5(2G)4p ^{3}H + 7 3d^5(2H)4p ^{1}G
433257.9	433681	−423	2	56 3d^5(4F)4p ^{3}F + 14 3d^5(4F)4p ^{3}D + 14 3d^5(2F)4p ^{3}F
434063.7	433893	171	5	24 3d^5(2F)4p ^{3}G + 21 3d^5(2H)4p ^{3}H + 18 3d^5(2G)4p ^{3}G
434264	434216	48	3	29 3d^5(2F)4p ^{3}G + 25 3d^5(4F)4p ^{3}G + 25 3d^5(2G)4p ^{3}G
434286.4	434177	109	4	25 3d^5(2F)4p ^{3}G + 15 3d^5(4F)4p ^{3}G + 12 3d^5(2H)4p ^{3}H
434722.8	434735	−12	6	44 3d^5(2G)4p ^{3}H + 36 3d^5(2H)4p ^{3}H + 15 3d^5(2H)4p ^{1}I
434812.2	434270	542	4	32 3d^5(2F)4p ^{1}G + 19 3d^5(2G)4p ^{3}G + 12 3d^5(2G)4p ^{1}G
435369.7	435912	−542	3	33 3d^5(2G)4p ^{1}F + 27 3d^5(2F)4p ^{3}F + 7 3d^5(4F)4p ^{3}F
435379.2	435701	−322	2	35 3d^5(2F)4p ^{1}D + 19 3d^5(4F)4p ^{3}F + 14 3d^5(4F)4p 3D
435676.7	435632	45	5	51 3d^5(2G)4p ^{1}H + 24 3d^5(2H)4p ^{1}H + 13 3d^5(2I)4p ^{1}H
436243.7	436572	−328	3	31 3d^5(2G)4p ^{1}F + 21 3d^5(2F)4p ^{3}F + 11 3d^5(2G)4p ^{3}F
436475.9	436626	−150	2	41 3d^5(2F)4p ^{3}F + 32 3d^5(2F)4p ^{1}D + 12 3d^5(2G)4p ^{3}F
436506.5	436937	−431	4	48 3d^5(2F)4p ^{3}F + 18 3d^5(4F)4p ^{3}F + 7 3d^5(2F)4p ^{1}G
437233.9	437113	121	5	63 3d^5(2H)4p ^{1}H + 27 3d^5(2G)4p ^{1}H
438607.7	438028	580	1	54 3d^5(2F)4p ^{3}D + 25 3d^5(2S)4p ^{3}P + 5 3d^5(2D)4p ^{3}P
439180.1	438670	510	3	56 3d^5(2F)4p ^{3}D + 17 3d^5(4F)4p ^{3}D + 9 3d^5(2F)4p ^{3}D
439327.1	438564	763	2	70 3d^5(2F)4p ^{3}D + 8 3d^5(2F)4p ^{3}D + 6 3d^5(4F)4p ^{3}D
439706.8	439557	150	3	45 3d^5(2H)4p ^{3}G + 31 3d^5(2F)4p ^{3}G + 11 3d^5(2G)4p ^{3}G
439775	439309	466	1	54 3d^5(2S)4p ^{3}P + 27 3d^5(2F)4p ^{3}D + 8 3d^5(2D)4p ^{3}P
440372.2	440206	166	4	40 3d^5(2H)4p ^{3}G + 41 3d^5(2F)4p ^{3}G + 9 3d^5(2G)4p ^{3}G
440896.3	440593	303	5	53 3d^5(2F)4p ^{3}G + 34 3d^5(2H)4p ^{3}G + 8 3d^5(2G)4p ^{3}G
441375.8	441168	208	2	72 3d^5(2S)4p ^{3}P + 16 3d^5(2D)4p ^{3}P
443432.9	443588	−155	4	42 3d^5(2H)4p ^{1}G + 32 3d^5(2F)4p ^{1}G + 22 3d^5(2G)4p ^{1}G
444432.7	444820	−387	1	68 3d^5(2S)4p ^{1}P + 18 3d^5(2D)4p ^{1}P + 7 3d^5(2D)4p ^{1}P
445290.5	445891	−601	3	82 3d^5(2F)4p ^{1}F + 8 3d^5(2F)4p ^{1}F
453663.5	453452	212	2	55 3d^5(2D)4p ^{3}F + 31 3d^5(2D)4p 3D + 5 3d^5(2G)4p ^{3}F
454176.3	454028	148	3	42 3d^5(2D)4p ^{3}F + 33 3d^5(2D)4p 3D + 11 3d^5(2D)4p ^{1}F
454317.5	453641	677	1	89 3d^5(2D)4p ^{3}D
454921.2	454443	478	2	54 3d^5(2D)4p ^{3}D + 30 3d^5(2D)4p ^{3}F
456264.2	455816	448	3	54 3d^5(2D)4p ^{3}D + 38 3d^5(2D)4p ^{3}F
456545.2	456543	2	4	90 3d^5(2D)4p ^{3}F + 6 3d^5(2G)4p ^{3}F
457544.9	457456	89	3	69 3d^5(2D)4p ^{1}F + 12 3d^5(2G)4p ^{1}F + 10 3d^5(2D)4p ^{3}F
458688.9	459139	−450	0	84 3d^5(2D)4p ^{3}P + 14 3d^5(2S)4p ^{3}P
458731.8	459104	−372	2	66 3d^5(2D)4p ^{3}P + 16 3d^5(2S)4p ^{3}P + 7 3d^5(2D)4p 3D
458778.9	459173	−394	1	72 3d^5(2D)4p ^{3}P + 15 3d^5(2S)4p ^{3}P + 5 3d^5(2D)4p 3D
460536.5	460634	−98	1	70 3d^5(2D)4p ^{1}P + 16 3d^5(2S)4p ^{1}P + 7 3d^5(2D)4p ^{3}P
461609.3	461150	459	2	82 3d^5(2D)4p ^{1}D + 7 3d^5(2D)4p ^{3}P + 5 3d^5(2F)4p ^{1}D
464741.7	464767	−25	4	53 3d^5(2G)4p ^{3}H + 24 3d^5(2G)4p ^{3}F + 17 3d^5(2G)4p ^{3}G
465130.4	465125	5	4	54 3d^5(2G)4p ^{3}F + 33 3d^5(2G)4p ^{3}H + 5 3d^5(2G)4p ^{1}G
465460	465330	130	5	73 3d^5(2G)4p ^{3}H + 16 3d^5(2G)4p ^{3}G + 8 3d^5(2G)4p ^{1}H
465803.6	465969	−165	3	50 3d^5(2G)4p ^{3}F + 40 3d^5(2G)4p ^{3}G
467531.5	467729	−198	2	89 3d^5(2G)4p ^{3}F + 7 3d^5(2D)4p ^{3}F
467599.8	467392	208	6	97 3d^5(2G)4p ^{3}H
467819.2	467954	−135	3	54 3d^5(2G)4p ^{3}G + 39 3d^5(2G)4p ^{3}F
468335.2	468448	−113	4	79 3d^5(2G)4p ^{3}G + 9 3d^5(2G)4p ^{3}F + 8 3d^5(2G)4p ^{3}H
468738.6	468841	−102	5	75 3d^5(2G)4p ^{3}G + 20 3d^5(2G)4p ^{3}H

Table A8: Continued

E^a_{exp}	E^b_{calc}	ΔE	J	Leading components (in %) in LS coupling ^{c}
471595.2	471450	145	5	88 $3d^5$(2G)4p ^{1}H + 5 $3d^5$(2G)4p ^{3}G
471769.3	471973	−204	4	91 $3d^5$(2G)4p ^{1}G
473212.1	473441	−229	3	76 $3d^5$(2G)4p ^{1}F + 10 $3d^5$(2D)4p ^{1}F + 5 $3d^5$(2D)4p ^{1}F
481411.7	481292	120	0	74 $3d^5$(2P)4p ^{3}P + 21 $3d^5$(2D)4p ^{3}P
481793.2	481612	181	1	72 $3d^5$(2P)4p ^{3}P + 22 $3d^5$(2D)4p ^{3}P
483006.9	482815	192	2	70 $3d^5$(2P)4p ^{3}P + 24 $3d^5$(2D)4p ^{3}P
488810.3	488641	169	2	55 $3d^5$(2P)4p ^{3}D + 28 $3d^5$(2P)4p ^{1}D + 6 $3d^5$(2D)4p ^{1}D
488869.4	488819	50	1	88 $3d^5$(2P)4p ^{3}D + 6 $3d^5$(2D)4p ^{3}D
491155.1	491019	136	3	87 $3d^5$(2P)4p ^{3}D + 8 $3d^5$(2D)4p ^{3}D
491878.9	491764	115	2	46 $3d^5$(2P)4p ^{1}D + 34 $3d^5$(2P)4p ^{3}D + 12 $3d^5$(2D)4p ^{1}D
493316.5	493517	−201	1	80 $3d^5$(2P)4p ^{3}S + 14 $3d^5$(2P)4p ^{1}P
495292.7	494929	364	1	59 $3d^5$(2P)4p ^{1}P + 17 $3d^5$(2P)4p ^{3}S + 16 $3d^5$(2D)4p ^{1}P
502689	502588	101	2	61 $3d^5$(2D)4p ^{3}F + 19 $3d^5$(2D)4p ^{3}F + 8 $3d^5$(2D)4p ^{3}D
503114.1	502969	145	3	58 $3d^5$(2D)4p ^{3}F + 18 $3d^5$(2D)4p ^{3}F + 9 $3d^5$(2D)4p ^{3}D
504630.2	504513	117	1	70 $3d^5$(2D)4p ^{3}D + 21 $3d^5$(2D)4p ^{3}D + 7 $3d^5$(2P)4p ^{3}D
505107.8	504938	170	4	71 $3d^5$(2D)4p ^{3}F + 23 $3d^5$(2D)4p ^{3}F + 6 $3d^5$(2G)4p ^{3}F
507108.1	507066	42	3	58 $3d^5$(2D)4p ^{3}D + 18 $3d^5$(2D)4p ^{3}D + 10 $3d^5$(2D)4p ^{3}F
507132.9	507310	−177	2	41 $3d^5$(2D)4p ^{1}D + 17 $3d^5$(2P)4p ^{1}D + 14 $3d^5$(2D)4p ^{1}D
509325.1	509521	−196	2	41 $3d^5$(2D)4p ^{3}P + 21 $3d^5$(2P)4p ^{3}P + 15 $3d^5$(2D)4p ^{3}P
509967.2	509818	149	3	68 $3d^5$(2D)4p ^{1}F + 21 $3d^5$(2D)4p ^{1}F + 6 $3d^5$(2G)4p ^{1}F
510178.2	510388	−210	1	54 $3d^5$(2D)4p ^{3}P + 25 $3d^5$(2P)4p ^{3}P + 19 $3d^5$(2D)4p ^{3}P
510942.6	511192	−249	0	55 $3d^5$(2D)4p ^{3}P + 24 $3d^5$(2P)4p ^{3}P + 19 $3d^5$(2D)4p ^{3}P

a: Experimental energies from [31]

b: This work

c: Only the components ≥ to 5% are given

Transitions

Table A9: Computed oscillator strengths and transition probabilities in Cu VI.

Wavelength	Lower Level	J_{low}	Upper Level	J_{up}	log gf	gA	CF
228.143	30418	6	468739	5	-0.8	2.02E+10	0.354
228.662	31009	5	468335	4	-0.96	1.39E+10	0.286
231.825	37378	5	468739	5	-0.93	1.45E+10	-0.2
232.621	77224	4	507108	3	-0.6	3.13E+10	0.256
232.91	38469	4	467819	3	-1	1.22E+10	-0.341
232.992	77909	2	507108	3	-0.98	1.27E+10	0.515
233.926	77145	2	504630	1	-0.79	1.96E+10	0.376
234.241	64968	3	491879	2	-0.98	1.26E+10	-0.286
235.189	46406	6	471595	5	-0.27	6.42E+10	-0.424
235.238	0	4	425102	4	-0.64	2.80E+10	-0.265
235.471	1196	3	425877	3	-0.77	2.06E+10	-0.256
235.937	64968	3	488810	2	-0.92	1.43E+10	-0.439
236.708	87506	4	509967	3	-0.3	5.95E+10	0.396
237.4	1196	3	422426	4	-0.91	1.45E+10	-0.273
237.962	1987	2	422221	3	-0.81	1.84E+10	-0.282
238.025	2489	1	422613	2	-0.95	1.31E+10	-0.29
238.568	37378	5	456545	4	-0.93	1.39E+10	-0.201
239.228	47119	3	465130	4	-0.98	1.22E+10	-0.352
240.727	77909	2	493317	1	-0.62	2.79E+10	-0.777
241.306	77468	3	491879	2	-0.75	2.03E+10	-0.659
241.586	77224	4	491155	3	-0.24	6.56E+10	0.73
242.881	77145	2	488869	1	-0.61	2.77E+10	0.749
243.106	77468	3	488810	2	-0.7	2.24E+10	0.471
244.244	47119	3	456545	4	-1	1.13E+10	-0.5
244.412	47119	3	456264	3	-0.99	1.14E+10	-0.228
245.56	75774	1	483007	2	-0.96	1.22E+10	0.703
245.783	54747	2	461609	2	-0.75	1.93E+10	-0.28
245.851	53787	0	460537	1	-0.95	1.24E+10	-0.491
246.611	31009	5	436507	4	-0.9	1.37E+10	-0.382
246.854	77909	2	483007	2	-0.56	3.00E+10	-0.643
247.646	31009	5	434812	4	-0.71	2.09E+10	0.566
247.742	30418	6	434064	5	-0.11	8.45E+10	-0.656
247.968	31009	5	434286	4	-0.43	4.05E+10	-0.413
248.153	31288	4	434264	3	-0.4	4.35E+10	-0.461
248.426	0	4	402534	4	-0.1	8.51E+10	-0.872
248.495	30418	6	432841	5	-0.47	3.68E+10	0.622
248.673	0	4	402134	3	-0.96	1.19E+10	-0.278
248.86	31009	5	432841	5	-0.78	1.81E+10	-0.239
248.972	31288	4	432939	4	-0.91	1.33E+10	-0.122
249.022	1196	3	402767	2	-0.97	1.16E+10	-0.285
249.166	1196	3	402534	4	-0.85	1.51E+10	0.648
249.212	0	4	401264	5	-0.64	2.46E+10	-0.503
249.415	1196	3	402134	3	-0.71	2.10E+10	-0.362
249.827	2489	1	402767	2	-0.84	1.54E+10	0.57
249.908	1987	2	402134	3	-0.71	2.09E+10	0.581
250.396	1196	3	400563	4	-0.73	1.97E+10	-0.424
250.418	30418	6	429750	7	-0.62	2.57E+10	-0.81
250.62	32756	4	431767	4	-0.97	1.14E+10	-0.085
250.824	1196	3	399881	3	-0.92	1.27E+10	-0.406
250.898	31009	5	429578	4	-0.98	1.10E+10	-0.542
251.248	30418	6	428431	6	-0.91	1.29E+10	-0.639
251.276	30418	6	428386	5	-0.59	2.68E+10	-0.2
251.323	1987	2	399881	3	-0.98	1.10E+10	-0.252
251.352	31288	4	429136	3	-0.81	1.62E+10	-0.145
251.399	38469	4	436244	3	-0.79	1.71E+10	-0.255
251.459	47612	4	445291	3	-0.81	1.63E+10	0.114
251.469	31009	5	428673	4	-0.85	1.48E+10	-0.127
251.529	38907	3	436476	2	-0.97	1.12E+10	-0.297
251.622	31009	5	428431	6	-0.97	1.12E+10	-0.402
251.671	37378	5	434723	6	-0.43	3.93E+10	-0.82
251.924	2489	1	399435	2	-0.96	1.16E+10	-0.419
251.947	37378	5	434286	4	-0.47	3.60E+10	0.602
252.002	32756	4	429578	4	-0.75	1.87E+10	-0.17
252.089	37378	5	434064	5	-0.67	2.27E+10	0.211
252.117	64968	3	461609	2	-0.3	5.19E+10	-0.772
252.157	33296	3	429873	3	-0.73	1.97E+10	-0.323
252.225	38907	3	435379	2	-0.72	1.99E+10	-0.393
252.284	2733	0	399113	1	-1	1.04E+10	-0.68
252.307	38469	4	434812	4	-0.87	1.40E+10	-0.206
252.32	31009	5	427331	5	-0.89	1.34E+10	-0.697
252.377	2489	1	398723	1	-0.96	1.14E+10	-0.821
252.498	31288	4	427331	5	-1	1.04E+10	-0.326
252.578	33740	2	429657	2	-0.63	2.48E+10	-0.242
252.627	33296	3	429136	3	-0.8	1.68E+10	-0.162
252.642	38469	4	434286	4	-0.84	1.52E+10	0.176
252.656	38469	4	434264	3	-0.71	2.05E+10	0.604
252.78	0	4	395601	3	-0.15	7.46E+10	-0.673
252.784	38469	4	434064	5	-0.62	2.49E+10	-0.438
252.805	37378	5	432939	4	-0.92	1.26E+10	-0.54
252.868	37378	5	432841	5	-0.65	2.34E+10	-0.267
252.922	38907	3	434286	4	-0.93	1.22E+10	-0.404
252.936	38907	3	434264	3	-0.51	3.25E+10	0.492
253.083	30418	6	425544	6	-0.51	3.25E+10	-0.448
253.108	1196	3	396284	2	-0.32	4.99E+10	-0.831
253.382	46714	2	441376	2	-0.66	2.27E+10	-0.62
253.414	32756	4	427367	4	-0.94	1.20E+10	-0.11
253.462	1987	2	396524	1	-0.71	2.04E+10	-0.88
253.463	31009	5	425544	6	-0.86	1.43E+10	0.524
253.546	1196	3	395601	3	-0.98	1.08E+10	0.176
253.557	37378	5	431767	4	-0.79	1.67E+10	0.215
253.568	38469	4	432840	3	-0.84	1.50E+10	0.169
253.568	38469	4	432841	5	-0.92	1.26E+10	-0.216
253.607	31288	4	425599	3	-0.81	1.59E+10	-0.146
253.616	1987	2	396284	2	-0.74	1.90E+10	0.428
253.642	47119	3	441376	2	-0.39	4.28E+10	0.505
253.671	1196	3	395407	4	-0.53	3.07E+10	-0.456
253.691	33868	0	428049	1	-0.94	1.18E+10	0.278

Table A9: Continued

Wavelength	Lower Level	J_{Low}	Upper level	J_{Up}	log gf	gA	CF
253.696	30418	6	424590	5	-0.7	2.08E+10	-0.133
253.732	0	4	394117	3	-0.98	1.09E+10	0.233
253.785	2489	1	396524	1	-0.83	1.52E+10	0.567
253.787	38907	3	432939	4	-0.83	1.52E+10	-0.365
254.008	31009	5	424698	4	-0.47	3.54E+10	-0.378
254.056	1987	2	395601	3	-0.94	1.20E+10	-0.451
254.26	38469	4	431767	4	-0.98	1.08E+10	-0.228
254.5	46848	1	439775	1	-0.51	3.19E+10	-0.76
254.504	1196	3	394117	3	-0.46	3.56E+10	-0.429
254.529	117084	2	509967	3	-0.72	1.97E+10	0.691
254.639	0	4	392713	4	-0.65	2.30E+10	-0.383
254.643	30418	6	423124	5	-0.49	3.35E+10	0.579
254.704	46714	2	439327	2	-0.59	2.66E+10	-0.363
254.706	31009	5	423618	5	-0.56	2.85E+10	-0.534
254.766	0	4	392517	5	0.03	1.11E+11	-0.762
254.882	29285	2	421623	3	-0.52	3.08E+10	0.353
254.936	0	4	392255	3	-0.82	1.57E+10	0.385
254.945	117084	2	509325	2	-0.96	1.14E+10	0.597
254.967	47119	3	439327	2	-0.63	2.41E+10	-0.755
254.972	37378	5	429578	4	-0.57	2.79E+10	-0.33
255.006	1987	2	394134	2	-0.67	2.21E+10	-0.485
255.017	1987	2	394117	3	-0.51	3.16E+10	-0.346
255.062	47119	3	439180	3	-0.2	6.44E+10	-0.607
255.171	46714	2	438608	1	-0.49	3.35E+10	-0.803
255.21	32756	4	424590	5	-0.39	4.19E+10	-0.342
255.215	32685	1	424512	2	-0.41	3.93E+10	0.699
255.303	0	4	391692	5	-0.53	3.06E+10	0.791
255.334	2489	1	394134	2	-0.7	2.03E+10	-0.363
255.378	32756	4	424333	4	-0.69	2.10E+10	-0.23
255.393	31288	4	422841	4	-0.33	4.83E+10	0.573
255.411	2489	1	394015	1	-0.83	1.53E+10	-0.553
255.417	1196	3	392713	4	-0.26	5.58E+10	-0.439
255.418	77224	4	468739	5	-0.43	3.80E+10	0.729
255.49	38469	4	429873	3	-0.88	1.36E+10	-0.183
255.492	33296	3	424698	4	-0.92	1.24E+10	-0.155
255.571	2733	0	394015	1	-0.92	1.22E+10	-0.401
255.682	77224	4	468335	4	-0.67	2.18E+10	0.765
255.708	29285	2	420356	3	-0.27	5.51E+10	0.668
255.73	33296	3	424333	4	-0.68	2.15E+10	0.33
255.841	77468	3	468335	4	-0.68	2.16E+10	0.412
255.867	46406	6	437234	5	-0.94	1.17E+10	-0.049
255.918	38907	3	429657	2	-0.8	1.61E+10	-0.143
255.958	32685	1	423375	2	-0.76	1.78E+10	-0.728
256.156	77145	2	467532	2	-0.26	5.54E+10	0.739
256.179	77468	3	467819	3	-0.33	4.72E+10	0.745
256.234	1987	2	392255	3	-0.94	1.16E+10	0.16
256.358	29285	2	419365	2	-0.39	4.09E+10	-0.554
256.359	32756	4	422834	5	-0.75	1.82E+10	0.465
256.378	117084	2	507133	2	-0.41	3.93E+10	0.665
256.417	37378	5	427367	4	-0.84	1.48E+10	-0.176
256.617	54747	2	444433	1	-0.21	6.22E+10	0.867
256.628	32756	4	422426	4	-0.79	1.63E+10	-0.475
256.631	33740	2	423403	3	-0.71	1.96E+10	0.629
256.65	33740	2	423375	2	-0.47	3.44E+10	0.617
256.659	47612	4	437234	5	-0.46	3.49E+10	0.515
256.676	38907	3	428504	2	-0.85	1.42E+10	-0.558
256.814	47119	3	436507	4	-0.77	1.74E+10	-0.242
256.891	46406	6	435677	5	0.45	2.82E+11	0.959
256.931	33868	0	423078	1	-0.76	1.74E+10	0.643
256.958	32756	4	421925	4	-0.75	1.80E+10	0.223
257.024	31288	4	420356	3	-0.87	1.38E+10	-0.426
257.137	38469	4	427367	4	-0.66	2.22E+10	0.214
257.157	32756	4	421623	3	-0.99	1.04E+10	-0.127
257.181	32685	1	421516	1	-0.8	1.60E+10	-0.546
257.242	32685	1	421424	0	-0.96	1.11E+10	-0.67
257.295	77145	2	465804	3	-0.56	2.80E+10	-0.708
257.313	47612	4	436244	3	-0.46	3.51E+10	0.491
257.35	31288	4	419864	3	-0.86	1.39E+10	-0.23
257.509	77468	3	465804	3	-0.52	3.05E+10	0.384
257.618	33296	3	421468	2	-0.25	5.67E+10	-0.843
257.794	77224	4	465130	4	-0.18	6.58E+10	0.748
257.881	33740	2	421516	1	-0.56	2.72E+10	-0.844
257.893	47612	4	435370	3	-0.59	2.62E+10	0.43
257.998	32756	4	420356	3	-0.25	5.67E+10	0.588
258.053	77224	4	464742	4	-0.64	2.32E+10	0.454
258.215	77468	3	464742	4	-0.81	1.57E+10	-0.645
258.256	37378	5	424590	5	0.01	1.03E+11	-0.739
258.264	47612	4	434812	4	-0.48	3.35E+10	0.264
258.428	37378	5	424333	4	-0.73	1.85E+10	0.378
258.451	32685	1	419606	1	-1	9.82E+09	-0.327
258.604	38907	3	425599	3	-0.23	5.88E+10	-0.683
258.688	29285	2	415852	2	-0.94	1.14E+10	0.547
258.776	46406	6	432841	5	-0.81	1.54E+10	0.595
258.914	38469	4	424698	4	-0.23	5.91E+10	-0.584
258.917	31288	4	417512	4	-0.22	6.03E+10	-0.405
258.925	31009	5	417221	5	-0.01	9.77E+10	-0.69
259.058	38469	4	424483	3	-0.97	1.06E+10	-0.241
259.072	30418	6	416411	6	0.22	1.66E+11	-0.886
259.157	33740	2	419606	1	-0.83	1.46E+10	0.573
259.238	37378	5	423124	5	-0.66	2.18E+10	0.38
259.265	87506	4	473212	3	0.03	1.06E+11	0.746
259.353	38907	3	424483	3	-0.82	1.51E+10	-0.266
259.519	47612	4	432939	4	-0.55	2.83E+10	-0.657
259.554	30418	6	415694	7	-0.28	5.17E+10	-0.797
259.73	31009	5	416025	5	-0.74	1.82E+10	0.565
259.784	38469	4	423403	3	-0.73	1.86E+10	0.335
259.867	46406	6	431218	6	-0.04	9.03E+10	-0.896
259.905	32756	4	417512	4	-0.85	1.39E+10	-0.248
260.047	37378	5	421925	4	-0.72	1.88E+10	-0.288
260.1	38907	3	423375	2	-0.69	2.00E+10	-0.425
260.238	87506	4	471769	4	0.12	1.30E+11	0.764
260.356	87506	4	471595	5	-0.64	2.25E+10	0.574
260.472	47612	4	431531	3	-0.74	1.81E+10	-0.449
260.913	32756	4	416025	5	-0.95	1.10E+10	0.349
261.227	46848	1	429657	2	-0.77	1.69E+10	0.411
261.436	32756	4	415258	3	-0.8	1.54E+10	0.252

Table A9: Continued

Wavelength	Lower Level	J_{Low}	Upper level	J_{Up}	log gf	gA	CF
261.466	47119	3	429578	4	-0.7	1.96E+10	0.468
261.492	46714	2	429136	3	-0.83	1.46E+10	0.4
261.601	47612	4	429873	3	-0.04	8.97E+10	-0.631
261.765	30418	6	412440	7	-0.64	2.24E+10	0.646
261.789	37378	5	419365	4	-1	9.75E+09	0.324
261.803	47612	4	429578	4	-0.38	4.10E+10	0.575
261.966	54747	2	436476	2	-0.91	1.20E+10	0.491
262.107	47612	4	429136	3	-0.76	1.71E+10	0.345
262.126	54747	2	436244	3	-0.88	1.27E+10	-0.218
262.425	47612	4	428673	4	-0.88	1.27E+10	-0.449
262.44	31288	4	412326	5	-0.33	4.55E+10	-0.552
262.465	29285	2	410289	1	-0.34	4.40E+10	0.654
262.539	38469	4	419365	4	-0.99	9.91E+09	-0.225
262.562	31009	5	411872	6	-0.87	1.30E+10	0.483
262.589	77909	2	458732	2	-0.53	2.88E+10	-0.735
262.721	54747	2	435379	2	-0.94	1.10E+10	-0.301
262.727	54747	2	435370	3	-0.8	1.54E+10	-0.281
262.93	47612	4	427941	3	-0.66	2.10E+10	-0.323
262.934	64968	3	445291	3	0.02	1.02E+11	0.74
262.986	47119	3	427367	4	-0.99	9.93E+09	0.495
263.327	47612	4	427367	4	-0.5	3.08E+10	-0.345
263.756	46406	6	425544	6	-0.22	5.72E+10	0.908
263.829	37378	5	416411	6	-0.32	4.61E+10	0.388
264.025	38469	4	417221	5	-0.4	3.78E+10	0.411
264.128	38907	3	417512	4	-0.48	3.14E+10	0.383
264.225	64968	3	443433	4	-0.59	2.48E+10	0.269
264.302	77909	2	456264	3	-0.92	1.15E+10	-0.567
264.404	117084	2	495293	1	-0.11	7.46E+10	-0.806
264.828	32685	1	410289	1	-0.8	1.50E+10	-0.363
265.191	47612	4	424698	4	-0.89	1.23E+10	-0.333
265.615	54747	2	431232	2	-0.81	1.44E+10	0.438
265.637	46406	6	422859	6	0.19	1.47E+11	0.711
265.768	77909	2	454176	3	-0.98	9.88E+09	0.585
265.793	117084	2	493317	1	-0.85	1.33E+10	0.757
266.054	46406	6	422270	6	-0.54	2.69E+10	-0.697
266.577	54747	2	429873	3	-0.56	2.59E+10	-0.591
266.805	47119	3	421925	4	-0.87	1.27E+10	0.651
267.192	53787	0	428049	1	-0.56	2.62E+10	0.864
267.382	32756	4	406753	3	-0.84	1.37E+10	-0.27
267.554	54747	2	428504	2	-0.27	4.93E+10	-0.525
267.957	54747	2	427941	3	-0.96	1.01E+10	-0.366
268.301	30418	6	403133	5	0.14	1.28E+11	0.575
268.761	31009	5	403087	4	0.04	1.01E+11	0.515
268.761	31288	4	403366	3	-0.79	1.50E+10	-0.412
269.033	31288	4	402989	3	-0.15	6.55E+10	0.426
269.341	64968	3	436244	3	-0.77	1.57E+10	-0.18
269.642	46406	6	417267	7	-0.36	4.04E+10	0.821
269.785	33296	3	403961	2	-0.54	2.66E+10	0.332
269.825	32756	4	403366	3	-0.54	2.62E+10	0.253
269.977	64968	3	435370	3	-0.28	4.80E+10	-0.717
269.995	32756	4	403133	5	-0.53	2.73E+10	-0.501
270.01	33740	2	404096	1	-0.8	1.45E+10	0.367
270.1	32756	4	402989	3	-0.82	1.40E+10	0.265
270.242	87506	4	457545	3	-0.91	1.13E+10	-0.111
270.286	37378	5	407356	4	-0.2	5.71E+10	-0.372
270.384	64968	3	434812	4	-0.48	3.01E+10	0.539
270.423	33296	3	403087	4	-0.57	2.48E+10	-0.457
270.483	38469	4	408178	3	-0.35	4.10E+10	-0.312
270.549	46406	6	416025	5	-0.96	9.98E+09	0.076
270.556	47612	4	417221	5	-0.83	1.37E+10	0.537
270.728	38907	3	408282	2	-0.46	3.13E+10	-0.282
270.789	53787	0	423078	1	-0.93	1.07E+10	-0.464
270.82	33740	2	402989	3	-0.61	2.24E+10	-0.573
271.011	29285	2	398273	2	-0.52	2.71E+10	0.519
271.434	47612	4	416025	5	-0.39	3.67E+10	0.488
272.346	47119	3	414299	2	-0.37	3.81E+10	0.458
272.414	31288	4	398377	4	-0.46	3.13E+10	0.346
272.469	31009	5	398023	5	-0.33	4.21E+10	0.358
272.489	30418	6	397404	6	-0.25	5.03E+10	0.377
272.957	46714	2	413073	1	-0.66	1.96E+10	0.409
273.027	64968	3	431232	2	-0.91	1.10E+10	-0.38
273.407	37378	5	403133	5	-0.33	4.16E+10	0.378
274.187	47612	4	412326	5	-0.92	1.08E+10	0.271
274.26	38469	4	403087	4	-0.56	2.46E+10	0.246
274.595	32756	4	396929	4	-0.43	3.29E+10	-0.345
274.664	38907	3	402989	3	-0.73	1.65E+10	0.218
274.804	74712	0	438608	1	-0.99	8.97E+09	0.458
274.973	77224	4	440896	5	-0.59	2.27E+10	-0.313
275.063	75774	1	439327	2	-0.63	2.08E+10	0.415
275.076	64968	3	428504	2	-0.98	9.17E+09	0.29
275.128	77909	2	441376	2	-0.8	1.41E+10	0.6
275.238	33296	3	396617	3	-0.6	2.24E+10	-0.265
275.555	77468	3	440372	4	-0.65	1.96E+10	-0.299
275.699	33740	2	396455	2	-0.7	1.76E+10	-0.315
275.815	77145	2	439707	3	-0.73	1.64E+10	0.298
276.276	77224	4	439180	3	-0.75	1.56E+10	-0.272
276.8	77909	2	439180	3	-0.32	4.16E+10	0.398
277.757	37378	5	397404	6	-0.68	1.79E+10	0.614
277.82	46714	2	406659	2	-0.73	1.63E+10	0.323
278.061	47119	3	406753	3	-0.7	1.73E+10	0.524
278.122	38469	4	398023	5	-0.84	1.24E+10	0.498
278.125	37378	5	396929	4	-0.7	1.74E+10	0.252
278.188	38907	3	398377	4	-0.96	9.37E+09	0.5
278.332	77224	4	436507	4	-0.4	3.41E+10	-0.294
278.522	77468	3	436507	4	-0.98	9.11E+09	0.305
278.726	77468	3	436244	3	-0.56	2.37E+10	-0.343
279.147	77145	2	435379	2	-0.52	2.62E+10	-0.55
279.214	38469	4	396617	3	-0.98	9.06E+09	0.148
279.256	47119	3	405214	3	-0.67	1.81E+10	0.348
279.498	87506	4	445291	3	-0.49	2.77E+10	0.376
279.673	74712	0	432272	1	-0.94	9.86E+09	-0.36
280.063	77224	4	434286	4	-0.88	1.13E+10	0.42
280.798	117084	2	473212	3	-0.07	7.25E+10	-0.661
280.81	77145	2	433258	2	-0.69	1.74E+10	0.231
280.956	87506	4	443433	4	-0.13	6.25E+10	-0.469
281.065	77468	3	433258	2	-0.69	1.71E+10	0.406

Table A9: Continued

Wavelength	Lower Level	J_{Low}	Upper level	J_{Up}	log gf	gA	CF
281.202	77224	4	432840	3	-0.57	2.28E+10	0.406
281.328	75774	1	431232	2	-1	8.54E+09	-0.226
281.395	77468	3	432840	3	-0.51	2.63E+10	0.246
281.485	0	4	355259	3	-0.07	7.19E+10	-0.63
281.589	77145	2	432272	1	-0.71	1.64E+10	0.382
281.737	1196	3	356137	2	-0.36	3.65E+10	-0.596
281.745	77909	2	432840	3	-0.97	9.02E+09	-0.37
281.939	1987	2	356674	1	-0.79	1.36E+10	-0.574
282.053	77224	4	431767	4	-0.31	4.13E+10	0.366
282.241	77224	4	431531	3	-0.93	9.77E+09	0.111
282.339	2489	1	356674	1	-0.68	1.74E+10	0.581
282.366	1987	2	356137	2	-0.57	2.26E+10	0.593
282.435	1196	3	355259	3	-0.66	1.83E+10	0.617
282.436	77468	3	431531	3	-0.83	1.24E+10	-0.202
282.674	77468	3	431232	2	-0.94	9.63E+09	0.162
282.788	77909	2	431531	3	-0.87	1.11E+10	-0.149
285.794	46714	2	396617	3	-0.76	1.41E+10	-0.336
285.869	47119	3	396929	4	-0.59	2.09E+10	-0.363
285.936	87506	4	437234	5	-0.54	2.34E+10	-0.365
286.036	46848	1	396455	2	-0.93	9.52E+09	-0.336
287.215	87506	4	435677	5	-0.39	3.28E+10	0.579
290.255	117084	2	461609	2	-0.71	1.53E+10	0.302
297.274	77909	2	414299	2	-0.88	9.95E+09	0.169
935.694	322877	7	429750	7	-0.88	1.00E+09	0.753
956.584	322792	5	427331	5	-0.94	8.29E+08	0.572
979.23	299143	6	401264	5	-0.76	1.20E+09	-0.599
987.102	299256	5	400563	4	-0.76	1.20E+09	-0.574
994.15	299293	4	399881	3	-0.75	1.20E+09	-0.586
998.477	299282	3	399435	2	-0.67	1.42E+09	-0.701
1001.38	299251	2	399113	1	-0.7	1.32E+09	-0.859
1017.694	299143	6	397404	6	-0.95	7.23E+08	0.87
1023.473	309046	3	406753	3	-0.68	1.33E+09	-0.701
1035.486	322792	5	419365	4	-0.57	1.70E+09	0.677
1039.853	309046	3	405214	3	-0.78	1.02E+09	0.367
1040.03	299256	5	395407	4	-0.48	2.04E+09	-0.638
1040.429	299293	4	395407	4	-0.94	7.02E+08	0.69
1053.927	299251	2	394134	2	-0.72	1.16E+09	0.892
1054.277	299282	3	394134	2	-0.26	3.28E+09	-0.72
1054.46	299282	3	394117	3	-0.55	1.68E+09	0.753
1054.58	299293	4	394117	3	-0.17	4.05E+09	-0.646
1055.252	299251	2	394015	1	-0.28	3.14E+09	-0.895
1055.748	322792	5	417512	4	0.25	1.07E+10	-0.925
1058.62	322805	6	417267	7	-0.62	1.41E+09	0.654
1058.992	322792	5	417221	5	-0.75	1.07E+09	0.914
1059.136	322805	6	417221	5	0.3	1.19E+10	-0.816
1059.434	322877	7	417267	7	-0.8	9.26E+08	0.941
1060.89	250877	3	345137	4	0.38	1.41E+10	-0.942
1062.3	308998	5	403133	5	0.41	1.51E+10	0.875
1062.822	308998	5	403087	4	-0.71	1.14E+09	0.884
1064.104	309111	4	403087	4	0.26	1.08E+10	0.802
1064.428	299143	6	393090	7	0.59	2.28E+10	-0.925
1064.479	309046	3	402989	3	-0.13	4.35E+09	0.7
1065.212	309111	4	402989	3	-0.79	9.50E+08	0.791
1067	309046	3	402767	2	-0.69	1.20E+09	-0.582
1068.159	322792	5	416411	6	-0.66	1.30E+09	-0.788
1068.305	322805	6	416411	6	0.02	6.16E+09	0.771
1069.135	322877	7	416411	6	0.29	1.13E+10	-0.665
1070.015	299256	5	392713	4	-0.01	5.66E+09	-0.599
1070.084	299143	6	392594	6	-0.96	6.34E+08	0.074
1070.314	299282	3	392713	4	-0.7	1.15E+09	-0.829
1070.438	299293	4	392713	4	-0.41	2.24E+09	0.54
1070.965	299143	6	392517	5	0.15	8.26E+09	-0.584
1071.38	299256	5	392594	6	0.51	1.85E+10	-0.92
1072.263	299256	5	392517	5	-0.33	2.70E+09	0.363
1072.582	322792	5	416025	5	0	5.88E+09	-0.848
1072.687	299293	4	392517	5	-0.17	3.96E+09	-0.89
1072.729	322805	6	416025	5	-0.94	6.66E+08	0.245
1074.252	309046	3	402134	3	-0.62	1.39E+09	-0.388
1075.581	299282	3	392255	3	-0.97	6.13E+08	-0.608
1075.706	299293	4	392255	3	-0.59	1.46E+09	0.629
1076.546	322805	6	415694	7	0.27	1.06E+10	-0.887
1077.388	322877	7	415694	7	0.3	1.15E+10	0.62
1079.416	322877	7	415520	8	0.64	2.50E+10	-0.935
1080.512	299143	6	391692	5	-0.19	3.68E+09	0.698
1082.251	250877	3	343277	3	0.25	1.01E+10	-0.942
1082.265	299293	4	391692	5	0.31	1.15E+10	-0.82
1087.641	299256	5	391198	4	-0.7	1.11E+09	0.478
1087.95	299282	3	391198	4	0.3	1.12E+10	-0.851
1092.698	309046	3	400563	4	-0.08	4.70E+09	0.816
1094.48	299251	2	390618	3	0.22	9.14E+09	-0.887
1094.708	250877	3	342225	2	0.1	7.06E+09	-0.942
1098.48	265639	2	356674	1	-0.12	4.24E+09	-0.935
1100.895	309046	3	399881	3	-0.95	6.12E+08	0.243
1104.996	265639	2	356137	2	0.1	6.86E+09	-0.936
1115.633	322805	6	412440	7	0.25	9.45E+09	-0.592
1115.821	265639	2	355259	3	0.24	9.21E+09	-0.933
1116.514	299143	6	388708	6	0.49	1.65E+10	0.948
1116.537	322877	7	412440	7	0.21	8.60E+09	-0.945
1116.888	322792	5	412326	5	0.19	8.23E+09	0.736
1117.048	322805	6	412326	5	-0.28	2.81E+09	0.928
1119.438	309046	3	398377	4	0.05	5.94E+09	-0.926
1119.832	299143	6	388442	5	-0.34	2.43E+09	0.934
1121.251	299256	5	388442	5	0.34	1.18E+10	0.792
1122.584	322792	5	411872	6	0.3	1.05E+10	-0.664
1122.745	322805	6	411872	6	0.05	5.86E+09	-0.852
1122.885	299256	5	388312	4	-0.29	2.73E+09	0.933
1123.351	299293	4	388312	4	0.23	8.91E+09	0.761
1123.661	322877	7	411872	6	-0.98	5.46E+08	-0.926
1124.177	299282	3	388236	3	0.1	6.67E+09	0.77
1124.313	299293	4	388236	3	-0.35	2.34E+09	0.936
1124.34	299251	2	388192	2	-0.04	4.83E+09	0.815
1124.708	309111	4	398023	5	0.39	1.29E+10	-0.907
1124.738	299282	3	388192	2	-0.56	1.47E+09	0.938
1131.133	308998	5	397404	6	0.48	1.57E+10	-0.937
1137.248	308998	5	396929	4	0.27	9.66E+09	-0.886
1138.715	309111	4	396929	4	-0.74	9.42E+08	0.866

Table A9: Continued

Wavelength	Lower Level	J_{Low}	Upper level	J_{Up}	log gf	gA	CF
1142.775	309111	4	396617	3	0.12	6.78E+09	-0.867
1144.055	309046	3	396455	2	-0.18	3.40E+09	-0.923
1146.295	309046	3	396284	2	-0.87	6.90E+08	0.378
1157.93	309046	3	395407	4	-1	4.96E+08	-0.234
1201.793	309046	3	392255	3	-1	4.55E+08	0.189
1254.548	308998	5	388708	6	-0.93	5.05E+08	0.848

Cu VII

Energy Levels

Table A10: Comparison between available experimental data and calculated odd energy levels (in cm^{-1}) in Cu VII

E^{a}_{exp}	E^{b}_{calc}	ΔE	J	Leading components (in %) in LS coupling [c]
0	−13	13	2.5	100 $3d^5\ ^6S$
46442.7	46565	−122	5.5	100 $3d^5\ ^4G$
46515.3	46383	132	2.5	99 $3d^5\ ^4G$
46575	46604	−29	4.5	100 $3d^5\ ^4G$
46578.2	46520	58	3.5	99 $3d^5\ ^4G$
50731.7	50742	−10	2.5	86 $3d^5\ ^4P$ + 12 $3d^5\ ^4D$
51066.6	51059	8	1.5	89 $3d^5\ ^4P$ + 10 $3d^5\ ^4D$
51406.6	51420	−13	0.5	96 $3d^5\ ^4P$
55742.2	55792	−50	3.5	99 $3d^5\ ^4D$
56209.9	56168	42	0.5	96 $3d^5\ ^4D$
56427.2	56473	−46	2.5	87 $3d^5\ ^4D$ + 12 $3d^5\ ^4P$
56428.5	56434	−6	1.5	89 $3d^5\ ^4D$ + 10 $3d^5\ ^4P$
67757.3	67660	97	5.5	98 $3d^5\ ^2I$
67917.9	67993	−75	6.5	100 $3d^5\ ^2I$
70875.6	70762	114	2.5	49 $3d^5\ ^2D$ + 32 $3d^5\ ^2F$ + 15 $3d^5\ ^2D$
72226.8	72213	14	1.5	68 $3d^5\ ^2D$ + 21 $3d^5\ ^2D$ + 11 $3d^5\ ^4F$
74407.6	74668	−260	3.5	92 $3d^5\ ^2F$ + 5 $3d^5\ ^4F$
75930.5	75980	−50	4.5	93 $3d^5\ ^4F$ + 6 $3d^5\ ^2G$
76019	76095	−76	2.5	73 $3d^5\ ^4F$ + 22 $3d^5\ ^2F$
76349.1	76277	72	3.5	91 $3d^5\ ^4F$ + 6 $3d^5\ ^2F$
76886	76876	10	1.5	89 $3d^5\ ^4F$ + 9 $3d^5\ ^2D$
77529.3	77389	140	2.5	44 $3d^5\ ^2F$ + 24 $3d^5\ ^2D$ + 23 $3d^5\ ^4F$
80717	80653	64	4.5	71 $3d^5\ ^2H$ + 25 $3d^5\ ^2G$
81954.4	81992	−38	5.5	97 $3d^5\ ^2H$
82745.5	82790	−45	3.5	97 $3d^5\ ^2G$
83910.4	83935	−25	4.5	68 $3d^5\ ^2G$ + 28 $3d^5\ ^2H$
87979.2	88025	−46	2.5	97 $3d^5\ ^2F$
88279.7	88128	152	3.5	97 $3d^5\ ^2F$
95875.4	95932	−57	0.5	100 $3d^5\ ^2S$
106957	106878	79	1.5	100 $3d^5\ ^2D$
107130.6	107135	−4	2.5	99 $3d^5\ ^2D$
119534	119545	−11	4.5	100 $3d^5\ ^2G$
119605.4	119648	−43	3.5	99 $3d^5\ ^2G$
143933.7	143910	24	1.5	99 $3d^5\ ^2P$
144077.2	144131	−54	0.5	100 $3d^5\ ^2P$
156224.4	156181	43	2.5	77 $3d^5\ ^2D$ + 23 $3d^5\ ^2D$
156373.6	156377	−3	1.5	76 $3d^5\ ^2D$ + 23 $3d^5\ ^2D$

a: Experimental energies from [105]
b: This work
c: Only the components ≥ to 5% are given

Table A11: Comparison between available experimental data and calculated odd energy levels (in cm^{-1}) in Cu VII

E^a_{exp}	E^b_{calc}	ΔE	J	Leading components (in %) in LS coupling ^{c}
497624	497489	135	1.5	90 $3d^4$(5D)4p ^{6}P + 7 $3d^4$(5D)4p 4P
497863	497657	206	2.5	93 $3d^4$(5D)4p ^{6}P
498317	498057	260	3.5	98 $3d^4$(5D)4p ^{6}P
498775	499069	−294	0.5	65 $3d^4$(5D)4p ^{4}P + 32 $3d^4$(5D)4p ^{6}D
500706	500802	−96	1.5	51 $3d^4$(5D)4p ^{4}P + 36 $3d^4$(5D)4p ^{6}D + 10 $3d^4$(5D)4p ^{6}P
502909	502882	27	2.5	58 $3d^4$(5D)4p ^{6}D + 34 $3d^4$(5D)4p 4P + 6 $3d^4$(5D)4p ^{6}P
504338	504276	62	0.5	68 $3d^4$(5D)4p ^{6}D + 31 $3d^4$(5D)4p 4P
504729	504631	98	1.5	60 $3d^4$(5D)4p ^{6}D + 38 $3d^4$(5D)4p 4P
505447	505280	167	2.5	59 $3d^4$(5D)4p ^{4}P + 38 $3d^4$(5D)4p ^{6}D
508524	508408	116	1.5	94 $3d^4$(5D)4p ^{4}F
508877	508703	174	2.5	92 $3d^4$(5D)4p ^{4}F
509418	509167	251	3.5	89 $3d^4$(5D)4p ^{4}F + 5 $3d^4$(5D)4p ^{6}D
510250	509928	322	4.5	81 $3d^4$(5D)4p ^{4}F + 14 $3d^4$(5D)4p ^{6}D
517847	518055	−208	0.5	96 $3d^4$(5D)4p ^{4}D
518282	518443	−161	1.5	96 $3d^4$(5D)4p ^{4}D
518863	518976	−113	2.5	96 $3d^4$(5D)4p ^{4}D
519415	519509	−94	3.5	96 $3d^4$(5D)4p ^{4}D
528494	528566	−72	3.5	74 $3d^4$(3H)4p ^{4}H + 21 $3d^4$(3G)4p ^{4}H
529027	529068	−41	4.5	69 $3d^4$(3H)4p ^{4}H + 19 $3d^4$(3G)4p ^{4}H + 8 $3d^4$(3H)4p ^{4}I
529891	529884	7	5.5	70 $3d^4$(3H)4p ^{4}H + 17 $3d^4$(3G)4p ^{4}H + 11 $3d^4$(3H)4p ^{4}I
531047	531008	39	6.5	76 $3d^4$(3H)4p ^{4}H + 13 $3d^4$(3G)4p ^{4}H + 9 $3d^4$(3H)4p ^{4}I
532460	532075	385	2.5	40 $3d^4$(3P)4p ^{4}D + 26 $3d^4$(3P)4p ^{4}D + 17 $3d^4$(3F)4p ^{4}D
533066	533079	−13	3.5	27 $3d^4$(3F)4p ^{4}G + 17 $3d^4$(3G)4p ^{4}G + 14 $3d^4$(3F)4p ^{4}G
533103	532965	138	4.5	58 $3d^4$(3H)4p ^{4}I + 8 $3d^4$(3H)4p ^{4}H + 7 $3d^4$(3H)4p ^{2}G
533685	533587	98	0.5	41 $3d^4$(3P)4p ^{4}P + 22 $3d^4$(3P)4p 4P + 15 $3d^4$(3P)4p ^{2}S
534128	533733	395	4.5	29 $3d^4$(3H)4p ^{4}I + 14 $3d^4$(3F)4p ^{4}G + 13 $3d^4$(3H)4p ^{4}G
534204	533796	408	3.5	31 $3d^4$(3F)4p ^{4}D + 25 $3d^4$(3P)4p ^{4}D + 16 $3d^4$(3P)4p ^{4}D
534912	534654	258	5.5	67 $3d^4$(3H)4p ^{4}I + 11 $3d^4$(3H)4p ^{4}G + 11 $3d^4$(3H)4p ^{4}H
535632	535162	470	5.5	38 $3d^4$(3H)4p ^{4}G + 25 $3d^4$(3G)4p ^{4}G + 19 $3d^4$(3H)4p ^{4}I
536229	536291	−62	1.5	55 $3d^4$(3P)4p ^{4}P + 29 $3d^4$(3P)4p ^{4}P
536650	536534	116	4.5	31 $3d^4$(3H)4p ^{2}G + 20 $3d^4$(3F)4p ^{2}G + 14 $3d^4$(3G)4p ^{4}G
537169	537180	−11	2.5	33 $3d^4$(3H)4p ^{4}G + 27 $3d^4$(3F)4p ^{4}G + 14 $3d^4$(3G)4p ^{4}G
537802	537633	169	3.5	46 $3d^4$(3H)4p ^{4}G + 32 $3d^4$(3F)4p ^{4}G + 14 $3d^4$(3G)4p ^{4}G
537874	537807	67	2.5	44 $3d^4$(3F)4p ^{4}F + 11 $3d^4$(3F)4p ^{2}D + 9 $3d^4$(3H)4p ^{4}G
538144	537939	205	4.5	42 $3d^4$(3F)4p ^{4}G + 36 $3d^4$(3H)4p ^{4}G + 7 $3d^4$(3F)4p ^{4}G
538624	538331	293	2.5	54 $3d^4$(3P)4p ^{4}P + 28 $3d^4$(3P)4p 4P + 5 $3d^4$(3P)4p ^{2}D
538749	538777	−28	3.5	60 $3d^4$(3F)4p ^{4}F + 11 $3d^4$(3F)4p ^{4}F + 10 $3d^4$(3G)4p ^{4}F
539041	538800	241	5.5	60 $3d^4$(3F)4p ^{4}G + 18 $3d^4$(3H)4p ^{4}G + 13 $3d^4$(3F)4p ^{4}G
539146	539272	−126	4.5	54 $3d^4$(3F)4p ^{4}F + 15 $3d^4$(3G)4p ^{4}F + 10 $3d^4$(3F)4p ^{4}F
539640	539940	−300	2.5	14 $3d^4$(3F)4p ^{2}D + 14 $3d^4$(3G)4p ^{4}F + 12 $3d^4$(3G)4p ^{2}F
540086	540131	−45	1.5	21 $3d^4$(3F)4p ^{2}D + 21 $3d^4$(3F)4p ^{4}F + 9 $3d^4$(3D)4p ^{2}D
540915	540877	38	1.5	37 $3d^4$(3F)4p ^{4}D + 13 $3d^4$(3F)4p ^{4}D + 10 $3d^4$(3G)4p ^{4}F
540925	540904	21	3.5	22 $3d^4$(3G)4p ^{4}F + 22 $3d^4$(3P)4p ^{4}D + 14 $3d^4$(3P)4p ^{4}D
541444	541807	−363	2.5	27 $3d^4$(3G)4p ^{2}F + 14 $3d^4$(3D)4p ^{2}F + 12 $3d^4$(3F)4p ^{4}D
541457	541680	−223	4.5	31 $3d^4$(3H)4p ^{2}H + 26 $3d^4$(3G)4p ^{4}H + 12 $3d^4$(3G)4p ^{2}H
541509	540981	528	6.5	82 $3d^4$(3H)4p ^{2}I + 11 $3d^4$(3G)4p ^{4}H
541884	541745	139	3.5	69 $3d^4$(3G)4p ^{4}H + 21 $3d^4$(3H)4p ^{4}H
542239	542259	−20	4.5	49 $3d^4$(3G)4p ^{4}F + 18 $3d^4$(3F)4p ^{4}F + 9 $3d^4$(3D)4p ^{4}F
542362	542676	−314	3.5	16 $3d^4$(3G)4p ^{2}F + 16 $3d^4$(3D)4p ^{2}F + 16 $3d^4$(3G)4p ^{4}F
542394	542133	261	1.5	21 $3d^4$(3G)4p ^{4}F + 14 $3d^4$(3F)4p ^{4}F
542776	542901	−125	2.5	37 $3d^4$(3G)4p ^{4}F + 15 $3d^4$(3F)4p ^{4}F + 15 $3d^4$(3F)4p ^{4}D
543188	543060	128	5.5	36 $3d^4$(3G)4p ^{4}H + 26 $3d^4$(3H)4p ^{2}H + 16 $3d^4$(3G)4p ^{2}H
543217	543139	78	3.5	24 $3d^4$(3F)4p ^{4}D + 19 $3d^4$(3G)4p ^{4}F + 10 $3d^4$(3F)4p ^{4}F
543244	543002	242	1.5	22 $3d^4$(3G)4p ^{4}F + 19 $3d^4$(3P)4p ^{2}P + 14 $3d^4$(3F)4p ^{4}D
543574	543293	281	4.5	48 $3d^4$(3G)4p ^{4}H + 23 $3d^4$(3H)4p ^{2}H + 11 $3d^4$(3H)4p ^{4}H
544873	544242	631	1.5	36 $3d^4$(3P)4p ^{2}D + 23 $3d^4$(3P)4p ^{2}D + 9 $3d^4$(3G)4p ^{4}F
546268	545746	522	2.5	41 $3d^4$(3P)4p ^{2}D + 26 $3d^4$(3P)4p ^{2}D + 5 $3d^4$(3P)4p 4P
546771	546378	393	2.5	55 $3d^4$(3F)4p ^{2}F + 20 $3d^4$(3G)4p ^{2}F + 5 $3d^4$(3P)4p ^{2}D
546881	546990	−109	3.5	26 $3d^4$(3F)4p ^{2}G + 15 $3d^4$(3F)4p ^{2}G + 14 $3d^4$(3H)4p ^{2}G
547090	547235	−145	5.5	38 $3d^4$(3G)4p ^{2}H + 18 $3d^4$(3H)4p ^{2}H + 16 $3d^4$(3G)4p ^{4}G
547381	547495	−114	4.5	23 $3d^4$(3F)4p ^{2}G + 12 $3d^4$(3F)4p ^{2}G + 12 $3d^4$(3G)4p ^{2}G
547565	547500	65	3.5	50 $3d^4$(3F)4p ^{2}F + 30 $3d^4$(3G)4p ^{2}F
548001	547913	88	2.5	52 $3d^4$(3G)4p ^{4}G + 32 $3d^4$(3H)4p ^{4}G + 5 $3d^4$(3F)4p ^{2}F
548491	548364	127	3.5	49 $3d^4$(3G)4p ^{4}G + 24 $3d^4$(3H)4p ^{4}G + 6 $3d^4$(3F)4p ^{2}G
549249	549135	114	4.5	40 $3d^4$(3G)4p ^{4}G + 18 $3d^4$(3H)4p ^{4}G + 13 $3d^4$(3G)4p ^{2}H
550007	549870	137	5.5	46 $3d^4$(3G)4p ^{4}G + 21 $3d^4$(3G)4p ^{2}H + 18 $3d^4$(3H)4p ^{4}G
550053	550667	−614	2.5	61 $3d^4$(3D)4p ^{4}P + 26 $3d^4$(3D)4p ^{4}D + 5 $3d^4$(3P)4p ^{4}P
551508	552407	−899	3.5	75 $3d^4$(3D)4p ^{4}D + 7 $3d^4$(3D)4p ^{4}F + 5 $3d^4$(3G)4p ^{4}F
551743	552463	−720	2.5	48 $3d^4$(3D)4p ^{4}D + 26 $3d^4$(3D)4p ^{4}P + 8 $3d^4$(3D)4p ^{4}F
551903	551648	255	6.5	60 $3d^4$(1I)4p ^{2}I + 34 $3d^4$(1I)4p ^{2}K + 6 $3d^4$(3H)4p ^{2}I
552334	553189	−855	3.5	46 $3d^4$(1G)4p ^{2}F + 20 $3d^4$(1G)4p ^{2}F + 18 $3d^4$(3G)4p ^{2}G
552359	552167	192	5.5	88 $3d^4$(1I)4p ^{2}I
553130	553419	−289	1.5	69 $3d^4$(3D)4p 4P + 11 $3d^4$(3D)4p ^{4}D + 7 $3d^4$(3D)4p ^{4}F
553490	553853	−363	4.5	51 $3d^4$(3G)4p ^{2}G + 21 $3d^4$(3H)4p ^{2}G + 11 $3d^4$(1G)4p ^{2}G
553703	553770	−67	3.5	49 $3d^4$(3G)4p ^{2}G + 17 $3d^4$(3H)4p ^{2}G + 9 $3d^4$(1G)4p ^{2}F
553950	554244	−294	0.5	87 $3d^4$(3D)4p ^{4}P + 7 $3d^4$(3P)4p ^{4}P
554123	554268	−145	4.5	47 $3d^4$(1G)4p ^{2}H + 21 $3d^4$(1G)4p ^{2}H + 10 $3d^4$(3G)4p ^{2}H
554201	555068	−867	0.5	39 $3d^4$(3D)4p ^{2}P + 35 $3d^4$(1S)4p ^{2}P + 9 $3d^4$(3D)4p ^{4}D
555069	555490	−421	5.5	54 $3d^4$(1G)4p ^{2}H + 18 $3d^4$(1G)4p ^{2}H + 11 $3d^4$(1I)4p ^{2}H
555137	556274	−1137	1.5	62 $3d^4$(3D)4p ^{2}P + 19 $3d^4$(1S)4p ^{2}P + 6 $3d^4$(3D)4p ^{4}D
555295	554827	468	6.5	64 $3d^4$(1I)4p ^{2}K + 35 $3d^4$(1I)4p ^{2}I
555314	555863	−549	2.5	49 $3d^4$(1G)4p ^{2}F + 23 $3d^4$(1G)4p ^{2}F + 6 $3d^4$(3G)4p ^{2}F
555395	555919	−524	3.5	63 $3d^4$(3D)4p ^{4}F + 19 $3d^4$(3G)4p ^{4}F + 12 $3d^4$(3D)4p ^{4}D
555800	556340	−540	4.5	76 $3d^4$(3D)4p ^{4}F + 19 $3d^4$(3G)4p ^{4}F
558348	559260	−912	3.5	45 $3d^4$(1G)4p ^{2}G + 30 $3d^4$(1G)4p ^{2}G + 9 $3d^4$(3G)4p ^{2}G
559339	560050	−711	4.5	42 $3d^4$(1G)4p ^{2}G + 32 $3d^4$(1G)4p ^{2}G + 18 $3d^4$(3G)4p ^{2}G
560328	560307	21	1.5	34 $3d^4$(1D)4p ^{2}D + 18 $3d^4$(1S)4p ^{2}P
560658	560942	−284	5.5	65 $3d^4$(1I)4p ^{2}H + 13 $3d^4$(1G)4p ^{2}H + 9 $3d^4$(3G)4p ^{2}H
561271	561860	−589	0.5	40 $3d^4$(3D)4p ^{2}P + 29 $3d^4$(1S)4p ^{2}P + 12 $3d^4$(1D)4p ^{2}P
561677	561998	−321	4.5	80 $3d^4$(1I)4p ^{2}H + 10 $3d^4$(3G)4p ^{2}H + 8 $3d^4$(1G)4p ^{2}H
561985	561596	389	2.5	47 $3d^4$(1D)4p ^{2}D + 19 $3d^4$(3D)4p ^{2}D + 17 $3d^4$(1D)4p ^{2}D
562178	562598	−420	3.5	62 $3d^4$(3D)4p ^{2}F + 10 $3d^4$(3G)4p ^{2}F + 7 $3d^4$(1F)4p ^{2}F

Table A11: Continued

E^a_{exp}	E^b_{calc}	ΔE	J	Leading components (in %) in LS coupling [c]
562816	563160	−344	2.5	49 $3d^4$(3D)4p ^{2}F + 19 $3d^4$(1F)4p ^{2}F + 16 $3d^4$(3G)4p ^{2}F
563705	564030	−325	1.5	25 $3d^4$(1D)4p ^{2}D + 24 $3d^4$(1S)4p ^{2}P + 12 $3d^4$(3D)4p ^{2}P
565170	565169	1	1.5	70 $3d^4$(3D)4p ^{2}D + 15 $3d^4$(3F)4p ^{2}D + 5 $3d^4$(1D)4p ^{2}D
565670	565238	432	2.5	35 $3d^4$(1D)4p ^{2}F + 20 $3d^4$(3D)4p ^{2}D + 16 $3d^4$(3D)4p ^{2}F
567069	566385	684	2.5	35 $3d^4$(3D)4p ^{2}D + 18 $3d^4$(1D)4p ^{2}F + 16 $3d^4$(1D)4p ^{2}D
567778	566943	835	3.5	49 $3d^4$(1D)4p ^{2}F + 28 $3d^4$(1F)4p ^{2}F + 12 $3d^4$(1D)4p ^{2}F
572310	571556	754	2.5	61 $3d^4$(1F)4p ^{2}F + 12 $3d^4$(1G)4p ^{2}F + 11 $3d^4$(1D)4p ^{2}F
573402	573064	338	0.5	68 $3d^4$(1D)4p ^{2}P + 14 $3d^4$(1D)4p ^{2}P + 9 $3d^4$(1S)4p ^{2}P
573463	572399	1064	3.5	46 $3d^4$(1F)4p ^{2}F + 23 $3d^4$(1D)4p ^{2}F + 10 $3d^4$(1G)4p ^{2}F
574043	573284	759	1.5	56 $3d^4$(1D)4p ^{2}P + 16 $3d^4$(1S)4p ^{2}P + 12 $3d^4$(1G)4p ^{2}P
575709	575410	299	3.5	84 $3d^4$(1F)4p ^{2}G + 6 $3d^4$(1F)4p ^{2}F
578193	577847	346	4.5	90 $3d^4$(1F)4p ^{2}G
582101	582247	−146	2.5	59 $3d^4$(3F)4p ^{4}F + 11 $3d^4$(3P)4p ^{4}D + 8 $3d^4$(3F)4p ^{4}F
582434	582473	−39	3.5	65 $3d^4$(3F)4p ^{4}F + 8 $3d^4$(3F)4p ^{4}D + 8 $3d^4$(3F)4p ^{4}F
582632	582763	−131	1.5	37 $3d^4$(3F)4p ^{4}F + 13 $3d^4$(1F)4p ^{2}D + 11 $3d^4$(3P)4p ^{4}D
583223	583285	−62	4.5	82 $3d^4$(3F)4p ^{4}F + 9 $3d^4$(3F)4p ^{4}F
583496	583891	−395	1.5	20 $3d^4$(3P)4p ^{4}P + 16 $3d^4$(3P)4p ^{4}D + 16 $3d^4$(3F)4p ^{4}F
583853	583914	−61	2.5	23 $3d^4$(3P)4p ^{4}D + 21 $3d^4$(3F)4p ^{4}F + 12 $3d^4$(3P)4p ^{4}D
584627	584697	−70	3.5	32 $3d^4$(3P)4p ^{4}D + 19 $3d^4$(3F)4p ^{4}D + 16 $3d^4$(3F)4p ^{4}F
586361	586509	−148	2.5	29 $3d^4$(3F)4p ^{4}G + 17 $3d^4$(3P)4p ^{4}P + 13 $3d^4$(3F)4p ^{2}F
587400	587450	−50	3.5	37 $3d^4$(3F)4p ^{4}G + 28 $3d^4$(3F)4p ^{2}F + 12 $3d^4$(3F)4p ^{4}G
588525	588525	0	2.5	26 $3d^4$(1F)4p ^{2}D + 19 $3d^4$(3P)4p ^{2}D + 13 $3d^4$(3P)4p ^{2}D
589098	589136	−38	3.5	39 $3d^4$(3F)4p ^{2}F + 31 $3d^4$(3F)4p ^{4}G + 10 $3d^4$(3F)4p ^{4}G
589132	589220	−88	1.5	33 $3d^4$(1F)4p ^{2}D + 21 $3d^4$(3P)4p ^{2}D + 17 $3d^4$(3F)4p ^{2}D
596473	596393	80	4.5	70 $3d^4$(3F)4p ^{2}G + 20 $3d^4$(3F)4p ^{2}G
596790	597023	−233	1.5	61 $3d^4$(3P)4p ^{2}P + 25 $3d^4$(3P)4p ^{2}P + 7 $3d^4$(3D)4p ^{2}P
597774	597560	214	3.5	72 $3d^4$(3F)4p ^{2}G + 22 $3d^4$(3F)4p ^{2}G
599993	599594	399	4.5	40 $3d^4$(1G)4p ^{2}H + 22 $3d^4$(1G)4p ^{2}G + 19 $3d^4$(1G)4p ^{2}H
600555	600479	76	3.5	51 $3d^4$(1G)4p ^{2}G + 31 $3d^4$(1G)4p ^{2}G + 7 $3d^4$(1G)4p ^{2}F
601692	601391	301	0.5	54 $3d^4$(3P)4p ^{2}S + 41 $3d^4$(3P)4p ^{2}S
603569	603112	457	4.5	37 $3d^4$(1G)4p ^{2}G + 23 $3d^4$(1G)4p ^{2}H + 22 $3d^4$(1G)4p ^{2}G
604021	603515	506	5.5	65 $3d^4$(1G)4p ^{2}H + 31 $3d^4$(1G)4p ^{2}H
604655	604594	61	3.5	53 $3d^4$(1G)4p ^{2}F + 16 $3d^4$(1G)4p ^{2}F + 8 $3d^4$(1G)4p ^{2}G
605306	605304	2	2.5	58 $3d^4$(1G)4p ^{2}F + 18 $3d^4$(1G)4p ^{2}F + 9 $3d^4$(1D)4p ^{2}F
608598	608701	−103	2.5	49 $3d^4$(3F)4p ^{2}D + 18 $3d^4$(3F)4p ^{2}D + 16 $3d^4$(3P)4p ^{2}D
609072	609176	−104	1.5	44 $3d^4$(3F)4p ^{2}D + 21 $3d^4$(3P)4p ^{2}D + 18 $3d^4$(3F)4p ^{2}D
634888	634813	75	3.5	72 $3d^4$(1D)4p ^{2}F + 19 $3d^4$(1D)4p ^{2}F + 5 $3d^4$(1G)4p ^{2}F

a: Experimental energies from [105]
b: This work
c: Only the components ≥ to 5% are given

Transitions

Table A12: Computed oscillator strengths and transition probabilities in Cu VII.

Wavelength	Lower Level	J_{low}	Upper Level	J_{up}	log gf	gA	CF
186.296	46443	5.5	583223	4.5	-0.89	2.47E+10	-0.623
189.077	55742	3.5	584627	3.5	-0.93	2.18E+10	0.374
191.546	81954	5.5	604021	5.5	-0.95	2.02E+10	0.152
191.712	81954	5.5	603569	4.5	-0.51	5.58E+10	0.276
192.368	80717	4.5	600555	3.5	-0.85	2.53E+10	0.176
193.402	80717	4.5	597774	3.5	-0.67	3.80E+10	-0.14
194.041	119534	4.5	634888	3.5	-0.44	6.50E+10	-0.391
194.164	82746	3.5	597774	3.5	-1	1.75E+10	0.355
194.356	81954	5.5	596473	4.5	-0.58	4.67E+10	-0.118
194.604	83910	4.5	597774	3.5	-0.92	2.11E+10	0.162
196.581	75931	4.5	584627	3.5	-0.08	1.44E+11	-0.682
197.043	76349	3.5	583853	2.5	-0.32	8.17E+10	-0.549
197.053	76019	2.5	583496	1.5	-0.86	2.40E+10	0.359
197.125	75931	4.5	583223	4.5	-0.17	1.17E+11	0.529
197.288	76349	3.5	583223	4.5	-0.91	2.09E+10	-0.506
197.595	76349	3.5	582434	3.5	-0.29	8.83E+10	0.477
197.596	76019	2.5	582101	2.5	-0.45	6.11E+10	0.522
197.641	77529	2.5	583496	1.5	-0.99	1.74E+10	0.372
197.728	76886	1.5	582632	1.5	-0.6	4.31E+10	0.536
198.614	83910	4.5	587400	3.5	-0.99	1.74E+10	0.309
199.54	87979	2.5	589132	1.5	-0.69	3.41E+10	-0.324
199.902	88280	3.5	588525	2.5	-0.59	4.32E+10	-0.336
200.272	50732	2.5	550053	2.5	-0.62	3.98E+10	0.351
200.675	0	2.5	498317	3.5	0.13	2.24E+11	0.984
200.858	0	2.5	497863	2.5	-0.01	1.61E+11	0.983
200.955	0	2.5	497624	1.5	-0.2	1.04E+11	0.982
200.995	107131	2.5	604655	3.5	-0.87	2.25E+10	-0.224
200.996	56429	1.5	553950	0.5	-0.77	2.78E+10	-0.663
201.015	80717	4.5	578193	4.5	-0.91	2.04E+10	-0.468
201.209	46578	3.5	543574	4.5	-0.79	2.68E+10	-0.54
201.328	56427	2.5	553130	1.5	-0.46	5.73E+10	-0.611
201.364	46575	4.5	543188	5.5	-0.67	3.55E+10	-0.791
201.516	81954	5.5	578193	4.5	-0.49	5.26E+10	0.618
201.613	55742	3.5	551743	2.5	-0.57	4.44E+10	-0.521
201.708	55742	3.5	551508	3.5	-0.6	4.12E+10	-0.24
201.87	46515	2.5	541884	3.5	-0.64	3.76E+10	-0.639
202.07	46578	3.5	541457	4.5	-0.92	1.97E+10	-0.739
202.286	46575	4.5	540925	3.5	-1	1.62E+10	-0.379
202.302	55742	3.5	550053	2.5	-0.72	3.15E+10	-0.266
202.313	83910	4.5	578193	4.5	-0.62	3.92E+10	-0.488
202.462	67757	5.5	561677	4.5	-0.21	1.01E+11	-0.507
202.583	56427	2.5	550053	2.5	-0.91	1.99E+10	0.158
202.605	46515	2.5	540086	1.5	-0.63	3.80E+10	0.749
202.814	46578	3.5	539640	2.5	-0.46	5.66E+10	-0.799
202.855	82746	3.5	575709	3.5	-0.59	4.21E+10	-0.483
202.947	67918	6.5	560658	5.5	-0.42	6.10E+10	-0.203
202.962	46443	5.5	539146	4.5	0.12	2.15E+11	-0.912
203.005	46443	5.5	539041	5.5	0.05	1.82E+11	-0.956
203.052	50732	2.5	543217	3.5	-0.87	2.18E+10	0.169
203.18	46575	4.5	538749	3.5	0.01	1.65E+11	-0.851
203.315	75931	4.5	567778	3.5	-0.99	1.63E+10	-0.661
203.335	83910	4.5	575709	3.5	-0.77	2.74E+10	-0.403
203.43	46575	4.5	538144	4.5	0.12	2.11E+11	-0.883
203.517	46515	2.5	537874	2.5	-0.44	5.87E+10	0.802
203.541	70876	2.5	562178	3.5	-0.73	3.00E+10	0.381
203.543	46578	3.5	537874	2.5	-0.53	4.73E+10	-0.392
203.572	46575	4.5	537802	3.5	-1	1.61E+10	0.37
203.573	46578	3.5	537802	3.5	0.08	1.91E+11	0.885
203.621	70876	2.5	561985	2.5	-0.74	2.90E+10	0.215
203.81	46515	2.5	537169	2.5	-0.18	1.06E+11	0.662
203.836	46578	3.5	537169	2.5	-0.6	4.04E+10	0.884
203.837	72227	1.5	562816	2.5	-0.8	2.55E+10	0.526
204.001	50732	2.5	540925	3.5	-0.62	3.84E+10	0.467
204.05	46575	4.5	536650	4.5	-0.63	3.74E+10	0.328
204.145	51067	1.5	540915	1.5	-0.64	3.65E+10	0.373
204.224	107131	2.5	596790	1.5	-0.52	4.82E+10	-0.401
204.263	82746	3.5	572310	2.5	-0.85	2.27E+10	-0.135
204.31	70876	2.5	560328	1.5	-0.42	6.04E+10	-0.498
204.42	46443	5.5	535632	5.5	-0.07	1.36E+11	0.494
204.48	72227	1.5	561271	0.5	-0.57	4.27E+10	0.807
204.721	46443	5.5	534912	5.5	-0.74	2.87E+10	-0.37
204.777	46575	4.5	534912	5.5	-0.82	2.40E+10	0.685
204.876	72227	1.5	560328	1.5	-0.66	3.46E+10	0.64
204.963	50732	2.5	538624	2.5	-0.82	2.43E+10	0.276
205.05	46443	5.5	534128	4.5	-0.73	2.94E+10	0.541
205.05	76019	2.5	563705	1.5	-0.86	2.20E+10	-0.638
205.096	74408	3.5	561985	2.5	-0.18	1.04E+11	0.648
205.104	51067	1.5	538624	2.5	-0.93	1.84E+10	-0.496
205.139	55742	3.5	543217	3.5	-0.32	7.64E+10	-0.728
205.18	67918	6.5	555295	6.5	-0.19	1.02E+11	-0.929
205.275	67918	6.5	555069	5.5	0.35	3.53E+11	-0.947
205.313	80717	4.5	567778	3.5	-0.67	3.40E+10	0.376
205.417	56429	1.5	543244	1.5	-0.94	1.81E+10	0.37
205.427	56427	2.5	543217	3.5	-0.7	3.14E+10	-0.22
205.551	55742	3.5	542239	4.5	-0.08	1.31E+11	0.83
205.554	46575	4.5	533066	3.5	-0.92	1.90E+10	0.375
205.607	67757	5.5	554123	4.5	0.15	2.24E+11	-0.779
205.614	56427	2.5	542776	2.5	-0.54	4.53E+10	0.553
205.614	56429	1.5	542776	2.5	-0.62	3.76E+10	0.331
205.683	56210	0.5	542394	1.5	-0.94	1.80E+10	0.585
205.687	77529	2.5	563705	1.5	-0.28	8.29E+10	0.719
205.789	56427	2.5	542362	3.5	-0.67	3.37E+10	-0.472
205.888	119605	3.5	605306	2.5	-0.17	1.07E+11	0.763
205.974	50732	2.5	536229	1.5	-0.53	4.65E+10	0.675
206.108	88280	3.5	573463	3.5	-0.13	1.17E+11	-0.606
206.134	119534	4.5	604655	3.5	-0.08	1.32E+11	0.777
206.172	82746	3.5	567778	3.5	-0.91	1.93E+10	-0.551

Table A12: Continued

Wavelength	Lower Level	J_{Low}	Upper level	J_{Up}	log gf	gA	CF
206.215	74408	3.5	559339	4.5	-0.82	2.38E+10	0.185
206.261	51407	0.5	536229	1.5	-0.97	1.67E+10	-0.439
206.311	56210	0.5	540915	1.5	-0.86	2.16E+10	0.451
206.335	77529	2.5	562178	3.5	-0.98	1.64E+10	0.278
206.354	46443	5.5	531047	6.5	-0.31	7.63E+10	0.528
206.355	67757	5.5	552359	5.5	0.24	2.71E+11	-0.848
206.399	56427	2.5	540925	3.5	-0.65	3.47E+10	0.327
206.404	119534	4.5	604021	5.5	-0.69	3.19E+10	0.711
206.404	56429	1.5	540915	1.5	-0.88	2.09E+10	-0.291
206.425	70876	2.5	555314	2.5	-0.85	2.23E+10	-0.16
206.47	87979	2.5	572310	2.5	-0.18	1.02E+11	-0.583
206.474	82746	3.5	567069	2.5	-0.64	3.59E+10	-0.576
206.549	67757	5.5	551903	6.5	-0.66	3.45E+10	0.771
206.597	119534	4.5	603569	4.5	-0.47	5.23E+10	0.42
206.618	67918	6.5	551903	6.5	0.15	2.20E+11	-0.852
206.668	83910	4.5	567778	3.5	-0.05	1.37E+11	0.746
206.837	50732	2.5	534204	3.5	-0.22	9.29E+10	0.744
206.904	46575	4.5	529891	5.5	-0.47	5.32E+10	0.432
207.072	82746	3.5	565670	2.5	-0.24	8.99E+10	0.628
207.09	55742	3.5	538624	2.5	-0.41	6.05E+10	0.607
207.203	51067	1.5	533685	0.5	-0.89	2.00E+10	0.619
207.276	46578	3.5	529027	4.5	-0.57	4.13E+10	0.393
207.384	56427	2.5	538624	2.5	-0.78	2.60E+10	-0.359
207.394	106957	1.5	589132	1.5	-0.58	4.09E+10	0.505
207.478	46515	2.5	528494	3.5	-0.62	3.69E+10	0.408
207.702	70876	2.5	552334	3.5	-0.83	2.31E+10	0.174
207.73	107131	2.5	588525	2.5	-0.43	5.76E+10	0.548
207.73	51067	1.5	532460	2.5	-0.73	2.86E+10	0.557
207.917	80717	4.5	561677	4.5	-0.2	9.85E+10	0.617
207.922	119605	3.5	600555	3.5	-0.19	9.96E+10	0.793
208.134	119534	4.5	599993	4.5	-0.59	3.92E+10	-0.576
208.165	119605	3.5	599993	4.5	-0.78	2.58E+10	0.659
208.39	75931	4.5	555800	4.5	-0.71	3.01E+10	-0.553
208.454	81954	5.5	561677	4.5	-0.99	1.58E+10	0.542
208.497	67757	5.5	547381	4.5	-0.51	4.70E+10	0.454
208.64	76019	2.5	555314	2.5	-0.82	2.34E+10	-0.289
208.64	74408	3.5	553703	3.5	-0.96	1.70E+10	0.167
208.748	76349	3.5	555395	3.5	-0.97	1.64E+10	-0.298
208.798	82746	3.5	561677	4.5	-0.64	3.53E+10	-0.307
208.86	88280	3.5	567069	2.5	-0.12	1.15E+11	0.698
208.898	81954	5.5	560658	5.5	0.17	2.26E+11	0.873
208.915	156224	2.5	634888	3.5	-1	1.53E+10	-0.517
209.131	119605	3.5	597774	3.5	-0.32	7.31E+10	0.589
209.132	95875	0.5	574043	1.5	-0.47	5.21E+10	-0.845
209.237	74408	3.5	552334	3.5	-0.08	1.28E+11	0.678
209.299	77529	2.5	555314	2.5	-0.31	7.52E+10	0.455
209.307	83910	4.5	561677	4.5	-0.46	5.32E+10	-0.594
209.367	80717	4.5	558348	3.5	-0.1	1.22E+11	-0.741
209.412	95875	0.5	573402	0.5	-0.75	2.72E+10	-0.844
209.472	88280	3.5	565670	2.5	-0.49	4.90E+10	0.478
209.475	81954	5.5	559339	4.5	-0.05	1.36E+11	-0.658
209.56	87979	2.5	565170	1.5	-0.13	1.13E+11	0.82
209.67	119534	4.5	596473	4.5	-0.09	1.25E+11	0.761
209.755	83910	4.5	560658	5.5	-0.82	2.31E+10	-0.176
210.165	67757	5.5	543574	4.5	-0.48	5.03E+10	-0.358
210.26	82746	3.5	558348	3.5	-0.42	5.80E+10	-0.442
210.271	75931	4.5	551508	3.5	-0.84	2.19E+10	-0.317
210.337	83910	4.5	559339	4.5	-0.23	9.01E+10	-0.552
210.353	70876	2.5	546268	2.5	-0.81	2.35E+10	0.186
210.407	67918	6.5	543188	5.5	-0.12	1.14E+11	0.35
210.456	76349	3.5	551508	3.5	-0.86	2.08E+10	0.476
210.756	67757	5.5	542239	4.5	-0.83	2.21E+10	0.356
210.936	75931	4.5	550007	5.5	-0.42	5.73E+10	-0.468
210.972	70876	2.5	544873	1.5	-0.89	1.93E+10	0.153
211.104	67757	5.5	541457	4.5	-0.26	8.29E+10	0.275
211.153	67918	6.5	541509	6.5	-0.21	9.12E+10	0.36
211.264	81954	5.5	555295	6.5	-0.77	2.54E+10	0.684
211.428	74408	3.5	547381	4.5	-0.73	2.80E+10	0.266
211.461	76349	3.5	549249	4.5	-0.5	4.74E+10	-0.485
211.518	80717	4.5	553490	4.5	-0.86	2.08E+10	-0.157
211.575	72227	1.5	544873	1.5	-0.81	2.32E+10	0.401
211.653	76019	2.5	548491	3.5	-0.7	2.95E+10	-0.326
211.701	74408	3.5	546771	2.5	-0.97	1.61E+10	0.252
211.789	81954	5.5	554123	4.5	-0.64	3.44E+10	0.388
211.872	76019	2.5	548001	2.5	-0.95	1.66E+10	-0.524
211.927	74408	3.5	546268	2.5	-0.34	6.81E+10	-0.318
212.025	80717	4.5	552359	5.5	-0.73	2.78E+10	0.331
212.081	70876	2.5	542394	1.5	-0.59	3.78E+10	0.475
212.095	70876	2.5	542362	3.5	-0.95	1.68E+10	-0.196
212.242	75931	4.5	547090	5.5	-0.48	4.90E+10	0.673
212.262	76886	1.5	548001	2.5	-0.5	4.64E+10	-0.65
212.331	77529	2.5	548491	3.5	-0.85	2.08E+10	-0.337
212.333	82746	3.5	553703	3.5	-0.59	3.81E+10	-0.182
212.376	76019	2.5	546881	3.5	-0.74	2.68E+10	-0.386
212.599	87979	2.5	558348	3.5	-0.86	2.05E+10	0.42
212.67	83910	4.5	554123	4.5	-0.53	4.36E+10	0.353
212.69	72227	1.5	542394	1.5	-0.98	1.53E+10	0.289
212.789	81954	5.5	551903	6.5	-0.97	1.57E+10	0.213
212.952	82746	3.5	552334	3.5	-0.86	2.04E+10	0.246
212.964	119534	4.5	589098	3.5	-0.49	4.80E+10	0.334
213.121	72227	1.5	541444	2.5	-0.74	2.69E+10	0.448
213.327	70876	2.5	539640	2.5	-0.66	3.21E+10	-0.322
213.338	77529	2.5	546268	2.5	-0.66	3.23E+10	0.283
213.433	80717	4.5	549249	4.5	-0.83	2.17E+10	-0.264
213.681	76886	1.5	544873	1.5	-1	1.44E+10	0.55
213.696	74408	3.5	542362	3.5	-0.81	2.28E+10	0.153
213.736	119534	4.5	587400	3.5	-0.56	3.99E+10	0.37
213.975	77529	2.5	544873	1.5	-0.83	2.17E+10	-0.155
213.979	87979	2.5	555314	2.5	-0.85	2.09E+10	0.205
214.173	107131	2.5	574043	1.5	-0.56	3.95E+10	-0.574
214.202	80717	4.5	547565	3.5	-0.39	5.89E+10	0.425
214.245	119605	3.5	586361	2.5	-0.98	1.51E+10	0.357
214.287	80717	4.5	547381	4.5	-0.78	2.44E+10	0.146
214.354	74408	3.5	540925	3.5	-1	1.44E+10	0.204
214.388	106957	1.5	573402	0.5	-0.94	1.66E+10	-0.524
214.45	75931	4.5	542239	4.5	-0.68	3.05E+10	-0.293

Table A12: Continued

Wavelength	Lower Level	J_{Low}	Upper level	J_{Up}	log gf	gA	CF
214.517	80717	4.5	546881	3.5	-0.39	5.96E+10	0.217
214.548	83910	4.5	550007	5.5	-0.72	2.75E+10	-0.548
214.72	87979	2.5	553703	3.5	-0.56	3.94E+10	-0.577
214.857	81954	5.5	547381	4.5	-0.17	9.81E+10	0.325
214.957	88280	3.5	553490	4.5	-0.46	5.06E+10	-0.659
214.991	81954	5.5	547090	5.5	-0.66	3.19E+10	-0.171
215.056	144077	0.5	609072	1.5	-0.85	2.04E+10	-0.472
215.131	77529	2.5	542362	3.5	-0.92	1.72E+10	-0.205
215.209	143934	1.5	608598	2.5	-0.58	3.76E+10	-0.425
215.454	82746	3.5	546881	3.5	-0.64	3.30E+10	0.223
215.492	88280	3.5	552334	3.5	-0.86	2.02E+10	0.231
215.505	82746	3.5	546771	2.5	-0.51	4.48E+10	0.238
215.607	46443	5.5	510250	4.5	-0.03	1.35E+11	-0.529
215.669	55742	3.5	519415	3.5	-0.4	5.73E+10	-0.457
215.678	83910	4.5	547565	3.5	-0.6	3.61E+10	0.155
215.763	83910	4.5	547381	4.5	-0.91	1.76E+10	0.088
215.882	75931	4.5	539146	4.5	-0.72	2.71E+10	-0.202
215.899	83910	4.5	547090	5.5	-1	1.45E+10	-0.187
215.988	56427	2.5	519415	3.5	-0.78	2.37E+10	0.522
215.996	83910	4.5	546881	3.5	-0.67	3.09E+10	-0.168
216.049	80717	4.5	543574	4.5	-0.89	1.83E+10	-0.246
216.056	46575	4.5	509418	3.5	-0.11	1.11E+11	-0.502
216.246	56427	2.5	518863	2.5	-0.89	1.82E+10	-0.216
216.247	56429	1.5	518863	2.5	-0.8	2.25E+10	0.517
216.263	76349	3.5	538749	3.5	-0.91	1.76E+10	-0.155
216.31	46578	3.5	508877	2.5	-0.22	8.51E+10	-0.485
216.337	74408	3.5	536650	4.5	-0.63	3.31E+10	0.386
216.446	46515	2.5	508524	1.5	-0.35	6.35E+10	-0.478
216.546	76349	3.5	538144	4.5	-0.96	1.55E+10	0.153
216.81	81954	5.5	543188	5.5	-0.88	1.89E+10	0.125
217.086	107131	2.5	567778	3.5	-0.69	2.86E+10	-0.575
217.42	107131	2.5	567069	2.5	-0.4	5.56E+10	0.449
217.532	75931	4.5	535632	5.5	-0.9	1.79E+10	-0.144
217.602	81954	5.5	541509	6.5	-0.6	3.53E+10	0.688
217.73	88280	3.5	547565	3.5	-0.78	2.33E+10	-0.29
217.741	95875	0.5	555137	1.5	-0.61	3.44E+10	0.786
217.964	87979	2.5	546771	2.5	-0.94	1.62E+10	-0.209
218.002	82746	3.5	541457	4.5	-0.93	1.65E+10	-0.504
218.084	107131	2.5	565670	2.5	-0.92	1.67E+10	0.288
218.239	106957	1.5	565170	1.5	-0.5	4.47E+10	0.559
218.346	88280	3.5	546268	2.5	-0.83	2.05E+10	0.209
218.456	143934	1.5	601692	0.5	-0.5	4.44E+10	0.746
218.524	144077	0.5	601692	0.5	-0.95	1.56E+10	-0.458
219.366	106957	1.5	562816	2.5	-0.67	2.98E+10	0.429
219.757	107131	2.5	562178	3.5	-0.94	1.60E+10	0.204
219.918	50732	2.5	505447	2.5	-0.88	1.84E+10	-0.29
220.112	106957	1.5	561271	0.5	-0.9	1.74E+10	0.35
220.224	88280	3.5	542362	3.5	-0.92	1.65E+10	0.19
220.299	119534	4.5	573463	3.5	-0.99	1.39E+10	-0.162
220.821	143934	1.5	596790	1.5	-0.8	2.17E+10	0.383
220.898	156374	1.5	609072	1.5	-0.33	6.44E+10	-0.647
221.056	156224	2.5	608598	2.5	-0.14	1.00E+11	-0.654
221.129	156374	1.5	608598	2.5	-0.74	2.50E+10	0.69
222.235	50732	2.5	500706	1.5	-0.95	1.53E+10	-0.432
222.368	55742	3.5	505447	2.5	-0.75	2.42E+10	-0.471
222.677	156224	2.5	605306	2.5	-0.88	1.77E+10	-0.721
222.751	156374	1.5	605306	2.5	-0.46	4.64E+10	-0.469
223	156224	2.5	604655	3.5	-0.27	7.25E+10	-0.675
223.03	88280	3.5	536650	4.5	-0.92	1.62E+10	-0.238
224.691	144077	0.5	589132	1.5	-0.7	2.63E+10	-0.596
224.926	143934	1.5	588525	2.5	-0.63	3.08E+10	-0.532
225.058	156224	2.5	600555	3.5	-0.98	1.40E+10	0.702
225.487	75931	4.5	519415	3.5	-0.18	8.77E+10	-0.592
225.626	119605	3.5	562816	2.5	-0.8	2.08E+10	0.169
225.7	76349	3.5	519415	3.5	-0.91	1.60E+10	0.475
225.813	76019	2.5	518863	2.5	-0.98	1.37E+10	0.497
225.915	119534	4.5	562178	3.5	-0.61	3.25E+10	0.179
225.982	76349	3.5	518863	2.5	-0.38	5.42E+10	-0.486
226.11	76019	2.5	518282	1.5	-0.67	2.80E+10	-0.468
226.208	119605	3.5	561677	4.5	-0.5	4.16E+10	-0.485
226.694	119534	4.5	560658	5.5	-0.6	3.28E+10	-0.317
226.777	76886	1.5	517847	0.5	-0.8	2.06E+10	-0.485
226.981	156224	2.5	596790	1.5	-0.52	3.90E+10	-0.477
227.049	107131	2.5	547565	3.5	-0.67	2.75E+10	-0.418
227.369	106957	1.5	546771	2.5	-0.9	1.62E+10	-0.325
227.373	119534	4.5	559339	4.5	-0.97	1.39E+10	0.076
229.603	119534	4.5	555069	5.5	-0.96	1.38E+10	-0.19
230.245	75931	4.5	510250	4.5	-0.64	2.87E+10	-0.395
230.363	119605	3.5	553703	3.5	-0.57	3.34E+10	0.221
230.438	119534	4.5	553490	4.5	-0.41	4.89E+10	0.247
230.91	76349	3.5	509418	3.5	-0.87	1.68E+10	-0.265

In IV-VII

In IV

Energy Levels

Table A13: Comparison between available experimental data and calculated even energy levels (in cm^{-1}) in In IV

E^a_{exp}	E^b_{calc}	ΔE	J	Leading components (in %) in LS coupling ^{c}
0	0	0	0	99.3 4d^{10} (^{1}S) ^{1}S
128641.4	128681	-39.6	3	99.4 4d^{9}5s (^{2}D) ^{3}D
130879.2	130833	46.2	2	72.7 4d^{9}5s (^{2}D) ^{3}D + 26.7 4d^{9}5s (^{2}D) ^{1}D
135791.4	135781	10.4	1	99.4 4d^{9}5s (^{2}D) ^{3}D +
138662.1	138679	-16.9	2	72.6 4d^{9}5s (^{2}D) ^{1}D + 26.7 4d^{9}5s (^{2}D) ^{3}D
277340.2	277373	-32.8	4	94.2 4d^{8}5s^2 (^{3}F) ^{3}F
283497.2	283379	118.2	3	93.9 4d^{8}5s^2 (^{3}F) ^{3}F
284985.4	285120	-134.6	2	65.2 4d^{8}5s^2 (^{3}F) ^{3}F + 21.3 4d^{8}5s^2 (^{1}D) ^{1}D + 5 4d^{8}5s^2 (^{3}P) ^{3}P
285946.9	285916	30.9	1	78.1 4d^{9}5d (^{2}D) ^{3}S + 18 4d^{9}5d (^{2}D) ^{3}P
288732.1	288772	-39.9	2	62.6 4d^{9}5d (^{2}D) ^{3}P + 18.8 4d^{9}5d (^{2}D) ^{3}D + 10.3 4d^{8}5s^2 (^{3}P) ^{3}P
289011.5	289036	-24.5	4	46.9 4d^{9}5d (^{2}D) ^{1}G + 50.7 4d^{9}5d (^{2}D) ^{3}G
289432.9	289421	11.9	5	99.5 4d^{9}5d (^{2}D) ^{3}G +
289515.2	289549	-33.8	1	48.9 4d^{9}5d (^{2}D) ^{1}P + 24.5 4d^{9}5d (^{2}D) ^{3}P + 22.3 4d^{9}5d (^{2}D) ^{3}D
290845.9	290863	-17.1	3	78.9 4d^{9}5d (^{2}D) ^{3}D + 17.3 4d^{9}5d (^{2}D) ^{3}F
291474.8	291422	52.8	2	33.9 4d^{9}5d (^{2}D) ^{3}D + 36.5 4d^{9}5d (^{2}D) ^{1}D + 12.2 4d^{8}5s^2 (^{3}F) ^{3}F
291620.6	291661	-40.4	3	48 4d^{9}5d (^{2}D) ^{1}F + 23.2 4d^{9}5d (^{2}D) ^{3}G + 20.1 4d^{9}5d (^{2}D) ^{3}F
292068.6	291950	118.6	0	84.7 4d^{9}5d (^{2}D) ^{3}P + 11.2 4d^{8}5s^2 (^{3}P) ^{3}P
292221.8	292195	26.8	4	74.2 4d^{9}5d (^{2}D) ^{3}F + 15.8 4d^{9}5d (^{2}D) ^{1}G + 7.6 4d^{9}5d (^{2}D) ^{3}G
293229.7	293267	-37.3	2	41 4d^{8}5s^2 (^{3}P) ^{3}P + 16.6 4d^{8}5s^2 (^{1}D) ^{1}D + 16.1 4d^{9}5d (^{2}D) ^{3}P
294544.8	294629	-84.2	1	36.6 4d^{9}5d (^{2}D) ^{3}P + 29.1 4d^{9}5d (^{2}D) ^{1}P + 17 4d^{9}5d (^{2}D) ^{3}S
296394.7	296359	35.7	3	74 4d^{9}5d (^{2}D) ^{3}G + 18.1 4d^{9}5d (^{2}D) ^{1}F + 7.2 4d^{9}5d (^{2}D) ^{3}F
296723.8	296782	-58.2	1	69.6 4d^{9}5d (^{2}D) ^{3}D + 19.2 4d^{9}5d (^{2}D) ^{1}P + 8.8 4d^{8}5s^2 (^{3}P) ^{3}P
296993.7	296970	23.7	4	40.3 4d^{9}5d (^{2}D) ^{3}G + 31.4 4d^{9}5d (^{2}D) ^{1}G + 22.2 4d^{9}5d (^{2}D) ^{3}F
297086.6	297157	-70.4	2	35.4 4d^{9}5d (^{2}D) ^{1}D + 27.2 4d^{9}5d (^{2}D) ^{3}D + 11.5 4d^{9}5d (^{2}D) ^{3}P
297850.5	297864	-13.5	0	79.3 4d^{8}5s^2 (^{3}P) ^{3}P + 11.3 4d^{9}5d (^{2}D) ^{3}P + 5.7 4d^{8}5s^2 (^{1}S) ^{1}S
298619.5	298588	31.5	1	70.1 4d^{8}5s^2 (^{3}P) ^{3}P + 18.8 4d^{9}5d (^{2}D) ^{3}P + 6.6 4d^{9}5d (^{2}D) ^{3}D
298643.9	298650	-6.1	3	99.8 4d^{9}6s (^{2}D) ^{3}D
298925.8	298873	52.8	2	69.2 4d^{9}5d (^{2}D) ^{3}F + 18.4 4d^{9}5d (^{2}D) ^{3}D
299322.9	299316	6.9	2	50.9 4d^{9}6s (^{2}D) ^{1}D + 47.6 4d^{9}6s (^{2}D) ^{3}D
299325.2	299330	-4.8	3	51.8 4d^{9}5d (^{2}D) ^{3}F + 33.1 4d^{9}5d (^{2}D) ^{1}F + 13.3 4d^{9}5d (^{2}D) ^{3}D
301456.6	301363	93.6	2	43.3 4d^{8}5s^2 (^{1}D) ^{1}D + 21.7 4d^{8}5s^2 (^{3}P) ^{3}P + 13.7 4d^{9}5d (^{2}D) ^{1}D
302457.9	302459	-1.1	4	88.7 4d^{8}5s^2 (^{1}G) ^{1}G + 5.3 4d^{9}5d (^{2}D) ^{1}G
305793.7	305788	5.7	1	99.9 4d^{9}6s (^{2}D) ^{3}D
306290.2	306296	-5.8	2	51.8 4d^{9}6s (^{2}D) ^{3}D + 48 4d^{9}6s (^{2}D) ^{1}D
309455.8	309459	-3.2	0	88.7 4d^{9}5d (^{2}D) ^{1}S + 5.5 4d^{9}6d (^{2}D) ^{1}S
356718.8	356766	-47.2	1	67.3 4d^{9}6d (^{2}D) ^{3}S + 27.2 4d^{9}6d (^{2}D) ^{3}P
357807.8	357815	-7.2	4	47.1 4d^{9}6d (^{2}D) ^{1}G + 51.1 4d^{9}6d (^{2}D) ^{3}G
357968.8	357879	89.8	2	63.7 4d^{9}6d (^{2}D) ^{3}P + 33.6 4d^{9}6d (^{2}D) ^{3}D
357920.8	357890	30.8	5	99.9 4d^{9}6d (^{2}D) ^{3}G
358005.8	357974	31.8	1	53.5 4d^{9}6d (^{2}D) ^{1}P + 26.8 4d^{9}6d (^{2}D) ^{3}D + 18 4d^{9}6d (^{2}D) ^{3}P
358397.6	358406	-8.4	3	68.9 4d^{9}6d (^{2}D) ^{3}D + 28.5 4d^{9}6d (^{2}D) ^{3}F
358745.8	358760	-14.2	3	56.3 4d^{9}6d (^{2}D) ^{1}F + 18.5 4d^{9}6d (^{2}D) ^{3}F + 13.5 4d^{9}6d (^{2}D) ^{3}D
358841	358843	-2	2	54.3 4d^{9}6d (^{2}D) ^{1}D + 17.4 4d^{9}6d (^{2}D) ^{3}D + 17 4d^{9}6d (^{2}D) ^{3}F
358944.4	358937	7.4	4	85.2 4d^{9}6d (^{2}D) ^{3}F + 11.9 4d^{9}6d (^{2}D) ^{1}G
360739.1	360859	-119.9	0	88.2 4d^{9}6d (^{2}D) ^{3}P + 10.2 4d^{9}6d (^{2}D) ^{1}S
360971.5	360980	-8.5	3	99.8 4d^{9}7s (^{2}D) ^{3}D
361238.1	361230	8.1	2	56.9 4d^{9}7s (^{2}D) ^{1}D + 42.9 4d^{9}7s (^{2}D) ^{3}D
364509.3	364477	32.3	1	39.6 4d^{9}6d (^{2}D) ^{3}P + 30.1 4d^{9}6d (^{2}D) ^{3}S + 28.8 4d^{9}6d (^{2}D) ^{1}P
364917.7	364912	5.7	3	85.8 4d^{9}6d (^{2}D) ^{3}G + 10.2 4d^{9}6d (^{2}D) ^{1}F
365226.7	365217	9.7	1	71.2 4d^{9}6d (^{2}D) ^{3}D + 14.9 4d^{9}6d (^{2}D) ^{3}P + 13.1 4d^{9}6d (^{2}D) ^{1}P
365353.4	365347	6.4	4	46.1 4d^{9}6d (^{2}D) ^{3}G + 40.9 4d^{9}6d (^{2}D) ^{1}G + 12.9 4d^{9}6d (^{2}D) ^{3}F
365644.3	365625	19.3	2	45.1 4d^{9}6d (^{2}D) ^{3}D + 28.1 4d^{9}6d (^{2}D) ^{1}D + 24.8 4d^{9}6d (^{2}D) ^{3}P
365914.3	365942	-27.7	2	78.8 4d^{9}6d (^{2}D) ^{3}F + 17 4d^{9}6d (^{2}D) ^{1}D
366067.7	366091	-23.3	3	49 4d^{9}6d (^{2}D) ^{3}F + 33.2 4d^{9}6d (^{2}D) ^{1}F + 17.2 4d^{9}6d (^{2}D) ^{3}D
368163	368152	11	1	99.8 4d^{9}7s (^{2}D) ^{3}D
368320.4	368331	-10.6	2	56.9 4d^{9}7s (^{2}D) ^{3}D + 42.9 4d^{9}7s (^{2}D) ^{1}D
370640.4	370624	16.4	0	76.8 4d^{9}6d (^{2}D) ^{1}S + 11.5 4d^{9}6d (^{2}D) ^{3}P + 7.9 4d^{9}7d (^{2}D) ^{1}S
391586.5	391246	340.5	2	60.4 4d^{9}7d (^{2}D) ^{3}P + 33.8 4d^{9}7d (^{2}D) ^{3}D
391446.1	391258	188.1	3	94.1 4d^{9}8s (^{2}D) ^{3}D

a: From Swapnil [32] and Ryabtsev [33]
b: This work
c: Only the component $\geq$ 5% are given

Table A14: Comparison between available experimental data and calculated odd energy levels (in cm^{-1}) in In IV

E^a_{exp}	E^b_{calc}	ΔE	J	Leading components (in %) in LS coupling ^{c}
193894.2	193941	-46.8	2	87.3 4d^{9}5p (^{2}D) ^{3}P + 9.9 4d^{9}5p (^{2}D) ^{3}D
196599.7	196561	38.7	3	57.7 4d^{9}5p (^{2}D) ^{3}F + 32.5 4d^{9}5p (^{2}D) ^{1}F + 9.3 4d^{9}5p (^{2}D) ^{3}D
200553.1	200542	11.1	1	88.9 4d^{9}5p (^{2}D) ^{3}P + 8.5 4d^{9}5p (^{2}D) ^{3}D
201051.4	201090	-38.6	4	99.6 4d^{9}5p (^{2}D) ^{3}F
202024.6	202009	15.6	2	83.4 4d^{9}5p (^{2}D) ^{3}F + 10.8 4d^{9}5p (^{2}D) ^{3}D
204947.6	204887	60.6	0	99.5 4d^{9}5p (^{2}D) ^{3}P
205252.2	205287	-34.8	2	65.8 4d^{9}5p (^{2}D) ^{1}D + 19.3 4d^{9}5p (^{2}D) ^{3}D + 9.1 4d^{9}5p (^{2}D) ^{3}F
205848.9	205789	59.9	3	71.6 4d^{9}5p (^{2}D) ^{3}D + 27.5 4d^{9}5p (^{2}D) ^{1}F
208598.5	208599	-0.5	1	76.1 4d^{9}5p (^{2}D) ^{1}P + 23.4 4d^{9}5p (^{2}D) ^{3}D
209781.2	209856	-74.8	3	39.5 4d^{9}5p (^{2}D) ^{1}F + 41.6 4d^{9}5p (^{2}D) ^{3}F + 18.5 4d^{9}5p (^{2}D) ^{3}D
211546.8	211541	5.8	1	67.6 4d^{9}5p (^{2}D) ^{3}D + 21.3 4d^{9}5p (^{2}D) ^{1}P + 10.6 4d^{9}5p (^{2}D) ^{3}P
212679.6	212674	5.6	2	59.4 4d^{9}5p (^{2}D) ^{3}D + 31.1 4d^{9}5p (^{2}D) ^{1}D + 6.4 4d^{9}5p (^{2}D) ^{3}F
321515.5	321331	184.5	2	82.9 4d^{9}6p (^{2}D) ^{3}P + 14.5 4d^{9}6p (^{2}D) ^{3}D
321925.8	321991	-65.2	3	50.6 4d^{9}6p (^{2}D) ^{3}F + 38.9 4d^{9}6p (^{2}D) ^{1}F + 10.1 4d^{9}6p (^{2}D) ^{3}D
323452.2	323530	-77.8	4	99.4 4d^{9}6p (^{2}D) ^{3}F + 0.2 4d^{9}4f (^{2}D) ^{3}F
323892.8	323899	-6.2	1	45.7 4d^{9}6p (^{2}D) ^{3}P + 44.7 4d^{9}6p (^{2}D) ^{1}P + 7.6 4d^{9}6p (^{2}D) ^{3}D
324424	324483	-59	2	51.1 4d^{9}6p (^{2}D) ^{1}D + 26.3 4d^{9}6p (^{2}D) ^{3}D + 11.1 4d^{9}6p (^{2}D) ^{3}F
324925.2	324907	18.2	3	79.8 4d^{9}6p (^{2}D) ^{3}D + 19.4 4d^{9}6p (^{2}D) ^{1}F
327893.1	327832	61.1	0	91.2 4d^{9}4f (^{2}D) ^{3}P + 7.6 4d^{9}6p (^{2}D) ^{3}P
328547.4	328596	-48.6	1	79.2 4d^{9}4f (^{2}D) ^{3}P + 8.7 4d^{9}4f (^{2}D) ^{3}D + 8.6 4d^{9}6p (^{2}D) ^{1}P
328806.5	328921	-114.5	2	80 4d^{9}6p (^{2}D) ^{3}F + 18.8 4d^{9}6p (^{2}D) ^{1}D
329330.2	329309	21.2	1	43 4d^{9}6p (^{2}D) ^{1}P + 32.7 4d^{9}6p (^{2}D) ^{3}P + 11.8 4d^{9}6p (^{2}D) ^{3}D
329640.5	329756	-115.5	2	64.6 4d^{9}4f (^{2}D) ^{3}P + 21.3 4d^{9}4f (^{2}D) ^{3}D + 12.6 4d^{9}4f (^{2}D) ^{1}D
329773.4	329817	-43.6	0	92.1 4d^{9}6p (^{2}D) ^{3}P + 7.5 4d^{9}4f (^{2}D) ^{3}P
330512.3	330543	-30.7	6	99.7 4d^{9}4f (^{2}D) ^{3}H
330858.3	330829	29.3	5	51.9 4d^{9}4f (^{2}D) ^{3}H + 47.3 4d^{9}4f (^{2}D) ^{1}H
331003.1	330953	50.1	3	40.5 4d^{9}6p (^{2}D) ^{1}F + 47.4 4d^{9}6p (^{2}D) ^{3}F + 9.4 4d^{9}6p (^{2}D) ^{3}D
331368.5	331309	59.5	1	78.3 4d^{9}6p (^{2}D) ^{3}D + 19.2 4d^{9}6p (^{2}D) ^{3}P
331916.2	331886	30.2	2	55.9 4d^{9}6p (^{2}D) ^{3}D + 27.6 4d^{9}6p (^{2}D) ^{1}D + 7.4 4d^{9}6p (^{2}D) ^{3}F
332072.4	331952	120.4	2	37.6 4d^{9}4f (^{2}D) ^{1}D + 34.1 4d^{9}4f (^{2}D) ^{3}F + 23.3 4d^{9}4f (^{2}D) ^{3}D
331945.4	332009	-63.6	3	57.8 4d^{9}4f (^{2}D) ^{3}D + 34.4 4d^{9}4f (^{2}D) ^{3}F
332541.6	332532	9.6	4	62.2 4d^{9}4f (^{2}D) ^{3}F + 30.6 4d^{9}4f (^{2}D) ^{3}G
332743.2	332743	0.2	4	48.4 4d^{9}4f (^{2}D) ^{1}G + 19.8 4d^{9}4f (^{2}D) ^{3}H + 16.2 4d^{9}4f (^{2}D) ^{3}F
332819.1	332809	10.1	5	75.4 4d^{9}4f (^{2}D) ^{3}G + 14 4d^{9}4f (^{2}D) ^{1}H + 8.8 4d^{9}4f (^{2}D) ^{3}H
333233.6	333228	5.6	3	47.5 4d^{9}4f (^{2}D) ^{1}F + 22.2 4d^{9}4f (^{2}D) ^{3}G + 19 4d^{9}4f (^{2}D) ^{3}F
333972.3	333970	2.3	1	78 4d^{9}4f (^{2}D) ^{3}D + 11.4 4d^{9}4f (^{2}D) ^{1}P + 5.9 4d^{9}4f (^{2}D) ^{3}P
335865.5	335838	27.5	3	69.1 4d^{8}5s5p (^{3}F) ^{5}D + 10.9 4d^{8}5s5p (^{3}F) ^{5}F + 9.2 4d^{8}5s5p (^{3}P) ^{5}D
337003.8	336981	22.8	2	38.1 4d^{9}4f (^{2}D) ^{3}D + 33.5 4d^{9}4f (^{2}D) ^{3}P + 26.6 4d^{9}4f (^{2}D) ^{1}D
337978.7	337829	149.7	4	60.4 4d^{9}4f (^{2}D) ^{3}H + 12.5 4d^{8}5s5p (^{3}F) ^{5}G + 7.3 4d^{9}4f (^{2}D) ^{1}G
338146.8	338216	-69.2	5	38 4d^{9}4f (^{2}D) ^{1}H + 38.6 4d^{9}4f (^{2}D) ^{3}H + 22.3 4d^{9}4f (^{2}D) ^{3}G
338200.7	338355	-154.3	4	43.3 4d^{8}5s5p (^{3}F) ^{5}G + 14.8 4d^{9}4f (^{2}D) ^{3}H + 11 4d^{8}5s5p (^{3}F) ^{5}F
339093.2	339083	10.2	2	62.7 4d^{9}4f (^{2}D) ^{3}F + 21.3 4d^{9}4f (^{2}D) ^{1}D + 14.3 4d^{9}4f (^{2}D) ^{3}D
339567.8	339446	121.8	3	42.3 4d^{9}4f (^{2}D) ^{3}F + 27.5 4d^{9}4f (^{2}D) ^{3}D + 16.5 4d^{9}4f (^{2}D) ^{1}F
339881.9	339853	28.9	2	68.8 4d^{8}5s5p (^{3}F) ^{5}D + 14.8 4d^{8}5s5p (^{3}P) ^{5}D + 7.7 4d^{8}5s5p (^{3}F) ^{5}F
339794.6	340105	-310.4	4	42.4 4d^{9}4f (^{2}D) ^{3}G + 36 4d^{9}4f (^{2}D) ^{1}G + 20 4d^{9}4f (^{2}D) ^{3}F
340333.8	340131	202.8	3	52.5 4d^{9}4f (^{2}D) ^{3}G + 30 4d^{9}4f (^{2}D) ^{1}F + 7.5 4d^{8}5s5p (^{3}F) ^{5}G
340919.3	341024	-104.7	3	62.4 4d^{8}5s5p (^{3}F) ^{5}G + 12.2 4d^{8}5s5p (^{3}F) ^{5}F + 8.2 4d^{9}4f (^{2}D) ^{3}G
341920.7	342117	-196.3	2	65 4d^{8}5s5p (^{3}F) ^{5}G + 10.4 4d^{8}5s5p (^{1}D) ^{3}F + 10.3 4d^{8}5s5p (^{3}F) ^{5}F
342526.8	342504	22.8	1	69.6 4d^{8}5s5p (^{3}F) ^{5}D + 19.6 4d^{8}5s5p (^{3}P) ^{5}D + 5 4d^{8}5s5p (^{3}F) ^{5}F
343003	342991	12	1	77.6 4d^{9}4f (^{2}D) ^{1}P + 10.1 4d^{9}4f (^{2}D) ^{3}D
344718.3	344490	228.3	4	55 4d^{8}5s5p (^{3}F) ^{5}F + 10.8 4d^{8}5s5p (^{3}F) ^{3}G + 9 4d^{8}5s5p (^{3}F) ^{1}G
344859	344847	12	2	27.7 4d^{8}5s5p (^{3}P) ^{5}P + 17.7 4d^{8}5s5p (^{3}F) ^{5}G + 15 4d^{8}5s5p (^{1}D) ^{3}D
345259	345176	83	1	34.1 4d^{8}5s5p (^{3}F) ^{5}F + 30 4d^{8}5s5p (^{1}D) ^{3}D + 7.3 4d^{8}5s5p (^{3}F) ^{3}D
345738.5	345866	-127.5	3	23.3 4d^{8}5s5p (^{3}F) ^{3}D + 19.3 4d^{8}5s5p (^{3}F) ^{3}F + 10.6 4d^{8}5s5p (^{3}F) ^{5}D
346271.9	346187	84.9	3	32.6 4d^{8}5s5p (^{3}F) ^{5}F + 15.4 4d^{8}5s5p (^{3}P) ^{5}P + 11.6 4d^{8}5s5p (^{1}D) ^{3}D
346388.9	346613	-224.1	4	16.5 4d^{8}5s5p (^{3}F) ^{3}G + 32.6 4d^{8}5s5p (^{3}F) ^{5}G + 19.5 4d^{8}5s5p (^{3}F) ^{1}G
348130.4	348046	84.4	2	54.2 4d^{8}5s5p (^{3}F) ^{5}F + 9 4d^{8}5s5p (^{3}F) ^{5}D + 7.1 4d^{8}5s5p (^{3}P) ^{5}P
348955.6	348673	282.6	3	38.8 4d^{8}5s5p (^{3}P) ^{5}P + 18.8 4d^{8}5s5p (^{3}F) ^{3}D + 9.7 4d^{8}5s5p (^{3}F) ^{5}F
349088.8	348976	112.8	2	22.2 4d^{8}5s5p (^{3}F) ^{3}D + 34.9 4d^{8}5s5p (^{3}P) ^{5}P + 11.8 4d^{8}5s5p (^{3}F) ^{3}D
350304.6	350402	-97.4	3	37.5 4d^{8}5s5p (^{3}F) ^{3}G + 19.9 4d^{8}5s5p (^{3}F) ^{3}G + 19.1 4d^{8}5s5p (^{3}P) ^{5}P
351714.5	351987	-272.5	4	35.9 4d^{8}5s5p (^{3}F) ^{3}F + 30.7 4d^{8}5s5p (^{3}F) ^{3}F + 17.8 4d^{8}5s5p (^{3}F) ^{5}F
352253.3	352066	187.3	3	17 4d^{8}5s5p (^{3}F) ^{3}F + 26.3 4d^{8}5s5p (^{3}F) ^{1}F + 16.6 4d^{8}5s5p (^{3}F) ^{5}F
352173.1	352149	24.1	1	5.1 4d^{8}5s5p (^{1}D) ^{3}P + 32 4d^{8}5s5p (^{3}F) ^{5}F + 22.9 4d^{8}5s5p (^{3}F) ^{3}D
354150.4	353660	490.4	2	43.6 4d^{8}5s5p (^{3}F) ^{1}D + 14.5 4d^{8}5s5p (^{3}F) ^{3}F + 12.4 4d^{8}5s5p (^{1}D) ^{3}D
354111.7	353770	341.7	4	27.1 4d^{8}5s5p (^{3}F) ^{1}G + 36.4 4d^{8}5s5p (^{1}D) ^{3}F + 17 4d^{8}5s5p (^{3}P) ^{5}D
354929.1	354803	126.1	2	35 4d^{8}5s5p (^{1}D) ^{3}F + 14 4d^{8}5s5p (^{3}F) ^{3}D + 10 4d^{8}5s5p (^{3}F) ^{5}G
356138.3	356388	-249.7	2	19.5 4d^{8}5s5p (^{3}F) ^{3}F + 17.7 4d^{8}5s5p (^{3}F) ^{3}F + 15.1 4d^{8}5s5p (^{3}F) ^{1}D
356309	356392	-83	3	22.4 4d^{8}5s5p (^{1}D) ^{3}D + 16 4d^{8}5s5p (^{3}P) ^{5}P + 14.2 4d^{8}5s5p (^{3}F) ^{1}F
356582.8	356720	-137.2	3	18.3 4d^{8}5s5p (^{3}F) ^{1}F + 28.1 4d^{8}5s5p (^{3}P) ^{5}D + 13.7 4d^{8}5s5p (^{1}D) ^{3}F
358034.5	357868	166.5	1	21.3 4d^{8}5s5p (^{3}F) ^{3}D + 22.3 4d^{8}5s5p (^{3}P) ^{3}P + 10.8 4d^{8}5s5p (^{3}F) ^{3}D
358628.7	358718	-89.3	0	62.9 4d^{8}5s5p (^{3}P) ^{5}D + 25.4 4d^{8}5s5p (^{3}F) ^{5}D
358751.6	358897	-145.4	4	47.5 4d^{8}5s5p (^{3}P) ^{5}D + 22.6 4d^{8}5s5p (^{3}F) ^{1}G + 11.2 4d^{8}5s5p (^{3}F) ^{3}G
358922.3	358942	-19.7	1	63.3 4d^{8}5s5p (^{3}P) ^{5}D + 19.4 4d^{8}5s5p (^{3}F) ^{5}D
359563.3	359447	116.3	2	20.1 4d^{8}5s5p (^{3}P) ^{3}P + 24.5 4d^{8}5s5p (^{3}P) ^{5}D + 19.9 4d^{8}5s5p (^{1}D) ^{3}D
360307	360039	268	2	36.2 4d^{8}5s5p (^{3}P) ^{5}D + 14.5 4d^{8}5s5p (^{1}D) ^{3}F + 10.8 4d^{8}5s5p (^{3}F) ^{5}D
360330.7	360148	182.7	4	60.5 4d^{8}5s5p (^{1}G) ^{3}F + 11.5 4d^{8}5s5p (^{3}P) ^{5}D + 10.9 4d^{8}5s5p (^{1}G) ^{3}H
360831.9	360388	443.9	1	32.5 4d^{8}5s5p (^{1}D) ^{3}D + 22.9 4d^{8}5s5p (^{1}D) ^{3}P + 14.6 4d^{8}5s5p (^{3}P) ^{1}P
360920.3	361014	-93.7	4	82 4d^{8}5s5p (^{1}G) ^{3}H + 8.2 4d^{8}5s5p (^{1}G) ^{3}F + 6.2 4d^{8}5s5p (^{3}F) ^{1}G
361284.1	361033	251.1	3	33.2 4d^{8}5s5p (^{1}G) ^{3}F + 30 4d^{8}5s5p (^{3}P) ^{5}D + 14.7 4d^{8}5s5p (^{1}D) ^{3}F
362115.9	361961	154.9	2	38.3 4d^{8}5s5p (^{1}D) ^{3}P + 12.3 4d^{8}5s5p (^{3}P) ^{3}D + 12.3 4d^{8}5s5p (^{3}F) ^{1}D
362278.5	362942	-663.5	3	7.2 4d^{8}5s5p (^{1}D) ^{3}F + 31.2 4d^{8}5s5p (^{1}D) ^{3}D + 26.2 4d^{8}5s5p (^{3}F) ^{1}F
362948.8	363323	-374.2	2	20.6 4d^{8}5s5p (^{1}D) ^{3}D + 18 4d^{8}5s5p (^{3}P) ^{3}P + 11.2 4d^{8}5s5p (^{3}P) ^{3}P
363895.5	364303	-407.5	1	33.7 4d^{8}5s5p (^{3}P) ^{3}D + 18.7 4d^{8}5s5p (^{1}D) ^{3}P + 15.7 4d^{8}5s5p (^{3}P) ^{3}P
364988.4	365408	-419.6	3	14.2 4d^{8}5s5p (^{3}P) ^{5}D + 28 4d^{8}5s5p (^{1}G) ^{3}F + 19.1 4d^{8}5s5p (^{3}P) ^{3}D
366418.6	365691	727.6	2	8.3 4d^{8}5s5p (^{3}P) ^{3}D + 31.7 4d^{8}5s5p (^{1}G) ^{3}F + 11.5 4d^{8}5s5p (^{3}P) ^{3}P
366197.3	365776	421.3	1	7.3 4d^{8}5s5p (^{3}P) ^{3}P + 29.8 4d^{8}5s5p (^{3}P) ^{1}P + 16.5 4d^{8}5s5p (^{3}P) ^{3}D
367240.2	367501	-260.8	0	43.4 4d^{8}5s5p (^{1}D) ^{3}P + 29.8 4d^{8}5s5p (^{3}P) ^{3}P + 14.2 4d^{8}5s5p (^{3}P) ^{1}S
367621.3	367617	4.3	2	70.1 4d^{8}5s5p (^{3}P) ^{5}S + 11.4 4d^{8}5s5p (^{1}D) ^{3}P + 5.9 4d^{8}5s5p (^{1}G) ^{3}F
368048.7	368260	-211.3	4	50.5 4d^{8}5s5p (^{1}D) ^{3}F + 15.4 4d^{8}5s5p (^{1}G) ^{3}F + 14.7 4d^{8}5s5p (^{3}P) ^{5}D
368820.4	368709	111.4	2	37.3 4d^{8}5s5p (^{1}G) ^{3}F + 12.7 4d^{8}5s5p (^{3}P) ^{3}D + 11 4d^{8}5s5p (^{1}D) ^{3}F
368857.8	368848	9.8	3	30.1 4d^{8}5s5p (^{3}P) ^{3}D + 13.6 4d^{8}5s5p (^{1}D) ^{3}F + 12.2 4d^{8}5s5p (^{3}F) ^{3}D
370001.4	369992	9.4	1	34 4d^{8}5s5p (^{3}P) ^{1}P + 12.7 4d^{8}5s5p (^{1}D) ^{3}P + 9.9 4d^{8}5s5p (^{3}P) ^{3}P

Table A14: Continued

E^{a}_{exp}	E^{b}_{calc}	ΔE	J	Leading components (in %) in LS coupling [c]
370806.6	371118	-311.4	2	56.7 $4d^8 5s5p$ (^3P) ^1D + 6.7 $4d^9 5F$ (^2D) ^1D + 5.6 $4d^8 5s5p$ (^3P) ^3D
371525.5	371494	31.5	2	69.6 $4d^9 7p$ (^2D) ^3P + 17.8 $4d^9 7p$ (^2D) ^3D
371915.9	371845	70.9	3	43.6 $4d^9 7p$ (^2D) ^1F + 47.5 $4d^9 7p$ (^2D) ^3F + 6.3 $4d^9 7p$ (^2D) ^3D
371655.4	372017	-361.6	1	27.9 $4d^8 5s5p$ (^3P) ^3S + 29.5 $4d^8 5s5p$ (^3P) ^3S + 19.2 $4d^9 5F$ (^2D) ^3P
372145.7	372246	-100.3	1	56.2 $4d^9 5F$ (^2D) ^3P + 9.6 $4d^9 5F$ (^2D) ^3D + 8.2 $4d^8 5s5p$ (^3P) ^3S
372549.3	372629	-79.7	4	77.3 $4d^9 7p$ (^2D) ^3F + 8.3 $4d^9 5F$ (^2D) ^3F + 5.4 $4d^9 5F$ (^2D) ^3G
372701.4	372717	-15.6	1	47.5 $4d^9 7p$ (^2D) ^1P + 32.1 $4d^9 7p$ (^2D) ^3P + 8.4 $4d^9 7p$ (^2D) ^3D
373535.4	373294	241.4	6	98.5 $4d^9 5F$ (^2D) ^3H
374448.1	374712	-263.9	4	79.4 $4d^8 5s5p$ (^1G) ^3G + 6.1 $4d^9 5F$ (^2D) ^3G

a: From Swapnil [32] and Ryabtsev [33]
b: This work
c: Only the component $\geq$ 5% are given

Transitions

Table A15: Computed oscillator strengths and transition probabilities in In IV.

Wavelength	Lower Level[a]	J_{Low}	Upper level[a]	J_{Up}	log gf	gA	CF
291.543	0	0	343003	1	-0.13	5.77E+10	0.335
299.426	0	0	333972	1	-0.89	9.61E+09	0.374
416.361	128681	3	368858	3	-0.6	9.68E+09	0.146
420.633	128681	3	366419	2	-0.91	4.57E+09	0.206
424.557	130879	2	366419	2	-0.99	3.79E+09	0.111
427.151	130879	2	364988	3	-0.67	7.89E+09	0.275
428.386	128681	3	362116	2	-0.98	3.80E+09	0.255
429.131	135791	1	368820	2	-0.59	9.29E+09	0.396
430.591	128681	3	360920	4	-0.92	4.29E+09	0.922
431.687	128681	3	360331	4	-0.02	3.39E+10	0.925
431.731	128681	3	360307	2	-1	3.58E+09	0.713
432.061	135791	1	367240	0	-0.91	4.40E+09	0.898
432.266	138662	2	370001	1	-0.47	1.22E+10	0.586
433.122	128681	3	359563	2	-0.34	1.62E+10	0.767
433.6	135791	1	366419	2	-0.87	4.77E+09	0.218
434.017	135791	1	366197	1	-0.73	6.54E+09	0.337
434.018	130879	2	361284	3	-0.51	1.09E+10	0.575
434.872	130879	2	360832	1	-0.98	3.66E+09	0.22
438.396	135791	1	363896	1	-0.83	5.18E+09	0.373
439.065	138662	2	366419	2	-0.45	1.23E+10	0.595
439.314	128681	3	356309	3	-0.9	4.40E+09	0.342
440.227	130879	2	358035	1	-0.69	7.09E+09	0.381
441.84	138662	2	364988	3	-0.89	4.46E+09	0.331
441.844	135791	1	362116	2	-0.87	4.56E+09	0.876
441.993	128681	3	354929	2	-0.97	3.69E+09	0.529
443.596	128681	3	354112	4	-0.92	4.07E+09	0.506
447.194	138662	2	362279	3	-0.7	6.75E+09	0.301
447.283	128681	3	352253	3	-0.33	1.54E+10	0.789
447.52	138662	2	362116	2	-0.52	1.01E+10	0.611
447.886	130879	2	354150	2	-0.17	2.26E+10	0.709
448.364	128681	3	351715	4	-0.46	1.16E+10	0.381
449.192	138662	2	361284	3	-0.9	4.14E+09	0.497
449.958	135791	1	358035	1	-0.86	4.51E+09	0.225
451.724	130879	2	352253	3	-0.79	5.29E+09	0.233
453.98	128681	3	348956	3	-0.38	1.34E+10	0.694
458.275	130879	2	349089	2	-0.51	9.82E+09	0.412
458.883	138662	2	356583	3	-0.93	3.77E+09	0.365
459.579	128681	3	346272	3	-0.89	4.04E+09	0.189
459.821	138662	2	356138	2	-0.64	7.18E+09	0.413
460.708	128681	3	345739	3	-0.65	6.97E+09	0.31
462.146	135791	1	352173	1	-0.93	3.68E+09	0.267
464.062	138662	2	354150	2	-0.67	6.54E+09	0.177
465.421	130879	2	345739	3	-0.82	4.69E+09	0.246
472.709	0	0	211547	1	-0.73	5.62E+09	0.733
479.39	0	0	208598	1	-0.18	1.93E+10	0.735
525.225	201051	4	391446	3	-0.95	2.69E+09	0.612
598.525	193894	2	360972	3	-0.82	2.83E+09	0.558
607.392	196600	3	361238	2	-0.83	2.70E+09	0.563
620.316	196600	3	357808	4	-0.93	2.05E+09	0.393
625.312	201051	4	360972	3	-0.57	4.60E+09	0.696
630.759	209781	3	368320	2	-0.7	3.35E+09	0.755
637.473	201051	4	357921	5	-0.77	2.80E+09	0.384
641.084	205252	2	361238	2	-0.96	1.79E+09	0.503
642.505	212680	2	368320	2	-0.98	1.69E+09	0.504
642.788	209781	3	365353	4	-0.89	2.07E+09	0.41
644.652	205849	3	360972	3	-0.87	2.15E+09	0.664
945.742	200553	1	306290	2	-0.74	1.36E+09	0.401
954.656	193894	2	298644	3	-0.06	6.40E+09	0.754
959.089	202025	2	306290	2	-0.71	1.42E+09	0.5
963.678	202025	2	305794	1	-0.36	3.14E+09	0.418
973.489	196600	3	299323	2	-0.05	6.24E+09	0.593
979.968	196600	3	298644	3	-0.4	2.74E+09	0.808
989.727	205252	2	306290	2	-0.93	8.07E+08	0.109
991.499	208598	1	309456	0	-0.36	2.97E+09	0.522
991.61	204948	0	305794	1	-0.77	1.15E+09	0.751
994.614	205252	2	305794	1	-0.68	1.41E+09	0.892
1012.455	200553	1	299323	2	-0.46	2.24E+09	0.724
1023.628	208598	1	306290	2	-0.48	2.09E+09	0.736
1024.669	201051	4	298644	3	0.2	1.01E+10	0.862
1024.793	193894	2	291475	2	-0.52	1.92E+09	0.358
1027.766	202025	2	299323	2	-0.57	1.71E+09	0.668
1028.857	208598	1	305794	1	-0.98	6.65E+08	0.945
1031.441	193894	2	290846	3	0.07	7.37E+09	0.455
1031.979	202025	2	298926	2	-0.26	3.48E+09	0.272
1035.911	200553	1	297087	2	-0.52	1.87E+09	0.232
1036.173	209781	3	306290	2	0.06	7.19E+09	0.868
1039.818	200553	1	296724	1	-0.56	1.69E+09	0.309
1045.795	193894	2	289515	1	-0.56	1.68E+09	0.338
1050.32	277340	4	372549	4	-0.81	9.49E+08	0.448
1051.945	202025	2	297087	2	-0.81	9.37E+08	0.182
1052.4	196600	3	291621	3	0.04	6.55E+09	0.52
1054.017	196600	3	291475	2	-0.55	1.69E+09	0.595
1054.43	193894	2	288732	2	0.22	9.88E+09	0.584
1055.975	202025	2	296724	1	-0.85	8.39E+08	0.336
1059.658	202025	2	296395	3	0.33	1.28E+10	0.53
1061.043	211547	1	305794	1	-0.37	2.50E+09	0.909
1061.051	196600	3	290846	3	-0.24	3.40E+09	0.425
1063.029	205252	2	299323	2	-0.15	4.19E+09	0.586
1063.924	200553	1	294545	1	-0.72	1.14E+09	0.205
1067.537	205252	2	298926	2	-0.95	6.62E+08	0.109
1067.556	204948	0	298620	1	-0.7	1.18E+09	0.526
1068.255	212680	2	306290	2	-0.17	3.96E+09	0.696
1069.816	205849	3	299323	2	-0.48	1.93E+09	0.596
1073.951	212680	2	305794	1	-0.58	1.54E+09	0.905
1076.912	208598	1	301457	2	-0.78	9.46E+08	0.335
1077.645	205849	3	298644	3	-0.07	4.90E+09	0.893

Table A15: Continued

Wavelength	Lower Level	J_{Low}	Upper level	J_{Up}	log gf	gA	CF
1079.02	209781	3	302458	4	-0.71	1.11E+09	0.354
1079.021	200553	1	293230	2	-0.77	9.83E+08	0.486
1082.113	196600	3	289011	4	0.7	2.84E+10	0.892
1085.394	196600	3	288732	2	-0.72	1.09E+09	0.613
1086.334	193894	2	285947	1	0.19	8.63E+09	0.802
1089.608	204948	0	296724	1	-0.5	1.78E+09	0.676
1092.686	277340	4	368858	3	-0.13	4.18E+09	0.538
1092.712	200553	1	292069	0	-0.28	2.91E+09	0.811
1096.429	202025	2	293230	2	-0.65	1.25E+09	0.599
1096.847	201051	4	292222	4	0.18	8.46E+09	0.743
1097.183	205252	2	296395	3	0.24	9.71E+09	0.883
1099.848	200553	1	291475	2	-0.37	2.33E+09	0.47
1107.085	208598	1	298926	2	-0.28	2.82E+09	0.867
1113.654	201051	4	290846	3	-0.44	1.96E+09	0.632
1116.107	204948	0	294545	1	-0.38	2.25E+09	0.81
1116.12	202025	2	291621	3	0.16	7.80E+09	0.582
1116.77	209781	3	299325	3	-0.03	5.03E+09	0.389
1117.94	202025	2	291475	2	-0.73	1.00E+09	0.237
1122.938	283497	3	372549	4	-0.96	5.85E+08	0.22
1124.074	200553	1	289515	1	-0.19	3.43E+09	0.657
1126.418	212680	2	301457	2	-0.74	9.56E+08	0.259
1130.096	208598	1	297087	2	-0.47	1.76E+09	0.348
1131.458	201051	4	289433	5	0.82	3.43E+10	0.91
1134.748	208598	1	296724	1	-0.13	3.86E+09	0.89
1136.654	205252	2	293230	2	-0.69	1.06E+09	0.283
1136.879	201051	4	289011	4	-0.55	1.46E+09	0.874
1140.925	277340	4	364988	3	-0.87	6.92E+08	0.306
1142.979	202025	2	289515	1	-0.97	5.49E+08	0.327
1144.44	211547	1	298926	2	0.17	7.50E+09	0.758
1145.405	209781	3	297087	2	-0.82	7.70E+08	0.23
1146.624	209781	3	296994	4	0.71	2.57E+10	0.921
1148.465	211547	1	298620	1	-0.89	6.59E+08	0.417
1154.127	212680	2	299325	3	0.47	1.48E+10	0.874
1154.555	209781	3	296395	3	-0.55	1.41E+09	0.303
1157.771	205849	3	292222	4	0.55	1.78E+10	0.873
1157.83	205252	2	291621	3	0.12	6.57E+09	0.403
1159.789	205252	2	291475	2	-0.07	4.18E+09	0.458
1163.517	208598	1	294545	1	-0.73	9.26E+08	0.335
1165.886	205849	3	291621	3	-0.6	1.24E+09	0.212
1169.047	211547	1	297087	2	-0.48	1.61E+09	0.258
1171.045	200553	1	285947	1	-0.69	9.91E+08	0.179
1176.513	205849	3	290846	3	0.26	8.77E+09	0.838
1184.737	212680	2	297087	2	0.06	5.45E+09	0.544
1186.76	205252	2	289515	1	-0.57	1.27E+09	0.358
1189.025	289433	5	373535	6	-0.25	2.63E+09	0.597
1189.85	212680	2	296724	1	-0.88	6.22E+08	0.242
1194.528	212680	2	296395	3	-0.91	5.76E+08	0.082
1202.465	205849	3	289011	4	-0.45	1.64E+09	0.297
1203.132	289433	5	372549	4	-0.76	8.01E+08	0.53
1204.848	211547	1	294545	1	-0.26	2.52E+09	0.844
1206.208	289011	4	371916	3	-0.92	5.48E+08	0.448
1206.517	205849	3	288732	2	-0.19	2.95E+09	0.899
1206.617	208598	1	291475	2	-0.52	1.38E+09	0.324
1221.52	212680	2	294545	1	-0.66	9.73E+08	0.434
1223.939	290846	3	372549	4	-0.96	4.94E+08	0.514
1233.583	209781	3	290846	3	-0.81	6.79E+08	0.108
1235.838	208598	1	289515	1	-0.41	1.71E+09	0.353
1267.395	130879	2	209781	3	-0.71	8.16E+08	0.087
1282.571	211547	1	289515	1	-0.85	5.78E+08	0.117
1295.882	128681	3	205849	3	0.08	4.80E+09	0.727
1300.59	135791	1	212680	2	-0.4	1.58E+09	0.775
1320.038	135791	1	211547	1	-0.22	2.29E+09	0.746
1322.26	293230	2	368858	3	-0.96	4.17E+08	0.087
1333.871	130879	2	205849	3	-0.39	1.52E+09	0.56
1344.573	130879	2	205252	2	-0.19	2.39E+09	0.464
1351.032	138662	2	212680	2	-0.1	2.92E+09	0.598
1373.494	135791	1	208598	1	-0.87	4.73E+08	0.729
1381.788	128681	3	201051	4	0.37	8.26E+09	0.848
1398.772	205849	3	277340	4	-0.94	3.91E+08	0.806
1405.572	130879	2	202025	2	-0.25	1.89E+09	0.799
1406.093	138662	2	209781	3	0.19	5.24E+09	0.831
1419.749	321152	2	391587	2	-0.7	6.48E+08	0.385
1422.584	321152	2	391446	3	-0.81	5.10E+08	0.371
1429.872	138662	2	208598	1	-0.24	1.86E+09	0.781
1435.256	130879	2	200553	1	-0.2	2.03E+09	0.83
1438.429	321926	3	391446	3	-1	3.18E+08	0.593
1439.662	135791	1	205252	2	-0.56	8.78E+08	0.801
1446.002	135791	1	204948	0	-0.59	8.26E+08	0.849
1470.72	323452	4	391446	3	-0.49	9.89E+08	0.611
1472.357	128681	3	196600	3	-0.31	1.50E+09	0.783
1488.387	138662	2	205849	3	-0.72	5.77E+08	0.24
1501.725	138662	2	205252	2	-0.49	9.59E+08	0.22
1503.287	324925	3	391446	3	-0.63	6.92E+08	0.626
1509.818	135791	1	202025	2	-0.24	1.70E+09	0.416
1521.594	130879	2	196600	3	0.06	3.29E+09	0.578
1533.442	128681	3	193894	2	0.07	3.36E+09	0.837
1802.489	277340	4	332819	5	-0.69	4.22E+08	0.722
1869.586	289515	1	343003	1	-0.62	4.57E+08	0.176
2062.975	294545	1	343003	1	-0.33	7.38E+08	0.568
2071.953	284985	2	333234	3	-0.67	3.33E+08	0.622
2160.119	296724	1	343003	1	-0.36	6.20E+08	0.712
2248.663	289515	1	333972	1	-0.1	1.06E+09	0.616
2275.172	296395	3	340334	3	-0.28	6.63E+08	0.549
2285.962	289011	4	332743	4	-0.12	9.76E+08	0.767
2287.962	285947	1	329640	2	-0.03	1.20E+09	0.397
2296.554	289011	4	332542	4	-0.54	3.63E+08	0.671
2304.175	289433	5	332819	5	0.06	1.45E+09	0.959
2304.326	285947	1	329330	1	-0.71	2.43E+08	0.204
2306.615	288732	2	332072	2	-0.46	4.31E+08	0.382
2311.574	297087	2	340334	3	-0.05	1.11E+09	0.716
2313.394	288732	2	331945	3	0.21	2.04E+09	0.573
2319.008	289433	5	332542	4	-0.8	1.98E+08	0.711
2335.689	296994	4	339795	4	-0.16	8.68E+08	0.475
2346.673	285947	1	328547	1	-0.03	1.13E+09	0.599
2349.062	289515	1	332072	2	0.1	1.52E+09	0.586
2353.26	297087	2	339568	3	0.17	1.77E+09	0.553

Table A15: Continued

Wavelength	Lower Level	J_{Low}	Upper level	J_{Up}	log gf	gA	CF
2354.494	294545	1	337004	2	0.25	2.10E+09	0.856
2359.472	296724	1	339093	2	0.26	2.16E+09	0.937
2379.849	297087	2	339093	2	-0.42	4.50E+08	0.36
2380.595	298926	2	340919	3	-0.68	2.50E+08	0.578
2383.283	285947	1	327893	0	-0.4	4.70E+08	0.511
2385.696	292069	0	333972	1	-0.17	7.92E+08	0.835
2388.94	289011	4	330858	5	0.8	7.40E+09	0.935
2391.271	296395	3	338201	4	0.11	1.53E+09	0.866
2393.974	291475	2	333234	3	0.32	2.46E+09	0.802
2397.601	290846	3	332542	4	0.51	3.74E+09	0.735
2402.365	291621	3	333234	3	0.07	1.34E+09	0.644
2404.038	296395	3	337979	4	0.58	4.36E+09	0.923
2413.247	289433	5	330858	5	-0.76	2.00E+08	0.934
2414.258	298926	2	340334	3	0.1	1.44E+09	0.689
2419.974	329330	1	370640	0	-0.26	6.19E+08	0.46
2424.889	290846	3	332072	2	-0.85	1.58E+08	0.365
2429.216	296994	4	338147	5	0.79	6.99E+09	0.949
2431.016	291621	3	332743	4	0.64	4.88E+09	0.892
2432.382	290846	3	331945	3	0.27	2.09E+09	0.744
2433.575	289433	5	330512	6	0.88	8.57E+09	0.932
2437.77	299325	3	340334	3	-0.37	4.78E+08	0.571
2443.749	288732	2	329640	2	0.01	1.14E+09	0.584
2459.765	298926	2	339568	3	0.27	2.04E+09	0.818
2462.457	291475	2	332072	2	-0.06	9.49E+08	0.526
2462.477	292222	4	332819	5	0.72	5.80E+09	0.883
2467.085	292222	4	332743	4	-0.91	1.36E+08	0.109
2469.996	298620	1	339093	2	-0.66	2.42E+08	0.741
2470.258	299325	3	339795	4	0.66	5.06E+09	0.969
2479.425	292222	4	332542	4	0.16	1.57E+09	0.786
2484.176	299325	3	339568	3	-0.25	6.11E+08	0.297
2488.831	298926	2	339093	2	-0.53	3.16E+08	0.235
2491.445	289515	1	329640	2	-0.62	2.62E+08	0.186
2499.003	293230	2	333234	3	-0.24	6.07E+08	0.63
2504.429	297087	2	337004	2	-0.31	5.17E+08	0.363
2510.545	321152	2	360972	3	0.16	1.50E+09	0.78
2510.844	288732	2	328547	1	-0.4	4.18E+08	0.585
2516.639	292222	4	331945	3	-0.53	3.11E+08	0.679
2529.994	328807	2	368320	2	-0.3	5.16E+08	0.86
2542.116	328807	2	368132	1	-0.01	9.96E+08	0.857
2542.969	321926	3	361238	2	0.14	1.42E+09	0.633
2560.334	321926	3	360972	3	-0.24	5.85E+08	0.79
2563.978	329330	1	368320	2	-0.14	7.31E+08	0.788
2571.43	301457	2	340334	3	-0.3	5.00E+08	0.611
2576.909	290846	3	329640	2	-0.51	3.13E+08	0.83
2582.161	293230	2	331945	3	-0.67	2.15E+08	0.348
2604.457	298620	1	337004	2	-0.5	3.12E+08	0.636
2606.199	329773	0	368132	1	-0.58	2.58E+08	0.788
2625.407	298926	2	337004	2	-0.96	1.07E+08	0.259
2656.198	301457	2	339093	2	-0.78	1.57E+08	0.505
2664.502	323452	4	360972	3	0.39	2.31E+09	0.879
2676.918	323893	1	361238	2	-0.14	6.76E+08	0.737
2678.926	331003	3	368320	2	0.26	1.69E+09	0.867
2684.048	321152	2	358398	3	0.2	1.45E+09	0.429
2694.052	328807	2	365914	2	0.17	1.35E+09	0.774
2694.843	328547	1	365644	2	-0.97	9.77E+07	0.164
2708.108	321926	3	358841	2	-0.53	2.67E+08	0.416
2712.583	321152	2	358006	1	-0.43	3.35E+08	0.395
2713.364	323893	1	360737	0	-0.16	6.25E+08	0.706
2714.838	294545	1	331369	1	-0.93	1.05E+08	0.425
2715.111	321926	3	358746	3	0.12	1.19E+09	0.46
2715.31	321152	2	357969	2	0.45	2.50E+09	0.619
2715.546	324424	2	361238	2	0.17	1.34E+09	0.917
2719.283	331369	1	368132	1	-0.1	7.14E+08	0.814
2732.619	329330	1	365914	2	-0.2	5.68E+08	0.537
2741.033	321926	3	358398	3	0.1	1.12E+09	0.629
2744.917	328807	2	365227	1	-0.78	1.46E+08	0.411
2745.63	293230	2	329640	2	-0.63	2.08E+08	0.5
2746.124	331916	2	368320	2	-0.03	8.29E+08	0.625
2752.937	329330	1	365644	2	-0.14	6.45E+08	0.316
2753.028	324925	3	361238	2	-0.28	4.65E+08	0.817
2760.41	331916	2	368132	1	-0.37	3.71E+08	0.835
2762.145	288732	2	324925	3	-0.63	2.06E+08	0.544
2768.406	328807	2	364918	3	0.73	4.66E+09	0.934
2773.391	324925	3	360972	3	0.11	1.11E+09	0.777
2773.645	321926	3	357969	2	-0.47	2.89E+08	0.614
2779.9	328547	1	364509	1	-0.93	1.01E+08	0.114
2783.629	289011	4	324925	3	-0.84	1.25E+08	0.357
2784.965	329330	1	365227	1	-0.18	5.68E+08	0.354
2786.091	321926	3	357808	4	0.84	5.98E+09	0.912
2801.166	302458	4	338147	5	-0.58	2.22E+08	0.563
2810.743	321152	2	356719	1	0.34	1.81E+09	0.775
2816.691	323452	4	358944	4	0.37	1.95E+09	0.858
2819.782	329773	0	365227	1	-0.12	6.41E+08	0.723
2837.769	294545	1	329773	0	-0.86	1.15E+08	0.375
2839.704	285947	1	321152	2	-0.25	4.67E+08	0.556
2841.761	329330	1	364509	1	0.01	8.49E+08	0.49
2851.041	331003	3	366068	3	0.18	1.25E+09	0.49
2860.538	323893	1	358841	2	0.17	1.20E+09	0.692
2860.767	323452	4	358398	3	-0.39	3.34E+08	0.486
2863.569	331003	3	365914	2	-0.86	1.14E+08	0.296
2863.768	289515	1	324424	2	-0.94	9.30E+07	0.255
2870.274	297087	2	331916	2	-0.34	3.66E+08	0.277
2873.927	294545	1	329330	1	-0.81	1.23E+08	0.171
2878.021	329773	0	364509	1	-0.33	3.74E+08	0.49
2885.598	296724	1	331369	1	-0.88	1.06E+08	0.219
2885.89	331003	3	365644	2	-0.84	1.16E+08	0.161
2888.622	296395	3	331003	3	-0.97	8.54E+07	0.198
2893.86	331369	1	365914	2	0.26	1.44E+09	0.759
2900.341	323452	4	357921	5	0.96	7.19E+09	0.939
2902.688	289011	4	323452	4	-0.87	1.07E+08	0.855
2904.69	324424	2	358841	2	0.36	1.81E+09	0.659
2908.021	289515	1	323893	1	-0.37	3.34E+08	0.506
2909.881	323452	4	357808	4	-0.33	3.66E+08	0.899
2910.33	331003	3	365353	4	0.87	5.80E+09	0.942
2912.747	324424	2	358746	3	0.59	3.05E+09	0.834
2916.656	331369	1	365644	2	0.11	1.01E+09	0.847

Table A15: Continued

Wavelength	Lower Level	J_{Low}	Upper level	J_{Up}	log gf	gA	CF
2927.272	331916	2	366068	3	0.61	3.19E+09	0.902
2930.576	323893	1	358006	1	0.18	1.18E+09	0.709
2933.474	290846	3	324925	3	-0.01	7.49E+08	0.899
2938.65	289433	5	323452	4	0.46	2.24E+09	0.868
2938.657	324925	3	358944	4	0.71	3.98E+09	0.956
2939.507	296994	4	331003	3	0.33	1.66E+09	0.831
2940.481	331916	2	365914	2	-0.92	9.40E+07	0.057
2940.721	332072	2	366068	3	-0.85	1.11E+08	0.308
2947.721	331003	3	364918	3	-0.45	2.76E+08	0.349
2952.631	331369	1	365227	1	-0.13	5.70E+08	0.343
2955.914	324925	3	358746	3	-0.17	5.13E+08	0.358
2964.021	331916	2	365644	2	0.26	1.37E+09	0.518
2976.934	324424	2	358006	1	-0.31	3.63E+08	0.419
2980.008	309456	0	343003	1	-0.1	5.92E+08	0.583
2986.665	324925	3	358398	3	0.43	2.02E+09	0.878
2992.421	331945	3	365353	4	-0.91	9.19E+07	0.413
3001.717	291621	3	324925	3	-0.91	9.06E+07	0.265
3016.55	331369	1	364509	1	-0.45	2.58E+08	0.439
3024.874	296724	1	329773	0	-0.88	9.65E+07	0.578
3025.424	324925	3	357969	2	0.02	7.51E+08	0.856
3029.283	331916	2	364918	3	-0.59	1.89E+08	0.165
3034.093	291475	2	324424	2	-0.38	3.04E+08	0.456
3037.306	289011	4	321926	3	0.3	1.45E+09	0.848
3040.237	324925	3	357808	4	-0.46	2.49E+08	0.279
3045.48	323893	1	356719	1	-0.73	1.35E+08	0.137
3047.582	291621	3	324424	2	0.07	8.41E+08	0.797
3056.898	292222	4	324925	3	0.19	1.10E+09	0.896
3065.991	296724	1	329330	1	-0.53	2.09E+08	0.498
3066.001	290846	3	323452	4	-0.99	7.24E+07	0.371
3067.243	331916	2	364509	1	-0.46	2.43E+08	0.316
3067.436	299325	3	331916	2	0.1	8.94E+08	0.775
3081.463	298926	2	331369	1	-0.07	6.03E+08	0.817
3083.681	288732	2	321152	2	-0.14	5.17E+08	0.586
3083.811	291475	2	323893	1	-0.48	2.34E+08	0.573
3084.397	296395	3	328807	2	0.2	1.11E+09	0.872
3095.575	324424	2	356719	1	-0.88	9.18E+07	0.174
3100.486	297087	2	329330	1	-0.51	2.14E+08	0.328
3141.351	292069	0	323893	1	-0.69	1.41E+08	0.815
3155.857	299325	3	331003	3	-0.29	3.43E+08	0.435
3160.013	289515	1	321152	2	-0.9	8.40E+07	0.339
3183.154	329330	1	360737	0	-0.98	6.98E+07	0.121
3201.084	292222	4	323452	4	-0.09	5.35E+08	0.955
3204.791	293230	2	324424	2	-0.62	1.56E+08	0.716
3216.584	290846	3	321926	3	-0.56	1.80E+08	0.544
3260.312	293230	2	323893	1	-0.8	1.00E+08	0.805
3283.02	291475	2	321926	3	-0.93	7.31E+07	0.579
3298.77	290846	3	321152	2	-0.36	2.71E+08	0.43
3298.818	291621	3	321926	3	-0.33	2.88E+08	0.601
3345.681	298926	2	328807	2	-0.56	1.67E+08	0.648
3368.68	291475	2	321152	2	-0.83	8.82E+07	0.44
3502.213	302458	4	331003	3	-0.78	9.00E+07	0.874
3529.026	329640	2	357969	2	-0.89	6.82E+07	0.198
3548.685	328547	1	356719	1	-0.71	1.02E+08	0.248
3586.6	301457	2	329330	1	-0.93	6.11E+07	0.518
3617.254	343003	1	370640	0	-0.95	5.78E+07	0.092
3634.599	337004	2	364509	1	-0.42	1.92E+08	0.533
3647.458	330512	6	357921	5	0.16	7.23E+08	0.669
3674.531	338147	5	365353	4	0.1	6.23E+08	0.76
3691.939	329640	2	356719	1	-0.67	1.05E+08	0.264
3709.586	330858	5	357808	4	0.08	5.86E+08	0.726
3711.033	337979	4	364918	3	-0.14	3.55E+08	0.694
3727.348	339093	2	365914	2	-0.92	5.76E+07	0.383
3734.655	332072	2	358841	2	-0.92	5.83E+07	0.162
3735.272	333972	1	360737	0	-0.8	7.62E+07	0.461
3741.871	338201	4	364918	3	-0.62	1.13E+08	0.664
3779.329	331945	3	358398	3	-0.54	1.34E+08	0.431
3786.396	332542	4	358944	4	-0.61	1.15E+08	0.551
3803.908	298644	3	324925	3	0.37	1.09E+09	0.89
3805.084	339795	4	366068	3	-0.02	4.33E+08	0.909
3825.421	339093	2	365227	1	-0.4	1.84E+08	0.844
3826.614	332819	5	358944	4	0.04	5.00E+08	0.858
3827.034	305794	1	331916	2	-0.11	3.53E+08	0.952
3833.783	339568	3	365644	2	-0.19	2.97E+08	0.847
3841.604	331945	3	357969	2	-0.41	1.76E+08	0.511
3844.683	332743	4	358746	3	-0.05	4.00E+08	0.828
3854.935	332072	2	358006	1	-0.56	1.23E+08	0.424
3866.472	332542	4	358398	3	-0.16	3.11E+08	0.681
3901.185	306290	2	331916	2	0.2	6.84E+08	0.664
3904.02	333234	3	358841	2	-0.21	2.68E+08	0.741
3904.805	299323	2	324925	3	-0.03	4.07E+08	0.894
3908.124	340334	3	365914	2	-0.28	2.33E+08	0.861
3908.995	305794	1	331369	1	0.14	6.05E+08	0.939
3911.428	339795	4	365353	4	-0.8	6.67E+07	0.533
3918.588	333234	3	358746	3	-0.67	9.35E+07	0.434
3982.659	332819	5	357921	5	-0.64	9.63E+07	0.916
3982.775	299323	2	324424	2	0.38	1.01E+09	0.907
3988.567	332743	4	357808	4	-0.81	6.44E+07	0.69
4029.772	298644	3	323452	4	0.63	1.78E+09	0.982
4045.33	306290	2	331003	3	0.5	1.29E+09	0.967
4066.558	340334	3	364918	3	-1	4.11E+07	0.6
4068.885	299323	2	323893	1	0.13	5.38E+08	0.87
4159.686	333972	1	358006	1	-0.62	9.18E+07	0.509
4169.022	305794	1	329773	0	-0.36	1.69E+08	0.982
4293.976	298644	3	321926	3	-0.06	3.20E+08	0.909
4339.062	306290	2	329330	1	0.06	4.02E+08	0.921
4344.19	305794	1	328807	2	0.18	5.35E+08	0.962
4422.985	299323	2	321926	3	0.33	7.36E+08	0.697
4425.828	368858	3	391446	3	-0.69	6.92E+07	0.757
4439.984	306290	2	328807	2	-0.15	2.40E+08	0.937
4441.699	298644	3	321152	2	0.34	7.48E+08	0.963
4491.672	306290	2	328547	1	-0.92	3.95E+07	0.877
4498.439	343003	1	365227	1	-0.99	3.40E+07	0.392
4648.499	343003	1	364509	1	-0.63	7.21E+07	0.587
4810.998	370807	2	391587	2	-0.58	7.16E+07	0.371
4983.406	371526	2	391587	2	0.55	9.27E+08	0.588
5018.529	371526	2	391446	3	0	2.59E+08	0.3

Table A15: Continued

Wavelength	Lower Level	J_{Low}	Upper level	J_{Up}	log gf	gA	CF
5030.203	309456	0	329330	1	-0.62	6.32E+07	0.751
5118.849	371916	3	391446	3	-0.06	2.19E+08	0.729
5142.388	372146	1	391587	2	-0.71	4.66E+07	0.227
5290.429	372549	4	391446	3	0.36	5.33E+08	0.62
6007.839	357808	4	374448	4	-0.82	2.89E+07	0.731
6228.608	358398	3	374448	4	-0.34	8.18E+07	0.722
6255.074	356719	1	372701	1	-0.39	6.93E+07	0.314
6366.729	358746	3	374448	4	-0.72	3.25E+07	0.265
6402.476	357921	5	373535	6	1.01	1.64E+09	0.952
6448.287	358944	4	374448	4	-0.93	1.95E+07	0.424
6480.393	356719	1	372146	1	-0.08	1.33E+08	0.475
6663.582	343003	1	358006	1	-0.81	2.31E+07	0.381
6693.116	356719	1	371655	1	-0.49	5.06E+07	0.663
6751.835	356719	1	371526	2	-0.1	1.15E+08	0.482
6781.698	357808	4	372549	4	-0.32	7.04E+07	0.831
6802.88	358006	1	372701	1	-0.23	8.48E+07	0.376
6834.085	357921	5	372549	4	0.52	4.76E+08	0.686
6924.751	309456	0	323893	1	-0.99	1.43E+07	0.533
7051.784	357969	2	372146	1	-0.28	7.25E+07	0.568
7064.341	358398	3	372549	4	-0.87	1.83E+07	0.063
7070.236	358006	1	372146	1	-0.7	2.73E+07	0.237
7086.173	357808	4	371916	3	0.53	4.48E+08	0.861
7212.811	358841	2	372701	1	-0.11	9.94E+07	0.593
7304.404	357969	2	371655	1	-0.78	2.23E+07	0.675
7348.268	358944	4	372549	4	0.36	2.86E+08	0.965
7374.395	357969	2	371526	2	0.21	2.02E+08	0.653
7394.577	358006	1	371526	2	-0.93	1.45E+07	0.18
7395.343	358398	3	371916	3	-0.26	6.59E+07	0.657
7590.867	358746	3	371916	3	-0.13	8.54E+07	0.551
7615.268	358398	3	371526	2	-0.28	5.96E+07	0.279
7646.137	358841	2	371916	3	-0.92	1.37E+07	0.314
7787.354	357969	2	370807	2	-0.6	2.96E+07	0.52
7809.863	358006	1	370807	2	-0.64	2.63E+07	0.5
8355.483	360737	0	372701	1	-0.57	2.53E+07	0.43
8634.847	360972	3	372549	4	0.63	3.89E+08	0.938
8721.096	361238	2	372701	1	0.2	1.40E+08	0.911
8762.45	360737	0	372146	1	-0.94	9.87E+06	0.179
9134.586	360972	3	371916	3	-0.07	6.78E+07	0.881
9165.404	361238	2	372146	1	-0.9	1.02E+07	0.768
9362.656	361238	2	371916	3	0.48	2.27E+08	0.769
9472.482	360972	3	371526	2	0.41	1.90E+08	0.958
9557.425	358398	3	368858	3	-0.83	1.08E+07	0.733
10164.878	360972	3	370807	2	-0.99	7.04E+06	0.867
12676.749	360972	3	368858	3	-0.95	4.61E+06	0.785

a: Experimental values from: [33, 32]

In V

Energy Levels

Table A16: Comparison between available experimental data and calculated even energy levels (in cm^{-1}) in In V

E$^a_{exp}$	E$^b_{calc}$	ΔE	J	Leading components (in %) in LS coupling ^{c}
0	0	0	2.5	99.5 4d^9 (^{2}D) ^{2}D
7171.8	7172	-0.2	1.5	99.5 4d^9 (^{2}D) ^{2}D
160428.2	160412	16.2	4.5	98.5 4d^8 5s (^{3}F) ^{4}F
163979.7	163935	44.7	3.5	82.4 4d^8 5s (^{3}F) ^{4}F + 16.2 4d^8 5s (^{3}F) ^{2}F
167760.8	167718	42.8	2.5	91.7 4d^8 5s (^{3}F) ^{4}F + 5 4d^8 5s (^{1}D) ^{2}D
169230.4	169174	56.4	1.5	81.4 4d^8 5s (^{3}F) ^{4}F + 16.6 4d^8 5s (^{1}D) ^{2}D
171289.7	171358	-68.3	3.5	81.5 4d^8 5s (^{3}F) ^{2}F + 17 4d^8 5s (^{3}F) ^{4}F
173370.9	173412	-41.1	2.5	36.8 4d^8 5s (^{3}P) ^{4}P + 31.9 4d^8 5s (^{1}D) ^{2}D + 29.6 4d^8 5s (^{3}F) ^{2}F
177669.8	177782	-112.2	2.5	52.7 4d^8 5s (^{3}F) ^{2}F + 43.9 4d^8 5s (^{3}P) ^{4}P
178288.8	178293	-4.2	1.5	54.2 4d^8 5s (^{3}P) ^{4}P + 23 4d^8 5s (^{1}D) ^{2}D + 12.2 4d^8 5s (^{3}P) ^{2}P
180492.8	180552	-59.2	0.5	97.1 4d^8 5s (^{3}P) ^{4}P
182194	182182	12	1.5	33.3 4d^8 5s (^{1}D) ^{2}D + 44.7 4d^8 5s (^{3}P) ^{4}P + 15.3 4d^8 5s (^{3}P) ^{2}P
185622.1	185652	-29.9	2.5	62.5 4d^8 5s (^{1}D) ^{2}D + 17.8 4d^8 5s (^{3}P) ^{4}P + 15.3 4d^8 5s (^{3}F) ^{2}F
188396.3	188434	-37.7	4.5	98.4 4d^8 5s (^{1}G) ^{2}G
188575.1	188537	38.1	3.5	97.4 4d^8 5s (^{1}G) ^{2}G
188639.6	188563	76.6	0.5	97.6 4d^8 5s (^{3}P) ^{2}P
188649.1	188583	66.1	1.5	70.9 4d^8 5s (^{3}P) ^{2}P + 26.6 4d^8 5s (^{1}D) ^{2}D
220693.6	220694	-0.4	0.5	95.2 4d^8 5s (^{1}S) ^{2}S + 2.3 4d^8 5s (^{3}P) ^{4}P
349273.3	349350	-76.7	3.5	79.6 4d^8 5d (^{3}F) ^{4}D + 13.7 4d^8 5d (^{3}F) ^{4}F
349569.3	349576	-6.7	2.5	41.3 4d^8 5d (^{3}F) ^{4}D + 48.3 4d^8 5d (^{3}F) ^{4}P
351039.2	351083	-43.8	5.5	50.5 4d^8 5d (^{3}F) ^{2}H + 39.9 4d^8 5d (^{3}F) ^{4}H + 7.6 4d^8 5d (^{3}F) ^{4}G
351397.5	351294	103.5	6.5	98.2 4d^8 5d (^{3}F) ^{4}H
351761.9	351678	83.9	1.5	40.4 4d^8 5d (^{3}F) ^{2}P + 27.8 4d^8 5d (^{3}F) ^{4}D
352433.9	352336	97.9	4.5	39.8 4d^8 5d (^{3}F) ^{4}G + 29.3 4d^8 5d (^{3}F) ^{2}G + 9.9 4d^8 5d (^{3}F) ^{4}F
352548.2	352438	110.2	5.5	78.2 4d^8 5d (^{3}F) ^{4}G + 19 4d^8 5d (^{3}F) ^{2}H
351571.7	352572	-1000.3	3.5	42.4 4d^8 5d (^{3}F) ^{2}F + 21.4 4d^8 5d (^{3}F) ^{4}F + 11.7 4d^7 5s^2 (^{4}F) ^{4}F
353886.1	353681	205.1	2.5	41.2 4d^8 5d (^{3}F) ^{4}P + 20.7 4d^8 5d (^{3}F) ^{4}D + 12 4d^8 5d (^{3}F) ^{4}F
353631.9	354257	-625.1	4.5	45.6 4d^8 5d (^{3}F) ^{4}F + 25 4d^8 5d (^{3}F) ^{2}G + 16.7 4d^7 5s^2 (^{4}F) ^{4}F
356232.8	356193	39.8	1.5	46.2 4d^8 5d (^{3}F) ^{2}P + 43.7 4d^8 5d (^{3}F) ^{4}D
356617.7	356477	140.7	0.5	73.3 4d^8 5d (^{3}F) ^{4}D + 13 4d^8 5d (^{3}F) ^{4}P + 8 4d^8 5d (^{3}F) ^{2}P
357392.6	356714	678.6	2.5	42.7 4d^7 5s^2 (^{4}F) ^{4}F + 25.7 4d^8 5d (^{3}F) ^{4}F + 12 4d^8 5d (^{3}F) ^{4}D
357537.3	357392	145.3	4.5	62.4 4d^8 5d (^{3}F) ^{4}H + 18.9 4d^8 5d (^{3}F) ^{2}G + 15.8 4d^8 5d (^{3}F) ^{2}H
358493.2	357859	634.2	1.5	34.4 4d^8 5d (^{3}F) ^{4}F + 33.7 4d^7 5s^2 (^{4}F) ^{4}F + 14 4d^8 5d (^{1}D) ^{2}D
357950.5	357904	46.5	3.5	40.3 4d^8 5d (^{3}F) ^{4}G + 33.8 4d^8 5d (^{3}F) ^{4}H + 18 4d^8 5d (^{3}F) ^{2}F
358242.2	357927	315.2	5.5	58.1 4d^8 5d (^{3}F) ^{4}H + 28.5 4d^8 5d (^{3}F) ^{2}H + 12.9 4d^8 5d (^{3}F) ^{4}G
358748.1	358004	744.1	1.5	67.6 4d^8 5d (^{3}F) ^{4}P + 5.5 4d^8 5d (^{3}F) ^{4}F + 5.1 4d^8 5d (^{3}F) ^{4}D
358143.7	358525	-381.3	2.5	50.4 4d^8 5d (^{3}F) ^{2}F + 11.5 4d^8 5d (^{3}F) ^{2}D + 11.5 4d^8 5d (^{3}F) ^{4}D
359123.8	358823	300.8	4.5	13.3 4d^8 5d (^{3}F) ^{2}G + 37.6 4d^8 5d (^{3}F) ^{4}G + 29.1 4d^8 5d (^{3}F) ^{2}H
358748	359102	-354	3.5	30.2 4d^8 5d (^{3}F) ^{4}H + 24.2 4d^8 5d (^{3}F) ^{4}F + 13.9 4d^8 5d (^{3}F) ^{2}F
359561.7	359285	276.7	0.5	51.6 4d^8 5d (^{3}F) ^{4}P + 17.5 4d^8 5d (^{3}F) ^{2}P + 16.6 4d^8 5d (^{3}F) ^{4}D
359254.2	359451	-196.8	2.5	63.7 4d^8 5d (^{3}F) ^{4}G + 15.7 4d^8 5d (^{1}D) ^{2}F + 7.8 4d^7 5s^2 (^{4}F) ^{4}F
360579.9	360090	489.9	3.5	27.1 4d^8 5d (^{3}F) ^{4}F + 19.8 4d^8 5d (^{3}F) ^{4}G + 18.8 4d^8 5d (^{3}F) ^{4}H
360413.7	360346	67.7	0.5	61.8 4d^8 5d (^{3}F) ^{2}P + 22.6 4d^8 5d (^{3}F) ^{4}P + 11.8 4d^8 5d (^{1}D) ^{2}S
359377.3	360422	-1044.7	2.5	32.3 4d^8 5d (^{3}F) ^{4}F + 23.8 4d^7 5s^2 (^{4}F) ^{4}F + 14.5 4d^8 5d (^{3}F) ^{2}D
359409.6	360769	-1359.4	1.5	28.5 4d^7 5s^2 (^{4}F) ^{4}F + 19.3 4d^8 5d (^{3}F) ^{2}D + 16.6 4d^8 5d (^{1}D) ^{2}D
360937.3	360789	148.3	4.5	36 4d^8 5d (^{3}F) ^{2}H + 16.2 4d^8 5d (^{3}F) ^{4}G + 15.4 4d^8 5d (^{1}D) ^{2}G
361097.4	360922	175.4	3.5	54.5 4d^8 5d (^{3}F) ^{2}G + 23.4 4d^8 5d (^{1}D) ^{2}F + 7.2 4d^8 5d (^{3}F) ^{4}G
362171.7	363111	-939.3	1.5	14.9 4d^8 5d (^{3}F) ^{2}D + 36.7 4d^8 5d (^{3}F) ^{4}F + 20.5 4d^7 5s^2 (^{4}F) ^{4}F
364260.1	363911	349.1	2.5	34.1 4d^8 5d (^{3}F) ^{2}D + 14.1 4d^8 5d (^{3}F) ^{2}F + 10.8 4d^8 5d (^{3}F) ^{4}F
365556.5	366198	-641.5	0.5	57.4 4d^8 5d (^{3}P) ^{4}D + 20.5 4d^8 5d (^{1}D) ^{2}P + 10.1 4d^8 5d (^{3}P) ^{4}P
366235.9	366371	-135.1	3.5	63.6 4d^8 5d (^{3}P) ^{4}D + 12.7 4d^8 5d (^{3}F) ^{2}G + 6.4 4d^8 5d (^{1}D) ^{2}F
366978.4	366401	577.4	1.5	25.7 4d^7 5s^2 (^{4}P) ^{4}P + 16.5 4d^8 5d (^{3}P) ^{4}D
368135.1	367155	980.1	1.5	39 4d^8 5d (^{3}P) ^{4}D + 18.8 4d^8 5d (^{3}P) ^{2}D + 14.8 4d^8 5d (^{3}F) ^{2}D
367398.2	368046	-647.8	3.5	38.7 4d^8 5d (^{3}P) ^{2}F + 30.2 4d^8 5d (^{1}D) ^{2}G + 13.8 4d^8 5d (^{3}P) ^{4}F
368096.6	368509	-412.4	4.5	55.3 4d^8 5d (^{3}P) ^{4}F + 26.8 4d^8 5d (^{1}D) ^{2}G + 8.3 4d^8 5d (^{3}F) ^{2}H
369302.5	368531	771.5	0.5	32 4d^8 5d (^{3}P) ^{4}P + 21.7 4d^8 5d (^{1}D) ^{2}S + 21.1 4d^7 5s^2 (^{4}P) ^{4}P
369553.4	368635	918.4	1.5	35.8 4d^7 5s^2 (^{4}P) ^{4}P + 23.3 4d^8 5d (^{3}P) ^{2}D + 10.6 4d^8 5d (^{3}P) ^{4}D
368011.6	368947	-935.4	2.5	30.2 4d^8 5d (^{3}P) ^{2}D + 20.8 4d^8 5d (^{3}P) ^{4}D + 17.9 4d^8 5d (^{1}G) ^{2}D
371725.9	372061	-335.1	0.5	27.4 4d^8 5d (^{3}P) ^{2}P + 19.2 4d^8 5d (^{3}P) ^{4}D + 18.6 4d^7 5s^2 (^{4}P) ^{4}P
372351.7	372766	-414.3	2.5	23.6 4d^8 5d (^{3}P) ^{4}F + 19.2 4d^8 5d (^{1}D) ^{2}F + 16.7 4d^8 5d (^{3}P) ^{2}D
372497.9	372792	-294.1	1.5	21.5 4d^8 5d (^{3}P) ^{4}P + 23.1 4d^8 5d (^{3}P) ^{4}F + 17.1 4d^8 5d (^{3}P) ^{4}D
373780.9	373258	522.9	2.5	27.5 4d^8 5d (^{1}D) ^{2}D + 23.5 4d^8 5d (^{3}P) ^{4}F + 16.5 4d^8 5d (^{3}P) ^{4}D
373670.2	373262	408.2	1.5	32.4 4d^8 5d (^{3}P) ^{4}F + 25.8 4d^8 5d (^{3}P) ^{4}P + 13.7 4d^8 5d (^{3}P) ^{2}D
373176.7	373447	-270.3	3.5	24.3 4d^8 5d (^{1}D) ^{2}F + 26.9 4d^8 5d (^{3}P) ^{4}F + 22.3 4d^8 5d (^{3}P) ^{4}D
375218	374248	970	2.5	32.7 4d^8 5d (^{1}D) ^{2}F + 27.6 4d^8 5d (^{3}P) ^{4}F + 13.5 4d^8 5d (^{3}P) ^{2}F
374804.6	374589	215.6	5.5	97.9 4d^8 5d (^{1}G) ^{2}I
374412.7	374610	-197.3	1.5	8.2 4d^8 5d (^{3}P) ^{2}D + 28.6 4d^8 5d (^{3}P) ^{4}F + 19.3 4d^8 5d (^{3}P) ^{2}P
374263.1	374654	-390.9	3.5	45.2 4d^8 5d (^{3}P) ^{4}F + 30.4 4d^8 5d (^{1}D) ^{2}F + 7.6 4d^8 5d (^{1}G) ^{2}F
375734.5	375305	429.5	6.5	98.2 4d^8 5d (^{1}G) ^{2}I
375831.9	375375	456.9	2.5	49.7 4d^8 5d (^{3}P) ^{2}F + 13.1 4d^8 5d (^{3}P) ^{4}P + 11.4 4d^8 5d (^{3}P) ^{4}F

Table A16: Continued

375279.5	375724	-444.5	3.5	37.9 4d^8 5d (^{1}D) ^{2}G + 42.3 4d^8 5d (^{3}P) ^{2}F + 8.6 4d^8 5d (^{1}G) ^{2}G
376554.5	376060	494.5	1.5	18.8 4d^8 5d (^{1}G) ^{2}D + 15.7 4d^8 5d (^{3}P) ^{4}P + 15.3 4d^8 5d (^{3}P) ^{2}P
377152.5	377629	-476.5	3.5	83.8 4d^8 5d (^{1}G) ^{2}F + 6.1 4d^8 5d (^{1}D) ^{2}F
378144.6	377928	216.6	2.5	82.3 4d^8 5d (^{1}G) ^{2}F + 7 4d^8 5d (^{1}D) ^{2}F
377971.2	378218	-246.8	3.5	62.9 4d^7 5s^2 (^{2}G) ^{2}G + 29.7 4d^8 5d (^{1}G) ^{2}G
377994.7	378354	-359.3	0.5	35.5 4d^8 5d (^{1}D) ^{2}S + 34.2 4d^8 5d (^{3}P) ^{2}P + 10.4 4d^8 5d (^{3}P) ^{4}P
379358.2	378999	359.2	4.5	98.9 4d^8 6s (^{3}F) ^{4}F
380026.2	380383	-356.8	3.5	57.3 4d^8 6s (^{3}F) ^{2}F + 39.2 4d^8 6s (^{3}F) ^{4}F
381614.9	381547	67.9	4.5	70.5 4d^8 5d (^{1}G) ^{2}G + 11 4d^8 5d (^{1}G) ^{2}H + 8.6 4d^8 5d (^{1}D) ^{2}G

a: From Swapnil [34] and Ryabtsev [35]

b: This work

c: Only the component $\geq$ 5% are given

Table A17: Comparison between available experimental data and calculated odd energy levels (in cm^{-1}) in In V

E$^a_{exp}$	E$^b_{calc}$	ΔE	J	Leading components (in %) in LS coupling ^{c}
235384.1	235446	-61.9	3.5	76.5 4d^{8}5p (^{3}F) ^{4}D + 11.2 4d^{8}5p (^{3}F) ^{4}F
238629.2	238589	40.2	4.5	35.9 4d^{8}5p (^{3}F) ^{2}G + 41.1 4d^{8}5p (^{3}F) ^{4}G + 21.4 4d^{8}5p (^{3}F) ^{4}F
241510.9	241550	-39.1	2.5	69.7 4d^{8}5p (^{3}F) ^{4}D + 11.1 4d^{8}5p (^{3}P) ^{4}D + 10.4 4d^{8}5p (^{3}F) ^{4}F
243798.3	243766	32.3	3.5	65.9 4d^{8}5p (^{3}F) ^{4}G + 15 4d^{8}5p (^{3}F) ^{4}F + 13.3 4d^{8}5p (^{3}F) ^{2}G
244282.5	244197	85.5	5.5	98.2 4d^{8}5p (^{3}F) ^{4}G + 1.5 4d^{8}5p (^{1}G) ^{2}H
245121.7	245136	-14.3	2.5	55.7 4d^{8}5p (^{3}F) ^{4}G + 12.9 4d^{8}5p (^{1}D) ^{2}F + 12.5 4d^{8}5p (^{3}F) ^{4}F
245554	245632	-78	1.5	34 4d^{8}5p (^{3}F) ^{4}D + 21.6 4d^{8}5p (^{3}F) ^{4}F + 12.7 4d^{8}5p (^{1}D) ^{2}D
246721.8	246823	-101.2	1.5	16.8 4d^{8}5p (^{1}D) ^{2}D + 36.9 4d^{8}5p (^{3}F) ^{4}D + 17.8 4d^{8}5p (^{3}P) ^{4}D
247254.7	247177	77.7	4.5	71.1 4d^{8}5p (^{3}F) ^{4}F + 25.4 4d^{8}5p (^{3}F) ^{2}G
248164.6	248173	-8.4	0.5	63.5 4d^{8}5p (^{3}F) ^{4}D + 24.2 4d^{8}5p (^{3}P) ^{4}D + 7.6 4d^{8}5p (^{1}D) ^{2}P
248507.3	248555	-47.7	3.5	54.6 4d^{8}5p (^{3}F) ^{2}F + 21.9 4d^{8}5p (^{3}F) ^{4}F + 10.2 4d^{8}5p (^{3}F) ^{4}D
249639.7	249672	-32.3	2.5	36 4d^{8}5p (^{3}F) ^{2}D + 24.1 4d^{8}5p (^{3}F) ^{4}G + 16.3 4d^{8}5p (^{3}F) ^{4}F
251868.1	251852	16.1	4.5	56.6 4d^{8}5p (^{3}F) ^{4}G + 36.7 4d^{8}5p (^{3}F) ^{2}G + 6.3 4d^{8}5p (^{3}F) ^{4}F
252621.8	252542	79.8	1.5	47.6 4d^{8}5p (^{3}P) ^{4}P + 26.2 4d^{8}5p (^{3}F) ^{4}F + 5.9 4d^{8}5p (^{1}D) ^{2}P
252690.6	252659	31.6	2.5	35 4d^{8}5p (^{3}F) ^{4}F + 21.7 4d^{8}5p (^{3}F) ^{2}F + 14.2 4d^{8}5p (^{3}F) ^{4}D
253298.3	253357	-58.7	0.5	86.3 4d^{8}5p (^{3}P) ^{4}P
253871.2	253842	29.2	2.5	46.6 4d^{8}5p (^{3}P) ^{4}P + 29.8 4d^{8}5p (^{3}F) ^{2}D + 6.1 4d^{8}5p (^{3}P) ^{4}D
253926.3	253959	-32.7	3.5	42.2 4d^{8}5p (^{3}F) ^{4}F + 25.7 4d^{8}5p (^{3}F) ^{2}F + 24.8 4d^{8}5p (^{3}F) ^{2}G
254804.6	254877	-72.4	3.5	38.3 4d^{8}5p (^{3}F) ^{2}G + 24.8 4d^{8}5p (^{1}D) ^{2}F + 16.4 4d^{8}5p (^{3}F) ^{4}G
257128.6	257306	-177.4	2.5	38.7 4d^{8}5p (^{3}F) ^{2}F + 19.8 4d^{8}5p (^{1}D) ^{2}F + 17.3 4d^{8}5p (^{3}P) ^{2}D
257290.6	257336	-45.4	1.5	42.6 4d^{8}5p (^{3}F) ^{4}F + 26.3 4d^{8}5p (^{3}F) ^{2}D + 14.1 4d^{8}5p (^{3}P) ^{4}P
258597.9	258502	95.9	2.5	21.7 4d^{8}5p (^{1}D) ^{2}F + 26.1 4d^{8}5p (^{3}P) ^{4}P + 13.6 4d^{8}5p (^{3}F) ^{4}G
261208.1	261157	51.1	0.5	35.1 4d^{8}5p (^{3}P) ^{2}P + 38 4d^{8}5p (^{1}D) ^{2}P + 9 4d^{8}5p (^{3}P) ^{4}P
261262.6	261226	36.6	3.5	25.3 4d^{8}5p (^{1}G) ^{2}F + 23 4d^{8}5p (^{1}D) ^{2}F + 20.9 4d^{8}5p (^{3}P) ^{4}F
262089.3	261902	187.3	1.5	19.3 4d^{8}5p (^{3}F) ^{2}D + 30.5 4d^{8}5p (^{3}P) ^{2}P + 20.1 4d^{8}5p (^{3}P) ^{4}F
262350.7	262404	-53.3	4.5	92.2 4d^{8}5p (^{1}G) ^{2}H + 5.8 4d^{8}5p (^{1}G) ^{2}G
263009.8	262814	195.8	0.5	62.3 4d^{8}5p (^{3}P) ^{4}D + 23.2 4d^{8}5p (^{3}F) ^{4}D + 5.2 4d^{8}5p (^{3}P) ^{2}P
262965.5	263145	-179.5	2.5	18 4d^{8}5p (^{3}P) ^{4}D + 24.8 4d^{8}5p (^{3}P) ^{2}D + 22.5 4d^{8}5p (^{1}D) ^{2}D
263558.6	263449	109.6	1.5	33.8 4d^{8}5p (^{3}P) ^{4}D + 22.6 4d^{8}5p (^{3}F) ^{2}D + 12.4 4d^{8}5p (^{1}D) ^{2}D
264126.5	264038	88.5	3.5	42.8 4d^{8}5p (^{3}P) ^{4}D + 46 4d^{8}5p (^{1}G) ^{2}F + 5.5 4d^{8}5p (^{3}F) ^{2}F
265905.4	265811	94.4	1.5	54 4d^{8}5p (^{1}D) ^{2}P + 17.7 4d^{8}5p (^{1}D) ^{2}D + 7.8 4d^{8}5p (^{3}P) ^{2}D
266067.6	265965	102.6	2.5	30.4 4d^{8}5p (^{1}D) ^{2}D + 21.1 4d^{8}5p (^{1}G) ^{2}F + 18 4d^{8}5p (^{3}P) ^{4}D
268230.5	268146	84.5	1.5	55.8 4d^{8}5p (^{3}P) ^{2}P + 19.9 4d^{8}5p (^{1}D) ^{2}D + 8.5 4d^{8}5p (^{3}P) ^{2}D
268861.1	268841	20.1	2.5	43 4d^{8}5p (^{3}P) ^{2}D + 36.3 4d^{8}5p (^{3}P) ^{4}D + 11.3 4d^{8}5p (^{1}G) ^{2}F
268957	268920	37	5.5	98.1 4d^{8}5p (^{1}G) ^{2}H
270201.1	270383	-181.9	1.5	66.8 4d^{8}5p (^{3}P) ^{2}D + 12.9 4d^{8}5p (^{3}P) ^{4}D + 5.3 4d^{8}5p (^{1}D) ^{2}P
270845.5	271154	-308.5	0.5	70.7 4d^{8}5p (^{3}P) ^{2}S + 16.2 4d^{8}5p (^{3}P) ^{2}P + 5 4d^{8}5p (^{3}P) ^{4}D
271234.4	271173	61.4	3.5	49 4d^{8}5p (^{1}D) ^{2}F + 24.4 4d^{8}5p (^{3}P) ^{4}D + 11.1 4d^{8}5p (^{1}G) ^{2}F
272573.9	272602	-28.1	2.5	56.2 4d^{8}5p (^{1}G) ^{2}F + 12.1 4d^{8}5p (^{1}D) ^{2}F + 9.8 4d^{8}5p (^{1}D) ^{2}D
272846.4	272655	191.4	1.5	86.3 4d^{8}5p (^{3}P) ^{4}S
275318.1	275486	-167.9	0.5	39.9 4d^{8}5p (^{1}D) ^{2}P + 34.4 4d^{8}5p (^{3}P) ^{2}P + 18.6 4d^{8}5p (^{3}P) ^{2}S
276576.3	276605	-28.7	3.5	87.7 4d^{8}5p (^{1}G) ^{2}G + 9.6 4d^{8}5p (^{1}G) ^{2}F
277481.7	277509	-27.3	4.5	92.6 4d^{8}5p (^{1}G) ^{2}G + 5.6 4d^{8}5p (^{1}G) ^{2}H
298294.7	298294	0.7	0.5	91.2 4d^{8}5p (^{1}S) ^{2}P
305344.3	305343	1.3	1.5	93.2 4d^{8}5p (^{1}S) ^{2}P
382835	382781	54	3.5	49.8 4d^{8}4f (^{3}F) ^{4}D + 38.1 4d^{8}4f (^{3}F) ^{4}F + 6.3 4d^{8}4f (^{3}P) ^{4}F
385365	385403	-38	0.5	24.9 4d^{8}4f (^{3}F) ^{2}S + 26.7 4d^{8}4f (^{3}F) ^{4}P + 25.4 4d^{8}4f (^{3}F) ^{4}D
386795	386890	-95	3.5	22.1 4d^{8}4f (^{3}F) ^{4}F + 39.9 4d^{8}4f (^{3}F) ^{4}D + 11.5 4d^{8}4f (^{3}P) ^{4}F
386943	386896	47	2.5	34.1 4d^{8}4f (^{3}F) ^{4}F + 31.2 4d^{8}4f (^{3}F) ^{4}P + 14.1 4d^{8}4f (^{3}P) ^{4}F
387648	387677	-29	1.5	24.4 4d^{8}4f (^{3}F) ^{4}S + 21.8 4d^{8}4f (^{3}F) ^{4}P + 20.8 4d^{8}4f (^{3}F) ^{4}F
390542	390635	-93	2.5	39.6 4d^{8}4f (^{3}F) ^{4}P + 32.7 4d^{8}4f (^{3}F) ^{4}D + 7.9 4d^{8}4f (^{1}D) ^{2}F
390542	390723	-181	1.5	45.6 4d^{8}4f (^{3}F) ^{4}F + 16.9 4d^{8}4f (^{3}P) ^{4}F + 16.5 4d^{8}4f (^{3}F) ^{4}D
391882	391903	-21	0.5	63.9 4d^{8}4f (^{3}F) ^{4}P + 15.7 4d^{8}4f (^{3}F) ^{2}S + 12.4 4d^{8}4f (^{3}F) ^{2}P
392278	392226	52	3.5	39.5 4d^{8}4f (^{3}F) ^{4}H + 24.1 4d^{8}4f (^{3}F) ^{4}G + 19.8 4d^{8}4f (^{3}F) ^{2}G
393914	393592	322	2.5	38 4d^{8}4f (^{3}F) ^{4}G + 26 4d^{8}4f (^{1}D) ^{2}F + 11.8 4d^{8}4f (^{3}F) ^{4}F
393573	393788	-215	1.5	26 4d^{8}4f (^{3}F) ^{4}P + 39.6 4d^{8}4f (^{3}F) ^{4}S + 9.4 4d^{8}4f (^{3}F) ^{4}D
394157	394331	-174	1.5	37.7 4d^{8}4f (^{3}F) ^{2}P + 13.6 4d^{8}4f (^{1}G) ^{2}P + 12.5 4d^{8}4f (^{3}F) ^{4}D
394644	394375	269	3.5	3.8 4d^{8}4f (^{1}D) ^{2}F + 28 4d^{8}4f (^{3}F) ^{4}H + 27 4d^{8}4f (^{3}F) ^{2}G
396177	396020	157	1.5	7.3 4d^{8}4f (^{1}G) ^{2}D + 26.7 4d^{8}4f (^{1}D) ^{2}D + 16.1 4d^{8}4f (^{3}F) ^{2}D
396509	396670	-161	2.5	2.9 4d^{8}4f (^{1}D) ^{2}F + 34.3 4d^{8}4f (^{3}F) ^{4}G + 21.3 4d^{8}4f (^{3}F) ^{2}F
399348	399231	117	3.5	35.3 4d^{8}4f (^{3}P) ^{4}F + 20.4 4d^{8}4f (^{3}F) ^{2}F + 14.8 4d^{8}4f (^{3}F) ^{4}H
399533	399687	-154	2.5	25.3 4d^{8}4f (^{3}F) ^{2}D + 13.4 4d^{8}4f (^{1}G) ^{2}D + 11.7 4d^{8}4f (^{1}D) ^{2}F
400853	400633	220	2.5	51.7 4d^{8}4f (^{3}P) ^{4}F + 15.7 4d^{8}4f (^{3}F) ^{4}F + 6 4d^{8}4f (^{3}F) ^{2}D
401318	401189	129	1.5	53.6 4d^{8}4f (^{3}P) ^{4}F + 13.4 4d^{8}4f (^{3}F) ^{4}F + 11.2 4d^{8}4f (^{1}G) ^{2}D
401352	401403	-51	3.5	58.5 4d^{8}6p (^{3}F) ^{4}D + 9.9 4d^{8}6p (^{3}F) ^{4}F + 6.1 4d^{8}4f (^{3}F) ^{2}G
401957	401559	398	3.5	19 4d^{8}4f (^{3}F) ^{2}G + 20 4d^{8}6p (^{3}F) ^{4}D + 13.9 4d^{8}4f (^{3}F) ^{2}F
403631	403746	-115	2.5	20.5 4d^{8}4f (^{3}F) ^{2}F + 27.5 4d^{8}4f (^{3}P) ^{2}F + 16.7 4d^{8}4f (^{1}G) ^{2}D
404022	403894	128	3.5	24.7 4d^{8}4f (^{3}P) ^{2}F + 23.5 4d^{8}4f (^{3}P) ^{4}F + 16.7 4d^{8}4f (^{1}D) ^{2}F
405584	404321	1263	2.5	50.7 4d^{8}6p (^{3}F) ^{2}D + 30.4 4d^{8}6p (^{3}F) ^{4}D
403778	404401	-623	1.5	35.8 4d^{8}4f (^{1}D) ^{2}P + 38 4d^{8}4f (^{3}P) ^{4}D + 14 4d^{8}4f (^{3}P) ^{2}D
405917	404931	986	3.5	55.8 4d^{8}6p (^{3}F) ^{2}F + 17.6 4d^{8}6p (^{3}F) ^{4}F + 11.8 4d^{8}6p (^{3}F) ^{4}D
407604	407340	264	3.5	42.7 4d^{8}4f (^{1}D) ^{2}G + 12.4 4d^{8}4f (^{3}P) ^{2}F + 10 4d^{8}4f (^{3}F) ^{2}F
408137	408025	112	2.5	44.9 4d^{8}4f (^{3}P) ^{4}D + 15.1 4d^{8}4f (^{3}P) ^{4}G + 10.4 4d^{8}4f (^{3}P) ^{4}F
408470	408354	116	3.5	53.8 4d^{8}4f (^{3}P) ^{4}G + 11.8 4d^{8}6p (^{3}F) ^{4}G + 7.7 4d^{8}4f (^{3}F) ^{4}G

Table A17: Continued

E^{a}_{exp}	E^{b}_{calc}	ΔE	J	Leading components (in %) in LS coupling ^{c}
408756	408731	25	2.5	39.1 4d^{8}4f (^{3}P) ^{4}G + 12.9 4d^{8}4f (^{3}P) ^{4}D + 10.3 4d^{8}4f (^{3}P) ^{2}F
409094	408909	185	1.5	23.4 4d^{8}4f (^{3}P) ^{4}D + 14.7 4d^{8}4f (^{3}P) ^{2}D + 14.7 4d^{8}4f (^{1}D) ^{2}D
409016	409117	-101	3.5	52.9 4d^{8}4f (^{3}P) ^{4}D + 8.9 4d^{8}6p (^{3}F) ^{4}G + 6.3 4d^{8}4f (^{3}P) ^{2}G
409174	409379	-205	2.5	39.1 4d^{8}6p (^{3}F) ^{4}D + 33.7 4d^{8}6p (^{3}F) ^{2}D + 11.3 4d^{8}6p (^{3}F) ^{4}F
409843	410000	-157	3.5	37 4d^{8}6p (^{3}F) ^{4}G + 21.1 4d^{8}4f (^{3}P) ^{4}G + 13.7 4d^{8}6p (^{3}F) ^{2}F
410603	410711	-108	2.5	36 4d^{8}6p (^{3}F) ^{4}G + 19.4 4d^{8}6p (^{3}F) ^{4}F + 10.7 4d^{8}6p (^{1}D) ^{2}F
410331	410853	-522	1.5	59.2 4d^{8}6p (^{3}F) ^{4}D + 17.8 4d^{8}6p (^{3}F) ^{4}F + 9.4 4d^{8}6p (^{1}D) ^{2}P
410963	411107	-144	3.5	65 4d^{8}4f (^{3}P) ^{2}G + 12.1 4d^{8}4f (^{3}P) ^{4}D + 8.3 4d^{8}4f (^{1}G) ^{2}G
411211	411138	73	2.5	27.6 4d^{8}4f (^{3}P) ^{2}D + 19 4d^{8}4f (^{1}G) ^{2}F + 12.4 4d^{8}4f (^{3}P) ^{4}G
411257	411963	-706	1.5	26.6 4d^{8}4f (^{1}D) ^{2}D + 26 4d^{8}4f (^{3}P) ^{4}D + 22.7 4d^{8}4f (^{1}G) ^{2}D
411182	412001	-819	3.5	49.7 4d^{8}6p (^{3}F) ^{4}F + 24.1 4d^{8}6p (^{3}F) ^{2}G + 9.6 4d^{8}6p (^{3}F) ^{2}F
412353	412158	195	2.5	33.9 4d^{8}6p (^{3}F) ^{4}F + 24 4d^{8}6p (^{3}F) ^{2}F + 10.8 4d^{8}6p (^{1}D) ^{2}F
412518	412271	247	2.5	41.5 4d^{8}4f (^{1}D) ^{2}D + 21.9 4d^{8}4f (^{3}P) ^{4}D + 8 4d^{8}4f (^{3}P) ^{2}D
412912	412608	304	0.5	28.1 4d^{8}4f (^{1}D) ^{2}P + 28.5 4d^{8}6p (^{3}F) ^{4}D + 24.8 4d^{8}4f (^{3}P) ^{4}D
413816	412999	817	2.5	28.3 4d^{8}6p (^{3}F) ^{2}F + 21.4 4d^{8}6p (^{1}D) ^{2}D + 18.2 4d^{8}6p (^{3}P) ^{4}P
413151	413044	107	3.5	36.9 4d^{8}4f (^{1}G) ^{2}F + 17.2 4d^{8}4f (^{1}D) ^{2}F + 10.2 4d^{8}6p (^{3}F) ^{2}G
413916	413330	586	3.5	19.7 4d^{8}6p (^{3}F) ^{2}G + 21.7 4d^{8}6p (^{1}D) ^{2}F + 13 4d^{8}6p (^{3}F) ^{4}G
412646	413528	-882	1.5	29.4 4d^{8}6p (^{3}F) ^{4}F + 29.5 4d^{8}6p (^{3}F) ^{2}D + 10.7 4d^{8}6p (^{1}D) ^{2}P
414465	414364	101	2.5	43.5 4d^{8}4f (^{1}G) ^{2}F + 28.2 4d^{8}4f (^{3}P) ^{2}D + 10.8 4d^{8}4f (^{1}D) ^{2}F
414310	414736	-426	1.5	42.9 4d^{8}4f (^{3}P) ^{2}D + 32.7 4d^{8}4f (^{1}D) ^{2}P + 8.2 4d^{8}4f (^{3}F) ^{2}D
415880	416248	-368	1.5	45.1 4d^{8}6p (^{3}P) ^{4}P + 19.8 4d^{8}6p (^{3}F) ^{2}D + 11.5 4d^{8}6p (^{3}F) ^{4}F
417549	416899	650	2.5	20.3 4d^{8}6p (^{3}P) ^{2}D + 21.3 4d^{8}6p (^{3}P) ^{4}P + 17.9 4d^{8}6p (^{3}F) ^{2}F
417225	417140	85	3.5	79.4 4d^{8}4f (^{1}G) ^{2}G + 9.1 4d^{8}4f (^{3}P) ^{2}G
417679	417608	71	0.5	20.5 4d^{8}6p (^{3}P) ^{2}P + 40.1 4d^{8}6p (^{3}P) ^{4}P + 15 4d^{8}6p (^{3}F) ^{4}D
417629	418384	-755	1.5	48.4 4d^{8}6p (^{3}P) ^{2}P + 13.6 4d^{8}6p (^{3}F) ^{4}F + 8.7 4d^{8}4f (^{1}G) ^{2}P
420075	419292	783	2.5	59.6 4d^{7}5s5p (^{4}F) ^{6}F + 22.5 4d^{7}5s5p (^{4}F) ^{6}D + 9.1 4d^{7}5s5p (^{4}F) ^{6}G
420008	420646	-638	0.5	51.8 4d^{8}6p (^{3}P) ^{4}P + 27.1 4d^{8}6p (^{3}P) ^{2}P + 9.9 4d^{8}6p (^{3}P) ^{2}S
421670	421908	-238	1.5	45.9 4d^{8}6p (^{3}P) ^{4}D + 23.6 4d^{8}6p (^{3}P) ^{2}D + 5.9 4d^{8}6p (^{3}F) ^{4}D
422872	423004	-132	0.5	81.4 4d^{7}5s5p (^{4}F) ^{6}F + 6.2 4d^{7}5s5p (^{4}F) ^{6}D
424036	423519	517	2.5	18.9 4d^{7}5s5p (^{4}F) ^{6}D + 31.7 4d^{7}5s5p (^{4}F) ^{6}G + 17.8 4d^{8}6p (^{3}P) ^{4}D
423531	424095	-564	0.5	48.3 4d^{8}6p (^{3}P) ^{2}S + 17.5 4d^{8}6p (^{3}P) ^{4}D + 9.5 4d^{8}6p (^{3}P) ^{2}P
423896	424224	-328	1.5	15.7 4d^{8}6p (^{3}P) ^{4}S + 24.5 4d^{8}4f (^{1}G) ^{2}P + 15.1 4d^{8}6p (^{3}P) ^{4}P
424800	424507	293	3.5	9.6 4d^{8}4f (^{3}F) ^{2}F + 30.8 4d^{8}4f (^{3}P) ^{2}F + 18.5 4d^{8}4f (^{1}G) ^{2}F
425311	424891	420	1.5	46.4 4d^{8}6p (^{3}P) ^{2}D + 30.3 4d^{8}6p (^{3}P) ^{4}S + 7.3 4d^{8}6p (^{3}P) ^{4}D
427028	425957	1071	1.5	27.9 4d^{7}5s5p (^{4}F) ^{6}D + 22.7 4d^{7}5s5p (^{4}F) ^{6}F + 20.2 4d^{7}5s5p (^{4}P) ^{6}D
425949	425971	-22	2.5	35 4d^{7}5s5p (^{4}F) ^{6}G + 28.1 4d^{7}5s5p (^{4}F) ^{6}F + 14.7 4d^{7}5s5p (^{4}F) ^{6}D
426592	426420	172	2.5	30.9 4d^{8}6p (^{1}D) ^{2}F + 14.2 4d^{8}6p (^{1}G) ^{2}F + 10 4d^{8}6p (^{3}P) ^{2}D
427070	426855	215	0.5	40.5 4d^{8}4f (^{1}G) ^{2}P + 18.5 4d^{8}4f (^{3}F) ^{2}P + 13.3 4d^{8}6p (^{3}P) ^{2}S
427199	426855	344	1.5	39.4 4d^{8}6p (^{1}D) ^{2}D + 12.7 4d^{8}6p (^{3}P) ^{2}P + 8.2 4d^{8}6p (^{3}F) ^{4}F
427721	427969	-248	3.5	23.6 4d^{7}5s5p (^{4}F) ^{4}F + 20.7 4d^{7}5s5p (^{4}F) ^{4}D + 11.5 4d^{7}5s5p (^{4}F) ^{4}F
428240	428019	221	2.5	47.3 4d^{8}6p (^{1}D) ^{2}D + 24.6 4d^{8}6p (^{1}G) ^{2}F + 7.5 4d^{8}6p (^{3}P) ^{4}P
429414	429178	236	1.5	51.4 4d^{8}6p (^{1}D) ^{2}P + 19.4 4d^{8}6p (^{3}P) ^{4}S + 9.7 4d^{8}6p (^{1}D) ^{2}D
429175	429192	-17	2.5	11.1 4d^{8}4f (^{3}P) ^{2}F + 27.6 4d^{8}6p (^{1}D) ^{2}F + 12.6 4d^{8}6p (^{1}G) ^{2}F
429575	429943	-368	3.5	46.8 4d^{8}6p (^{1}D) ^{2}F + 25.6 4d^{8}6p (^{1}G) ^{2}F + 13.5 4d^{8}6p (^{3}P) ^{4}D
430484	430603	-119	0.5	57.2 4d^{8}6p (^{1}D) ^{2}P + 12.8 4d^{8}6p (^{3}P) ^{2}S + 12.2 4d^{8}6p (^{3}P) ^{2}P
430469	430661	-192	1.5	23.3 4d^{8}4f (^{3}F) ^{2}D + 19.5 4d^{8}4f (^{1}G) ^{2}D + 11.1 4d^{8}6p (^{1}D) ^{2}D
431126	431081	45	2.5	26.6 4d^{7}5s5p (^{4}F) ^{4}F + 16.8 4d^{7}5s5p (^{4}F) ^{4}D + 14.3 4d^{7}5s5p (^{4}F) ^{4}F
432769	433336	-567	3.5	30.6 4d^{7}5s5p (^{4}F) ^{4}G + 18.9 4d^{7}5s5p (^{4}F) ^{4}G + 14.4 4d^{7}5s5p (^{4}F) ^{4}D

a: From Swapnil [34] and Ryabtsev [35]
b: This work
c: Only the component $\geq$ 5% are given

Transitions

Table A18: Computed oscillator strengths and transition probabilities in In V.

Wavelength Å	Lower Level[a] cm^{-1}	J_{Low}	Upper level[a] cm^{-1}	J_{Up}	log gf	gA s^{-1}	CF
204.985	0	2.5	487840	3.5	-0.73	2.92E+10	0.213
209.781	0	2.5	476687	3.5	-0.88	2.02E+10	0.267
210.637	0	2.5	474750	2.5	-0.92	1.83E+10	0.116
214.361	0	2.5	466502	1.5	-0.97	1.58E+10	0.181
223.995	0	2.5	446439	3.5	-0.77	2.26E+10	0.196
227.108	7172	1.5	447491	2.5	-0.43	4.81E+10	0.32
234.083	0	2.5	427199	1.5	-0.89	1.58E+10	0.333
234.416	0	2.5	426592	2.5	-0.54	3.52E+10	0.321
235.405	0	2.5	424800	3.5	0.33	2.57E+11	0.369
235.907	0	2.5	423896	1.5	-0.22	7.30E+10	0.453
236.232	7172	1.5	430484	0.5	-0.9	1.52E+10	0.483
236.241	7172	1.5	430469	1.5	0.18	1.82E+11	0.475
236.965	7172	1.5	429175	2.5	-0.11	9.23E+10	0.308
237.152	0	2.5	421670	1.5	-1	1.20E+10	0.326
238.08	7172	1.5	427199	1.5	-0.8	1.87E+10	0.15
238.153	7172	1.5	427070	0.5	-0.26	6.49E+10	0.508
238.424	7172	1.5	426592	2.5	-1	1.17E+10	0.065
337.028	185622	2.5	482333	3.5	-0.9	7.42E+09	0.339
340.209	188396	4.5	482333	3.5	-0.23	3.41E+10	0.611
341.367	178289	1.5	471229	2.5	-0.76	1.00E+10	0.212
345.979	182194	1.5	471229	2.5	-0.77	9.47E+09	0.23
346.713	178289	1.5	466712	2.5	-0.79	9.04E+09	0.28
349.586	171290	3.5	457343	3.5	-0.98	5.71E+09	0.174
350.132	185622	2.5	471229	2.5	-0.69	1.11E+10	0.351
357.561	177670	2.5	457343	3.5	-0.93	6.20E+09	0.314
367.187	160428	4.5	432769	3.5	-0.57	1.34E+10	0.528
367.842	188575	3.5	460431	3.5	-0.71	9.62E+09	0.635
368.025	185622	2.5	457343	3.5	-0.51	1.52E+10	0.414
370.095	0	2.5	270201	1.5	-0.82	7.37E+09	0.441
371.822	188396	4.5	457343	3.5	-0.85	6.77E+09	0.342
372.814	0	2.5	268230	1.5	-0.41	1.89E+10	0.33
372.931	7172	1.5	275318	0.5	-0.33	2.24E+10	0.841
375.844	0	2.5	266068	2.5	-0.77	8.03E+09	0.478
376.074	0	2.5	265905	1.5	-0.64	1.08E+10	0.539
376.787	7172	1.5	272574	2.5	-0.12	3.61E+10	0.49
378.606	0	2.5	264127	3.5	-0.1	3.71E+10	0.715
379.159	163980	3.5	427721	3.5	-0.52	1.40E+10	0.219
379.257	7172	1.5	270846	0.5	-1	4.68E+09	0.669
379.701	167761	2.5	431126	2.5	-0.73	8.57E+09	0.158
380.278	0	2.5	262966	2.5	-0.79	7.43E+09	0.262
381.549	0	2.5	262089	1.5	-0.32	2.21E+10	0.599
382.133	7172	1.5	268861	2.5	-0.83	6.77E+09	0.437
382.757	0	2.5	261263	3.5	-0.33	2.11E+10	0.711
383.056	7172	1.5	268230	1.5	-0.23	2.69E+10	0.697
386.256	7172	1.5	266068	2.5	-0.97	4.79E+09	0.242
386.701	0	2.5	258598	2.5	-0.69	9.19E+09	0.317
388.91	0	2.5	257129	2.5	-0.29	2.27E+10	0.625
390.036	7172	1.5	263559	1.5	-0.52	1.33E+10	0.362
390.94	7172	1.5	262966	2.5	-0.64	9.93E+09	0.53
392.284	7172	1.5	262089	1.5	-0.55	1.21E+10	0.265
392.458	0	2.5	254805	3.5	-0.76	7.53E+09	0.722
393.901	0	2.5	253871	2.5	-0.3	2.15E+10	0.464
395.741	0	2.5	252691	2.5	-0.85	5.98E+09	0.224
399.81	7172	1.5	257291	1.5	-0.73	7.78E+09	0.285
400.069	7172	1.5	257129	2.5	-0.91	5.13E+09	0.157
400.577	0	2.5	249640	2.5	-0.35	1.84E+10	0.324
402.403	0	2.5	248507	3.5	-0.58	1.08E+10	0.31
694.567	235384	3.5	379359	4.5	0.15	1.92E+10	0.802
707.228	238629	4.5	380026	3.5	0.07	1.56E+10	0.582
710.584	238629	4.5	379359	4.5	-0.1	1.04E+10	0.914
719.514	349273	3.5	488256	3.5	-0.43	4.81E+09	0.442
721.05	349569	2.5	488256	3.5	-1	1.28E+09	0.154
721.942	241511	2.5	380026	3.5	-0.35	5.68E+09	0.67
734.064	243798	3.5	380026	3.5	-0.47	4.25E+09	0.657
740.323	244283	5.5	379359	4.5	0.35	2.70E+10	0.87
753.173	247255	4.5	380026	3.5	-0.14	8.56E+09	0.828
756.98	247255	4.5	379359	4.5	0.06	1.33E+10	0.784
760.347	248507	3.5	380026	3.5	0.04	1.28E+10	0.626
766.95	249640	2.5	380026	3.5	-0.84	1.66E+09	0.251
785.326	252691	2.5	380026	3.5	-0.92	1.31E+09	0.149
792.675	253871	2.5	380026	3.5	-0.45	3.76E+09	0.647
794.362	241511	2.5	367398	3.5	-0.82	1.64E+09	0.188
795.989	246722	1.5	372352	2.5	-0.91	1.31E+09	0.059
796.777	248165	0.5	373670	1.5	-0.94	1.19E+09	0.142
804.29	248165	0.5	372498	1.5	-0.93	1.22E+09	0.174
816.143	252691	2.5	375218	2.5	-0.7	1.96E+09	0.269
822.555	252691	2.5	374263	3.5	-0.89	1.29E+09	0.128
823.633	246722	1.5	368135	1.5	-0.92	1.16E+09	0.086
830.759	253298	0.5	373670	1.5	-0.62	2.31E+09	0.28
836.215	241511	2.5	361097	3.5	-0.96	1.04E+09	0.139
838.477	257291	1.5	376555	1.5	-0.84	1.35E+09	0.198
838.929	253298	0.5	372498	1.5	-0.49	3.08E+09	0.291
841.505	246722	1.5	365557	0.5	-0.77	1.61E+09	0.314
842.417	245554	1.5	364260	2.5	-0.69	1.90E+09	0.145
845.682	235384	3.5	353632	4.5	-0.56	2.58E+09	0.112
846.105	360937	4.5	479126	3.5	-0.9	1.17E+09	0.447
847.441	351572	3.5	469574	3.5	-0.85	1.29E+09	0.18
847.978	257291	1.5	375218	2.5	-0.6	2.29E+09	0.28
848.419	241511	2.5	359377	2.5	-0.47	3.21E+09	0.384
849.196	249640	2.5	367398	3.5	-0.65	2.09E+09	0.164
851.148	264127	3.5	381615	4.5	-0.96	1.02E+09	0.059
852.54	366978	1.5	484275	1.5	-0.41	3.53E+09	0.211
852.97	241511	2.5	358748	3.5	-0.19	5.91E+09	0.383
852.972	241511	2.5	358748	1.5	-0.55	2.56E+09	0.146
852.995	258598	2.5	375832	2.5	-1	9.07E+08	0.128

Table A18: Continued

Wavelength	Lower Level	J_{Low}	Upper level	J_{Up}	log gf	gA	CF
853.81	257291	1.5	374413	1.5	-0.89	1.17E+09	0.245
854.337	235384	3.5	352434	4.5	0.05	1.02E+10	0.603
857.033	258598	2.5	375280	3.5	-0.42	3.48E+09	0.189
857.04	252622	1.5	369303	0.5	-0.78	1.50E+09	0.286
857.484	258598	2.5	375218	2.5	-0.88	1.19E+09	0.123
857.661	249640	2.5	366236	3.5	-0.64	2.06E+09	0.142
858.815	241511	2.5	357951	3.5	-0.87	1.22E+09	0.26
860.677	235384	3.5	351572	3.5	-0.61	2.24E+09	0.127
862.038	253298	0.5	369303	0.5	-0.64	2.02E+09	0.607
862.25	245122	2.5	361097	3.5	-0.68	1.87E+09	0.173
862.888	261263	3.5	377153	3.5	-0.31	4.39E+09	0.243
863.91	248507	3.5	364260	2.5	-0.59	2.30E+09	0.188
864.565	258598	2.5	374263	3.5	-0.87	1.22E+09	0.101
864.899	262351	4.5	377971	3.5	-0.63	2.11E+09	0.625
865.209	243798	3.5	359377	2.5	-0.91	1.11E+09	0.278
865.702	252622	1.5	368135	1.5	-0.21	5.39E+09	0.533
866.115	245122	2.5	360580	3.5	-0.25	4.93E+09	0.159
866.132	243798	3.5	359254	2.5	-0.87	1.21E+09	0.406
867.111	243798	3.5	359124	4.5	-0.93	1.03E+09	0.032
867.881	257129	2.5	372352	2.5	-0.88	1.18E+09	0.095
870.628	245554	1.5	360414	0.5	-0.31	4.27E+09	0.799
870.801	253298	0.5	368135	1.5	-0.42	3.29E+09	0.434
871.066	262351	4.5	377153	3.5	-0.99	9.14E+08	0.555
871.674	241511	2.5	356233	1.5	-0.26	4.86E+09	0.617
871.675	369553	1.5	484275	1.5	-0.63	2.08E+09	0.156
871.782	252691	2.5	367398	3.5	-0.96	9.72E+08	0.093
874.458	252622	1.5	366978	1.5	-0.61	2.11E+09	0.27
874.984	245122	2.5	359410	1.5	-0.74	1.63E+09	0.379
875.167	253871	2.5	368135	1.5	-0.98	9.04E+08	0.221
875.757	262966	2.5	377153	3.5	-0.73	1.62E+09	0.374
875.77	235384	3.5	349569	2.5	0.53	2.91E+10	0.853
876.024	243798	3.5	357951	3.5	0.23	1.46E+10	0.826
876.175	245122	2.5	359254	2.5	0.18	1.31E+10	0.721
877.138	248165	0.5	362172	1.5	-0.41	3.47E+09	0.572
878.046	235384	3.5	349273	3.5	0.42	2.29E+10	0.619
878.306	245554	1.5	359410	1.5	-0.18	5.81E+09	0.48
878.39	264127	3.5	377971	3.5	-0.91	1.07E+09	0.555
878.698	238629	4.5	352434	4.5	0.46	2.47E+10	0.772
879.092	258598	2.5	372352	2.5	-0.74	1.60E+09	0.156
879.206	243798	3.5	357537	4.5	0.58	3.26E+10	0.746
879.506	245554	1.5	359254	2.5	-0.1	6.84E+09	0.531
880.075	245122	2.5	358748	3.5	0.04	9.48E+09	0.31
880.326	243798	3.5	357393	2.5	-0.93	1.01E+09	0.159
880.367	262966	2.5	376555	1.5	-0.71	1.68E+09	0.48
880.848	253871	2.5	367398	3.5	-0.29	4.42E+09	0.421
882.056	245122	2.5	358493	1.5	-0.63	1.98E+09	0.528
883.438	245554	1.5	358748	1.5	-0.34	3.83E+09	0.329
883.947	262089	1.5	375218	2.5	-0.15	5.98E+09	0.419
884.117	253871	2.5	366978	1.5	-0.93	9.91E+08	0.202
884.752	264127	3.5	377153	3.5	-0.04	7.82E+09	0.401
884.952	261263	3.5	374263	3.5	-0.68	1.81E+09	0.13
884.988	263559	1.5	376555	1.5	-0.81	1.30E+09	0.194
885.406	238629	4.5	351572	3.5	-0.44	3.18E+09	0.377
885.432	245554	1.5	358493	1.5	-0.34	3.82E+09	0.352
885.468	252622	1.5	365557	0.5	-0.54	2.47E+09	0.571
886.211	246722	1.5	359562	0.5	-0.73	1.58E+09	0.217
886.299	245122	2.5	357951	3.5	0.28	1.62E+10	0.475
887.643	268957	5.5	381615	4.5	-0.45	3.02E+09	0.372
887.662	246722	1.5	359377	2.5	-0.18	5.74E+09	0.578
888.633	246722	1.5	359254	2.5	-0.59	2.19E+09	0.365
889.277	262351	4.5	374802	5.5	0.86	6.08E+10	0.914
889.601	238629	4.5	351039	5.5	0.81	5.50E+10	0.848
889.876	241511	2.5	353886	2.5	0.24	1.45E+10	0.639
889.959	253871	2.5	366236	3.5	0.11	1.10E+10	0.457
890.286	262089	1.5	374413	1.5	-0.69	1.73E+09	0.197
890.361	262966	2.5	375280	3.5	0.12	1.12E+10	0.464
890.703	245122	2.5	357393	2.5	-0.62	1.99E+09	0.265
890.804	253298	0.5	365557	0.5	-0.37	3.62E+09	0.446
890.847	262966	2.5	375218	2.5	-0.04	7.44E+09	0.718
892.244	266068	2.5	378145	2.5	-0.6	2.11E+09	0.23
892.279	248507	3.5	360580	3.5	-0.96	9.10E+08	0.068
892.648	246722	1.5	358748	1.5	-0.32	3.96E+09	0.431
893.543	261263	3.5	373177	3.5	-0.52	2.52E+09	0.184
894.027	368012	2.5	479865	3.5	-0.87	1.10E+09	0.097
894.146	245554	1.5	357393	2.5	-0.64	1.91E+09	0.191
894.683	246722	1.5	358493	1.5	-0.69	1.68E+09	0.246
895.75	252622	1.5	364260	2.5	-0.47	2.82E+09	0.275
896.211	262089	1.5	373670	1.5	-0.69	1.70E+09	0.198
897.202	249640	2.5	361097	3.5	-0.77	1.40E+09	0.124
897.49	246722	1.5	358144	2.5	-0.84	1.22E+09	0.258
897.643	263010	0.5	374413	1.5	-0.75	1.49E+09	0.164
897.689	248165	0.5	359562	0.5	-0.24	4.73E+09	0.783
898.492	262966	2.5	374263	3.5	0.14	1.14E+10	0.416
900	245122	2.5	356233	1.5	-0.52	2.47E+09	0.64
900.384	245554	1.5	356618	0.5	-0.31	4.01E+09	0.478
900.848	257129	2.5	368135	1.5	-0.89	1.03E+09	0.249
901.387	249640	2.5	360580	3.5	0.2	1.30E+10	0.799
901.852	257129	2.5	368012	2.5	-0.8	1.32E+09	0.205
902.165	257291	1.5	368135	1.5	-1	8.13E+08	0.093
903.171	257291	1.5	368012	2.5	-0.57	2.26E+09	0.362
903.444	377153	3.5	487840	3.5	-0.55	2.24E+09	0.366
903.581	246722	1.5	357393	2.5	-0.56	2.20E+09	0.321
903.666	263010	0.5	373670	1.5	-0.32	3.90E+09	0.401
903.799	238629	4.5	349273	3.5	-0.2	5.19E+09	0.809
904.025	248507	3.5	359124	4.5	-0.87	1.11E+09	0.042
904.832	261208	0.5	371726	0.5	-0.24	4.67E+09	0.693
905.085	266068	2.5	376555	1.5	-0.49	2.62E+09	0.352
905.726	262089	1.5	372498	1.5	-0.88	1.09E+09	0.132
905.888	253871	2.5	364260	2.5	-0.19	5.22E+09	0.376
905.957	271234	3.5	381615	4.5	-0.1	6.52E+09	0.374
906.383	248165	0.5	358493	1.5	-0.39	3.29E+09	0.772
906.868	257129	2.5	367398	3.5	0.29	1.60E+10	0.725
906.872	356233	1.5	466502	1.5	-0.71	1.62E+09	0.294
906.927	262089	1.5	372352	2.5	-0.25	4.64E+09	0.227
907.022	241511	2.5	351762	1.5	0.08	9.72E+09	0.825
907.258	263559	1.5	373781	2.5	-0.37	3.45E+09	0.21

Table A18: Continued

Wavelength	Lower Level	J_{Low}	Upper level	J_{Up}	log gf	gA	CF
907.964	264127	3.5	374263	3.5	-0.24	4.69E+09	0.567
908.366	243798	3.5	353886	2.5	-0.37	3.42E+09	0.494
908.589	241511	2.5	351572	3.5	-0.21	5.02E+09	0.433
909.801	268230	1.5	378145	2.5	-0.75	1.43E+09	0.485
909.952	246722	1.5	356618	0.5	-0.53	2.36E+09	0.41
910.468	243798	3.5	353632	4.5	-0.2	5.11E+09	0.455
911.01	358144	2.5	467912	2.5	-0.83	1.19E+09	0.2
911.265	249640	2.5	359377	2.5	-0.24	4.71E+09	0.372
911.679	257291	1.5	366978	1.5	-0.73	1.46E+09	0.331
912.827	252622	1.5	362172	1.5	-0.79	1.32E+09	0.184
913.15	246722	1.5	356233	1.5	-0.43	2.95E+09	0.508
913.341	263010	0.5	372498	1.5	-0.08	6.72E+09	0.772
913.4	252691	2.5	362172	1.5	-0.77	1.39E+09	0.182
913.613	254805	3.5	364260	2.5	-0.97	8.51E+08	0.167
913.716	248507	3.5	357951	3.5	-0.54	2.28E+09	0.17
913.963	258598	2.5	368012	2.5	-0.66	1.77E+09	0.264
914.5	244283	5.5	353632	4.5	-0.65	1.83E+09	0.508
915.007	367398	3.5	476687	3.5	-0.95	8.91E+08	0.261
915.051	268861	2.5	378145	2.5	-0.91	9.69E+08	0.181
915.651	266068	2.5	375280	3.5	-0.04	7.30E+09	0.807
916.166	266068	2.5	375218	2.5	-0.9	9.83E+08	0.083
916.517	249640	2.5	358748	3.5	-0.09	6.43E+09	0.346
916.849	251868	4.5	360937	4.5	-0.67	1.68E+09	0.115
917.179	248507	3.5	357537	4.5	0.28	1.49E+10	0.91
918.617	351572	3.5	460431	3.5	-0.39	3.14E+09	0.284
919.115	258598	2.5	367398	3.5	0.17	1.19E+10	0.718
919.176	263559	1.5	372352	2.5	0.15	1.14E+10	0.694
920.171	368012	2.5	476687	3.5	-0.51	2.38E+09	0.303
920.509	243798	3.5	352434	4.5	-0.2	4.92E+09	0.188
921.597	265905	1.5	374413	1.5	-0.92	9.51E+08	0.183
921.625	249640	2.5	358144	2.5	-0.71	1.56E+09	0.18
922.452	252691	2.5	361097	3.5	-0.91	9.54E+08	0.063
922.676	258598	2.5	366978	1.5	-0.99	7.98E+08	0.277
922.864	358144	2.5	466502	1.5	-0.94	9.01E+08	0.243
922.975	261208	0.5	369553	1.5	-0.32	3.69E+09	0.639
923.156	268230	1.5	376555	1.5	-0.52	2.33E+09	0.288
923.269	249640	2.5	357951	3.5	-0.96	8.67E+08	0.037
923.648	244283	5.5	352549	5.5	0.34	1.72E+10	0.846
923.999	264127	3.5	372352	2.5	-1	7.90E+08	0.248
924.63	244283	5.5	352434	4.5	-0.63	1.82E+09	0.685
924.732	378145	2.5	486284	3.5	-0.19	5.04E+09	0.672
925.117	261208	0.5	369303	0.5	-0.92	9.24E+08	0.28
926.754	365557	0.5	473460	1.5	-0.43	2.89E+09	0.55
926.876	252691	2.5	360580	3.5	0.13	1.05E+10	0.464
926.994	265905	1.5	373781	2.5	0.13	1.04E+10	0.764
927.873	243798	3.5	351572	3.5	-0.24	4.58E+09	0.374
928.05	249640	2.5	357393	2.5	-0.49	2.45E+09	0.354
928.391	266068	2.5	373781	2.5	-0.55	2.16E+09	0.162
928.562	268861	2.5	376555	1.5	-0.91	9.43E+08	0.271
928.856	360414	0.5	468073	0.5	-0.73	1.46E+09	0.531
929.04	258598	2.5	366236	3.5	0.09	9.54E+09	0.498
929.281	351762	1.5	459372	1.5	-0.36	3.39E+09	0.421
929.356	268230	1.5	375832	2.5	-0.81	1.18E+09	0.172
930.117	372352	2.5	479865	3.5	-0.25	4.31E+09	0.452
930.543	262089	1.5	369553	1.5	-0.99	7.78E+08	0.151
932.351	251868	4.5	359124	4.5	0.23	1.30E+10	0.671
932.608	253871	2.5	361097	3.5	-0.46	2.64E+09	0.37
933.088	253926	3.5	361097	3.5	-0.48	2.55E+09	0.227
933.432	257129	2.5	364260	2.5	-0.54	2.18E+09	0.173
933.576	244283	5.5	351398	6.5	0.93	6.55E+10	0.928
933.578	375218	2.5	482333	3.5	-0.84	1.12E+09	0.273
933.628	266068	2.5	373177	3.5	0.4	1.94E+10	0.819
934.687	268230	1.5	375218	2.5	-0.09	6.11E+09	0.578
934.834	268861	2.5	375832	2.5	-0.35	3.36E+09	0.574
934.846	257291	1.5	364260	2.5	-0.36	3.33E+09	0.342
935.217	261208	0.5	368135	1.5	-0.87	1.00E+09	0.151
935.364	271234	3.5	378145	2.5	-0.93	8.95E+08	0.329
935.617	356618	0.5	463499	1.5	-0.44	2.78E+09	0.584
935.626	251868	4.5	358748	3.5	-0.74	1.39E+09	0.307
935.659	358748	3.5	465625	3.5	-0.9	9.40E+08	0.122
936.032	261263	3.5	368097	4.5	0.59	2.96E+10	0.865
936.527	268957	5.5	375735	6.5	0.93	6.46E+10	0.926
936.709	244283	5.5	351039	5.5	-0.15	5.36E+09	0.876
936.72	252622	1.5	359377	2.5	-0.62	1.84E+09	0.427
936.777	261263	3.5	368012	2.5	-0.84	1.12E+09	0.223
936.87	368012	2.5	474750	2.5	-0.76	1.31E+09	0.301
936.884	271234	3.5	377971	3.5	-0.79	1.23E+09	0.687
937.31	373177	3.5	479865	3.5	-0.86	1.04E+09	0.204
937.369	366978	1.5	473660	2.5	-0.41	2.98E+09	0.333
937.604	358493	1.5	465148	2.5	-0.59	1.96E+09	0.182
937.615	253926	3.5	360580	3.5	-0.4	3.00E+09	0.213
937.802	252622	1.5	359254	2.5	-0.58	2.03E+09	0.229
937.955	368135	1.5	474750	2.5	-0.37	3.32E+09	0.403
938.147	249640	2.5	356233	1.5	-0.18	4.96E+09	0.599
938.152	265905	1.5	372498	1.5	-0.91	9.32E+08	0.135
938.571	353886	2.5	460431	3.5	-0.2	4.74E+09	0.446
938.957	375832	2.5	482333	3.5	-0.41	2.90E+09	0.563
939.441	265905	1.5	372352	2.5	-0.56	2.12E+09	0.226
939.492	357951	3.5	464391	3.5	-0.63	1.81E+09	0.492
939.687	268861	2.5	375280	3.5	0.12	1.02E+10	0.648
940.051	247255	4.5	353632	4.5	0.35	1.70E+10	0.711
940.079	251868	4.5	358242	5.5	0.86	5.45E+10	0.937
940.108	359254	2.5	465625	3.5	-0.05	6.63E+09	0.473
940.261	270201	1.5	376555	1.5	-0.85	1.06E+09	0.341
940.797	254805	3.5	361097	3.5	0.12	9.81E+09	0.582
941.197	359377	2.5	465625	3.5	-0.01	7.22E+09	0.759
942.216	254805	3.5	360937	4.5	0.75	4.24E+10	0.927
942.284	351762	1.5	457887	0.5	-0.42	2.81E+09	0.719
942.663	251868	4.5	357951	3.5	-0.74	1.37E+09	0.567
942.882	252691	2.5	358748	3.5	-0.74	1.38E+09	0.079
942.885	252691	2.5	358748	1.5	-0.26	4.12E+09	0.534
944.088	262089	1.5	368012	2.5	-0.46	2.63E+09	0.234
944.126	271234	3.5	377153	3.5	-0.09	6.13E+09	0.645
944.342	359254	2.5	465148	2.5	-0.21	4.62E+09	0.758
944.543	252622	1.5	358493	1.5	-0.93	8.65E+08	0.159
944.781	268957	5.5	374802	5.5	-0.79	1.22E+09	0.867

Table A18: Continued

Wavelength	Lower Level	J_{Low}	Upper level	J_{Up}	log gf	gA	CF
945.445	261208	0.5	366978	1.5	-0.66	1.61E+09	0.374
945.52	358748	1.5	464510	0.5	-0.98	8.01E+08	0.322
945.73	359410	1.5	465148	2.5	-0.24	4.14E+09	0.614
945.993	270846	0.5	376555	1.5	-0.65	1.64E+09	0.325
946.35	251868	4.5	357537	4.5	-0.44	2.71E+09	0.279
946.413	258598	2.5	364260	2.5	-0.4	2.95E+09	0.214
946.536	368012	2.5	473660	2.5	-0.66	1.61E+09	0.406
946.635	359562	0.5	465199	1.5	-0.84	1.10E+09	0.567
946.693	270201	1.5	375832	2.5	0.32	1.53E+10	0.799
946.953	374263	3.5	479865	3.5	-0.83	1.08E+09	0.296
947.232	272574	2.5	378145	2.5	0.19	1.14E+10	0.735
947.415	268230	1.5	373781	2.5	-0.73	1.38E+09	0.161
947.812	253871	2.5	359377	2.5	-0.9	9.50E+08	0.172
947.994	353886	2.5	459372	1.5	-0.44	2.75E+09	0.36
948.289	252691	2.5	358144	2.5	0.09	9.08E+09	0.617
948.308	253926	3.5	359377	2.5	-0.77	1.28E+09	0.351
948.748	268861	2.5	374263	3.5	0.14	1.04E+10	0.591
948.791	272574	2.5	377971	3.5	-0.45	2.62E+09	0.501
948.958	248507	3.5	353886	2.5	-0.19	4.74E+09	0.39
949.443	368135	1.5	473460	1.5	-0.67	1.60E+09	0.322
949.72	247255	4.5	352549	5.5	0.7	3.71E+10	0.888
950.03	252691	2.5	357951	3.5	-0.47	2.52E+09	0.164
950.593	253926	3.5	359124	4.5	0.57	2.72E+10	0.773
950.601	369553	1.5	474750	2.5	-0.92	9.08E+08	0.183
951.038	272846	1.5	377995	0.5	-0.93	8.79E+08	0.355
951.142	359254	2.5	464391	3.5	-0.49	2.44E+09	0.373
951.252	248507	3.5	353632	4.5	0	7.52E+09	0.376
951.972	360580	3.5	465625	3.5	-0.75	1.31E+09	0.149
952.031	276576	3.5	381615	4.5	0.19	1.13E+10	0.803
952.623	261263	3.5	366236	3.5	-0.06	6.41E+09	0.716
953.461	257291	1.5	362172	1.5	-0.24	4.28E+09	0.456
953.997	253926	3.5	358748	3.5	0	7.40E+09	0.539
954.465	252622	1.5	357393	2.5	-0.73	1.35E+09	0.268
954.646	358748	1.5	463499	1.5	-0.76	1.29E+09	0.264
955.092	252691	2.5	357393	2.5	-0.23	4.22E+09	0.363
956.218	272574	2.5	377153	3.5	-0.92	8.84E+08	0.241
956.238	263559	1.5	368135	1.5	-0.48	2.38E+09	0.241
956.569	362172	1.5	466712	2.5	-0.97	7.63E+08	0.28
957.369	263559	1.5	368012	2.5	-0.39	3.01E+09	0.479
957.555	262966	2.5	367398	3.5	-0.43	2.70E+09	0.123
958.448	372352	2.5	476687	3.5	-0.27	3.87E+09	0.353
958.596	254805	3.5	359124	4.5	-0.76	1.24E+09	0.04
958.629	268861	2.5	373177	3.5	0.09	8.99E+09	0.477
959.533	253926	3.5	358144	2.5	-0.19	4.68E+09	0.744
960.084	369303	0.5	473460	1.5	-0.71	1.44E+09	0.432
960.309	277482	4.5	381615	4.5	0.42	1.90E+10	0.616
960.419	268230	1.5	372352	2.5	-0.71	1.43E+09	0.088
960.554	369553	1.5	473660	2.5	-0.45	2.60E+09	0.427
960.713	359410	1.5	463499	1.5	-0.65	1.58E+09	0.371
961.315	253926	3.5	357951	3.5	-0.71	1.41E+09	0.163
961.371	373781	2.5	477799	3.5	-0.91	9.05E+08	0.527
961.718	272574	2.5	376555	1.5	-0.81	1.11E+09	0.181
961.815	264127	3.5	368097	4.5	0.26	1.32E+10	0.784
961.827	257129	2.5	361097	3.5	0.25	1.26E+10	0.664
962.058	254805	3.5	358748	3.5	-0.43	2.71E+09	0.265
962.218	248507	3.5	352434	4.5	0	7.13E+09	0.244
962.392	375218	2.5	479126	3.5	-0.98	7.75E+08	0.285
962.602	264127	3.5	368012	2.5	-0.31	3.62E+09	0.657
963.535	247255	4.5	351039	5.5	-0.32	3.46E+09	0.154
964.245	272846	1.5	376555	1.5	-0.7	1.42E+09	0.283
964.804	265905	1.5	369553	1.5	-0.73	1.33E+09	0.247
965.149	253926	3.5	357537	4.5	-0.59	1.83E+09	0.121
965.439	270201	1.5	373781	2.5	-0.27	3.83E+09	0.383
965.557	270846	0.5	374413	1.5	-0.09	5.81E+09	0.875
966.271	268861	2.5	372352	2.5	-0.59	1.86E+09	0.229
966.472	270201	1.5	373670	1.5	-0.45	2.51E+09	0.525
967.145	265905	1.5	369303	0.5	-0.82	1.06E+09	0.286
968.11	375832	2.5	479126	3.5	-0.7	1.44E+09	0.488
968.114	361097	3.5	464391	3.5	-0.85	1.02E+09	0.36
968.332	262966	2.5	366236	3.5	-0.44	2.59E+09	0.315
969.563	356233	1.5	459372	1.5	-0.83	1.06E+09	0.237
969.715	257291	1.5	360414	0.5	-0.57	1.89E+09	0.563
970.267	248507	3.5	351572	3.5	0.27	1.34E+10	0.524
970.603	271234	3.5	374263	3.5	-0.22	4.29E+09	0.373
971.01	272846	1.5	375832	2.5	-0.51	2.16E+09	0.391
971.097	362172	1.5	465148	2.5	-0.54	2.00E+09	0.314
971.76	373781	2.5	476687	3.5	-0.65	1.61E+09	0.205
973.657	272574	2.5	375280	3.5	-0.18	4.73E+09	0.335
973.932	275318	0.5	377995	0.5	-0.16	4.92E+09	0.868
975.615	258598	2.5	361097	3.5	-0.46	2.43E+09	0.206
976.929	253871	2.5	356233	1.5	-0.51	2.17E+09	0.379
977.699	257129	2.5	359410	1.5	-0.9	9.08E+08	0.21
978.073	364260	2.5	466502	1.5	-0.98	7.43E+08	0.156
978.189	265905	1.5	368135	1.5	-0.89	8.79E+08	0.223
979.22	249640	2.5	351762	1.5	-0.67	1.48E+09	0.22
979.25	257291	1.5	359410	1.5	-0.75	1.27E+09	0.171
979.342	264127	3.5	366236	3.5	-0.22	4.17E+09	0.722
980.213	247255	4.5	349273	3.5	0.07	8.12E+09	0.78
980.412	263559	1.5	365557	0.5	-0.95	7.87E+08	0.203
980.566	258598	2.5	360580	3.5	-0.9	8.64E+08	0.06
980.742	257291	1.5	359254	2.5	-0.59	1.78E+09	0.168
980.947	271234	3.5	373177	3.5	-0.61	1.73E+09	0.155
981.046	249640	2.5	351572	3.5	-0.79	1.13E+09	0.122
981.944	272574	2.5	374413	1.5	-0.49	2.24E+09	0.516
983.389	272574	2.5	374263	3.5	-0.77	1.18E+09	0.159
983.452	358748	3.5	460431	3.5	-0.85	9.65E+08	0.133
984.559	276576	3.5	378145	2.5	0	6.78E+09	0.612
986.243	276576	3.5	377971	3.5	-0.14	5.05E+09	0.539
986.901	362172	1.5	463499	1.5	-0.76	1.19E+09	0.24
987.22	262966	2.5	364260	2.5	-0.8	1.08E+09	0.169
989.156	272574	2.5	373670	1.5	-0.93	7.93E+08	0.385
989.384	265905	1.5	366978	1.5	-0.66	1.47E+09	0.269
989.951	257129	2.5	358144	2.5	-0.71	1.33E+09	0.128
991.273	270846	0.5	371726	0.5	-0.98	7.10E+08	0.176
991.541	257291	1.5	358144	2.5	-0.52	2.07E+09	0.398

Table A18: Continued

Wavelength	Lower Level	J_{Low}	Upper level	J_{Up}	log gf	gA	CF
991.829	272846	1.5	373670	1.5	-0.61	1.65E+09	0.307
991.848	257129	2.5	357951	3.5	-0.98	7.00E+08	0.117
991.949	258598	2.5	359410	1.5	-0.92	8.39E+08	0.205
992.399	248507	3.5	349273	3.5	-0.73	1.28E+09	0.131
994.008	272574	2.5	373177	3.5	-0.98	7.10E+08	0.124
994.271	276576	3.5	377153	3.5	-0.3	3.38E+09	0.652
998.666	264127	3.5	364260	2.5	-0.97	7.21E+08	0.166
999.851	253871	2.5	353886	2.5	-0.91	8.23E+08	0.128
1000.102	373670	1.5	473660	2.5	-0.92	8.13E+08	0.136
1000.76	272574	2.5	372498	1.5	-0.95	7.45E+08	0.229
1001.491	360580	3.5	460431	3.5	-0.9	8.27E+08	0.123
1002.194	268230	1.5	368012	2.5	-0.36	2.94E+09	0.262
1002.953	253926	3.5	353632	4.5	-0.66	1.46E+09	0.124
1003.303	277482	4.5	377153	3.5	0.18	1.01E+10	0.86
1003.497	272846	1.5	372498	1.5	-0.64	1.52E+09	0.315
1006.775	257291	1.5	356618	0.5	-0.72	1.26E+09	0.447
1008.568	268861	2.5	368012	2.5	-0.38	2.81E+09	0.522
1009.137	275318	0.5	374413	1.5	-0.67	1.40E+09	0.235
1009.375	252691	2.5	351762	1.5	-0.68	1.36E+09	0.137
1013.138	276576	3.5	375280	3.5	-0.74	1.18E+09	0.38
1013.768	276576	3.5	375218	2.5	-0.73	1.19E+09	0.647
1015.829	375218	2.5	473660	2.5	-0.98	7.01E+08	0.18
1016.728	265905	1.5	364260	2.5	-0.92	7.80E+08	0.24
1017.041	262089	1.5	360414	0.5	-0.66	1.43E+09	0.5
1021.548	253871	2.5	351762	1.5	-0.28	3.33E+09	0.541
1023.536	253871	2.5	351572	3.5	-0.49	2.10E+09	0.412
1024.616	377153	3.5	474750	2.5	-0.68	1.32E+09	0.636
1027.539	277482	4.5	374802	5.5	-0.56	1.74E+09	0.498
1033.256	277482	4.5	374263	3.5	-0.86	8.78E+08	0.665
1035.712	263010	0.5	359562	0.5	-0.7	1.24E+09	0.637
1036.741	272846	1.5	369303	0.5	-0.93	7.16E+08	0.236
1043.866	167761	2.5	263559	1.5	-0.91	7.47E+08	0.306
1050.679	177670	2.5	272846	1.5	-0.85	8.40E+08	0.305
1057.556	178289	1.5	272846	1.5	-0.78	9.86E+08	0.278
1066.332	169230	1.5	263010	0.5	-0.8	9.36E+08	0.596
1073.377	258598	2.5	351762	1.5	-0.87	7.80E+08	0.238
1074.586	263559	1.5	356618	0.5	-0.9	7.26E+08	0.319
1080.679	173371	2.5	265905	1.5	-0.93	6.72E+08	0.15
1082.795	180493	0.5	272846	1.5	-0.6	1.41E+09	0.603
1096.596	177670	2.5	268861	2.5	-0.84	7.99E+08	0.635
1101.861	173371	2.5	264127	3.5	-0.53	1.63E+09	0.413
1103.115	182194	1.5	272846	1.5	-0.58	1.45E+09	0.497
1111.771	163980	3.5	253926	3.5	-0.88	7.12E+08	0.071
1112.453	163980	3.5	253871	2.5	-0.6	1.35E+09	0.593
1116.947	167761	2.5	257291	1.5	-0.98	5.56E+08	0.337
1122.518	188396	4.5	277482	4.5	0.36	1.20E+10	0.639
1124.776	188575	3.5	277482	4.5	-0.38	2.19E+09	0.805
1135.586	169230	1.5	257291	1.5	-0.56	1.43E+09	0.429
1136.348	188575	3.5	276576	3.5	0.31	1.05E+10	0.746
1137.679	169230	1.5	257129	2.5	-0.74	9.38E+08	0.664
1137.765	173371	2.5	261263	3.5	-0.54	1.48E+09	0.159
1137.807	163980	3.5	251868	4.5	-0.19	3.30E+09	0.209
1141.336	178289	1.5	265905	1.5	-0.52	1.55E+09	0.451
1143.574	264127	3.5	351572	3.5	-0.98	5.43E+08	0.271
1146.47	185622	2.5	272846	1.5	-0.87	6.88E+08	0.338
1148.848	167761	2.5	254805	3.5	-0.24	2.92E+09	0.462
1150.063	185622	2.5	272574	2.5	-0.76	8.80E+08	0.307
1151.723	160428	4.5	247255	4.5	0.22	8.23E+09	0.678
1153.815	188649	1.5	275318	0.5	-0.32	2.41E+09	0.779
1153.841	182194	1.5	268861	2.5	-0.34	2.30E+09	0.478
1156.648	177670	2.5	264127	3.5	-0.24	2.86E+09	0.776
1160.558	167761	2.5	253926	3.5	-0.52	1.52E+09	0.54
1168.057	185622	2.5	271234	3.5	0.23	8.23E+09	0.814
1170.787	180493	0.5	265905	1.5	-0.95	5.47E+08	0.711
1172.748	178289	1.5	263559	1.5	-0.54	1.38E+09	0.367
1177.443	167761	2.5	252691	2.5	-0.11	3.76E+09	0.621
1180.962	178289	1.5	262966	2.5	-0.71	9.31E+08	0.195
1181.326	220694	0.5	305344	1.5	0.02	5.00E+09	0.844
1183.046	163980	3.5	248507	3.5	-0.01	4.71E+09	0.51
1190.493	188575	3.5	272574	2.5	0	4.67E+09	0.811
1191.543	188649	1.5	272574	2.5	-0.51	1.45E+09	0.715
1191.616	173371	2.5	257291	1.5	-1	4.75E+08	0.157
1192.27	182194	1.5	266068	2.5	-0.18	3.08E+09	0.756
1192.545	160428	4.5	244283	5.5	0.52	1.54E+10	0.89
1193.921	173371	2.5	257129	2.5	-0.5	1.48E+09	0.28
1194.581	182194	1.5	265905	1.5	-0.68	9.81E+08	0.3
1196.275	177670	2.5	261263	3.5	-0.09	3.74E+09	0.672
1199.163	169230	1.5	252622	1.5	-0.48	1.54E+09	0.643
1200.842	163980	3.5	247255	4.5	-0.1	3.72E+09	0.854
1203.864	180493	0.5	263559	1.5	-0.5	1.44E+09	0.667
1207.174	188396	4.5	271234	3.5	-0.55	1.30E+09	0.668
1210.117	171290	3.5	253926	3.5	0.08	5.52E+09	0.731
1210.531	185622	2.5	268230	1.5	-0.92	5.41E+08	0.46
1210.925	171290	3.5	253871	2.5	-0.54	1.32E+09	0.419
1211.871	180493	0.5	263010	0.5	-0.54	1.31E+09	0.767
1216.457	188640	0.5	270846	0.5	-0.45	1.61E+09	0.783
1221.316	167761	2.5	249640	2.5	-0.93	5.25E+08	0.153
1226.068	188640	0.5	270201	1.5	-0.14	3.21E+09	0.821
1227.994	173371	2.5	254805	3.5	0	4.43E+09	0.629
1228.487	171290	3.5	252691	2.5	-0.49	1.42E+09	0.39
1235.664	177670	2.5	258598	2.5	-0.35	1.94E+09	0.574
1238.444	167761	2.5	248507	3.5	-0.42	1.67E+09	0.723
1241.027	171290	3.5	251868	4.5	0.31	8.81E+09	0.875
1241.3	188396	4.5	268957	5.5	0.51	1.39E+10	0.895
1241.382	173371	2.5	253926	3.5	-0.56	1.19E+09	0.49
1242.233	173371	2.5	253871	2.5	-0.21	2.65E+09	0.725
1243.077	185622	2.5	266068	2.5	-0.47	1.45E+09	0.293
1243.636	169230	1.5	249640	2.5	-0.24	2.51E+09	0.742
1245.188	178289	1.5	258598	2.5	-0.19	2.77E+09	0.725
1245.548	188575	3.5	268861	2.5	-0.74	7.79E+08	0.751
1245.59	185622	2.5	265905	1.5	-0.66	9.40E+08	0.23
1246.697	188649	1.5	268861	2.5	-0.22	2.58E+09	0.803
1251.639	182194	1.5	262089	1.5	-0.49	1.36E+09	0.427
1252.841	163980	3.5	243798	3.5	-0.05	3.82E+09	0.797
1255.953	177670	2.5	257291	1.5	-0.48	1.39E+09	0.622
1256.576	188649	1.5	268230	1.5	-0.09	3.44E+09	0.73

Table A18: Continued

Wavelength	Lower Level	J_{Low}	Upper level	J_{Up}	log gf	gA	CF
1258.514	177670	2.5	257129	2.5	-0.42	1.61E+09	0.43
1260.722	173371	2.5	252691	2.5	-0.7	8.38E+08	0.359
1261.815	173371	2.5	252622	1.5	-0.91	5.15E+08	0.196
1265.597	182194	1.5	261208	0.5	-0.49	1.34E+09	0.678
1266.448	167761	2.5	246722	1.5	-0.72	7.92E+08	0.301
1266.878	169230	1.5	248165	0.5	-0.43	1.55E+09	0.8
1268.395	178289	1.5	257129	2.5	-0.32	2.02E+09	0.693
1276.323	171290	3.5	249640	2.5	-0.3	2.03E+09	0.656
1278.756	160428	4.5	238629	4.5	-0.01	4.03E+09	0.836
1283.096	185622	2.5	263559	1.5	-0.73	7.47E+08	0.349
1285.46	167761	2.5	245554	1.5	-0.22	2.43E+09	0.669
1288.642	220694	0.5	298295	0.5	-0.32	1.91E+09	0.843
1289.803	163980	3.5	241511	2.5	0.06	4.56E+09	0.862
1290.447	188575	3.5	266068	2.5	-0.49	1.29E+09	0.783
1290.465	169230	1.5	246722	1.5	-0.54	1.18E+09	0.724
1291.68	188649	1.5	266068	2.5	-1	3.98E+08	0.734
1292.643	167761	2.5	245122	2.5	-0.28	2.12E+09	0.621
1292.935	185622	2.5	262966	2.5	-0.13	2.95E+09	0.722
1295.041	171290	3.5	248507	3.5	-0.34	1.80E+09	0.216
1296.432	177670	2.5	254805	3.5	-0.34	1.80E+09	0.398
1307.751	185622	2.5	262089	1.5	-0.72	7.46E+08	0.634
1312.312	177670	2.5	253871	2.5	-0.56	1.06E+09	0.398
1315.141	167761	2.5	243798	3.5	-0.08	3.21E+09	0.413
1316.396	171290	3.5	247255	4.5	-0.6	9.56E+08	0.228
1317.673	169230	1.5	245122	2.5	-0.21	2.39E+09	0.412
1320.477	188396	4.5	264127	3.5	-0.03	3.60E+09	0.796
1322.043	185622	2.5	261263	3.5	-0.49	1.23E+09	0.217
1330.914	173371	2.5	248507	3.5	-0.87	5.12E+08	0.652
1331.618	182194	1.5	257291	1.5	-0.78	6.25E+08	0.458
1333.164	178289	1.5	253298	0.5	-0.48	1.25E+09	0.758
1334.118	160428	4.5	235384	3.5	0.25	6.73E+09	0.867
1334.186	177670	2.5	252622	1.5	-0.49	1.22E+09	0.64
1334.498	182194	1.5	257129	2.5	-0.97	4.02E+08	0.141
1339.594	163980	3.5	238629	4.5	0.07	4.35E+09	0.484
1345.598	188649	1.5	262966	2.5	-0.38	1.56E+09	0.524
1352.185	188396	4.5	262351	4.5	-0.47	1.24E+09	0.799
1354.425	171290	3.5	245122	2.5	-0.75	6.52E+08	0.817
1355.462	188575	3.5	262351	4.5	0.32	7.66E+09	0.771
1361.475	188640	0.5	262089	1.5	-0.69	7.31E+08	0.804
1363.311	173371	2.5	246722	1.5	-0.45	1.28E+09	0.803
1365.592	351572	3.5	424800	3.5	-0.55	9.68E+08	0.363
1372.376	188396	4.5	261263	3.5	-0.24	2.05E+09	0.835
1379.146	171290	3.5	243798	3.5	-0.93	4.08E+08	0.363
1382.642	358144	2.5	430469	1.5	-0.92	4.17E+08	0.153
1385.367	173371	2.5	245554	1.5	-0.8	5.50E+08	0.343
1386.403	180493	0.5	252622	1.5	-0.84	5.06E+08	0.429
1389.469	177670	2.5	249640	2.5	-0.78	5.69E+08	0.431
1393.713	173371	2.5	245122	2.5	-0.98	3.58E+08	0.288
1395.144	182194	1.5	253871	2.5	-0.95	3.83E+08	0.166
1406.385	182194	1.5	253298	0.5	-1	3.42E+08	0.264
1407.83	358144	2.5	429175	2.5	-0.91	4.14E+08	0.16
1424.07	171290	3.5	241511	2.5	-0.96	3.61E+08	0.319
1427.444	360414	0.5	430469	1.5	-0.61	8.14E+08	0.423
1461.283	178289	1.5	246722	1.5	-0.84	4.59E+08	0.236
1467.567	173371	2.5	241511	2.5	-0.86	4.32E+08	0.494
1477.72	180493	0.5	248165	0.5	-0.97	3.31E+08	0.841
1477.908	356233	1.5	423896	1.5	-0.85	4.38E+08	0.41
1485.012	171290	3.5	238629	4.5	-0.56	8.36E+08	0.148
1495.898	357951	3.5	424800	3.5	-0.86	4.07E+08	0.365
1513.968	358748	3.5	424800	3.5	-0.9	3.57E+08	0.336
1569.795	361097	3.5	424800	3.5	-0.84	3.87E+08	0.293
1720.658	372352	2.5	430469	1.5	-0.97	2.42E+08	0.163
1738.629	369553	1.5	427070	0.5	-0.98	2.37E+08	0.441
1759.841	372352	2.5	429175	2.5	-0.82	3.24E+08	0.133
1765.421	349273	3.5	405917	3.5	-0.84	2.96E+08	0.203
1783.444	374413	1.5	430484	0.5	-0.85	2.96E+08	0.297
1783.921	374413	1.5	430469	1.5	-0.89	2.68E+08	0.169
1784.685	351572	3.5	407604	3.5	-0.97	2.14E+08	0.139
1789.407	368012	2.5	423896	1.5	-0.33	9.61E+08	0.464
1796.225	358144	2.5	413816	2.5	-0.62	4.76E+08	0.302
1807.929	374263	3.5	429575	3.5	-0.77	3.43E+08	0.21
1808.714	353886	2.5	409174	2.5	-0.68	4.29E+08	0.146
1809.929	375218	2.5	430469	1.5	-0.45	7.46E+08	0.559
1812.658	358748	3.5	413916	3.5	-0.54	5.70E+08	0.333
1815.95	358748	3.5	413816	2.5	-0.96	2.11E+08	0.167
1816.092	373177	3.5	428240	2.5	-0.51	6.16E+08	0.272
1819.492	357393	2.5	412353	2.5	-0.57	5.53E+08	0.316
1823.244	372352	2.5	427199	1.5	-0.7	3.86E+08	0.213
1836.24	373781	2.5	428240	2.5	-0.89	2.58E+08	0.166
1838.019	359410	1.5	413816	2.5	-0.98	1.90E+08	0.254
1840.086	351572	3.5	405917	3.5	-0.02	1.74E+09	0.525
1844.702	358144	2.5	412353	2.5	-0.64	4.42E+08	0.262
1850.92	359124	4.5	413151	3.5	-0.82	2.99E+08	0.258
1851.43	351572	3.5	405584	2.5	-0.32	8.50E+08	0.516
1852.644	374263	3.5	428240	2.5	-0.27	1.03E+09	0.559
1853.335	375218	2.5	429175	2.5	-0.5	6.35E+08	0.261
1855.442	375280	3.5	429175	2.5	-0.26	1.05E+09	0.363
1857.972	351762	1.5	405584	2.5	-0.01	1.79E+09	0.75
1861.736	356618	0.5	410331	1.5	-0.37	8.42E+08	0.793
1863.64	368012	2.5	421670	1.5	-0.91	2.29E+08	0.221
1864.117	357537	4.5	411182	3.5	-0.66	4.37E+08	0.256
1865.501	358748	1.5	412353	2.5	-0.96	2.16E+08	0.241
1867.94	368135	1.5	421670	1.5	-0.87	2.71E+08	0.254
1869.75	352434	4.5	405917	3.5	-0.13	1.38E+09	0.391
1872.947	359254	2.5	412646	1.5	-0.72	3.75E+08	0.255
1873.75	364260	2.5	417629	1.5	-0.77	3.40E+08	0.213
1874.404	359562	0.5	412912	0.5	-0.78	3.15E+08	0.396
1877.275	359377	2.5	412646	1.5	-0.76	3.27E+08	0.354
1878.425	360580	3.5	413816	2.5	-0.93	2.19E+08	0.131
1879.332	357393	2.5	410603	2.5	-0.7	3.85E+08	0.315
1885.43	358144	2.5	411182	3.5	-0.64	4.33E+08	0.388
1887.551	360937	4.5	413916	3.5	0.3	3.66E+09	0.862
1887.658	359377	2.5	412353	2.5	-0.73	3.31E+08	0.26
1888.2	375280	3.5	428240	2.5	-0.48	6.05E+08	0.706
1888.888	356233	1.5	409174	2.5	-0.22	1.13E+09	0.571

Table A18: Continued

Wavelength	Lower Level	J_{Low}	Upper level	J_{Up}	log gf	gA	CF
1888.988	357393	2.5	410331	1.5	-0.66	4.32E+08	0.372
1891.808	376555	1.5	429414	1.5	-0.88	2.47E+08	0.21
1893.272	361097	3.5	413916	3.5	-0.27	9.86E+08	0.46
1896.864	361097	3.5	413816	2.5	0.03	1.95E+09	0.775
1898.12	349273	3.5	401957	3.5	-0.61	4.43E+08	0.138
1899.072	374413	1.5	427070	0.5	-0.6	4.54E+08	0.509
1899.245	357951	3.5	410603	2.5	-0.17	1.25E+09	0.461
1905.15	377995	0.5	430484	0.5	-0.59	4.74E+08	0.661
1907.174	358748	3.5	411182	3.5	-0.42	7.13E+08	0.353
1907.578	377153	3.5	429575	3.5	-0.18	1.20E+09	0.694
1908.102	375832	2.5	428240	2.5	-0.92	2.23E+08	0.21
1908.845	349569	2.5	401957	3.5	-0.33	8.42E+08	0.257
1910.99	374263	3.5	426592	2.5	-0.35	8.06E+08	0.413
1911.838	357537	4.5	409843	3.5	0.16	2.69E+09	0.795
1912.591	353632	4.5	405917	3.5	-0.05	1.54E+09	0.736
1914.524	360414	0.5	412646	1.5	-0.75	3.33E+08	0.35
1915.206	360937	4.5	413151	3.5	-0.47	6.19E+08	0.412
1918.557	365557	0.5	417679	0.5	-0.64	4.03E+08	0.616
1920.171	349273	3.5	401352	3.5	0.01	1.84E+09	0.456
1920.927	359124	4.5	411182	3.5	0.25	3.36E+09	0.769
1921.097	361097	3.5	413151	3.5	-0.86	2.51E+08	0.136
1921.935	353886	2.5	405917	3.5	-0.4	7.06E+08	0.461
1923.787	375218	2.5	427199	1.5	-0.62	4.43E+08	0.274
1927.061	357951	3.5	409843	3.5	-0.15	1.28E+09	0.762
1928.469	358748	3.5	410603	2.5	-0.26	9.77E+08	0.399
1931.147	349569	2.5	401352	3.5	0.05	2.03E+09	0.519
1931.505	360580	3.5	412353	2.5	0.15	2.54E+09	0.874
1934.315	353886	2.5	405584	2.5	-0.18	1.14E+09	0.591
1934.779	376555	1.5	428240	2.5	-0.52	5.39E+08	0.474
1936.453	373670	1.5	425311	1.5	-0.6	4.51E+08	0.491
1938.627	358748	1.5	410331	1.5	-0.43	6.86E+08	0.514
1940.079	372352	2.5	423896	1.5	-0.9	2.21E+08	0.186
1942.551	357537	4.5	409016	3.5	-0.35	8.06E+08	0.787
1944.795	377995	0.5	429414	1.5	-0.89	2.23E+08	0.363
1945.597	372498	1.5	423896	1.5	-0.93	2.07E+08	0.245
1946.517	375218	2.5	426592	2.5	-0.74	3.30E+08	0.152
1947.465	359254	2.5	410603	2.5	-0.24	1.01E+09	0.621
1948.82	366236	3.5	417549	2.5	-0.26	9.40E+08	0.468
1948.843	375280	3.5	426592	2.5	0	1.73E+09	0.632
1952.229	357951	3.5	409174	2.5	-0.76	3.09E+08	0.385
1952.98	377971	3.5	429175	2.5	-0.99	1.78E+08	0.428
1957.813	357393	2.5	408470	3.5	-0.94	2.03E+08	0.246
1957.836	359254	2.5	410331	1.5	-0.69	3.58E+08	0.481
1959.616	378145	2.5	429175	2.5	-0.94	2.00E+08	0.103
1959.62	358144	2.5	409174	2.5	-0.74	3.12E+08	0.243
1963.375	357537	4.5	408470	3.5	-0.27	9.42E+08	0.822
1963.811	359410	1.5	410331	1.5	-0.79	2.73E+08	0.384
1966.209	373177	3.5	424036	2.5	-0.39	6.81E+08	0.722
1968.291	357951	3.5	408756	2.5	-0.7	3.47E+08	0.482
1974.31	366978	1.5	417629	1.5	-0.73	3.37E+08	0.526
1974.548	376555	1.5	427199	1.5	-0.54	4.92E+08	0.293
1976.203	360580	3.5	411182	3.5	-0.66	3.93E+08	0.189
1981.206	362172	1.5	412646	1.5	-0.54	4.93E+08	0.361
1981.98	369553	1.5	420008	0.5	-0.9	2.27E+08	0.42
1983.108	358748	1.5	409174	2.5	-0.78	2.94E+08	0.183
1983.12	358748	3.5	409174	2.5	-0.61	4.13E+08	0.338
1987.143	365557	0.5	415880	1.5	-0.67	3.56E+08	0.68
1993.986	367398	3.5	417549	2.5	-0.11	1.25E+09	0.61
1995.407	373781	2.5	423896	1.5	-0.69	3.55E+08	0.299
1996.191	378145	2.5	428240	2.5	-0.9	2.13E+08	0.165
1996.622	361097	3.5	411182	3.5	-0.73	3.26E+08	0.237
2002.565	359254	2.5	409174	2.5	-0.98	1.75E+08	0.33
2007.516	359377	2.5	409174	2.5	-0.55	4.50E+08	0.374
2008.476	374263	3.5	424036	2.5	-0.86	2.19E+08	0.361
2014.77	368012	2.5	417629	1.5	-0.57	4.38E+08	0.277
2017.272	364260	2.5	413816	2.5	-0.69	3.29E+08	0.239
2017.761	368135	1.5	417679	0.5	-0.64	3.90E+08	0.399
2018.608	352434	4.5	401957	3.5	-0.89	2.09E+08	0.169
2019.322	361097	3.5	410603	2.5	-0.97	1.78E+08	0.225
2020.404	375832	2.5	425311	1.5	0.02	1.70E+09	0.849
2023.07	368135	1.5	417549	2.5	-0.99	1.70E+08	0.322
2026.992	372352	2.5	421670	1.5	-0.22	9.72E+08	0.571
2035.247	374413	1.5	423531	0.5	-0.66	3.61E+08	0.349
2037.898	378145	2.5	427199	1.5	-0.71	3.13E+08	0.572
2043.577	352434	4.5	401352	3.5	-0.48	5.34E+08	0.366
2044.267	366978	1.5	415880	1.5	-0.85	2.35E+08	0.317
2066.058	364260	2.5	412646	1.5	-0.73	3.03E+08	0.269
2066.459	369303	0.5	417679	0.5	-0.92	1.94E+08	0.574
2070.5	371726	0.5	420008	0.5	-0.65	3.53E+08	0.775
2079.395	369553	1.5	417629	1.5	-0.96	1.81E+08	0.403
2084.403	381615	4.5	429575	3.5	-0.32	7.55E+08	0.519
2092.423	351572	3.5	399348	3.5	-0.83	2.16E+08	0.174
2093.799	368135	1.5	415880	1.5	-0.43	6.04E+08	0.569
2104.148	372498	1.5	420008	0.5	-0.84	2.20E+08	0.369
2107.244	358144	2.5	405584	2.5	-0.92	1.69E+08	0.148
2128.052	376555	1.5	423531	0.5	-1	1.55E+08	0.256
2152.092	375218	2.5	421670	1.5	-0.55	4.27E+08	0.318
2181.799	368097	4.5	413916	3.5	-0.81	2.08E+08	0.101
2225.79	364260	2.5	409174	2.5	-0.85	1.96E+08	0.136
2314.902	381615	4.5	424800	3.5	-0.71	2.39E+08	0.332
2414.871	357951	3.5	399348	3.5	-0.89	1.47E+08	0.19
2446.664	361097	3.5	401957	3.5	-0.96	1.20E+08	0.124
2455.879	351572	3.5	392278	3.5	-0.59	2.70E+08	0.323
2489.555	359377	2.5	399533	2.5	-0.94	1.18E+08	0.2
2546.759	377971	3.5	417225	3.5	-0.3	5.09E+08	0.861
2558.06	378145	2.5	417225	3.5	0.01	1.05E+09	0.789
2580.732	373781	2.5	412518	2.5	-0.85	1.45E+08	0.206
2584.455	362172	1.5	400853	2.5	-0.79	1.53E+08	0.368
2589.141	372352	2.5	410963	3.5	-0.78	1.65E+08	0.221
2605.744	358144	2.5	396509	2.5	-0.28	5.13E+08	0.659
2613.558	361097	3.5	399348	3.5	-0.89	1.27E+08	0.388
2625.357	349569	2.5	387648	1.5	-0.97	1.04E+08	0.109
2629.701	358493	1.5	396509	2.5	-0.86	1.39E+08	0.214
2636.053	356233	1.5	394157	1.5	-0.56	2.68E+08	0.553
2637.006	376555	1.5	414465	2.5	-0.26	5.36E+08	0.789
2651.948	364260	2.5	401957	3.5	-0.48	3.10E+08	0.241

Table A18: Continued

Wavelength	Lower Level	J_{Low}	Upper level	J_{Up}	log gf	gA	CF
2666.492	372352	2.5	409843	3.5	-0.87	1.24E+08	0.24
2675.284	371726	0.5	409094	1.5	-0.35	4.03E+08	0.812
2675.771	362172	1.5	399533	2.5	-0.97	9.52E+07	0.243
2678.797	375832	2.5	413151	3.5	-0.73	1.77E+08	0.199
2695.206	364260	2.5	401352	3.5	-0.85	1.32E+08	0.182
2716.616	366978	1.5	403778	1.5	-0.62	2.32E+08	0.629
2716.712	374413	1.5	411211	2.5	-0.09	7.19E+08	0.764
2718.995	359410	1.5	396177	1.5	-0.48	2.72E+08	0.572
2719.283	377153	3.5	413916	3.5	-0.73	1.57E+08	0.283
2724.471	357951	3.5	394644	3.5	-0.79	1.45E+08	0.254
2727.266	353886	2.5	390542	2.5	-0.85	1.28E+08	0.091
2731.962	364260	2.5	400853	2.5	-0.56	2.51E+08	0.38
2737.311	357393	2.5	393914	2.5	-0.75	1.61E+08	0.351
2738.893	358144	2.5	394644	3.5	-0.52	2.60E+08	0.306
2752.46	378145	2.5	414465	2.5	-0.28	4.68E+08	0.657
2752.846	377995	0.5	414310	1.5	-0.2	5.51E+08	0.799
2767.862	372352	2.5	408470	3.5	-0.15	5.93E+08	0.627
2775.932	358144	2.5	394157	1.5	-0.75	1.51E+08	0.6
2776.154	368012	2.5	404022	3.5	-0.11	6.27E+08	0.584
2777.074	377153	3.5	413151	3.5	-0.15	5.96E+08	0.599
2779.777	376555	1.5	412518	2.5	-0.95	9.77E+07	0.128
2785.77	351762	1.5	387648	1.5	-0.43	3.20E+08	0.517
2795.338	360414	0.5	396177	1.5	-0.59	2.18E+08	0.847
2795.479	365557	0.5	401318	1.5	-0.47	2.76E+08	0.704
2796.785	375218	2.5	410963	3.5	-0.76	1.58E+08	0.221
2798.641	366236	3.5	401957	3.5	-0.57	2.23E+08	0.364
2804.286	356233	1.5	391882	0.5	-0.69	1.75E+08	0.764
2805.08	372498	1.5	408137	2.5	-0.05	7.44E+08	0.729
2806.63	368012	2.5	403631	2.5	-0.72	1.53E+08	0.419
2816.397	368135	1.5	403631	2.5	-0.21	5.51E+08	0.668
2822.369	358493	1.5	393914	2.5	-0.63	1.98E+08	0.288
2823.318	358748	1.5	394157	1.5	-0.68	1.82E+08	0.425
2824.842	359254	2.5	394644	3.5	0	8.20E+08	0.739
2826.319	351572	3.5	386943	2.5	-1	7.95E+07	0.412
2834.204	364260	2.5	399533	2.5	-0.61	2.10E+08	0.289
2834.702	359377	2.5	394644	3.5	-0.82	1.17E+08	0.288
2835.86	372352	2.5	407604	3.5	-0.08	6.59E+08	0.598
2837.245	373781	2.5	409016	3.5	-0.45	3.02E+08	0.329
2838.195	351572	3.5	386795	3.5	-0.24	4.55E+08	0.596
2841.597	351762	1.5	386943	2.5	-0.67	1.77E+08	0.361
2845.644	375832	2.5	410963	3.5	0.18	1.28E+09	0.814
2846.86	366236	3.5	401352	3.5	-0.8	1.31E+08	0.272
2849.148	364260	2.5	399348	3.5	-0.11	6.46E+08	0.59
2849.318	373670	1.5	408756	2.5	-0.02	7.98E+08	0.809
2865.687	357393	2.5	392278	3.5	-0.33	3.97E+08	0.645
2870.666	358748	1.5	393573	1.5	-0.82	1.30E+08	0.195
2880.792	376555	1.5	411257	1.5	-0.4	3.46E+08	0.567
2881.904	373781	2.5	408470	3.5	-0.31	4.01E+08	0.515
2882.553	374413	1.5	409094	1.5	-0.99	7.98E+07	0.272
2884.341	359254	2.5	393914	2.5	-0.36	3.36E+08	0.626
2887.257	375218	2.5	409843	3.5	-0.66	1.89E+08	0.48
2897.332	359410	1.5	393914	2.5	-0.57	1.92E+08	0.442
2899.761	369303	0.5	403778	1.5	-0.36	3.76E+08	0.874
2911.432	362172	1.5	396509	2.5	-0.39	3.10E+08	0.467
2912.263	357951	3.5	392278	3.5	-0.41	3.04E+08	0.403
2913.817	356233	1.5	390542	2.5	-0.88	1.03E+08	0.335
2922.531	374263	3.5	408470	3.5	-0.95	8.54E+07	0.273
2928.748	358144	2.5	392278	3.5	-0.44	2.73E+08	0.528
2933.621	369553	1.5	403631	2.5	-0.7	1.64E+08	0.384
2934.783	360580	3.5	394644	3.5	-0.73	1.46E+08	0.23
2939.34	359562	0.5	393573	1.5	-0.26	4.35E+08	0.873
2939.858	362172	1.5	396177	1.5	-0.89	9.23E+07	0.368
2945.044	368012	2.5	401957	3.5	-0.96	7.79E+07	0.228
2946.878	356618	0.5	390542	1.5	-0.56	2.16E+08	0.456
2951.202	366978	1.5	400853	2.5	-0.85	1.11E+08	0.303
2955.696	373781	2.5	407604	3.5	-0.49	2.54E+08	0.641
2957.908	375218	2.5	409016	3.5	-0.37	3.47E+08	0.561
2961.054	353886	2.5	387648	1.5	-0.47	2.62E+08	0.4
2964.355	374413	1.5	408137	2.5	-0.72	1.42E+08	0.412
2975.045	351762	1.5	385365	0.5	-0.31	3.71E+08	0.838
2978.717	349273	3.5	382835	3.5	0.06	8.49E+08	0.631
2980.058	361097	3.5	394644	3.5	-0.7	1.48E+08	0.334
3005.223	349569	2.5	382835	3.5	-0.53	2.16E+08	0.218
3006.48	375218	2.5	408470	3.5	-0.59	2.01E+08	0.292
3012.723	368135	1.5	401318	1.5	-0.63	1.80E+08	0.536
3015.767	357393	2.5	390542	2.5	-0.76	1.34E+08	0.32
3017.178	358748	1.5	391882	0.5	-0.72	1.45E+08	0.52
3019.137	378145	2.5	411257	1.5	-0.89	9.99E+07	0.597
3019.165	366236	3.5	399348	3.5	-0.92	8.58E+07	0.267
3023.337	378145	2.5	411211	2.5	-0.55	2.09E+08	0.5
3024.206	353886	2.5	386943	2.5	-0.16	5.04E+08	0.626
3027.238	359254	2.5	392278	3.5	-0.52	2.17E+08	0.233
3037.808	353886	2.5	386795	3.5	-0.16	5.10E+08	0.503
3055.542	368135	1.5	400853	2.5	-0.53	2.23E+08	0.363
3070.87	366978	1.5	399533	2.5	-0.56	2.04E+08	0.669
3086.877	375218	2.5	407604	3.5	-0.38	3.02E+08	0.359
3092.731	375280	3.5	407604	3.5	-0.67	1.44E+08	0.472
3094.588	375832	2.5	408137	2.5	-1	7.07E+07	0.233
3119.016	371726	0.5	403778	1.5	-0.98	7.27E+07	0.311
3119.337	358493	1.5	390542	2.5	-0.67	1.53E+08	0.759
3129.003	367398	3.5	399348	3.5	-0.82	9.86E+07	0.446
3144.347	358748	1.5	390542	2.5	-0.31	3.44E+08	0.604
3144.347	358748	1.5	390542	1.5	-0.83	1.06E+08	0.307
3170.052	381615	4.5	413151	3.5	-0.82	1.00E+08	0.358
3182.252	356233	1.5	387648	1.5	-1	6.69E+07	0.234
3288.407	352434	4.5	382835	3.5	-0.96	6.78E+07	0.537
3305.806	373781	2.5	404022	3.5	-0.46	2.20E+08	0.41
3334.642	369553	1.5	399533	2.5	-0.68	1.35E+08	0.541
3343.867	364260	2.5	394157	1.5	-1	6.11E+07	0.271
3359.374	374263	3.5	404022	3.5	-0.49	1.83E+08	0.604
3400.107	357393	2.5	386795	3.5	-0.79	9.86E+07	0.235
3423.312	353632	4.5	382835	3.5	-0.83	8.06E+07	0.588
3473.604	373177	3.5	401957	3.5	-0.96	5.76E+07	0.17
3516.22	377153	3.5	405584	2.5	-0.96	5.22E+07	0.456
3564.477	358748	3.5	386795	3.5	-0.99	5.30E+07	0.153

Table A18: Continued

Wavelength	Lower Level	J_{Low}	Upper level	J_{Up}	log gf	gA	CF
3813.513	360580	3.5	386795	3.5	-0.96	5.28E+07	0.187
3861.296	380026	3.5	405917	3.5	0.43	1.09E+09	0.948
3911.607	380026	3.5	405584	2.5	0.27	7.16E+08	0.91
4235.252	380026	3.5	403631	2.5	-0.98	3.82E+07	0.898
4423.85	379359	4.5	401957	3.5	-0.18	2.26E+08	0.98
4545.544	379359	4.5	401352	3.5	0.29	6.49E+08	0.989

a: Experimental values from [35, 34]

In VI

Energy Levels

Table A19: Comparison between available experimental data and calculated even energy levels (in cm^{-1}) in In VI

E^{a}_{exp}	E^{b}_{calc}	Δ E	J	Leading components (in %) in LS coupling [c]
0	-10	10	4	98.3 $4d^8$ (^{3}F) ^{3}F
6465.3	6473	-7.7	3	99.7 $4d^8$ (^{3}F) ^{3}F
8154	8151	3	2	68.3 $4d^8$ (^{3}F) ^{3}F + 25.7 $4d^8$ (^{1}D) ^{1}D + 5.7 $4d^8$ (^{3}P) ^{3}P
15160.7	15180	-19.3	2	59.5 $4d^8$ (^{3}P) ^{3}P + 22.9 $4d^8$ (^{3}F) ^{3}F + 17.3 $4d^8$ (^{1}D) ^{1}D
20606.8	20618	-11.2	0	95.6 $4d^8$ (^{3}P) ^{3}P
20649.2	20629	20.2	1	99.6 $4d^8$ (^{3}P) ^{3}P
23255.1	23251	4.1	2	56.6 $4d^8$ (^{1}D) ^{1}D + 34.5 $4d^8$ (^{3}P) ^{3}P + 8.6 $4d^8$ (^{3}F) ^{3}F
25865.9	25866	-0.1	4	98.3 $4d^8$ (^{1}G) ^{1}G
58627.3	58627	0.3	0	95.5 $4d^8$ (^{1}S) ^{1}S
201884	201914	-30	5	95.3 $4d^75s$ (^{4}F) ^{5}F
205958	205952	6	4	90.7 $4d^75s$ (^{4}F) ^{5}F + 6 $4d^75s$ (^{4}F) ^{3}F
209225.9	209217	8.9	3	95.1 $4d^75s$ (^{4}F) ^{5}F
211177.7	211163	14.7	2	93.7 $4d^75s$ (^{4}F) ^{5}F
212336.5	212317	19.5	1	91.8 $4d^75s$ (^{4}F) ^{5}F + 5.5 $4d^75s$ (^{2}D) ^{3}D
214364.3	214368	-3.7	4	84.7 $4d^75s$ (^{4}F) ^{3}F + 7.6 $4d^75s$ (^{4}F) ^{5}F
219074	218999	75	3	54.7 $4d^75s$ (^{4}P) ^{5}P + 36.9 $4d^75s$ (^{4}F) ^{3}F
219005.8	219042	-36.2	2	68.5 $4d^75s$ (^{4}P) ^{5}P + 24.8 $4d^75s$ (^{2}P) ^{3}P
220287.1	220214	73.1	3	54.1 $4d^75s$ (^{4}F) ^{3}F + 41.8 $4d^75s$ (^{4}P) ^{5}P
221971.3	221971	0.3	1	75.9 $4d^75s$ (^{4}P) ^{5}P + 17.8 $4d^75s$ (^{2}P) ^{3}P
222582.1	222604	-21.9	2	82.8 $4d^75s$ (^{4}F) ^{3}F + 7.3 $4d^75s$ (^{4}P) ^{5}P + 5.1 $4d^75s$ (^{2}D) ^{1}D
225122.4	225104	18.4	5	79.5 $4d^75s$ (^{2}G) ^{3}G + 12.9 $4d^75s$ (^{2}H) ^{3}H
226765.2	226695	70.2	4	61.2 $4d^75s$ (^{2}G) ^{3}G + 20.6 $4d^75s$ (^{2}H) ^{3}H + 10 $4d^75s$ (^{2}G) ^{1}G
228283.9	228380	-96.1	1	31.7 $4d^75s$ (^{2}P) ^{1}P + 29.4 $4d^75s$ (^{4}P) ^{3}P + 15 $4d^75s$ (^{4}P) ^{5}P
228806.9	228705	101.9	2	24.3 $4d^75s$ (^{2}P) ^{3}P + 44.3 $4d^75s$ (^{4}P) ^{3}P + 11.8 $4d^75s$ (^{2}D) ^{3}D
230497.2	230395	102.2	3	94.2 $4d^75s$ (^{2}G) ^{3}G
230738.1	231064	-325.9	0	59.6 $4d^75s$ (^{2}P) ^{3}P + 40 $4d^75s$ (^{4}P) ^{3}P
231741.8	231835	-93.2	6	99.7 $4d^75s$ (^{2}H) ^{3}H
233207.3	233171	36.3	2	48.4 $4d^75s$ (^{4}P) ^{3}P + 23.5 $4d^75s$ (^{2}P) ^{3}P + 9.8 $4d^75s$ (^{4}P) ^{5}P
233167.7	233176	-8.3	4	49.8 $4d^75s$ (^{2}G) ^{1}G + 28.4 $4d^75s$ (^{2}G) ^{3}G + 16.7 $4d^75s$ (^{2}H) ^{3}H
233903	233924	-21	5	73 $4d^75s$ (^{2}H) ^{3}H + 20.5 $4d^75s$ (^{2}H) ^{1}H + 6 $4d^75s$ (^{2}G) ^{3}G
234615.5	234475	140.5	3	71.2 $4d^75s$ (^{2}D) ^{3}D + 19 $4d^75s$ (^{2}D) ^{3}D
234581.9	234564	17.9	1	40.6 $4d^75s$ (^{4}P) ^{3}P + 33.4 $4d^75s$ (^{2}P) ^{3}P + 15.4 $4d^75s$ (^{2}D) ^{3}D
237469.8	237310	159.8	2	40.8 $4d^75s$ (^{2}D) ^{3}D + 23.6 $4d^75s$ (^{2}D) ^{1}D + 8.6 $4d^75s$ (^{2}D) ^{3}D
237876	238092	-216	1	35.7 $4d^75s$ (^{2}P) ^{3}P + 23.2 $4d^75s$ (^{2}D) ^{3}D + 20.3 $4d^75s$ (^{2}P) ^{1}P
238975.3	238983	-7.7	4	61.9 $4d^75s$ (^{2}H) ^{3}H + 31.9 $4d^75s$ (^{2}G) ^{1}G
239157.9	239198	-40.1	0	59.5 $4d^75s$ (^{4}P) ^{3}P + 40.1 $4d^75s$ (^{2}P) ^{3}P
240989.6	241128	-138.4	5	76 $4d^75s$ (^{2}H) ^{1}H + 13.7 $4d^75s$ (^{2}H) ^{3}H + 9.8 $4d^75s$ (^{2}G) ^{3}G
245366.1	245307	59.1	2	53.6 $4d^75s$ (^{2}F) ^{3}F + 14.3 $4d^75s$ (^{2}D) ^{3}D + 13.8 $4d^75s$ (^{2}D) ^{1}D
245508.9	245555	-46.1	1	34.8 $4d^75s$ (^{2}D) ^{3}D + 43.7 $4d^75s$ (^{2}P) ^{1}P + 15.2 $4d^75s$ (^{4}P) ^{3}P
245979.1	245873	106.1	2	35.7 $4d^75s$ (^{2}D) ^{1}D + 41.9 $4d^75s$ (^{2}F) ^{3}F + 9.3 $4d^75s$ (^{2}P) ^{3}P
246405.3	246397	8.3	3	89.6 $4d^75s$ (^{2}F) ^{3}F + 5.6 $4d^75s$ (^{2}F) ^{1}F
248693.5	248754	-60.5	4	94.6 $4d^75s$ (^{2}F) ^{3}F
253378.5	253204	174.5	3	90.1 $4d^75s$ (^{2}F) ^{1}F + 6.1 $4d^75s$ (^{2}F) ^{3}F
269705	269807	-102	1	90 $4d^75s$ (^{2}D) ^{3}D + 8.6 $4d^75s$ (^{2}D) ^{3}D
270483	270584	-101	2	82 $4d^75s$ (^{2}D) ^{3}D + 11.5 $4d^75s$ (^{2}D) ^{3}D
272270.5	272206	64.5	3	74.3 $4d^75s$ (^{2}D) ^{3}D + 20.3 $4d^75s$ (^{2}D) ^{3}D
277076	276987	89	2	77.2 $4d^75s$ (^{2}D) ^{1}D + 16.2 $4d^75s$ (^{2}D) ^{1}D

a: From Ryabtsev [37]
b: This work
c: Only the component ≥ 5% are given

Table A20: Comparison between available experimental data and calculated odd energy levels (in cm^{-1}) in In VI

E$^a_{exp}$	E$^b_{calc}$	Δ E	J	Leading components (in %) in LS coupling ^{c}
286626.1	286628	-1.9	4	48.7 4d^{7}5p (^{4}F) ^{5}D + 28.5 4d^{7}5p (^{4}F) ^{5}F + 8.5 4d^{7}5p (^{4}F) ^{3}F
288303.7	288202	101.7	5	53.3 4d^{7}5p (^{4}F) ^{5}F + 21.7 4d^{7}5p (^{4}F) ^{5}G + 19.9 4d^{7}5p (^{4}F) ^{3}G
291912.1	291928	-15.9	3	36.1 4d^{7}5p (^{4}F) ^{5}D + 45.6 4d^{7}5p (^{4}F) ^{5}F + 5.9 4d^{7}5p (^{4}P) ^{5}D
294223.8	294127	96.8	4	41.4 4d^{7}5p (^{4}F) ^{5}G + 22.1 4d^{7}5p (^{4}F) ^{5}F + 15 4d^{7}5p (^{4}F) ^{5}D
294997.7	295016	-18.3	2	55.1 4d^{7}5p (^{4}F) ^{5}F + 19.4 4d^{7}5p (^{4}F) ^{5}D + 6.5 4d^{7}5p (^{4}F) ^{5}G
296630.6	296574	56.6	3	44.1 4d^{7}5p (^{4}F) ^{5}G + 14.3 4d^{7}5p (^{4}F) ^{5}D + 8.7 4d^{7}5p (^{4}F) ^{5}F
296786.5	296804	-17.5	1	57.1 4d^{7}5p (^{4}F) ^{5}F + 12 4d^{7}5p (^{4}F) ^{5}D + 7.8 4d^{7}5p (^{4}F) ^{3}D
297246	297165	81	5	34.2 4d^{7}5p (^{4}F) ^{3}G + 42.3 4d^{7}5p (^{4}F) ^{5}F + 16.9 4d^{7}5p (^{4}F) ^{5}G
297392.4	297325	67.4	6	93.8 4d^{7}5p (^{4}F) ^{5}G + 5.8 4d^{7}5p (^{2}G) ^{3}H
298738.2	298767	-28.8	2	0 4d^{6}5s5p (^{3}F) ^{3}P + 37.8 4d^{7}5p (^{4}P) ^{5}S + 27.4 4d^{7}5p (^{4}F) ^{5}G
298945.5	298955	-9.5	2	43.8 4d^{7}5p (^{4}P) ^{5}S + 27.8 4d^{7}5p (^{4}F) ^{5}G + 6.3 4d^{7}5p (^{4}F) ^{5}D
299666	299670	-4	2	23.3 4d^{7}5p (^{4}P) ^{5}D + 13.6 4d^{7}5p (^{4}F) ^{5}G + 12.5 4d^{7}5p (^{4}F) ^{5}D
299836.1	299771	65.1	4	31.4 4d^{7}5p (^{4}F) ^{3}F + 22.4 4d^{7}5p (^{4}F) ^{5}D + 16.5 4d^{7}5p (^{4}F) ^{5}F
300502.8	300556	-53.2	1	25.5 4d^{7}5p (^{4}F) ^{5}D + 36.4 4d^{7}5p (^{4}P) ^{5}D + 17.3 4d^{7}5p (^{4}F) ^{5}F
300850.9	300956	-105.1	0	45.6 4d^{7}5p (^{4}P) ^{5}D + 42.1 4d^{7}5p (^{4}F) ^{5}D + 7.9 4d^{7}5p (^{2}P) ^{3}P
301111.2	300979	132.2	3	22.5 4d^{7}5p (^{4}F) ^{5}F + 24.6 4d^{7}5p (^{4}F) ^{5}G + 13.4 4d^{7}5p (^{4}P) ^{5}D
303053.2	303056	-2.8	4	30.9 4d^{7}5p (^{4}F) ^{5}F + 27.6 4d^{7}5p (^{4}F) ^{3}F + 14 4d^{7}5p (^{4}F) ^{5}G
304156.8	304145	11.8	5	59.1 4d^{7}5p (^{4}F) ^{5}G + 36.3 4d^{7}5p (^{4}F) ^{3}G
304448.8	304630	-181.2	3	44.6 4d^{7}5p (^{4}F) ^{3}D + 17.8 4d^{7}5p (^{4}F) ^{3}F + 9 4d^{7}5p (^{4}F) ^{5}D
306757	306935	-178	1	22.6 4d^{7}5p (^{2}P) ^{3}P + 17.1 4d^{7}5p (^{4}P) ^{3}S + 12.1 4d^{7}5p (^{2}P) ^{3}S
307655.3	307793	-137.7	2	29.4 4d^{7}5p (^{4}F) ^{3}D + 17.4 4d^{7}5p (^{4}F) ^{5}F + 10.8 4d^{7}5p (^{4}F) ^{5}D
308184.9	308271	-86.1	4	62 4d^{7}5p (^{4}F) ^{3}G + 23.4 4d^{7}5p (^{4}F) ^{5}G
308432.1	308419	13.1	3	37.5 4d^{7}5p (^{4}F) ^{3}F + 16.9 4d^{7}5p (^{4}F) ^{5}F + 13.1 4d^{7}5p (^{4}F) ^{3}D
308868.2	308844	24.2	2	16.6 4d^{7}5p (^{4}F) ^{5}G + 26 4d^{7}5p (^{4}F) ^{3}F + 9.2 4d^{7}5p (^{4}F) ^{5}D
309215	309144	71	5	37.3 4d^{7}5p (^{2}G) ^{3}H + 18.6 4d^{7}5p (^{2}H) ^{3}I + 18 4d^{7}5p (^{2}G) ^{1}H
310570.9	310475	95.9	4	27.6 4d^{7}5p (^{2}G) ^{3}F + 24.1 4d^{7}5p (^{4}F) ^{3}F + 10.5 4d^{7}5p (^{2}G) ^{3}G
310899.4	310905	-5.6	3	63.7 4d^{7}5p (^{4}F) ^{3}G + 7.3 4d^{7}5p (^{4}F) ^{5}G
310800.6	310959	-158.4	1	33.2 4d^{7}5p (^{4}F) ^{3}D + 16.8 4d^{7}5p (^{2}P) ^{3}D + 15.4 4d^{7}5p (^{4}F) ^{5}D
311484.8	311430	54.8	3	9 4d^{7}5p (^{4}P) ^{5}P + 19.5 4d^{7}5p (^{4}P) ^{5}D + 18.6 4d^{7}5p (^{4}F) ^{3}D
312153	312239	-86	2	28.2 4d^{7}5p (^{4}F) ^{3}F + 12.1 4d^{7}5p (^{4}F) ^{3}D + 11.5 4d^{7}5p (^{4}F) ^{5}D
313493.4	313414	79.4	4	65.9 4d^{7}5p (^{2}G) ^{3}H + 9.9 4d^{7}5p (^{2}G) ^{1}G + 5.3 4d^{7}5p (^{2}G) ^{3}G
314286.6	314052	234.6	1	14.8 4d^{7}5p (^{2}P) ^{3}D + 15.6 4d^{7}5p (^{4}P) ^{3}S + 15 4d^{7}5p (^{4}P) ^{5}P
314464.2	314662	-197.8	0	36.8 4d^{7}5p (^{4}F) ^{5}D + 24.2 4d^{7}5p (^{4}P) ^{5}D + 14.9 4d^{7}5p (^{2}P) ^{1}S
314565.8	315107	-541.2	0	64 4d^{7}5p (^{2}P) ^{3}P + 13.4 4d^{7}5p (^{2}D) ^{3}P + 7.1 4d^{7}5p (^{4}P) ^{3}P
315135.6	315147	-11.4	6	59 4d^{7}5p (^{2}H) ^{3}I + 20 4d^{7}5p (^{2}H) ^{1}I + 9.9 4d^{7}5p (^{2}G) ^{3}H
315321.2	315184	137.2	2	20.7 4d^{7}5p (^{4}P) ^{5}P + 21.9 4d^{7}5p (^{4}P) ^{5}D + 10.9 4d^{7}5p (^{2}D) ^{3}F
315206.8	315229	-22.2	5	80.5 4d^{7}5p (^{2}H) ^{3}G + 6.4 4d^{7}5p (^{2}F) ^{3}G + 5 4d^{7}5p (^{2}H) ^{3}H
316098.1	315824	274.1	4	81.6 4d^{7}5p (^{4}P) ^{5}D + 9.7 4d^{7}5p (^{4}F) ^{5}D
315985.8	315942	43.8	3	30.1 4d^{7}5p (^{2}G) ^{3}G + 22.6 4d^{7}5p (^{2}G) ^{3}F + 14 4d^{7}5p (^{2}G) ^{1}F
316391.7	316417	-25.3	1	28 4d^{7}5p (^{4}P) ^{5}D + 18.6 4d^{7}5p (^{4}P) ^{5}P + 14.5 4d^{7}5p (^{4}F) ^{3}D
316277	316587	-310	2	23.3 4d^{7}5p (^{2}P) ^{3}P + 26.9 4d^{7}5p (^{4}F) ^{3}D + 11.8 4d^{7}5p (^{4}P) ^{5}P
316886.1	316888	-1.9	3	30.4 4d^{7}5p (^{2}P) ^{3}D + 18.3 4d^{7}5p (^{4}P) ^{5}P + 17.3 4d^{7}5p (^{4}P) ^{5}D
317795.4	317722	73.4	6	64.8 4d^{7}5p (^{2}G) ^{3}H + 29.8 4d^{7}5p (^{2}H) ^{1}I
318711.2	318636	75.2	4	26.8 4d^{7}5p (^{2}G) ^{1}G + 26 4d^{7}5p (^{2}G) ^{3}F + 13.4 4d^{7}5p (^{2}H) ^{1}G
318650.7	318704	-53.3	3	21.9 4d^{7}5p (^{2}H) ^{3}G + 19.1 4d^{7}5p (^{2}G) ^{1}F + 11.6 4d^{7}5p (^{2}F) ^{3}G
318954.2	318867	87.2	2	16 4d^{7}5p (^{4}P) ^{3}P + 20 4d^{7}5p (^{4}P) ^{5}P + 11.8 4d^{7}5p (^{2}P) ^{1}D
319588	319586	2	5	52 4d^{7}5p (^{2}G) ^{3}G + 37.1 4d^{7}5p (^{2}H) ^{3}I
320269.7	320057	212.7	3	32.2 4d^{7}5p (^{2}D) ^{3}D + 10.3 4d^{7}5p (^{2}D) ^{3}F + 7.3 4d^{7}5p (^{2}D) ^{3}D
320117.5	320192	-74.5	1	35.1 4d^{7}5p (^{4}P) ^{3}S + 16.8 4d^{7}5p (^{2}P) ^{3}P + 10 4d^{7}5p (^{4}P) ^{3}D
320046.1	320270	-223.9	0	46.1 4d^{7}5p (^{2}P) ^{1}S + 21 4d^{7}5p (^{4}P) ^{5}D + 13.9 4d^{7}5p (^{4}P) ^{3}P
320949.8	320766	183.8	3	49.7 4d^{7}5p (^{4}P) ^{3}D + 27.3 4d^{7}5p (^{4}P) ^{5}P + 8 4d^{7}5p (^{4}P) ^{5}D
321145.7	321008	137.7	1	28 4d^{7}5p (^{4}P) ^{5}P + 14.3 4d^{7}5p (^{2}P) ^{3}D + 11.8 4d^{7}5p (^{4}P) ^{3}S
321423.7	321263	160.7	2	30.1 4d^{7}5p (^{4}P) ^{3}D + 19.1 4d^{7}5p (^{2}D) ^{3}P + 15.9 4d^{7}5p (^{4}P) ^{3}P
321497.1	321545	-47.9	4	55.5 4d^{7}5p (^{2}H) ^{3}G + 16 4d^{7}5p (^{2}G) ^{3}F + 12 4d^{7}5p (^{2}F) ^{3}G
321946.6	322018	-71.4	5	36.3 4d^{7}5p (^{2}H) ^{3}I + 20.6 4d^{7}5p (^{2}G) ^{1}H + 14.7 4d^{7}5p (^{2}G) ^{3}H
322528.8	322680	-151.2	1	28.4 4d^{7}5p (^{2}P) ^{1}P + 24.1 4d^{7}5p (^{4}P) ^{3}P + 19.5 4d^{7}5p (^{2}P) ^{3}D
322915.1	322940	-24.9	7	99.7 4d^{7}5p (^{2}H) ^{3}I
323218.9	323120	98.9	3	39.7 4d^{7}5p (^{2}G) ^{3}F + 16.1 4d^{7}5p (^{2}G) ^{3}G + 12.8 4d^{7}5p (^{2}F) ^{3}G
323559.1	323456	103.1	2	23.7 4d^{7}5p (^{2}D) ^{3}F + 23.3 4d^{7}5p (^{2}G) ^{3}F + 14.2 4d^{7}5p (^{4}P) ^{3}P
323562.4	323511	51.4	4	59 4d^{7}5p (^{2}G) ^{3}G + 17.6 4d^{7}5p (^{2}G) ^{3}H + 12.2 4d^{7}5p (^{2}H) ^{1}G
324393.5	324325	68.5	5	45.8 4d^{7}5p (^{2}G) ^{1}H + 41.3 4d^{7}5p (^{2}G) ^{3}H + 8.6 4d^{7}5p (^{2}G) ^{3}G
324358.9	324345	13.9	2	42.2 4d^{7}5p (^{2}G) ^{3}F + 9.1 4d^{7}5p (^{4}P) ^{3}D + 7.2 4d^{7}5p (^{2}D) ^{3}F
324595.7	324541	54.7	2	9.2 4d^{7}5p (^{2}D) ^{3}D + 18.4 4d^{7}5p (^{4}P) ^{3}P + 17.1 4d^{7}5p (^{4}P) ^{5}P
324826	324749	77	3	9.1 4d^{7}5p (^{4}P) ^{5}D + 19.3 4d^{7}5p (^{2}D) ^{3}F + 15.8 4d^{7}5p (^{2}P) ^{3}D
325370.5	325297	73.5	1	32.7 4d^{7}5p (^{2}D) ^{3}D + 20.1 4d^{7}5p (^{4}P) ^{3}D + 8.1 4d^{7}5p (^{4}F) ^{3}D
326277.1	326115	162.1	3	7.2 4d^{7}5p (^{2}F) ^{3}D + 15.8 4d^{7}5p (^{2}H) ^{3}G + 15.6 4d^{7}5p (^{2}G) ^{3}G
326243.8	326357	-113.2	1	36.7 4d^{7}5p (^{4}P) ^{3}P + 16.7 4d^{7}5p (^{2}P) ^{3}S + 16.7 4d^{7}5p (^{4}P) ^{3}D
327152.7	327044	108.7	2	13.4 4d^{7}5p (^{2}D) ^{3}P + 23 4d^{7}5p (^{2}P) ^{3}D + 14.5 4d^{7}5p (^{2}F) ^{3}D
328090.9	327913	177.9	4	69.7 4d^{7}5p (^{2}D) ^{3}F + 12.8 4d^{7}5p (^{2}D) ^{3}F + 5 4d^{7}5p (^{2}F) ^{3}F
329406.5	329520	-113.5	6	84.2 4d^{7}5p (^{2}H) ^{3}H + 15 4d^{7}5p (^{2}H) ^{3}I
329895.2	330019	-123.8	6	49.7 4d^{7}5p (^{2}H) ^{1}I + 25.7 4d^{7}5p (^{2}H) ^{3}I + 18.9 4d^{7}5p (^{2}G) ^{3}H
330022	330059	-37	2	20.3 4d^{7}5p (^{2}P) ^{3}D + 16 4d^{7}5p (^{2}D) ^{1}D + 12.5 4d^{7}5p (^{2}D) ^{3}P
330374.9	330424	-49.1	5	66.1 4d^{7}5p (^{2}H) ^{3}H + 18.6 4d^{7}5p (^{2}H) ^{1}H + 6.4 4d^{7}5p (^{2}H) ^{3}G
330633.4	330603	30.4	3	33.6 4d^{7}5p (^{2}G) ^{1}F + 10.9 4d^{7}5p (^{2}P) ^{3}D + 10.2 4d^{7}5p (^{2}D) ^{3}F
330914.7	330967	-52.3	1	23.1 4d^{7}5p (^{2}P) ^{3}S + 22.8 4d^{7}5p (^{2}P) ^{3}P + 21.8 4d^{7}5p (^{2}D) ^{3}P
331579.1	331559	20.1	1	17.9 4d^{7}5p (^{4}P) ^{3}D + 23.2 4d^{7}5p (^{2}D) ^{1}P + 12 4d^{7}5p (^{2}P) ^{1}P
331200.2	331588	-387.8	0	66.8 4d^{7}5p (^{4}P) ^{3}P + 26 4d^{7}5p (^{2}P) ^{1}S
331952.1	332165	-212.9	2	22.3 4d^{7}5p (^{2}P) ^{1}D + 22.4 4d^{7}5p (^{2}F) ^{3}F + 10.2 4d^{7}5p (^{4}P) ^{3}D
332306.3	332463	-156.7	4	50.3 4d^{7}5p (^{2}H) ^{1}G + 20.7 4d^{7}5p (^{2}G) ^{1}G + 15.7 4d^{7}5p (^{2}H) ^{3}H
332847.9	332832	15.9	4	51.5 4d^{7}5p (^{2}H) ^{3}H + 22.7 4d^{7}5p (^{2}G) ^{1}G + 14.7 4d^{7}5p (^{2}F) ^{3}G
333541.4	333427	114.4	3	19.4 4d^{7}5p (^{2}D) ^{1}F + 19.7 4d^{7}5p (^{2}F) ^{3}F + 13 4d^{7}5p (^{2}F) ^{3}G
334172.8	333928	244.8	2	0.7 4d^{7}5p (^{4}F) ^{5}D + 18.2 4d^{7}5p (^{2}P) ^{1}D + 15.9 4d^{7}5p (^{2}F) ^{1}D
335891.7	335876	15.7	2	18.9 4d^{7}5p (^{2}D) ^{1}D + 12.5 4d^{7}5p (^{2}F) ^{3}F + 12.3 4d^{7}5p (^{2}P) ^{3}P
336395.2	336339	56.2	1	50.2 4d^{7}5p (^{2}D) ^{1}P + 20.7 4d^{7}5p (^{2}P) ^{3}S + 9.8 4d^{7}5p (^{2}P) ^{1}P
336758.1	336619	139.1	3	20 4d^{7}5p (^{2}F) ^{3}G + 24.7 4d^{7}5p (^{2}H) ^{3}G + 16.5 4d^{7}5p (^{2}F) ^{3}D
337132.5	337181	-48.5	4	17.7 4d^{7}5p (^{2}F) ^{3}G + 21.8 4d^{7}5p (^{2}F) ^{1}G + 19.1 4d^{7}5p (^{2}F) ^{3}F
338400.4	338476	-75.6	5	71.4 4d^{7}5p (^{2}H) ^{1}H + 12.8 4d^{7}5p (^{2}H) ^{3}H + 5.4 4d^{7}5p (^{2}G) ^{3}G
339553	339549	4	1	37.2 4d^{7}5p (^{2}D) ^{3}P + 17.8 4d^{7}5p (^{2}P) ^{1}P + 11.5 4d^{7}5p (^{2}F) ^{3}D
340106.5	339953	153.5	0	73.2 4d^{7}5p (^{2}D) ^{3}P + 11.4 4d^{7}5p (^{2}P) ^{3}P + 10.2 4d^{7}5p (^{2}P) ^{1}S
341214.1	341205	9.1	3	56.7 4d^{7}5p (^{2}F) ^{3}F + 15.5 4d^{7}5p (^{2}F) ^{3}G + 6.9 4d^{7}5p (^{2}F) ^{3}D
341053.9	341249	-195.1	2	31.6 4d^{7}5p (^{2}F) ^{3}F + 20.7 4d^{7}5p (^{2}F) ^{1}D + 18.3 4d^{7}5p (^{2}F) ^{3}D
342178.7	342010	168.7	3	11 4d^{7}5p (^{2}D) ^{3}F + 24.3 4d^{7}5p (^{2}F) ^{3}D + 18 4d^{7}5p (^{2}P) ^{3}D

Table A20: Continued

E^a_{exp}	E^b_{calc}	ΔE	J	Leading components (in %) in LS coupling ^{c}
342064.9	342193	-128.1	4	47.8 4d^{7}5p (^{2}F) ^{1}G + 33.8 4d^{7}5p (^{2}F) ^{3}G + 6 4d^{7}5p (^{2}H) ^{3}G
343271.8	343174	97.8	1	64.4 4d^{7}5p (^{2}F) ^{3}D + 9.9 4d^{7}5p (^{2}D) ^{3}D + 9.3 4d^{7}5p (^{2}D) ^{3}D
343896.6	343862	34.6	2	47.8 4d^{7}5p (^{2}F) ^{3}D + 22.2 4d^{7}5p (^{2}F) ^{1}D + 6.2 4d^{7}5p (^{2}D) ^{3}D
344138	344089	49	5	84.3 4d^{7}5p (^{2}F) ^{3}G + 8.2 4d^{7}5p (^{2}H) ^{3}G
344200.9	344236	-35.1	4	61.9 4d^{7}5p (^{2}F) ^{3}F + 12.5 4d^{7}5p (^{2}F) ^{1}G + 11.5 4d^{7}5p (^{2}F) ^{3}G
350223.5	350319	-95.5	3	79.7 4d^{7}5p (^{2}F) ^{1}F + 9.7 4d^{7}5p (^{2}F) ^{3}D
355484	355523	-39	2	69.2 4d^{7}5p (^{2}D) ^{3}P + 15.3 4d^{7}5p (^{2}D) ^{3}P
356225.6	356397	-171.4	2	71.1 4d^{7}5p (^{2}D) ^{3}F + 8.1 4d^{7}5p (^{2}F) ^{3}F + 6.9 4d^{7}5p (^{2}D) ^{3}F
357557.3	357608	-50.7	1	67.2 4d^{7}5p (^{2}D) ^{3}P + 10.8 4d^{7}5p (^{2}D) ^{1}P + 8.3 4d^{7}5p (^{2}D) ^{3}D
359371.2	359296	75.2	3	54 4d^{7}5p (^{2}D) ^{3}F + 12.4 4d^{7}5p (^{2}D) ^{1}F + 11.1 4d^{7}5p (^{2}D) ^{3}F
360811.4	360915	-103.6	0	90 4d^{7}5p (^{2}D) ^{3}P
365620.4	365497	123.4	4	70.1 4d^{7}5p (^{2}D) ^{3}F + 19 4d^{7}5p (^{2}D) ^{3}F
365630.9	365545	85.9	1	31.6 4d^{7}5p (^{2}D) ^{1}P + 28.4 4d^{7}5p (^{2}D) ^{3}D + 18.6 4d^{7}5p (^{2}D) ^{3}P
366355.3	366389	-33.7	3	58.6 4d^{7}5p (^{2}D) ^{1}F + 20.7 4d^{7}5p (^{2}D) ^{3}F + 7.8 4d^{7}5p (^{2}D) ^{1}F
369896.8	369849	47.8	2	61.6 4d^{7}5p (^{2}D) ^{3}D + 13.4 4d^{7}5p (^{2}D) ^{3}D + 12.4 4d^{7}5p (^{2}D) ^{1}D
370177.8	370228	-50.2	1	40.9 4d^{7}5p (^{2}D) ^{3}D + 42.9 4d^{7}5p (^{2}D) ^{1}P + 7.5 4d^{7}5p (^{2}D) ^{3}D
373995.4	373904	91.4	3	59.6 4d^{7}5p (^{2}D) ^{3}D + 21.2 4d^{7}5p (^{2}D) ^{3}D + 8.3 4d^{7}5p (^{2}D) ^{1}F
433093.2	433279	-185.8	1	75.7 4d^{7}4f (^{4}F) ^{5}F + 9.8 4d^{7}4f (^{4}P) ^{5}F
436667.9	437204	-536.1	1	65.2 4d^{7}4f (^{4}F) ^{5}P + 20.2 4d^{7}4f (4f) ^{5}D + 5.2 4d^{7}4f (^{4}P) ^{5}D
440559.7	440621	-61.3	1	54 4d^{7}4f (^{4}P) ^{5}D + 19.6 4d^{7}4f (4f) ^{5}P + 15.2 4d^{7}4f (^{4}F) ^{5}D
441387	441600	-213	3	10.4 4d^{7}4f (^{4}F) ^{3}G + 20.5 4d^{7}4f (4f) ^{5}D + 11.7 4d^{7}4f (^{4}F) ^{3}D
442751.3	442904	-152.7	1	52.4 4d^{7}4f (^{4}F) ^{3}D + 12.8 4d^{7}4f (4f) ^{3}P + 9 4d^{7}4f (^{2}H) ^{3}D
443097.1	443434	-336.9	1	49.3 4d^{7}4f (^{4}F) ^{5}D + 32.2 4d^{7}4f (^{4}P) ^{5}D + 7.5 4d^{7}4f (^{4}F) ^{5}P
444346	443535	811	5	43.6 4d^{7}4f (^{4}F) ^{3}H + 13.7 4d^{7}4f (^{4}F) ^{3}G + 11.1 4d^{7}4f (^{2}G) ^{3}G
445014	444588	426	3	21.2 4d^{7}4f (^{4}F) ^{5}D + 32.1 4d^{7}4f (^{4}P) ^{5}D + 9.9 4d^{7}4f (^{4}F) ^{3}G
448754	448180	574	2	29.3 4d^{7}4f (^{2}P) ^{3}F + 13.3 4d^{7}4f (^{2}D) ^{3}F + 10 4d^{7}4f (^{4}P) ^{5}D
450428	451273	-845	2	21.1 4d^{7}4f (^{4}F) ^{3}P + 24.6 4d^{7}4f (^{2}H) ^{1}D + 17 4d^{7}4f (^{4}F) ^{3}D
453642	453098	544	1	39.3 4d^{7}4f (^{2}P) ^{3}D + 13.1 4d^{7}4f (^{4}F) ^{3}P + 8.5 4d^{7}4f (^{4}F) ^{3}S
454009	454778	-769	4	17.2 4d^{7}4f (^{2}H) ^{3}G + 16.3 4d^{7}4f (^{2}H) ^{3}F + 15.6 4d^{7}4f (^{2}G) ^{3}H
454321	455487	-1166	2	31.3 4d^{7}4f (^{2}H) ^{3}F + 16.3 4d^{7}4f (^{2}G) ^{3}F + 13.6 4d^{7}4f (^{4}P) ^{3}D
456827	456867	-40	4	19.2 4d^{7}4f (^{2}P) ^{3}F + 13.5 4d^{7}4f (^{2}H) ^{3}G + 10.1 4d^{7}4f (^{2}P) ^{1}G
457848	457456	392	3	15.1 4d^{7}4f (^{2}H) ^{3}F + 11.6 4d^{7}4f (^{4}P) ^{3}D + 8 4d^{7}4f (^{4}P) ^{3}G
459103	458581	522	4	14.8 4d^{7}4f (^{2}G) ^{3}G + 19.5 4d^{7}4f (^{2}P) ^{3}G + 12.2 4d^{7}4f (^{4}P) ^{5}G
458311	459004	-693	1	29.6 4d^{7}4f (^{4}F) ^{3}S + 17.9 4d^{7}4f (^{2}G) ^{3}D + 11.2 4d^{7}4f (^{2}F) ^{3}S
459774	459039	735	4	25.2 4d^{7}4f (^{2}D) ^{3}F + 24.1 4d^{7}4f (^{2}G) ^{1}G + 10.5 4d^{7}4f (^{2}D) ^{3}F
460440	460262	178	4	23.2 4d^{7}4f (^{2}H) ^{3}F + 18.9 4d^{7}4f (^{2}G) ^{3}F + 16.6 4d^{7}4f (^{2}H) ^{3}G
460841	461582	-741	1	35.9 4d^{7}4f (^{2}G) ^{3}D + 17.2 4d^{7}4f (^{2}G) ^{3}P + 9.4 4d^{7}4f (^{4}F) ^{3}S
461717	461617	100	4	12.3 4d^{7}4f (^{2}D) ^{3}G + 17.6 4d^{7}4f (^{2}G) ^{3}H + 15.4 4d^{7}4f (^{4}P) ^{5}F
464406	464503	-97	2	21.2 4d^{7}4f (^{2}P) ^{1}D + 15.2 4d^{7}4f (^{4}P) ^{3}F + 12.5 4d^{7}4f (^{2}G) ^{3}D
465968	464881	1087	2	39.4 4d^{7}4f (^{4}P) ^{5}F + 10.6 4d^{7}4f (^{2}G) ^{1}D + 8.7 4d^{7}4f (^{2}D) ^{1}D
465777	465436	341	4	14.7 4d^{7}4f (^{2}H) ^{3}H + 23.7 4d^{7}4f (^{4}P) ^{3}F + 17.9 4d^{7}4f (^{2}P) ^{1}G
465997	466345	-348	1	35.9 4d^{7}4f (^{2}D) ^{1}P + 27.3 4d^{7}4f (^{2}F) ^{1}P + 9.6 4d^{7}4f (^{2}G) ^{1}P
468330	467632	698	3	4.9 4d^{7}4f (^{2}D) ^{3}D + 15 4d^{7}4f (^{4}P) ^{5}F + 13.8 4d^{7}4f (^{4}P) ^{3}F
470177	470011	166	4	22.2 4d^{7}4f (^{2}P) ^{3}G + 12.7 4d^{7}4f (^{2}D) ^{1}G + 9.7 4d^{7}4f (^{2}P) ^{1}G
470312	470998	-686	3	38.7 4d^{7}4f (^{4}P) ^{3}F + 9.5 4d^{7}4f (^{2}D) ^{3}G + 9 4d^{7}4f (^{2}P) ^{3}G
472704	472484	220	0	37.3 4d^{7}4f (^{2}D) ^{3}P + 35.5 4d^{7}4f (^{2}D) ^{3}P + 11.9 4d^{7}4f (^{4}F) ^{3}P
471669	473000	-1331	1	33.9 4d^{7}4f (^{2}D) ^{3}P + 27.3 4d^{7}4f (^{2}D) ^{3}P + 8.9 4d^{7}4f (^{4}F) ^{3}P
480137	478704	1433	5	51.8 4d^{7}4f (^{2}F) ^{3}I + 18.9 4d^{7}4f (^{2}H) ^{3}I + 6 4d^{7}4f (^{2}H) ^{1}H
478443	478844	-401	3	15.5 4d^{7}4f (^{2}D) ^{3}D + 12.2 4d^{7}4f (^{2}H) ^{3}D + 11.1 4d^{7}4f (^{2}F) ^{3}D
480376	479822	554	2	13.5 4d^{7}4f (^{2}D) ^{1}D + 13.5 4d^{7}4f (^{2}F) ^{3}F + 12.5 4d^{7}4f (^{2}F) ^{1}D
479867	480712	-845	3	36.6 4d^{7}4f (^{2}F) ^{3}G + 22.2 4d^{7}4f (^{2}F) ^{3}F + 5.2 4d^{7}4f (^{2}H) ^{3}G
482000	481649	351	5	42.1 4d^{7}4f (^{2}F) ^{3}G + 8.7 4d^{7}4f (^{2}F) ^{3}H + 7.4 4d^{7}6p (^{4}F) ^{3}G
482451	481884	567	4	15.2 4d^{7}4f (^{2}F) ^{3}H + 18.9 4d^{7}4f (^{2}F) ^{1}G + 14.7 4d^{7}4f (^{2}D) ^{3}H
481700	482657	-957	2	57.9 4d^{7}4f (^{2}F) ^{3}F + 5.7 4d^{7}4f (^{2}H) ^{3}F + 5 4d^{7}4f (^{2}D) ^{3}F
482984	482983	1	3	30.7 4d^{7}4f (^{2}H) ^{3}D + 16.3 4d^{7}4f (^{2}F) ^{3}F + 7.1 4d^{7}4f (^{4}F) ^{3}D
485789	484606	1183	5	28.3 4d^{7}4f (^{2}F) ^{3}H + 11.8 4d^{7}4f (^{2}H) ^{3}H + 11.7 4d^{7}4f (^{2}D) ^{3}H
484659	485333	-674	2	19.6 4d^{7}4f (^{2}D) ^{1}D + 19.2 4d^{7}4f (^{2}F) ^{1}D + 17.5 4d^{7}4f (^{2}F) ^{3}D
492097	492563	-466	5	3.6 4d^{7}4f (^{2}H) ^{3}G + 20.9 4d^{7}4f (^{4}F) ^{3}G + 17.6 4d^{7}4f (^{4}P) ^{3}G
494861	494692	169	5	68.1 4d^{7}6p (^{4}F) ^{5}F + 17.9 4d^{7}6p (^{4}F) ^{5}G + 5 4d^{7}6p (^{4}F) ^{3}G
495646	495380	266	2	8.4 4d^{7}4f (^{2}G) ^{3}F + 11.9 4d^{7}4f (^{4}F) ^{3}F + 10.5 4d^{7}4f (^{2}F) ^{3}P
495623	495868	-245	3	28.7 4d^{7}4f (^{2}H) ^{1}F + 10.6 4d^{7}4f (^{4}F) ^{3}F + 8.4 4d^{7}4f (^{2}G) ^{3}F
496515	497749	-1234	4	11.3 4d^{7}4f (^{4}P) ^{3}G + 14.9 4d^{7}4f (^{2}D) ^{3}H + 14.3 4d^{7}4f (^{4}F) ^{3}G
497593	497904	-311	3	18.1 4d^{7}4f (^{2}F) ^{3}D + 14.5 4d^{7}4f (^{2}F) ^{1}F + 10.6 4d^{7}6p (^{4}F) ^{3}D
498091	498710	-619	3	37.2 4d^{7}6p (^{4}F) ^{5}F + 39.6 4d^{7}6p (^{4}F) ^{5}D + 5 4d^{7}6p (^{4}F) ^{3}F
500115	499643	472	5	42.4 4d^{7}4f (^{2}D) ^{3}H + 15 4d^{7}4f (^{2}F) ^{3}H + 11.9 4d^{7}4f (^{2}D) ^{3}H
504304	503572	732	4	41.7 4d^{7}6p (^{4}F) ^{5}F + 20.8 4d^{7}6p (^{4}F) ^{5}G + 13.2 4d^{7}6p (^{4}F) ^{3}G
505151	505298	-147	4	23.4 4d^{7}4f (^{2}D) ^{1}G + 12 4d^{7}4f (^{2}H) ^{1}G + 11.9 4d^{7}4f (^{2}G) ^{1}G
506788	506159	629	3	17.6 4d^{7}4f (^{2}D) ^{3}F + 19.3 4d^{7}6p (^{4}F) ^{5}F + 15.1 4d^{7}6p (^{4}F) ^{3}F
506753	507197	-444	4	50.7 4d^{7}6p (^{4}F) ^{3}G + 20.8 4d^{7}6p (^{4}F) ^{5}G + 9.3 4d^{7}4f (^{2}D) ^{3}G
510338	509837	501	4	34.6 4d^{7}4f (^{2}D) ^{3}F + 14.8 4d^{7}4f (^{2}D) ^{3}F + 14 4d^{7}4f (^{2}D) ^{3}G
511308	510572	736	3	33.7 4d^{7}6p (^{4}F) ^{3}G + 12.8 4d^{7}4f (^{2}D) ^{3}D + 6.9 4d^{7}4f (^{2}D) ^{3}D
510313	512017	-1704	5	44 4d^{7}4f (^{2}D) ^{3}G + 13.6 4d^{7}4f (^{2}D) ^{3}G + 12.3 4d^{7}6p (^{2}G) ^{1}H
512945	512680	265	3	28.4 4d^{7}4f (^{2}D) ^{1}F + 16 4d^{7}6p (^{4}F) ^{3}G + 15.7 4d^{7}4f (^{2}D) ^{3}G
513093	512729	364	4	25.9 4d^{7}4f (^{2}D) ^{3}G + 22 4d^{7}6p (^{2}G) ^{3}F + 6.3 4d^{7}4f (^{2}D) ^{3}G
513229	513045	184	4	35.7 4d^{7}6p (^{2}G) ^{3}F + 16.4 4d^{7}4f (^{2}D) ^{3}G + 9 4d^{7}6p (^{2}G) ^{3}G
513638	513584	54	4	62.9 4d^{6}5s5p (^{5}D) ^{7}F + 24 4d^{6}5s5p (^{5}D) ^{7}P
512690	513904	-1214	2	71.9 4d^{6}5s5p (^{5}D) ^{7}F
514520	514458	62	3	6.6 4d^{7}4f (^{2}D) ^{1}F + 17.5 4d^{7}4f (^{2}D) ^{3}G + 16.2 4d^{7}4f (^{2}D) ^{1}F
515813	516591	-778	4	31.8 4d^{7}6p (^{2}G) ^{3}H + 30.9 4d^{7}6p (^{2}G) ^{3}G + 12.8 4d^{7}6p (^{2}G) ^{3}F
517431	517357	74	4	53.9 4d^{6}5s5p (^{5}D) ^{7}P + 21 4d^{6}5s5p (^{5}D) ^{7}D + 18.3 4d^{6}5s5p (^{5}D) ^{7}F
518987	520141	-1154	5	82.8 4d^{7}6p (^{2}H) ^{3}G + 9.2 4d^{7}6p (^{2}H) ^{3}H
522188	521267	921	5	33 4d^{7}6p (^{2}G) ^{1}H + 35.5 4d^{7}6p (^{2}G) ^{3}H + 5.8 4d^{7}4f (^{2}F) ^{1}H
523207	522055	1152	4	38 4d^{7}6p (^{2}G) ^{3}G + 32.2 4d^{7}6p (^{2}G) ^{1}G + 9.5 4d^{7}6p (^{2}G) ^{3}H
522551	522979	-428	5	25.4 4d^{7}4f (^{2}D) ^{1}H + 15.7 4d^{7}4f (^{2}D) ^{1}H + 9 4d^{7}4f (^{2}F) ^{1}H
524913	525538	-625	5	42.5 4d^{7}6p (^{2}H) ^{3}I + 32.9 4d^{7}6p (^{2}H) ^{3}H + 8.3 4d^{7}6p (^{2}G) ^{1}H
526265	525629	636	4	58.3 4d^{7}6p (^{2}D) ^{3}F + 20.7 4d^{7}6p (^{2}D) ^{3}F + 11.9 4d^{7}6p (^{4}P) ^{5}D
526016	525900	116	2	16.1 4d^{7}6p (^{2}D) ^{3}F + 15.4 4d^{7}6p (^{4}P) ^{3}D + 12.6 4d^{7}6p (^{2}P) ^{3}P
526056	526418	-362	5	45.7 4d^{6}5s5p (^{5}D) ^{5}F + 36 4d^{6}5s5p (^{5}D) ^{5}F + 9.8 4d^{6}5s5p (^{5}D) ^{7}F
527054	527469	-415	3	30.6 4d^{6}5s5p (^{5}D) ^{5}F + 22.2 4d^{6}5s5p (^{5}D) ^{5}F + 10 4d^{6}5s5p (^{5}D) ^{3}D
531754	531989	-235	5	52.7 4d^{7}6p (^{2}H) ^{1}H + 24.8 4d^{7}6p (^{2}H) ^{3}H + 9.4 4d^{7}6p (^{2}G) ^{3}G
537980	538376	-396	3	70.3 4d^{7}6p (^{2}F) ^{3}G + 7.1 4d^{7}6p (^{2}F) ^{3}F + 5.2 4d^{7}6p (^{2}F) ^{1}F
538218	539206	-988	2	22.7 4d^{6}5s5p (^{3}F) ^{5}F + 16.2 4d^{6}5s5p (^{3}D) ^{5}F + 8.2 4d^{6}5s5p (^{4}F) ^{5}F

a: From Ryabtsev [37]

b: This work

c: Only the component $\geq$ 5% are given

Transitions

Table A21: Computed oscillator strengths and transition probabilities in In VI.

Wavelength Å	Lower Level[a] cm^{-1}	J_{Low}	Upper level[a] cm^{-1}	J_{Up}	log gf	gA s^{-1}	CF
207.046	0	4	482984	3	-0.23	9.21E+10	0.389
207.469	0	4	482000	5	-0.69	3.17E+10	0.114
209.011	0	4	478443	3	-0.4	6.12E+10	0.303
209.855	6465	3	482984	3	-0.91	1.87E+10	0.116
211.244	6465	3	479853	2	-0.88	1.98E+10	0.194
293.695	25866	4	366355	3	-0.29	3.97E+10	0.464
293.838	15161	2	355484	2	-0.89	9.87E+09	0.183
296.357	6465	3	343897	2	-0.98	8.04E+09	0.221
298.403	8154	2	343272	1	-0.91	9.14E+09	0.225
298.655	20649	1	355484	2	-0.68	1.58E+10	0.6
299.845	25866	4	359371	3	-0.85	1.05E+10	0.349
300.997	23255	2	355484	2	-0.78	1.22E+10	0.298
304.794	0	4	328091	4	-0.95	8.03E+09	0.208
305.84	23255	2	350224	3	-0.67	1.53E+10	0.326
307.857	0	4	324826	3	-0.66	1.54E+10	0.171
308.302	25866	4	350224	3	0.12	9.17E+10	0.819
309.065	6465	3	330022	2	-0.98	7.39E+09	0.145
309.196	8154	2	331573	1	-0.94	8.11E+09	0.116
309.361	20649	1	343897	2	-0.56	1.90E+10	0.434
309.919	20607	0	343272	1	-0.66	1.52E+10	0.44
310.948	15161	2	336758	3	-0.23	4.03E+10	0.52
311.575	0	4	320950	3	-0.48	2.27E+10	0.343
311.875	23255	2	343897	2	-0.64	1.57E+10	0.283
312.237	0	4	320270	3	-0.31	3.34E+10	0.354
312.903	0	4	319588	5	-0.62	1.62E+10	0.471
313.031	20649	1	340107	0	-0.91	8.37E+09	0.718
313.481	8154	2	327153	2	-0.78	1.13E+10	0.351
313.555	23255	2	342179	3	-0.41	2.63E+10	0.312
313.574	20649	1	339553	1	-0.61	1.65E+10	0.517
313.764	0	4	318711	4	-0.47	2.30E+10	0.318
314.089	15161	2	333541	3	-1	6.82E+09	0.113
314.109	6465	3	324826	3	-0.76	1.17E+10	0.202
314.337	6465	3	324596	2	-0.43	2.49E+10	0.61
314.344	8154	2	326277	3	-0.73	1.26E+10	0.175
314.571	6465	3	324359	2	-0.62	1.62E+10	0.352
315.361	6465	3	323562	4	-0.64	1.53E+10	0.38
315.571	0	4	316886	3	-0.66	1.47E+10	0.295
315.703	6465	3	323219	3	-0.2	4.20E+10	0.445
316.014	8154	2	324596	2	-0.86	9.21E+09	0.199
316.143	25866	4	342179	3	-0.32	3.20E+10	0.56
316.158	23255	2	339553	1	-0.52	2.02E+10	0.421
316.251	8154	2	324359	2	-0.16	4.58E+10	0.428
316.47	0	4	315986	3	-0.81	1.03E+10	0.434
316.702	15161	2	330915	1	-0.66	1.47E+10	0.316
317.053	8154	2	323559	2	-0.76	1.16E+10	0.239
317.216	20649	1	335892	2	-0.72	1.26E+10	0.684
317.252	0	4	315207	5	0.24	1.16E+11	0.75
317.395	8154	2	323219	3	-0.98	7.02E+09	0.158
317.428	6465	3	321497	4	0.1	8.29E+10	0.749
317.502	6465	3	321424	2	-0.44	2.38E+10	0.499
317.6	15161	2	330022	2	-0.11	5.10E+10	0.625
318.092	8154	2	322529	1	-0.35	2.98E+10	0.539
318.67	6465	3	320270	3	-0.81	1.02E+10	0.227
318.986	0	4	313493	4	-0.65	1.46E+10	0.469
319.346	23255	2	336395	1	-0.2	4.13E+10	0.506
319.697	8154	2	320950	3	-0.92	7.79E+09	0.376
319.86	23255	2	335892	2	-0.55	1.86E+10	0.22
319.965	25866	4	338400	5	0.02	6.74E+10	0.58
320.26	6465	3	318711	4	-0.7	1.31E+10	0.29
320.322	6465	3	318651	3	-0.27	3.53E+10	0.654
320.394	8154	2	320270	3	-0.46	2.24E+10	0.509
320.521	15161	2	327153	2	-0.89	8.33E+09	0.15
321.423	15161	2	326277	3	-0.41	2.51E+10	0.44
321.458	15161	2	326244	1	-0.44	2.36E+10	0.381
321.629	23255	2	334173	2	-0.27	3.49E+10	0.462
321.988	0	4	310571	4	0.22	1.07E+11	0.636
322.065	8154	2	318651	3	-0.43	2.40E+10	0.231
322.776	6465	3	316277	2	-0.75	1.14E+10	0.214
322.929	15161	2	324826	3	-0.98	6.71E+09	0.203
323.08	6465	3	315986	3	-0.67	1.36E+10	0.2
323.17	15161	2	324596	2	-1	6.38E+09	0.111
324.22	0	4	308432	3	-0.26	3.48E+10	0.466
324.853	8154	2	315986	3	-0.63	1.47E+10	0.204
325.018	25866	4	333541	3	-0.71	1.23E+10	0.278
325.332	23255	2	330633	3	-0.08	5.27E+10	0.623
325.752	25866	4	332848	4	-0.2	3.99E+10	0.622
325.98	23255	2	330022	2	-0.77	1.06E+10	0.15
326.328	25866	4	332306	4	0.47	1.85E+11	0.692
327.131	6465	3	312153	2	-0.71	1.22E+10	0.273
327.915	15161	2	320118	1	-0.66	1.37E+10	0.184
328.119	25866	4	330633	3	-0.7	1.25E+10	0.577
328.123	20607	0	325371	1	-0.73	1.14E+10	0.369
328.398	25866	4	330375	5	-0.48	2.04E+10	0.713
328.462	0	4	304449	3	-0.42	2.34E+10	0.199
328.948	8154	2	312153	2	-0.82	9.36E+09	0.133
329.005	20649	1	324596	2	-0.93	7.32E+09	0.321
329.975	0	4	303053	4	-0.63	1.45E+10	0.159
330.045	23255	2	326244	1	-1	6.19E+09	0.138
330.418	8154	2	310801	1	-0.68	1.27E+10	0.287
331.162	6465	3	308432	3	-0.82	9.15E+09	0.091
332.016	6465	3	307655	2	-0.82	9.16E+09	0.122
332.097	15161	2	316277	2	-0.66	1.34E+10	0.234
332.103	0	4	301111	3	-0.92	7.32E+09	0.197
332.542	8154	2	308868	2	-0.89	7.77E+09	0.12
333.516	0	4	299836	4	-0.37	2.57E+10	0.32
333.925	20649	1	320118	1	-0.61	1.46E+10	0.314

Table A21: Continued

Wavelength	Lower Level	J_{Low}	Upper level	J_{Up}	log gf	gA	CF
334.977	25866	4	324394	5	-0.69	1.21E+10	0.641
335.227	20649	1	318954	2	-0.75	1.06E+10	0.435
335.589	6465	3	304449	3	-0.66	1.29E+10	0.164
335.913	25866	4	323562	4	-0.91	7.22E+09	0.173
337.468	15161	2	311485	3	-0.97	6.24E+09	0.196
337.502	8154	2	304449	3	-0.92	7.05E+09	0.214
337.746	25866	4	321947	5	-0.69	1.20E+10	0.565
340.981	15161	2	308432	3	-0.84	8.32E+09	0.262
345.676	15161	2	304449	3	-0.86	7.69E+09	0.121
855.235	248694	4	365620	4	-0.92	1.10E+09	0.514
875.549	201884	5	316098	4	-0.71	1.70E+09	0.418
889.71	231742	6	344138	5	-0.7	1.67E+09	0.383
947.498	226765	4	332306	4	-0.95	8.39E+08	0.136
947.627	205958	4	311485	3	-0.47	2.54E+09	0.506
950.444	211178	2	316392	1	-0.9	9.31E+08	0.602
955.029	237470	2	342179	3	-0.99	7.50E+08	0.082
962.759	226765	4	330633	3	-1	7.13E+08	0.184
968.715	233903	5	337133	4	-0.53	2.12E+09	0.36
968.96	238975	4	342179	3	-0.91	8.76E+08	0.38
969.848	211178	2	314287	1	-0.96	7.78E+08	0.447
971.561	209226	3	312153	2	-0.74	1.30E+09	0.36
972.872	222582	2	325371	1	-0.97	7.46E+08	0.429
974.366	228284	1	330915	1	-0.85	9.83E+08	0.304
974.427	221971	1	324596	2	-0.95	7.96E+08	0.16
977.91	209226	3	311485	3	-0.81	1.09E+09	0.444
979.023	234616	3	336758	3	-0.89	9.02E+08	0.657
979.166	212337	1	314464	0	-0.93	8.29E+08	0.66
979.593	237470	2	339553	1	-0.84	9.99E+08	0.272
981.587	219074	3	320950	3	-0.43	2.58E+09	0.568
983.043	272271	3	373995	3	0.15	9.80E+09	0.686
984.931	248694	4	350224	3	-0.82	1.04E+09	0.529
987.399	234616	3	335892	2	-0.85	9.63E+08	0.476
987.519	219006	2	320270	3	-0.87	9.13E+08	0.431
989.361	240990	5	342065	4	-0.93	8.04E+08	0.437
993.417	220287	3	320950	3	-0.44	2.44E+09	0.699
995.294	269705	1	370178	1	-0.49	2.17E+09	0.718
996.277	233168	4	333541	3	-0.67	1.44E+09	0.472
998.64	230497	3	330633	3	-0.91	8.32E+08	0.4
999.56	269705	1	369749	2	-0.38	2.77E+09	0.802
1002.791	211178	2	310899	3	-0.82	1.01E+09	0.376
1004.447	234616	3	334173	2	-0.93	7.80E+08	0.176
1004.775	230497	3	330022	2	-0.92	7.91E+08	0.595
1005.782	238975	4	338400	5	-0.45	2.36E+09	0.744
1008.689	233168	4	332306	4	-0.03	6.09E+09	0.737
1010.52	209226	3	308185	4	-0.44	2.40E+09	0.352
1010.858	234616	3	333541	3	-0.88	8.61E+08	0.381
1010.863	237470	2	336395	1	-1	6.48E+08	0.195
1012.712	233207	2	331952	2	-0.87	8.93E+08	0.321
1015.599	212337	1	310801	1	-0.61	1.60E+09	0.762
1016.034	237470	2	335892	2	-0.78	1.08E+09	0.138
1016.226	233903	5	332306	4	-0.4	2.59E+09	0.633
1018.342	205958	4	304157	5	0.02	6.78E+09	0.372
1018.774	238975	4	337133	4	-0.21	4.00E+09	0.745
1018.813	231742	6	329895	6	-0.47	2.20E+09	0.812
1019.775	226765	4	324826	3	-0.94	7.42E+08	0.308
1020.245	237876	1	335892	2	-0.62	1.53E+09	0.511
1020.907	201884	5	299836	4	-0.69	1.30E+09	0.164
1021.391	245366	2	343272	1	-0.57	1.72E+09	0.364
1021.656	219006	2	316886	3	0.08	7.66E+09	0.709
1022.541	246405	3	344201	4	-0.38	2.69E+09	0.342
1022.675	238975	4	336758	3	-0.28	3.36E+09	0.707
1022.883	245509	1	343272	1	-0.89	8.17E+08	0.649
1023.912	231742	6	329406	6	0.41	1.64E+10	0.615
1024.293	226765	4	324394	5	-0.43	2.37E+09	0.164
1025.733	246405	3	343897	2	-0.31	3.11E+09	0.381
1025.955	228807	2	326277	3	-0.88	8.44E+08	0.301
1026.58	240990	5	338400	5	0.41	1.63E+10	0.724
1026.843	219006	2	316392	1	-0.75	1.12E+09	0.297
1027.826	245979	2	343272	1	-0.52	1.90E+09	0.483
1028.231	211178	2	308432	3	-0.44	2.32E+09	0.731
1028.773	219074	3	316277	2	-0.72	1.21E+09	0.286
1029.649	214364	4	311485	3	-0.88	8.30E+08	0.164
1030.672	219074	3	316098	4	0.03	6.74E+09	0.581
1031.11	221971	1	318954	2	-0.54	1.80E+09	0.367
1032.578	253379	3	350224	3	0.2	1.00E+10	0.778
1032.8	225122	5	321947	5	-0.24	3.59E+09	0.476
1032.901	233207	2	330022	2	-0.67	1.33E+09	0.298
1032.923	245366	2	342179	3	-0.61	1.54E+09	0.26
1033.088	226765	4	323562	4	-0.26	3.47E+09	0.312
1034.094	237470	2	334173	2	-0.66	1.38E+09	0.278
1035.929	212337	1	308868	2	-0.5	1.96E+09	0.58
1036.51	211178	2	307655	2	-0.53	1.86E+09	0.542
1036.571	233903	5	330375	5	0.41	1.61E+10	0.735
1036.767	226765	4	323219	3	-0.65	1.37E+09	0.181
1038.068	234582	1	330915	1	-0.79	1.01E+09	0.351
1038.256	219006	2	315321	2	-0.62	1.49E+09	0.326
1038.294	228284	1	324596	2	-0.52	1.88E+09	0.354
1039.43	214364	4	310571	4	-0.61	1.51E+09	0.198
1039.505	245979	2	342179	3	-0.15	4.35E+09	0.686
1040.923	222582	2	318651	3	-0.7	1.23E+09	0.322
1041.459	228807	2	324826	3	-0.36	2.70E+09	0.379
1041.751	233903	5	329895	6	-0.88	8.20E+08	0.04
1042.471	269705	1	365631	1	-0.35	2.74E+09	0.761
1043.319	245366	2	341214	3	-0.15	4.32E+09	0.759
1043.721	220287	3	316098	4	0.05	6.86E+09	0.795
1044.06	230497	3	326277	3	-0.59	1.56E+09	0.476
1044.946	220287	3	315986	3	-0.85	8.71E+08	0.342
1045.065	245366	2	341054	2	-0.67	1.32E+09	0.244
1045.373	246405	3	342065	4	0.16	8.92E+09	0.822
1047.028	201884	5	297392	6	0.57	2.26E+10	0.91
1047.039	248694	4	344201	4	0.09	7.51E+09	0.546
1047.058	230738	0	326244	1	-0.81	9.48E+08	0.252
1047.083	233903	5	329406	6	-0.05	5.44E+09	0.883
1047.729	248694	4	344138	5	0.43	1.64E+10	0.846
1047.778	234582	1	330022	2	-0.71	1.19E+09	0.259
1048.636	201884	5	297246	5	-0.11	4.72E+09	0.382

Table A21: Continued

Wavelength	Lower Level	J_{Low}	Upper level	J_{Up}	log gf	gA	CF
1050.034	245979	2	341214	3	-1	6.04E+08	0.126
1050.168	209226	3	304449	3	-0.61	1.51E+09	0.498
1050.625	226765	4	321947	5	-0.6	1.52E+09	0.103
1051.803	245979	2	341054	2	-0.29	3.10E+09	0.62
1054.754	246405	3	341214	3	-0.06	5.18E+09	0.462
1055.384	228807	2	323559	2	-0.97	6.47E+08	0.134
1056.54	246405	3	341054	2	-0.81	9.32E+08	0.178
1057.109	245509	1	340107	0	-0.76	1.03E+09	0.752
1058.586	225122	5	319588	5	0.16	8.57E+09	0.693
1060.122	230497	3	324826	3	-0.53	1.75E+09	0.595
1060.379	221971	1	316277	2	-0.45	2.12E+09	0.767
1061.065	228284	1	322529	1	-0.91	7.28E+08	0.166
1061.719	245366	2	339553	1	-0.68	1.23E+09	0.443
1062.662	237470	2	331573	1	-0.4	2.38E+09	0.66
1062.969	237876	1	331952	2	-0.75	1.05E+09	0.253
1063.331	245509	1	339553	1	-0.39	2.38E+09	0.767
1065.211	205958	4	299836	4	-0.2	3.69E+09	0.336
1065.274	238975	4	332848	4	0.23	9.87E+09	0.75
1065.397	230497	3	324359	2	-0.18	3.89E+09	0.774
1065.788	209226	3	303053	4	-0.05	5.24E+09	0.765
1065.864	214364	4	308185	4	-0.78	9.70E+08	0.515
1066.986	228807	2	322529	1	-0.98	6.15E+08	0.261
1068.504	225122	5	318711	4	-0.3	2.92E+09	0.324
1069.688	248694	4	342179	3	-0.25	3.23E+09	0.718
1069.8	234616	3	328091	4	0.35	1.32E+10	0.883
1071.238	272271	3	365620	4	0.37	1.36E+10	0.853
1071.238	221971	1	315321	2	-0.97	6.19E+08	0.1
1073.381	237470	2	330633	3	-0.39	2.38E+09	0.772
1074.462	233207	2	326277	3	-0.84	8.36E+08	0.28
1074.516	230497	3	323562	4	-0.1	4.59E+09	0.756
1074.554	230497	3	323559	2	-0.44	2.11E+09	0.807
1076.869	228284	1	321146	1	-0.97	6.14E+08	0.225
1077.322	226765	4	319588	5	-0.31	2.81E+09	0.429
1078.496	230497	3	323219	3	-0.23	3.42E+09	0.664
1079.063	225122	5	317795	6	0.44	1.56E+10	0.909
1079.718	228807	2	321424	2	-0.46	1.97E+09	0.35
1080.254	234582	1	327153	2	-0.73	1.07E+09	0.369
1080.646	234616	3	327153	2	-1	5.74E+08	0.226
1081.327	219006	2	311485	3	-0.96	6.20E+08	0.146
1082.073	239158	0	331573	1	-0.73	1.06E+09	0.702
1082.125	219074	3	311485	3	-0.25	3.23E+09	0.596
1082.968	228807	2	321146	1	-0.66	1.25E+09	0.374
1083.244	221971	1	314287	1	-0.65	1.27E+09	0.5
1085.271	228807	2	320950	3	-0.3	2.84E+09	0.461
1087.595	226765	4	318711	4	0.03	6.10E+09	0.838
1088.311	226765	4	318651	3	-0.17	3.86E+09	0.786
1088.313	209226	3	301111	3	-0.63	1.32E+09	0.157
1088.926	228284	1	320118	1	-0.68	1.17E+09	0.364
1089.023	219074	3	310899	3	-0.69	1.15E+09	0.639
1089.435	230738	0	322529	1	-0.94	6.45E+08	0.276
1089.837	239158	0	330915	1	-0.96	6.19E+08	0.641
1090.459	222582	2	314287	1	-0.96	6.14E+08	0.437
1091.011	238975	4	330633	3	-0.26	3.11E+09	0.703
1091.48	233207	2	324826	3	-0.14	4.01E+09	0.777
1092.933	219074	3	310571	4	-0.96	6.17E+08	0.651
1094.097	238975	4	330375	5	-0.65	1.26E+09	0.814
1094.231	233207	2	324596	2	-0.77	9.46E+08	0.149
1095.09	240990	5	332306	4	-0.03	5.20E+09	0.634
1095.434	205958	4	297246	5	0.23	9.51E+09	0.906
1096.181	233168	4	324394	5	0.36	1.27E+10	0.858
1096.812	231742	6	322915	7	0.63	2.34E+10	0.933
1097.618	269705	1	360811	0	-0.57	1.48E+09	0.877
1098.55	245366	2	336395	1	-0.64	1.26E+09	0.688
1101.05	253379	3	344201	4	-0.21	3.41E+09	0.823
1101.46	234582	1	325371	1	-0.59	1.41E+09	0.495
1101.576	245979	2	336758	3	-0.38	2.28E+09	0.457
1102.897	228284	1	318954	2	-0.47	1.84E+09	0.355
1103.629	209226	3	299836	4	-0.11	4.25E+09	0.839
1104.66	245366	2	335892	2	-0.24	3.17E+09	0.507
1104.751	253379	3	343897	2	-0.23	3.23E+09	0.806
1105.998	245979	2	336395	1	-0.59	1.41E+09	0.531
1106.102	230738	0	321146	1	-0.85	7.70E+08	0.334
1106.26	233168	4	323562	4	-0.19	3.52E+09	0.553
1106.773	246405	3	336758	3	-0.59	1.41E+09	0.636
1107.618	220287	3	310571	4	-0.82	8.19E+08	0.695
1108.518	234616	3	324826	3	-0.96	6.02E+08	0.119
1109.296	228807	2	318954	2	-0.63	1.28E+09	0.3
1110.069	214364	4	304449	3	0.13	7.30E+09	0.766
1110.479	233168	4	323219	3	-0.52	1.63E+09	0.431
1110.948	225122	5	315136	6	-0.09	4.41E+09	0.458
1110.968	233207	2	323219	3	-0.98	5.69E+08	0.54
1111.933	211178	2	301111	3	0.02	5.65E+09	0.881
1112.812	219006	2	308868	2	-0.81	8.32E+08	0.381
1113.679	214364	4	304157	5	0.28	1.04E+10	0.891
1113.871	234582	1	324359	2	-0.46	1.87E+09	0.757
1113.927	230497	3	320270	3	-0.94	6.21E+08	0.386
1116.434	222582	2	312153	2	-0.31	2.64E+09	0.543
1119.093	219074	3	308432	3	-0.55	1.50E+09	0.35
1120.113	237876	1	327153	2	-0.33	2.45E+09	0.692
1120.817	226765	4	315986	3	-0.4	2.10E+09	0.355
1122.197	219074	3	308185	4	-0.07	4.49E+09	0.838
1123.883	234582	1	323559	2	-0.48	1.77E+09	0.526
1124.789	240990	5	329895	6	0.49	1.62E+10	0.872
1124.825	222582	2	311485	3	-0.92	6.40E+08	0.24
1126.034	237470	2	326277	3	-0.38	2.19E+09	0.692
1126.124	253379	3	342179	3	-1	5.27E+08	0.345
1127.537	214364	4	303053	4	0.07	6.12E+09	0.653
1127.569	253379	3	342065	4	-0.13	3.88E+09	0.378
1127.855	245509	1	334173	2	-0.23	3.06E+09	0.782
1128.906	219074	3	307655	2	-0.6	1.31E+09	0.538
1128.909	220287	3	308868	2	-0.87	7.11E+08	0.526
1129.76	212337	1	300851	0	-0.87	7.13E+08	0.859
1130.093	211178	2	299666	2	-0.95	5.83E+08	0.16
1130.723	248694	4	337133	4	-0.21	3.24E+09	0.635
1131.007	240990	5	329406	6	-0.88	6.90E+08	0.551
1131.634	237876	1	326244	1	-0.8	8.30E+08	0.344

Table A21: Continued

Wavelength	Lower Level	J_{Low}	Upper level	J_{Up}	log gf	gA	CF
1132.281	222582	2	310899	3	0.09	6.42E+09	0.761
1132.942	205958	4	294224	4	0.14	7.10E+09	0.714
1133.549	222582	2	310801	1	-0.48	1.71E+09	0.772
1133.576	233207	2	321424	2	-0.93	6.05E+08	0.126
1134.104	245366	2	333541	3	-0.34	2.35E+09	0.372
1134.22	212337	1	300503	1	-0.48	1.74E+09	0.777
1134.494	220287	3	308432	3	-0.07	4.42E+09	0.76
1135.342	228807	2	316886	3	-0.59	1.34E+09	0.185
1135.53	248694	4	336758	3	-0.67	1.10E+09	0.442
1135.801	233903	5	321947	5	-1	5.19E+08	0.093
1136.45	228284	1	316277	2	-0.94	5.98E+08	0.215
1137.685	220287	3	308185	4	-0.09	4.21E+09	0.601
1139.37	211178	2	298946	2	-0.49	1.67E+09	0.732
1139.586	219006	2	306757	1	-0.65	1.17E+09	0.508
1139.699	233207	2	320950	3	-0.37	2.17E+09	0.39
1140.571	253379	3	341054	2	-0.67	1.12E+09	0.353
1141.629	233903	5	321497	4	0.14	7.01E+09	0.77
1141.751	228807	2	316392	1	-0.84	7.51E+08	0.434
1142.067	211178	2	298738	2	-0.75	9.04E+08	0.445
1142.929	237876	1	325371	1	-0.64	1.16E+09	0.527
1144.103	209226	3	296631	3	-0.02	4.85E+09	0.748
1144.581	220287	3	307655	2	-0.39	2.09E+09	0.703
1144.738	237470	2	324826	3	-0.81	7.92E+08	0.162
1145.088	212337	1	299666	2	-0.32	2.47E+09	0.874
1145.452	238975	4	326277	3	-0.36	2.22E+09	0.855
1147.63	246405	3	333541	3	-0.4	2.01E+09	0.407
1147.764	237470	2	324596	2	-0.32	2.44E+09	0.494
1148.079	233168	4	320270	3	-0.96	5.50E+08	0.358
1148.096	272271	3	359371	3	-0.46	1.74E+09	0.73
1148.292	239158	0	326244	1	-0.51	1.57E+09	0.485
1148.933	228284	1	315321	2	-0.98	5.23E+08	0.129
1150.613	233207	2	320118	1	-0.75	8.95E+08	0.299
1151.965	234616	3	321424	2	-0.42	1.90E+09	0.647
1153.028	226765	4	313493	4	-0.84	7.31E+08	0.181
1154.614	212337	1	298946	2	-0.8	8.01E+08	0.287
1155.794	269705	1	356226	2	-0.09	4.03E+09	0.75
1155.878	228807	2	315321	2	-0.55	1.39E+09	0.615
1156.829	245509	1	331952	2	-0.61	1.23E+09	0.468
1156.837	246405	3	332848	4	-0.81	7.66E+08	0.266
1157.136	233168	4	319588	5	-0.31	2.43E+09	0.471
1157.144	201884	5	288304	5	0.33	1.06E+10	0.908
1157.385	212337	1	298738	2	-0.57	1.35E+09	0.522
1158.935	222582	2	308868	2	-0.44	1.79E+09	0.546
1158.992	228284	1	314566	0	-0.83	7.44E+08	0.864
1161.585	237470	2	323559	2	-0.9	6.21E+08	0.306
1163.156	245979	2	331952	2	-0.4	1.97E+09	0.564
1163.412	205958	4	291912	3	0.11	6.39E+09	0.79
1165.884	209226	3	294998	2	-0.08	4.05E+09	0.768
1166.223	233207	2	318954	2	-0.79	8.02E+08	0.211
1167.065	233903	5	319588	5	-0.81	7.67E+08	0.311
1167.485	234616	3	320270	3	0.03	5.17E+09	0.828
1168.104	211178	2	296787	1	-0.35	2.18E+09	0.792
1168.951	246405	3	331952	2	-0.98	5.12E+08	0.466
1168.996	233168	4	318711	4	-0.71	9.51E+08	0.128
1169.747	230497	3	315986	3	-0.4	1.93E+09	0.367
1169.823	233168	4	318651	3	-0.47	1.65E+09	0.339
1169.977	214364	4	299836	4	-0.4	1.94E+09	0.241
1170.235	211178	2	296631	3	-0.5	1.54E+09	0.232
1170.296	225122	5	310571	4	0.06	5.53E+09	0.847
1170.711	238975	4	324394	5	-0.64	1.12E+09	0.232
1176.5	209226	3	294224	4	-0.41	1.87E+09	0.203
1178.58	248694	4	333541	3	-0.57	1.28E+09	0.548
1179.131	233903	5	318711	4	-0.73	8.96E+08	0.178
1180.051	201884	5	286626	4	0.25	8.58E+09	0.875
1181.253	245366	2	330022	2	-0.56	1.32E+09	0.464
1181.275	245979	2	330633	3	-0.53	1.41E+09	0.598
1181.296	237876	1	322529	1	-0.97	5.07E+08	0.174
1183.249	245509	1	330022	2	-0.78	7.86E+08	0.367
1184.133	212337	1	296787	1	-0.79	7.76E+08	0.238
1188.292	248694	4	332848	4	-0.73	8.69E+08	0.796
1189.092	225122	5	309220	5	-0.08	3.92E+09	0.8
1189.869	245979	2	330022	2	-0.81	7.39E+08	0.254
1192.003	233903	5	317795	6	-0.17	3.19E+09	0.834
1193.033	211178	2	294998	2	-0.6	1.17E+09	0.206
1193.236	226765	4	310571	4	-0.37	1.99E+09	0.324
1193.973	253379	3	337133	4	-0.22	2.85E+09	0.592
1198.107	231742	6	315207	5	0.39	1.13E+10	0.893
1199.13	231742	6	315136	6	-0.21	2.85E+09	0.842
1199.816	228807	2	312153	2	-0.75	8.27E+08	0.297
1201.728	272271	3	355484	2	0.08	5.57E+09	0.88
1202.148	233207	2	316392	1	-0.73	8.58E+08	0.664
1203.805	233207	2	316277	2	-1	4.67E+08	0.141
1203.913	225122	5	308185	4	-0.81	7.21E+08	0.707
1204.874	230497	3	313493	4	0.13	6.18E+09	0.689
1205.236	238975	4	321947	5	0.24	8.00E+09	0.741
1206.539	214364	4	297246	5	-0.28	2.41E+09	0.291
1207.466	233168	4	315986	3	-0.29	2.32E+09	0.505
1207.731	237470	2	320270	3	-0.77	7.77E+08	0.177
1209.392	209226	3	291912	3	-0.66	9.97E+08	0.133
1209.513	228807	2	311485	3	-0.56	1.26E+09	0.365
1211.053	240990	5	323562	4	-0.48	1.48E+09	0.697
1212.783	226765	4	309220	5	0.24	7.90E+09	0.643
1214.392	205958	4	288304	5	-0.53	1.34E+09	0.16
1215.501	234616	3	316886	3	-0.79	7.40E+08	0.358
1217.821	233207	2	315321	2	-0.97	4.78E+08	0.287
1220.407	248694	4	330633	3	-0.55	1.28E+09	0.662
1224.269	248694	4	330375	5	-0.92	5.38E+08	0.735
1224.564	234616	3	316277	2	-0.62	1.07E+09	0.664
1227.039	219006	2	300503	1	-0.85	6.29E+08	0.553
1231.033	233903	5	315136	6	0.24	7.61E+09	0.512
1231.817	237470	2	318651	3	-0.62	1.06E+09	0.619
1235.224	240990	5	321947	5	-0.74	7.97E+08	0.249
1237.255	220287	3	301111	3	-0.62	1.04E+09	0.356
1237.711	253379	3	334173	2	-0.66	9.57E+08	0.628
1238.205	219074	3	299836	4	-0.54	1.24E+09	0.645
1238.43	246405	3	327153	2	-0.46	1.49E+09	0.678

Table A21: Continued

Wavelength	Lower Level	J_{Low}	Upper level	J_{Up}	log gf	gA	CF
1239.647	205958	4	286626	4	-0.57	1.17E+09	0.162
1239.769	219006	2	299666	2	-0.59	1.12E+09	0.501
1240.499	238975	4	319588	5	-0.5	1.36E+09	0.233
1240.818	219074	3	299666	2	-0.84	6.26E+08	0.488
1242.12	240990	5	321497	4	-0.29	2.20E+09	0.884
1244.932	233168	4	313493	4	-0.29	2.20E+09	0.687
1245.361	245979	2	326277	3	-0.95	4.82E+08	0.151
1249.024	230738	0	310801	1	-0.98	4.48E+08	0.524
1250.943	219006	2	298946	2	-0.46	1.49E+09	0.572
1252.011	219074	3	298946	2	-0.93	5.00E+08	0.264
1252.199	214364	4	294224	4	-0.72	8.16E+08	0.327
1254.631	234582	1	314287	1	-0.83	6.23E+08	0.318
1255.269	219074	3	298738	2	-0.44	1.54E+09	0.822
1258.346	253379	3	332848	4	-0.63	9.91E+08	0.654
1259.487	248694	4	328091	4	-0.88	5.50E+08	0.657
1259.9	228284	1	307655	2	-0.7	8.37E+08	0.711
1266.981	253379	3	332306	4	-0.95	4.74E+08	0.475
1267.755	221971	1	300851	0	-0.94	4.81E+08	0.662
1271.32	220287	3	298946	2	-0.73	7.76E+08	0.481
1273.374	221971	1	300503	1	-0.68	8.54E+08	0.47
1273.626	237470	2	315986	3	-0.95	4.63E+08	0.351
1274.322	228284	1	306757	1	-0.94	4.77E+08	0.281
1274.679	220287	3	298738	2	-0.81	6.45E+08	0.404
1282.872	228807	2	306757	1	-0.67	8.82E+08	0.363
1283.19	225122	5	303053	4	-0.64	9.36E+08	0.769
1286.644	240990	5	318711	4	-0.51	1.23E+09	0.301
1287.089	221971	1	299666	2	-0.82	6.10E+08	0.31
1288.248	219006	2	296631	3	-0.91	4.99E+08	0.479
1288.932	248694	4	326277	3	-0.86	5.49E+08	0.537
1289.381	219074	3	296631	3	-0.77	6.87E+08	0.441
1289.527	214364	4	291912	3	-0.96	4.36E+08	0.353
1301.853	246405	3	323219	3	-0.83	5.80E+08	0.374
1301.985	240990	5	317795	6	-0.82	5.92E+08	0.081
1302.645	221971	1	298738	2	-1	3.93E+08	0.204
1309.528	222582	2	298946	2	-0.95	4.41E+08	0.607
1331.703	246405	3	321497	4	-0.67	8.04E+08	0.536
1338.443	225122	5	299836	4	-0.86	5.18E+08	0.546
1348.69	240990	5	315136	6	-0.79	5.94E+08	0.08
1352.459	214364	4	288304	5	-0.43	1.36E+09	0.33
1352.508	220287	3	294224	4	-0.58	9.66E+08	0.441
1364.543	245366	2	318651	3	-0.74	6.48E+08	0.326
1372.908	219074	3	291912	3	-0.99	3.60E+08	0.603
1383.857	214364	4	286626	4	-0.98	3.66E+08	0.167
1503.459	248694	4	315207	5	-0.82	4.44E+08	0.581

a: Exprimental values taken from [37, 36]

In VII

Energy Levels

Table A22: Comparison between available experimental data and calculated even energy levels (in cm^{-1}) in In VII

E^a_{exp}	E^b_{calc}	ΔE	J	Leading components (in %) in LS coupling ^{c}
0	30	-30	4.5	94.1 $4d^7$ (^{4}F) ^{4}F + 5.6 $4d^7$ (^{2}G) ^{2}G
5736	5757	-21	3.5	98.3 $4d^7$ (^{4}F) ^{4}F
10382	10412	-30	1.5	87.9 $4d^7$ (^{4}F) ^{4}F + 7.5 $4d^7$ (^{2}D) ^{2}D
16903	17056	-153	1.5	60.4 $4d^7$ (^{4}P) ^{4}P + 34.2 $4d^7$ (^{2}P) ^{2}P
18509	18288	221	2.5	94.6 $4d^7$ (^{4}P) ^{4}P
20666	20638	28	4.5	75.8 $4d^7$ (^{2}G) ^{2}G + 18.7 $4d^7$ (^{2}H) ^{2}H + 5.3 $4d^7$ (^{4}F) ^{4}F
21571	21571	0	0.5	82.2 $4d^7$ (^{4}P) ^{4}P + 17.6 $4d^7$ (^{2}P) ^{2}P
26023	25982	41	3.5	95.5 $4d^7$ (^{2}G) ^{2}G
27420	27556	-136	1.5	34.2 $4d^7$ (^{2}P) ^{2}P + 33.9 $4d^7$ (^{4}P) ^{4}P + 22.9 $4d^7$ (^{2}D) ^{2}D
27662	27679	-17	5.5	99.8 $4d^7$ (^{2}H) ^{2}H
30441	30289	152	2.5	71.2 $4d^7$ (^{2}D) ^{2}D + 19.4 $4d^7$ (^{2}D) ^{2}D
33744	33753	-9	4.5	81 $4d^7$ (^{2}H) ^{2}H + 18.4 $4d^7$ (^{2}G) ^{2}G
39221	39235	-14	1.5	58.1 $4d^7$ (^{2}D) ^{2}D + 29.2 $4d^7$ (^{2}P) ^{2}P + 5 $4d^7$ (^{4}P) ^{4}P
41865	41850	15	2.5	95.5 $4d^7$ (^{2}F) ^{2}F
45079	45093	-14	3.5	96.4 $4d^7$ (^{2}F) ^{2}F
66339	66371	-32	1.5	89.8 $4d^7$ (^{2}D) ^{2}D + 9.3 $4d^7$ (^{2}D) ^{2}D

a: From Ryabtsev [38]
b: This work
c: Only the component $\geq$ 5% are given

Table A23: Comparison between available experimental data and calculated odd energy levels (in cm^{-1}) in In VII

E^a_{exp}	E^b_{calc}	ΔE	J	Leading components (in %) in LS coupling ^{c}
347961	347613	348	3.5	44.9 4d^{6}5p (^{5}D) ^{6}F + 21.2 4d^{6}5p (^{5}D) ^{4}D + 16.2 4d^{6}5p (^{5}D) ^{6}P
348264	348164	100	2.5	56.1 4d^{6}5p (^{5}D) ^{6}F + 18.7 4d^{6}5p (^{5}D) ^{4}D + 5.7 4d^{6}5p (^{5}D) ^{4}F
351191	350831	360	4.5	0.1 4d^{6}5p (^{1}G) ^{2}H + 40.4 4d^{6}5p (^{5}D) ^{6}F + 27.5 4d^{6}5p (^{5}D) ^{4}F
353170	354663	-1493	3.5	1.6 4d^{6}5p (^{3}F) ^{4}D + 31.2 4d^{6}5p (^{5}D) ^{6}D + 29.4 4d^{6}5p (^{5}D) ^{6}P
357547	357404	143	3.5	34.8 4d^{6}5p (^{5}D) ^{6}P + 44.3 4d^{6}5p (^{5}D) ^{4}D + 5.3 4d^{6}5p (^{5}D) ^{4}F
358516	358205	311	2.5	19.8 4d^{6}5p (^{5}D) ^{4}D + 30.5 4d^{6}5p (^{5}D) ^{6}P + 17.6 4d^{6}5p (^{5}D) ^{6}D
358496	358361	135	4.5	50 4d^{6}5p (^{5}D) ^{4}F + 42.8 4d^{6}5p (^{5}D) ^{6}F
360085	359956	129	2.5	34.3 4d^{6}5p (^{5}D) ^{6}P + 30.8 4d^{6}5p (^{5}D) ^{4}D + 14.7 4d^{6}5p (^{5}D) ^{4}P
361026	361061	-35	1.5	61.5 4d^{6}5p (^{5}D) ^{4}D + 16.1 4d^{6}5p (^{5}D) ^{6}F
361620	361647	-27	0.5	61.6 4d^{6}5p (^{5}D) ^{4}D + 15.2 4d^{6}5p (^{5}D) ^{6}F + 7.1 4d^{6}5p (^{3}F) ^{4}D
362040	362073	-33	3.5	64.5 4d^{6}5p (^{5}D) ^{4}F + 18.5 4d^{6}5p (^{5}D) ^{6}F + 4.6 4d^{6}5p (^{3}G) ^{4}F
363519	363584	-65	2.5	46.5 4d^{6}5p (^{5}D) ^{4}P + 20.2 4d^{6}5p (^{5}D) ^{4}F + 16.3 4d^{6}5p (^{5}D) ^{6}P
363801	363757	44	3.5	13.9 4d^{6}5p (^{5}D) ^{4}D + 13.8 4d^{6}5p (^{3}H) ^{4}H + 12.4 4d^{6}5p (^{3}H) ^{2}G
363857	363941	-84	2.5	47.1 4d^{6}5p (^{5}D) ^{4}F + 18 4d^{6}5p (^{5}D) ^{4}P + 10.5 4d^{6}5p (^{5}D) ^{6}F
365647	365754	-107	1.5	76.7 4d^{6}5p (^{5}D) ^{4}F + 4 4d^{6}5p (^{3}G) ^{4}F
367434	367200	234	5.5	51.5 4d^{6}5p (^{3}H) ^{4}G + 13.7 4d^{6}5p (^{3}G) ^{4}G + 9.9 4d^{6}5p (^{3}H) ^{4}I
367647	367427	220	1.5	71.6 4d^{6}5p (^{5}D) ^{4}P + 8.4 4d^{6}5p (^{3}P) ^{4}P + 5.1 4d^{6}5p (^{3}P) ^{4}S
367590	367513	77	4.5	26.6 4d^{6}5p (^{3}H) ^{4}G + 15 4d^{6}5p (^{3}H) ^{2}G + 13.8 4d^{6}5p (^{3}G) ^{4}F
367570	367664	-94	0.5	83.8 4d^{6}5p (^{5}D) ^{4}P + 5.7 4d^{6}5p (^{5}D) ^{6}D
367959	368218	-259	2.5	14.9 4d^{6}5p (^{3}P) ^{4}D + 9.4 4d^{6}5p (^{5}D) ^{4}D + 9 4d^{6}5p (^{5}D) ^{4}F
368796	368873	-77	3.5	31.2 4d^{6}5p (^{3}F) ^{4}G + 12.5 4d^{6}5p (^{3}G) ^{4}H + 11 4d^{6}5p (^{3}H) ^{4}G
368956	369089	-133	2.5	37.4 4d^{6}5p (^{3}F) ^{4}G + 8.3 4d^{6}5p (^{3}F) ^{4}F + 7.2 4d^{6}5p (^{3}H) ^{4}G
371041	370999	42	4.5	42.7 4d^{6}5p (^{3}H) ^{4}I + 10.5 4d^{6}5p (^{3}G) ^{4}G + 10.1 4d^{6}5p (^{3}F) ^{4}F
371496	371628	-132	1.5	39.6 4d^{6}5p (^{3}F) ^{4}F + 22.2 4d^{6}5p (^{3}D) ^{4}F + 11 4d^{6}5p (^{3}F) ^{2}D
371734	371749	-15	3.5	26.5 4d^{6}5p (^{3}H) ^{4}H + 20.5 4d^{6}5p (^{3}F) ^{4}D + 9.1 4d^{6}5p (^{3}G) ^{4}H
374317	374228	89	3.5	14.8 4d^{6}5p (^{3}D) ^{4}F + 25.6 4d^{6}5p (^{3}H) ^{4}G + 9.4 4d^{6}5p (^{3}G) ^{4}F
374461	374486	-25	4.5	12.1 4d^{6}5p (^{3}H) ^{2}G + 16 4d^{6}5p (^{3}H) ^{4}G + 15 4d^{6}5p (^{3}H) ^{4}I
374950	374947	3	5.5	42.1 4d^{6}5p (^{3}H) ^{4}I + 26.8 4d^{6}5p (^{3}G) ^{4}G + 8.6 4d^{6}5p (^{3}G) ^{4}H
376194	376071	123	4.5	15.5 4d^{6}5p (^{3}H) ^{4}H + 18 4d^{6}5p (^{3}H) ^{4}G + 13.9 4d^{6}5p (^{3}G) ^{4}F
376235	376181	54	3.5	23.9 4d^{6}5p (^{3}G) ^{4}H + 22.6 4d^{6}5p (^{3}F) ^{4}D + 12.6 4d^{6}5p (^{3}D) ^{4}D
376198	376272	-74	2.5	14.8 4d^{6}5p (^{3}P) ^{4}P + 9.7 4d^{6}5p (^{3}P) ^{4}P + 9 4d^{6}5p (^{3}D) ^{4}P
376936	376680	256	4.5	26.1 4d^{6}5p (^{3}G) ^{4}F + 12.5 4d^{6}5p (^{3}F) ^{4}F + 8.7 4d^{6}5p (^{3}F) ^{4}F
377141	377057	84	2.5	25.4 4d^{6}5p (^{3}F) ^{4}D + 18.5 4d^{6}5p (^{3}D) ^{4}D + 12.7 4d^{6}5p (^{3}D) ^{4}F
377145	377224	-79	5.5	19.6 4d^{6}5p (^{3}F) ^{4}G + 26.1 4d^{6}5p (^{3}H) ^{2}I + 18.5 4d^{6}5p (^{3}G) ^{2}H
377189	377287	-98	6.5	36.9 4d^{6}5p (^{3}H) ^{2}I + 27.8 4d^{6}5p (^{3}G) ^{4}H + 25.9 4d^{6}5p (^{3}H) ^{4}H
377873	377913	-40	3.5	36.2 4d^{6}5p (^{3}G) ^{4}G + 15.6 4d^{6}5p (^{3}F) ^{4}G + 9.2 4d^{6}5p (^{3}H) ^{2}G
378221	378251	-30	3.5	38.9 4d^{6}5p (^{3}P) ^{4}D + 17.6 4d^{6}5p (^{3}P) ^{4}D + 11.5 4d^{6}5p (^{3}F) ^{4}F
378650	378627	23	4.5	16.2 4d^{6}5p (^{3}G) ^{4}G + 18.2 4d^{6}5p (^{3}F) ^{4}G + 9.4 4d^{6}5p (^{3}H) ^{2}G
378630	378663	-33	2.5	32.7 4d^{6}5p (^{3}G) ^{4}G + 10.4 4d^{6}5p (^{3}F) ^{4}D + 7.6 4d^{6}5p (^{3}P) ^{4}P
378726	378735	-9	1.5	7.3 4d^{6}5p (^{3}P) ^{4}D + 14 4d^{6}5p (^{3}F) ^{4}D + 13.8 4d^{6}5p (^{3}D) ^{4}D
378995	379131	-136	5.5	40.4 4d^{6}5p (^{3}H) ^{4}H + 19.9 4d^{6}5p (^{3}G) ^{2}H + 13.6 4d^{6}5p (^{1}I) ^{2}H
380519	380331	188	3.5	28.9 4d^{6}5p (^{3}G) ^{4}F + 11.1 4d^{6}5p (^{3}P) ^{4}D + 10.2 4d^{6}5p (^{3}F) ^{4}G
380707	380770	-63	0.5	5.6 4d^{6}5p (^{1}S) ^{2}P + 20 4d^{6}5p (^{3}F) ^{4}D + 14.3 4d^{6}5p (^{3}P) ^{4}D
381246	381010	236	2.5	21.7 4d^{6}5p (^{3}G) ^{4}F + 21.7 4d^{6}5p (^{3}H) ^{4}G + 11.5 4d^{6}5p (^{3}F) ^{4}F
382193	382187	6	5.5	9.3 4d^{6}5p (^{1}I) ^{2}H + 14.2 4d^{6}5p (^{3}H) ^{4}H + 13.5 4d^{6}5p (^{3}F) ^{4}G
382010	382270	-260	1.5	14.5 4d^{6}5p (^{3}P) ^{4}S + 16.6 4d^{6}5p (^{3}P) ^{2}P + 10.1 4d^{6}5p (^{3}P) ^{4}D
382362	382336	26	4.5	19.8 4d^{6}5p (^{3}G) ^{2}H + 15.2 4d^{6}5p (^{3}F) ^{4}G + 8.3 4d^{6}5p (^{3}G) ^{2}G
382111	382521	-410	0.5	40.9 4d^{6}5p (^{3}P) ^{2}S + 14.9 4d^{6}5p (^{3}D) ^{2}P + 13.1 4d^{6}5p (^{3}P) ^{4}P
383254	383192	62	2.5	22.8 4d^{6}5p (^{3}H) ^{4}G + 17.2 4d^{6}5p (^{3}D) ^{4}F + 14.5 4d^{6}5p (^{3}D) ^{4}P
383076	383296	-220	6.5	74 4d^{6}5p (^{1}I) ^{2}K + 11 4d^{6}5p (^{1}I) ^{2}I + 8.8 4d^{6}5p (^{3}H) ^{2}I
383934	383858	76	2.5	15.9 4d^{6}5p (^{3}D) ^{4}P + 11.4 4d^{6}5p (^{3}G) ^{4}F + 9.9 4d^{6}5p (^{3}P) ^{4}P
384525	384626	-101	4.5	27.9 4d^{6}5p (^{3}G) ^{4}H + 26.9 4d^{6}5p (^{3}H) ^{4}H + 20.5 4d^{6}5p (^{3}H) ^{2}G
384701	384766	-65	2.5	7.1 4d^{6}5p (^{1}D) ^{2}F + 13.4 4d^{6}5p (^{3}D) ^{4}P + 9.2 4d^{6}5p (^{3}F) ^{2}F
384721	384811	-90	5.5	23 4d^{6}5p (^{3}H) ^{2}I + 17.3 4d^{6}5p (^{1}I) ^{2}H + 15.6 4d^{6}5p (^{3}G) ^{4}H
384926	384879	47	3.5	30.6 4d^{6}5p (^{3}H) ^{4}G + 13 4d^{6}5p (^{3}D) ^{4}F + 8.5 4d^{6}5p (^{3}H) ^{4}H
385231	385587	-356	3.5	29.5 4d^{6}5p (^{3}F) ^{2}G + 15 4d^{6}5p (^{3}H) ^{2}G + 9.7 4d^{6}5p (^{3}F) ^{2}G
385902	385698	204	5.5	23.6 4d^{6}5p (^{3}G) ^{4}G + 13.6 4d^{6}5p (^{3}G) ^{4}H + 12.8 4d^{6}5p (^{3}H) ^{2}I
385876	385731	145	1.5	25.3 4d^{6}5p (^{3}F) ^{4}D + 14.7 4d^{6}5p (^{3}D) ^{2}P + 9.9 4d^{6}5p (^{3}D) ^{4}P
385749	385753	-4	0.5	29.5 4d^{6}5p (^{3}D) ^{4}P + 24.4 4d^{6}5p (^{3}P) ^{4}D + 14.6 4d^{6}5p (^{3}P) ^{2}S
385969	385869	100	4.5	19.3 4d^{6}5p (^{3}H) ^{2}H + 8.6 4d^{6}5p (^{3}F) ^{4}F + 7.6 4d^{6}5p (^{3}G) ^{4}G
386607	386674	-67	2.5	12.7 4d^{6}5p (^{3}F) ^{2}F + 13.3 4d^{6}5p (^{3}G) ^{4}G + 12.5 4d^{6}5p (^{3}G) ^{2}F
386775	386860	-85	3.5	19.1 4d^{6}5p (^{3}H) ^{2}G + 13.5 4d^{6}5p (^{3}G) ^{4}G + 12.1 4d^{6}5p (^{3}F) ^{2}F
387346	387011	335	1.5	18.7 4d^{6}5p (^{3}F) ^{2}D + 12.8 4d^{6}5p (^{3}F) ^{4}F + 9.7 4d^{6}5p (^{3}P) ^{4}P
387444	387232	212	4.5	15.3 4d^{6}5p (^{3}F) ^{4}G + 16.9 4d^{6}5p (^{3}G) ^{4}G + 14.6 4d^{6}5p (^{3}H) ^{4}G
387772	387685	87	3.5	9.4 4d^{6}5p (^{3}F) ^{4}F + 20.3 4d^{6}5p (^{3}D) ^{2}F + 15.9 4d^{6}5p (^{3}F) ^{2}G
388005	388100	-95	2.5	27.1 4d^{6}5p (^{3}F) ^{2}D + 10.5 4d^{6}5p (^{3}F) ^{4}F + 8 4d^{6}5p (^{3}G) ^{4}F
388322	388304	18	4.5	27.2 4d^{6}5p (^{3}F) ^{2}G + 24.1 4d^{6}5p (^{1}G) ^{2}H + 19 4d^{6}5p (^{1}I) ^{2}H
389002	389085	-83	2.5	8.9 4d^{6}5p (^{3}P) ^{2}D + 16.3 4d^{6}5p (^{3}F) ^{2}D + 14.3 4d^{6}5p (^{3}P) ^{4}D
389679	389733	-54	5.5	43.6 4d^{6}5p (^{3}H) ^{2}H + 24.6 4d^{6}5p (^{1}I) ^{2}H + 9.9 4d^{6}5p (^{3}G) ^{4}H
390689	390618	71	3.5	24.4 4d^{6}5p (^{3}G) ^{2}G + 14 4d^{6}5p (^{1}G) ^{2}F + 11 4d^{6}5p (^{3}G) ^{4}H
391658	391687	-29	1.5	10.2 4d^{6}5p (^{3}P) ^{2}D + 12.7 4d^{6}5p (^{3}G) ^{4}F + 9.8 4d^{6}5p (^{3}D) ^{4}D
391912	391947	-35	5.5	30.7 4d^{6}5p (^{3}G) ^{2}H + 19.5 4d^{6}5p (^{3}H) ^{2}H + 14.1 4d^{6}5p (^{3}G) ^{4}H
392432	392337	95	2.5	24.6 4d^{6}5p (^{3}D) ^{4}D + 12.2 4d^{6}5p (^{1}F) ^{2}D + 11.5 4d^{6}5p (^{3}F) ^{4}D
392332	392475	-143	1.5	8.7 4d^{6}5p (^{1}D) ^{2}P + 14.4 4d^{6}5p (^{3}D) ^{4}D + 8.9 4d^{6}5p (^{3}F) ^{4}D
392612	392571	41	3.5	15.2 4d^{6}5p (^{1}G) ^{2}G + 18.2 4d^{6}5p (^{3}G) ^{2}F + 11.5 4d^{6}5p (^{3}G) ^{4}F
393179	393162	17	4.5	26 4d^{6}5p (^{3}G) ^{2}G + 26.3 4d^{6}5p (^{3}G) ^{2}H + 11.6 4d^{6}5p (^{3}G) ^{4}H
393202	393170	32	3.5	27.2 4d^{6}5p (^{1}F) ^{2}G + 12.4 4d^{6}5p (^{1}G) ^{2}F + 11.4 4d^{6}5p (^{3}F) ^{2}F
393373	393526	-153	2.5	7.3 4d^{6}5p (^{3}D) ^{4}F + 18.1 4d^{6}5p (^{3}G) ^{4}F + 13.7 4d^{6}5p (^{3}F) ^{4}D
393595	393688	-93	1.5	26.7 4d^{6}5p (^{3}D) ^{2}P + 17.5 4d^{6}5p (^{3}G) ^{4}F + 7.7 4d^{6}5p (^{3}P) ^{2}D
394009	393815	194	3.5	19.2 4d^{6}5p (^{3}D) ^{4}D + 25.7 4d^{6}5p (^{3}D) ^{4}F + 5.4 4d^{6}5p (^{3}G) ^{4}F
394078	393917	161	4.5	0.4 4d^{6}5p (^{5}D) ^{6}F + 31.5 4d^{6}5p (^{3}D) ^{4}F + 14 4d^{6}5p (^{3}G) ^{2}G
394267	394151	116	2.5	11.5 4d^{6}5p (^{3}D) ^{2}F + 16.3 4d^{6}5p (^{3}G) ^{4}F + 15.9 4d^{6}5p (^{3}D) ^{4}F
394901	395136	-235	0.5	4.6 4d^{6}5p (^{3}D) ^{4}D + 24.6 4d^{6}5p (^{3}D) ^{4}P + 16.1 4d^{6}5p (^{3}P) ^{2}S
395387	395477	-90	2.5	2.7 4d^{6}5p (^{1}F) ^{2}D + 25.4 4d^{6}5p (^{3}D) ^{2}D + 20.4 4d^{6}5p (^{3}D) ^{2}F
396039	395870	169	4.5	31.3 4d^{6}5p (^{3}D) ^{4}F + 16.3 4d^{6}5p (^{3}H) ^{2}H + 12.9 4d^{6}5p (^{3}G) ^{2}G
396255	396329	-74	1.5	10.1 4d^{6}5p (^{3}P) ^{2}P + 22.8 4d^{6}5p (^{1}D) ^{2}D + 12.4 4d^{6}5p (^{1}D) ^{2}P
396772	396758	14	3.5	0.6 4d^{6}5p (^{3}P) ^{4}D + 20.9 4d^{6}5p (^{1}G) ^{2}G + 11.8 4d^{6}5p (^{1}D) ^{2}F
397464	397152	312	3.5	30.5 4d^{6}5p (^{3}D) ^{2}F + 19.6 4d^{6}5p (^{3}D) ^{4}D + 12 4d^{6}5p (^{3}F) ^{4}D
397273	397305	-32	2.5	27 4d^{6}5p (^{3}G) ^{2}F + 24.5 4d^{6}5p (^{3}F) ^{2}F + 11.2 4d^{6}5p (^{3}D) ^{2}F
397612	397723	-111	4.5	47.8 4d^{6}5p (^{1}I) ^{2}H + 17.6 4d^{6}5p (^{3}G) ^{2}H + 8.1 4d^{6}5p (^{3}F) ^{2}G
397953	397980	-27	5.5	64.2 4d^{6}5p (^{1}I) ^{2}I + 9.5 4d^{6}5p (^{1}I) ^{2}H + 8.3 4d^{6}5p (^{3}H) ^{2}H
398110	398173	-63	6.5	83.4 4d^{6}5p (^{1}I) ^{2}I + 11.5 4d^{6}5p (^{1}I) ^{2}K + 3.9 4d^{6}5p (^{3}H) ^{4}H

Table A23: Continued

E^a_{exp}	E^b_{calc}	ΔE	J	Leading components (in %) in LS coupling ^{c}
398952	398896	56	2.5	36.9 4d^{6}5p (^{3}D) ^{2}D + 9 4d^{6}5p (^{1}D) ^{2}F + 8.9 4d^{6}5p (^{1}F) ^{2}D
399514	399439	75	1.5	15.9 4d^{6}5p (^{3}P) ^{4}D + 13.5 4d^{6}5p (^{1}S) ^{2}P + 12.7 4d^{6}5p (^{3}D) ^{2}D
400183	400010	173	4.5	34.3 4d^{6}5p (^{1}G) ^{2}G + 23.2 4d^{6}5p (^{3}H) ^{2}H + 8.6 4d^{6}5p (^{1}G) ^{2}H
400538.4	400349	189.4	5.5	47.6 4d^{6}5p (^{1}G) ^{2}H + 24 4d^{6}5p (^{1}G) ^{2}H + 8.4 4d^{6}5p (^{3}F) ^{4}G
400870	400764	106	3.5	5.8 4d^{6}5p (^{1}G) ^{2}F + 24.2 4d^{6}5p (^{3}G) ^{2}G + 14.2 4d^{6}5p (^{1}F) ^{2}G
401788	401778	10	3.5	43.6 4d^{6}5p (^{3}F) ^{4}D + 13.7 4d^{6}5p (^{3}P) ^{4}D + 10.8 4d^{6}5p (^{3}G) ^{2}F
404002	403760	242	2.5	24.9 4d^{6}5p (^{1}G) ^{2}F + 15.2 4d^{6}5p (^{3}D) ^{2}F + 11.3 4d^{6}5p (^{1}G) ^{2}F
404466	404396	70	4.5	53.9 4d^{6}5p (^{1}F) ^{2}G + 17.5 4d^{6}5p (^{3}F) ^{4}G + 3.5 4d^{6}5p (^{3}F) ^{4}G
404853	404799	54	1.5	22.5 4d^{6}5p (^{1}D) ^{2}D + 17.6 4d^{6}5p (^{3}P) ^{4}D + 10.4 4d^{6}5p (^{1}D) ^{2}P
405249	405005	244	1.5	19.7 4d^{6}5p (^{1}S) ^{2}P + 13.6 4d^{6}5p (^{3}P) ^{2}D + 13.3 4d^{6}5p (^{3}P) ^{4}S
406806	407182	-376	3.5	30.4 4d^{6}5p (^{1}D) ^{2}F + 12 4d^{6}5p (^{1}G) ^{2}F + 10.4 4d^{6}5p (^{3}F) ^{4}D
407640	407442	198	2.5	46.3 4d^{6}5p (^{3}F) ^{4}G + 13.2 4d^{6}5p (^{1}F) ^{2}F + 7.2 4d^{6}5p (^{1}F) ^{2}D
408551	408601	-50	3.5	41 4d^{6}5p (^{1}F) ^{2}F + 13.7 4d^{6}5p (^{1}D) ^{2}F + 11.7 4d^{6}5p (^{1}G) ^{2}F
408655	408914	-259	1.5	40.1 4d^{6}5p (^{1}F) ^{2}D + 7.3 4d^{6}5p (^{3}F) ^{4}F + 5.8 4d^{6}5p (^{3}P) ^{4}D
409420	409438	-18	4.5	34.1 4d^{6}5p (^{3}F) ^{2}G + 20.1 4d^{6}5p (^{1}F) ^{2}G + 13.4 4d^{6}5p (^{3}F) ^{4}G
410057	410015	42	2.5	38.9 4d^{6}5p (^{1}F) ^{2}F + 14.4 4d^{6}5p (^{3}F) ^{4}G + 9 4d^{6}5p (^{1}F) ^{2}D
411076	411035	41	3.5	50.5 4d^{6}5p (^{3}F) ^{4}G + 8.6 4d^{6}5p (^{1}F) ^{2}G + 6.5 4d^{6}5p (^{3}F) ^{4}G
413681	413798	-117	1.5	26 4d^{6}5p (^{3}P) ^{4}S + 24.3 4d^{6}5p (^{3}F) ^{2}D + 9 4d^{6}5p (^{1}D) ^{2}D
416462	416141	321	1.5	32.3 4d^{6}5p (^{3}P) ^{4}P + 18.7 4d^{6}5p (^{3}P) ^{4}S + 11.4 4d^{6}5p (^{1}S) ^{2}P
416206	416271	-65	2.5	19.6 4d^{6}5p (^{3}F) ^{4}F + 17.2 4d^{6}5p (^{3}P) ^{4}D + 9.7 4d^{6}5p (^{3}F) ^{4}D
417097	416997	100	0.5	49.4 4d^{6}5p (^{3}F) ^{4}D + 15.8 4d^{6}5p (^{3}P) ^{2}S + 7.6 4d^{6}5p (^{3}P) ^{4}P
417531	417640	-109	3.5	33.9 4d^{6}5p (^{3}F) ^{4}F + 12.2 4d^{6}5p (^{1}G) ^{2}F + 11.1 4d^{6}5p (^{1}G) ^{2}G
417677	417926	-249	2.5	9.2 4d^{6}5p (^{3}P) ^{4}P + 30.4 4d^{6}5p (^{3}P) ^{2}D + 14.5 4d^{6}5p (^{3}P) ^{2}D
418393	418439	-46	1.5	21.8 4d^{6}5p (^{3}P) ^{2}D + 17.1 4d^{6}5p (^{3}F) ^{4}F + 14.2 4d^{6}5p (^{3}F) ^{4}D
419771	419942	-171	3.5	43.9 4d^{6}5p (^{3}F) ^{2}G + 17.9 4d^{6}5p (^{1}G) ^{2}F + 5.9 4d^{6}5p (^{1}F) ^{2}F
420288	420263	25	4.5	26.2 4d^{6}5p (^{1}G) ^{2}H + 19 4d^{6}5p (^{3}F) ^{4}F + 13.2 4d^{6}5p (^{1}G) ^{2}H
420923	420518	405	1.5	25 4d^{6}5p (^{3}F) ^{4}D + 21 4d^{6}5p (^{3}P) ^{2}D + 10.6 4d^{6}5p (^{3}F) ^{2}D
421363	421296	67	2.5	45.2 4d^{6}5p (^{3}F) ^{2}D + 14.1 4d^{6}5p (^{3}F) ^{4}F + 10.9 4d^{6}5p (^{3}P) ^{4}P
421229	421329	-100	3.5	2.8 4d^{6}5p (^{1}G) ^{2}F + 22.6 4d^{6}5p (^{3}F) ^{2}G + 20.2 4d^{6}5p (^{3}P) ^{4}D
422052	422076	-24	2.5	22.7 4d^{6}5p (^{3}F) ^{4}D + 21.4 4d^{6}5p (^{3}F) ^{4}F + 7.7 4d^{6}5p (^{3}P) ^{4}D
423109	423090	19	4.5	37.9 4d^{6}5p (^{3}F) ^{4}F + 30 4d^{6}5p (^{3}F) ^{2}G + 13.3 4d^{6}5p (^{3}F) ^{4}F
424983	425071	-88	3.5	26 4d^{6}5p (^{3}F) ^{2}F + 19.5 4d^{6}5p (^{1}G) ^{2}G + 11.7 4d^{6}5p (^{3}P) ^{4}D
426759	426604	155	2.5	14.2 4d^{6}5p (^{3}P) ^{2}D + 14.5 4d^{6}5p (^{1}G) ^{2}F + 13 4d^{6}5p (^{3}P) ^{4}P
427084	427113	-29	2.5	46.7 4d^{6}5p (^{3}F) ^{2}F + 12.6 4d^{6}5p (^{3}F) ^{2}F + 7 4d^{6}5p (^{3}P) ^{2}D
427155	427549	-394	5.5	60.9 4d^{6}5p (^{1}G) ^{2}H + 28.9 4d^{6}5p (^{1}G) ^{2}H
430363	430560	-197	4.5	55.9 4d^{6}5p (^{1}G) ^{2}G + 15.6 4d^{6}5p (^{1}G) ^{2}G + 8.5 4d^{6}5p (^{1}G) ^{2}H
432957	432999	-42	3.5	9.6 4d^{6}5p (^{3}F) ^{2}F + 19.7 4d^{6}5p (^{3}F) ^{2}F + 18.5 4d^{6}5p (^{1}G) ^{2}G
436247	436217	30	1.5	66.6 4d^{6}5p (^{1}D) ^{2}D + 9.8 4d^{6}5p (^{1}D) ^{2}P + 6.8 4d^{6}5p (^{1}D) ^{2}D
447561	447476	85	2.5	46.7 4d^{6}5p (^{1}D) ^{2}F + 24.1 4d^{6}5p (^{1}D) ^{2}D + 12.5 4d^{6}5p (^{1}D) ^{2}F

a: From Ryabtsev [38]
b: This work
c: Only the component $\geq$ 5% are given

Transitions

Table A24: Computed oscillator strengths and transition probabilities in In VII.

Wavelength Å	Lower Level[a] cm^{-1}	J_{Low}	Upper level[a] cm^{-1}	J_{Up}	log gf	gA s^{-1}	CF
248.323	27662	5.5	430363	4.5	-0.54	3.14E+10	0.241
248.458	45079	3.5	447561	2.5	-0.94	1.24E+10	0.275
250.493	33744	4.5	432957	3.5	-0.52	3.25E+10	0.185
251.286	18509	2.5	416462	1.5	-0.87	1.43E+10	0.2
252.878	27662	5.5	423109	4.5	-0.4	4.15E+10	0.275
253.561	41865	2.5	436247	1.5	-0.64	2.38E+10	0.406
255.598	33744	4.5	424983	3.5	-0.58	2.68E+10	0.24
257.502	16903	1.5	405249	1.5	-0.97	1.07E+10	0.179
258.075	33744	4.5	421229	3.5	-0.56	2.78E+10	0.174
258.572	18509	2.5	405249	1.5	-0.73	1.86E+10	0.512
259.049	33744	4.5	419771	3.5	-0.42	3.79E+10	0.219
259.549	45079	3.5	430363	4.5	-0.37	4.22E+10	0.682
259.929	0	4.5	384721	5.5	-0.78	1.63E+10	0.239
260.666	8699	2.5	392332	1.5	-0.95	1.09E+10	0.17
260.907	18509	2.5	401788	3.5	-0.39	4.03E+10	0.581
260.915	5736	3.5	389002	2.5	-0.67	2.12E+10	0.408
260.951	10382	1.5	393595	1.5	-0.87	1.33E+10	0.149
261.532	0	4.5	382362	4.5	-0.75	1.74E+10	0.23
261.946	27662	5.5	409420	4.5	0.04	1.06E+11	0.621
261.98	5736	3.5	387444	4.5	-0.7	1.94E+10	0.15
261.984	39221	1.5	420923	1.5	-0.51	3.00E+10	0.326
262.277	10382	1.5	391658	1.5	-0.89	1.24E+10	0.132
262.305	27420	1.5	408655	1.5	-0.87	1.31E+10	0.118
262.948	8699	2.5	389002	2.5	-0.74	1.77E+10	0.311
263.017	20666	4.5	400870	3.5	-0.98	1.01E+10	0.036
263.028	41865	2.5	422052	2.5	-0.93	1.12E+10	0.239
263.224	45079	3.5	424983	3.5	-0.58	2.53E+10	0.356
263.493	20666	4.5	400183	4.5	-0.71	1.88E+10	0.064
263.812	41865	2.5	420923	1.5	-0.73	1.79E+10	0.315
263.856	0	4.5	378995	5.5	-0.9	1.20E+10	0.546
263.884	18509	2.5	397464	3.5	-0.39	3.92E+10	0.582
264.366	18509	2.5	396772	3.5	-0.98	9.90E+09	0.394
264.396	0	4.5	378221	3.5	-0.07	8.22E+10	0.701
264.412	5736	3.5	383934	2.5	-0.88	1.27E+10	0.319
264.473	30441	2.5	408551	3.5	-0.51	2.96E+10	0.296
264.529	45079	3.5	423109	4.5	-0.85	1.35E+10	0.592
264.565	26023	3.5	404002	2.5	-0.3	4.76E+10	0.374
264.616	41865	2.5	419771	3.5	-0.86	1.30E+10	0.324
265.019	33744	4.5	411076	3.5	-0.51	2.92E+10	0.465
265.05	20666	4.5	397953	5.5	-0.97	1.02E+10	0.068
265.128	8699	2.5	385876	1.5	-0.97	1.01E+10	0.197
265.15	0	4.5	377145	5.5	-0.56	2.64E+10	0.715
265.277	10382	1.5	387346	1.5	-0.95	1.07E+10	0.243
265.297	0	4.5	376936	4.5	-0.08	7.96E+10	0.44
265.39	27662	5.5	404466	4.5	-0.04	8.66E+10	0.579
265.394	20666	4.5	397464	3.5	-0.63	2.21E+10	0.135
265.546	27420	1.5	404002	2.5	-0.74	1.71E+10	0.183
265.584	41865	2.5	418393	1.5	-0.86	1.32E+10	0.168
265.791	0	4.5	376235	3.5	-0.77	1.61E+10	0.253
265.797	8699	2.5	384926	3.5	-0.28	4.98E+10	0.415
265.798	10382	1.5	386607	2.5	-0.91	1.17E+10	0.176
265.82	0	4.5	376194	4.5	-0.59	2.44E+10	0.22
265.882	20666	4.5	396772	3.5	-0.72	1.78E+10	0.097
266.291	16903	1.5	392432	2.5	-0.83	1.38E+10	0.125
266.304	5736	3.5	381246	2.5	-0.76	1.63E+10	0.556
266.362	16903	1.5	392332	1.5	-0.86	1.31E+10	0.15
266.5	8699	2.5	383934	2.5	-0.85	1.32E+10	0.144
266.702	0	4.5	374950	5.5	-0.94	1.07E+10	0.319
266.821	5736	3.5	380519	3.5	0.15	1.33E+11	0.799
266.886	45079	3.5	419771	3.5	-0.79	1.52E+10	0.143
267.051	0	4.5	374461	4.5	-0.81	1.45E+10	0.187
267.153	0	4.5	374317	3.5	-0.97	9.92E+09	0.176
267.265	26023	3.5	400183	4.5	-0.81	1.46E+10	0.161
267.435	18509	2.5	392432	2.5	-0.42	3.55E+10	0.496
267.7	10382	1.5	383934	2.5	-0.85	1.31E+10	0.214
267.801	20666	4.5	394078	4.5	-0.73	1.74E+10	0.074
267.85	20666	4.5	394009	3.5	-0.16	6.51E+10	0.533
267.873	8699	2.5	382010	1.5	-0.93	1.11E+10	0.237
268.052	33744	4.5	406806	3.5	-0.79	1.52E+10	0.161
268.148	26023	3.5	398952	2.5	-1	9.35E+09	0.154
268.158	5736	3.5	378650	4.5	-0.9	1.16E+10	0.231
268.189	10382	1.5	383254	2.5	-0.38	3.88E+10	0.556
268.386	45079	3.5	417677	2.5	0.02	9.72E+10	0.651
268.423	8699	2.5	381246	2.5	-0.18	6.12E+10	0.564
268.43	20666	4.5	393202	3.5	-0.21	5.73E+10	0.306
268.447	20666	4.5	393179	4.5	-0.51	2.87E+10	0.121
268.491	45079	3.5	417531	3.5	-0.61	2.30E+10	0.282
268.746	16903	1.5	389002	2.5	-0.92	1.10E+10	0.099
268.856	20666	4.5	392612	3.5	-0.89	1.20E+10	0.086
268.95	41865	2.5	413681	1.5	-0.37	3.90E+10	0.625
269.01	0	4.5	371734	3.5	-0.27	4.99E+10	0.481
269.115	26023	3.5	397612	4.5	-0.57	2.46E+10	0.15
269.222	26023	3.5	397464	3.5	-0.51	2.82E+10	0.33
269.248	5736	3.5	377141	2.5	-0.15	6.57E+10	0.587
269.36	26023	3.5	397273	2.5	-0.02	8.88E+10	0.325
269.363	20666	4.5	391912	5.5	-0.66	2.03E+10	0.197
269.397	5736	3.5	376936	4.5	-0.24	5.28E+10	0.747
269.45	45079	3.5	416206	2.5	-0.71	1.81E+10	0.385
269.468	16903	1.5	388005	2.5	-0.95	1.02E+10	0.156
269.661	39221	1.5	410057	2.5	-0.8	1.47E+10	0.176
269.911	18509	2.5	389002	2.5	-0.71	1.81E+10	0.277
269.936	5736	3.5	376194	4.5	-0.25	5.20E+10	0.472
269.943	27662	5.5	398110	6.5	-0.05	8.15E+10	0.716
270.033	10382	1.5	380707	0.5	-0.31	4.47E+10	0.772
270.251	8699	2.5	378726	1.5	-0.06	7.96E+10	0.774
270.253	20666	4.5	390689	3.5	-0.79	1.47E+10	0.08

Table A24: Continued

Wavelength	Lower Level	J_{Low}	Upper level	J_{Up}	log gf	gA	CF
270.337	66339	1.5	436247	1.5	-0.18	6.00E+10	0.665
270.62	8699	2.5	378221	3.5	-0.82	1.38E+10	0.336
270.684	39221	1.5	408655	1.5	-0.52	2.75E+10	0.229
270.736	26023	3.5	395387	2.5	-0.18	6.09E+10	0.528
270.81	18509	2.5	387772	3.5	-0.86	1.26E+10	0.547
270.875	8699	2.5	377873	3.5	-0.24	5.20E+10	0.746
270.949	30441	2.5	399514	1.5	-0.32	4.40E+10	0.492
271.023	16903	1.5	385876	1.5	-1	9.04E+09	0.104
271.116	16903	1.5	385749	0.5	-0.85	1.28E+10	0.3
271.124	27420	1.5	396255	1.5	-0.84	1.31E+10	0.106
271.153	0	4.5	368796	3.5	-0.91	1.11E+10	0.39
271.205	5736	3.5	374461	4.5	-0.36	3.98E+10	0.61
271.311	5736	3.5	374317	3.5	-0.6	2.26E+10	0.233
271.362	30441	2.5	398952	2.5	0.06	1.04E+11	0.607
271.413	8699	2.5	377141	2.5	-0.62	2.16E+10	0.315
271.461	27662	5.5	396039	4.5	-0.45	3.23E+10	0.441
271.556	10382	1.5	378630	2.5	-0.43	3.38E+10	0.503
271.559	26023	3.5	394267	2.5	-0.51	2.80E+10	0.369
271.597	41865	2.5	410057	2.5	-0.16	6.30E+10	0.55
271.707	33744	4.5	401788	3.5	-0.3	4.56E+10	0.502
271.749	26023	3.5	394009	3.5	-0.93	1.06E+10	0.245
271.888	16903	1.5	384701	2.5	-0.7	1.78E+10	0.258
271.993	20666	4.5	388322	4.5	0.03	9.59E+10	0.503
272.042	0	4.5	367590	4.5	0.08	1.07E+11	0.762
272.082	8699	2.5	376235	3.5	-0.85	1.28E+10	0.404
272.123	27420	1.5	394901	0.5	-0.71	1.78E+10	0.242
272.158	0	4.5	367434	5.5	0.27	1.69E+11	0.803
272.364	26023	3.5	393179	4.5	-0.84	1.31E+10	0.179
272.386	33744	4.5	400870	3.5	0.11	1.16E+11	0.468
272.401	20666	4.5	387772	3.5	-0.35	4.00E+10	0.271
272.457	16903	1.5	383934	2.5	-0.65	2.02E+10	0.254
272.593	27420	1.5	394267	2.5	-0.98	9.36E+09	0.121
272.636	41865	2.5	408655	1.5	-0.93	1.06E+10	0.149
272.785	26023	3.5	392612	3.5	-0.05	7.94E+10	0.584
272.897	33744	4.5	400183	4.5	-0.06	7.79E+10	0.297
272.913	18509	2.5	384926	3.5	-0.75	1.60E+10	0.548
272.914	27662	5.5	394078	4.5	-0.19	5.83E+10	0.442
272.977	30441	2.5	396772	3.5	-0.74	1.62E+10	0.179
273.081	18509	2.5	384701	2.5	-0.92	1.07E+10	0.166
273.143	20666	4.5	386775	3.5	-0.18	5.94E+10	0.369
273.226	45079	3.5	411076	3.5	-0.43	3.36E+10	0.636
273.226	5736	3.5	371734	3.5	-0.89	1.16E+10	0.209
273.259	27420	1.5	393373	2.5	-0.62	2.16E+10	0.237
273.361	10382	1.5	376198	2.5	-0.83	1.34E+10	0.291
273.363	30441	2.5	396255	1.5	-0.77	1.53E+10	0.169
273.499	39221	1.5	404853	1.5	-0.44	3.27E+10	0.285
273.51	8699	2.5	374317	3.5	-0.58	2.32E+10	0.239
273.585	27662	5.5	393179	4.5	-0.14	6.49E+10	0.502
273.654	18509	2.5	383934	2.5	-0.48	2.92E+10	0.345
273.744	5736	3.5	371041	4.5	-0.68	1.86E+10	0.298
273.745	20666	4.5	385969	4.5	-0.8	1.40E+10	0.076
273.817	16903	1.5	382111	0.5	-0.64	2.05E+10	0.335
274.137	39221	1.5	404002	2.5	-0.63	2.10E+10	0.206
274.164	18509	2.5	383254	2.5	-0.53	2.60E+10	0.498
274.224	26023	3.5	390689	3.5	-0.16	6.19E+10	0.344
274.3	20666	4.5	385231	3.5	-0.64	2.02E+10	0.086
274.495	21571	0.5	385876	1.5	-0.43	3.32E+10	0.49
274.529	20666	4.5	384926	3.5	-0.69	1.83E+10	0.294
274.537	27662	5.5	391912	5.5	-0.87	1.20E+10	0.057
274.546	27420	1.5	391658	1.5	-0.67	1.89E+10	0.157
274.568	33744	4.5	397953	5.5	0.13	1.19E+11	0.735
274.591	21571	0.5	385749	0.5	-0.85	1.24E+10	0.761
274.684	20666	4.5	384721	5.5	-0.01	8.62E+10	0.861
274.825	33744	4.5	397612	4.5	0.47	2.59E+11	0.766
274.876	0	4.5	363801	3.5	-0.17	5.98E+10	0.514
275.124	45079	3.5	408551	3.5	-0.61	2.14E+10	0.181
275.191	41865	2.5	405249	1.5	-0.96	9.60E+09	0.147
275.365	30441	2.5	393595	1.5	-0.51	2.74E+10	0.343
275.437	5736	3.5	368796	3.5	-0.77	1.49E+10	0.254
275.461	33744	4.5	396772	3.5	-0.93	1.03E+10	0.092
275.664	30441	2.5	393202	3.5	-0.79	1.42E+10	0.173
276.015	26023	3.5	388322	4.5	-0.19	5.68E+10	0.707
276.018	33744	4.5	396039	4.5	-0.45	3.10E+10	0.147
276.073	5736	3.5	367959	2.5	-0.28	4.59E+10	0.437
276.113	30441	2.5	392612	3.5	-0.65	1.98E+10	0.325
276.139	41865	2.5	404002	2.5	-0.56	2.38E+10	0.199
276.213	0	4.5	362040	3.5	-0.81	1.34E+10	0.266
276.23	27662	5.5	389679	5.5	0.63	3.76E+11	0.883
276.326	30441	2.5	392332	1.5	-0.57	2.34E+10	0.226
276.355	5736	3.5	367590	4.5	-0.96	9.48E+09	0.092
276.452	45079	3.5	406806	3.5	0.07	1.04E+11	0.57
276.452	16903	1.5	378630	2.5	-0.75	1.55E+10	0.244
276.475	20666	4.5	382362	4.5	-0.13	6.54E+10	0.365
276.562	27420	1.5	389002	2.5	-0.53	2.60E+10	0.198
276.605	20666	4.5	382193	5.5	-0.43	3.25E+10	0.325
276.842	30441	2.5	391658	1.5	-0.8	1.39E+10	0.145
276.921	10382	1.5	371496	1.5	-0.99	8.83E+09	0.148
277.199	26023	3.5	386775	3.5	-0.41	3.39E+10	0.354
277.269	27662	5.5	388322	4.5	-0.66	1.90E+10	0.183
277.454	66339	1.5	426759	2.5	-0.34	3.93E+10	0.478
277.58	8699	2.5	368956	2.5	-0.86	1.21E+10	0.179
278.197	33744	4.5	393202	3.5	-0.82	1.32E+10	0.097
278.407	27420	1.5	386607	2.5	-0.72	1.63E+10	0.204
278.548	41865	2.5	400870	3.5	-0.38	3.55E+10	0.307
278.611	45079	3.5	404002	2.5	-0.99	8.77E+09	0.141
278.802	26023	3.5	384701	2.5	-0.96	9.40E+09	0.084
278.837	18509	2.5	377141	2.5	-0.89	1.10E+10	0.192
278.938	26023	3.5	384525	4.5	-0.69	1.73E+10	0.561
278.943	0	4.5	358496	4.5	-0.46	2.98E+10	0.322
279.073	20666	4.5	378995	5.5	-0.82	1.30E+10	0.177
279.142	27662	5.5	385902	5.5	-0.24	4.93E+10	0.709
279.342	20666	4.5	378650	4.5	-0.06	7.52E+10	0.499
279.544	18509	2.5	376235	3.5	-0.93	1.01E+10	0.133
279.684	0	4.5	357547	3.5	-0.13	6.27E+10	0.349
279.853	30441	2.5	387772	3.5	-0.55	2.42E+10	0.331
279.892	27420	1.5	384701	2.5	-0.88	1.12E+10	0.121

Table A24: Continued

Wavelength	Lower Level	J_{Low}	Upper level	J_{Up}	log gf	gA	CF
280.044	41865	2.5	398952	2.5	-0.89	1.10E+10	0.13
280.066	27662	5.5	384721	5.5	-0.93	1.00E+10	0.127
280.22	27662	5.5	384525	4.5	-0.69	1.73E+10	0.177
280.341	45079	3.5	401788	3.5	-0.48	2.79E+10	0.434
280.632	26023	3.5	382362	4.5	-1	8.49E+09	0.108
280.636	30441	2.5	386775	3.5	-0.56	2.32E+10	0.426
280.659	5736	3.5	362040	3.5	-0.71	1.67E+10	0.151
281.362	27662	5.5	383076	6.5	-0.48	2.81E+10	0.915
281.367	41865	2.5	397273	2.5	-0.31	4.16E+10	0.205
281.48	10382	1.5	365647	1.5	-0.94	9.68E+09	0.157
281.555	0	4.5	355170	3.5	-0.93	9.92E+09	0.25
281.565	8699	2.5	363857	2.5	-0.88	1.10E+10	0.179
281.671	66339	1.5	421363	2.5	-0.69	1.71E+10	0.477
281.764	41865	2.5	396772	3.5	-0.74	1.53E+10	0.186
281.936	27420	1.5	382111	0.5	-0.58	2.20E+10	0.302
282.021	66339	1.5	420923	1.5	-0.74	1.52E+10	0.258
282.099	30441	2.5	384926	3.5	-0.93	9.78E+09	0.2
282.208	5736	3.5	360085	2.5	-0.52	2.55E+10	0.293
282.259	20666	4.5	374950	5.5	-0.85	1.19E+10	0.331
282.365	39221	1.5	393373	2.5	-0.96	9.14E+09	0.136
282.587	45079	3.5	398952	2.5	-0.91	1.03E+10	0.095
283.106	18509	2.5	371734	3.5	-0.74	1.52E+10	0.183
283.463	5736	3.5	358516	2.5	-0.7	1.64E+10	0.311
283.661	45079	3.5	397612	4.5	-1	8.39E+09	0.178
283.827	8699	2.5	361026	1.5	-0.37	3.52E+10	0.328
283.909	33744	4.5	385969	4.5	-0.81	1.28E+10	0.061
284.244	5736	3.5	357547	3.5	-0.81	1.28E+10	0.236
284.707	10382	1.5	361620	0.5	-0.57	2.21E+10	0.332
284.745	0	4.5	351191	4.5	-0.67	1.74E+10	0.352
284.933	45079	3.5	396039	4.5	-0.54	2.37E+10	0.557
285.171	16903	1.5	367570	0.5	-0.51	2.55E+10	0.572
285.19	10382	1.5	361026	1.5	-0.89	1.06E+10	0.263
285.883	41865	2.5	391658	1.5	-0.96	9.06E+09	0.163
286.101	27662	5.5	377189	6.5	-0.65	1.84E+10	0.901
286.534	45079	3.5	394078	4.5	-0.48	2.70E+10	0.359
286.71	39221	1.5	388005	2.5	-0.79	1.32E+10	0.171
286.715	27420	1.5	376198	2.5	-0.97	8.69E+09	0.109
286.854	18509	2.5	367119	1.5	-0.43	3.00E+10	0.364
287.274	45079	3.5	393179	4.5	-0.41	3.11E+10	0.401
287.389	0	4.5	347961	3.5	-0.4	3.22E+10	0.349
287.742	45079	3.5	392612	3.5	-0.98	8.37E+09	0.097
287.826	30441	2.5	377873	3.5	-0.96	8.81E+09	0.187
287.901	66339	1.5	413681	1.5	-0.31	3.98E+10	0.571
288.248	20666	4.5	367590	4.5	-0.83	1.18E+10	0.108
289.395	21571	0.5	367119	1.5	-0.73	1.50E+10	0.226
289.563	18509	2.5	363857	2.5	-0.94	9.25E+09	0.199
289.61	18509	2.5	363801	3.5	-0.9	9.92E+09	0.246
289.847	18509	2.5	363519	2.5	-0.32	3.83E+10	0.364
291.234	41865	2.5	385231	3.5	-0.26	4.32E+10	0.43
291.391	16903	1.5	360085	2.5	-0.76	1.35E+10	0.263
291.947	5736	3.5	348264	2.5	-0.77	1.32E+10	0.2
294.598	45079	3.5	384525	4.5	-0.7	1.52E+10	0.368
294.952	18509	2.5	357547	3.5	-0.79	1.23E+10	0.336

a: Experimental values from [38]

Cs IV-VII

Cs IV

Energy Levels

Table A25: Comparison between available experimental data and calculated energy levels (in cm^{-1}) in Cs IV

E^a_{exp}	E^b_{calc}	ΔE	J	Leading components (in %) in LS coupling ^{c}
Even Parity				
0	-96	96	2	82.8 $5s^25p^4$ (^3P) ^3P + 13.1 $5s^25p^4$ (^1D) ^1D
9749.4	9857	-107.6	0	72.6 $5s^25p^4$ (^3P) ^3P + 23.2 $5s^25p^4$ (^1S) ^1S
12902	12910	-8	1	95.8 $5s^25p^4$ (^3P) ^3P
20754	20769	-15	2	82 $5s^25p^4$ (^1D) ^1D + 13.1 $5s^25p^4$ (^3P) ^3P
43279.4	43245	34.4	0	71.8 $5s^25p^4$ (^1S) ^1S + 23.1 $5s^25p^4$ (^3P) ^3P
Odd Parity				
114307.7	114559	-251.3	2	76 $5s5p^5$ (^2S) ^3P + 14.8 $5s^25p^35d$ (^2D) ^3P + 6.2 $5s^25p^35d$ (^2P) ^3P
121242.5	121377	-134.5	1	65.3 $5s5p^5$ (^2S) ^3P + 14.4 $5s^25p^35d$ (^2D) ^3P + 5.9 $5s^25p^35d$ (^2P) ^3P
128086.3	127893	193.3	0	70.2 $5s5p^5$ (^2S) ^3P + 16.7 $5s^25p^35d$ (^2D) ^3P + 5.9 $5s^25p^35d$ (^2P) ^3P
136143.1	136175	-31.9	2	69.8 $5s^25p^35d$ (^4S) ^5D + 7.1 $5s^25p^35d$ (^2P) ^3D + 5.7 $5s^25p^35d$ (^4S) ^3D
135979.9	136185	-205.1	3	73 $5s^25p^35d$ (^4S) ^5D + 6.8 $5s^25p^35d$ (^2P) ^3F + 6.5 $5s^25p^35d$ (^2P) ^3D
136625.7	136529	96.7	0	80.3 $5s^25p^35d$ (^4S) ^5D + 6.8 $5s^25p^35d$ (^2P) ^3P
136868.6	136871	-2.4	1	82.8 $5s^25p^35d$ (^4S) ^5D
141402.9	141043	359.9	1	41.3 $5s^25p^35d$ (^2D) ^1P + 35.2 $5s5p^5$ (^2S) ^1P + 6.5 $5s5p^5$ (^2S) ^3P
142167	142307	-140	2	22.8 $5s^25p^35d$ (^4S) ^3D + 19.1 $5s^25p^35d$ (^2D) ^3D + 18.9 $5s^25p^35d$ (^4S) ^5D
147695.5	147934	-238.5	3	33.1 $5s^25p^35d$ (^4S) ^3D + 27.7 $5s^25p^35d$ (^2D) ^3D + 17.5 $5s^25p^35d$ (^4S) ^5D
148640	148616	24	1	49.5 $5s^25p^35d$ (^4S) ^3D + 36.4 $5s^25p^35d$ (^2D) ^3D
150982.7	151200	-217.3	2	50.7 $5s^25p^35d$ (^2D) ^3F + 20.5 $5s^25p^35d$ (^2D) ^3D + 12.9 $5s^25p^35d$ (^4S) ^3D
152832.1	151413	1419.1	0	81.2 $5s^25p^35d$ (^2D) ^1S + 7.1 $5s^25p^35d$ (^2P) ^3P + 5.6 $5s^25p^35d$ (^4S) ^5D
152776.7	153154	-377.3	3	63.8 $5s^25p^35d$ (^2D) ^3F + 8.9 $5s^25p^35d$ (^2D) ^3D + 7.8 $5s^25p^35d$ (^2P) ^3F
155045.5	155818	-772.5	3	62.5 $5s^25p^35d$ (^2D) ^3G + 13.8 $5s^25p^35d$ (^2D) ^3F + 7.1 $5s^25p^35d$ (^2P) ^1F
162425.9	162117	308.9	1	40.8 $5s^25p^35d$ (^2D) ^3D + 34.1 $5s^25p^35d$ (^2P) ^3D + 8.9 $5s^25p^35d$ (^4S) ^3D
164609.5	164599	10.5	2	74.2 $5s^25p^36s$ (^4S) ^5S + 14.3 $5s^25p^36s$ (^2P) ^3P
166472.1	166537	-64.9	2	29 $5s^25p^35d$ (^2P) ^1D + 17.4 $5s^25p^35d$ (^2D) ^1D + 16.7 $5s^25p^35d$ (^2P) ^3F
167553.8	167863	-309.2	1	46.2 $5s^25p^36s$ (^4S) ^3S + 13.5 $5s^25p^35d$ (^2P) ^3P + 10.3 $5s^25p^35d$ (^2D) ^3S
169843.8	169324	519.8	0	43.6 $5s^25p^35d$ (^2P) ^3P + 31.8 $5s^25p^35d$ (^2D) ^3P + 12 $5s^25p^35d$ (^2D) ^1S
170401.9	170004	397.9	2	30.1 $5s^25p^35d$ (^2P) ^3D + 17.9 $5s^25p^35d$ (^4S) ^3D + 17.1 $5s^25p^35d$ (^2D) ^3D
171449.5	170569	880.5	1	34.5 $5s^25p^35d$ (^2P) ^3P + 25.1 $5s^25p^36s$ (^4S) ^3S + 13.5 $5s^25p^35d$ (^2D) ^3P
173942.4	173752	190.4	3	41.9 $5s^25p^35d$ (^2D) ^3D + 20.7 $5s^25p^35d$ (^4S) ^3D + 12.1 $5s^25p^35d$ (^2P) ^1F
174718.7	175394	-675.3	2	56 $5s^25p^35d$ (^2P) ^3F + 17.7 $5s^25p^35d$ (^2D) ^3F + 12 $5s^25p^35d$ (^2P) ^3P
174789.4	175490	-700.6	3	61.2 $5s^25p^35d$ (^2P) ^3F + 21.7 $5s^25p^35d$ (^2P) ^3D + 8.3 $5s^25p^35d$ (^2D) ^3G
179159.8	178997	162.8	2	32 $5s^25p^35d$ (^2D) ^3P + 23.2 $5s^25p^35d$ (^2P) ^3P + 13.7 $5s5p^5$ (^2S) ^3P
179477.8	179928	-450.2	1	19.6 $5s^25p^35d$ (^2D) ^3P + 33 $5s^25p^35d$ (^2D) ^3S + 21.6 $5s^25p^36s$ (^2D) ^3D
180538.2	180199	339.2	3	31.4 $5s^25p^35d$ (^2D) ^1F + 26.1 $5s^25p^35d$ (^2P) ^3D + 20 $5s^25p^35d$ (^4S) ^3D
181944.8	182111	-166.2	2	50.2 $5s^25p^36s$ (^2D) ^3D + 13.6 $5s^25p^36s$ (^2P) ^3P + 9.4 $5s^25p^36s$ (^4S) ^5S
182511	182390	121	2	35.5 $5s^25p^35d$ (^2P) ^3P + 25.6 $5s^25p^35d$ (^2D) ^3P + 7.7 $5s^25p^35d$ (^4S) ^3D
182573.3	182975	-401.7	1	48 $5s^25p^36s$ (^2D) ^3D + 14.3 $5s^25p^36s$ (^4S) ^3S + 12.6 $5s^25p^35d$ (^2D) ^3P
185718.8	185618	100.8	3	73.2 $5s^25p^36s$ (^2D) ^3D + 10.1 $5s^25p^35d$ (^2P) ^1F + 9.2 $5s^25p^35d$ (^2D) ^1F
185913.9	186673	-759.1	1	31.8 $5s^25p^35d$ (^2D) ^3S + 19.6 $5s5p^5$ (^2S) ^1P + 16 $5s^25p^35d$ (^2D) ^1P
187266.6	187287	-20.4	2	9.1 $5s^25p^35d$ (^2D) ^3D + 19.4 $5s^25p^35d$ (^2P) ^3D + 16.2 $5s^25p^36s$ (^2D) ^1D
189217.8	188884	333.8	2	50.6 $5s^25p^36s$ (^2D) ^1D + 17 $5s^25p^36s$ (^2D) ^3D + 11.3 $5s^25p^35d$ (^2P) ^3D
189391.7	189194	197.7	1	31 $5s^25p^35d$ (^2P) ^3D + 14.8 $5s^25p^35d$ (^2P) ^1P + 13.3 $5s^25p^35d$ (^4S) ^3D
190309.8	190123	186.8	3	27.6 $5s^25p^35d$ (^2P) ^3D + 21.4 $5s^25p^36s$ (^2D) ^3D + 21.2 $5s^25p^35d$ (^2P) ^1F
192952	192246	706	0	33.2 $5s^25p^35d$ (^2D) ^3P + 32.2 $5s^25p^35d$ (^2P) ^3P + 16.2 $5s5p^5$ (^2S) ^3P
194685.9	194638	47.9	1	18.3 $5s^25p^35d$ (^2D) ^1P + 18.2 $5s5p^5$ (^2S) ^1P
198135.3	198085	50.3	0	86.8 $5s^25p^36s$ (^2P) ^3P + 7.5 $5s^25p^35d$ (^2D) ^3P
197380.8	198310	-929.2	2	45.4 $5s^25p^35d$ (^2D) ^1D + 18.5 $5s^25p^35d$ (^2P) ^1D + 15.9 $5s^25p^35d$ (^2P) ^3D
198514.1	198580	-65.9	1	63 $5s^25p^36s$ (^2P) ^3P + 21.7 $5s^25p^36s$ (^2P) ^1P
199392.1	199058	334.1	3	40.9 $5s^25p^35d$ (^2P) ^1F + 34.9 $5s^25p^35d$ (^2D) ^1F + 6.7 $5s^25p^35d$ (^4S) ^3D
207937.6	207733	204.6	2	67.7 $5s^25p^36s$ (^2P) ^3P + 12.9 $5s^25p^36s$ (^2D) ^3D + 11.3 $5s^25p^36s$ (^2D) ^1D
208500	208754	-254	1	48.9 $5s^25p^36s$ (^2P) ^1P + 18.9 $5s^25p^36s$ (^2D) ^3D + 17.7 $5s^25p^36s$ (^2P) ^3P
246061	245994	67	2	70.5 $5s^25p^36d$ (^4S) ^5D + 9 $5s^25p^36d$ (^2P) ^3D + 6.8 $5s^25p^36d$ (^4S) ^3D
246089.4	246060	29.4	3	72.2 $5s^25p^36d$ (^4S) ^5D + 7.6 $5s^25p^36d$ (^2P) ^3D + 7.2 $5s^25p^36d$ (^2P) ^3F
246233	246183	50	1	80.3 $5s^25p^36d$ (^4S) ^5D + 9.5 $5s^25p^36d$ (^2P) ^3P
248688	248744	-56	2	56.7 $5s^25p^36d$ (^4S) ^3D + 11.1 $5s^25p^36d$ (^2P) ^1D + 10.1 $5s^25p^36d$ (^4S) ^5D
250634.2	250479	155.2	1	77.5 $5s^25p^36d$ (^4S) ^3D + 7.6 $5s^25p^36d$ (^2P) ^1P + 5.6 $5s^25p^36d$ (^2P) ^3D
250415.4	250690	-274.6	3	68.1 $5s^25p^36d$ (^4S) ^3D + 10.4 $5s^25p^36d$ (^2P) ^1F + 7.9 $5s^25p^36d$ (^4S) ^5D
251551.7	251582	-30.3	2	70.2 $5s^25p^37s$ (^4S) ^5S + 20.5 $5s^25p^37s$ (^2P) ^3P + 5.5 $5s^25p^37s$ (^2D) ^3D
253194.4	253181	13.4	1	64.8 $5s^25p^37s$ (^4S) ^3S + 14.6 $5s^25p^37s$ (^2P) ^1P + 11.8 $5s^25p^37s$ (^2D) ^3D
261177.8	261224	-46.2	2	58.5 $5s^25p^36d$ (^2D) ^3F + 11.6 $5s^25p^36d$ (^4S) ^3D + 7 $5s^25p^36d$ (^4S) ^5D
261868.3	261761	107.3	1	53.1 $5s^25p^36d$ (^2D) ^3D + 17.6 $5s^25p^36d$ (^2D) ^1P + 8 $5s^25p^36d$ (^4S) ^5D
261644.7	261763	-118.3	3	46.6 $5s^25p^36d$ (^2D) ^3F + 16.2 $5s^25p^36d$ (^2D) ^3D + 8.8 $5s^25p^36d$ (^2P) ^3D
262150.2	262160	-9.8	3	59.2 $5s^25p^36d$ (^2D) ^3G + 12.4 $5s^25p^36d$ (^4S) ^3D + 7.8 $5s^25p^36d$ (^2P) ^3F
262537	262218	319	0	54.4 $5s^25p^36d$ (^2D) ^1S + 20.5 $5s^25p^36d$ (^2D) ^3P + 13.1 $5s^25p^36d$ (^2P) ^3P
264175.5	264280	-104.5	2	24.4 $5s^25p^36d$ (^2D) ^3P + 31.8 $5s^25p^36d$ (^2D) ^3D + 14 $5s^25p^36d$ (^4S) ^3D
265107.3	265152	-44.7	1	29.8 $5s^25p^36d$ (^2D) ^3P + 25.4 $5s^25p^36d$ (^2D) ^3S + 15.1 $5s^25p^36d$ (^2D) ^1P
267056.1	266938	118.1	2	43.5 $5s^25p^37s$ (^2D) ^3D + 21 $5s^25p^37s$ (^4S) ^5S + 19.9 $5s^25p^37s$ (^2D) ^1D
267199.4	267145	54.4	3	63.7 $5s^25p^36d$ (^2D) ^3D + 27.6 $5s^25p^36d$ (^2D) ^3F
267211	267258	-47	1	62.9 $5s^25p^37s$ (^2D) ^3D + 25.8 $5s^25p^37s$ (^4S) ^3S + 5 $5s^25p^37s$ (^2P) ^1P
268007.3	268056	-48.7	2	43.7 $5s^25p^36d$ (^2D) ^3D + 32.6 $5s^25p^36d$ (^2D) ^3P + 10.7 $5s^25p^36d$ (^2D) ^1D
268328	268130	198	0	62 $5s^25p^36d$ (^2D) ^3P + 33.9 $5s^25p^36d$ (^2D) ^1S

Table A25: Continued

E^a_{exp}	E^b_{calc}	ΔE	J	Leading components (in %) in LS coupling [c]
268521.1	268496	25.1	1	35.4 $5s^25p^36d$ (^{2}D) ^{1}P + 32.9 $5s^25p^36d$ (^{2}D) ^{3}P + 24.6 $5s^25p^36d$ (^{2}D) ^{3}D
269477.7	269838	-360.3	1	59.6 $5s^25p^36d$ (^{2}D) ^{3}S + 21.1 $5s^25p^36d$ (^{2}D) ^{3}P + 16.4 $5s^25p^36d$ (^{2}D) ^{1}P
270015.6	270145	-129.4	2	58.4 $5s^25p^36d$ (^{2}D) ^{1}D + 26.8 $5s^25p^36d$ (^{2}D) ^{3}P + 6.6 $5s^25p^36d$ (^{2}D) ^{3}F
270688.4	270491	197.4	3	72.9 $5s^25p^36d$ (^{2}D) ^{1}F + 11.6 $5s^25p^36d$ (^{2}D) ^{3}D + 5.3 $5s^25p^36d$ (^{2}D) ^{3}G
272133.7	272152	-18.3	3	98.8 $5s^25p^37s$ (^{2}D) ^{3}D
272805.3	272831	-25.7	2	64.9 $5s^25p^37s$ (^{2}D) ^{1}D + 33.6 $5s^25p^37s$ (^{2}D) ^{3}D
278199.8	278247	-47.2	2	71.4 $5s^25p^36d$ (^{2}P) ^{3}F + 17.9 $5s^25p^36d$ (^{2}P) ^{1}D
279262.5	279238	24.5	2	39.3 $5s^25p^36d$ (^{2}P) ^{3}P + 38.5 $5s^25p^36d$ (^{2}P) ^{3}D + 17.7 $5s^25p^36d$ (^{2}P) ^{1}D
279539.7	279471	68.7	3	52.2 $5s^25p^36d$ (^{2}P) ^{3}F + 22.9 $5s^25p^36d$ (^{2}P) ^{3}D + 20.7 $5s^25p^36d$ (^{2}P) ^{1}F
280241.9	280361	-119.1	1	56.9 $5s^25p^36d$ (^{2}P) ^{3}D + 21.5 $5s^25p^36d$ (^{2}P) ^{1}P + 15.5 $5s^25p^36d$ (^{2}P) ^{3}P
283542	283545	-3	0	98.4 $5s^25p^37s$ (^{2}P) ^{3}P
283908	283915	-7	1	67.7 $5s^25p^37s$ (^{2}P) ^{3}P + 31 $5s^25p^37s$ (^{2}P) ^{1}P
288142	287995	147	1	55 $5s^25p^36d$ (^{2}P) ^{3}P + 10.7 $5s^25p^36d$ (^{2}P) ^{3}D + 8.9 $5s^25p^36d$ (^{2}D) ^{1}P
289119	289209	-90	3	58.6 $5s^25p^36d$ (^{2}P) ^{1}F + 15.6 $5s^25p^36d$ (^{2}D) ^{3}G + 10.6 $5s^25p^36d$ (^{2}P) ^{3}F
289400.1	289563	-162.9	3	45.6 $5s^25p^36d$ (^{2}P) ^{3}D + 16.9 $5s^25p^36d$ (^{2}P) ^{3}F + 11.1 $5s^25p^36d$ (^{2}D) ^{1}F
289626	289807	-181	0	64.2 $5s^25p^37d$ (^{4}S) ^{5}D + 20.7 $5s5p^44f$ (^{3}P) ^{5}D + 7.7 $5s^25p^37d$ (^{2}P) ^{3}P
289723	290023	-300	2	21.6 $5s^25p^36d$ (^{2}P) ^{3}D + 23.8 $5s^25p^36d$ (^{2}P) ^{1}D + 13.6 $5s^25p^36d$ (^{2}D) ^{3}F
290157	290433	-276	3	73.7 $5s^25p^37d$ (^{4}S) ^{5}D + 5.6 $5s^25p^37d$ (^{2}P) ^{3}D
293926.5	291738	2188.5	2	80.3 $5s^25p^35g$ (^{4}S) ^{5}G + 10 $5s^25p^35g$ (^{2}P) ^{3}F + 5.7 $5s5p^44f$ (^{3}P) ^{5}G
292768.2	292384	384.2	1	41 $5s^25p^36d$ (^{2}P) ^{1}P + 33.6 $5s^25p^37d$ (^{4}S) ^{3}D
294402.4	293916	486.4	1	46.9 $5s^25p^37d$ (^{4}S) ^{3}D + 15.7 $5s^25p^36d$ (^{2}P) ^{1}P + 10.9 $5s^25p^36d$ (^{2}P) ^{3}D

a: Energy Levels from Sansonetti [39]
b: This work
c: Only the components $\geq$ 5% are given

Transitions

Table A26: Computed oscillator strengths and transition probabilities Cs IV.

λ_{Ritz} Å	E^a_{low} cm^{-1}	J_{low}	E_{up} cm^{-1}	J_{up}	log gf	gA s^{-1}	CF
367.466	0	2	272134	3	-0.73	9.12E+09	0.403
372.627	20754	2	289119	3	-0.89	6.18E+09	-0.182
373.124	0	2	268007	2	-0.92	5.72E+09	0.127
374.252	0	2	267199	3	-0.88	6.34E+09	0.201
374.453	0	2	267056	2	-0.81	7.35E+09	0.451
393.222	12902	1	267211	1	-0.75	7.64E+09	0.495
394.953	0	2	253194	1	-0.56	1.17E+10	-0.55
396.745	20754	2	272805	2	-0.39	1.74E+10	-0.533
397.973	12902	1	264176	2	-0.88	5.59E+09	0.138
399.336	0	2	250415	3	-0.61	1.04E+10	-0.208
400.105	20754	2	270688	3	-0.61	1.03E+10	-0.158
400.82	43279	0	292768	1	-0.92	5.00E+09	0.176
401.185	20754	2	270016	2	-0.92	5.05E+09	0.114
512.727	12902	1	207938	2	-0.63	5.98E+09	0.202
528.492	0	2	189218	2	-0.5	7.46E+09	-0.051
529.76	9749	0	198514	1	-0.59	6.06E+09	0.119
532.635	20754	2	208500	1	-0.56	6.45E+09	-0.164
534.235	20754	2	207938	2	-0.28	1.22E+10	0.337
538.448	0	2	185719	3	-0.15	1.64E+10	0.152
542.068	12902	1	197381	2	0.06	2.63E+10	-0.402
547.725	0	2	182573	1	0.23	3.75E+10	-0.341
547.912	0	2	182511	2	-0.44	8.12E+09	-0.034
549.617	0	2	181945	2	-0.67	4.79E+09	0.066
550.104	12902	1	194686	1	0.25	3.94E+10	0.504
553.899	0	2	180538	3	0.9	1.71E+11	-0.549
555.401	12902	1	192952	0	0.2	3.37E+10	-0.504
556.662	9749	0	189392	1	0.55	7.54E+10	-0.485
557.172	0	2	179478	1	0.35	4.88E+10	0.327
558.161	0	2	179160	2	0.85	1.50E+11	-0.508
559.791	20754	2	199392	3	1.02	2.23E+11	-0.532
566.165	20754	2	197381	2	0.66	9.54E+10	0.462
567.164	12902	1	189218	2	-0.13	1.55E+10	-0.178
567.651	9749	0	185914	1	-0.42	8.01E+09	0.103
572.117	0	2	174789	3	-0.27	1.11E+10	-0.25
573.511	12902	1	187267	2	0.68	9.69E+10	-0.556
574.903	0	2	173942	3	0.36	4.63E+10	0.154
574.938	20754	2	194686	1	0.4	5.11E+10	-0.401
577.995	12902	1	185914	1	0.32	4.22E+10	-0.477
578.624	9749	0	182573	1	-0.7	3.96E+09	0.072
583.262	0	2	171450	1	-0.09	1.59E+10	0.153
589.375	12902	1	182573	1	-0.54	5.51E+09	0.076
591.566	12902	1	181945	2	-0.36	8.42E+09	0.167
592.987	20754	2	189392	1	-0.54	5.52E+09	-0.153
593.599	20754	2	189218	2	0.43	5.11E+10	-0.406
596.823	0	2	167554	1	-0.67	4.04E+09	-0.041
600.327	12902	1	179478	1	-0.53	5.46E+09	0.054
600.701	0	2	166472	2	-0.92	2.21E+09	-0.028
605.474	20754	2	185914	1	0.19	2.82E+10	-0.238
606.19	20754	2	185719	3	-0.48	6.05E+09	-0.06
607.498	0	2	164610	2	-0.63	4.24E+09	-0.199
617.973	20754	2	182573	1	-0.97	1.90E+09	0.062
617.983	12902	1	174719	2	-0.38	7.35E+09	-0.33
618.429	9749	0	171450	1	-0.59	4.39E+09	0.072
625.844	20754	2	180538	3	-0.49	5.52E+09	-0.033
630.726	12902	1	171450	1	-0.49	5.31E+09	-0.087
631.29	20754	2	179160	2	-0.78	2.78E+09	0.042
634.921	12902	1	170402	2	-0.54	4.78E+09	0.032
637.179	12902	1	169844	0	-0.99	1.66E+09	-0.058
644.972	0	2	155046	3	-0.66	3.57E+09	0.108
649.201	20754	2	174789	3	-0.7	3.17E+09	0.225
649.5	20754	2	174719	2	-0.94	1.82E+09	0.083
652.791	20754	2	173942	3	-0.48	5.21E+09	-0.042
654.98	9749	0	162426	1	-0.73	2.87E+09	0.042

a: Energy Levels from [39]

Cs V

Energy Levels

Table A27: Comparison between available experimental data and calculated energy levels (in cm^{-1}) in Cs V

E^a_{exp}	E^b_{calc}	ΔE	J	Leading components (in %) in LS coupling ^{c}
Odd Parity				
0	-297	297	1.5	76.5 $5s^25p^3$ (^{4}S) ^{4}S + 15.4 $5s^25p^3$ (^{2}P) ^{2}P + 5.4 $5s^25p^3$ (^{2}D) ^{2}D
15077.4	15294	-216.6	1.5	68.3 $5s^25p^3$ (^{2}D) ^{2}D + 14.9 $5s^25p^3$ (^{4}S) ^{4}S + 13.3 $5s^25p^3$ (^{2}P) ^{2}P
20373.5	20797	-423.5	2.5	96.3 $5s^25p^3$ (^{2}D) ^{2}D
31951.1	31750	201.1	0.5	96 $5s^25p^3$ (^{2}P) ^{2}P
42273.7	42133	140.7	1.5	67.2 $5s^25p^3$ (^{2}P) ^{2}P + 22.6 $5s^25p^3$ (^{2}D) ^{2}D + 6 $5s^25p^3$ (^{4}S) ^{4}S
Even Parity				
113901.7	113715	186.7	2.5	84 $5s5p^4$ (^{3}P) ^{4}P + 8.3 $5s^25p^25d$ (^{3}P) ^{4}P + 5 $5s5p^4$ (^{1}D) ^{2}D
123192.4	123104	88.4	1.5	82.7 $5s5p^4$ (^{3}P) ^{4}P + 9.2 $5s^25p^25d$ (^{3}P) ^{4}P
125858.3	125954	-95.7	0.5	81 $5s5p^4$ (^{3}P) ^{4}P + 9.2 $5s^25p^25d$ (^{3}P) ^{4}P + 7.1 $5s5p^4$ (^{1}S) ^{2}S
139959.2	140458	-498.8	1.5	55.7 $5s5p^4$ (^{1}D) ^{2}D + 14.6 $5s^25p^25d$ (^{1}D) ^{2}D + 8.1 $5s5p^4$ (^{3}P) ^{2}P
144333	144743	-410	2.5	69.5 $5s5p^4$ (^{1}D) ^{2}D + 18.9 $5s^25p^25d$ (^{1}D) ^{2}D + 5.7 $5s5p^4$ (^{3}P) ^{4}P
154971.2	154583	388.2	1.5	33.7 $5s^25p^25d$ (^{3}P) ^{2}P + 18.4 $5s5p^4$ (^{3}P) ^{2}P + 16.7 $5s5p^4$ (^{1}D) ^{2}D
158248.8	157799	449.8	0.5	30.9 $5s^25p^25d$ (^{3}P) ^{2}P + 31.2 $5s5p^4$ (^{3}P) ^{2}P + 20.8 $5s5p^4$ (^{1}S) ^{2}S
157903	158258	-355	1.5	66.4 $5s^25p^25d$ (^{3}P) ^{4}F + 11.7 $5s5p^4$ (^{3}P) ^{2}P + 8.7 $5s^25p^25d$ (^{3}P) ^{2}P
160327.9	160329	-1.1	2.5	54 $5s^25p^25d$ (^{3}P) ^{4}F + 25.7 $5s^25p^25d$ (^{3}P) ^{4}D + 6.2 $5s^25p^25d$ (^{1}S) ^{2}D
166800.2	166980	-179.8	2.5	39.8 $5s^25p^25d$ (^{1}D) ^{2}F + 27 $5s^25p^25d$ (^{3}P) ^{2}F + 24.1 $5s^25p^25d$ (^{3}P) ^{4}F
167231.1	167718	-486.9	3.5	71.9 $5s^25p^25d$ (^{3}P) ^{4}F + 22 $5s^25p^25d$ (^{3}P) ^{4}D
169557.9	169711	-153.1	0.5	63.3 $5s^25p^25d$ (^{3}P) ^{4}D + 19.4 $5s5p^4$ (^{1}S) ^{2}S + 5.9 $5s^25p^25d$ (^{1}D) ^{2}S
170736.7	170595	141.7	3.5	36.4 $5s^25p^25d$ (^{1}D) ^{2}F + 27.3 $5s^25p^25d$ (^{3}P) ^{4}D + 14.8 $5s^25p^25d$ (^{3}P) ^{2}F
171936.7	172220	-283.3	1.5	74.9 $5s^25p^25d$ (^{3}P) ^{4}D + 11.4 $5s^25p^25d$ (^{3}P) ^{4}F
175576.8	175111	465.8	0.5	27.7 $5s5p^4$ (^{1}S) ^{2}S + 25.7 $5s^25p^25d$ (^{3}P) ^{4}D + 19.5 $5s^25p^25d$ (^{3}P) ^{2}P
175405	175415	-10	2.5	47.7 $5s^25p^25d$ (^{3}P) ^{4}D + 14.9 $5s^25p^25d$ (^{3}P) ^{4}F + 11.8 $5s^25p^25d$ (^{3}P) ^{2}F
184244.5	184647	-402.5	3.5	33.8 $5s^25p^25d$ (^{3}P) ^{4}D + 31.1 $5s^25p^25d$ (^{1}D) ^{2}G + 17 $5s^25p^25d$ (^{3}P) ^{2}F
187619.8	187180	439.8	2.5	66.2 $5s^25p^25d$ (^{3}P) ^{4}P + 11.9 $5s^25p^25d$ (^{3}P) ^{4}D + 6.8 $5s^25p^25d$ (^{1}D) ^{2}D
188245.8	187859	386.8	1.5	38.2 $5s5p^4$ (^{3}P) ^{2}P + 28.1 $5s^25p^25d$ (^{1}D) ^{2}P + 12.8 $5s^25p^25d$ (^{3}P) ^{2}P
189415.9	189230	185.9	3.5	50.1 $5s^25p^25d$ (^{1}D) ^{2}G + 30.1 $5s^25p^25d$ (^{1}D) ^{2}F + 14 $5s^25p^25d$ (^{3}P) ^{4}D
189992.1	189967	25.1	1.5	49.6 $5s^25p^25d$ (^{3}P) ^{4}P + 8.2 $5s^25p^25d$ (^{3}P) ^{2}D + 6.6 $5s^25p^25d$ (^{1}S) ^{2}D
191236.7	190783	453.7	0.5	58.9 $5s^25p^25d$ (^{3}P) ^{4}P + 14.9 $5s^25p^25d$ (^{1}D) ^{2}P + 10 $5s^25p^25d$ (^{1}D) ^{2}S
195328.4	195100	228.4	1.5	40.4 $5s^25p^25d$ (^{3}P) ^{2}D + 18.9 $5s^25p^25d$ (^{1}S) ^{2}D + 12.7 $5s^25p^25d$ (^{3}P) ^{4}P
199403.5	198863	540.5	2.5	44.5 $5s^25p^25d$ (^{3}P) ^{2}D + 19.3 $5s^25p^25d$ (^{3}P) ^{2}F + 13.9 $5s^25p^25d$ (^{1}D) ^{2}D
200123.6	199740	383.6	0.5	40.8 $5s^25p^26s$ (^{3}P) ^{4}P + 29 $5s^25p^25d$ (^{1}D) ^{2}P + 15 $5s^25p^26s$ (^{3}P) ^{2}P
201141.6	201077	64.6	0.5	24.2 $5s5p^4$ (^{3}P) ^{2}P + 16.5 $5s^25p^25d$ (^{3}P) ^{4}P + 14.8 $5s^25p^25d$ (^{1}D) ^{2}P
206375.9	206299	76.9	1.5	55.3 $5s^25p^25d$ (^{1}D) ^{2}D + 13.3 $5s5p^4$ (^{1}D) ^{2}D + 9.8 $5s^25p^25d$ (^{1}D) ^{2}P
205203.2	206523	-1319.8	0.5	25.4 $5s^25p^25d$ (^{1}D) ^{2}P + 24.2 $5s^25p^26s$ (^{3}P) ^{4}P + 15 $5s^25p^25d$ (^{1}D) ^{2}S
206712	206534	178	2.5	26 $5s^25p^25d$ (^{1}D) ^{2}D + 21.5 $5s^25p^25d$ (^{1}D) ^{2}F + 16.2 $5s^25p^25d$ (^{3}P) ^{2}F
211084.4	210013	1071.4	2.5	41.6 $5s^25p^25d$ (^{1}S) ^{2}D + 20.9 $5s^25p^25d$ (^{1}D) ^{2}D + 17.7 $5s^25p^25d$ (^{3}P) ^{2}D
210475.3	210247	228.3	3.5	60.4 $5s^25p^25d$ (^{3}P) ^{2}F + 25.4 $5s^25p^25d$ (^{1}D) ^{2}F + 7 $5s^25p^25d$ (^{1}D) ^{2}G
211476.1	211137	339.1	1.5	77.7 $5s^25p^26s$ (^{3}P) ^{4}P + 10.7 $5s^25p^26s$ (^{3}P) ^{2}P
214163.1	215561	-1397.9	1.5	24.8 $5s^25p^25d$ (^{1}D) ^{2}P + 15.6 $5s^25p^25d$ (^{3}P) ^{2}P + 15.4 $5s^25p^26s$ (^{3}P) ^{2}P
216635.5	215996	639.5	0.5	57.5 $5s^25p^26s$ (^{3}P) ^{2}P + 18.5 $5s^25p^25d$ (^{1}D) ^{2}S + 9 $5s^25p^26s$ (^{3}P) ^{4}P
217754.6	217690	64.6	2.5	67.7 $5s^25p^26s$ (^{3}P) ^{4}P + 21.5 $5s^25p^26s$ (^{1}D) ^{2}D + 5.8 $5s^25p^25d$ (^{1}S) ^{2}D
220013.2	220236	-222.8	0.5	27.4 $5s^25p^25d$ (^{1}D) ^{2}S + 15 $5s^25p^25d$ (^{3}P) ^{2}P + 12.5 $5s5p^4$ (^{3}P) ^{2}P
221933.8	222642	-708.2	1.5	32.3 $5s^25p^26s$ (^{3}P) ^{2}P + 34.1 $5s^25p^26s$ (^{1}D) ^{2}D + 9.8 $5s^25p^25d$ (^{1}D) ^{2}P
224000.6	223990	10.6	2.5	14.6 $5s^25p^25d$ (^{3}P) ^{2}F + 30.4 $5s^25p^25d$ (^{1}S) ^{2}D + 28.9 $5s^25p^25d$ (^{3}P) ^{2}D
223839.4	224621	-781.6	1.5	48.4 $5s^25p^25d$ (^{1}S) ^{2}D + 36.1 $5s^25p^25d$ (^{3}P) ^{2}D
235192.8	235205	-12.2	2.5	69.9 $5s^25p^26s$ (^{1}D) ^{2}D + 26.4 $5s^25p^26s$ (^{3}P) ^{4}P
237340	237087	253	1.5	53.3 $5s^25p^26s$ (^{1}D) ^{2}D + 37.7 $5s^25p^26s$ (^{3}P) ^{2}P
252603.3	252564	39.3	0.5	86.2 $5s^25p^26s$ (^{1}S) ^{2}S + 6.5 $5s^25p^26s$ (^{3}P) ^{4}P

a: Energy Levels from Sansonetti [39]
b: This work
c: Only the components $\geq$ 5% are given

Transitions

Table A28: Computed oscillator strengths and transition probabilities Cs V.

λ_{Ritz} Å	E^{a}_{low} cm^{-1}	J_{low}	E_{up} cm^{-1}	J_{up}	log gf	gA s^{-1}	CF
449.918	15077	1.5	237340	1.5	-0.99	3.38E+09	-0.032
453.202	31951	0.5	252603	0.5	-0.53	9.70E+09	-0.408
454.307	15077	1.5	235193	2.5	-0.32	1.54E+10	0.382
459.233	0	1.5	217755	2.5	-0.11	2.46E+10	0.319
460.901	20374	2.5	237340	1.5	-0.49	1.01E+10	0.135
465.508	20374	2.5	235193	2.5	-0.05	2.74E+10	-0.354
472.867	0	1.5	211476	1.5	-0.39	1.22E+10	0.183
475.444	42274	1.5	252603	0.5	-0.73	5.56E+09	0.169
483.427	15077	1.5	221934	1.5	-0.57	7.74E+09	-0.04
487.958	15077	1.5	220013	0.5	-0.25	1.59E+10	0.103
491.094	20374	2.5	224001	2.5	-0.96	3.02E+09	0.017
496.129	20374	2.5	221934	1.5	-0.24	1.57E+10	-0.113
496.135	15077	1.5	216636	0.5	-0.42	1.02E+10	0.14
499.691	0	1.5	200124	0.5	-0.43	9.99E+09	0.21
501.496	0	1.5	199404	2.5	-0.07	2.24E+10	-0.264
511.958	0	1.5	195328	1.5	-0.06	2.23E+10	-0.19
512.646	42274	1.5	237340	1.5	0.3	5.07E+10	-0.599
516.024	20374	2.5	214163	1.5	-0.19	1.64E+10	0.108
518.352	42274	1.5	235193	2.5	-0.29	1.27E+10	-0.279
521.137	31951	0.5	223839	1.5	0.33	5.30E+10	0.285
521.826	15077	1.5	206712	2.5	0.52	8.11E+10	0.255
522.743	15077	1.5	206376	1.5	0.54	8.51E+10	0.391
522.912	0	1.5	191237	0.5	0.38	5.83E+10	0.543
523.279	20374	2.5	211476	1.5	-0.39	9.91E+09	-0.287
524.354	20374	2.5	211084	2.5	-0.25	1.34E+10	0.09
525.968	15077	1.5	205203	0.5	-0.91	2.98E+09	0.028
526.034	20374	2.5	210475	3.5	1.02	2.53E+11	0.62
526.338	0	1.5	189992	1.5	0.62	1.00E+11	0.497
526.364	31951	0.5	221934	1.5	0.41	6.29E+10	-0.641
531.739	31951	0.5	220013	0.5	-0.95	2.64E+09	-0.024
532.993	0	1.5	187620	2.5	0.77	1.38E+11	0.597
536.658	20374	2.5	206712	2.5	0.65	1.02E+11	0.553
537.449	15077	1.5	201142	0.5	0.17	3.38E+10	0.269
537.627	20374	2.5	206376	1.5	-0.08	1.91E+10	0.4
541.464	31951	0.5	216636	0.5	-0.01	2.20E+10	-0.508
542.517	15077	1.5	199404	2.5	0.64	9.72E+10	0.402
548.811	31951	0.5	214163	1.5	-0.63	5.32E+09	-0.06
550.276	42274	1.5	224001	2.5	0.87	1.64E+11	0.511
550.765	42274	1.5	223839	1.5	0.22	3.65E+10	0.335
556.607	42274	1.5	221934	1.5	-0.21	1.33E+10	0.077
558.566	20374	2.5	199404	2.5	0.2	3.35E+10	-0.179
562.621	42274	1.5	220013	0.5	0.29	4.17E+10	-0.294
570.109	0	1.5	175405	2.5	-0.18	1.37E+10	0.253
571.576	20374	2.5	195328	1.5	-0.84	2.90E+09	-0.09
573.313	31951	0.5	206376	1.5	-0.56	5.59E+09	-0.101
573.52	42274	1.5	216636	0.5	-0.5	6.34E+09	0.1
577.194	31951	0.5	205203	0.5	0.04	2.24E+10	0.325
577.473	15077	1.5	188246	1.5	0.19	3.05E+10	0.259
579.568	15077	1.5	187620	2.5	-0.49	6.46E+09	0.084
581.609	0	1.5	171937	1.5	-0.75	3.51E+09	0.228
581.769	42274	1.5	214163	1.5	0.02	2.11E+10	0.108
591.008	42274	1.5	211476	1.5	-0.96	2.07E+09	-0.044
591.05	31951	0.5	201142	0.5	-0.85	2.72E+09	0.057
591.568	20374	2.5	189416	3.5	-0.24	1.09E+10	-0.151
592.38	42274	1.5	211084	2.5	-0.7	3.74E+09	-0.021
595.691	20374	2.5	188246	1.5	0.34	4.09E+10	-0.34
597.921	20374	2.5	187620	2.5	-0.23	1.09E+10	-0.43
608.131	42274	1.5	206712	2.5	-1	1.81E+09	-0.01
610.236	20374	2.5	184245	3.5	-0.37	7.60E+09	0.129
612.08	31951	0.5	195328	1.5	-0.37	7.66E+09	-0.071
623.722	0	1.5	160328	2.5	-0.51	5.38E+09	0.316
623.723	15077	1.5	175405	2.5	-0.86	2.34E+09	0.033
629.454	42274	1.5	201142	0.5	-0.83	2.51E+09	0.035
645.03	20374	2.5	175405	2.5	-0.79	2.57E+09	0.194
659.791	20374	2.5	171937	1.5	-0.82	2.30E+09	0.381
698.464	15077	1.5	158249	0.5	-0.76	2.34E+09	-0.057
727.117	20374	2.5	157903	1.5	-1	1.26E+09	0.084
742.955	20374	2.5	154971	1.5	-0.79	1.96E+09	-0.048
750.17	42274	1.5	175577	0.5	-1	1.17E+09	-0.034
800.757	15077	1.5	139959	1.5	-0.65	2.34E+09	-0.039
806.715	20374	2.5	144333	2.5	-0.65	2.30E+09	-0.037
811.738	0	1.5	123192	1.5	-0.81	1.59E+09	0.047
877.95	0	1.5	113902	2.5	-0.74	1.57E+09	0.045

a: Energy Levels from [39]

Cs VI

Energy Levels

Table A29: Comparison between available experimental data and calculated energy levels (in cm^{-1}) in Cs VI

E^{a}_{exp}	E^{b}_{calc}	ΔE	J	Leading components (in %) in LS coupling ^{c}
Even Parity				
0	45	-45	0	86.3 $5s^25p^2$ (^{3}P) ^{3}P + 11.1 $5s^25p^2$ (^{1}S) ^{1}S
12176	12006	170	1	97.4 $5s^25p^2$ (^{3}P) ^{3}P
17628.2	17723	-94.8	2	63.5 $5s^25p^2$ (^{3}P) ^{3}P + 33.7 $5s^25p^2$ (^{1}D) ^{1}D
35061.4	35134	-72.6	2	62.8 $5s^25p^2$ (^{1}D) ^{1}D + 33.8 $5s^25p^2$ (^{3}P) ^{3}P
52410.3	52368	42.3	0	84.7 $5s^25p^2$ (^{1}S) ^{1}S + 11.2 $5s^25p^2$ (^{3}P) ^{3}P
Odd Parity				
106878.6	106911	-32.4	2	90.9 $5s5p^3$ (^{4}S) ^{5}S + 7.3 $5s5p^3$ (^{2}P) ^{3}P
131766.8	131977	-210.2	1	73 $5s5p^3$ (^{2}D) ^{3}D + 12.3 $5s5p^3$ (^{2}P) ^{3}P + 7.2 $5s^25p5d$ (^{2}P) ^{3}D
133089.4	133160	-70.6	2	71 $5s5p^3$ (^{2}D) ^{3}D + 14 $5s5p^3$ (^{2}P) ^{3}P + 6.6 $5s^25p5d$ (^{2}P) ^{3}D
138042.8	138025	17.8	3	89.8 $5s5p^3$ (^{2}D) ^{3}D + 7.8 $5s^25p5d$ (^{2}P) ^{3}D
152634.7	152692	-57.3	0	91.3 $5s5p^3$ (^{2}P) ^{3}P + 6.9 $5s^25p5d$ (^{2}P) ^{3}P
154198.2	154083	115.2	1	73.7 $5s5p^3$ (^{2}P) ^{3}P + 12.1 $5s5p^3$ (^{2}D) ^{3}D + 5.8 $5s^25p5d$ (^{2}P) ^{3}P
154775.8	154559	216.8	2	39.8 $5s5p^3$ (^{2}P) ^{3}P + 23.2 $5s5p^3$ (^{2}D) ^{1}D + 14.3 $5s5p^3$ (^{2}D) ^{3}D
168730.2	168396	334.2	2	32 $5s5p^3$ (^{2}D) ^{1}D + 28.1 $5s5p^3$ (^{2}P) ^{3}P + 26.4 $5s^25p5d$ (^{2}P) ^{1}D
175645.3	175441	204.3	1	64.3 $5s5p^3$ (^{4}S) ^{3}S + 25.7 $5s5p^3$ (^{2}P) ^{1}P
181755.2	181684	71.2	2	85.5 $5s^25p5d$ (^{2}P) ^{3}F + 8.1 $5s5p^3$ (^{2}D) ^{1}D
187270	187505	-235	3	88.1 $5s^25p5d$ (^{2}P) ^{3}F
194461	194979	-518	1	50.5 $5s5p^3$ (^{2}P) ^{1}P + 22.9 $5s5p^3$ (^{4}S) ^{3}S + 13.3 $5s^25p5d$ (^{2}P) ^{1}P
197579.4	197530	49.4	2	21.6 $5s^25p5d$ (^{2}P) ^{3}D + 44 $5s^25p5d$ (^{2}P) ^{3}P + 14.6 $5s^25p5d$ (^{2}P) ^{1}D
199798.6	199665	133.6	1	59.7 $5s^25p5d$ (^{2}P) ^{3}D + 15.8 $5s^25p5d$ (^{2}P) ^{3}P + 7 $5s5p^3$ (^{2}P) ^{1}P
209795.3	209937	-141.7	2	34.1 $5s^25p5d$ (^{2}P) ^{1}D + 37.1 $5s^25p5d$ (^{2}P) ^{3}D + 14.9 $5s5p^3$ (^{2}D) ^{1}D
212146.6	212162	-15.4	3	75.2 $5s^25p5d$ (^{2}P) ^{3}D + 7.3 $5s^25p5d$ (^{2}P) ^{3}F + 6.7 $5s^25p5d$ (^{2}P) ^{1}F
212928.1	212908	20.1	0	89.1 $5s^25p5d$ (^{2}P) ^{3}P + 6.6 $5s5p^3$ (^{2}P) ^{3}P
214185.9	214144	41.9	1	64.9 $5s^25p5d$ (^{2}P) ^{3}P + 20.2 $5s^25p5d$ (^{2}P) ^{3}D + 6.1 $5s5p^3$ (^{2}P) ^{3}P
216002.8	215978	24.8	2	43.4 $5s^25p5d$ (^{2}P) ^{3}P + 26.2 $5s^25p5d$ (^{2}P) ^{3}D + 11.5 $5s^25p5d$ (^{2}P) ^{1}D
226523.4	226643	-119.6	3	85.2 $5s^25p5d$ (^{2}P) ^{1}F + 8.3 $5s^25p5d$ (^{2}P) ^{3}D + 1.1 $5p^35d$ (^{2}P) ^{1}F
232014.9	231831	183.9	1	72.7 $5s^25p5d$ (^{2}P) ^{1}P + 8.5 $5s5p^3$ (^{2}P) ^{1}P + 5.8 $5s^25p5d$ (^{2}P) ^{3}D
242213.3	242174	39.3	0	96.5 $5s^25p6s$ (^{2}P) ^{3}P
243719.2	243768	-48.8	1	72.6 $5s^25p6s$ (^{2}P) ^{3}P + 20.5 $5s^25p6s$ (^{2}P) ^{1}P
260952	260958	-6	2	96.2 $5s^25p6s$ (^{2}P) ^{3}P
264226.7	264221	5.7	1	72.2 $5s^25p6s$ (^{2}P) ^{1}P + 22.6 $5s^25p6s$ (^{2}P) ^{3}P

a: Energy Levels from Sansonetti [39]
b: This work
c: Only the components ≥ 5% are given

Transitions

Table A30: Computed oscillator strengths and transition probabilities Cs VI.

λ_{Ritz} Å	E^{a}_{low} cm^{-1}	J_{low}	E_{up} cm^{-1}	J_{up}	log gf	gA s^{-1}	CF
401.968	12176	1	260952	2	-0.33	1.92E+10	-0.758
405.517	17628	2	264227	1	-0.68	8.46E+09	-0.154
410.308	0	0	243719	1	-0.41	1.54E+10	-0.476
410.975	17628	2	260952	2	-0.06	3.44E+10	0.749
431.885	12176	1	243719	1	-0.7	7.08E+09	0.557
434.712	12176	1	242213	0	-0.5	1.12E+10	0.677
436.366	35061	2	264227	1	0.11	4.50E+10	0.704
442.3	17628	2	243719	1	-0.19	2.19E+10	0.528
442.692	35061	2	260952	2	-0.37	1.44E+10	0.73
472.107	52410	0	264227	1	-0.23	1.78E+10	0.76
478.709	17628	2	226523	3	-0.03	2.74E+10	-0.114
490.613	12176	1	216003	2	-0.68	5.75E+09	-0.036
495.025	12176	1	214186	1	0.15	3.85E+10	-0.474
498.127	12176	1	212928	0	-0.11	2.09E+10	-0.606
500.504	0	0	199799	1	0.36	6.10E+10	0.487
504.097	17628	2	216003	2	-0.02	2.51E+10	-0.13
506.023	12176	1	209795	2	0.32	5.42E+10	0.669
508.756	17628	2	214186	1	-0.17	1.75E+10	-0.403
514.09	17628	2	212147	3	0.81	1.64E+11	0.674
514.242	0	0	194461	1	-0.45	8.92E+09	-0.148
520.38	17628	2	209795	2	0.32	5.17E+10	0.449
522.297	35061	2	226523	3	0.85	1.75E+11	0.676
522.715	52410	0	243719	1	-0.81	3.82E+09	-0.23
532.985	12176	1	199799	1	-0.16	1.63E+10	0.203
539.364	12176	1	197579	2	0.43	6.17E+10	0.647
548.591	12176	1	194461	1	-0.67	4.74E+09	0.139
552.665	35061	2	216003	2	0.52	7.26E+10	-0.593
555.706	17628	2	197579	2	0.1	2.72E+10	-0.185
556.779	52410	0	232015	1	0.37	5.04E+10	0.527
558.271	35061	2	214186	1	-0.28	1.12E+10	-0.528
564.7	35061	2	212147	3	-0.12	1.59E+10	0.121
569.329	0	0	175645	1	-0.49	6.64E+09	0.178
572.299	35061	2	209795	2	-0.1	1.63E+10	-0.154
589.477	17628	2	187270	3	-0.2	1.22E+10	0.657
589.695	12176	1	181755	2	-0.95	2.17E+09	0.556
607.027	35061	2	199799	1	-0.65	4.07E+09	-0.158
609.284	17628	2	181755	2	-0.69	3.63E+09	0.351
611.736	12176	1	175645	1	-0.18	1.18E+10	-0.29
615.316	35061	2	197579	2	-0.4	7.08E+09	0.07
627.354	35061	2	194461	1	0.08	2.04E+10	-0.312
632.843	17628	2	175645	1	0.23	2.84E+10	0.429
681.692	35061	2	181755	2	-0.78	2.36E+09	-0.244
703.974	52410	0	194461	1	-0.69	2.79E+09	0.071
704.115	12176	1	154198	1	-0.52	4.07E+09	0.155
711.953	12176	1	152635	0	-0.95	1.47E+09	0.141
729.141	17628	2	154776	2	-0.29	6.40E+09	0.101
748.118	35061	2	168730	2	-0.36	5.20E+09	0.08
758.917	0	0	131767	1	-0.7	2.31E+09	0.097
827.038	12176	1	133089	2	-0.58	2.60E+09	0.079
830.464	17628	2	138043	3	-0.67	2.05E+09	0.064
971.049	35061	2	138043	3	-0.9	8.95E+08	0.079

a: Energy Levels from [39]

Cs VII

Energy Levels

Table A31: Comparison between available experimental data and calculated energy levels (in cm^{-1}) in Cs VII

E^a_{exp}	E^b_{calc}	ΔE	J	Leading components (in %) in LS coupling [c]
Odd Parity				
0	-2	2	0.5	97.9 $5s^25p$ (^{1}S) ^{2}P
19379.3	19383	-3.7	1.5	97.7 $5s^25p$ (^{1}S) ^{2}P
166536.9	166537	-0.1	2.5	99.6 $5s^24f$ (^{1}S) ^{2}F
167296.5	167296	0.5	3.5	99.6 $5s^24f$ (^{1}S) ^{2}F
260637.9	260489	148.9	1.5	29.2 $5p^3$ (^{2}D) ^{2}D + 35.9 $5p^3$ (^{4}S) ^{4}S + 21.5 $5p^3$ (^{2}P) ^{2}P
270870.2	271020	-149.8	1.5	52.4 $5p^3$ (^{4}S) ^{4}S + 32.9 $5p^3$ (^{2}D) ^{2}D + 12.9 5s5p5d (^{3}P) ^{2}D
272400.9	272341	59.9	2.5	71.8 $5p^3$ (^{2}D) ^{2}D + 25.7 5s5p5d (^{3}P) ^{2}D
293283.2	293298	-14.8	1.5	91.5 5s5p5d (^{3}P) ^{4}F
293209.4	293379	-169.6	0.5	83 $5p^3$ (^{2}P) ^{2}P + 10.3 5s5p5d (^{3}P) ^{2}P
297070.8	297358	-287.2	2.5	90.4 5s5p5d (^{3}P) ^{4}F
302522.8	302270	252.8	1.5	54 $5p^3$ (^{2}P) ^{2}P + 12.6 5s5p5d (^{3}P) ^{2}P + 10 $5p^3$ (^{4}S) ^{4}S
302858.4	303676	-817.6	3.5	89 5s5p5d (^{3}P) ^{4}F + 7.8 5s5p5d (^{3}P) ^{4}D
310692.9	310460	232.9	2.5	51.2 5s5p5d (^{3}P) ^{4}P + 26.9 5s5p5d (^{3}P) ^{4}D + 8.8 5s5p5d (^{1}P) ^{2}D
312206.3	311930	276.3	1.5	60.7 5s5p5d (^{3}P) ^{4}D + 27.3 5s5p5d (^{3}P) ^{4}P + 3.3 5s5p5d (^{1}P) ^{2}D
312626.8	312342	284.8	0.5	85.8 5s5p5d (^{3}P) ^{4}D + 7.6 5s5p5d (^{3}P) ^{4}P
320848.6	320846	2.6	0.5	93.6 $5s^26p$ (^{1}S) ^{2}P
322850.6	322908	-57.4	2.5	25.6 5s5p5d (^{3}P) ^{2}F + 21.1 5s5p5d (^{3}P) ^{4}D + 17.5 5s5p5d (^{1}P) ^{2}F
324129.9	323877	252.9	1.5	36.7 5s5p5d (^{3}P) ^{2}D + 16 $5s^26p$ (^{1}S) ^{2}P + 11 5s5p5d (^{1}P) ^{2}D
324722.6	324859	-136.4	3.5	87.9 5s5p5d (^{3}P) ^{4}D + 9.2 5s5p5d (^{3}P) ^{4}F
326029.5	325976	53.5	2.5	43.7 5s5p5d (^{3}P) ^{4}D + 22.2 5s5p5d (^{3}P) ^{4}P + 21.2 5s5p5d (^{3}P) ^{2}F
326357.4	326556	-198.6	0.5	90.5 5s5p5d (^{3}P) ^{4}P + 8.3 5s5p5d (^{3}P) ^{4}D
326711.9	326660	51.9	1.5	49.7 5s5p5d (^{3}P) ^{4}P + 23.7 $5s^26p$ (^{1}S) ^{2}P + 21.6 5s5p5d (^{3}P) ^{4}D
328057.7	328165	-107.3	1.5	50.9 $5s^26p$ (^{1}S) ^{2}P + 16.6 5s5p5d (^{3}P) ^{4}P + 14.3 5s5p5d (^{3}P) ^{2}D
332409.5	331502	907.5	2.5	27.6 5s5p5d (^{3}P) ^{2}D + 25 5s5p5d (^{3}P) ^{4}P + 17.4 5s5p5d (^{1}P) ^{2}D
342601.4	342153	448.4	3.5	57.3 5s5p5d (^{3}P) ^{2}F + 40 5s5p5d (^{1}P) ^{2}F
348210.7	348178	32.7	1.5	50.8 5s5p5d (^{3}P) ^{2}P + 28.3 5s5p5d (^{1}P) ^{2}D + 8.9 $5p^3$ (^{2}P) ^{2}P
356097.4	356127	-29.6	3.5	46.1 5s5p5d (^{1}P) ^{2}F + 38.2 5s5p5d (^{3}P) ^{2}F + 8.3 $5s^25f$ (^{1}S) ^{2}F
356019.7	356421	-401.3	0.5	63.6 5s5p5d (^{3}P) ^{2}P + 21.8 5s5p5d (^{1}P) ^{2}P
357398.5	357204	194.5	2.5	52.8 5s5p5d (^{1}P) ^{2}F + 26.3 5s5p5d (^{3}P) ^{2}F + 9.8 $5s^25f$ (^{1}S) ^{2}F
365025	364524	501	1.5	48.2 5s5p5d (^{1}P) ^{2}P + 22.5 5s5p5d (^{1}P) ^{2}D + 15.5 5s5p5d (^{3}P) ^{2}P
364989.8	364956	33.8	0.5	65.9 5s5p5d (^{1}P) ^{2}P + 18.9 5s5p5d (^{3}P) ^{2}P + 9.3 $5p^3$ (^{2}P) ^{2}P
366610.1	367646	-1035.9	2.5	60.7 5s5p5d (^{1}P) ^{2}D + 16.7 5s5p5d (^{3}P) ^{2}D + 10.5 $5p^3$ (^{2}D) ^{2}D
368265.1	368590	-324.9	1.5	21.9 5s5p5d (^{1}P) ^{2}D + 37.6 5s5p5d (^{1}P) ^{2}P + 11.7 5s5p5d (^{3}P) ^{2}D
379095	379026	69	0.5	93.7 sp6s (^{3}P) ^{4}P
383877.1	383868	9.1	1.5	87.1 sp6s (^{3}P) ^{4}P + 6.5 sp6s (^{3}P) ^{2}P
384897	384908	-11	2.5	88 $5s^25f$ (^{1}S) ^{2}F + 8.4 5s5p5d (^{1}P) ^{2}F
385051.8	385054	-2.2	3.5	89.8 $5s^25f$ (^{1}S) ^{2}F + 7.7 5s5p5d (^{1}P) ^{2}F
390998.4	391082	-83.6	0.5	89.4 sp6s (^{3}P) ^{2}P
398620.2	398699	-78.8	2.5	98.7 sp6s (^{3}P) ^{4}P
406417.6	406333	84.6	1.5	86.6 sp6s (^{3}P) ^{2}P + 8.6 sp6s (^{3}P) ^{4}P
434063.6	434150	-86.4	0.5	88.4 sp6s (^{1}P) ^{2}P
435440	435353	87	1.5	88.3 sp6s (^{1}P) ^{2}P
Even Parity				
104226.2	104221	5.2	0.5	92.6 $5s5p^2$ (^{3}P) ^{4}P + 6 $5s5p^2$ (^{1}S) ^{2}S
114254.9	114308	-53.1	1.5	98 $5s5p^2$ (^{3}P) ^{4}P
122261.3	122240	21.3	2.5	84.6 $5s5p^2$ (^{3}P) ^{4}P + 13.9 $5s5p^2$ (^{1}D) ^{2}D
141168.5	141335	-166.5	1.5	82.7 $5s5p^2$ (^{1}D) ^{2}D + 9.5 $5s^25d$ (^{1}S) ^{2}D + 5.1 $5s5p^2$ (^{3}P) ^{2}P
147182.2	147001	181.2	2.5	74.4 $5s5p^2$ (^{1}D) ^{2}D + 14.8 $5s5p^2$ (^{3}P) ^{4}P + 9.1 $5s^25d$ (^{1}S) ^{2}D
158091.3	157986	105.3	0.5	64 $5s5p^2$ (^{3}P) ^{2}P + 29.1 $5s5p^2$ (^{1}S) ^{2}S
178190.9	178240	-49.1	0.5	63.3 $5s5p^2$ (^{1}S) ^{2}S + 32.5 $5s5p^2$ (^{3}P) ^{2}P
179339.4	179387	-47.6	1.5	90.8 $5s5p^2$ (^{3}P) ^{2}P
205994.2	205972	22.2	1.5	83 $5s^25d$ (^{1}S) ^{2}D + 10.2 $5s5p^2$ (^{1}D) ^{2}D
208786.9	208804	-17.1	2.5	85.3 $5s^25d$ (^{1}S) ^{2}D + 8.8 $5s5p^2$ (^{1}D) ^{2}D
263007.7	263214	-206.3	2.5	67.8 5s5p4f (^{3}F) ^{4}G + 20 5s5p4f (^{3}F) ^{4}F + 5.6 5s5p4f (^{3}F) ^{2}F
265224.4	264989	235.4	3.5	44.8 5s5p4f (^{3}F) ^{4}G + 43.6 5s5p4f (^{3}F) ^{4}F + 9.1 5s5p4f (^{3}F) ^{4}D
268166.6	268286	-119.4	1.5	87 5s5p4f (^{3}F) ^{4}F + 7.3 5s5p4f (^{3}F) ^{4}D
268650	268773	-123	2.5	49.3 5s5p4f (^{3}F) ^{4}F + 18.5 5s5p4f (^{3}F) ^{4}D + 11.9 5s5p4f (^{3}F) ^{2}F
268882.9	268843	39.9	4.5	49.3 5s5p4f (^{3}F) ^{4}F + 43.6 5s5p4f (^{3}F) ^{4}G + 6.5 5s5p4f (^{3}F) ^{2}G
269022.7	268854	168.7	3.5	26.9 5s5p4f (^{3}F) ^{4}D + 23.1 5s5p4f (^{3}F) ^{2}F + 21.4 5s5p4f (^{3}F) ^{4}G
273351.5	273351	0.5	0.5	97 $5s^26s$ (^{1}S) ^{2}S
274950.7	275180	-229.3	2.5	49.5 5s5p4f (^{1}F) ^{2}F + 19.1 5s5p4f (^{3}F) ^{4}G + 15.3 5s5p4f (^{1}F) ^{2}D
276972.2	276854	118.2	3.5	28.5 5s5p4f (^{1}F) ^{2}F + 31.8 5s5p4f (^{1}F) ^{2}G + 14.4 5s5p4f (^{3}F) ^{4}G
284435.5	284391	44.5	3.5	38.9 5s5p4f (^{3}F) ^{4}F + 36 5s5p4f (^{3}F) ^{4}D + 14.9 5s5p4f (^{3}F) ^{4}G
286808.3	286764	44.3	2.5	67.8 5s5p4f (^{3}F) ^{4}D + 24.5 5s5p4f (^{3}F) ^{4}F
289470.5	289848	-377.5	3.5	43.8 5s5p4f (^{1}F) ^{2}G + 16.4 5s5p4f (^{3}F) ^{2}F + 15.1 5s5p4f (^{3}F) ^{4}D
295868.7	295303	565.7	2.5	58.2 5s5p4f (^{1}F) ^{2}D + 17.1 5s5p4f (^{3}F) ^{2}F + 9.1 5s5p4f (^{3}F) ^{2}D
302199	302337	-138	1.5	68.3 5s5p4f (^{1}F) ^{2}D + 25 5s5p4f (^{3}F) ^{2}D
313168.4	312989	179.4	2.5	56.6 5s5p4f (^{3}F) ^{2}F + 31.7 5s5p4f (^{1}F) ^{2}F + 7.6 5s5p4f (^{1}F) ^{2}D
313848.9	313861	-12.1	3.5	54.7 5s5p4f (^{3}F) ^{2}F + 36.7 5s5p4f (^{1}F) ^{2}F
317249.8	317257	-7.2	4.5	68 5s5p4f (^{3}F) ^{2}G + 27.3 5s5p4f (^{1}F) ^{2}G
317726.7	317650	76.7	3.5	88.3 5s5p4f (^{3}F) ^{2}G + 7.3 5s5p4f (^{1}F) ^{2}G
323933.7	323956	-22.3	1.5	65.1 5s5p4f (^{3}F) ^{2}D + 29.7 5s5p4f (^{1}F) ^{2}D
325157.4	325401	-243.6	2.5	80 5s5p4f (^{3}F) ^{2}D + 13.8 5s5p4f (^{1}F) ^{2}D

a: Energy Levels from Husain [40]
b: This work
c: Only the components ≥ 5% are given

Transitions

Table A32: Computed oscillator strengths and transition probabilities Cs VII.

λ_{Ritz} Å	E^a_{low} cm^{-1}	J_{low}	E_{up} cm^{-1}	J_{up}	log gf	gA s^{-1}	CF
365.829	0	0.5	273352	0.5	-0.4	1.99E+10	-0.895
393.744	19379	1.5	273352	0.5	-0.13	3.19E+10	0.898
485.451	0	0.5	205994	1.5	0.42	7.36E+10	0.617
527.962	19379	1.5	208787	2.5	0.67	1.12E+11	0.746
535.863	19379	1.5	205994	1.5	-0.1	1.85E+10	0.71
546.998	114255	1.5	297071	2.5	-0.83	3.28E+09	-0.582
557.602	0	0.5	179339	1.5	-0.2	1.37E+10	-0.314
572.051	122261	2.5	297071	2.5	-0.84	2.98E+09	0.692
600.082	104226	0.5	270870	1.5	-0.57	5.04E+09	-0.442
625.156	19379	1.5	179339	1.5	0.4	4.26E+10	0.497
629.677	19379	1.5	178191	0.5	-0.04	1.52E+10	-0.553
632.546	0	0.5	158091	0.5	0.08	2.01E+10	0.607
638.507	114255	1.5	270870	1.5	-0.18	1.08E+10	-0.581
639.338	104226	0.5	260638	1.5	-0.53	4.80E+09	-0.414
657.718	141169	1.5	293209	0.5	-0.27	8.32E+09	0.28
672.907	122261	2.5	270870	1.5	-0.21	9.02E+09	-0.454
683.139	114255	1.5	260638	1.5	-0.45	5.08E+09	-0.399
708.373	0	0.5	141169	1.5	-0.41	5.24E+09	-0.146
722.666	122261	2.5	260638	1.5	-0.09	1.04E+10	-0.556
773.205	166537	2.5	295869	2.5	-0.66	2.41E+09	-0.179
782.455	19379	1.5	147182	2.5	-0.53	3.23E+09	-0.095
798.603	147182	2.5	272401	2.5	-0.25	5.91E+09	0.169
808.486	147182	2.5	270870	1.5	-0.67	2.21E+09	-0.376
818.505	167297	3.5	289471	3.5	-0.82	1.52E+09	-0.083
837.034	141169	1.5	260638	1.5	-0.85	1.33E+09	-0.062
869.425	178191	0.5	293209	0.5	-0.61	2.16E+09	0.124
975.166	158091	0.5	260638	1.5	-0.84	1.03E+09	-0.067
975.745	166537	2.5	269023	3.5	-0.98	7.26E+08	-0.402
983.031	167297	3.5	269023	3.5	-0.93	8.04E+08	0.074
984.384	167297	3.5	268883	4.5	-0.87	9.25E+08	-0.42
1074.558	179339	1.5	272401	2.5	-0.62	1.40E+09	0.066
2409.463	167297	3.5	208787	2.5	-0.69	2.35E+08	0.246
2533.624	166537	2.5	205994	1.5	-0.9	1.31E+08	0.234
3139.163	265224	3.5	297071	2.5	-0.64	1.60E+08	-0.813
3302.05	263008	2.5	293283	1.5	-0.71	1.17E+08	-0.797

a: Energy Levels from [40]

Ag IV-VII

Ag IV

Energy Levels

Table A33: Comparison between available experimental data and calculated even energy levels (in cm^{-1}) in Ag IV

E^a_{exp}	E^b_{calc}	Δ E	J	Leading components (in %) in LS Coupling^c
0	-15	15	4	98.4 $4d^8$ (^{3}F) ^{3}F
4172.5	4177	-4.5	3	99.4 $4d^8$ (^{3}F) ^{3}F
5829.6	5838	-8.4	2	82.1 $4d^8$ (^{3}F) ^{3}F + 15.3 $4d^8$ (^{1}D) ^{1}D
11871.5	11887	-15.5	2	58.8 $4d^8$ (^{3}P) ^{3}P + 28.1 $4d^8$ (^{1}D) ^{1}D + 12.1 $4d^8$ (^{3}F) ^{3}F
15899.8	15889	10.8	1	99 $4d^8$ (^{3}P) ^{3}P
16092.4	16096	-3.6	0	96.5 $4d^8$ (^{3}P) ^{3}P
17397.7	17388	9.7	2	55.8 $4d^8$ (^{1}D) ^{1}D + 38.2 $4d^8$ (^{3}P) ^{3}P + 5.1 $4d^8$ (^{3}F) ^{3}F
20570	20572	-2	4	98.2 $4d^8$ (^{1}G) ^{1}G
47138.6	47140	-1.4	0	96.5 $4d^8$ (^{1}S) ^{1}S
96396.69	96411	-14.31	5	96.7 $4d^75d$ (^{4}F) ^{5}F
99147.15	99148	-0.85	4	95.1 $4d^75d$ (^{4}F) ^{5}F
101260.51	101269	-8.49	3	96.8 $4d^75d$ (^{4}F) ^{5}F
102632.67	102643	-10.33	2	96.1 $4d^75d$ (^{4}F) ^{5}F
103471.58	103482	-10.42	1	95.2 $4d^75d$ (^{4}F) ^{5}F
107022.3	106993	29.3	4	90.2 $4d^75d$ (^{4}F) ^{3}F
110376.64	110333	43.64	3	47.2 $4d^75d$ (^{4}F) ^{3}F + 46.3 $4d^75d$ (^{4}P) ^{5}P
110778.97	110773	5.97	2	78.7 $4d^75d$ (^{4}P) ^{5}P + 17.1 $4d^75d$ (^{2}P) ^{3}P
111004.7	110945	59.7	3	51 $4d^75d$ (^{4}P) ^{5}P + 46.3 $4d^75d$ (^{4}F) ^{3}F
112611.74	112591	20.74	1	86.3 $4d^75d$ (^{4}P) ^{5}P + 11.1 $4d^75d$ (^{2}P) ^{3}P
112688.86	112724	-35.14	2	89 $4d^75d$ (^{4}F) ^{3}F
115550.39	115522	28.39	5	84 $4d^75d$ (^{2}G) ^{3}G + 10.4 $4d^75d$ (^{2}H) ^{3}H
116806	116732	74	4	70.7 $4d^75d$ (^{2}G) ^{3}G + 16.1 $4d^75d$ (^{2}H) ^{3}H + 7.2 $4d^75d$ (^{2}G) ^{1}G
118603.01	118602	1.01	2	35.2 $4d^75d$ (^{2}P) ^{3}P + 34.5 $4d^75d$ (^{4}P) ^{3}P + 14 $4d^75d$ (^{2}D) ^{3}D
118613.78	118725	-111.22	1	13.4 $4d^75d$ (^{2}D) ^{3}D + 29.2 $4d^75d$ (^{4}P) ^{3}P + 27.6 $4d^75d$ (^{2}P) ^{1}P
119119.24	119036	83.24	3	95.8 $4d^75d$ (^{2}G) ^{3}G
120216.19	120504	-287.81	0	60.8 $4d^75d$ (^{2}P) ^{3}P + 38.3 $4d^75d$ (^{4}P) ^{3}P
120871.27	120938	-66.73	6	99.5 $4d^75d$ (^{2}H) ^{3}H
121766.62	121780	-13.38	4	49.9 $4d^75d$ (^{2}G) ^{1}G + 24.4 $4d^75d$ (^{2}H) ^{3}H + 22.1 $4d^75d$ (^{2}G) ^{3}G
121832.93	121771	61.93	2	59.7 $4d^75d$ (^{4}P) ^{3}P + 21.1 $4d^75d$ (^{2}P) ^{3}P + 5.5 $4d^75d$ (^{4}P) ^{5}P
122456.21	122460	-3.79	5	80.5 $4d^75d$ (^{2}H) ^{3}H + 12.6 $4d^75d$ (^{2}H) ^{1}H + 6.3 $4d^75d$ (^{2}G) ^{3}G
122676.15	122661	15.15	1	45.1 $4d^75d$ (^{4}P) ^{3}P + 32.9 $4d^75d$ (^{2}P) ^{3}P + 12.8 $4d^75d$ (^{2}D) ^{3}D
122820.45	122674	146.45	3	73.9 $4d^75d$ (^{2}D) ^{3}D + 19.6 $4d^75d$ (^{2}D) ^{3}D
125076.99	125239	-162.01	1	34.6 $4d^75d$ (^{2}P) ^{3}P + 28.8 $4d^75d$ (^{2}D) ^{3}D + 18.8 $4d^75d$ (^{2}P) ^{1}P
125077.14	124942	135.14	2	46.7 $4d^75d$ (^{2}D) ^{3}D + 18.7 $4d^75d$ (^{2}D) ^{1}D + 11.3 $4d^75d$ (^{2}P) ^{3}P
125735.19	125754	-18.81	4	58.7 $4d^75d$ (^{2}H) ^{3}H + 36.8 $4d^75d$ (^{2}G) ^{1}G
125857.9	125808	49.9	0	60.7 $4d^75d$ (^{4}P) ^{3}P + 38.4 $4d^75d$ (^{2}P) ^{3}P
127929.34	128045	-115.66	5	84.4 $4d^75d$ (^{2}H) ^{1}H + 8.6 $4d^75d$ (^{2}H) ^{3}H + 6.3 $4d^75d$ (^{2}G) ^{3}G
130570.62	130656	-85.38	1	49.7 $4d^75d$ (^{2}P) ^{1}P + 29.8 $4d^75d$ (^{2}D) ^{3}D + 14.7 $4d^75d$ (^{4}P) ^{3}P
131005.72	130922	83.72	2	52.7 $4d^75d$ (^{2}D) ^{1}D + 14.7 $4d^75d$ (^{2}D) ^{3}D + 14.2 $4d^75d$ (^{2}P) ^{3}P
132758.38	132711	47.38	2	94.6 $4d^75d$ (^{2}F) ^{3}F +
133265.26	133263	2.26	3	93.2 $4d^75d$ (^{2}F) ^{3}F +
134577.89	134630	-52.11	4	96.2 $4d^75d$ (^{2}F) ^{3}F +
138852.05	138696	156.05	3	93.4 $4d^75d$ (^{2}F) ^{1}F +
152454.1	152526	-71.9	1	87.8 $4d^75d$ (^{2}D) ^{3}D + 10.9 $4d^75d$ (^{2}D) ^{3}D
153025.9	153064	-38.1	2	81.9 $4d^75d$ (^{2}D) ^{3}D + 13.5 $4d^75d$ (^{2}D) ^{3}D
154125.9	154104	21.9	3	75.6 $4d^75d$ (^{2}D) ^{3}D + 20.2 $4d^75d$ (^{2}D) ^{3}D
158398	158358	40	2	78.6 $4d^75d$ (^{2}D) ^{1}D + 16.5 $4d^75d$ (^{2}D) ^{1}D
246679.7	246668	11.7	5	75.1 $4d^75d$ (^{4}F) ^{5}F + 15.8 $4d^75d$ (^{4}F) ^{5}G
247262	247243	19	4	55.7 $4d^75d$ (^{4}F) ^{5}F + 25 $4d^75d$ (^{4}F) ^{5}D + 8.4 $4d^75d$ (^{4}F) ^{5}G
247618	247689	-71	6	85.4 $4d^75d$ (^{4}F) ^{5}G + 10.5 $4d^75d$ (^{4}F) ^{5}H
250366.9	250240	126.9	2	38.2 $4d^75d$ (^{4}F) ^{5}F + 24.7 $4d^75d$ (^{4}F) ^{5}D + 14.3 $4d^75d$ (^{4}F) ^{5}P
250505.6	250438	67.6	4	46 $4d^75d$ (^{4}F) ^{5}D + 30.2 $4d^75d$ (^{4}F) ^{5}G + 10.9 $4d^75d$ (^{4}F) ^{3}G
251310.2	251342	-31.8	3	53.5 $4d^75d$ (^{4}F) ^{3}D + 24.3 $4d^75d$ (^{4}F) ^{5}F + 12.8 $4d^75d$ (^{4}F) ^{5}G
252092.8	252325	-232.2	5	25.2 $4d^75d$ (^{4}F) ^{5}G + 28.8 $4d^75d$ (^{4}F) ^{3}H + 18.4 $4d^75d$ (^{4}F) ^{5}H
253120.5	252903	217.5	4	27 $4d^75d$ (^{4}F) ^{5}G + 29.8 $4d^75d$ (^{4}F) ^{3}G + 10.6 $4d^75d$ (^{4}F) ^{3}F
261776.2	261795	-18.8	3	80.1 $4d^76s$ (^{4}F) ^{5}F + 17.9 $4d^76s$ (^{4}F) ^{3}F
262823.8	263055	-231.2	5	94.3 $4d^75d$ (^{4}P) ^{5}F + 1.6 $4d^75d$ (^{4}F) ^{5}F
263413.8	263104	309.8	2	54.9 $4d^75d$ (^{4}P) ^{5}F + 10 $4d^75d$ (^{2}P) ^{3}D + 8 $4d^75d$ (^{4}P) ^{5}D
265006.2	265053	-46.8	7	78.2 $4d^75d$ (^{2}G) ^{3}I + 10.5 $4d^75d$ (^{2}H) ^{3}K + 7.1 $4d^75d$ (^{2}H) ^{1}K
265332.4	265481	-148.6	4	76 $4d^75d$ (^{4}P) ^{5}D + 9.6 $4d^75d$ (^{2}P) ^{3}F + 6.8 $4d^75d$ (^{4}P) ^{3}F
265345.3	265411	-65.7	5	42.4 $4d^75d$ (^{2}G) ^{3}G + 25.8 $4d^75d$ (^{2}G) ^{3}H + 8 $4d^75d$ (^{2}G) ^{1}H
266079.3	266089	-9.7	5	24 $4d^75d$ (^{2}G) ^{1}H + 36.8 $4d^75d$ (^{2}G) ^{3}G + 11.3 $4d^75d$ (^{2}G) ^{3}H
267820.7	267885	-64.3	4	37.1 $4d^75d$ (^{2}G) ^{3}F + 31.7 $4d^75d$ (^{2}H) ^{3}G + 16.1 $4d^75d$ (^{2}H) ^{3}F
269345.3	269557	-211.7	5	37.3 $4d^75d$ (^{2}G) ^{3}H + 30.5 $4d^75d$ (^{2}G) ^{1}H + 21 $4d^75d$ (^{2}H) ^{3}G
269391.3	269281	110.3	6	44.1 $4d^75d$ (^{2}G) ^{1}I + 39.2 $4d^75d$ (^{2}G) ^{3}I + 11.7 $4d^75d$ (^{2}G) ^{3}H
269452.5	269619	-166.5	7	50.7 $4d^75d$ (^{2}H) ^{3}K + 48.1 $4d^75d$ (^{2}H) ^{1}K
270208.7	270284	-75.3	5	71.3 $4d^75d$ (^{2}H) ^{3}G + 11.4 $4d^75d$ (^{2}G) ^{1}H + 10.8 $4d^75d$ (^{2}G) ^{3}H
272280.4	272071	209.4	7	96.9 $4d^75d$ (^{2}H) ^{3}I
272423.91	272266	157.91	6	36.3 $4d^75d$ (^{2}H) ^{3}I + 50.4 $4d^75d$ (^{2}H) ^{3}H + 7.9 $4d^75d$ (^{2}H) ^{1}I
273195.6	273001	194.6	6	40.4 $4d^75d$ (^{2}H) ^{3}H + 22.2 $4d^75d$ (^{2}H) ^{3}I + 16.2 $4d^75d$ (^{2}H) ^{1}I
273420.8	273459	-38.2	6	64.4 $4d^75d$ (^{2}H) ^{3}K + 9.3 $4d^75d$ (^{2}G) ^{1}I + 8.2 $4d^75d$ (^{2}H) ^{1}I
274634.3	274715	-80.7	5	81.3 $4d^76s$ (^{2}G) ^{3}G + 8.9 $4d^76s$ (^{2}H) ^{3}H + 5.1 $4d^76s$ (^{2}H) ^{1}H
278215.8	278145	70.8	3	96.3 $4d^76s$ (^{2}G) ^{3}G
280700.6	280693	7.6	5	56.8 $4d^76s$ (^{2}H) ^{3}H + 42 $4d^76s$ (^{2}H) ^{1}H

a: From Ankita [41]
b: This work
c: Only the component ≥ 5% are given

Table A34: Comparison between available experimental data and calculated odd energy levels (in cm^{-1}) in Ag IV

E$^{a}_{exp}$	E$^{b}_{calc}$	Δ E	J	Leading components (in %) in LS Coupling^{c}
159220.05	159200	20.05	4	50.7 4d^{7}5p (^{4}F) ^{5}D + 29.8 4d^{7}5p (^{4}F) ^{5}F + 6.7 4d^{7}5p (^{4}F) ^{3}F
160255.4	160177	78.4	5	64.4 4d^{7}5p (^{4}F) ^{5}F + 18.1 4d^{7}5p (^{4}F) ^{5}G + 13.9 4d^{7}5p (^{4}F) ^{3}G
162487.2	162516	-28.8	3	37.7 4d^{7}5p (^{4}F) ^{5}D + 46.6 4d^{7}5p (^{4}F) ^{5}F + 5.7 4d^{7}5p (^{4}P) ^{5}D
164107.86	164046	61.86	4	30.7 4d^{7}5p (^{4}F) ^{5}F + 32.4 4d^{7}5p (^{4}F) ^{5}G + 21.6 4d^{7}5p (^{4}F) ^{5}D
164677.68	164724	-46.32	2	60.3 4d^{7}5p (^{4}F) ^{5}F + 22.7 4d^{7}5p (^{4}F) ^{5}D
165602.1	165581	21.1	6	95.6 4d^{7}5p (^{4}F) ^{5}G
165602.4	165490	112.4	5	38.8 4d^{7}5p (^{4}F) ^{3}G + 32.2 4d^{7}5p (^{4}F) ^{5}F + 24.2 4d^{7}5p (^{4}F) ^{5}G
166005.9	165993	12.9	3	37 4d^{7}5p (^{4}F) ^{5}G + 22.4 4d^{7}5p (^{4}F) ^{5}D + 16.2 4d^{7}5p (^{4}F) ^{5}F
166077.8	166105	-27.2	1	69.4 4d^{7}5p (^{4}F) ^{5}F + 12.6 4d^{7}5p (^{4}F) ^{5}D + 5.1 4d^{7}5p (^{4}F) ^{3}D
167533.2	167561	-27.8	2	29.8 4d^{7}5p (^{4}F) ^{5}D + 36.8 4d^{7}5p (^{4}F) ^{5}G + 15.1 4d^{7}5p (^{4}P) ^{5}D
167566.07	167471	95.07	4	28.6 4d^{7}5p (^{4}F) ^{5}G + 23.5 4d^{7}5p (^{4}F) ^{3}F + 18.5 4d^{7}5p (^{4}F) ^{5}F
168370.19	168417	-46.81	2	24.2 4d^{7}5p (^{4}F) ^{5}G + 32.1 4d^{7}5p (^{4}P) ^{5}S + 12.4 4d^{7}5p (^{4}F) ^{5}F
168493.34	168531	-37.66	2	56.7 4d^{7}5p (^{4}P) ^{5}S + 17.2 4d^{7}5p (^{4}F) ^{5}G + 5.2 4d^{7}5p (^{4}F) ^{5}D
168595.64	168516	79.64	3	23.4 4d^{7}5p (^{4}F) ^{5}F + 36.7 4d^{7}5p (^{4}F) ^{5}G + 12.6 4d^{7}5p (^{4}F) ^{5}D
168599.51	168622	-22.49	1	45.4 4d^{7}5p (^{4}F) ^{5}D + 29.4 4d^{7}5p (^{4}P) ^{5}D + 14.8 4d^{7}5p (^{4}F) ^{5}F
168748.31	168813	-64.69	0	57.8 4d^{7}5p (^{4}F) ^{5}D + 34.5 4d^{7}5p (^{4}P) ^{5}D
169735.47	169708	27.47	4	48.2 4d^{7}5p (^{4}F) ^{3}F + 19.1 4d^{7}5p (^{4}F) ^{5}F + 11.2 4d^{7}5p (^{4}F) ^{3}G
170092.43	170084	8.43	5	55.7 4d^{7}5p (^{4}F) ^{5}G + 40.9 4d^{7}5p (^{4}F) ^{3}G
171201.77	171288	-86.23	3	43.4 4d^{7}5p (^{4}F) ^{3}D + 26 4d^{7}5p (^{4}F) ^{3}F + 6.6 4d^{7}5p (^{2}G) ^{3}F
173069.05	173074	-4.95	4	66.3 4d^{7}5p (^{4}F) ^{3}G + 26 4d^{7}5p (^{4}F) ^{5}G
173560.58	173634	-73.42	2	36 4d^{7}5p (^{4}F) ^{3}D + 28.8 4d^{7}5p (^{4}F) ^{3}F + 6.8 4d^{7}5p (^{2}G) ^{3}F
173713.49	173729	-15.51	3	37.1 4d^{7}5p (^{4}F) ^{3}F + 27.4 4d^{7}5p (^{4}F) ^{3}D + 12.1 4d^{7}5p (^{4}F) ^{3}G
174638.9	174641	-2.1	2	32.1 4d^{7}5p (^{4}F) ^{3}F + 11.7 4d^{7}5p (^{4}F) ^{3}D + 10.8 4d^{7}5p (^{4}F) ^{5}F
175020.93	175135	-114.07	1	19.3 4d^{7}5p (^{2}P) ^{3}P + 24.1 4d^{7}5p (^{4}F) ^{3}D + 10.7 4d^{7}5p (^{4}P) ^{3}S
175057.11	175042	15.11	3	70.4 4d^{7}5p (^{4}F) ^{3}G + 11.2 4d^{7}5p (^{4}F) ^{5}G
176497.56	176581	-83.44	1	31.1 4d^{7}5p (^{4}F) ^{3}D + 12.9 4d^{7}5p (^{4}F) ^{5}D + 10.3 4d^{7}5p (^{2}P) ^{3}D
177602.49	177533	69.49	5	42.6 4d^{7}5p (^{2}G) ^{3}H + 19.6 4d^{7}5p (^{2}G) ^{1}H + 16.1 4d^{7}5p (^{2}H) ^{3}I
177872.52	177837	35.52	2	1.1 4d^{7}5p (^{2}D) ^{3}F + 20.6 4d^{7}5p (^{4}P) ^{5}D + 16.7 4d^{7}5p (^{4}F) ^{5}D
178004.8	177876	128.8	3	38.4 4d^{7}5p (^{4}P) ^{5}D + 20.3 4d^{7}5p (^{4}P) ^{3}D + 15.3 4d^{7}5p (^{4}F) ^{5}D
178319.66	178276	43.66	4	34.2 4d^{7}5p (^{2}G) ^{3}F + 16.3 4d^{7}5p (^{4}F) ^{3}F + 12.6 4d^{7}5p (^{2}G) ^{3}G
179820.39	179909	-88.61	0	37.7 4d^{7}5p (^{4}P) ^{5}D + 34.2 4d^{7}5p (^{4}F) ^{5}D + 20.5 4d^{7}5p (^{2}P) ^{3}P
179913.67	179774	139.67	1	31 4d^{7}5p (^{4}P) ^{5}D + 15.8 4d^{7}5p (^{4}F) ^{5}D + 13.4 4d^{7}5p (^{4}P) ^{3}S
180280.87	180202	78.87	4	43.1 4d^{7}5p (^{4}P) ^{5}D + 35.3 4d^{7}5p (^{2}G) ^{3}H
180529.11	180390	139.11	4	33.7 4d^{7}5p (^{2}G) ^{3}H + 40.2 4d^{7}5p (^{4}P) ^{5}D + 8.8 4d^{7}5p (^{2}G) ^{1}G
180542.7	181002	-459.3	0	47.6 4d^{7}5p (^{2}P) ^{3}P + 18.3 4d^{7}5p (^{2}D) ^{3}P + 11.1 4d^{7}5p (^{4}P) ^{3}P
181163.79	181061	102.79	2	26.5 4d^{7}5p (^{4}P) ^{5}P + 16.6 4d^{7}5p (^{4}P) ^{5}D + 12.8 4d^{7}5p (^{2}P) ^{1}D
181404.63	181630	-225.37	2	32.7 4d^{7}5p (^{2}P) ^{3}P + 17.5 4d^{7}5p (^{4}F) ^{3}D + 13.4 4d^{7}5p (^{4}P) ^{3}D
181552.93	181466	86.93	6	61 4d^{7}5p (^{2}G) ^{3}H + 32.3 4d^{7}5p (^{2}H) ^{3}I
181823.22	181832	-8.78	1	32.7 4d^{7}5p (^{4}P) ^{5}P + 15.5 4d^{7}5p (^{4}P) ^{5}D + 12.8 4d^{7}5p (^{2}P) ^{3}P
181942.22	181883	59.22	3	38.6 4d^{7}5p (^{4}P) ^{5}P + 26.6 4d^{7}5p (^{2}P) ^{3}D + 12.3 4d^{7}5p (^{4}P) ^{5}D
182242.73	182198	44.73	3	29.5 4d^{7}5p (^{2}G) ^{3}G + 29.6 4d^{7}5p (^{2}G) ^{3}F + 6.7 4d^{7}5p (^{2}G) ^{1}F
182317.58	182377	-59.42	5	80.5 4d^{7}5p (^{2}H) ^{3}G + 7.7 4d^{7}5p (^{2}F) ^{3}G
182910.1	182948	-37.9	6	48.9 4d^{7}5p (^{2}H) ^{1}I + 27.1 4d^{7}5p (^{2}H) ^{3}I + 18.4 4d^{7}5p (^{2}G) ^{3}H
183023.82	182897	126.82	4	30.6 4d^{7}5p (^{2}G) ^{1}G + 29.6 4d^{7}5p (^{2}G) ^{3}F + 12.5 4d^{7}5p (^{2}H) ^{1}G
183234.89	183147	87.89	2	13.3 4d^{7}5p (^{4}P) ^{5}D + 25.1 4d^{7}5p (^{4}P) ^{5}P + 15.2 4d^{7}5p (^{4}P) ^{3}P
183395.67	183414	-18.33	3	0 d^{6}S6p (^{3}P) ^{5}P + 17.2 4d^{7}5p (^{4}P) ^{3}D + 15.8 4d^{7}5p (^{2}G) ^{1}F
183927.65	183930	-2.35	1	25.5 4d^{7}5p (^{4}P) ^{3}S + 21.7 4d^{7}5p (^{4}P) ^{3}D + 20.5 4d^{7}5p (^{2}P) ^{3}P
183962.99	183915	47.99	5	65 4d^{7}5p (^{2}G) ^{3}G + 14.7 4d^{7}5p (^{2}H) ^{3}I + 11.5 4d^{7}5p (^{2}G) ^{1}H
184078.3	184501	-422.7	0	45.1 4d^{7}5p (^{2}P) ^{1}S + 21.6 4d^{7}5p (^{4}P) ^{3}P + 15.3 4d^{7}5p (^{4}P) ^{5}D
184379.86	184250	129.86	3	34.6 4d^{7}5p (^{4}P) ^{3}D + 22.7 4d^{7}5p (^{2}G) ^{1}F + 13.4 4d^{7}5p (^{4}P) ^{5}P
184576.17	184455	121.17	1	7.7 4d^{7}5p (^{2}P) ^{3}D + 29.9 4d^{7}5p (^{4}P) ^{5}P + 25.3 4d^{7}5p (^{4}P) ^{3}S
185280.63	185270	10.63	2	34.8 4d^{7}5p (^{4}P) ^{3}P + 17.3 4d^{7}5p (^{2}D) ^{3}P + 11.5 4d^{7}5p (^{4}P) ^{3}D
185599.89	185443	156.89	3	33.8 4d^{7}5p (^{2}D) ^{3}D + 12.5 4d^{7}5p (^{2}G) ^{3}G + 11.4 4d^{7}5p (^{2}D) ^{3}F
185894.25	185928	-33.75	4	33.6 4d^{7}5p (^{2}H) ^{3}G + 18.4 4d^{7}5p (^{2}G) ^{3}G + 16 4d^{7}5p (^{2}G) ^{3}H
186269.64	186363	-93.36	5	42.5 4d^{7}5p (^{2}H) ^{3}I + 42.6 4d^{7}5p (^{2}G) ^{3}H + 8.7 4d^{7}5p (^{2}G) ^{3}G
186411.3	186451	-39.7	7	99.6 4d^{7}5p (^{2}H) ^{3}I
186418.2	186561	-142.8	1	46.1 4d^{7}5p (^{4}P) ^{3}P + 17.3 4d^{7}5p (^{2}P) ^{1}P + 14.9 4d^{7}5p (^{2}P) ^{3}D
186593.36	186491	102.36	3	34.9 4d^{7}5p (^{2}G) ^{3}F + 23.3 4d^{7}5p (^{2}G) ^{3}G + 6 4d^{7}5p (^{2}F) ^{3}G
186616.09	186498	118.09	2	43.7 4d^{7}5p (^{2}G) ^{3}F + 15.5 4d^{7}5p (^{2}D) ^{3}F + 9.5 4d^{7}5p (^{4}P) ^{3}P
186710.07	186709	1.07	4	47 4d^{7}5p (^{2}G) ^{3}G + 29.4 4d^{7}5p (^{2}H) ^{3}G + 6.5 4d^{7}5p (^{2}H) ^{1}G
186740.29	186711	29.29	5	59.2 4d^{7}5p (^{2}G) ^{1}H + 20.2 4d^{7}5p (^{2}H) ^{3}I + 11 4d^{7}5p (^{2}G) ^{3}H
187354.94	187352	2.94	3	29.3 4d^{7}5p (^{2}P) ^{3}D + 19.7 4d^{7}5p (^{2}D) ^{3}F + 10.3 4d^{7}5p (^{2}D) ^{3}D
187417.14	187426	-8.86	2	21.8 4d^{7}5p (^{4}P) ^{3}D + 32 4d^{7}5p (^{2}G) ^{3}F + 10.6 4d^{7}5p (^{4}P) ^{3}P
187875.22	187794	81.22	1	36 4d^{7}5p (^{2}D) ^{3}D + 17.1 4d^{7}5p (^{4}P) ^{3}D + 8.1 4d^{7}5p (^{4}F) ^{3}D
187965.5	187818	147.5	2	18.1 4d^{7}5p (^{2}D) ^{3}D + 17.2 4d^{7}5p (^{2}P) ^{3}P + 13.2 4d^{7}5p (^{4}P) ^{5}P
188922.26	188825	97.26	3	30.1 4d^{7}5p (^{2}H) ^{3}G + 16.2 4d^{7}5p (^{2}D) ^{1}F + 13.3 4d^{7}5p (^{2}G) ^{3}G
189103.2	189199	-95.8	1	14.4 4d^{7}5p (^{4}P) ^{3}D + 26.6 4d^{7}5p (^{4}P) ^{3}P + 23.2 4d^{7}5p (^{2}P) ^{3}D
189963.65	190034	-70.35	2	39.8 4d^{7}5p (^{2}P) ^{3}D + 11.3 4d^{7}5p (^{2}P) ^{1}D + 10.4 4d^{7}5p (^{2}D) ^{3}P
190120.3	189961	159.3	4	73.8 4d^{7}5p (^{2}D) ^{3}F + 14.3 4d^{7}5p (^{2}D) ^{3}F
190754	190921	-167	6	39.4 4d^{7}5p (^{2}H) ^{3}I + 41.6 4d^{7}5p (^{2}H) ^{1}I + 14.3 4d^{7}5p (^{2}G) ^{3}H
191361.65	191500	-138.35	6	87.7 4d^{7}5p (^{2}H) ^{3}H + 8.9 4d^{7}5p (^{2}H) ^{1}I
191677.8	192067	-389.2	0	60.9 4d^{7}5p (^{4}P) ^{3}P + 34.8 4d^{7}5p (^{2}P) ^{1}S
192003.49	191969	34.49	3	30.3 4d^{7}5p (^{2}G) ^{1}F + 15.3 4d^{7}5p (^{2}D) ^{3}F + 15 4d^{7}5p (^{2}P) ^{3}D
192182.72	192251	-68.28	5	73.7 4d^{7}5p (^{2}H) ^{3}H + 14.6 4d^{7}5p (^{2}H) ^{1}H
192212.87	192340	-127.13	1	48.6 4d^{7}5p (^{2}P) ^{3}S + 18.1 4d^{7}5p (^{2}P) ^{3}P + 11.7 4d^{7}5p (^{2}D) ^{1}P
192372.78	192406	-33.22	2	24.9 4d^{7}5p (^{2}D) ^{3}P + 17 4d^{7}5p (^{2}D) ^{1}D + 14.7 4d^{7}5p (^{2}P) ^{3}D
192830.9	192732	98.9	1	15.3 4d^{7}5p (^{2}P) ^{1}P + 18 4d^{7}5p (^{2}D) ^{3}P + 17.3 4d^{7}5p (^{2}D) ^{1}P
193210.83	193149	61.83	2	31.3 4d^{7}5p (^{2}P) ^{1}D + 16 4d^{7}5p (^{2}D) ^{3}F + 10.3 4d^{7}5p (^{2}P) ^{3}P
193641.49	193794	-152.51	4	68.6 4d^{7}5p (^{2}H) ^{3}H + 20.5 4d^{7}5p (^{2}H) ^{1}G
194622.62	194655	-32.38	4	36.9 4d^{7}5p (^{2}H) ^{1}G + 39.8 4d^{7}5p (^{2}G) ^{1}G + 13.4 4d^{7}5p (^{2}H) ^{3}H
195399.42	195405	-5.58	2	23.3 4d^{7}5p (^{2}D) ^{1}D + 16.2 4d^{7}5p (^{2}F) ^{1}D + 13.8 4d^{7}5p (^{2}D) ^{3}P
195561.29	195414	147.29	3	30.9 4d^{7}5p (^{2}D) ^{1}F + 13.4 4d^{7}5p (^{2}F) ^{3}F + 9.2 4d^{7}5p (^{2}D) ^{3}F
196892.5	196894	-1.5	2	26.1 4d^{7}5p (^{2}F) ^{1}D + 30.9 4d^{7}5p (^{2}F) ^{3}F + 7.5 4d^{7}5p (^{2}D) ^{1}D
197185.75	197105	80.75	1	52.4 4d^{7}5p (^{2}D) ^{1}P + 15.3 4d^{7}5p (^{2}P) ^{3}S + 13.5 4d^{7}5p (^{2}P) ^{1}P
197847.4	197902	-54.6	5	78.5 4d^{7}5p (^{2}H) ^{1}H + 10.7 4d^{7}5p (^{2}H) ^{3}H
198486.52	198395	91.52	3	40.7 4d^{7}5p (^{2}F) ^{3}G + 22.3 4d^{7}5p (^{2}H) ^{3}G + 8.1 4d^{7}5p (^{2}D) ^{1}F
198660.9	198641	19.9	1	40.6 4d^{7}5p (^{2}D) ^{3}P + 18.6 4d^{7}5p (^{2}P) ^{1}P + 7.6 4d^{7}5p (^{2}P) ^{3}S
198990.4	199026	-35.6	4	32.7 4d^{7}5p (^{2}F) ^{3}G + 22.9 4d^{7}5p (^{2}F) ^{1}G + 22.4 4d^{7}5p (^{2}F) ^{3}F
199028	198887	141	0	70.9 4d^{7}5p (^{2}D) ^{3}P + 13.6 4d^{7}5p (^{2}P) ^{3}P + 8.1 4d^{7}5p (^{2}P) ^{1}S
201269.41	201193	76.41	3	62.4 4d^{7}5p (^{2}F) ^{3}F + 10.5 4d^{7}5p (^{2}F) ^{3}G + 6.1 4d^{7}5p (^{2}D) ^{3}F
201341.9	201422	-80.1	2	40.3 4d^{7}5p (^{2}F) ^{3}F + 27.6 4d^{7}5p (^{2}F) ^{1}D + 12.5 4d^{7}5p (^{2}F) ^{3}D

Table A34: Continued

E^a_{exp}	E^b_{calc}	Δ E	J	Leading components (in %) in LS Coupling[c]
201957.65	201885	72.65	3	52.8 $4d^7 5p$ (^2F) ^3D + 8.2 $4d^7 5p$ (^2P) ^3D + 6.8 $4d^7 5p$ (^2D) ^3D
201962	202036	-74	4	53 $4d^7 5p$ (^2F) ^1G + 32.7 $4d^7 5p$ (^2F) ^3G + 5 $4d^7 5p$ (^2H) ^3G
203084.6	203019	65.6	1	76.1 $4d^7 5p$ (^2F) ^3D + 7.4 $4d^7 5p$ (^2D) ^3D + 7.3 $4d^7 5p$ (^2D) ^3D
203154.5	203085	69.5	5	86.7 $4d^7 5p$ (^2F) ^3G + 8.2 $4d^7 5p$ (^2H) ^3G
203236.5	203222	14.5	4	62.8 $4d^7 5p$ (^2F) ^3F + 14.9 $4d^7 5p$ (^2F) ^1G + 10.8 $4d^7 5p$ (^2F) ^3G
203284.2	203222	62.2	2	61 $4d^7 5p$ (^2F) ^3D + 16.3 $4d^7 5p$ (^2F) ^1D + 5.9 $4d^7 5p$ (^2D) ^3D
208471.3	208530	-58.7	3	85.3 $4d^7 5p$ (^2F) ^1F + 7.1 $4d^7 5p$ (^2F) ^3D
215234.5	215218	16.5	2	72.7 $4d^7 5p$ (^2D) ^3P + 16.6 $4d^7 5p$ (^2D) ^3P
215899	216010	-111	2	75.2 $4d^7 5p$ (^2D) ^3F + 8.9 $4d^7 5p$ (^2D) ^3F + 5.9 $4d^7 5p$ (^2F) ^3F
216295	216283	12	1	75.4 $4d^7 5p$ (^2D) ^3P + 7.4 $4d^7 5p$ (^2D) ^3P + 7 $4d^7 5p$ (^2D) ^1P
217731.7	217711	20.7	0	88.8 $4d^7 5p$ (^2D) ^3P + 6.2 $4d^7 5p$ (^2D) ^3P
217970.8	217899	71.8	3	65.1 $4d^7 5p$ (^2D) ^3F + 12.7 $4d^7 5p$ (^2D) ^3F + 7.2 $4d^7 5p$ (^2D) ^1F
221125	221099	26	4	72.5 $4d^7 5p$ (^2D) ^3F + 18.5 $4d^7 5p$ (^2D) ^3F
222038.4	222260	-221.6	1	41.1 $4d^7 5p$ (^2D) ^1P + 30.1 $4d^7 5p$ (^2D) ^3D + 9.5 $4d^7 5p$ (^2D) ^3P
222519.6	222446	73.6	3	66 $4d^7 5p$ (^2D) ^1F + 11.8 $4d^7 5p$ (^2D) ^3F + 11.5 $4d^7 5p$ (^2D) ^1F
224873	225200	-327	1	44.3 $4d^7 5p$ (^2D) ^3D + 39.1 $4d^7 5p$ (^2D) ^1P + 8.9 $4d^7 5p$ (^2D) ^3D
224987.6	225025	-37.4	2	60.7 $4d^7 5p$ (^2D) ^3D + 14.9 $4d^7 5p$ (^2D) ^1D + 13.5 $4d^7 5p$ (^2D) ^3D
226882.1	226511	371.1	2	51.7 $4d^7 5p$ (^2D) ^1D + 17.8 $4d^7 5p$ (^2D) ^1D + 12 $4d^7 5p$ (^2D) ^3D
227643.2	227547	96.2	3	63.2 $4d^7 5p$ (^2D) ^3D + 21.1 $4d^7 5p$ (^2D) ^3D + 6.6 $4d^7 5p$ (^2D) ^1F

a: From Ankita [41]
b: This work
c: Only the component ≥ 5% are given

Transitions

Table A35: Computed oscillator strengths and transition probabilities Ag IV.

Wavelength Å	Lower Level[a] cm^{-1}	J_{Low}	Upper level[a] cm^{-1}	J_{Up}	log gf	gA s^{-1}	CF
491.732	11872	2	215235	2	-0.93	3.26E+09	0.186
495.153	0	4	201958	3	-0.92	3.25E+09	0.121
495.173	20570	4	222520	3	-0.22	1.62E+10	0.563
499.494	16092	0	216295	1	-0.99	2.74E+09	-0.419
501.669	15900	1	215235	2	-0.74	4.78E+09	-0.548
502.231	4173	3	203284	2	-0.9	3.32E+09	0.251
505.467	17398	2	215235	2	-0.81	4.05E+09	-0.316
506.584	20570	4	217971	3	-0.97	2.81E+09	0.556
506.958	5830	2	203085	1	-0.89	3.32E+09	0.307
523.359	17398	2	208471	3	-0.85	3.48E+09	-0.25
525.983	0	4	190120	4	-0.88	3.15E+09	-0.269
526.077	11872	2	201958	3	-0.65	5.42E+09	0.157
531.349	4173	3	192373	2	-0.99	2.41E+09	-0.199
532.194	20570	4	208471	3	0.05	2.66E+10	-0.785
533.662	15900	1	203284	2	-0.56	6.41E+09	0.417
533.746	0	4	187355	3	-0.4	9.42E+09	-0.441
534.231	15900	1	203085	1	-0.94	2.71E+09	0.388
534.756	5830	2	192831	1	-0.95	2.59E+09	0.152
534.782	16092	0	203085	1	-0.8	3.72E+09	0.402
535.863	11872	2	198487	3	-0.65	5.26E+09	-0.403
537.94	0	4	185894	4	-1	2.29E+09	0.144
537.963	17398	2	203284	2	-0.69	4.71E+09	-0.344
538.239	4173	3	189964	2	-0.79	3.78E+09	-0.403
538.793	0	4	185600	3	-0.3	1.14E+10	-0.391
539.624	11872	2	197186	1	-0.94	2.64E+09	-0.11
541.829	17398	2	201958	3	-0.42	8.55E+09	-0.324
543.083	5830	2	189964	2	-0.55	6.45E+09	0.598
543.588	0	4	183963	5	-0.36	9.86E+09	-0.529
544.09	4173	3	187966	2	-0.99	2.32E+09	-0.24
544.396	11872	2	195561	3	-0.65	4.99E+09	-0.28
545.269	0	4	183396	3	-1	2.24E+09	0.111
545.632	5830	2	189103	1	-0.67	4.83E+09	0.356
545.719	4173	3	187417	2	-0.29	1.15E+10	-0.626
546.066	15900	1	199028	0	-0.98	2.34E+09	0.551
546.172	5830	2	188922	3	-0.35	1.00E+10	-0.388
546.377	0	4	183024	4	-0.42	8.47E+09	-0.493
547.162	15900	1	198661	1	-0.81	3.45E+09	0.384
547.832	4173	3	186710	4	-0.01	2.18E+10	-0.657
548.183	4173	3	186593	3	-0.24	1.28E+10	-0.446
548.493	0	4	182318	5	0.11	2.86E+10	-0.677
549.041	5830	2	187966	2	-0.97	2.38E+09	0.284
549.625	0	4	181942	3	-0.69	4.51E+09	-0.332
550.292	4173	3	185894	4	-0.53	6.53E+09	-0.205
550.699	5830	2	187417	2	-0.57	5.94E+09	-0.222
551.305	20570	4	201958	3	-0.71	4.31E+09	0.519
551.684	17398	2	198661	1	-0.6	5.51E+09	-0.365
552.156	4173	3	185281	2	-0.87	2.98E+09	-0.351
553.139	5830	2	186616	2	-0.43	8.18E+09	-0.393
553.745	5830	2	186418	1	-0.72	4.16E+09	-0.589
554.013	11872	2	192373	2	-0.2	1.37E+10	0.505
554.504	11872	2	192213	1	-0.72	4.16E+09	0.265
554.916	4173	3	184380	3	-0.78	3.59E+09	-0.525
556.21	17398	2	197186	1	-0.3	1.09E+10	-0.407
557.104	15900	1	195399	2	-0.98	2.23E+09	-0.347
557.964	4173	3	183396	3	-0.63	5.08E+09	0.319
559.124	4173	3	183024	4	-0.92	2.58E+09	-0.23
560.066	5830	2	184380	3	-0.52	6.39E+09	-0.398
560.791	0	4	178320	4	0.06	2.42E+10	-0.55
561.576	4173	3	182243	3	-0.52	6.36E+09	-0.292
561.792	17398	2	195399	2	-0.09	1.70E+10	-0.492
562.637	47139	0	224873	1	-0.48	7.06E+09	0.674
563.171	5830	2	183396	3	-0.83	3.15E+09	0.152
563.981	15900	1	193211	2	-1	2.11E+09	-0.401
564.088	20570	4	197847	5	-0.02	2.02E+10	0.566
564.233	11872	2	189103	1	-0.94	2.40E+09	0.121
564.81	11872	2	188922	3	-0.67	4.48E+09	-0.331
571.457	20570	4	195561	3	-0.62	4.84E+09	0.283
571.756	47139	0	222038	1	-0.47	6.91E+09	-0.622
572.719	17398	2	192003	3	-0.22	1.22E+10	0.542
574.539	20570	4	194623	4	0.37	4.78E+10	-0.572
575.661	0	4	173713	3	-0.28	1.06E+10	-0.45
575.705	4173	3	177873	2	-0.99	2.08E+09	-0.16
577.796	20570	4	193641	4	-0.29	1.03E+10	-0.626
581.173	15900	1	187966	2	-0.86	2.74E+09	0.323
581.206	11872	2	183928	1	-0.98	2.08E+09	0.117
582.13	16092	0	187875	1	-0.94	2.27E+09	0.286
582.393	17398	2	189103	1	-1	1.95E+09	-0.123
582.707	20570	4	192183	5	-0.64	4.46E+09	0.67
583.317	20570	4	192003	3	-0.83	2.87E+09	-0.37
584.106	0	4	171202	3	-0.63	4.61E+09	-0.138
585.933	5830	2	176498	1	-0.74	3.54E+09	-0.313
586.626	4173	3	174639	2	-0.71	3.77E+09	-0.263
589.152	0	4	169735	4	-0.35	8.63E+09	-0.244
589.828	4173	3	173713	3	-0.92	2.32E+09	-0.084
589.855	11872	2	181405	2	-0.84	2.75E+09	0.216
590.36	4173	3	173561	2	-0.97	2.04E+09	-0.081
592.384	5830	2	174639	2	-0.99	1.96E+09	-0.088
592.851	15900	1	184576	1	-0.93	2.22E+09	0.264
595.139	15900	1	183928	1	-0.77	3.17E+09	-0.275
596.193	5830	2	173561	2	-0.69	3.81E+09	0.171
596.78	0	4	167566	4	-0.56	5.19E+09	-0.313
598.697	4173	3	171202	3	-0.57	5.00E+09	0.196
601.792	20570	4	186740	5	-0.59	4.75E+09	-0.594
602.417	17398	2	183396	3	-0.97	1.96E+09	-0.118
617.887	11872	2	173713	3	-0.74	3.20E+09	0.322
627.627	11872	2	171202	3	-0.89	2.18E+09	0.142

Table A35: Continued

Wavelength	Lower Level	J_{Low}	Upper level	J_{Up}	log gf	gA	CF
953.299	169735	4	274634	5	-0.92	8.90E+08	-0.404
965.216	159220	4	262824	5	-0.74	1.32E+09	-0.171
1007.161	162487	3	261776	3	-0.77	1.13E+09	-0.122
1008.597	181553	6	280701	5	-0.55	1.84E+09	0.32
1021.086	180281	4	278216	3	-0.31	3.15E+09	-0.555
1022.594	182910	6	280701	5	0.22	1.07E+10	0.687
1023.681	180529	4	278216	3	-0.3	3.23E+09	0.668
1023.785	183024	4	280701	5	-0.7	1.28E+09	0.287
1023.873	164108	4	261776	3	-0.65	1.42E+09	0.145
1027.369	166078	1	263414	2	-0.77	1.06E+09	0.269
1029.882	164678	2	261776	3	-0.31	3.05E+09	-0.524
1030.59	177602	5	274634	5	-0.23	3.75E+09	0.773
1038.264	178320	4	274634	5	0.01	6.30E+09	0.808
1041.959	182243	3	278216	3	-0.62	1.46E+09	0.277
1042.964	167533	2	263414	2	-0.47	2.07E+09	-0.325
1044.165	166006	3	261776	3	-0.18	4.03E+09	0.513
1045.918	169735	4	265345	5	-0.85	8.69E+08	-0.137
1049.784	167566	4	262824	5	-0.94	7.05E+08	-0.164
1053.514	168493	2	263414	2	-0.66	1.29E+09	-0.248
1054.65	168596	3	263414	2	-0.73	1.13E+09	-0.328
1054.693	168600	1	263414	2	-0.49	1.94E+09	-0.188
1054.782	185894	4	280701	5	-0.29	3.08E+09	0.639
1061.457	167566	4	261776	3	0.03	6.34E+09	0.792
1063.937	186710	4	280701	5	-0.97	6.32E+08	0.128
1073.185	168596	3	261776	3	-0.82	8.70E+08	-0.107
1074.329	181553	6	274634	5	0.25	1.03E+10	0.735
1079.728	185600	3	278216	3	-0.67	1.23E+09	-0.541
1083.171	185894	4	278216	3	-0.4	2.24E+09	-0.654
1086.476	169735	4	261776	3	-0.47	1.92E+09	-0.419
1090.225	182910	6	274634	5	-0.36	2.44E+09	-0.291
1091.436	186593	3	278216	3	-0.29	2.87E+09	-0.658
1091.578	183024	4	274634	5	-0.55	1.58E+09	0.248
1091.707	186616	2	278216	3	-0.4	2.21E+09	0.61
1092.828	186710	4	278216	3	-0.77	9.56E+08	0.556
1100.376	182318	5	273196	6	-0.6	1.37E+09	0.088
1100.461	181553	6	272424	6	-0.25	3.09E+09	-0.282
1101.338	187417	2	278216	3	-0.53	1.61E+09	0.563
1102.885	183963	5	274634	5	0.11	7.13E+09	-0.79
1103.347	162487	3	253121	4	-0.63	1.26E+09	-0.133
1104.064	171202	3	261776	3	-0.9	6.87E+08	0.275
1104.842	182910	6	273421	6	-0.86	7.62E+08	0.103
1107.598	182910	6	273196	6	-0.09	4.40E+09	0.257
1108.424	177602	5	267821	4	-0.51	1.68E+09	-0.368
1109.8	182318	5	272424	6	0.21	8.73E+09	0.591
1117.146	182910	6	272424	6	0.25	9.41E+09	-0.622
1117.305	178320	4	267821	4	-0.33	2.49E+09	0.16
1117.845	183963	5	273421	6	-0.47	1.81E+09	0.129
1119.333	191362	6	280701	5	-0.51	1.65E+09	0.725
1119.902	188922	3	278216	3	-0.96	5.78E+08	-0.287
1123.436	164108	4	253121	4	-0.56	1.47E+09	-0.145
1125.835	162487	3	251310	3	0.02	5.50E+09	0.492
1127.958	181553	6	270209	5	-0.74	9.59E+08	-0.362
1129.715	192183	5	280701	5	0.27	9.76E+09	-0.864
1130.24	177602	5	266079	5	-0.35	2.35E+09	0.12
1131.674	186270	5	274634	5	-0.9	6.58E+08	-0.207
1135.822	159220	4	247262	4	0.51	1.65E+10	-0.577
1136.126	162487	3	250506	4	0.07	6.08E+09	-0.402
1136.558	164108	4	252093	5	-0.84	7.60E+08	0.029
1137.662	181553	6	269453	7	0.15	7.35E+09	0.583
1137.771	182318	5	270209	5	0.33	1.10E+10	0.516
1137.919	162487	3	250367	2	0.31	1.04E+10	-0.707
1139.476	178320	4	266079	5	-0.84	7.44E+08	-0.042
1139.695	177602	5	265345	5	0.41	1.32E+10	-0.657
1143.384	159220	4	246680	5	0.06	5.87E+09	0.286
1144.655	160255	5	247618	6	0.57	1.91E+10	0.598
1145.494	182910	6	270209	5	-0.94	5.79E+08	-0.276
1146.758	164108	4	251310	3	-0.37	2.19E+09	0.419
1147.432	186270	5	273421	6	0.56	1.85E+10	-0.623
1147.913	166006	3	253121	4	-0.01	4.93E+09	0.403
1148.452	182318	5	269391	6	-0.63	1.18E+09	-0.444
1148.645	193641	4	280701	5	-0.61	1.24E+09	-0.504
1149.059	182318	5	269345	5	0.05	5.70E+09	0.619
1149.087	178320	4	265345	5	0.27	9.53E+09	0.562
1149.338	160255	5	247262	4	0.22	8.36E+09	-0.741
1150.404	186270	5	273196	6	-0.24	2.89E+09	0.234
1150.533	176498	1	263414	2	-0.46	1.74E+09	-0.302
1152.282	186411	7	273196	6	-0.61	1.24E+09	0.275
1153.662	186740	5	273421	6	0.34	1.10E+10	-0.406
1154.301	164678	2	251310	3	-0.96	5.48E+08	-0.061
1155.503	182910	6	269453	7	0.88	3.83E+10	0.916
1156.667	186740	5	273196	6	-0.05	4.40E+09	0.327
1157.082	160255	5	246680	5	0.51	1.60E+10	0.648
1157.438	164108	4	250506	4	0.43	1.34E+10	-0.619
1159.478	183963	5	270209	5	-0.93	5.80E+08	0.094
1160.709	186270	5	272424	6	-0.63	1.15E+09	-0.182
1161.737	194623	4	280701	5	-0.61	1.22E+09	-0.396
1162.62	186411	7	272424	6	-0.11	3.81E+09	0.677
1164.563	186411	7	272280	7	0.53	1.66E+10	0.751
1165.522	180281	4	266079	5	-0.53	1.45E+09	0.16
1167.008	164678	2	250367	2	-0.59	1.27E+09	0.091
1168.847	167566	4	253121	4	-0.4	1.95E+09	-0.146
1168.904	180529	4	266079	5	-0.78	8.07E+08	-0.101
1169.026	177873	2	263414	2	-0.18	3.17E+09	-0.46
1169.548	182318	5	267821	4	0.2	7.67E+09	-0.72
1170.837	178005	3	263414	2	-0.89	6.19E+08	0.295
1172.274	166006	3	251310	3	-0.44	1.79E+09	-0.171
1175.579	180281	4	265345	5	-0.85	6.89E+08	-0.081
1175.758	180281	4	265332	4	-0.24	2.81E+09	0.602
1177.812	165602	5	250506	4	-0.29	2.45E+09	0.424
1179.2	180529	4	265332	4	-0.32	2.32E+09	0.539
1179.289	183024	4	267821	4	0.14	6.72E+09	0.519
1179.596	162487	3	247262	4	-0.99	4.89E+08	-0.028
1183.058	167566	4	252093	5	0.33	1.03E+10	0.444
1183.063	181553	6	266079	5	-0.87	6.46E+08	0.214
1183.236	190120	4	274634	5	-0.95	5.42E+08	-0.568
1183.374	178320	4	262824	5	-0.97	5.18E+08	0.516

Table A35: Continued

Wavelength	Lower Level	J_{Low}	Upper level	J_{Up}	log gf	gA	CF
1184.483	183396	3	267821	4	-0.67	1.01E+09	-0.323
1186.036	185894	4	270209	5	-0.49	1.54E+09	0.318
1191.34	186270	5	270209	5	-0.54	1.37E+09	-0.365
1191.843	177873	2	261776	3	-0.86	6.52E+08	0.318
1192.12	96397	5	180281	4	-1	4.74E+08	-0.356
1192.496	183963	5	267821	4	-0.29	2.41E+09	0.332
1193.426	181553	6	265345	5	-0.36	2.04E+09	0.583
1193.645	167533	2	251310	3	-0.87	6.30E+08	-0.132
1194.114	167566	4	251310	3	-0.65	1.05E+09	0.14
1197.603	179914	1	263414	2	-0.7	9.36E+08	0.113
1197.624	186710	4	270209	5	-0.63	1.11E+09	-0.181
1198.058	186740	5	270209	5	-0.19	3.01E+09	0.505
1198.275	181553	6	265006	7	0.88	3.54E+10	0.877
1198.307	185894	4	269345	5	-0.03	4.34E+09	-0.479
1199.182	181942	3	265332	4	0.32	9.83E+09	0.454
1199.256	169735	4	253121	4	-0.22	2.81E+09	-0.221
1203.056	186270	5	269391	6	0.48	1.38E+10	-0.851
1203.722	186270	5	269345	5	-0.33	2.17E+09	0.324
1204.014	183024	4	266079	5	0.36	1.07E+10	0.716
1204.222	186411	7	269453	7	-0.71	8.98E+08	-0.851
1204.412	170092	5	253121	4	-0.67	9.90E+08	0.479
1205.698	167566	4	250506	4	-0.66	1.02E+09	0.059
1206.954	197847	5	280701	5	-0.57	1.23E+09	-0.149
1208.977	168596	3	251310	3	-0.93	5.43E+08	0.053
1209.907	186740	5	269391	6	0.65	2.03E+10	0.717
1210.138	186710	4	269345	5	0.17	6.76E+09	0.565
1210.58	186740	5	269345	5	-0.06	3.96E+09	-0.395
1211.067	164108	4	246680	5	-0.51	1.42E+09	-0.095
1211.491	180281	4	262824	5	0.5	1.43E+10	0.862
1212.98	190754	6	273196	6	-0.53	1.33E+09	-0.096
1213.074	182910	6	265345	5	-0.92	5.42E+08	-0.227
1214.221	169735	4	252093	5	0.42	1.20E+10	-0.675
1215.145	180529	4	262824	5	0.46	1.31E+10	0.841
1215.314	120871	6	203155	5	-0.7	8.95E+08	-0.342
1217.785	183963	5	266079	5	0.32	9.40E+09	0.59
1218.085	182910	6	265006	7	0.19	6.97E+09	-0.269
1218.633	191362	6	273421	6	-0.73	8.30E+08	0.274
1219.276	165602	6	247618	6	0.51	1.44E+10	0.875
1219.28	165602	5	247618	6	-0.06	3.91E+09	0.219
1219.507	170092	5	252093	5	-0.3	2.28E+09	0.227
1220.454	183396	3	265332	4	-0.1	3.60E+09	0.435
1220.722	171202	3	253121	4	-0.33	2.06E+09	-0.23
1221.987	191362	6	273196	6	0.28	8.38E+09	0.441
1225.87	169735	4	251310	3	-0.34	2.06E+09	0.311
1226.226	186270	5	267821	4	-0.83	6.51E+08	0.381
1228.768	183963	5	265345	5	0.07	5.19E+09	0.331
1230.677	166006	3	247262	4	-0.81	6.85E+08	-0.065
1230.95	192183	5	273421	6	0.2	6.96E+09	0.849
1233.386	165602	6	246680	5	-0.18	2.92E+09	0.745
1233.391	165602	5	246680	5	-0.05	3.91E+09	0.297
1233.62	191362	6	272424	6	0.3	8.76E+09	0.41
1234.372	192183	5	273196	6	0.36	9.95E+09	0.577
1235.292	184380	3	265332	4	0.01	4.47E+09	0.487
1235.808	191362	6	272280	7	0.74	2.39E+10	0.944
1238.081	169735	4	250506	4	-0.89	5.62E+08	0.061
1246.243	192183	5	272424	6	-0.09	3.46E+09	-0.197
1248.308	171202	3	251310	3	-0.18	2.84E+09	0.3
1249.197	173069	4	253121	4	-0.04	3.90E+09	0.454
1252.981	186270	5	266079	5	-0.56	1.18E+09	0.117
1259.335	173713	3	253121	4	-0.66	9.09E+08	0.08
1263.182	171202	3	250367	2	-0.73	7.77E+08	0.181
1264.005	167566	4	246680	5	-0.82	6.37E+08	0.067
1264.612	186270	5	265345	5	-0.98	4.42E+08	0.037
1268.108	99147	4	178005	3	-0.62	9.90E+08	-0.395
1268.278	191362	6	270209	5	0.24	7.15E+09	0.75
1280.56	191362	6	269453	7	-0.4	1.61E+09	0.376
1281.624	192183	5	270209	5	-0.96	4.43E+08	0.092
1282.32	191362	6	269345	5	-0.27	2.19E+09	0.663
1288.714	173713	3	251310	3	-0.57	1.07E+09	0.12
1293.979	102633	2	179914	1	-0.92	4.75E+08	-0.492
1301.482	116806	4	193641	4	-0.98	4.14E+08	0.108
1303.029	101261	3	178005	3	-0.98	4.08E+08	0.404
1305.278	101261	3	177873	2	-0.7	7.87E+08	-0.456
1306.606	122456	5	198990	4	-0.67	8.32E+08	-0.346
1319.065	115550	5	191362	6	-1	3.83E+08	-0.246
1320.937	193641	4	269345	5	-0.84	5.55E+08	-0.422
1322.087	192183	5	267821	4	-0.82	5.73E+08	0.101
1322.995	194623	4	270209	5	-0.76	6.69E+08	0.386
1327.172	197847	5	273196	6	-0.52	1.13E+09	0.11
1338.282	194623	4	269345	5	-0.15	2.66E+09	-0.691
1340.172	153026	2	227643	3	-0.76	6.50E+08	-0.405
1351.293	110377	3	184380	3	-0.97	3.91E+08	-0.216
1352.247	125077	1	199028	0	-0.95	4.05E+08	0.34
1353.982	153026	2	226882	2	-0.76	6.28E+08	0.244
1355.111	121767	4	195561	3	-0.84	5.22E+08	0.358
1358.712	118614	1	192213	1	-0.86	5.01E+08	0.34
1358.996	125077	2	198661	1	-0.73	6.72E+08	-0.265
1360.224	154126	3	227643	3	0.14	5.03E+09	0.612
1362.859	111005	3	184380	3	-0.62	8.69E+08	0.518
1364.156	178005	3	251310	3	-0.92	4.29E+08	0.16
1365.091	125735	4	198990	4	-0.8	5.71E+08	0.542
1369.376	103472	1	176498	1	-0.93	4.23E+08	-0.651
1369.506	110377	3	183396	3	-0.73	6.62E+08	-0.255
1372.571	121767	4	194623	4	-0.69	7.25E+08	0.12
1374.545	125735	4	198487	3	-0.43	1.32E+09	-0.542
1376.105	112612	1	185281	2	-0.88	4.70E+08	0.36
1377.81	122820	3	195399	2	-0.68	7.46E+08	-0.417
1378.673	152454	1	224988	2	-0.46	1.21E+09	-0.705
1380.495	193641	4	266079	5	-0.71	6.73E+08	0.188
1380.749	102633	2	175057	3	-0.76	6.09E+08	0.403
1380.855	152454	1	224873	1	-0.48	1.16E+09	0.64
1381.388	111005	3	183396	3	-0.94	4.02E+08	0.165
1381.939	178005	3	250367	2	-0.76	6.02E+08	0.241
1385.686	122456	5	194623	4	-0.94	3.98E+08	0.249
1386.728	125735	4	197847	5	-0.68	7.30E+08	0.577

Table A35: Continued

Wavelength	Lower Level	J_{Low}	Upper level	J_{Up}	log gf	gA	CF
1389.575	112612	1	184576	1	-0.9	4.31E+08	-0.286
1389.628	153026	2	224988	2	-0.13	2.54E+09	0.482
1391.307	121767	4	193641	4	-0.13	2.58E+09	0.656
1392.457	125077	1	196893	2	-0.68	7.21E+08	0.551
1392.592	101261	3	173069	4	-0.37	1.46E+09	0.385
1399.449	194623	4	266079	5	-0.54	9.74E+08	0.203
1402.576	107022	4	178320	4	-0.74	6.24E+08	0.189
1403.745	111005	3	182243	3	-0.94	3.89E+08	0.314
1404.785	122456	5	193641	4	-0.89	4.40E+08	0.227
1405.099	96397	5	167566	4	-0.97	3.60E+08	-0.108
1405.139	103472	1	174639	2	-0.59	8.77E+08	0.622
1405.22	110779	2	181942	3	0.08	4.06E+09	-0.696
1406.849	102633	2	173713	3	-0.81	5.18E+08	0.58
1407.573	110779	2	181823	1	-0.69	6.88E+08	0.279
1407.896	110377	3	181405	2	-0.8	5.39E+08	-0.243
1409.405	131006	2	201958	3	-0.79	5.47E+08	-0.332
1409.537	99147	4	170092	5	0.06	3.84E+09	-0.438
1409.691	111005	3	181942	3	-0.82	5.12E+08	0.151
1409.882	102633	2	173561	2	-0.92	4.07E+08	-0.416
1412.686	110377	3	181164	2	-0.99	3.43E+08	-0.181
1414.042	115550	5	186270	5	-0.71	6.52E+08	0.19
1415.966	112612	1	183235	2	-0.4	1.34E+09	-0.464
1417.638	121833	2	192373	2	-0.62	8.03E+08	0.313
1418.633	120871	6	191362	6	0.46	9.47E+09	0.684
1420.761	110779	2	181164	2	-0.64	7.62E+08	0.299
1420.859	121833	2	192213	1	-0.85	4.67E+08	-0.212
1421.945	132758	2	203085	1	-0.2	2.06E+09	-0.69
1422.024	125077	2	195399	2	-0.76	5.73E+08	0.193
1423.21	131006	2	201269	3	-0.47	1.12E+09	0.658
1425.467	110377	3	180529	4	-0.36	1.44E+09	0.474
1428.185	133265	3	203284	2	-0.18	2.18E+09	-0.469
1429.159	133265	3	203237	4	-0.36	1.41E+09	-0.363
1429.771	101261	3	171202	3	-0.96	3.57E+08	-0.4
1429.914	116806	4	186740	5	-0.7	6.56E+08	0.102
1430.246	127929	5	197847	5	0.42	8.48E+09	0.675
1430.529	110377	3	180281	4	-0.3	1.63E+09	0.427
1430.532	116806	4	186710	4	-0.33	1.54E+09	0.233
1432.603	119119	3	188922	3	-0.73	6.10E+08	0.364
1432.924	116806	4	186593	3	-0.74	5.94E+08	-0.126
1434.175	122456	5	192183	5	0.4	8.14E+09	0.663
1434.79	122676	1	192373	2	-0.89	4.17E+08	0.193
1436.384	138852	3	208471	3	0.22	5.35E+09	0.717
1437.106	152454	1	222038	1	-0.42	1.22E+09	0.675
1437.766	122820	3	192373	2	-0.9	4.06E+08	-0.158
1438.344	111005	3	180529	4	-0.23	1.88E+09	-0.627
1438.979	153026	2	222520	3	-0.26	1.76E+09	0.708
1439.602	116806	4	186270	5	-0.46	1.13E+09	-0.117
1441.925	118614	1	187966	2	-0.79	5.15E+08	0.227
1443.498	111005	3	180281	4	-0.24	1.84E+09	-0.491
1444.143	158398	2	227643	3	-0.64	7.30E+08	-0.745
1444.967	96397	5	165602	5	-0.34	1.46E+09	0.252
1444.974	96397	5	165602	6	0.55	1.13E+10	-0.832
1445.102	132758	2	201958	3	-0.58	8.36E+08	-0.641
1447.424	116806	4	185894	4	-0.62	7.71E+08	-0.172
1451.264	122456	5	191362	6	-0.51	9.84E+08	-0.499
1451.644	125735	4	194623	4	0.05	3.52E+09	-0.667
1453.639	112612	1	181405	2	-0.68	6.61E+08	-0.48
1454.505	118603	2	187355	3	-0.04	2.91E+09	-0.686
1455.673	133265	3	201962	4	0.1	3.96E+09	0.744
1455.765	133265	3	201958	3	-0.6	7.87E+08	0.337
1456.482	134578	4	203237	4	0.07	3.67E+09	0.491
1458.076	132758	2	201342	2	-0.14	2.30E+09	0.704
1458.223	134578	4	203155	5	0.41	8.09E+09	-0.761
1458.746	112612	1	181164	2	-0.87	4.21E+08	-0.12
1459.619	132758	2	201269	3	-0.38	1.30E+09	-0.471
1460.193	158398	2	226882	2	0.02	3.26E+09	0.699
1460.388	101261	3	169735	4	-0.3	1.55E+09	0.631
1460.763	130571	1	199028	0	-0.87	4.22E+08	0.589
1461.584	99147	4	167566	4	-0.55	8.83E+08	0.143
1461.719	115550	5	183963	5	0.27	5.79E+09	0.696
1464.174	119119	3	187417	2	-0.34	1.43E+09	-0.7
1464.176	122456	5	190754	6	-0.13	2.31E+09	0.206
1467.767	121833	2	189964	2	-0.99	3.19E+08	-0.245
1468.638	130571	1	198661	1	-0.39	1.26E+09	-0.682
1470.498	133265	3	201269	3	-0.2	1.94E+09	0.322
1472.617	125735	4	193641	4	-0.06	2.70E+09	0.516
1475.933	125077	2	192831	1	-0.37	1.32E+09	-0.639
1476.861	96397	5	164108	4	-0.98	3.22E+08	0.076
1478.674	110377	3	178005	3	-0.27	1.63E+09	0.651
1479.491	119119	3	186710	4	-0.53	9.11E+08	-0.662
1479.862	116806	4	184380	3	-0.83	4.47E+08	-0.383
1481.551	119119	3	186616	2	-0.19	1.95E+09	-0.753
1482.05	119119	3	186593	3	-0.15	2.17E+09	0.636
1482.065	115550	5	183024	4	-0.26	1.68E+09	-0.347
1484.125	134578	4	201958	3	-0.08	2.49E+09	-0.527
1484.567	115550	5	182910	6	-0.34	1.39E+09	0.226
1485.109	101261	3	168596	3	-0.82	4.57E+08	0.087
1485.841	112612	1	179914	1	-0.48	9.94E+08	-0.573
1485.887	122820	3	190120	4	0.35	6.71E+09	-0.804
1486.16	122676	1	189964	2	-0.75	5.41E+08	0.243
1487.523	110779	2	178005	3	-0.65	6.73E+08	-0.195
1487.904	112612	1	179820	0	-0.9	3.85E+08	-0.601
1489.048	116806	4	183963	5	-0.33	1.42E+09	-0.721
1489.078	121767	4	188922	3	-0.77	5.09E+08	-0.251
1489.354	122820	3	189964	2	-0.77	5.17E+08	0.507
1489.516	125077	1	192213	1	-1	3.01E+08	0.229
1490.456	110779	2	177873	2	-0.57	8.00E+08	-0.335
1491.331	203155	5	270209	5	-0.99	3.12E+08	0.131
1492.535	111005	3	178005	3	-0.69	6.10E+08	-0.246
1492.557	154126	3	221125	4	0.35	6.68E+09	-0.77
1494.18	125077	2	192003	3	-0.19	1.93E+09	0.712
1495.488	111005	3	177873	2	-0.78	4.91E+08	-0.273
1497.566	119119	3	185894	4	-0.27	1.60E+09	0.605
1499.401	127929	5	194623	4	-0.11	2.32E+09	0.612
1499.441	134578	4	201269	3	-0.72	5.66E+08	0.518
1499.448	107022	4	173713	3	-0.83	4.37E+08	-0.11

Table A35: Continued

Wavelength	Lower Level	J_{Low}	Upper level	J_{Up}	log gf	gA	CF
1499.754	118603	2	185281	2	-0.61	7.27E+08	-0.236
1501.734	116806	4	183396	3	-0.37	1.26E+09	0.658
1501.736	158398	2	224988	2	-0.89	3.84E+08	-0.251
1504.197	119119	3	185600	3	-0.61	7.31E+08	0.5
1504.325	158398	2	224873	1	-0.41	1.17E+09	0.729
1504.772	99147	4	165602	5	0.23	4.95E+09	-0.829
1504.947	125735	4	192183	5	-0.65	6.63E+08	-0.68
1507.046	125858	0	192213	1	-0.81	4.58E+08	0.534
1508.169	101261	3	167566	4	0.11	3.78E+09	-0.804
1509.017	125735	4	192003	3	-0.23	1.73E+09	0.675
1510.168	116806	4	183024	4	-0.06	2.53E+09	0.749
1510.528	120216	0	186418	1	-0.75	5.13E+08	-0.406
1511.03	131006	2	197186	1	-0.25	1.64E+09	-0.697
1515.093	115550	5	181553	6	0.46	8.43E+09	-0.797
1515.768	118603	2	184576	1	-0.8	4.63E+08	-0.292
1516.002	102633	2	168596	3	0.11	3.74E+09	-0.817
1517.755	131006	2	196893	2	-0.64	6.64E+08	-0.33
1520.292	118603	2	184380	3	-0.87	3.90E+08	0.161
1521.418	132758	2	198487	3	-0.23	1.71E+09	-0.425
1521.488	133265	3	198990	4	-0.57	7.84E+08	-0.146
1521.789	127929	5	193641	4	-0.38	1.19E+09	0.499
1525.785	120871	6	186411	7	0.6	1.15E+10	-0.859
1526.205	121833	2	187355	3	-0.29	1.49E+09	-0.719
1528.194	116806	4	182243	3	-0.16	1.98E+09	-0.497
1531.068	118614	1	183928	1	-0.71	5.58E+08	0.325
1531.919	152454	1	217732	0	-0.59	7.33E+08	-0.797
1531.939	103472	1	168748	0	-0.78	4.72E+08	-0.775
1532.318	119119	3	184380	3	-0.96	3.13E+08	0.555
1533.242	133265	3	198487	3	-0.33	1.33E+09	-0.678
1533.764	122676	1	187875	1	-0.83	4.23E+08	-0.284
1534.127	112689	2	177873	2	-0.67	6.07E+08	0.437
1535.44	103472	1	168600	1	-0.39	1.16E+09	0.773
1537.947	103472	1	168493	2	-0.49	9.17E+08	0.81
1539.085	121767	4	186740	5	-0.1	2.23E+09	-0.245
1539.392	99147	4	164108	4	0.23	4.80E+09	-0.765
1539.767	153026	2	217971	3	0	2.81E+09	-0.517
1539.801	121767	4	186710	4	-0.4	1.12E+09	-0.329
1540.819	102633	2	167533	2	-0.12	2.15E+09	-0.754
1540.865	103472	1	168370	2	-0.25	1.60E+09	-0.806
1541.149	125077	1	189964	2	-0.24	1.60E+09	-0.587
1542.524	130571	1	195399	2	-0.69	5.65E+08	0.555
1542.573	121767	4	186593	3	-0.48	9.35E+08	0.41
1543.385	118603	2	183396	3	-0.77	4.73E+08	0.251
1544.512	101261	3	166006	3	0.08	3.38E+09	-0.744
1544.616	122676	1	187417	2	-0.23	1.64E+09	0.669
1546.403	203155	5	267821	4	-0.94	3.22E+08	-0.245
1547.224	118603	2	183235	2	-0.79	4.49E+08	-0.217
1547.482	118614	1	183235	2	-0.57	7.44E+08	0.29
1549.053	131006	2	195561	3	-0.04	2.54E+09	-0.625
1550.315	121767	4	186270	5	0.13	3.73E+09	0.735
1552.02	138852	3	203284	2	-0.4	1.11E+09	-0.723
1552.493	134578	4	198990	4	-0.08	2.29E+09	-0.698
1552.947	131006	2	195399	2	-0.57	7.40E+08	0.288
1553.17	138852	3	203237	4	-0.24	1.59E+09	-0.751
1555.595	122456	5	186740	5	-1	2.77E+08	0.241
1556.327	122456	5	186710	4	-0.24	1.59E+09	-0.421
1556.615	110779	2	175021	1	-0.73	5.15E+08	-0.618
1558.131	107022	4	171202	3	0.11	3.57E+09	-0.753
1559.232	132758	2	196893	2	-0.56	7.53E+08	0.414
1559.39	121767	4	185894	4	-0.77	4.68E+08	0.217
1559.537	158398	2	222520	3	0.09	3.36E+09	-0.63
1560.997	103472	1	167533	2	-0.88	3.65E+08	-0.146
1561.86	125077	1	189103	1	-0.67	5.90E+08	0.364
1563.968	122676	1	186616	2	-0.54	7.77E+08	-0.578
1565.927	110779	2	174639	2	-0.99	2.81E+08	0.56
1565.957	96397	5	160255	5	0.37	6.34E+09	0.833
1566.29	125077	2	188922	3	-0.32	1.30E+09	0.663
1566.296	154126	3	217971	3	-0.52	8.30E+08	-0.703
1567.184	112689	2	176498	1	-0.54	7.82E+08	-0.673
1568.064	122820	3	186593	3	-0.8	4.28E+08	-0.468
1568.823	122676	1	186418	1	-0.71	5.28E+08	0.378
1569.576	120216	0	183928	1	-0.78	4.46E+08	0.332
1571.329	158398	2	222038	1	-0.46	9.42E+08	-0.6
1571.654	133265	3	196893	2	-0.92	3.27E+08	0.54
1575.427	116806	4	180281	4	-0.74	4.89E+08	0.321
1576.101	121833	2	185281	2	-0.52	8.14E+08	0.279
1576.165	102633	2	166078	1	-0.33	1.27E+09	0.752
1576.171	152454	1	215899	2	-0.07	2.28E+09	-0.69
1576.341	122456	5	185894	4	0.01	2.76E+09	-0.679
1576.484	127929	5	191362	6	-0.71	5.19E+08	-0.311
1576.86	101261	3	164678	2	-0.05	2.42E+09	0.744
1577.953	102633	2	166006	3	-0.82	4.08E+08	-0.106
1578.78	99147	4	162487	3	0.14	3.66E+09	0.768
1578.801	118603	2	181942	3	-0.64	6.15E+08	-0.163
1578.86	110377	3	173713	3	-0.29	1.37E+09	0.553
1580.55	153026	2	216295	1	-0.17	1.82E+09	-0.781
1581.145	125858	0	189103	1	-0.38	1.12E+09	-0.615
1581.773	118603	2	181823	1	-0.73	4.93E+08	-0.436
1582.602	125735	4	188922	3	-0.26	1.47E+09	-0.769
1582.681	110377	3	173561	2	-0.42	1.01E+09	-0.522
1584.196	119119	3	182243	3	-0.5	8.47E+08	-0.277
1584.536	138852	3	201962	4	-0.05	2.39E+09	-0.442
1585.537	107022	4	170092	5	0.22	4.42E+09	0.807
1590.119	125077	2	187966	2	-0.13	1.97E+09	0.596
1590.505	153026	2	215899	2	-0.62	6.33E+08	-0.608
1591.157	101261	3	164108	4	-0.76	4.61E+08	-0.095
1591.732	127929	5	190754	6	0.42	6.93E+09	-0.848
1591.765	96397	5	159220	4	0.25	4.69E+09	-0.793
1592.316	118603	2	181405	2	-0.56	7.33E+08	0.297
1592.402	125077	1	187875	1	-0.56	7.13E+08	-0.429
1592.589	118614	1	181405	2	-0.84	3.82E+08	-0.244
1592.878	122820	3	185600	3	0.01	2.67E+09	0.752
1593.136	115550	5	178320	4	0.11	3.41E+09	-0.784
1593.797	121833	2	184576	1	-0.75	4.70E+08	0.289
1594.561	107022	4	169735	4	0.18	3.93E+09	0.67
1594.673	111005	3	173713	3	-0.17	1.77E+09	0.732

Table A35: Continued

Wavelength	Lower Level	J_{Low}	Upper level	J_{Up}	log gf	gA	CF
1595.089	110377	3	173069	4	-0.01	2.58E+09	-0.81
1596.419	130571	1	193211	2	-0.09	2.14E+09	-0.746
1597.106	121767	4	184380	3	-0.41	1.01E+09	-0.526
1597.285	103472	1	166078	1	-0.72	4.99E+08	0.242
1598.446	118603	2	181164	2	-0.51	8.00E+08	-0.54
1598.571	111005	3	173561	2	-0.34	1.21E+09	-0.71
1598.721	118614	1	181164	2	-0.66	5.64E+08	-0.243
1598.799	121833	2	184380	3	-0.42	9.81E+08	-0.369
1600.26	138852	3	201342	2	-0.49	8.46E+08	0.474
1601.02	122820	3	185281	2	-0.5	8.32E+08	0.551
1603.38	112689	2	175057	3	0.15	3.63E+09	-0.792
1604.311	112689	2	175021	1	-0.72	4.93E+08	-0.494
1605.239	133265	3	195561	3	-0.67	5.54E+08	0.304
1606.16	130571	1	192831	1	-0.79	4.16E+08	0.293
1607.585	131006	2	193211	2	-0.87	3.53E+08	0.232
1607.811	121767	4	183963	5	-0.39	1.04E+09	-0.408
1610.443	121833	2	183928	1	-0.89	3.36E+08	-0.266
1611.231	111005	3	173069	4	-0.12	1.94E+09	-0.637
1611.549	115550	5	177602	5	-0.12	1.94E+09	-0.722
1611.733	102633	2	164678	2	-0.67	5.48E+08	0.163
1611.894	120871	6	182910	6	-0.58	6.77E+08	-0.722
1614.204	112689	2	174639	2	-0.24	1.48E+09	0.661
1614.754	118614	1	180543	0	-0.68	5.39E+08	0.756
1622.611	121767	4	183396	3	-0.54	7.34E+08	0.332
1624.359	121833	2	183396	3	-0.56	6.90E+08	-0.344
1625.655	116806	4	178320	4	-0.4	9.97E+08	-0.276
1627.437	120871	6	182318	5	0.37	5.96E+09	-0.82
1628.403	119119	3	180529	4	-0.17	1.68E+09	-0.679
1628.607	122676	1	184078	0	-0.98	2.68E+08	-0.564
1628.613	121833	2	183235	2	-0.63	5.93E+08	0.297
1629.539	131006	2	192373	2	-0.33	1.17E+09	-0.456
1632.461	121767	4	183024	4	-0.57	6.75E+08	0.171
1632.613	122676	1	183928	1	-0.92	2.99E+08	0.193
1633.275	101261	3	162487	3	-0.71	4.88E+08	0.112
1635.012	119119	3	180281	4	-0.17	1.68E+09	0.58
1636.431	154126	3	215235	2	0.06	2.88E+09	-0.794
1636.44	99147	4	160255	5	-0.9	3.13E+08	0.074
1636.469	130571	1	191678	0	-0.98	2.65E+08	-0.492
1639.207	125735	4	186740	5	0.18	3.75E+09	0.578
1639.404	131006	2	192003	3	-1	2.46E+08	-0.178
1639.791	134578	4	195561	3	-0.63	5.72E+08	0.496
1642.799	112689	2	173561	2	-0.92	3.00E+08	-0.137
1644.832	116806	4	177602	5	0.23	4.19E+09	-0.594
1647.944	120871	6	181553	6	-0.62	5.81E+08	-0.664
1651.047	122456	5	183024	4	-0.93	2.87E+08	-0.125
1651.501	121767	4	182318	5	-0.9	3.11E+08	0.515
1651.698	107022	4	167566	4	-0.55	6.89E+08	0.216
1651.952	125735	4	186270	5	-0.11	1.91E+09	0.524
1652.271	125077	2	185600	3	-0.86	3.37E+08	0.142
1653.546	121767	4	182243	3	-0.6	6.09E+08	0.263
1654.153	122456	5	182910	6	0.31	4.93E+09	-0.732
1662.832	138852	3	198990	4	-0.2	1.55E+09	-0.598
1664.644	99147	4	159220	4	-0.64	5.46E+08	-0.13
1666.936	121833	2	181823	1	-0.82	3.65E+08	-0.59
1678.618	158398	2	217971	3	-0.5	7.48E+08	-0.712
1683.451	118603	2	178005	3	-0.75	4.13E+08	0.209
1686.263	125077	2	184380	3	-0.91	2.86E+08	-0.375
1687.208	118603	2	177873	2	-0.93	2.77E+08	-0.151
1692.141	122456	5	181553	6	-0.6	5.90E+08	-0.125
1700.364	127929	5	186740	5	-0.89	2.93E+08	-0.471
1701.238	127929	5	186710	4	-0.29	1.17E+09	0.796
1701.766	121767	4	180529	4	-0.59	5.83E+08	0.656
1706.945	122820	3	181405	2	-0.64	5.35E+08	0.61
1707.064	107022	4	165602	5	-0.16	1.60E+09	-0.379
1708.985	121767	4	180281	4	-0.83	3.35E+08	-0.386
1714.721	125077	2	183396	3	-0.89	2.96E+08	0.255
1720.676	110377	3	168493	2	-0.44	8.15E+08	0.592
1722.936	138852	3	196893	2	-0.55	6.31E+08	-0.534
1736.376	110779	2	168370	2	-0.4	8.89E+08	0.693
1736.384	111005	3	168596	3	-0.83	3.28E+08	0.312
1739.474	111005	3	168493	2	-0.59	5.71E+08	-0.407
1741.384	134578	4	192003	3	-0.81	3.42E+08	0.558
1743.208	111005	3	168370	2	-0.97	2.34E+08	-0.232
1748.575	110377	3	167566	4	-0.56	5.99E+08	-0.508
1761.983	110779	2	167533	2	-1	2.16E+08	-0.505
1763.719	133265	3	189964	2	-0.92	2.59E+08	0.56
1768.429	138852	3	195399	2	-0.75	3.84E+08	-0.473
1769.675	125735	4	182243	3	-0.98	2.25E+08	-0.219
1772.486	118603	2	175021	1	-0.78	3.56E+08	-0.295
1780.251	121833	2	178005	3	-0.76	3.63E+08	-0.208
1780.504	132758	2	188922	3	-0.81	3.27E+08	0.423
1784.914	118614	1	174639	2	-0.83	3.09E+08	0.466
1786.104	112612	1	168600	1	-0.8	3.31E+08	0.536
1788.692	112689	2	168596	3	-1	2.08E+08	-0.366
1789.498	112612	1	168493	2	-0.79	3.42E+08	-0.298
1790.963	121767	4	177602	5	-0.9	2.63E+08	-0.053
1793.06	138852	3	194623	4	-0.86	2.88E+08	-0.59
1797.615	110377	3	166006	3	-0.95	2.30E+08	0.335
1810.711	110779	2	166006	3	-0.95	2.28E+08	-0.517
1815.064	127929	5	183024	4	-0.51	6.21E+08	-0.352
1818.818	127929	5	182910	6	-0.33	9.36E+08	-0.16
1845.526	115550	5	169735	4	-0.77	3.30E+08	0.645
1878.53	107022	4	160255	5	-0.54	5.48E+08	0.386
1883.127	111005	3	164108	4	-0.65	4.25E+08	-0.482
1900.093	133265	3	185894	4	-0.72	3.56E+08	0.455
2094.028	134578	4	182318	5	-0.76	2.65E+08	0.517

a: Energy Levels from [41]

Ag V

Energy Levels

Table A36: Comparison between available experimental data and calculated even energy levels (in cm^{-1}) in Ag V

E^a_{exp}	E^b_{calc}	Δ E	J	Leading components (in %) in LS Coupling^c
0	52	-52	4.5	95.8 $4d^7$ (^{4}F) ^{4}F
3690.5	3720	-29.5	3.5	98.6 $4d^7$ (^{4}F) ^{4}F
5815.6	5839	-23.4	2.5	96.4 $4d^7$ (^{4}F) ^{4}F
7097.3	7119	-21.7	1.5	93.5 $4d^7$ (^{4}F) ^{4}F
14204.4	14256	-51.6	1.5	67.7 $4d^7$ (^{4}P) ^{4}P + 29.1 $4d^7$ (^{2}P) ^{2}P
14899.4	14742	157.4	2.5	96.1 $4d^7$ (^{4}P) ^{4}P
16874.7	16822	52.7	4.5	81.2 $4d^7$ (^{2}G) ^{2}G + 14.8 $4d^7$ (^{2}H) ^{2}H
17067.2	17013	54.2	0.5	86.5 $4d^7$ (^{4}P) ^{4}P + 13 $4d^7$ (^{2}P) ^{2}P
20442.1	20350	92.1	3.5	96.9 $4d^7$ (^{2}G) ^{2}G
21570.7	21644	-73.3	1.5	41.9 $4d^7$ (^{2}P) ^{2}P + 27.7 $4d^7$ (^{4}P) ^{4}P + 23.1 $4d^7$ (^{2}D) ^{2}D
22531.9	22597	-65.1	5.5	99.6 $4d^7$ (^{2}H) ^{2}H
24361.2	24142	219.2	2.5	74.2 $4d^7$ (^{2}D) ^{2}D + 19.5 $4d^7$ (^{2}D) ^{2}D
24599.1	24932	-332.9	0.5	86.6 $4d^7$ (^{2}P) ^{2}P + 13 $4d^7$ (^{4}P) ^{4}P
26367.7	26392	-24.3	4.5	84.7 $4d^7$ (^{2}H) ^{2}H + 14.6 $4d^7$ (^{2}G) ^{2}G
30134.4	29990	144.4	1.5	58.9 $4d^7$ (^{2}D) ^{2}D + 27.9 $4d^7$ (^{2}P) ^{2}P + 6.3 $4d^7$ (^{2}D) ^{2}D
34634.7	34635	-0.3	2.5	96.7 $4d^7$ (^{2}F) ^{2}F
36593.8	36589	4.8	3.5	97.4 $4d^7$ (^{2}F) ^{2}F
55041.2	55152	-110.8	1.5	87.7 $4d^7$ (^{2}D) ^{2}D + 11.3 $4d^7$ (^{2}D) ^{2}D
56771.9	56712	59.9	2.5	76.2 $4d^7$ (^{2}D) ^{2}D + 20.5 $4d^7$ (^{2}D) ^{2}D
132745	132725	20	4.5	96.9 $4d^65s$ (^{5}D) ^{6}D
135036.4	135044	-7.6	3.5	97.5 $4d^65s$ (^{5}D) ^{6}D
136401	136423	-22	2.5	96.3 $4d^65s$ (^{5}D) ^{6}D
137349.7	137384	-34.3	1.5	96 $4d^65s$ (^{5}D) ^{6}D
137913.8	137955	-41.2	0.5	96 $4d^65s$ (^{5}D) ^{6}D
146216.3	146173	43.3	3.5	93.8 $4d^65s$ (^{5}D) ^{4}D
148667.4	148684	-16.6	2.5	92.5 $4d^65s$ (^{5}D) ^{4}D
150005.7	150069	-63.3	1.5	92.2 $4d^65s$ (^{5}D) ^{4}D
150869.3	150959	-89.7	0.5	93.3 $4d^65s$ (^{5}D) ^{4}D
156155	156054	101	4.5	36.5 $4d^65s$ (^{3}H) ^{4}H + 26.2 $4d^65s$ (^{3}G) ^{4}G + 20.3 $4d^65s$ (^{3}F) ^{4}F
156445.1	156503	-57.9	2.5	56 $4d^65s$ (^{3}P) ^{4}P + 30.8 $4d^65s$ (^{3}P) ^{4}P
156645	156747	-102	6.5	96 $4d^65s$ (^{3}H) ^{4}H
156797.8	156827	-29.2	5.5	75.4 $4d^65s$ (^{3}H) ^{4}H + 23.5 $4d^65s$ (^{3}G) ^{4}G
156901.5	156789	112.5	3.5	51.2 $4d^65s$ (^{3}H) ^{4}H + 19.8 $4d^65s$ (^{3}G) ^{4}G + 11.4 $4d^65s$ (^{3}F) ^{4}F
159226.1	159228	-1.9	4.5	32.5 $4d^65s$ (^{3}F) ^{4}F + 47.5 $4d^65s$ (^{3}H) ^{4}H + 9.8 $4d^65s$ (^{3}F) ^{4}F
159922.5	159873	49.5	2.5	62.5 $4d^65s$ (^{3}F) ^{4}F + 19.9 $4d^65s$ (^{3}G) ^{4}G + 13 $4d^65s$ (^{3}F) ^{4}F
160022.6	160022	0.6	3.5	46.3 $4d^65s$ (^{3}F) ^{4}F + 30.8 $4d^65s$ (^{3}H) ^{4}H + 11.9 $4d^65s$ (^{3}F) ^{4}F
160124.6	160298	-173.4	1.5	42.6 $4d^65s$ (^{3}F) ^{4}F + 19.6 $4d^65s$ (^{3}P) ^{4}P + 9.4 $4d^65s$ (^{3}P) ^{4}P
160703.6	160726	-22.4	1.5	23.8 $4d^65s$ (^{3}P) ^{4}P + 39.8 $4d^65s$ (^{3}F) ^{4}F + 10.4 $4d^65s$ (^{3}P) ^{4}P
161490.5	161478	12.5	5.5	61.2 $4d^65s$ (^{3}G) ^{4}G + 18.2 $4d^65s$ (^{3}H) ^{2}H + 17.3 $4d^65s$ (^{3}H) ^{4}H
163952.4	163906	46.4	0.5	51.9 $4d^65s$ (^{3}P) ^{4}P + 23.2 $4d^65s$ (^{3}P) ^{4}P + 9.8 $4d^65s$ (^{1}S) ^{2}S
164031.7	164007	24.7	2.5	65.7 $4d^65s$ (^{3}G) ^{4}G + 17.5 $4d^65s$ (^{3}F) ^{4}F + 9.4 $4d^65s$ (^{3}F) ^{2}F
164077.6	164049	28.6	4.5	71 $4d^65s$ (^{3}G) ^{4}G + 12.6 $4d^65s$ (^{3}H) ^{4}H + 8.5 $4d^65s$ (^{3}F) ^{4}F
164685.3	164678	7.3	3.5	60.6 $4d^65s$ (^{3}G) ^{4}G + 18.4 $4d^65s$ (^{3}F) ^{4}F + 8.8 $4d^65s$ (^{3}H) ^{4}H
165333.7	165403	-69.3	4.5	67.4 $4d^65s$ (^{3}H) ^{2}H + 15.3 $4d^65s$ (^{3}G) ^{2}G + 9.7 $4d^65s$ (^{3}F) ^{4}F
165594.7	165717	-122.3	5.5	69.2 $4d^65s$ (^{3}H) ^{2}H + 14.8 $4d^65s$ (^{3}G) ^{4}G + 9.2 $4d^65s$ (^{1}I) ^{2}I
166466.5	166347	119.5	3.5	38.4 $4d^65s$ (^{3}F) ^{2}F + 12 $4d^65s$ (^{3}F) ^{2}F + 10.8 $4d^65s$ (^{3}G) ^{2}G
167020.6	167206	-185.4	1.5	37.8 $4d^65s$ (^{3}P) ^{2}P + 21.2 $4d^65s$ (^{3}P) ^{4}P + 18 $4d^65s$ (^{3}P) ^{2}P
167526.5	167353	173.5	2.5	82.6 $4d^65s$ (^{3}D) ^{4}D
167978.2	167781	197.2	1.5	83.8 $4d^65s$ (^{3}D) ^{4}D + 5.3 $4d^65s$ (^{3}P) ^{2}P
168321.8	168134	187.8	3.5	84.8 $4d^65s$ (^{3}D) ^{4}D + 6.1 $4d^65s$ (^{3}F) ^{2}F
169166.4	169171	-4.6	2.5	66 $4d^65s$ (^{3}F) ^{2}F + 11 $4d^65s$ (^{3}F) ^{2}F + 9.7 $4d^65s$ (^{3}G) ^{4}G
170864.7	170877	-12.3	4.5	75.4 $4d^65s$ (^{3}G) ^{2}G + 13.6 $4d^65s$ (^{3}H) ^{2}H + 4.4 $4d^65s$ (^{1}G) ^{2}G
171530.2	171632	-101.8	6.5	95.9 $4d^65s$ (^{1}I) ^{2}I
171713.4	171610	103.4	0.5	39.5 $4d^65s$ (^{3}P) ^{2}P + 21.9 $4d^65s$ (^{3}P) ^{2}P + 15.8 $4d^65s$ (^{1}S) ^{2}S
172070.3	172101	-30.7	5.5	86.7 $4d^65s$ (^{1}I) ^{2}I + 12.2 $4d^65s$ (^{3}H) ^{2}H
172346.3	172296	50.3	3.5	75.1 $4d^65s$ (^{3}G) ^{2}G + 8 $4d^65s$ (^{1}G) ^{2}G + 6.6 $4d^65s$ (^{1}G) ^{2}G
175085.4	174729	356.4	4.5	57.4 $4d^65s$ (^{1}G) ^{2}G + 17.7 $4d^65s$ (^{1}G) ^{2}G + 14.8 $4d^65s$ (^{3}H) ^{2}H
175241.7	175169	72.7	1.5	75.8 $4d^65s$ (^{3}D) ^{2}D + 7.5 $4d^65s$ (^{1}D) ^{2}D
175532.8	175180	352.8	3.5	50.3 $4d^65s$ (^{1}G) ^{2}G + 21.5 $4d^65s$ (^{3}F) ^{2}F + 14 $4d^65s$ (^{1}G) ^{2}G
175621.8	175363	258.8	2.5	84.7 $4d^65s$ (^{3}D) ^{2}D + 5 $4d^65s$ (^{1}D) ^{2}D
178946.2	179475	-528.8	2.5	61.2 $4d^65s$ (^{1}D) ^{2}D + 12.8 $4d^65s$ (^{1}D) ^{2}D + 6.8 $4d^65s$ (^{3}D) ^{2}D
179242	179623	-381	1.5	63.4 $4d^65s$ (^{1}D) ^{2}D + 13.9 $4d^65s$ (^{3}D) ^{2}D + 12.9 $4d^65s$ (^{1}D) ^{2}D
181638.7	181737	-98.3	3.5	77 $4d^65s$ (^{1}F) ^{2}F + 16 $4d^65s$ (^{3}F) ^{4}F
181871.6	181975	-103.4	2.5	77.3 $4d^65s$ (^{1}F) ^{2}F + 13.7 $4d^65s$ (^{3}F) ^{4}F
185621.8	185331	290.8	0.5	65.7 $4d^65s$ (^{3}P) ^{4}P + 15 $4d^65s$ (^{1}S) ^{2}S + 13.6 $4d^65s$ (^{3}P) ^{4}P
186287.9	186349	-61.1	1.5	64.3 $4d^65s$ (^{3}P) ^{4}P + 30.2 $4d^65s$ (^{3}P) ^{4}P
188223.5	188196	27.5	4.5	76.9 $4d^65s$ (^{3}F) ^{4}F + 18.5 $4d^65s$ (^{3}F) ^{4}F
188493.6	188504	-10.4	1.5	82.7 $4d^65s$ (^{3}F) ^{4}F + 13.3 $4d^65s$ (^{3}F) ^{4}F
189621.1	189679	-57.9	2.5	68.2 $4d^65s$ (^{3}F) ^{4}F + 12.8 $4d^65s$ (^{1}F) ^{2}F + 11.7 $4d^65s$ (^{3}F) ^{4}F
189943.9	189959	-15.1	3.5	63.3 $4d^65s$ (^{3}F) ^{4}F + 16.1 $4d^65s$ (^{1}F) ^{2}F + 12.8 $4d^65s$ (^{3}F) ^{4}F
190694.4	190882	-187.6	2.5	58.4 $4d^65s$ (^{3}P) ^{4}P + 32.8 $4d^65s$ (^{3}P) ^{4}P
196026.9	196024	2.9	3.5	59.5 $4d^65s$ (^{3}F) ^{2}F + 16.7 $4d^65s$ (^{1}G) ^{2}G + 11.3 $4d^65s$ (^{3}F) ^{2}F
197022.4	196962	60.4	2.5	78.5 $4d^65s$ (^{3}F) ^{2}F + 13.5 $4d^65s$ (^{3}F) ^{2}F
198032.6	198047	-14.4	1.5	60.1 $4d^65s$ (^{3}P) ^{2}P + 33.5 $4d^65s$ (^{3}P) ^{2}P
198329.2	198502	-172.8	4.5	67.8 $4d^65s$ (^{1}G) ^{2}G + 27.9 $4d^65s$ (^{1}G) ^{2}G
199047.5	199081	-33.5	3.5	52.1 $4d^65s$ (^{1}G) ^{2}G + 22.4 $4d^65s$ (^{1}G) ^{2}G + 16.8 $4d^65s$ (^{3}F) ^{2}F
215969.7	215921	48.7	2.5	79.2 $4d^65s$ (^{1}D) ^{2}D + 19.1 $4d^65s$ (^{1}D) ^{2}D
216022.7	215923	99.7	1.5	79.1 $4d^65s$ (^{1}D) ^{2}D + 19.2 $4d^65s$ (^{1}D) ^{2}D

a: From Van Kleef [30] and Kildiyarova [42]
b: This work
c: Only the component ≥ 5% are given

Table A37: Comparison between available experimental data and calculated even energy levels (in cm^{-1}) in Ag V

E^a_{exp}	E^b_{calc}	Δ E	J	Leading components (in %) in LS Coupling^c
203717.6	203736	-18.4	3.5	73.4 4d^{6}5p (^{5}D) ^{6}D + 10.8 4d^{6}5p (^{5}D) ^{6}P + 6.3 4d^{6}5p (^{5}D) ^{6}F
203754.6	203717	37.6	4.5	79.8 4d^{6}5p (^{5}D) ^{6}D + 10.3 4d^{6}5p (^{5}D) ^{6}F + 6.5 4d^{6}5p (^{5}D) ^{4}F
205222	205319	-97	2.5	82.4 4d^{6}5p (^{5}D) ^{6}D + 6 4d^{6}5p (^{5}D) ^{6}F + 5.6 4d^{6}5p (^{5}D) ^{6}P
206213	206334	-121	1.5	86.6 4d^{6}5p (^{5}D) ^{6}D
206960	207101	-141	0.5	91.6 4d^{6}5p (^{5}D) ^{6}D
211036.8	210841	195.8	3.5	49.7 4d^{6}5p (^{5}D) ^{6}F + 19 4d^{6}5p (^{5}D) ^{4}D + 16.7 4d^{6}5p (^{5}D) ^{6}P
211406.6	211285	121.6	2.5	64.9 4d^{6}5p (^{5}D) ^{6}F + 15.8 4d^{6}5p (^{5}D) ^{4}D + 5.4 4d^{6}5p (^{5}D) ^{4}F
211707.2	211631	76.2	1.5	75.3 4d^{6}5p (^{5}D) ^{6}F + 12.6 4d^{6}5p (^{5}D) ^{4}D
211735.3	211683	52.3	0.5	81.2 4d^{6}5p (^{5}D) ^{6}F + 11.2 4d^{6}5p (^{5}D) ^{4}D
212362	212197	165	4.5	52.7 4d^{6}5p (^{5}D) ^{6}F + 25.1 4d^{6}5p (^{5}D) ^{4}F + 17.6 4d^{6}5p (^{5}D) ^{6}D
212913.5	212758	155.5	5.5	96.1 4d^{6}5p (^{5}D) ^{6}F
214916	214736	180	3.5	37.6 4d^{6}5p (^{5}D) ^{6}P + 24.2 4d^{6}5p (^{5}D) ^{6}D + 22.3 4d^{6}5p (^{5}D) ^{6}F
217207.5	217163	44.5	3.5	52.8 4d^{6}5p (^{5}D) ^{4}D + 30.8 4d^{6}5p (^{5}D) ^{6}P + 6.2 4d^{6}5p (^{5}D) ^{4}F
217509.8	217489	20.8	4.5	59.7 4d^{6}5p (^{5}D) ^{4}F + 34.7 4d^{6}5p (^{5}D) ^{6}F
217602.8	217494	108.8	2.5	24.9 4d^{6}5p (^{5}D) ^{4}D + 37.8 4d^{6}5p (^{5}D) ^{6}P + 13.1 4d^{6}5p (^{5}D) ^{6}D
218960	218934	26	2.5	41.4 4d^{6}5p (^{5}D) ^{6}P + 37.2 4d^{6}5p (^{5}D) ^{4}D + 7.2 4d^{6}5p (^{5}D) ^{4}P
219501	219562	-61	1.5	60 4d^{6}5p (^{5}D) ^{4}D + 12.5 4d^{6}5p (^{5}D) ^{6}F + 10.6 4d^{6}5p (^{5}D) ^{6}P
220038.1	220157	-118.9	0.5	69.5 4d^{6}5p (^{5}D) ^{4}D + 13.3 4d^{6}5p (^{5}D) ^{6}F + 5.6 4d^{6}5p (^{3}F) ^{4}D
220181	220211	-30	3.5	70.6 4d^{6}5p (^{5}D) ^{4}F + 17.9 4d^{6}5p (^{5}D) ^{6}F
220259.6	220050	209.6	1.5	69.6 4d^{6}5p (^{5}D) ^{6}P + 9.5 4d^{6}5p (^{5}D) ^{4}D + 5.8 4d^{6}5p (^{3}P) ^{4}S
221491.8	221543	-51.2	2.5	75.7 4d^{6}5p (^{5}D) ^{4}F + 8.3 4d^{6}5p (^{5}D) ^{6}F
221974.2	222260	-285.8	2.5	75.7 4d^{6}5p (^{5}D) ^{4}P + 8.6 4d^{6}5p (^{5}D) ^{6}P
222687.9	222713	-25.1	1.5	83.4 4d^{6}5p (^{5}D) ^{4}F
223839.7	223850	-10.3	1.5	58.5 4d^{6}5p (^{5}D) ^{4}P + 11.2 4d^{6}5p (^{5}D) ^{6}P + 5.2 4d^{6}5p (^{3}P) ^{4}P
224933.7	225169	-235.3	0.5	87.9 4d^{6}5p (^{5}D) ^{4}P
225565.2	225491	74.2	3.5	2.8 4d^{6}5p (^{3}F) ^{2}F + 15.6 4d^{6}5p (^{3}H) ^{4}H + 14.2 4d^{6}5p (^{3}H) ^{2}G
226047.1	225903	144.1	4.5	3.1 4d^{6}5p (^{3}F) ^{2}G + 21.7 4d^{6}5p (^{3}H) ^{4}I + 16.3 4d^{6}5p (^{3}G) ^{4}H
226128.1	226457	-328.9	1.5	19.4 4d^{6}5p (^{3}P) ^{4}P + 24.7 4d^{6}5p (^{5}D) ^{4}P + 21.4 4d^{6}5p (^{3}P) ^{4}S
226921.4	226990	-68.6	5.5	2.1 4d^{6}5p (^{1}I) ^{2}H + 30.4 4d^{6}5p (^{3}H) ^{4}I + 27.4 4d^{6}5p (^{3}H) ^{4}H
227669.1	227709	-39.9	6.5	28 4d^{6}5p (^{3}H) ^{4}H + 38.3 4d^{6}5p (^{3}H) ^{4}I + 24.7 4d^{6}5p (^{3}H) ^{2}I
227841.1	227850	-8.9	5.5	58 4d^{6}5p (^{3}H) ^{4}G + 11.6 4d^{6}5p (^{3}G) ^{4}G + 9.8 4d^{6}5p (^{3}F) ^{4}G
228205.9	228325	-119.1	4.5	14.5 4d^{6}5p (^{3}H) ^{4}H + 30.6 4d^{6}5p (^{3}H) ^{4}G + 14.9 4d^{6}5p (^{3}H) ^{2}G
228296.2	228331	-34.8	2.5	16.8 4d^{6}5p (^{3}P) ^{4}D + 13.3 4d^{6}5p (^{3}P) ^{2}D + 8.2 4d^{6}5p (^{3}P) ^{4}P
228811.9	228864	-52.1	3.5	35 4d^{6}5p (^{3}F) ^{4}G + 15.5 4d^{6}5p (^{3}H) ^{4}G + 9.1 4d^{6}5p (^{3}G) ^{4}H
228957.4	229010	-52.6	2.5	43.1 4d^{6}5p (^{3}F) ^{4}G + 11.5 4d^{6}5p (^{3}H) ^{4}G + 8 4d^{6}5p (^{3}F) ^{4}F
230133.6	230107	26.6	4.5	44.1 4d^{6}5p (^{3}H) ^{4}I + 9.9 4d^{6}5p (^{3}G) ^{4}G + 9.7 4d^{6}5p (^{3}F) ^{4}F
230157.9	230147	10.9	2.5	21.4 4d^{6}5p (^{3}F) ^{4}F + 10.2 4d^{6}5p (^{3}D) ^{4}F + 7.8 4d^{6}5p (^{3}F) ^{4}D
230847.9	230865	-17.1	3.5	27.8 4d^{6}5p (^{3}H) ^{4}H + 19.4 4d^{6}5p (^{3}F) ^{4}D + 9.8 4d^{6}5p (^{3}G) ^{4}H
230950.4	231012	-61.6	1.5	43.3 4d^{6}5p (^{3}F) ^{4}F + 23.9 4d^{6}5p (^{3}D) ^{4}F + 11.5 4d^{6}5p (^{3}F) ^{4}F
232359.2	232510	-150.8	0.5	18.6 4d^{6}5p (^{3}P) ^{4}P + 17.7 4d^{6}5p (^{3}P) ^{4}P + 17.5 4d^{6}5p (^{3}P) ^{4}D
232379.3	232427	-47.7	3.5	12.2 4d^{6}5p (^{3}D) ^{4}F + 25.4 4d^{6}5p (^{3}H) ^{4}G + 7.7 4d^{6}5p (^{3}G) ^{4}F
232641.2	232768	-126.8	1.5	19.8 4d^{6}5p (^{3}P) ^{4}S + 17.4 4d^{6}5p (^{3}P) ^{4}D + 13.3 4d^{6}5p (^{3}F) ^{4}D
232648.2	232763	-114.8	4.5	19.4 4d^{6}5p (^{3}H) ^{4}G + 19.8 4d^{6}5p (^{3}H) ^{2}G + 13.2 4d^{6}5p (^{3}H) ^{4}I
232966.3	232962	4.3	5.5	43 4d^{6}5p (^{3}H) ^{4}I + 23 4d^{6}5p (^{3}G) ^{4}G + 9.9 4d^{6}5p (^{3}H) ^{4}H
233297.3	233320	-22.7	7.5	94.5 4d^{6}5p (^{3}H) ^{4}I + 5.3 4d^{6}5p (^{1}I) ^{2}K + 0.1 4d^{5}5s5f (^{4}G) ^{4}I
233624.6	233574	50.6	2.5	21.2 4d^{6}5p (^{3}P) ^{4}P + 18 4d^{6}5p (^{3}P) ^{4}P + 16.7 4d^{6}5p (^{3}P) ^{2}D
233689.1	233662	27.1	4.5	12.1 4d^{6}5p (^{3}F) ^{4}F + 19.7 4d^{6}5p (^{3}H) ^{4}H + 14.4 4d^{6}5p (^{3}G) ^{4}F
233938.4	233992	-53.6	3.5	26.6 4d^{6}5p (^{3}F) ^{4}D + 20.9 4d^{6}5p (^{3}G) ^{4}H + 12.3 4d^{6}5p (^{3}D) ^{4}D
233966.1	234005	-38.9	6.5	40.6 4d^{6}5p (^{3}H) ^{2}I + 29.3 4d^{6}5p (^{3}H) ^{4}H + 24.4 4d^{6}5p (^{3}G) ^{4}H
234222.4	234076	146.4	0.5	19.3 4d^{6}5p (^{1}S) ^{2}P + 14 4d^{6}5p (^{3}P) ^{4}D + 10.3 4d^{6}5p (^{3}P) ^{4}P
234472.1	234426	46.1	5.5	7.1 4d^{6}5p (^{3}G) ^{4}G + 27 4d^{6}5p (^{3}H) ^{2}I + 20 4d^{6}5p (^{3}G) ^{2}H
234862.8	234952	-89.2	3.5	45.5 4d^{6}5p (^{3}P) ^{4}D + 22.7 4d^{6}5p (^{3}P) ^{4}D + 7.4 4d^{6}5p (^{3}F) ^{4}F
234924.5	234878	46.5	2.5	28.5 4d^{6}5p (^{3}F) ^{4}D + 14.8 4d^{6}5p (^{3}D) ^{4}D + 11.1 4d^{6}5p (^{3}D) ^{4}F
234990.5	234934	56.5	4.5	29 4d^{6}5p (^{3}G) ^{4}F + 16.5 4d^{6}5p (^{3}F) ^{4}F + 11.4 4d^{6}5p (^{3}F) ^{4}F
235354.3	235474	-119.7	6.5	50 4d^{6}5p (^{3}H) ^{4}I + 31.6 4d^{6}5p (^{3}H) ^{4}H + 11.5 4d^{6}5p (^{3}H) ^{2}I
235669.8	235662	7.8	2.5	33.3 4d^{6}5p (^{3}G) ^{4}G + 14.4 4d^{6}5p (^{3}F) ^{4}D + 8 4d^{6}5p (^{3}G) ^{2}F
235732.5	235674	58.5	4.5	29.6 4d^{6}5p (^{3}G) ^{4}G + 15.6 4d^{6}5p (^{3}F) ^{4}G + 11.1 4d^{6}5p (^{3}F) ^{2}G
235881.9	235905	-23.1	3.5	36.3 4d^{6}5p (^{3}G) ^{4}G + 14.9 4d^{6}5p (^{3}F) ^{4}G + 8.6 4d^{6}5p (^{3}H) ^{2}G
235915	236132	-217	5.5	36.6 4d^{6}5p (^{3}H) ^{4}H + 25.2 4d^{6}5p (^{3}G) ^{2}H + 11.9 4d^{6}5p (^{1}I) ^{2}H
236095.4	236068	27.4	1.5	25.8 4d^{6}5p (^{3}F) ^{4}D + 14.2 4d^{6}5p (^{3}D) ^{4}D + 7.5 4d^{6}5p (^{3}P) ^{4}D
237217.6	237183	34.6	0.5	25.7 4d^{6}5p (^{3}F) ^{4}D + 13.6 4d^{6}5p (^{5}D) ^{4}D + 11.6 4d^{6}5p (^{3}P) ^{4}D
237351.1	237243	108.1	3.5	34.6 4d^{6}5p (^{3}G) ^{4}F + 14.4 4d^{6}5p (^{3}F) ^{4}F + 8.4 4d^{6}5p (^{3}F) ^{4}F
237665.2	237745	-79.8	1.5	16.6 4d^{6}5p (^{3}D) ^{4}F + 23.3 4d^{6}5p (^{3}F) ^{2}D + 14.7 4d^{6}5p (^{3}P) ^{4}D
237757.5	237823	-65.5	5.5	21.5 4d^{6}5p (^{3}F) ^{4}G + 21.8 4d^{6}5p (^{3}H) ^{2}I + 19.9 4d^{6}5p (^{3}G) ^{4}G
237864	237715	149	2.5	24.7 4d^{6}5p (^{3}H) ^{4}G + 14.8 4d^{6}5p (^{3}G) ^{4}F + 12.8 4d^{6}5p (^{3}F) ^{4}F
237958.5	238087	-128.5	4.5	4.5 4d^{6}5p (^{3}H) ^{2}G + 25.8 4d^{6}5p (^{3}G) ^{2}H + 13.1 4d^{6}5p (^{3}F) ^{4}G
238116.8	238112	4.8	1.5	16.9 4d^{6}5p (^{3}P) ^{4}D + 13.7 4d^{6}5p (^{3}P) ^{2}P + 10.9 4d^{6}5p (^{3}P) ^{4}S
238944.8	238935	9.8	3.5	21.7 4d^{6}5p (^{3}G) ^{4}H + 23.4 4d^{6}5p (^{3}H) ^{4}H + 9 4d^{6}5p (^{3}F) ^{2}F
239288.9	239651	-362.1	0.5	36.9 4d^{6}5p (^{3}P) ^{2}S + 13.4 4d^{6}5p (^{3}D) ^{2}P + 12.9 4d^{6}5p (^{3}P) ^{4}D
239519.2	239419	100.2	2.5	17.9 4d^{6}5p (^{3}D) ^{4}F + 18.5 4d^{6}5p (^{3}G) ^{4}F + 11.7 4d^{6}5p (^{3}H) ^{4}G
239754.7	239770	-15.3	5.5	23.3 4d^{6}5p (^{3}H) ^{2}I + 18.9 4d^{6}5p (^{3}H) ^{4}G + 11.6 4d^{6}5p (^{3}F) ^{4}G
239856.5	240014	-157.5	4.5	33 4d^{6}5p (^{3}G) ^{4}H + 21 4d^{6}5p (^{3}H) ^{4}H + 13.2 4d^{6}5p (^{3}F) ^{2}G
239997.5	240085	-87.5	2.5	7.7 4d^{6}5p (^{1}D) ^{2}F + 14.3 4d^{6}5p (^{3}H) ^{4}G + 10.2 4d^{6}5p (^{3}P) ^{4}D
240318.7	240380	-61.3	6.5	73.8 4d^{6}5p (^{1}I) ^{2}K + 12.4 4d^{6}5p (^{3}G) ^{4}H + 5.7 4d^{6}5p (^{1}I) ^{2}I
240447.9	240337	110.9	3.5	34.2 4d^{6}5p (^{3}H) ^{4}G + 14.2 4d^{6}5p (^{3}D) ^{4}F + 9.5 4d^{6}5p (^{3}F) ^{4}G
240625.4	240859	-233.6	3.5	38.5 4d^{6}5p (^{3}F) ^{2}G + 12.3 4d^{6}5p (^{3}H) ^{2}G + 9.5 4d^{6}5p (^{3}F) ^{2}G
240655.4	240572	83.4	4.5	19.6 4d^{6}5p (^{3}H) ^{2}H + 12.5 4d^{6}5p (^{3}G) ^{4}G + 8 4d^{6}5p (^{3}H) ^{4}H
240673.9	240575	98.9	5.5	41.6 4d^{6}5p (^{3}G) ^{4}H + 16.7 4d^{6}5p (^{1}I) ^{2}H + 16.7 4d^{6}5p (^{3}G) ^{4}G
240681.8	240603	78.8	2.5	11.7 4d^{6}5p (^{3}F) ^{2}F + 21.8 4d^{6}5p (^{3}G) ^{4}G + 12.1 4d^{6}5p (^{3}D) ^{4}P
240975.4	241086	-110.6	6.5	53.8 4d^{6}5p (^{3}G) ^{4}H + 21.3 4d^{6}5p (^{3}H) ^{2}I + 8.5 4d^{6}5p (^{1}I) ^{2}K
241006.9	241008	-1.1	1.5	16.9 4d^{6}5p (^{3}P) ^{2}D + 10.5 4d^{6}5p (^{3}G) ^{4}F + 10.3 4d^{6}5p (^{3}F) ^{4}F
241149.8	241110	39.8	2.5	34.3 4d^{6}5p (^{3}D) ^{4}P + 14.5 4d^{6}5p (^{3}P) ^{4}D + 5 4d^{6}5p (^{1}F) ^{2}D
241220.5	241324	-103.5	3.5	19 4d^{6}5p (^{3}H) ^{2}G + 17.8 4d^{6}5p (^{3}H) ^{4}H + 15.8 4d^{6}5p (^{3}G) ^{4}G
241485.7	241256	229.7	4.5	17.5 4d^{6}5p (^{3}F) ^{4}G + 15.3 4d^{6}5p (^{3}G) ^{4}G + 14 4d^{6}5p (^{3}H) ^{4}G
241549.2	241566	-16.8	0.5	17.8 4d^{6}5p (^{3}P) ^{4}D + 28.8 4d^{6}5p (^{3}D) ^{4}P + 21.4 4d^{6}5p (^{3}P) ^{2}S
241934	241807	127	1.5	9.4 4d^{6}5p (^{3}P) ^{2}P + 17.6 4d^{6}5p (^{3}D) ^{2}P + 13.5 4d^{6}5p (^{3}D) ^{2}D
242472.5	242571	-98.5	2.5	13.8 4d^{6}5p (^{3}D) ^{2}F + 13.4 4d^{6}5p (^{3}G) ^{2}F + 12.1 4d^{6}5p (^{3}F) ^{2}D
242570.4	242607	-36.6	1.5	29.1 4d^{6}5p (^{3}D) ^{4}P + 18.5 4d^{6}5p (^{3}P) ^{2}P + 12.5 4d^{6}5p (^{3}F) ^{2}D
243101.5	242919	182.5	3.5	4.1 4d^{6}5p (^{1}G) ^{2}F + 26.9 4d^{6}5p (^{3}D) ^{2}F + 13.2 4d^{6}5p (^{3}F) ^{2}G
243373.6	243440	-66.4	2.5	37.7 4d^{6}5p (^{3}F) ^{2}D + 9.7 4d^{6}5p (^{3}P) ^{4}D + 7.5 4d^{6}5p (^{3}P) ^{2}D
243972.8	243767	205.8	4.5	28.8 4d^{6}5p (^{1}G) ^{2}H + 19.1 4d^{6}5p (^{3}F) ^{2}G + 17.1 4d^{6}5p (^{1}I) ^{2}H
244336.2	244238	98.2	1.5	18.9 4d^{6}5p (^{3}F) ^{2}D + 23.7 4d^{6}5p (^{3}D) ^{4}P + 14.4 4d^{6}5p (^{3}P) ^{2}D

Table A37: Continued

E^{a}_{exp}	E^{b}_{calc}	Δ E	J	Leading components (in %) in LS Coupling^{c}
244815.5	244836	-20.5	5.5	50.5 $4d^6 5p$ (^{3}H) ^{2}H + 37.3 $4d^6 5p$ (^{1}I) ^{2}H
245016.1	244841	175.1	0.5	26 $4d^6 5p$ (^{3}D) ^{4}D + 33.9 $4d^6 5p$ (^{3}F) ^{4}D + 17 $4d^6 5p$ (^{3}D) ^{2}P
245073.3	245094	-20.7	3.5	28.9 $4d^6 5p$ (^{3}G) ^{2}G + 12 $4d^6 5p$ (^{3}G) ^{2}F + 10.7 $4d^6 5p$ (^{1}G) ^{2}F
245179.9	245051	128.9	5.5	38.5 $4d^6 5p$ (^{3}G) ^{2}H + 15.3 $4d^6 5p$ (^{3}G) ^{4}H + 11 $4d^6 5p$ (^{1}I) ^{2}I
245878.2	245960	-81.8	7.5	94.4 $4d^6 5p$ (^{1}I) ^{2}K + 5.3 $4d^6 5p$ (^{3}H) ^{4}I
246010.1	245916	94.1	1.5	37.8 $4d^6 5p$ (^{3}G) ^{4}F + 11.9 $4d^6 5p$ (^{3}D) ^{4}F + 10.1 $4d^6 5p$ (^{3}D) ^{2}P
246376.2	246356	20.2	4.5	33.8 $4d^6 5p$ (^{3}G) ^{2}H + 18 $4d^6 5p$ (^{3}G) ^{2}G + 12.2 $4d^6 5p$ (^{3}H) ^{2}H
246420.2	246533	-112.8	1.5	31.3 $4d^6 5p$ (^{3}D) ^{4}D + 10.4 $4d^6 5p$ (^{3}F) ^{4}D + 8.6 $4d^6 5p$ (^{1}D) ^{2}P
246450.7	246496	-45.3	0.5	33.6 $4d^6 5p$ (^{3}D) ^{4}P + 10.3 $4d^6 5p$ (^{3}P) ^{2}P + 8 $4d^6 5p$ (^{3}P) ^{4}P
246935.2	246771	164.2	2.5	49.5 $4d^6 5p$ (^{3}D) ^{4}D + 20.6 $4d^6 5p$ (^{3}F) ^{4}D + 6.5 $4d^6 5p$ (^{3}D) ^{4}P
246978.2	246857	121.2	3.5	10.4 $4d^6 5p$ (^{3}G) ^{2}F + 16.1 $4d^6 5p$ (^{1}G) ^{2}G + 14.7 $4d^6 5p$ (^{3}G) ^{4}F
247257.8	247104	153.8	3.5	28.4 $4d^6 5p$ (^{3}D) ^{4}D + 20.2 $4d^6 5p$ (^{3}D) ^{4}F + 8.4 $4d^6 5p$ (^{3}G) ^{2}G
247302.8	247214	88.8	2.5	34.1 $4d^6 5p$ (^{3}G) ^{4}F + 29.6 $4d^6 5p$ (^{3}D) ^{4}F + 7.9 $4d^6 5p$ (^{3}G) ^{2}F
247444.2	247358	86.2	1.5	36.3 $4d^6 5p$ (^{3}D) ^{2}P + 13.9 $4d^6 5p$ (^{3}G) ^{4}F + 6.5 $4d^6 5p$ (^{3}P) ^{2}D
247525.9	247376	149.9	4.5	35.4 $4d^6 5p$ (^{3}D) ^{4}F + 15.4 $4d^6 5p$ (^{3}G) ^{2}G + 8.3 $4d^6 5p$ (^{3}H) ^{2}G
247919.3	248060	-140.7	0.5	11.5 $4d^6 5p$ (^{3}P) ^{2}P + 16.6 $4d^6 5p$ (^{3}D) ^{4}P + 14.7 $4d^6 5p$ (^{3}D) ^{4}D
248496.3	248438	58.3	1.5	44.9 $4d^6 5p$ (^{3}D) ^{2}D + 9.6 $4d^6 5p$ (^{3}D) ^{4}D + 6.9 $4d^6 5p$ (^{3}D) ^{4}F
248566.7	248749	-182.3	2.5	21.2 $4d^6 5p$ (^{1}F) ^{2}D + 12.8 $4d^6 5p$ (^{1}D) ^{2}D + 10.9 $4d^6 5p$ (^{3}D) ^{2}F
248656.6	248522	134.6	3.5	21.2 $4d^6 5p$ (^{1}G) ^{2}F + 18 $4d^6 5p$ (^{1}F) ^{2}G + 12.2 $4d^6 5p$ (^{3}F) ^{2}F
248732.1	248605	127.1	4.5	22.5 $4d^6 5p$ (^{3}G) ^{2}G + 31.6 $4d^6 5p$ (^{3}D) ^{4}F + 11.9 $4d^6 5p$ (^{3}H) ^{2}H
249209.7	249196	13.7	2.5	33.3 $4d^6 5p$ (^{3}D) ^{2}D + 27.2 $4d^6 5p$ (^{3}D) ^{2}F + 5 $4d^6 5p$ (^{3}D) ^{4}P
249480.9	249252	228.9	3.5	35.3 $4d^6 5p$ (^{1}G) ^{2}G + 10.3 $4d^6 5p$ (^{3}D) ^{4}F + 7.2 $4d^6 5p$ (^{1}D) ^{2}F
250353.6	250552	-198.4	1.5	22.1 $4d^6 5p$ (^{1}D) ^{2}D + 19.9 $4d^6 5p$ (^{1}D) ^{2}P + 8.6 $4d^6 5p$ (^{3}F) ^{2}D
250358.3	250436	-77.7	5.5	59.8 $4d^6 5p$ (^{1}I) ^{2}I + 17.2 $4d^6 5p$ (^{1}G) ^{2}H + 5.5 $4d^6 5p$ (^{3}H) ^{2}H
250411	250372	39	4.5	44 $4d^6 5p$ (^{1}I) ^{2}H + 15.2 $4d^6 5p$ (^{3}G) ^{2}H + 12.5 $4d^6 5p$ (^{1}G) ^{2}H
250439.6	250534	-94.4	2.5	21.8 $4d^6 5p$ (^{3}G) ^{2}F + 19.9 $4d^6 5p$ (^{3}F) ^{2}F + 12.4 $4d^6 5p$ (^{1}D) ^{2}F
250483.9	250435	48.9	3.5	37.3 $4d^6 5p$ (^{3}D) ^{2}F + 23.3 $4d^6 5p$ (^{3}D) ^{4}D + 6.8 $4d^6 5p$ (^{1}D) ^{2}F
250486.7	250589	-102.3	6.5	87.9 $4d^6 5p$ (^{1}I) ^{2}I + 8.6 $4d^6 5p$ (^{1}I) ^{2}K + 2.8 $4d^6 5p$ (^{3}H) ^{4}H
251385.9	251131	254.9	4.5	36.8 $4d^6 5p$ (^{1}G) ^{2}G + 25.8 $4d^6 5p$ (^{3}H) ^{2}H + 10.4 $4d^6 5p$ (^{1}I) ^{2}H
251797.6	251328	469.6	5.5	36.5 $4d^6 5p$ (^{1}G) ^{2}H + 25 $4d^6 5p$ (^{1}G) ^{2}H + 15.5 $4d^6 5p$ (^{1}I) ^{2}I
252246.3	252233	13.3	2.5	0.8 $4d^6 5p$ (^{3}P) ^{4}P + 22.8 $4d^6 5p$ (^{3}D) ^{2}D + 18 $4d^6 5p$ (^{1}D) ^{2}F
252985.8	252813	172.8	1.5	19 $4d^6 5p$ (^{1}S) ^{2}P + 13.9 $4d^6 5p$ (^{3}D) ^{2}D + 11.5 $4d^6 5p$ (^{1}D) ^{2}D
253412.1	253058	354.1	0.5	33 $4d^6 5p$ (^{3}D) ^{2}P + 21 $4d^6 5p$ (^{1}S) ^{2}P + 11.7 $4d^6 5p$ (^{3}D) ^{4}D
254041.7	253978	63.7	3.5	31.2 $4d^6 5p$ (^{1}F) ^{2}G + 22.2 $4d^6 5p$ (^{3}G) ^{2}G + 9.8 $4d^6 5p$ (^{3}H) ^{2}G
255444.7	255544	-99.3	3.5	35.2 $4d^6 5p$ (^{3}F) ^{4}D + 14.7 $4d^6 5p$ (^{3}P) ^{4}D + 10.6 $4d^6 5p$ (^{3}G) ^{2}F
255608.3	255392	216.3	0.5	42.4 $4d^6 5p$ (^{3}P) ^{4}D + 17.7 $4d^6 5p$ (^{3}F) ^{4}D + 12.9 $4d^6 5p$ (^{1}S) ^{2}P
255752.6	255496	256.6	2.5	32.5 $4d^6 5p$ (^{1}G) ^{2}F + 16.7 $4d^6 5p$ (^{3}D) ^{2}F + 15.2 $4d^6 5p$ (^{1}G) ^{2}F
256377.2	256598	-220.8	1.5	29.2 $4d^6 5p$ (^{3}P) ^{4}D + 18.3 $4d^6 5p$ (^{1}D) ^{2}D + 12.6 $4d^6 5p$ (^{3}F) ^{4}D
256402.5	256757	-354.5	0.5	40.8 $4d^6 5p$ (^{1}D) ^{2}P + 18.4 $4d^6 5p$ (^{3}P) ^{2}P + 13.4 $4d^6 5p$ (^{1}D) ^{2}P
256959.1	257052	-92.9	4.5	64.8 $4d^6 5p$ (^{1}F) ^{2}G + 13.3 $4d^6 5p$ (^{3}F) ^{4}G
257015.9	257178	-162.1	2.5	31.1 $4d^6 5p$ (^{3}P) ^{4}D + 34.1 $4d^6 5p$ (^{3}F) ^{4}D + 7.1 $4d^6 5p$ (^{3}P) ^{4}D
257568.4	257274	294.4	1.5	13.4 $4d^6 5p$ (^{1}D) ^{2}P + 23.5 $4d^6 5p$ (^{1}S) ^{2}P + 9.6 $4d^6 5p$ (^{3}P) ^{2}D
258005.8	258178	-172.2	3.5	35.1 $4d^6 5p$ (^{1}D) ^{2}F + 24.5 $4d^6 5p$ (^{3}F) ^{4}D + 7.2 $4d^6 5p$ (^{1}G) ^{2}F
258708.7	259045	-336.3	2.5	37.2 $4d^6 5p$ (^{1}D) ^{2}D + 11.1 $4d^6 5p$ (^{1}D) ^{2}F + 7.7 $4d^6 5p$ (^{1}F) ^{2}D
260126.4	260199	-72.6	2.5	41 $4d^6 5p$ (^{3}F) ^{4}G + 25 $4d^6 5p$ (^{1}F) ^{2}F + 9.6 $4d^6 5p$ (^{1}F) ^{2}D
260314	260480	-166	1.5	54.1 $4d^6 5p$ (^{1}F) ^{2}D + 6.3 $4d^6 5p$ (^{1}D) ^{2}D + 5.7 $4d^6 5p$ (^{3}P) ^{2}D
260437.3	260576	-138.7	3.5	58 $4d^6 5p$ (^{1}F) ^{2}F + 6.1 $4d^6 5p$ (^{1}G) ^{2}F + 5.9 $4d^6 5p$ (^{1}F) ^{2}G
261991.2	262063	-71.8	2.5	32.3 $4d^6 5p$ (^{1}F) ^{2}F + 29.2 $4d^6 5p$ (^{3}F) ^{4}G + 7.8 $4d^6 5p$ (^{1}G) ^{2}F
262557.3	262539	18.3	4.5	27.9 $4d^6 5p$ (^{3}F) ^{2}G + 25 $4d^6 5p$ (^{3}F) ^{4}G + 15.9 $4d^6 5p$ (^{1}F) ^{2}G
262987	262965	22	3.5	59.7 $4d^6 5p$ (^{3}F) ^{4}G + 8.6 $4d^6 5p$ (^{3}F) ^{4}G + 7.3 $4d^6 5p$ (^{1}F) ^{2}G
265034.4	264978	56.4	1.5	11.8 $4d^6 5p$ (^{3}F) ^{2}D + 14.6 $4d^6 5p$ (^{3}P) ^{4}S + 13.5 $4d^6 5p$ (^{3}F) ^{4}D
265241.5	265105	136.5	5.5	75.6 $4d^6 5p$ (^{3}F) ^{4}G + 15.4 $4d^6 5p$ (^{3}F) ^{4}G
265642.1	265517	125.1	1.5	38.4 $4d^6 5p$ (^{3}P) ^{4}S + 22.9 $4d^6 5p$ (^{3}F) ^{2}D + 6.7 $4d^6 5p$ (^{3}P) ^{4}S
266306.3	266216	90.3	1.5	36.5 $4d^6 5p$ (^{3}P) ^{4}P + 20 $4d^6 5p$ (^{3}P) ^{4}P + 10.2 $4d^6 5p$ (^{3}P) ^{4}S
267191.2	267166	25.2	4.5	35.8 $4d^6 5p$ (^{3}F) ^{4}G + 20.8 $4d^6 5p$ (^{3}F) ^{2}G + 9.8 $4d^6 5p$ (^{1}G) ^{2}G
267326.5	267227	99.5	2.5	21.4 $4d^6 5p$ (^{3}F) ^{4}F + 16.9 $4d^6 5p$ (^{3}P) ^{4}D + 12.4 $4d^6 5p$ (^{3}F) ^{4}D
267493.2	267375	118.2	0.5	62.3 $4d^6 5p$ (^{3}F) ^{4}D + 9.2 $4d^6 5p$ (^{3}P) ^{4}D + 6.9 $4d^6 5p$ (^{3}F) ^{4}D
268208.4	268253	-44.6	2.5	29 $4d^6 5p$ (^{3}P) ^{2}D + 13.7 $4d^6 5p$ (^{3}P) ^{2}D + 13.2 $4d^6 5p$ (^{3}P) ^{4}P
268262.7	268212	50.7	3.5	37.6 $4d^6 5p$ (^{3}F) ^{4}F + 12.2 $4d^6 5p$ (^{3}F) ^{2}G + 12 $4d^6 5p$ (^{3}F) ^{4}F
268610.3	268660	-49.7	1.5	24.1 $4d^6 5p$ (^{3}P) ^{2}D + 26.5 $4d^6 5p$ (^{3}F) ^{4}F + 10.4 $4d^6 5p$ (^{3}P) ^{2}D
269623	269549	74	1.5	31.7 $4d^6 5p$ (^{3}F) ^{4}D + 13.9 $4d^6 5p$ (^{3}F) ^{2}D + 11.9 $4d^6 5p$ (^{3}P) ^{2}D
269889.7	269949	-59.3	3.5	54.9 $4d^6 5p$ (^{3}F) ^{2}G + 10.9 $4d^6 5p$ (^{1}G) ^{2}F + 8.8 $4d^6 5p$ (^{3}F) ^{2}G
270214.4	270284	-69.6	2.5	33.9 $4d^6 5p$ (^{3}F) ^{2}D + 18.8 $4d^6 5p$ (^{3}F) ^{4}F + 15.5 $4d^6 5p$ (^{3}P) ^{4}P
270353.3	270385	-31.7	4.5	37.4 $4d^6 5p$ (^{1}G) ^{2}H + 23 $4d^6 5p$ (^{3}F) ^{4}F + 18.8 $4d^6 5p$ (^{1}G) ^{2}H
270766.2	270842	-75.8	3.5	16.1 $4d^6 5p$ (^{3}F) ^{2}F + 20.7 $4d^6 5p$ (^{1}G) ^{2}F + 15.4 $4d^6 5p$ (^{3}P) ^{4}D
271217.8	271171	46.8	2.5	24.1 $4d^6 5p$ (^{3}F) ^{4}D + 21.5 $4d^6 5p$ (^{3}F) ^{4}F + 9.7 $4d^6 5p$ (^{3}P) ^{4}D
271392.3	271541	-148.7	1.5	29.1 $4d^6 5p$ (^{3}F) ^{4}F + 24.9 $4d^6 5p$ (^{3}F) ^{2}D + 7.9 $4d^6 5p$ (^{3}F) ^{4}F
271792.5	271738	54.5	4.5	33.6 $4d^6 5p$ (^{3}F) ^{4}F + 27 $4d^6 5p$ (^{3}F) ^{2}G + 11.8 $4d^6 5p$ (^{3}F) ^{4}F
273408.9	273446	-37.1	3.5	16.5 $4d^6 5p$ (^{3}P) ^{4}D + 17.7 $4d^6 5p$ (^{3}F) ^{2}F + 14.9 $4d^6 5p$ (^{3}F) ^{4}D
273965.5	274237	-271.5	2.5	16.6 $4d^6 5p$ (^{3}P) ^{2}D + 23.8 $4d^6 5p$ (^{3}P) ^{2}D + 14.2 $4d^6 5p$ (^{3}P) ^{4}P
274684.2	274884	-199.8	2.5	60.7 $4d^6 5p$ (^{3}F) ^{2}F + 19.8 $4d^6 5p$ (^{3}F) ^{2}F
274797.5	274790	7.5	3.5	4.5 $4d^6 5p$ (^{3}F) ^{4}F + 35.7 $4d^6 5p$ (^{1}G) ^{2}G + 12.6 $4d^6 5p$ (^{3}F) ^{4}F
275204.8	275354	-149.2	5.5	61.1 $4d^6 5p$ (^{1}G) ^{2}H + 30.2 $4d^6 5p$ (^{1}G) ^{2}H
275971.8	276197	-225.2	1.5	34 $4d^6 5p$ (^{3}P) ^{2}P + 22.3 $4d^6 5p$ (^{3}P) ^{2}P + 7.4 $4d^6 5p$ (^{3}P) ^{2}D
276014.8	276142	-127.2	2.5	45.9 $4d^6 5p$ (^{1}G) ^{2}F + 12.7 $4d^6 5p$ (^{1}G) ^{2}F + 11.9 $4d^6 5p$ (^{1}F) ^{2}F
277850.2	277950	-99.8	4.5	59.4 $4d^6 5p$ (^{1}G) ^{2}G + 18.2 $4d^6 5p$ (^{1}G) ^{2}G + 6.7 $4d^6 5p$ (^{1}G) ^{2}H
279626.8	279731	-104.2	3.5	22.6 $4d^6 5p$ (^{1}G) ^{2}G + 18.4 $4d^6 5p$ (^{3}F) ^{2}F + 16.1 $4d^6 5p$ (^{1}G) ^{2}F
286032.1	285926	106.1	1.5	69.1 $4d^6 5p$ (^{1}D) ^{2}D + 9.5 $4d^6 5p$ (^{1}D) ^{2}D + 8.3 $4d^6 5p$ (^{1}D) ^{2}P
287725.2	287653	72.2	2.5	62.6 $4d^6 5p$ (^{1}D) ^{2}D + 11.3 $4d^6 5p$ (^{1}D) ^{2}F + 8.3 $4d^6 5p$ (^{1}D) ^{2}D
293238.9	293171	67.9	2.5	52.2 $4d^6 5p$ (^{1}D) ^{2}F + 18.3 $4d^6 5p$ (^{1}D) ^{2}D + 14.4 $4d^6 5p$ (^{1}D) ^{2}F
294884.3	294728	156.3	1.5	51.6 $4d^6 5p$ (^{1}D) ^{2}P + 20.4 $4d^6 5p$ (^{1}D) ^{2}P + 10.5 $4d^6 5p$ (^{1}D) ^{2}D
295024.7	294942	82.7	0.5	54.9 $4d^6 5p$ (^{1}D) ^{2}P + 22.4 $4d^6 5p$ (^{1}D) ^{2}P + 17.4 $4d^6 5p$ (^{1}S) ^{2}P
296253.4	296106	147.4	3.5	70.1 $4d^6 5p$ (^{1}D) ^{2}F + 19.8 $4d^6 5p$ (^{1}D) ^{2}F + 5.2 $4d^6 5p$ (^{1}G) ^{2}F

a: From Van Kleef [30] and Kildiyarova [42]
b: This work
c: Only the component ≥ 5% are given

Transitions

Table A38: Computed oscillator strengths and transition probabilities Ag V.

Wavelength Å	Lower Level[a] cm^{-1}	J_{Low}	Upper level[a] cm^{-1}	J_{Up}	log gf	gA s^{-1}	CF
391.668	22532	5.5	277850	4.5	-0.38	1.83E+10	-0.323
394.853	26368	4.5	279627	3.5	-0.47	1.46E+10	-0.225
397.762	14899	2.5	266306	1.5	-0.96	4.59E+09	0.172
397.777	34635	2.5	286032	1.5	-0.6	1.06E+10	0.394
398.198	36594	3.5	287725	2.5	-0.52	1.28E+10	0.307
398.815	14899	2.5	265642	1.5	-0.87	5.65E+09	0.305
401.187	22532	5.5	271793	4.5	-0.37	1.76E+10	0.337
402.528	26368	4.5	274798	3.5	-0.63	9.71E+09	-0.231
403.279	17067	0.5	265034	1.5	-0.94	4.70E+09	0.199
404.791	26368	4.5	273409	3.5	-0.87	5.52E+09	0.215
410.641	26368	4.5	269890	3.5	-0.23	2.33E+10	0.339
410.907	14204	1.5	257568	1.5	-0.93	4.66E+09	-0.178
411.343	14899	2.5	258006	3.5	-0.76	6.86E+09	0.418
412.084	14899	2.5	257568	1.5	-0.96	4.35E+09	0.376
414.284	34635	2.5	276015	2.5	-0.86	5.38E+09	0.085
414.497	36594	3.5	277850	4.5	-0.42	1.48E+10	0.528
415.722	14899	2.5	255445	3.5	-0.39	1.59E+10	0.444
416.384	34635	2.5	274798	3.5	-0.9	4.89E+09	0.187
416.581	34635	2.5	274684	2.5	-0.77	6.50E+09	-0.145
416.623	22532	5.5	262557	4.5	-0.08	3.19E+10	0.586
416.695	55041	1.5	295025	0.5	-0.46	1.34E+10	-0.643
417.093	0	4.5	239755	5.5	-0.86	5.26E+09	-0.088
417.556	30134	1.5	269623	1.5	-0.73	7.13E+09	0.209
418.563	7097	1.5	246010	1.5	-0.78	6.30E+09	-0.191
419.97	56772	2.5	294884	1.5	-0.16	2.59E+10	-0.576
420.241	0	4.5	237959	4.5	-0.76	6.62E+09	0.241
420.53	3691	3.5	241486	4.5	-0.81	5.85E+09	0.119
420.95	5816	2.5	243374	2.5	-0.86	5.16E+09	-0.273
421.28	36594	3.5	273966	2.5	-0.85	5.32E+09	-0.097
422.27	36594	3.5	273409	3.5	-0.84	5.43E+09	-0.214
422.62	26368	4.5	262987	3.5	-0.69	7.63E+09	0.502
422.892	56772	2.5	293239	2.5	-1	3.71E+09	-0.183
423.431	3691	3.5	239857	4.5	-1	3.70E+09	-0.416
423.592	24361	2.5	260437	3.5	-0.77	6.34E+09	0.147
424.037	3691	3.5	239519	2.5	-0.7	7.37E+09	-0.408
424.476	14899	2.5	250484	3.5	-0.66	8.12E+09	0.442
424.727	21571	1.5	257016	2.5	-0.6	9.33E+09	-0.37
424.97	20442	3.5	255753	2.5	-0.35	1.64E+10	0.276
425.172	36594	3.5	271793	4.5	-0.95	4.13E+09	-0.376
425.549	0	4.5	234991	4.5	0.04	4.02E+10	-0.583
425.553	34635	2.5	269623	1.5	-0.95	4.09E+09	-0.261
425.78	0	4.5	234863	3.5	-0.09	2.97E+10	-0.682
426.199	5816	2.5	240448	3.5	-0.33	1.70E+10	-0.305
426.419	16875	4.5	251386	4.5	-0.66	7.95E+09	0.067
426.49	0	4.5	234472	5.5	-0.5	1.16E+10	0.489
426.572	22532	5.5	256959	4.5	-0.06	3.17E+10	0.55
426.69	14204	1.5	248567	2.5	-0.99	3.79E+09	-0.174
427.036	36594	3.5	270766	3.5	-0.46	1.29E+10	0.257
427.255	7097	1.5	241150	2.5	-0.96	4.06E+09	0.341
427.395	34635	2.5	268610	1.5	-0.82	5.58E+09	0.216
427.463	0	4.5	233938	3.5	-0.79	5.94E+09	0.223
427.516	7097	1.5	241007	1.5	-0.83	5.41E+09	0.333
427.892	5816	2.5	239519	2.5	-0.76	6.34E+09	-0.153
427.919	0	4.5	233689	4.5	-0.96	4.04E+09	-0.102
427.971	3691	3.5	237351	3.5	0.06	4.13E+10	-0.603
428.065	16875	4.5	250484	3.5	-0.18	2.41E+10	0.325
428.199	16875	4.5	250411	4.5	-0.97	3.90E+09	0.054
429.681	14204	1.5	246935	2.5	-0.84	5.23E+09	0.149
430.252	7097	1.5	239519	2.5	-0.42	1.36E+10	0.497
430.476	5816	2.5	238117	1.5	-0.69	7.41E+09	-0.405
430.634	14204	1.5	246420	1.5	-0.67	7.75E+09	0.29
430.945	5816	2.5	237864	2.5	-0.3	1.80E+10	-0.484
430.956	3691	3.5	235733	4.5	-0.34	1.63E+10	-0.466
430.968	14899	2.5	246935	2.5	-0.47	1.22E+10	0.5
431.073	3691	3.5	235670	2.5	-0.84	5.21E+09	-0.363
431.399	20442	3.5	252246	2.5	-0.34	1.63E+10	0.419
431.4	24599	0.5	256402	0.5	-0.69	7.37E+09	0.382
431.44	16875	4.5	248657	3.5	-0.04	3.24E+10	0.364
431.645	34635	2.5	266306	1.5	-1	3.56E+09	0.414
431.752	36594	3.5	268208	2.5	-0.06	3.13E+10	-0.516
431.899	5816	2.5	237351	3.5	-0.95	4.02E+09	0.137
432.339	3691	3.5	234991	4.5	-0.68	7.53E+09	0.426
432.462	3691	3.5	234925	2.5	-0.32	1.70E+10	0.413
432.744	24361	2.5	255445	3.5	-0.98	3.76E+09	0.127
432.887	34635	2.5	265642	1.5	-0.67	7.58E+09	-0.402
432.917	55041	1.5	286032	1.5	-0.35	1.59E+10	-0.44
432.988	56772	2.5	287725	2.5	-0.32	1.72E+10	-0.297
433.186	0	4.5	230848	3.5	-0.41	1.39E+10	-0.362
433.712	7097	1.5	237665	1.5	-0.44	1.29E+10	0.557
434.254	5816	2.5	236095	1.5	-0.23	2.08E+10	0.593
434.443	30134	1.5	260314	1.5	-0.47	1.19E+10	0.255
434.555	7097	1.5	237218	0.5	-0.48	1.18E+10	0.554
434.657	5816	2.5	235882	3.5	-0.33	1.65E+10	-0.518
434.785	3691	3.5	233689	4.5	-0.65	7.85E+09	-0.282
434.787	20442	3.5	250440	2.5	-0.01	3.43E+10	0.425
434.841	20442	3.5	250411	4.5	-0.56	9.72E+09	-0.167
435.727	16875	4.5	246376	4.5	-0.55	9.84E+09	0.122
435.85	14899	2.5	244336	1.5	-0.92	4.22E+09	0.337
436.175	22532	5.5	251798	5.5	-0.47	1.19E+10	0.27
436.474	5816	2.5	234925	2.5	-0.81	5.49E+09	-0.21
436.534	26368	4.5	255445	3.5	-0.74	6.35E+09	-0.237
436.607	20442	3.5	249481	3.5	-0.37	1.50E+10	0.272
436.762	3691	3.5	232648	4.5	-0.43	1.29E+10	-0.518
437.038	24599	0.5	253412	0.5	-0.96	3.82E+09	0.356
437.096	21571	1.5	250354	1.5	-0.84	5.02E+09	-0.094
437.125	20442	3.5	249210	2.5	-0.84	5.11E+09	-0.142

Table A38: Continued

Wavelength	Lower Level	J_{Low}	Upper level	J_{Up}	log gf	gA	CF
437.275	3691	3.5	232379	3.5	-0.93	4.13E+09	-0.122
437.398	24361	2.5	252986	1.5	-0.42	1.32E+10	-0.414
437.495	30134	1.5	258709	2.5	-0.77	5.89E+09	-0.147
437.498	7097	1.5	235670	2.5	-0.51	1.09E+10	-0.427
437.894	14204	1.5	242570	1.5	-0.8	5.50E+09	0.258
438.01	16875	4.5	245180	5.5	-0.42	1.32E+10	0.323
438.081	14204	1.5	242473	2.5	-0.95	3.92E+09	-0.191
438.184	20442	3.5	248657	3.5	-0.92	4.16E+09	-0.129
438.201	0	4.5	228206	4.5	-0.14	2.53E+10	-0.618
438.208	14899	2.5	243102	3.5	-0.98	3.63E+09	-0.468
438.215	16875	4.5	245073	3.5	-0.52	1.05E+10	-0.152
438.683	22532	5.5	250487	6.5	-0.1	2.77E+10	0.605
438.695	17067	0.5	245016	0.5	-0.78	5.80E+09	0.442
438.818	24361	2.5	252246	2.5	-0.16	2.38E+10	0.376
438.902	0	4.5	227841	5.5	0.17	5.15E+10	-0.583
439.225	26368	4.5	254042	3.5	0.07	4.09E+10	0.464
439.23	14899	2.5	242570	1.5	-0.85	4.90E+09	0.322
439.688	30134	1.5	257568	1.5	-0.79	5.54E+09	0.134
439.838	34635	2.5	261991	2.5	-0.29	1.76E+10	0.529
439.861	14204	1.5	241549	0.5	-0.79	5.55E+09	0.33
440.007	17067	0.5	244336	1.5	-0.87	4.65E+09	-0.285
440.338	16875	4.5	243973	4.5	-0.02	3.29E+10	-0.393
440.536	21571	1.5	248567	2.5	-0.63	7.99E+09	-0.201
440.635	14204	1.5	241150	2.5	-0.75	6.13E+09	-0.215
440.673	21571	1.5	248496	1.5	-0.75	6.17E+09	0.163
440.799	20442	3.5	247303	2.5	-0.97	3.69E+09	0.237
441.377	5816	2.5	232379	3.5	-0.68	7.12E+09	-0.208
441.431	20442	3.5	246978	3.5	-0.04	3.10E+10	0.51
441.545	14204	1.5	240682	2.5	-0.87	4.57E+09	-0.269
441.612	3691	3.5	230134	4.5	-0.86	4.69E+09	-0.218
441.709	36594	3.5	262987	3.5	-0.74	6.26E+09	-0.5
441.796	21571	1.5	247919	0.5	-0.93	4.00E+09	-0.135
441.954	30134	1.5	256402	0.5	-0.51	1.06E+10	-0.335
441.988	14899	2.5	241150	2.5	-0.5	1.09E+10	0.299
442.003	30134	1.5	256377	1.5	-0.84	4.92E+09	0.168
442.034	16875	4.5	243102	3.5	-0.17	2.28E+10	0.275
442.086	22532	5.5	248732	4.5	-0.26	1.87E+10	0.475
442.324	24361	2.5	250440	2.5	-0.83	5.12E+09	-0.162
442.493	24361	2.5	250354	1.5	-0.73	6.38E+09	0.152
442.607	20442	3.5	246376	4.5	-0.61	8.42E+09	0.268
442.904	14899	2.5	240682	2.5	-0.79	5.51E+09	0.281
442.959	24599	0.5	250354	1.5	-0.3	1.70E+10	0.582
443.227	30134	1.5	255753	2.5	-0.43	1.27E+10	-0.253
443.331	0	4.5	225565	3.5	-0.65	7.67E+09	0.29
444.205	3691	3.5	228812	3.5	-0.82	5.10E+09	-0.244
444.208	24361	2.5	249481	3.5	-0.78	5.57E+09	-0.229
444.278	14204	1.5	239289	0.5	-0.95	3.80E+09	0.209
444.408	26368	4.5	251386	4.5	0.25	5.94E+10	-0.523
444.456	22532	5.5	247526	4.5	-0.25	1.91E+10	-0.378
444.682	21571	1.5	246451	0.5	-0.9	4.24E+09	-0.161
444.744	24361	2.5	249210	2.5	-0.88	4.47E+09	0.092
445.174	20442	3.5	245073	3.5	-0.73	6.24E+09	0.146
445.225	3691	3.5	228296	2.5	-0.46	1.18E+10	-0.383
445.404	3691	3.5	228206	4.5	-0.82	5.05E+09	-0.128
445.555	21571	1.5	246010	1.5	-0.93	3.97E+09	-0.122
445.74	16875	4.5	241221	3.5	-0.56	9.21E+09	0.187
445.841	24361	2.5	248657	3.5	-0.69	6.93E+09	-0.142
446.342	26368	4.5	250411	4.5	0.09	4.10E+10	0.412
446.447	26368	4.5	250358	5.5	0	3.32E+10	0.575
446.549	17067	0.5	241007	1.5	-0.86	4.65E+09	0.33
446.739	22532	5.5	246376	4.5	-0.46	1.15E+10	-0.306
446.741	36594	3.5	260437	3.5	-0.33	1.56E+10	0.322
446.829	16875	4.5	240674	5.5	-0.21	2.05E+10	0.601
447.366	20442	3.5	243973	4.5	-0.4	1.32E+10	0.345
447.873	30134	1.5	253412	0.5	-0.51	1.03E+10	0.37
448.146	5816	2.5	228957	2.5	-0.92	3.96E+09	-0.192
448.264	24361	2.5	247444	1.5	-0.49	1.09E+10	0.317
448.438	5816	2.5	228812	3.5	-0.94	3.81E+09	-0.114
448.672	16875	4.5	239755	5.5	-0.63	7.72E+09	0.294
448.722	56772	2.5	279627	3.5	-0.06	2.91E+10	-0.508
449.116	20442	3.5	243102	3.5	-0.98	3.48E+09	0.119
449.202	24361	2.5	246978	3.5	-0.84	4.84E+09	0.293
449.712	26368	4.5	248732	4.5	-0.86	4.55E+09	0.073
449.865	26368	4.5	248657	3.5	-0.72	6.32E+09	-0.136
449.876	22532	5.5	244816	5.5	0.54	1.14E+11	0.651
450.217	36594	3.5	258709	2.5	-0.85	4.62E+09	0.101
450.331	24361	2.5	246420	1.5	-0.93	3.86E+09	0.16
450.389	20442	3.5	242473	2.5	-0.96	3.63E+09	0.136
450.752	24599	0.5	246451	0.5	-0.95	3.67E+09	0.348
450.851	21571	1.5	243374	2.5	-0.6	8.32E+09	-0.18
451.588	22532	5.5	243973	4.5	-0.86	4.51E+09	-0.12
451.647	36594	3.5	258006	3.5	-0.35	1.47E+10	0.322
452.247	34635	2.5	255753	2.5	-0.52	9.85E+09	0.173
452.317	16875	4.5	237959	4.5	-0.2	2.06E+10	-0.322
452.489	21571	1.5	242570	1.5	-0.92	3.93E+09	0.128
452.543	55041	1.5	276015	2.5	-0.25	1.86E+10	-0.392
452.943	20442	3.5	241221	3.5	-0.64	7.45E+09	0.252
453.062	14204	1.5	234925	2.5	-1	3.27E+09	0.114
454.105	20442	3.5	240655	4.5	-0.83	4.78E+09	0.156
454.172	0	4.5	220181	3.5	-0.63	7.55E+09	-0.387
455.284	55041	1.5	274684	2.5	-0.55	9.03E+09	-0.301
455.417	21571	1.5	241150	2.5	-0.9	4.07E+09	0.144
455.774	34635	2.5	254042	3.5	-0.52	9.79E+09	0.23
456.115	56772	2.5	276015	2.5	-0.89	4.13E+09	-0.216
456.205	56772	2.5	275972	1.5	-0.68	6.65E+09	-0.127
456.29	36594	3.5	255753	2.5	-0.9	4.05E+09	0.176
456.537	16875	4.5	235915	5.5	-0.87	4.31E+09	-0.141
456.54	14899	2.5	233938	3.5	-0.92	3.89E+09	0.13
456.595	24361	2.5	243374	2.5	-0.79	5.18E+09	-0.13
456.918	16875	4.5	235733	4.5	-0.35	1.44E+10	-0.285
456.932	36594	3.5	255445	3.5	-0.37	1.38E+10	-0.408
457.163	24361	2.5	243102	3.5	-0.54	9.12E+09	0.249
457.784	22532	5.5	240975	6.5	-0.62	7.73E+09	0.71
458.276	24361	2.5	242570	1.5	-0.84	4.63E+09	-0.189
458.662	56772	2.5	274798	3.5	-0.71	6.23E+09	0.352
459.309	21571	1.5	239289	0.5	-0.58	8.38E+09	0.307

Table A38: Continued

Wavelength	Lower Level	J_{Low}	Upper level	J_{Up}	log gf	gA	CF
459.534	34635	2.5	252246	2.5	-0.85	4.45E+09	-0.108
459.749	0	4.5	217510	4.5	-0.45	1.13E+10	-0.313
460.357	22532	5.5	239755	5.5	-0.79	5.09E+09	0.198
460.389	0	4.5	217208	3.5	-0.16	2.20E+10	-0.312
460.472	30134	1.5	247303	2.5	-0.84	4.58E+09	0.295
461.128	24361	2.5	241221	3.5	-0.71	6.08E+09	-0.341
461.602	56772	2.5	273409	3.5	-0.99	3.22E+09	-0.173
461.914	3691	3.5	220181	3.5	-0.78	5.23E+09	-0.141
462.212	55041	1.5	271392	1.5	-0.77	5.34E+09	0.183
463.073	14899	2.5	230848	3.5	-0.9	3.95E+09	-0.145
463.382	34635	2.5	250440	2.5	-0.51	9.72E+09	-0.141
463.449	16875	4.5	232648	4.5	-0.95	3.49E+09	0.051
463.658	5816	2.5	221492	2.5	-0.84	4.52E+09	-0.168
463.744	24361	2.5	239998	2.5	-0.92	3.72E+09	-0.14
463.842	7097	1.5	222688	1.5	-0.9	3.94E+09	-0.188
464.534	3691	3.5	218960	2.5	-0.51	9.49E+09	-0.279
464.742	55041	1.5	270214	2.5	-0.97	3.33E+09	0.368
465.298	0	4.5	214916	3.5	-0.98	3.19E+09	0.239
466.023	55041	1.5	269623	1.5	-0.78	5.12E+09	-0.253
466.662	26368	4.5	240655	4.5	-0.78	5.05E+09	0.069
467.481	3691	3.5	217603	2.5	-0.68	6.31E+09	0.284
467.592	34635	2.5	248496	1.5	-0.88	4.02E+09	0.246
467.978	5816	2.5	219501	1.5	-0.47	1.04E+10	-0.305
468.347	3691	3.5	217208	3.5	-0.79	4.89E+09	0.249
468.51	56772	2.5	270214	2.5	-0.31	1.48E+10	-0.35
469.614	7097	1.5	220038	0.5	-0.6	7.57E+09	-0.319
470.316	34635	2.5	247258	3.5	-0.98	3.17E+09	-0.237
470.802	7097	1.5	219501	1.5	-0.98	3.17E+09	0.273
470.894	0	4.5	212362	4.5	-0.83	4.48E+09	-0.305
470.947	30134	1.5	242473	2.5	-0.66	6.55E+09	0.235
471.391	36594	3.5	248732	4.5	-0.41	1.18E+10	0.495
472.955	56772	2.5	268208	2.5	-0.28	1.58E+10	-0.318
472.96	22532	5.5	233966	6.5	-0.66	6.47E+09	0.661
473.191	16875	4.5	228206	4.5	-0.95	3.37E+09	-0.095
473.421	14899	2.5	226128	1.5	-0.67	6.45E+09	-0.205
473.851	0	4.5	211037	3.5	-0.55	8.35E+09	-0.29
474.086	36594	3.5	247526	4.5	-0.52	8.86E+09	-0.307
474.542	14204	1.5	224934	0.5	-0.62	7.11E+09	-0.44
474.832	55041	1.5	265642	1.5	-0.47	9.95E+09	-0.424
474.936	56772	2.5	267327	2.5	-0.71	5.76E+09	-0.387
476.206	55041	1.5	265034	1.5	-1	2.97E+09	0.213
476.684	36594	3.5	246376	4.5	-0.72	5.64E+09	-0.261
478.606	14899	2.5	223840	1.5	-0.97	3.14E+09	-0.116
481.302	14204	1.5	221974	2.5	-0.93	3.43E+09	0.162
481.426	3691	3.5	211407	2.5	-0.91	3.56E+09	-0.19
482.917	14899	2.5	221974	2.5	-0.26	1.58E+10	-0.34
483.623	17067	0.5	223840	1.5	-0.89	3.64E+09	0.168
485.459	34635	2.5	240625	3.5	-0.43	1.06E+10	-0.369
488.387	14204	1.5	218960	2.5	-0.94	3.23E+09	-0.241
491.974	36594	3.5	239857	4.5	-0.82	4.20E+09	-0.34
494.296	14899	2.5	217208	3.5	-0.82	4.14E+09	-0.303
964.556	171530	6.5	275205	5.5	-0.89	9.23E+08	-0.344
1017.47	172070	5.5	270353	4.5	-0.92	7.82E+08	-0.423
1021.198	198329	4.5	296253	3.5	-0.85	8.95E+08	0.369
1061.668	199048	3.5	293239	2.5	-0.99	6.09E+08	0.335
1062.212	181872	2.5	276015	2.5	-0.91	7.35E+08	-0.189
1127.294	165334	4.5	254042	3.5	-0.81	8.20E+08	-0.221
1127.679	199048	3.5	287725	2.5	-0.81	8.20E+08	-0.552
1146.242	161491	5.5	248732	4.5	-0.45	1.81E+09	0.494
1147.564	170865	4.5	258006	3.5	-0.74	9.17E+08	0.516
1150.248	135036	3.5	221974	2.5	-0.88	6.72E+08	-0.434
1150.581	160023	3.5	246935	2.5	-0.88	6.58E+08	-0.259
1154.414	181639	3.5	268263	3.5	-0.88	6.63E+08	-0.229
1157.492	189621	2.5	276015	2.5	-0.7	9.92E+08	-0.511
1157.527	181872	2.5	268263	3.5	-0.87	6.70E+08	0.281
1161.516	170865	4.5	256959	4.5	-0.98	5.19E+08	-0.289
1168.873	181639	3.5	267191	4.5	-0.78	8.09E+08	0.168
1173.91	188224	4.5	273409	3.5	-0.69	9.82E+08	-0.192
1174.034	189621	2.5	274798	3.5	-0.6	1.21E+09	-0.588
1174.473	135036	3.5	220181	3.5	-0.69	9.92E+08	0.557
1177.442	186288	1.5	271218	2.5	-0.94	5.53E+08	0.25
1178.5	189944	3.5	274798	3.5	-0.71	9.34E+08	0.132
1179.735	132745	4.5	217510	4.5	-0.65	1.08E+09	0.76
1180.806	156798	5.5	241486	4.5	-0.82	7.24E+08	0.134
1182.313	170865	4.5	255445	3.5	-0.65	1.07E+09	-0.359
1183.957	132745	4.5	217208	3.5	-0.28	2.50E+09	-0.592
1185.812	156645	6.5	240975	6.5	-0.35	2.14E+09	0.726
1186.064	160704	1.5	245016	0.5	-0.89	6.12E+08	-0.313
1186.34	156155	4.5	240448	3.5	-1	4.75E+08	-0.079
1187.964	156798	5.5	240975	6.5	-0.98	5.00E+08	-0.05
1190.23	166467	3.5	250484	3.5	-0.89	6.10E+08	0.23
1191.56	135036	3.5	218960	2.5	-0.7	9.30E+08	-0.254
1192.235	156798	5.5	240674	5.5	-0.91	5.79E+08	0.212
1192.484	136401	2.5	220260	1.5	-0.99	4.79E+08	-0.16
1193.602	136401	2.5	220181	3.5	-0.72	8.94E+08	0.372
1196.174	196027	3.5	279627	3.5	-0.93	5.50E+08	0.052
1196.616	188224	4.5	271793	4.5	0.13	6.30E+09	0.723
1198.107	189944	3.5	273409	3.5	-0.1	3.67E+09	0.639
1198.347	164078	4.5	247526	4.5	-0.93	5.40E+08	-0.147
1198.861	164032	2.5	247444	1.5	-0.96	5.12E+08	0.249
1199.064	165334	4.5	248732	4.5	-1	4.68E+08	0.065
1199.975	186288	1.5	269623	1.5	-0.96	5.12E+08	0.241
1200.12	161491	5.5	244816	5.5	-0.92	5.64E+08	-0.106
1200.897	190694	2.5	273966	2.5	-0.34	2.12E+09	0.574
1202.227	159923	2.5	243102	3.5	-0.94	5.25E+08	0.269
1202.271	175533	3.5	258709	2.5	-0.85	6.65E+08	-0.563
1203.229	156645	6.5	239755	5.5	-0.43	1.69E+09	-0.301
1205.445	156798	5.5	239755	5.5	-0.9	5.79E+08	0.105
1205.473	156902	3.5	239857	4.5	-0.61	1.13E+09	-0.202
1205.976	175085	4.5	258006	3.5	-0.9	5.89E+08	-0.236
1206.129	137350	1.5	220260	1.5	-0.32	2.17E+09	0.689
1206.264	164078	4.5	246978	3.5	-0.44	1.67E+09	-0.423
1206.292	188494	1.5	271392	1.5	-0.37	1.98E+09	0.659
1208.836	188494	1.5	271218	2.5	-0.74	8.34E+08	-0.651
1208.978	190694	2.5	273409	3.5	-0.2	2.84E+09	0.634
1210.397	164685	3.5	247303	2.5	-0.37	1.92E+09	-0.364

Table A38: Continued

Wavelength	Lower Level	J_{Low}	Upper level	J_{Up}	log gf	gA	CF
1211.146	135036	3.5	217603	2.5	-0.79	7.29E+08	-0.114
1211.255	136401	2.5	218960	2.5	-0.29	2.33E+09	0.671
1212.512	135036	3.5	217510	4.5	-0.2	2.86E+09	0.499
1212.518	175533	3.5	258006	3.5	-0.9	5.80E+08	0.528
1212.594	163952	0.5	246420	1.5	-0.78	7.60E+08	-0.541
1212.918	160125	1.5	242570	1.5	-0.9	5.70E+08	0.243
1214.391	137914	0.5	220260	1.5	-0.51	1.40E+09	-0.518
1216.973	135036	3.5	217208	3.5	-0.61	1.10E+09	0.469
1216.974	132745	4.5	214916	3.5	-0.53	1.33E+09	-0.141
1217.106	168322	3.5	250484	3.5	-0.36	1.97E+09	0.451
1217.585	188224	4.5	270353	4.5	-0.21	2.79E+09	-0.449
1218.869	156902	3.5	238945	3.5	-0.58	1.19E+09	0.176
1219.341	159923	2.5	241934	1.5	-0.87	6.10E+08	-0.397
1219.834	164032	2.5	246010	1.5	-0.56	1.22E+09	-0.334
1220.191	167527	2.5	249481	3.5	-0.93	5.29E+08	-0.244
1220.536	165595	5.5	247526	4.5	-0.61	1.11E+09	0.349
1220.696	186288	1.5	268208	2.5	-0.42	1.70E+09	0.715
1222.146	196027	3.5	277850	4.5	-0.36	1.97E+09	0.678
1222.959	160704	1.5	242473	2.5	-0.79	7.20E+08	0.366
1223.679	188494	1.5	270214	2.5	-0.99	4.54E+08	0.607
1224.059	172346	3.5	254042	3.5	-0.29	2.28E+09	-0.474
1224.127	164685	3.5	246376	4.5	-0.86	6.10E+08	0.162
1224.497	188224	4.5	269890	3.5	-0.99	4.56E+08	0.598
1225.54	189621	2.5	271218	2.5	-0.12	3.35E+09	0.569
1225.682	137914	0.5	219501	1.5	-0.55	1.25E+09	0.678
1227.128	178946	2.5	260437	3.5	-0.96	4.86E+08	0.243
1230.049	198329	4.5	279627	3.5	-0.5	1.41E+09	-0.31
1230.407	189944	3.5	271218	2.5	-0.86	6.06E+08	-0.105
1230.418	169166	2.5	250440	2.5	-0.79	7.10E+08	0.192
1231.197	159226	4.5	240448	3.5	-0.4	1.76E+09	-0.407
1231.5	136401	2.5	217603	2.5	-0.87	5.93E+08	0.094
1231.559	160023	3.5	241221	3.5	-0.72	8.48E+08	-0.244
1231.586	156155	4.5	237351	3.5	-0.64	1.00E+09	-0.227
1232.123	156798	5.5	237959	4.5	-0.76	7.58E+08	0.37
1232.588	167527	2.5	248657	3.5	-0.88	5.82E+08	0.361
1232.632	160023	3.5	241150	2.5	-0.79	7.13E+08	0.499
1233.011	164078	4.5	245180	5.5	-0.55	1.24E+09	0.192
1233.92	165334	4.5	246376	4.5	-0.31	2.13E+09	0.31
1233.98	186288	1.5	267327	2.5	-0.26	2.42E+09	-0.667
1235.14	156902	3.5	237864	2.5	-0.18	2.87E+09	-0.493
1235.591	170865	4.5	251798	5.5	-0.63	1.01E+09	0.299
1235.81	181639	3.5	262557	4.5	-0.77	7.47E+08	-0.096
1236.002	156445	2.5	237351	3.5	-0.72	8.34E+08	0.56
1236.364	160125	1.5	241007	1.5	-0.79	6.99E+08	0.221
1237.907	165595	5.5	246376	4.5	-0.77	7.46E+08	0.365
1239.395	185622	0.5	266306	1.5	-0.25	2.47E+09	-0.692
1240.227	159226	4.5	239857	4.5	-0.28	2.30E+09	0.56
1240.652	160023	3.5	240625	3.5	-0.85	6.22E+08	0.362
1240.798	189621	2.5	270214	2.5	-0.85	6.19E+08	-0.236
1241.014	199048	3.5	279627	3.5	0.18	6.63E+09	0.715
1241.795	159226	4.5	239755	5.5	-0.53	1.26E+09	0.208
1242.056	166467	3.5	246978	3.5	-0.87	5.81E+08	0.131
1242.068	175242	1.5	255753	2.5	-0.56	1.20E+09	-0.485
1243.014	156902	3.5	237351	3.5	-0.58	1.15E+09	0.228
1243.067	160704	1.5	241150	2.5	-0.97	4.58E+08	-0.18
1243.39	160023	3.5	240448	3.5	-0.54	1.26E+09	0.467
1243.622	168322	3.5	248732	4.5	-0.12	3.25E+09	-0.518
1243.636	189944	3.5	270353	4.5	-0.46	1.49E+09	0.609
1244.791	168322	3.5	248657	3.5	-0.72	8.25E+08	-0.269
1245.26	164032	2.5	244336	1.5	-0.98	4.54E+08	0.27
1245.583	215970	2.5	296253	3.5	0.31	8.75E+09	-0.769
1245.788	189944	3.5	270214	2.5	-0.78	7.19E+08	-0.482
1245.836	171530	6.5	251798	5.5	-0.54	1.22E+09	-0.393
1246.058	137350	1.5	217603	2.5	-0.09	3.47E+09	-0.729
1246.575	175533	3.5	255753	2.5	0	4.30E+09	-0.656
1247.373	132745	4.5	212914	5.5	0.54	1.48E+10	-0.855
1248.134	181872	2.5	261991	2.5	-0.31	2.10E+09	0.415
1248.179	188494	1.5	268610	1.5	-0.34	1.98E+09	0.69
1248.879	190694	2.5	270766	3.5	-0.25	2.41E+09	0.686
1249.388	188224	4.5	268263	3.5	-0.74	7.75E+08	0.473
1249.713	186288	1.5	266306	1.5	-0.6	1.06E+09	0.477
1249.97	189621	2.5	269623	1.5	-0.53	1.27E+09	-0.401
1250.075	161491	5.5	241486	4.5	-0.6	1.07E+09	-0.271
1250.189	196027	3.5	276015	2.5	-0.81	6.60E+08	0.199
1250.341	160704	1.5	240682	2.5	-0.62	1.02E+09	0.562
1251.287	167527	2.5	247444	1.5	-0.89	5.49E+08	-0.408
1251.378	175533	3.5	255445	3.5	-0.92	5.14E+08	-0.502
1251.413	166467	3.5	246376	4.5	-0.96	4.71E+08	0.106
1251.884	135036	3.5	214916	3.5	-0.65	9.57E+08	0.096
1251.989	160125	1.5	239998	2.5	-0.82	6.45E+08	-0.206
1252.408	165334	4.5	245180	5.5	-0.9	5.36E+08	-0.085
1253.722	178946	2.5	258709	2.5	-0.21	2.58E+09	0.381
1253.761	156155	4.5	235915	5.5	-0.13	3.21E+09	-0.75
1254.082	165334	4.5	245073	3.5	-0.93	5.02E+08	0.341
1254.213	167527	2.5	247258	3.5	0.04	4.62E+09	-0.746
1254.276	172070	5.5	251798	5.5	-0.24	2.42E+09	0.679
1255.978	170865	4.5	250484	3.5	-0.84	6.13E+08	0.36
1256.333	159923	2.5	239519	2.5	-0.47	1.42E+09	-0.538
1256.515	165595	5.5	245180	5.5	-0.05	3.72E+09	0.621
1256.637	156155	4.5	235733	4.5	-0.92	5.12E+08	0.093
1257.529	198329	4.5	277850	4.5	0.3	8.39E+09	0.616
1257.545	190694	2.5	270214	2.5	-0.39	1.71E+09	0.634
1258.101	161491	5.5	240975	6.5	0.02	4.41E+09	-0.244
1258.389	179242	1.5	258709	2.5	-0.37	1.78E+09	-0.533
1258.626	167527	2.5	246978	3.5	-0.84	6.13E+08	0.226
1259.308	167527	2.5	246935	2.5	-0.26	2.29E+09	0.419
1259.532	160125	1.5	239519	2.5	-1	4.19E+08	-0.123
1260.643	167978	1.5	247303	2.5	-0.35	1.90E+09	0.629
1260.786	172070	5.5	251386	4.5	-0.34	1.91E+09	0.733
1262.295	165595	5.5	244816	5.5	0.14	5.72E+09	0.571
1262.561	168322	3.5	247526	4.5	0.1	5.23E+09	-0.715
1262.701	190694	2.5	269890	3.5	-0.77	7.03E+08	-0.545
1263.948	156798	5.5	235915	5.5	-0.05	3.71E+09	0.554
1264.705	164032	2.5	243102	3.5	-0.66	9.18E+08	0.562
1264.869	178946	2.5	258006	3.5	-0.03	3.89E+09	-0.593
1265.466	159923	2.5	238945	3.5	-0.68	8.68E+08	0.518

Table A38: Continued

Wavelength	Lower Level	J_{Low}	Upper level	J_{Up}	log gf	gA	CF
1265.791	216023	1.5	295025	0.5	-0.37	1.80E+09	-0.719
1265.829	188494	1.5	267493	0.5	-0.41	1.61E+09	-0.749
1266.137	156902	3.5	235882	3.5	-0.92	5.03E+08	0.129
1266.512	167978	1.5	246935	2.5	-0.42	1.60E+09	-0.674
1266.52	171530	6.5	250487	6.5	0.52	1.37E+10	0.711
1266.523	175085	4.5	254042	3.5	-0.62	1.00E+09	0.384
1266.849	168322	3.5	247258	3.5	-0.68	8.77E+08	0.121
1266.968	190694	2.5	269623	1.5	-0.77	6.98E+08	0.587
1267.193	215970	2.5	294884	1.5	-0.28	2.17E+09	-0.409
1268.044	216023	1.5	294884	1.5	-0.35	1.84E+09	0.774
1268.464	156155	4.5	234991	4.5	-0.24	2.39E+09	0.311
1268.536	156902	3.5	235733	4.5	-0.8	6.59E+08	-0.144
1268.582	161491	5.5	240319	6.5	-0.56	1.16E+09	-0.178
1268.992	199048	3.5	277850	4.5	-0.56	1.14E+09	-0.334
1269.058	181639	3.5	260437	3.5	0.09	5.07E+09	0.566
1269.509	196027	3.5	274798	3.5	0.08	4.97E+09	-0.647
1269.546	156902	3.5	235670	2.5	-0.78	6.86E+08	-0.244
1270.498	156645	6.5	235354	6.5	-0.15	2.94E+09	0.307
1271.352	168322	3.5	246978	3.5	-0.71	8.10E+08	0.246
1271.592	189621	2.5	268263	3.5	-0.32	1.99E+09	-0.505
1271.632	165334	4.5	243973	4.5	-0.73	7.58E+08	-0.55
1271.905	178946	2.5	257568	1.5	-0.72	7.78E+08	0.291
1272.155	166467	3.5	245073	3.5	-0.4	1.66E+09	-0.311
1272.82	181872	2.5	260437	3.5	-0.62	9.95E+08	-0.393
1272.969	156798	5.5	235354	6.5	0.42	1.09E+10	-0.848
1273.376	159226	4.5	237758	5.5	-0.14	2.96E+09	0.439
1273.642	136401	2.5	214916	3.5	0.15	5.76E+09	-0.821
1274.332	167978	1.5	246451	0.5	-0.65	9.18E+08	-0.618
1274.821	181872	2.5	260314	1.5	-0.14	2.99E+09	-0.744
1274.827	167978	1.5	246420	1.5	-0.47	1.40E+09	0.505
1274.847	164032	2.5	242473	2.5	-0.5	1.32E+09	-0.535
1275.222	156445	2.5	234863	3.5	0.17	6.06E+09	-0.752
1275.243	172070	5.5	250487	6.5	-0.23	2.45E+09	-0.832
1275.247	164685	3.5	243102	3.5	-0.66	8.97E+08	-0.312
1275.867	165595	5.5	243973	4.5	-0.98	4.30E+08	0.439
1276.476	172070	5.5	250411	4.5	0.12	5.33E+09	-0.775
1276.709	179242	1.5	257568	1.5	-0.72	7.60E+08	-0.471
1276.833	189944	3.5	268263	3.5	-0.29	2.10E+09	0.327
1276.86	156155	4.5	234472	5.5	0.12	5.35E+09	0.757
1277.273	132745	4.5	211037	3.5	-0.84	5.84E+08	0.217
1277.335	172070	5.5	250358	5.5	0.37	9.62E+09	0.791
1277.723	161491	5.5	239755	5.5	-0.03	3.83E+09	-0.598
1277.877	181872	2.5	260126	2.5	-0.2	2.61E+09	0.629
1279.257	175242	1.5	253412	0.5	-0.8	6.42E+08	-0.441
1279.813	169166	2.5	247303	2.5	-0.78	6.78E+08	0.41
1280.52	172346	3.5	250440	2.5	-0.36	1.80E+09	-0.526
1280.59	156902	3.5	234991	4.5	-0.54	1.17E+09	-0.407
1280.989	172346	3.5	250411	4.5	-0.78	6.71E+08	0.115
1282.354	163952	0.5	241934	1.5	-0.84	5.85E+08	0.386
1283.051	198033	1.5	275972	1.5	-0.06	3.55E+09	0.708
1283.061	196027	3.5	273966	2.5	-0.48	1.35E+09	0.599
1283.106	160023	3.5	237959	4.5	-0.14	2.92E+09	-0.746
1284.234	170865	4.5	248732	4.5	-0.01	3.99E+09	-0.63
1284.663	160023	3.5	237864	2.5	-0.96	4.41E+08	-0.132
1284.899	156645	6.5	234472	5.5	-0.91	4.97E+08	0.499
1285.621	156155	4.5	233938	3.5	-0.88	5.38E+08	0.176
1285.863	169166	2.5	246935	2.5	-0.95	4.53E+08	0.34
1286.349	160125	1.5	237864	2.5	-0.51	1.24E+09	0.621
1286.912	189621	2.5	267327	2.5	-0.94	4.63E+08	0.107
1287.634	197022	2.5	274684	2.5	0.14	5.57E+09	0.732
1288.713	163952	0.5	241549	0.5	-1	4.06E+08	0.34
1289.186	190694	2.5	268263	3.5	-0.61	9.83E+08	-0.568
1289.755	156155	4.5	233689	4.5	-0.73	7.45E+08	0.086
1290.09	190694	2.5	268208	2.5	-0.57	1.07E+09	-0.402
1291.512	159923	2.5	237351	3.5	-0.57	1.07E+09	0.35
1291.854	164078	4.5	241486	4.5	-0.38	1.65E+09	0.257
1292.28	189944	3.5	267327	2.5	-0.28	2.11E+09	0.526
1292.29	196027	3.5	273409	3.5	-0.47	1.37E+09	0.282
1293.233	135036	3.5	212362	4.5	0.35	8.80E+09	-0.857
1293.308	156645	6.5	233966	6.5	0.03	4.28E+09	0.766
1294.177	215970	2.5	293239	2.5	-0.98	4.20E+08	0.114
1294.544	189944	3.5	267191	4.5	-0.03	3.70E+09	-0.425
1295.065	216023	1.5	293239	2.5	0.13	5.38E+09	-0.763
1295.525	164032	2.5	241221	3.5	-0.98	4.18E+08	0.176
1295.681	156445	2.5	233625	2.5	-0.28	2.06E+09	-0.555
1296	179242	1.5	256402	0.5	-0.54	1.14E+09	-0.601
1296.425	179242	1.5	256377	1.5	-0.6	9.91E+08	-0.41
1297.522	181639	3.5	258709	2.5	-0.73	7.41E+08	-0.484
1298.398	188224	4.5	265242	5.5	0.51	1.27E+10	-0.836
1299.253	199048	3.5	276015	2.5	-0.06	3.42E+09	-0.636
1299.349	160704	1.5	237665	1.5	-0.87	5.30E+08	0.338
1300.27	166467	3.5	243374	2.5	-0.27	2.14E+09	-0.51
1300.537	156798	5.5	233689	4.5	-0.52	1.20E+09	-0.247
1300.803	198329	4.5	275205	5.5	0.5	1.26E+10	-0.834
1301.343	169166	2.5	246010	1.5	-0.59	1.01E+09	-0.513
1301.892	156155	4.5	232966	5.5	-0.65	8.91E+08	-0.105
1301.919	167527	2.5	244336	1.5	-0.67	8.38E+08	-0.395
1302.077	164685	3.5	241486	4.5	0.11	5.02E+09	-0.734
1303.574	175085	4.5	251798	5.5	0.33	8.32E+09	-0.782
1304.441	170865	4.5	247526	4.5	-0.12	3.00E+09	0.652
1304.592	156645	6.5	233297	7.5	0.66	1.78E+10	-0.899
1305.066	175622	2.5	252246	2.5	-0.61	9.60E+08	0.232
1305.546	164078	4.5	240674	5.5	0.32	8.23E+09	-0.852
1305.861	164078	4.5	240655	4.5	-0.17	2.64E+09	-0.449
1306.588	164685	3.5	241221	3.5	-0.31	1.91E+09	0.361
1306.95	160704	1.5	237218	0.5	-0.64	8.90E+08	-0.515
1307.215	178946	2.5	255445	3.5	-0.32	1.87E+09	0.647
1308.623	164032	2.5	240448	3.5	-0.43	1.45E+09	0.622
1309.132	197022	2.5	273409	3.5	-0.64	8.86E+08	-0.697
1309.144	172346	3.5	248732	4.5	-0.86	5.39E+08	-0.254
1309.41	164078	4.5	240448	3.5	-0.6	9.80E+08	0.274
1309.706	167021	1.5	243374	2.5	-0.41	1.50E+09	-0.586
1310.439	172346	3.5	248657	3.5	-0.9	4.92E+08	0.309
1310.607	175085	4.5	251386	4.5	0.27	7.25E+09	0.669
1311.183	161491	5.5	237758	5.5	0.13	5.27E+09	0.671
1311.918	156155	4.5	232379	3.5	-0.36	1.69E+09	-0.479

Table A38: Continued

Wavelength	Lower Level	J_{Low}	Upper level	J_{Up}	log gf	gA	CF
1312.234	171713	0.5	247919	0.5	-0.76	6.80E+08	-0.609
1312.803	159923	2.5	236095	1.5	-0.73	7.20E+08	-0.36
1312.879	156798	5.5	232966	5.5	-0.31	1.90E+09	0.276
1313.163	165334	4.5	241486	4.5	-0.76	6.67E+08	0.313
1313.827	170865	4.5	246978	3.5	-0.92	4.59E+08	-0.177
1315.783	135036	3.5	211037	3.5	-0.11	3.01E+09	-0.669
1316.295	160125	1.5	236095	1.5	-0.45	1.37E+09	0.475
1316.493	159923	2.5	235882	3.5	-0.77	6.59E+08	0.187
1316.93	156445	2.5	232379	3.5	-0.54	1.10E+09	-0.606
1316.952	198033	1.5	273966	2.5	-0.15	2.72E+09	-0.653
1317.403	169166	2.5	245073	3.5	-0.59	9.78E+08	0.448
1317.752	165334	4.5	241221	3.5	-0.9	4.89E+08	-0.153
1318.338	175533	3.5	251386	4.5	-0.65	8.55E+08	-0.598
1318.385	156798	5.5	232648	4.5	-0.37	1.64E+09	-0.571
1319.86	196027	3.5	271793	4.5	-0.5	1.22E+09	-0.179
1319.881	159226	4.5	234991	4.5	-0.89	4.91E+08	-0.083
1319.994	146216	3.5	221974	2.5	-0.04	3.55E+09	-0.558
1320.132	199048	3.5	274798	3.5	-0.47	1.31E+09	0.174
1320.831	160023	3.5	235733	4.5	-0.22	2.29E+09	0.568
1321.404	164078	4.5	239755	5.5	-0.85	5.40E+08	0.257
1323.63	167021	1.5	242570	1.5	-0.67	8.03E+08	0.374
1326.026	189621	2.5	265034	1.5	-0.45	1.36E+09	-0.611
1326.6	165595	5.5	240975	6.5	0.2	6.03E+09	-0.504
1327.639	165334	4.5	240655	4.5	-0.07	3.18E+09	0.625
1327.662	181639	3.5	256959	4.5	0.34	8.34E+09	-0.789
1328.168	165334	4.5	240625	3.5	-0.6	9.54E+08	0.402
1328.499	175085	4.5	250358	5.5	-0.05	3.40E+09	0.756
1328.974	159226	4.5	234472	5.5	-0.2	2.37E+09	-0.34
1329.824	175242	1.5	250440	2.5	-0.72	7.16E+08	0.463
1330.277	148667	2.5	223840	1.5	-0.35	1.67E+09	-0.543
1330.297	164685	3.5	239857	4.5	-0.59	9.76E+08	-0.154
1330.321	169166	2.5	244336	1.5	-0.79	6.15E+08	-0.277
1331.927	165595	5.5	240674	5.5	-0.46	1.28E+09	0.297
1332.255	165595	5.5	240655	4.5	-0.74	6.86E+08	0.342
1332.413	168322	3.5	243374	2.5	-0.88	4.99E+08	0.328
1332.553	167527	2.5	242570	1.5	-0.76	6.51E+08	-0.333
1333.234	136401	2.5	211407	2.5	-0.21	2.28E+09	-0.565
1333.298	159923	2.5	234925	2.5	-0.76	6.57E+08	0.278
1333.904	160023	3.5	234991	4.5	-0.57	1.01E+09	0.351
1334.107	172346	3.5	247303	2.5	-0.91	4.60E+08	-0.351
1334.264	190694	2.5	265642	1.5	-0.4	1.48E+09	-0.75
1334.396	159923	2.5	234863	3.5	-0.7	7.49E+08	0.537
1334.615	150006	1.5	224934	0.5	-0.63	8.75E+08	-0.643
1334.875	167021	1.5	241934	1.5	-0.98	3.90E+08	0.186
1334.88	164032	2.5	238945	3.5	-0.32	1.78E+09	-0.481
1334.909	172346	3.5	247258	3.5	-0.75	6.64E+08	0.341
1335.08	160023	3.5	234925	2.5	-0.49	1.21E+09	-0.337
1335.502	175533	3.5	250411	4.5	-0.06	3.29E+09	-0.706
1335.789	175622	2.5	250484	3.5	0.05	4.17E+09	-0.738
1336.18	160023	3.5	234863	3.5	-0.73	6.90E+08	-0.373
1336.293	164685	3.5	239519	2.5	-0.5	1.18E+09	-0.393
1336.58	175622	2.5	250440	2.5	-0.91	4.68E+08	-0.377
1337.261	168322	3.5	243102	3.5	-0.82	5.62E+08	-0.309
1337.721	166467	3.5	241221	3.5	-0.82	5.69E+08	0.123
1337.984	196027	3.5	270766	3.5	-0.68	7.72E+08	-0.182
1338.258	165595	5.5	240319	6.5	-0.35	1.67E+09	-0.322
1338.566	171713	0.5	246420	1.5	-0.77	6.41E+08	0.414
1338.815	156155	4.5	230848	3.5	-0.81	5.73E+08	-0.145
1339.84	136401	2.5	211037	3.5	-0.25	2.06E+09	-0.447
1339.91	172346	3.5	246978	3.5	-0.33	1.75E+09	0.5
1340.623	167978	1.5	242570	1.5	-0.83	5.52E+08	0.233
1342.949	159226	4.5	233689	4.5	-0.03	3.48E+09	0.6
1343.707	165334	4.5	239755	5.5	-0.07	3.15E+09	-0.492
1344.63	197022	2.5	271392	1.5	-0.51	1.14E+09	0.637
1344.854	137350	1.5	211707	1.5	-0.28	1.92E+09	-0.729
1345.026	171530	6.5	245878	7.5	0.65	1.65E+10	-0.908
1345.171	190694	2.5	265034	1.5	-0.53	1.09E+09	-0.408
1345.283	188224	4.5	262557	4.5	-0.24	2.15E+09	-0.731
1345.62	170865	4.5	245180	5.5	0.19	5.66E+09	-0.71
1346.587	165595	5.5	239857	4.5	-0.46	1.27E+09	0.507
1346.629	164685	3.5	238945	3.5	-0.94	4.21E+08	-0.1
1346.946	161491	5.5	235733	4.5	-0.76	6.42E+08	0.178
1347.553	170865	4.5	245073	3.5	-0.72	7.01E+08	0.256
1347.911	166467	3.5	240655	4.5	-0.69	7.50E+08	0.166
1347.936	196027	3.5	270214	2.5	-0.29	1.91E+09	-0.612
1348.356	163952	0.5	238117	1.5	-0.23	2.17E+09	-0.796
1348.456	166467	3.5	240625	3.5	-0.75	6.58E+08	-0.248
1348.996	167021	1.5	241150	2.5	-0.47	1.25E+09	-0.605
1349.275	181639	3.5	255753	2.5	-1	3.61E+08	0.547
1350.176	150869	0.5	224934	0.5	-0.61	9.03E+08	0.719
1350.313	137350	1.5	211407	2.5	-0.22	2.21E+09	-0.576
1350.806	172346	3.5	246376	4.5	0.16	5.25E+09	-0.766
1351.061	159923	2.5	233938	3.5	-0.54	1.07E+09	-0.597
1351.602	167021	1.5	241007	1.5	-0.76	6.30E+08	-0.419
1351.742	156155	4.5	230134	4.5	-0.62	8.85E+08	0.192
1351.936	175242	1.5	249210	2.5	-0.91	4.51E+08	0.113
1352.3	175533	3.5	249481	3.5	0.07	4.25E+09	0.76
1352.331	156902	3.5	230848	3.5	-0.55	1.04E+09	0.195
1352.538	169166	2.5	243102	3.5	-0.8	5.70E+08	-0.206
1352.891	160023	3.5	233938	3.5	-0.49	1.18E+09	0.333
1353.53	164078	4.5	237959	4.5	-0.51	1.14E+09	-0.345
1354.39	150006	1.5	223840	1.5	-0.67	7.73E+08	0.411
1354.619	137914	0.5	211735	0.5	-0.4	1.44E+09	-0.833
1355.135	137914	0.5	211707	1.5	-0.46	1.24E+09	-0.656
1356.046	179242	1.5	252986	1.5	-0.46	1.24E+09	0.654
1356.112	159226	4.5	232966	5.5	0.07	4.29E+09	-0.709
1357.469	160023	3.5	233689	4.5	-0.56	9.84E+08	-0.402
1357.779	171530	6.5	245180	5.5	-0.82	5.41E+08	0.598
1358.078	164032	2.5	237665	1.5	-0.55	1.02E+09	0.598
1358.491	165334	4.5	238945	3.5	-0.81	5.61E+08	0.631
1358.919	175622	2.5	249210	2.5	-0.02	3.50E+09	0.693
1359.228	175085	4.5	248657	3.5	-0.08	3.02E+09	-0.731
1359.971	166467	3.5	239998	2.5	-0.44	1.33E+09	-0.586
1360.544	161491	5.5	234991	4.5	-0.27	1.93E+09	-0.462
1360.544	160125	1.5	233625	2.5	-0.88	4.72E+08	0.181
1360.589	188494	1.5	261991	2.5	-0.27	1.96E+09	0.788

Table A38: Continued

Wavelength	Lower Level	J_{Low}	Upper level	J_{Up}	log gf	gA	CF
1361.988	159226	4.5	232648	4.5	-0.85	5.09E+08	0.159
1362.583	166467	3.5	239857	4.5	-0.01	3.54E+09	-0.671
1363.031	189621	2.5	262987	3.5	0.07	4.22E+09	-0.556
1363.791	175242	1.5	248567	2.5	-0.78	6.05E+08	0.286
1363.896	164032	2.5	237351	3.5	-0.81	5.53E+08	0.387
1364.13	148667	2.5	221974	2.5	-0.62	8.68E+08	0.369
1364.53	171530	6.5	244816	5.5	0.1	4.49E+09	-0.795
1364.75	164078	4.5	237351	3.5	-0.23	2.10E+09	-0.455
1365.068	156902	3.5	230158	2.5	-0.32	1.71E+09	-0.569
1365.102	175242	1.5	248496	1.5	-0.33	1.68E+09	0.624
1365.521	156902	3.5	230134	4.5	-0.12	2.75E+09	-0.416
1366.133	175533	3.5	248732	4.5	-0.83	5.37E+08	-0.388
1366.518	164685	3.5	237864	2.5	-0.76	6.20E+08	-0.17
1366.794	168322	3.5	241486	4.5	-0.72	6.81E+08	-0.369
1366.994	159226	4.5	232379	3.5	-0.42	1.35E+09	-0.459
1367.544	175533	3.5	248657	3.5	-0.94	4.16E+08	-0.181
1367.809	172070	5.5	245180	5.5	-0.99	3.64E+08	0.108
1368.875	166467	3.5	239519	2.5	-0.91	4.42E+08	-0.246
1369.055	189944	3.5	262987	3.5	-0.35	1.59E+09	-0.643
1369.227	175533	3.5	248567	2.5	-0.97	3.86E+08	-0.319
1369.782	179242	1.5	252246	2.5	-0.23	2.06E+09	0.663
1370.208	161491	5.5	234472	5.5	-0.96	3.86E+08	-0.194
1370.297	167021	1.5	239998	2.5	-0.95	4.02E+08	0.197
1370.419	150869	0.5	223840	1.5	-0.99	3.66E+08	-0.654
1371.34	167527	2.5	240448	3.5	-0.7	7.14E+08	0.31
1371.347	160704	1.5	233625	2.5	-0.44	1.29E+09	-0.515
1371.767	168322	3.5	241221	3.5	-0.83	5.34E+08	-0.35
1372.222	175622	2.5	248496	1.5	-0.87	4.77E+08	0.502
1372.358	197022	2.5	269890	3.5	0.14	4.92E+09	-0.77
1373.098	168322	3.5	241150	2.5	-0.34	1.61E+09	-0.516
1373.166	148667	2.5	221492	2.5	-0.34	1.62E+09	-0.791
1374.661	172070	5.5	244816	5.5	-0.62	8.53E+08	-0.327
1374.665	199048	3.5	271793	4.5	-0.04	3.20E+09	-0.698
1374.689	146216	3.5	218960	2.5	-0.28	1.88E+09	0.762
1375.005	172346	3.5	245073	3.5	-0.44	1.29E+09	0.269
1375.853	150006	1.5	222688	1.5	-0.48	1.16E+09	-0.765
1376.332	156155	4.5	228812	3.5	-0.9	4.50E+08	-0.201
1376.94	165334	4.5	237959	4.5	-0.4	1.40E+09	-0.396
1377.156	189944	3.5	262557	4.5	0.09	4.30E+09	-0.54
1377.399	197022	2.5	269623	1.5	-0.63	8.21E+08	-0.775
1378.995	160125	1.5	232641	1.5	-0.79	5.71E+08	0.26
1379.337	167021	1.5	239519	2.5	-0.82	5.24E+08	0.351
1379.723	166467	3.5	238945	3.5	-0.51	1.09E+09	0.26
1379.775	161491	5.5	233966	6.5	0.35	7.76E+09	0.873
1379.862	167527	2.5	239998	2.5	-0.88	4.67E+08	0.319
1380.51	198329	4.5	270766	3.5	-0.1	2.75E+09	-0.734
1380.762	165334	4.5	237758	5.5	-0.02	3.33E+09	-0.649
1381.158	181639	3.5	254042	3.5	-0.74	6.40E+08	-0.564
1381.786	189621	2.5	261991	2.5	-0.66	7.58E+08	0.348
1381.979	168322	3.5	240682	2.5	-0.56	9.54E+08	-0.458
1383.733	167021	1.5	239289	0.5	-0.55	9.96E+08	-0.498
1384.336	170865	4.5	243102	3.5	-0.56	9.47E+08	-0.424
1384.378	160125	1.5	232359	0.5	-0.45	1.24E+09	0.755
1385.397	196027	3.5	268208	2.5	-0.72	6.60E+08	-0.552
1385.612	199048	3.5	271218	2.5	-0.74	6.35E+08	-0.62
1385.615	181872	2.5	254042	3.5	-0.09	2.80E+09	-0.66
1387.846	169166	2.5	241221	3.5	-0.88	4.55E+08	-0.252
1388.424	198329	4.5	270353	4.5	-0.68	7.23E+08	-0.655
1388.517	167978	1.5	239998	2.5	-0.83	5.17E+08	0.436
1389.497	150006	1.5	221974	2.5	-0.76	6.03E+08	-0.725
1390.094	160704	1.5	232641	1.5	-0.42	1.31E+09	-0.626
1390.619	156902	3.5	228812	3.5	-0.49	1.13E+09	0.477
1390.772	172070	5.5	243973	4.5	-0.4	1.37E+09	0.626
1390.96	175085	4.5	246978	3.5	-0.82	5.23E+08	0.389
1391.767	156445	2.5	228296	2.5	-0.17	2.33E+09	-0.689
1391.972	169166	2.5	241007	1.5	-0.9	4.29E+08	0.428
1392.033	164078	4.5	235915	5.5	-0.94	3.98E+08	-0.1
1392.323	175622	2.5	247444	1.5	-0.39	1.40E+09	-0.595
1392.397	150869	0.5	222688	1.5	-0.18	2.25E+09	-0.74
1392.674	164078	4.5	235882	3.5	-0.57	9.16E+08	0.527
1393.621	215970	2.5	287725	2.5	0.13	4.62E+09	0.805
1394.214	175533	3.5	247258	3.5	-1	3.42E+08	-0.343
1394.336	199048	3.5	270766	3.5	-0.67	7.39E+08	-0.276
1394.971	156155	4.5	227841	5.5	-0.34	1.56E+09	0.468
1395.578	164078	4.5	235733	4.5	-0.49	1.11E+09	0.207
1395.905	164032	2.5	235670	2.5	-0.22	2.09E+09	0.503
1396.009	188494	1.5	260126	2.5	-0.27	1.85E+09	-0.568
1396.223	159226	4.5	230848	3.5	-0.17	2.33E+09	0.647
1396.8	148667	2.5	220260	1.5	-0.72	6.43E+08	0.77
1397.419	198329	4.5	269890	3.5	-0.57	9.09E+08	-0.549
1397.8	167978	1.5	239519	2.5	-0.8	5.46E+08	-0.293
1398.3	169166	2.5	240682	2.5	-0.35	1.53E+09	0.471
1398.335	148667	2.5	220181	3.5	0.2	5.41E+09	-0.825
1398.731	178946	2.5	250440	2.5	-0.58	8.89E+08	0.428
1398.758	166467	3.5	237959	4.5	-0.42	1.30E+09	0.391
1398.873	150006	1.5	221492	2.5	-0.03	3.21E+09	-0.704
1399.075	161491	5.5	232966	5.5	-0.5	1.07E+09	0.171
1399.404	169166	2.5	240625	3.5	0.05	3.82E+09	-0.657
1399.67	175533	3.5	246978	3.5	-0.73	6.34E+08	0.192
1400.401	156798	5.5	228206	4.5	0.12	4.44E+09	-0.819
1400.415	178946	2.5	250354	1.5	-0.26	1.84E+09	0.686
1402.41	199048	3.5	270353	4.5	0.09	4.16E+09	-0.708
1402.438	156902	3.5	228206	4.5	-0.82	5.18E+08	0.42
1402.532	196027	3.5	267327	2.5	-0.96	3.71E+08	-0.35
1402.652	146216	3.5	217510	4.5	0.26	6.12E+09	-0.828
1403.7	197022	2.5	268263	3.5	-0.63	7.93E+08	0.48
1404.542	179242	1.5	250440	2.5	-0.92	4.05E+08	0.193
1404.561	164685	3.5	235882	3.5	-0.13	2.49E+09	0.516
1404.571	156645	6.5	227841	5.5	0.28	6.40E+09	-0.835
1405.199	196027	3.5	267191	4.5	0.05	3.79E+09	0.707
1405.329	161491	5.5	232648	4.5	-0.24	1.96E+09	0.705
1406.189	181872	2.5	252986	1.5	-0.94	3.87E+08	0.463
1406.545	167021	1.5	238117	1.5	-0.84	4.86E+08	0.17
1407.592	156798	5.5	227841	5.5	-0.39	1.38E+09	0.622
1407.897	159923	2.5	230950	1.5	-0.52	1.02E+09	0.685
1407.973	156645	6.5	227669	6.5	0.2	5.26E+09	-0.855

Table A38: Continued

Wavelength	Lower Level	J_{Low}	Upper level	J_{Up}	log gf	gA	CF
1408.26	132745	4.5	203755	4.5	0.4	8.48E+09	0.88
1408.625	146216	3.5	217208	3.5	0.11	4.36E+09	0.727
1408.758	164685	3.5	235670	2.5	-0.71	6.61E+08	0.277
1408.994	132745	4.5	203718	3.5	0.07	3.95E+09	0.832
1410.181	164078	4.5	234991	4.5	-0.65	7.54E+08	-0.197
1410.288	159226	4.5	230134	4.5	-0.52	1.02E+09	-0.343
1410.58	164032	2.5	234925	2.5	-0.73	6.21E+08	0.503
1411.008	156798	5.5	227669	6.5	0.05	3.79E+09	-0.5
1411.293	171713	0.5	242570	1.5	-0.9	4.25E+08	-0.368
1411.759	148667	2.5	219501	1.5	-0.58	8.73E+08	0.707
1411.809	169166	2.5	239998	2.5	-0.98	3.54E+08	-0.172
1411.915	160125	1.5	230950	1.5	-0.86	4.59E+08	0.231
1411.925	160023	3.5	230848	3.5	-0.59	8.58E+08	0.177
1413.1	156155	4.5	226921	5.5	-0.3	1.69E+09	-0.283
1413.32	185622	0.5	256377	1.5	-0.67	7.19E+08	-0.637
1413.867	186288	1.5	257016	2.5	-0.4	1.34E+09	-0.612
1415.536	167021	1.5	237665	1.5	-0.84	4.84E+08	0.477
1415.969	168322	3.5	238945	3.5	-0.73	6.29E+08	-0.483
1416.278	181639	3.5	252246	2.5	-0.54	9.49E+08	-0.59
1417.742	178946	2.5	249481	3.5	-0.56	8.99E+08	0.541
1420.479	165334	4.5	235733	4.5	-0.9	4.16E+08	-0.247
1420.691	175622	2.5	246010	1.5	-0.72	6.29E+08	-0.535
1421.347	170865	4.5	241221	3.5	-0.4	1.30E+09	0.675
1422.064	165595	5.5	235915	5.5	-0.56	9.04E+08	-0.361
1422.625	148667	2.5	218960	2.5	-0.6	8.36E+08	0.294
1422.953	156645	6.5	226921	5.5	-0.22	1.97E+09	-0.825
1423.082	163952	0.5	234222	0.5	-0.56	8.96E+08	0.745
1423.552	160704	1.5	230950	1.5	-0.58	8.68E+08	0.487
1423.783	159923	2.5	230158	2.5	-0.86	4.51E+08	0.108
1424.562	167021	1.5	237218	0.5	-1	3.23E+08	-0.581
1424.794	135036	3.5	205222	2.5	0.04	3.61E+09	0.829
1424.993	198033	1.5	268208	2.5	-0.26	1.83E+09	-0.547
1425.765	165595	5.5	235733	4.5	-0.33	1.52E+09	0.591
1425.816	160023	3.5	230158	2.5	-0.7	6.59E+08	0.23
1426.001	172346	3.5	242473	2.5	-0.5	1.05E+09	-0.644
1426.053	156798	5.5	226921	5.5	0.1	4.11E+09	-0.607
1426.31	160023	3.5	230134	4.5	-0.25	1.83E+09	-0.348
1426.751	186288	1.5	256377	1.5	-0.61	8.03E+08	-0.607
1427.299	215970	2.5	286032	1.5	-0.41	1.28E+09	0.769
1427.892	160125	1.5	230158	2.5	-0.7	6.56E+08	-0.323
1427.911	150006	1.5	220038	0.5	-0.63	7.62E+08	0.801
1428.38	216023	1.5	286032	1.5	-0.24	1.88E+09	0.49
1428.818	175085	4.5	245073	3.5	-0.61	8.08E+08	0.549
1428.847	185622	0.5	255608	0.5	-0.58	8.54E+08	-0.644
1429.231	179242	1.5	249210	2.5	-0.95	3.65E+08	-0.208
1429.93	198329	4.5	268263	3.5	-0.99	3.35E+08	-0.365
1430.478	164032	2.5	233938	3.5	-0.64	7.47E+08	0.322
1430.777	156155	4.5	226047	4.5	0.16	4.74E+09	-0.761
1431.418	164078	4.5	233938	3.5	-0.81	5.09E+08	-0.366
1431.93	171713	0.5	241549	0.5	-0.9	4.11E+08	0.351
1432.418	136401	2.5	206213	1.5	-0.08	2.74E+09	0.848
1433.028	188224	4.5	258006	3.5	-0.27	1.77E+09	-0.667
1433.494	165595	5.5	235354	6.5	-0.23	1.92E+09	0.408
1434.101	175085	4.5	244816	5.5	-0.8	5.25E+08	0.551
1435.07	156445	2.5	226128	1.5	-0.08	2.73E+09	0.802
1436.359	178946	2.5	248567	2.5	-0.5	1.02E+09	-0.417
1436.544	164078	4.5	233689	4.5	-0.55	9.12E+08	0.187
1436.569	137350	1.5	206960	0.5	-0.35	1.47E+09	0.864
1437.075	159226	4.5	228812	3.5	-0.98	3.40E+08	-0.164
1438.946	150006	1.5	219501	1.5	-0.48	1.06E+09	0.711
1440.71	156155	4.5	225565	3.5	-0.2	2.03E+09	0.771
1441.009	165595	5.5	234991	4.5	-0.38	1.32E+09	-0.778
1442.577	186288	1.5	255608	0.5	-1	3.15E+08	-0.741
1443.137	171713	0.5	241007	1.5	-0.63	7.58E+08	-0.474
1443.71	166467	3.5	235733	4.5	-0.37	1.38E+09	0.398
1445.739	150869	0.5	220038	0.5	-0.72	6.15E+08	0.702
1446.224	156902	3.5	226047	4.5	-0.05	2.81E+09	-0.38
1446.263	171530	6.5	240674	5.5	-0.24	1.83E+09	0.804
1446.374	165334	4.5	234472	5.5	-0.06	2.77E+09	-0.331
1448.543	159923	2.5	228957	2.5	-0.25	1.81E+09	-0.679
1449.196	164685	3.5	233689	4.5	-0.94	3.69E+08	0.111
1449.7	159226	4.5	228206	4.5	-0.42	1.22E+09	-0.328
1450.633	148667	2.5	217603	2.5	-0.38	1.33E+09	-0.757
1450.646	160023	3.5	228957	2.5	-0.57	8.60E+08	-0.683
1451.271	172070	5.5	240975	6.5	-0.19	2.04E+09	0.64
1451.589	170865	4.5	239755	5.5	-0.51	9.70E+08	0.469
1451.602	159923	2.5	228812	3.5	-0.2	2.00E+09	-0.388
1451.617	164078	4.5	232966	5.5	-0.38	1.31E+09	0.266
1451.644	175085	4.5	243973	4.5	-0.31	1.55E+09	-0.529
1451.855	165595	5.5	234472	5.5	-0.99	3.20E+08	-0.379
1452.18	198329	4.5	267191	4.5	-0.43	1.18E+09	-0.506
1452.534	181639	3.5	250484	3.5	-0.89	4.05E+08	-0.536
1452.796	160125	1.5	228957	2.5	-0.93	3.71E+08	-0.1
1453.045	136401	2.5	205222	2.5	-0.56	8.66E+08	0.303
1453.714	160023	3.5	228812	3.5	-0.36	1.38E+09	-0.496
1453.731	171530	6.5	240319	6.5	-0.36	1.37E+09	-0.829
1455.61	146216	3.5	214916	3.5	-0.56	8.68E+08	-0.631
1456.003	135036	3.5	203718	3.5	-0.12	2.37E+09	0.385
1456.085	179242	1.5	247919	0.5	-0.99	3.18E+08	-0.37
1456.374	156902	3.5	225565	3.5	-0.11	2.46E+09	0.486
1456.811	161491	5.5	230134	4.5	-0.36	1.38E+09	0.75
1457.053	150869	0.5	219501	1.5	-0.91	3.87E+08	-0.406
1457.307	197022	2.5	265642	1.5	-0.77	5.27E+08	-0.437
1457.524	164032	2.5	232641	1.5	-0.88	4.16E+08	0.682
1457.626	165334	4.5	233938	3.5	-0.64	7.27E+08	0.458
1458.387	167527	2.5	236095	1.5	-0.86	4.34E+08	-0.445
1459.88	169166	2.5	237665	1.5	-0.86	4.32E+08	-0.233
1461.134	175533	3.5	243973	4.5	0.08	3.73E+09	-0.609
1462.6	165595	5.5	233966	6.5	-0.29	1.58E+09	-0.18
1463.109	164032	2.5	232379	3.5	-0.56	8.51E+08	-0.604
1463.368	172346	3.5	240682	2.5	-0.76	5.43E+08	0.478
1463.934	172346	3.5	240655	4.5	-0.53	9.23E+08	0.526
1464.146	137914	0.5	206213	1.5	-0.77	5.34E+08	-0.229
1465.12	160704	1.5	228957	2.5	-0.43	1.14E+09	-0.334
1465.236	172070	5.5	240319	6.5	0.39	7.55E+09	-0.765
1465.749	171530	6.5	239755	5.5	-0.83	4.61E+08	0.614

Table A38: Continued

Wavelength	Lower Level	J_{Low}	Upper level	J_{Up}	log gf	gA	CF
1466.887	160125	1.5	228296	2.5	-0.4	1.22E+09	-0.33
1468.058	167978	1.5	236095	1.5	-0.93	3.69E+08	-0.298
1470.24	175085	4.5	243102	3.5	-0.85	4.37E+08	0.283
1471.391	164685	3.5	232648	4.5	-0.26	1.72E+09	-0.654
1473.355	137350	1.5	205222	2.5	-0.74	5.67E+08	-0.149
1477.207	159226	4.5	226921	5.5	-0.37	1.31E+09	-0.319
1481.258	172346	3.5	239857	4.5	-0.99	3.11E+08	-0.401
1481.927	175622	2.5	243102	3.5	-0.36	1.35E+09	-0.534
1483.724	167527	2.5	234925	2.5	-0.48	1.01E+09	-0.487
1484.305	165595	5.5	232966	5.5	-0.67	6.48E+08	0.246
1485.518	136401	2.5	203718	3.5	-0.92	3.64E+08	-0.088
1485.632	190694	2.5	258006	3.5	-0.65	6.74E+08	-0.682
1487.414	175242	1.5	242473	2.5	-0.44	1.10E+09	-0.652
1487.626	188224	4.5	255445	3.5	-0.03	2.83E+09	-0.801
1489.024	166467	3.5	233625	2.5	-0.82	4.61E+08	-0.461
1490.935	189944	3.5	257016	2.5	-0.17	2.03E+09	-0.794
1491.346	165595	5.5	232648	4.5	-0.56	8.31E+08	-0.239
1491.522	165334	4.5	232379	3.5	-0.93	3.54E+08	-0.318
1494.143	181639	3.5	248567	2.5	-0.32	1.43E+09	-0.711
1496.643	164032	2.5	230848	3.5	-0.97	3.23E+08	0.287
1497.342	181872	2.5	248657	3.5	-0.51	9.23E+08	-0.513
1497.99	189621	2.5	256377	1.5	-0.65	6.67E+08	-0.656
1498.902	169166	2.5	235882	3.5	-0.79	4.78E+08	0.304
1499.423	175242	1.5	241934	1.5	-0.76	5.12E+08	0.3
1501.411	167021	1.5	233625	2.5	-0.73	5.49E+08	0.193
1501.441	168322	3.5	234925	2.5	-0.92	3.54E+08	-0.36
1503.072	196027	3.5	262557	4.5	-0.29	1.50E+09	-0.311
1507.145	161491	5.5	227841	5.5	-0.52	8.89E+08	0.31
1507.807	190694	2.5	257016	2.5	-0.6	7.30E+08	-0.6
1508.018	175622	2.5	241934	1.5	-0.89	3.77E+08	-0.228
1509.951	171530	6.5	237758	5.5	-0.91	3.58E+08	-0.604
1511.062	161491	5.5	227669	6.5	-0.5	9.21E+08	0.162
1511.814	146216	3.5	212362	4.5	-0.3	1.45E+09	-0.489
1515.965	197022	2.5	262987	3.5	-0.81	4.55E+08	-0.652
1517.156	166467	3.5	232379	3.5	-0.61	7.09E+08	-0.342
1517.722	172070	5.5	237959	4.5	-0.62	6.96E+08	-0.648
1522.355	175533	3.5	241221	3.5	-0.81	4.50E+08	-0.382
1524.005	168322	3.5	233938	3.5	-0.43	1.07E+09	-0.471
1524.107	172346	3.5	237959	4.5	-0.72	5.57E+08	-0.155
1526.387	165334	4.5	230848	3.5	-0.77	4.89E+08	-0.322
1529.375	181872	2.5	247258	3.5	-0.96	3.13E+08	-0.379
1529.817	168322	3.5	233689	4.5	-0.51	8.89E+08	-0.566
1535.752	167527	2.5	232641	1.5	-0.94	3.24E+08	0.491
1537.272	170865	4.5	235915	5.5	-0.15	2.00E+09	-0.556
1538.055	170865	4.5	235882	3.5	-0.58	7.37E+08	-0.616
1542.722	146216	3.5	211037	3.5	-0.64	6.44E+08	0.294
1543.212	165334	4.5	230134	4.5	-0.84	4.01E+08	0.347
1544.263	175242	1.5	239998	2.5	-0.79	4.56E+08	0.363
1544.394	190694	2.5	255445	3.5	-0.63	6.49E+08	-0.316
1544.776	164078	4.5	228812	3.5	-0.91	3.42E+08	0.364
1553.162	171530	6.5	235915	5.5	-0.41	1.08E+09	-0.731
1553.244	166467	3.5	230848	3.5	-1	2.80E+08	0.191
1558.718	178946	2.5	243102	3.5	-0.7	5.38E+08	-0.505
1565.94	175085	4.5	238945	3.5	-0.87	3.75E+08	0.508
1579.193	172346	3.5	235670	2.5	-0.69	5.52E+08	-0.714
1582.236	181872	2.5	245073	3.5	-0.92	3.16E+08	-0.325
1597.158	165595	5.5	228206	4.5	-0.54	7.60E+08	0.258
1603.35	148667	2.5	211037	3.5	-0.51	7.91E+08	-0.611
1603.968	166467	3.5	228812	3.5	-0.84	3.74E+08	0.296
1608.242	167978	1.5	230158	2.5	-0.8	4.08E+08	-0.582
1610.096	198329	4.5	260437	3.5	-0.54	7.46E+08	-0.713
1610.264	170865	4.5	232966	5.5	-0.68	5.38E+08	0.523
1610.97	165595	5.5	227669	6.5	-0.24	1.47E+09	-0.286
1618.555	170865	4.5	232648	4.5	-0.54	7.30E+08	0.353
1623.701	165334	4.5	226921	5.5	-0.84	3.68E+08	-0.324
1628.641	150006	1.5	211407	2.5	-0.66	5.50E+08	-0.621
1631.971	167021	1.5	228296	2.5	-0.76	4.34E+08	-0.149
1660.261	165334	4.5	225565	3.5	-0.61	5.98E+08	-0.302
1666.886	216023	1.5	276015	2.5	-0.84	3.49E+08	-0.508
1692.085	166467	3.5	225565	3.5	-0.98	2.47E+08	-0.105
1737.973	146216	3.5	203755	4.5	-0.82	3.35E+08	0.569
1946.908	199048	3.5	250411	4.5	-0.92	2.11E+08	0.183

a: Energy Levels from [42]

Ag VI

Energy Levels

Table A39: Comparison between available experimental data and calculated even energy levels (in cm^{-1}) in Ag VI

E^a_{exp}	E^b_{calc}	Δ E	J	Leading components (in %) in LS Coupling^c
0	-60	60	4	96.2 $4d^6$ (^{5}D) ^{5}D
2692.5	2696	-3.5	3	98 $4d^6$ (^{5}D) ^{5}D
3953	3979	-26	2	94.7 $4d^6$ (^{5}D) ^{5}D
4941	4995	-54	1	95.3 $4d^6$ (^{5}D) ^{5}D
5380	5442	-62	0	95.1 $4d^6$ (^{5}D) ^{5}D
20494.5	20345	149.5	4	20.8 $4d^6$ (^{3}F) ^{3}F + 34.2 $4d^6$ (^{3}H) ^{3}H + 22.5 $4d^6$ (^{3}G) ^{3}G
21041.5	21191	-149.5	2	56.4 $4d^6$ (^{3}P) ^{3}P + 31.5 $4d^6$ (^{3}P) ^{3}P
21512.5	21565	-52.5	6	94.3 $4d^6$ (^{3}H) ^{3}H + 5.5 $4d^6$ (^{1}I) ^{1}I
21812	21817	-5	5	69.7 $4d^6$ (^{3}H) ^{3}H + 30.1 $4d^6$ (^{3}G) ^{3}G
24441	24422	19	3	57.4 $4d^6$ (^{3}F) ^{3}F + 24.9 $4d^6$ (^{3}G) ^{3}G + 14.9 $4d^6$ (^{3}F) ^{3}F
25144.5	25221	-76.5	4	52.4 $4d^6$ (^{3}H) ^{3}H + 34.6 $4d^6$ (^{3}F) ^{3}F + 10.2 $4d^6$ (^{3}F) ^{3}F
25306.5	25374	-67.5	2	81.2 $4d^6$ (^{3}F) ^{3}F + 11.8 $4d^6$ (^{3}F) ^{3}F
27958.5	27989	-30.5	5	69.7 $4d^6$ (^{3}G) ^{3}G + 30.1 $4d^6$ (^{3}H) ^{3}H
28232	28491	-259	1	58.5 $4d^6$ (^{3}P) ^{3}P + 22.3 $4d^6$ (^{3}P) ^{3}P + 14.9 $4d^6$ (^{3}D) ^{3}D
29659.5	29638	21.5	4	74.4 $4d^6$ (^{3}G) ^{3}G + 12.1 $4d^6$ (^{3}F) ^{3}F + 5.1 $4d^6$ (^{1}G) ^{1}G
30361	30409	-48	3	72.5 $4d^6$ (^{3}G) ^{3}G + 23.6 $4d^6$ (^{3}F) ^{3}F
32650.5	32475	175.5	2	84.8 $4d^6$ (^{3}D) ^{3}D
33509	33260	249	3	94.4 $4d^6$ (^{3}D) ^{3}D
33558	33379	179	1	83.7 $4d^6$ (^{3}D) ^{3}D + 8 $4d^6$ (^{3}P) ^{3}P + 7.9 $4d^6$ (^{3}P) ^{3}P
34194.5	34221	-26.5	6	94.3 $4d^6$ (^{1}I) ^{1}I + 5.5 $4d^6$ (^{3}H) ^{3}H
37481	37089	392	4	60.7 $4d^6$ (^{1}G) ^{1}G + 19.9 $4d^6$ (^{1}G) ^{1}G + 9.4 $4d^6$ (^{3}F) ^{3}F
41372	42041	-669	2	67.9 $4d^6$ (^{1}D) ^{1}D + 14.7 $4d^6$ (^{1}D) ^{1}D + 6.3 $4d^6$ (^{3}D) ^{3}D
41638.5	41140	498.5	0	45.5 $4d^6$ (^{1}S) ^{1}S + 41.8 $4d^6$ (^{3}P) ^{3}P + 12.1 $4d^6$ (^{1}S) ^{1}S
44724.5	44864	-139.5	3	82.9 $4d^6$ (^{1}F) ^{1}F + 12.5 $4d^6$ (^{3}F) ^{3}F
51664.5	51587	77.5	1	67.1 $4d^6$ (^{3}P) ^{3}P + 31.5 $4d^6$ (^{3}P) ^{3}P
53990.5	53891	99.5	4	75.7 $4d^6$ (^{3}F) ^{3}F + 18.3 $4d^6$ (^{3}F) ^{3}F
54223	54213	10	2	83.8 $4d^6$ (^{3}F) ^{3}F + 13.6 $4d^6$ (^{3}F) ^{3}F
55982	56003	-21	3	69.2 $4d^6$ (^{3}F) ^{3}F + 13.5 $4d^6$ (^{1}F) ^{1}F + 13.2 $4d^6$ (^{3}F) ^{3}F
56519	56637	-118	2	60 $4d^6$ (^{3}P) ^{3}P + 34.4 $4d^6$ (^{3}P) ^{3}P
61726	61850	-124	4	66.1 $4d^6$ (^{1}G) ^{1}G + 27.9 $4d^6$ (^{1}G) ^{1}G

a: From Kleef [43] and Joshi [44]
b: This work
c: Only the component ≥ 5% are given

Table A40: Comparison between available experimental data and calculated odd energy levels (in cm^{-1}) in Ag VI

E^a_{exp}	E^b_{calc}	Δ E	J	Leading components (in %) in LS Coupling^c
245839.5	245691	148.5	3	83.4 4d^{5}5p (^{6}S) ^{7}P + 12.8 4d^{5}5p (^{6}S) ^{5}P
258553	258518	35	3	79.1 4d^{5}5p (^{6}S) ^{5}P + 14.7 4d^{5}5p (^{6}S) ^{7}P
259764.5	259775	-10.5	2	84.8 4d^{5}5p (^{6}S) ^{5}P + 5.9 4d^{5}5p (^{6}S) ^{7}P
260687	260702	-15	1	90.8 4d^{5}5p (^{6}S) ^{5}P
272741	272797	-56	2	49.8 4d^{5}5p (^{4}G) ^{5}G + 14.9 4d^{5}5p (^{4}G) ^{3}F + 7.4 4d^{5}5p (^{2}F) ^{3}F
274565.5	274652	-86.5	5	49.1 4d^{5}5p (^{4}G) ^{5}G + 31.3 4d^{5}5p (^{4}G) ^{5}H + 7.5 4d^{5}5p (^{4}G) ^{3}H
275049.5	275078	-28.5	2	20.4 4d^{5}5p (^{4}D) ^{5}F + 24.4 4d^{5}5p (^{4}P) ^{5}D + 17.2 4d^{5}5p (^{4}D) ^{5}D
275073.5	275094	-20.5	3	11.7 4d^{5}5p (^{4}G) ^{3}F + 22.1 4d^{5}5p (^{4}G) ^{5}G + 11.5 4d^{5}5p (^{4}D) ^{5}F
275162	275233	-71	6	49.7 4d^{5}5p (^{4}G) ^{5}G + 25.9 4d^{5}5p (^{4}G) ^{5}H + 17.5 4d^{5}5p (^{4}G) ^{3}H
276281.5	276135	146.5	3	45.1 4d^{5}5p (^{4}G) ^{5}H + 11.1 4d^{5}5p (^{4}D) ^{5}F + 9.7 4d^{5}5p (^{4}G) ^{5}G
276960	276917	43	4	29.6 4d^{5}5p (^{4}G) ^{5}F + 14.2 4d^{5}5p (^{4}G) ^{5}H
277162.5	277205	-42.5	2	23.3 4d^{5}5p (^{4}P) ^{5}S + 17.4 4d^{5}5p (^{4}P) ^{3}P + 10.4 4d^{5}5p (^{4}D) ^{5}F
277685.5	277524	161.5	5	59.2 4d^{5}5p (^{4}G) ^{5}F + 14.7 4d^{5}5p (^{4}G) ^{5}H + 8.6 4d^{5}5p (^{4}G) ^{3}G
279095.5	278988	107.5	4	31.8 4d^{5}5p (^{4}G) ^{5}H + 20.1 4d^{5}5p (^{4}D) ^{5}F + 13.8 4d^{5}5p (^{4}G) ^{5}G
280376.5	280308	68.5	3	38.9 4d^{5}5p (^{4}D) ^{5}P + 16.7 4d^{5}5p (^{4}P) ^{5}P + 9.8 4d^{5}5p (^{4}D) ^{3}D
281607	281546	61	5	39.2 4d^{5}5p (^{4}G) ^{5}H + 36.6 4d^{5}5p (^{4}G) ^{5}G + 10 4d^{5}5p (^{4}G) ^{5}F
282186.5	282105	81.5	1	23.9 4d^{5}5p (^{4}P) ^{3}P + 20.7 4d^{5}5p (^{4}P) ^{5}D + 14.2 4d^{5}5p (^{4}P) ^{5}P
282348.5	282319	29.5	3	0.6 4d^{5}5p (^{2}D) ^{3}F + 28.2 4d^{5}5p (^{4}G) ^{5}F + 16.4 4d^{5}5p (^{4}P) ^{5}D
282545.5	282488	57.5	6	52.3 4d^{5}5p (^{4}G) ^{5}H + 40.8 4d^{5}5p (^{4}G) ^{5}G
283032.5	283210	-177.5	2	33.8 4d^{5}5p (^{4}G) ^{3}F + 16.2 4d^{5}5p (^{4}G) ^{5}G + 14.1 4d^{5}5p (^{4}P) ^{5}S
283558.5	283448	110.5	4	43.9 4d^{5}5p (^{4}G) ^{5}F + 16.4 4d^{5}5p (^{4}P) ^{5}D + 9.9 4d^{5}5p (^{4}D) ^{5}D
284053	284018	35	3	23.3 4d^{5}5p (^{4}G) ^{5}F + 11.5 4d^{5}5p (^{4}G) ^{3}F + 10 4d^{5}5p (^{4}P) ^{5}P
284235.5	284186	49.5	2	14.5 4d^{5}5p (^{4}P) ^{5}P + 18.4 4d^{5}5p (^{4}D) ^{5}P + 11.9 4d^{5}5p (^{4}D) ^{5}D
284406	284356	50	2	20.9 4d^{5}5p (^{4}G) ^{5}F + 24 4d^{5}5p (^{4}D) ^{5}P + 13.4 4d^{5}5p (^{4}P) ^{5}S
284578.5	284639	-60.5	3	22.7 4d^{5}5p (^{4}D) ^{5}F + 23.9 4d^{5}5p (^{4}G) ^{3}F + 12 4d^{5}5p (^{4}G) ^{5}G
284659.5	284756	-96.5	4	43.9 4d^{5}5p (^{4}G) ^{3}F + 12 4d^{5}5p (^{4}G) ^{5}G + 8.4 4d^{5}5p (^{4}D) ^{5}F
284990	285066	-76	1	46.2 4d^{5}5p (^{4}G) ^{5}F + 17.6 4d^{5}5p (^{4}D) ^{5}F + 15.2 4d^{5}5p (^{4}P) ^{5}P
285564.5	285611	-46.5	6	63.9 4d^{5}5p (^{4}G) ^{3}H + 19.4 4d^{5}5p (^{4}G) ^{5}H + 5 4d^{5}5p (^{2}I) ^{3}H
285714	285803	-89	4	46.4 4d^{5}5p (^{4}G) ^{3}H + 11.4 4d^{5}5p (^{4}G) ^{3}F + 8.6 4d^{5}5p (^{4}D) ^{3}F
285791	285707	84	1	31.8 4d^{5}5p (^{4}P) ^{5}P + 16.2 4d^{5}5p (^{4}D) ^{5}P + 15.1 4d^{5}5p (^{4}G) ^{5}F
285968	285989	-21	5	64.4 4d^{5}5p (^{4}G) ^{3}H + 13.4 4d^{5}5p (^{4}D) ^{5}F + 8.7 4d^{5}5p (^{4}G) ^{5}H
286575.5	286646	-70.5	4	17.1 4d^{5}5p (^{4}P) ^{5}D + 17.3 4d^{5}5p (^{4}D) ^{3}F + 13.3 4d^{5}5p (^{4}D) ^{5}F
286636	286635	1	2	10.9 4d^{5}5p (^{4}P) ^{3}P + 25.5 4d^{5}5p (^{4}G) ^{5}F + 15.8 4d^{5}5p (^{4}P) ^{5}S
287055.5	286906	149.5	3	31.3 4d^{5}5p (^{4}D) ^{5}D + 15.1 4d^{5}5p (^{4}P) ^{3}D + 12.6 4d^{5}5p (^{4}G) ^{3}F
287589.5	287536	53.5	4	34.7 4d^{5}5p (^{4}D) ^{5}D + 18.5 4d^{5}5p (^{4}P) ^{5}D + 16.9 4d^{5}5p (^{4}G) ^{3}H
288183.5	288170	13.5	5	44.2 4d^{5}5p (^{4}D) ^{5}F + 10.4 4d^{5}5p (^{4}G) ^{3}H + 7.5 4d^{5}5p (^{2}I) ^{3}I
288704	288735	-31	3	25.5 4d^{5}5p (^{4}P) ^{5}D + 25.2 4d^{5}5p (^{4}D) ^{3}F + 11.9 4d^{5}5p (^{4}P) ^{3}D
288743	288734	9	1	26.6 4d^{5}5p (^{4}D) ^{3}D + 19.1 4d^{5}5p (^{4}D) ^{5}D + 13.7 4d^{5}5p (^{4}P) ^{3}D
288801.5	288905	-103.5	5	12.4 4d^{5}5p (^{2}I) ^{1}H + 24.9 4d^{5}5p (^{4}D) ^{5}F + 19 4d^{5}5p (^{2}I) ^{3}I
289143	289188	-45	6	60.2 4d^{5}5p (^{2}I) ^{3}K + 21 4d^{5}5p (^{2}I) ^{3}I + 6.4 4d^{5}5p (^{2}H) ^{3}I
289488.5	289453	35.5	3	46.8 4d^{5}5p (^{4}G) ^{3}G + 9 4d^{5}5p (^{4}P) ^{5}D + 6.3 4d^{5}5p (^{4}G) ^{5}H
289567	289626	-59	4	47.6 4d^{5}5p (^{4}G) ^{3}G + 6.2 4d^{5}5p (^{4}F) ^{3}G + 6 4d^{5}5p (^{2}F) ^{3}G
290297	290320	-23	1	61.3 4d^{5}5p (^{4}D) ^{5}P + 17.9 4d^{5}5p (^{4}P) ^{5}P + 7.5 4d^{5}5p (^{4}P) ^{3}P
290416	290471	-55	2	25.8 4d^{5}5p (^{4}D) ^{3}F + 12.8 4d^{5}5p (^{4}P) ^{5}D + 11.4 4d^{5}5p (^{4}P) ^{3}D
290705	290596	109	3	34.8 4d^{5}5p (^{4}D) ^{3}D + 9.7 4d^{5}5p (^{4}G) ^{3}F + 8.6 4d^{5}5p (^{4}D) ^{5}D
291127	291157	-30	7	50.3 4d^{5}5p (^{2}I) ^{3}K + 29.2 4d^{5}5p (^{2}I) ^{3}I + 18.8 4d^{5}5p (^{2}I) ^{1}K
291283.5	291338	-54.5	2	15.2 4d^{5}5p (^{4}D) ^{3}D + 14 4d^{5}5p (^{4}P) ^{5}P + 12.4 4d^{5}5p (^{4}P) ^{3}P
292117	292062	55	5	62.2 4d^{5}5p (^{4}G) ^{3}G + 12.8 4d^{5}5p (^{2}I) ^{3}I + 5 4d^{5}5p (^{2}I) ^{3}H
292500	292681	-181	4	17.6 4d^{5}5p (^{4}D) ^{5}F + 25.6 4d^{5}5p (^{4}D) ^{3}F + 17.3 4d^{5}5p (^{4}P) ^{5}D
292607	292593	14	1	22.6 4d^{5}5p (^{4}D) ^{5}D + 19.2 4d^{5}5p (^{4}P) ^{3}P + 14.1 4d^{5}5p (^{4}P) ^{5}D
293265	293324	-59	3	14.3 4d^{5}5p (^{4}D) ^{3}F + 11.3 4d^{5}5p (^{4}G) ^{3}G + 8.7 4d^{5}5p (^{4}P) ^{5}D
293275	293231	44	2	14.5 4d^{5}5p (^{2}D) ^{3}F + 21.7 4d^{5}5p (^{4}D) ^{3}D + 14.3 4d^{5}5p (^{4}D) ^{3}F
293586.5	293554	32.5	2	21.2 4d^{5}5p (^{4}D) ^{5}P + 15.7 4d^{5}5p (^{4}P) ^{5}P + 12.4 4d^{5}5p (^{4}P) ^{5}S
293765.5	293681	84.5	3	26.1 4d^{5}5p (^{4}P) ^{5}P + 21.1 4d^{5}5p (^{4}D) ^{5}P + 15.7 4d^{5}5p (^{4}D) ^{3}F
293848	293720	128	6	46.6 4d^{5}5p (^{2}I) ^{3}H + 22.7 4d^{5}5p (^{2}I) ^{3}I + 12.2 4d^{5}5p (^{2}I) ^{3}K
295023	295165	-142	2	23.3 4d^{5}5p (^{4}P) ^{3}D + 15.6 4d^{5}5p (^{2}D) ^{3}P + 11.2 4d^{5}5p (^{4}G) ^{3}F
295372	295402	-30	4	34.1 4d^{5}5p (^{2}G) ^{3}H + 22.5 4d^{5}5p (^{4}G) ^{3}G + 10.9 4d^{5}5p (^{2}I) ^{3}H
295431	295355	76	1	28.3 4d^{5}5p (^{4}D) ^{3}P + 25 4d^{5}5p (^{4}P) ^{3}S + 12.4 4d^{5}5p (^{4}P) ^{3}P
295629	295804	-175	2	0.1 4d^{5}5p (^{2}D) ^{3}P + 17.3 4d^{5}5p (^{4}F) ^{5}G + 10.5 4d^{5}5p (^{4}D) ^{3}F
296114.5	295913	201.5	5	23.9 4d^{5}5p (^{2}G) ^{3}H + 18.3 4d^{5}5p (^{2}G) ^{3}G + 9.2 4d^{5}5p (^{4}F) ^{5}G
296416.5	296824	-407.5	3	16.7 4d^{5}5p (^{2}F) ^{3}D + 11.8 4d^{5}5p (^{2}F) ^{3}F + 7.8 4d^{5}5p (^{2}F) ^{3}D
297076.5	297160	-83.5	5	30.8 4d^{5}5p (^{2}I) ^{3}I + 14.7 4d^{5}5p (^{2}I) ^{1}H + 10.8 4d^{5}5p (^{2}H) ^{3}I
297761.5	297626	135.5	4	10.5 4d^{5}5p (^{2}G) ^{1}G + 12.3 4d^{5}5p (^{2}H) ^{1}G + 11.6 4d^{5}5p (^{4}D) ^{3}F
297929.5	298101	-171.5	2	35.6 4d^{5}5p (^{4}F) ^{5}G + 12 4d^{5}5p (^{2}F) ^{3}F + 9.6 4d^{5}5p (^{2}D) ^{3}P
298069	298244	-175	1	24.3 4d^{5}5p (^{2}D) ^{3}P + 18.2 4d^{5}5p (^{4}P) ^{3}S + 9.1 4d^{5}5p (^{4}D) ^{3}D
298133.5	298128	5.5	6	33.4 4d^{5}5p (^{2}I) ^{3}I + 24.7 4d^{5}5p (^{2}I) ^{3}H + 16.2 4d^{5}5p (^{2}I) ^{3}K
298167.5	297975	192.5	4	16.5 4d^{5}5p (^{4}F) ^{5}G + 12.9 4d^{5}5p (^{2}F) ^{3}G + 9.7 4d^{5}5p (^{2}F) ^{3}G
298237.5	298354	-116.5	4	14.5 4d^{5}5p (^{2}I) ^{3}H + 15.4 4d^{5}5p (^{4}F) ^{5}G + 10.3 4d^{5}5p (^{2}G) ^{3}H
298289	298291	-2	3	44.2 4d^{5}5p (^{4}F) ^{5}G + 7.4 4d^{5}5p (^{4}G) ^{3}G + 6.9 4d^{5}5p (^{2}F) ^{3}D
298375.5	298378	-2.5	7	54.9 4d^{5}5p (^{2}I) ^{1}K + 29.8 4d^{5}5p (^{2}I) ^{3}K + 10.3 4d^{5}5p (^{2}H) ^{3}I
298421	298681	-260	2	32.5 4d^{5}5p (^{4}D) ^{3}P + 15.6 4d^{5}5p (^{4}P) ^{3}P + 11.2 4d^{5}5p (^{4}F) ^{5}G
298870	299014	-144	5	43.9 4d^{5}5p (^{2}I) ^{3}H + 21 4d^{5}5p (^{2}I) ^{1}H + 9.2 4d^{5}5p (^{2}G) ^{1}H
299164	299220	-56	7	64.6 4d^{5}5p (^{2}I) ^{3}I + 17.7 4d^{5}5p (^{2}I) ^{1}K + 14.7 4d^{5}5p (^{2}I) ^{3}K
299638.5	299527	111.5	4	24.9 4d^{5}5p (^{4}F) ^{5}D + 19.5 4d^{5}5p (^{4}F) ^{5}F + 11.3 4d^{5}5p (^{4}F) ^{5}G
300101	300091	10	2	21.6 4d^{5}5p (^{4}F) ^{5}F + 11.4 4d^{5}5p (^{4}F) ^{5}D + 8.8 4d^{5}5p (^{2}F) ^{3}D
300460	300236	224	3	20.5 4d^{5}5p (^{2}F) ^{3}F + 22.9 4d^{5}5p (^{2}F) ^{3}G + 11.1 4d^{5}5p (^{2}F) ^{3}F
300570.5	300597	-26.5	4	18.4 4d^{5}5p (^{2}D) ^{3}F + 12.1 4d^{5}5p (^{2}I) ^{3}H + 10.4 4d^{5}5p (^{2}F) ^{3}G
300965.5	301021	-55.5	5	23.2 4d^{5}5p (^{4}F) ^{5}G + 19.8 4d^{5}5p (^{2}I) ^{3}I + 10.6 4d^{5}5p (^{2}G) ^{3}H
300975	300868	107	3	19.5 4d^{5}5p (^{2}F) ^{3}G + 16.4 4d^{5}5p (^{2}D) ^{3}F + 7.6 4d^{5}5p (^{2}H) ^{3}G
301167	301055	112	2	10.3 4d^{5}5p (^{2}D) ^{1}D + 14.5 4d^{5}5p (^{4}F) ^{5}F + 6.9 4d^{5}5p (^{2}F) ^{3}F
301314	301237	77	6	41.2 4d^{5}5p (^{4}F) ^{5}G + 31.4 4d^{5}5p (^{2}G) ^{3}H + 9.7 4d^{5}5p (^{2}I) ^{3}I
301320	301217	103	3	16.3 4d^{5}5p (^{2}G) ^{3}G + 14.1 4d^{5}5p (^{4}F) ^{5}F + 10.5 4d^{5}5p (^{4}F) ^{5}D
301607	301604	3	3	23.1 4d^{5}5p (^{4}F) ^{5}F + 14.7 4d^{5}5p (^{2}G) ^{3}G + 14.3 4d^{5}5p (^{2}F) ^{3}D
301903.5	301810	93.5	5	21.9 4d^{5}5p (^{4}F) ^{5}F + 23.1 4d^{5}5p (^{4}F) ^{5}G + 12.5 4d^{5}5p (^{2}G) ^{3}G
302080.5	302279	-198.5	4	23.4 4d^{5}5p (^{2}F) ^{1}G + 12.7 4d^{5}5p (^{4}F) ^{5}G + 8 4d^{5}5p (^{2}I) ^{3}H
302808.5	302776	32.5	1	45.6 4d^{5}5p (^{4}F) ^{5}F + 10.8 4d^{5}5p (^{2}D) ^{1}P + 9.2 4d^{5}5p (^{4}F) ^{5}D
302947.5	303012	-64.5	2	12.3 4d^{5}5p (^{2}F) ^{1}D + 17.2 4d^{5}5p (^{2}D) ^{3}F + 15.4 4d^{5}5p (^{2}D) ^{3}D
303440	303433	7	1	18.1 4d^{5}5p (^{2}D) ^{3}D + 24 4d^{5}5p (^{4}F) ^{5}D + 10.7 4d^{5}5p (^{2}F) ^{3}D
303558.5	303479	79.5	6	13.3 4d^{5}5p (^{2}H) ^{3}H + 29.4 4d^{5}5p (^{4}F) ^{5}G + 23.5 4d^{5}5p (^{2}I) ^{1}I
303646.5	303706	-59.5	5	23.9 4d^{5}5p (^{2}H) ^{3}G + 19 4d^{5}5p (^{2}H) ^{3}I + 18.7 4d^{5}5p (^{4}F) ^{5}F
304144	303927	217	4	21.5 4d^{5}5p (^{2}F) ^{3}F + 9.9 4d^{5}5p (^{2}F) ^{3}F + 7.7 4d^{5}5p (^{2}F) ^{1}G

Table A40: Continued

E^a_{exp}	E^b_{calc}	Δ E	J	Leading components (in %) in LS Coupling^c
304450.5	304422	28.5	4	24.4 4d^{5}5p (^{2}G) ^{3}G + 14.4 4d^{5}5p (^{2}I) ^{3}H + 9.7 4d^{5}5p (^{4}F) ^{5}D
304878.5	305068	-189.5	4	19.1 4d^{5}5p (^{4}F) ^{5}F + 21.6 4d^{5}5p (^{2}F) ^{3}F + 10.6 4d^{5}5p (^{4}F) ^{5}G
304953.5	304914	39.5	5	29.4 4d^{5}5p (^{2}H) ^{3}I + 29.4 4d^{5}5p (^{2}H) ^{3}H + 9.8 4d^{5}5p (^{2}G) ^{3}H
305145.5	305122	23.5	1	19 4d^{5}5p (^{4}P) ^{3}S + 22.5 4d^{5}5p (^{2}F) ^{3}D + 10.9 4d^{5}5p (^{2}D) ^{3}P
305356.5	305600	-243.5	2	23 4d^{5}5p (^{2}G) ^{3}F + 12.4 4d^{5}5p (^{2}F) ^{3}F + 10.3 4d^{5}5p (^{4}D) ^{3}F
305641.5	305588	53.5	6	46.6 4d^{5}5p (^{2}I) ^{1}I + 35.7 4d^{5}5p (^{2}H) ^{3}I
306147.5	306248	-100.5	5	64.3 4d^{5}5p (^{2}F) ^{3}G + 8.5 4d^{5}5p (^{4}F) ^{5}F
306210	306261	-51	4	1.5 4d^{5}5p (^{4}D) ^{3}F + 26.5 4d^{5}5p (^{2}G) ^{3}F + 13.5 4d^{5}5p (^{2}F) ^{3}F
306474	306508	-34	3	17.7 4d^{5}5p (^{2}G) ^{3}F + 12.4 4d^{5}5p (^{4}F) ^{3}G + 10.2 4d^{5}5p (^{2}F) ^{3}D
306715.5	306629	86.5	3	25.1 4d^{5}5p (^{2}F) ^{3}G + 13 4d^{5}5p (^{2}D) ^{3}F + 8.3 4d^{5}5p (^{4}F) ^{5}F
306850	306964	-114	2	17.4 4d^{5}5p (^{2}D) ^{3}D + 19.4 4d^{5}5p (^{4}F) ^{5}F + 12.4 4d^{5}5p (^{2}F) ^{3}D
307337.5	307112	225.5	4	17.6 4d^{5}5p (^{2}F) ^{3}G + 9 4d^{5}5p (^{4}F) ^{3}G + 7.5 4d^{5}5p (^{2}F) ^{3}F
307892	307817	75	6	38.6 4d^{5}5p (^{2}H) ^{1}I + 32.7 4d^{5}5p (^{2}G) ^{3}H + 16.2 4d^{5}5p (^{4}F) ^{5}G
308266	308256	10	5	39.4 4d^{5}5p (^{4}F) ^{3}G + 12 4d^{5}5p (^{4}F) ^{5}G + 9.8 4d^{5}5p (^{4}F) ^{5}F
308404.5	308144	260.5	2	33.4 4d^{5}5p (^{2}F) ^{1}D + 10.1 4d^{5}5p (^{2}F) ^{1}D + 7.8 4d^{5}5p (^{2}F) ^{3}F
309083	309155	-72	2	22.2 4d^{5}5p (^{4}F) ^{5}D + 13.4 4d^{5}5p (^{2}F) ^{3}D + 11.2 4d^{5}5p (^{2}D) ^{3}P
309234	309110	124	1	53.2 4d^{5}5p (^{2}S) ^{3}P + 9.8 4d^{5}5p (^{2}D) ^{3}P + 7.4 4d^{5}5p (^{4}F) ^{3}D
309388.5	309281	107.5	5	34.9 4d^{5}5p (^{2}G) ^{3}G + 23.7 4d^{5}5p (^{2}G) ^{3}H + 16.6 4d^{5}5p (^{2}F) ^{3}G
309526.5	309596	-69.5	4	12 4d^{5}5p (^{4}F) ^{3}G + 13.6 4d^{5}5p (^{4}F) ^{5}D + 10.9 4d^{5}5p (^{2}F) ^{3}F
310253	310198	55	3	16.2 4d^{5}5p (^{4}F) ^{3}G + 15.9 4d^{5}5p (^{4}F) ^{3}F + 10.6 4d^{5}5p (^{2}F) ^{1}F
310303	310695	-392	2	9.7 4d^{5}5p (^{2}F) ^{3}D + 17.7 4d^{5}5p (^{4}F) ^{3}D + 14 4d^{5}5p (^{2}D) ^{1}D
310335.5	310339	-3.5	6	35 4d^{5}5p (^{2}H) ^{3}I + 33.4 4d^{5}5p (^{2}H) ^{3}H + 19.1 4d^{5}5p (^{2}H) ^{1}I
310470	310490	-20	4	24.6 4d^{5}5p (^{4}F) ^{3}F + 15.3 4d^{5}5p (^{4}F) ^{3}G + 12.1 4d^{5}5p (^{2}H) ^{3}H
310673.5	310912	-238.5	1	52.7 4d^{5}5p (^{4}F) ^{3}D + 11.6 4d^{5}5p (^{4}D) ^{3}D + 8.4 4d^{5}5p (^{2}F) ^{3}D
310967.5	311102	-134.5	4	27.5 4d^{5}5p (^{2}H) ^{3}H + 20.1 4d^{5}5p (^{2}F) ^{3}G + 11.9 4d^{5}5p (^{4}F) ^{3}F
311185.5	311184	1.5	7	82.6 4d^{5}5p (^{2}H) ^{3}I + 8.4 4d^{5}5p (^{2}I) ^{1}K + 4.7 4d^{5}5p (^{2}I) ^{3}K
311683	311631	52	4	10.5 4d^{5}5p (^{2}F) ^{1}G + 17.9 4d^{5}5p (^{2}G) ^{3}G + 13.5 4d^{5}5p (^{2}G) ^{1}G
311962	311852	110	5	23 4d^{5}5p (^{2}H) ^{3}H + 23 4d^{5}5p (^{2}F) ^{3}G + 15.3 4d^{5}5p (^{4}F) ^{3}G
312169	312263	-94	3	18.6 4d^{5}5p (^{4}F) ^{3}F + 15.9 4d^{5}5p (^{2}F) ^{1}F + 11.3 4d^{5}5p (^{2}G) ^{1}F
312431.5	312581	-149.5	2	34.3 4d^{5}5p (^{4}F) ^{3}D + 18.5 4d^{5}5p (^{2}S) ^{3}P + 9.1 4d^{5}5p (^{2}D) ^{3}P
312636	312440	196	3	5.4 4d^{5}5p (^{2}F) ^{3}D + 22.8 4d^{5}5p (^{4}F) ^{3}F + 16.9 4d^{5}5p (^{2}F) ^{1}F
313983.5	313803	180.5	2	15 4d^{5}5p (^{2}F) ^{3}D + 27.8 4d^{5}5p (^{2}F) ^{3}D + 15.1 4d^{5}5p (^{2}S) ^{3}P
314053.5	314334	-280.5	3	16.7 4d^{5}5p (^{2}F) ^{3}F + 13.2 4d^{5}5p (^{4}F) ^{3}G + 9.1 4d^{5}5p (^{2}F) ^{3}F
314172.5	314219	-46.5	4	6.1 4d^{5}5p (^{2}F) ^{3}G + 19.8 4d^{5}5p (^{2}F) ^{1}G + 15.3 4d^{5}5p (^{4}F) ^{3}F
314360	314294	66	1	24.1 4d^{5}5p (^{2}F) ^{3}D + 19.1 4d^{5}5p (^{2}S) ^{1}P + 10.7 4d^{5}5p (^{2}D) ^{1}P
314439	314398	41	5	43.9 4d^{5}5p (^{2}G) ^{1}H + 9.9 4d^{5}5p (^{2}H) ^{3}H + 9 4d^{5}5p (^{2}G) ^{3}H
314553.5	314736	-182.5	2	15.9 4d^{5}5p (^{2}F) ^{3}F + 28.8 4d^{5}5p (^{4}F) ^{3}F + 9 4d^{5}5p (^{2}F) ^{1}D
314675	314565	110	3	11.6 4d^{5}5p (^{2}F) ^{1}F + 19.1 4d^{5}5p (^{2}F) ^{3}G + 16.2 4d^{5}5p (^{2}G) ^{1}F
315274	315321	-47	6	30.7 4d^{5}5p (^{2}G) ^{3}H + 28.5 4d^{5}5p (^{2}H) ^{3}H + 27.5 4d^{5}5p (^{2}H) ^{1}I
315411.5	315313	98.5	4	23.6 4d^{5}5p (^{2}F) ^{3}F + 13.6 4d^{5}5p (^{4}F) ^{3}G + 13.4 4d^{5}5p (^{2}F) ^{1}G
315481.5	315361	120.5	3	26 4d^{5}5p (^{4}F) ^{3}D + 13.1 4d^{5}5p (^{2}F) ^{3}D + 12.4 4d^{5}5p (^{2}D) ^{3}D
316355.5	316291	64.5	5	59.5 4d^{5}5p (^{2}H) ^{1}H + 9 4d^{5}5p (^{2}G) ^{1}H + 7.7 4d^{5}5p (^{2}G) ^{3}G
317080.5	316985	95.5	3	34.3 4d^{5}5p (^{2}H) ^{3}G + 10.1 4d^{5}5p (^{2}G) ^{3}G + 7.9 4d^{5}5p (^{4}F) ^{3}G
317357	317341	16	4	32 4d^{5}5p (^{2}H) ^{3}G + 18.1 4d^{5}5p (^{2}F) ^{3}G + 7.5 4d^{5}5p (^{2}G) ^{3}G
317484.5	317382	102.5	2	19.5 4d^{5}5p (^{2}S) ^{3}P + 12.9 4d^{5}5p (^{2}F) ^{3}D + 12.7 4d^{5}5p (^{2}F) ^{3}D
318262.5	317996	266.5	5	31.6 4d^{5}5p (^{2}F) ^{3}G + 32.1 4d^{5}5p (^{2}H) ^{3}G + 10.1 4d^{5}5p (^{2}H) ^{1}H
320038	320226	-188	4	39 4d^{5}5p (^{2}H) ^{1}G + 20.2 4d^{5}5p (^{2}G) ^{1}G + 8.3 4d^{5}5p (^{2}F) ^{1}G
320974	321188	-214	3	37.4 4d^{5}5p (^{2}F) ^{1}F + 7.8 4d^{5}5p (^{2}F) ^{1}F + 6.6 4d^{5}5p (^{2}G) ^{3}F
322424.5	322143	281.5	1	58.5 4d^{5}5p (^{2}D) ^{3}D + 22.4 4d^{5}5p (^{2}S) ^{1}P
324022	324130	-108	3	16.6 4d^{5}5p (^{2}D) ^{1}F + 21.8 4d^{5}5p (^{2}D) ^{3}F + 10.7 4d^{5}5p (^{2}F) ^{1}F
326026	326148	-122	3	30.2 4d^{5}5p (^{2}D) ^{3}F + 23.2 4d^{5}5p (^{2}D) ^{1}F + 18.1 4d^{5}5p (^{2}G) ^{1}F
327004	326798	206	3	51 4d^{5}5p (^{2}D) ^{3}D + 16.6 4d^{5}5p (^{2}D) ^{3}F
327145	327142	3	4	55.8 4d^{5}5p (^{2}G) ^{3}F + 13.1 4d^{5}5p (^{2}G) ^{3}G + 5.6 4d^{5}5p (^{2}D) ^{3}F
327517	327459	58	5	50.8 4d^{5}5p (^{2}G) ^{3}H + 19.1 4d^{5}5p (^{2}G) ^{1}H + 17.2 4d^{5}5p (^{2}G) ^{3}G
327971.5	328015	-43.5	4	52.5 4d^{5}5p (^{2}G) ^{3}H + 10.4 4d^{5}5p (^{2}D) ^{3}F + 6.7 4d^{5}5p (^{2}G) ^{1}G
328367.5	328400	-32.5	4	69.2 4d^{5}5p (^{2}D) ^{3}F + 6.5 4d^{5}5p (^{2}G) ^{3}F + 6.4 4d^{5}5p (^{2}G) ^{3}H
329699.5	329674	25.5	3	34.5 4d^{5}5p (^{2}G) ^{3}G + 20.7 4d^{5}5p (^{2}G) ^{3}F + 15 4d^{5}5p (^{2}D) ^{1}F
331605.5	331553	52.5	2	55.9 4d^{5}5p (^{2}D) ^{1}D + 12.4 4d^{5}5p (^{2}D) ^{3}P + 7.8 4d^{5}5p (^{2}G) ^{3}F
332893	332834	59	6	94.5 4d^{5}5p (^{2}G) ^{3}H
333194.5	333237	-42.5	3	45 4d^{5}5p (^{2}G) ^{3}F + 29.8 4d^{5}5p (^{2}G) ^{3}G + 6.2 4d^{5}5p (^{2}D) ^{1}F
333270	333347	-77	2	62.5 4d^{5}5p (^{2}G) ^{3}F + 12.2 4d^{5}5p (^{2}D) ^{3}F + 7.4 4d^{5}5p (^{2}D) ^{1}D
333800.5	333799	1.5	4	69.9 4d^{5}5p (^{2}G) ^{3}G + 13.5 4d^{5}5p (^{2}G) ^{3}H + 9.4 4d^{5}5p (^{2}G) ^{3}F
334948.5	334923	25.5	5	62 4d^{5}5p (^{2}G) ^{3}G + 27.7 4d^{5}5p (^{2}G) ^{3}H
336829	336893	-64	4	79.2 4d^{5}5p (^{2}G) ^{1}G + 6 4d^{5}5p (^{2}G) ^{3}F
337029	337032	-3	5	72.8 4d^{5}5p (^{2}G) ^{1}H + 9.6 4d^{5}5p (^{2}G) ^{3}H + 9.1 4d^{5}5p (^{2}G) ^{3}G
337558	337714	-156	2	54.1 4d^{5}5p (^{2}P) ^{3}P + 23 4d^{5}5p (^{2}D) ^{3}P + 7.1 4d^{5}5p (^{2}P) ^{3}D
338182.5	338165	17.5	3	53 4d^{5}5p (^{2}G) ^{1}F + 15.5 4d^{5}5p (^{2}D) ^{1}F + 9.6 4d^{5}5p (^{2}G) ^{3}G
341727	341775	-48	2	28.6 4d^{5}5p (^{2}P) ^{3}D + 26.3 4d^{5}5p (^{2}P) ^{1}D + 9.6 4d^{5}5p (^{2}D) ^{3}P
342518.5	342556	-37.5	1	76.2 4d^{5}5p (^{2}P) ^{3}D + 5.4 4d^{5}5p (^{2}F) ^{3}D + 5.3 4d^{5}5p (^{2}D) ^{3}D
347274	347237	37	3	80.6 4d^{5}5p (^{2}P) ^{3}D + 8.7 4d^{5}5p (^{2}D) ^{3}D + 2.7 4d^{5}5p (^{2}F) ^{3}D
347842	347900	-58	2	0 4d^{5}5p (^{2}F) ^{3}F + 46 4d^{5}5p (^{2}P) ^{3}D + 24.5 4d^{5}5p (^{2}P) ^{1}D
353721	353650	71	3	44.3 4d^{5}5p (^{2}D) ^{3}F + 12.8 4d^{5}5p (^{2}D) ^{3}D + 12 4d^{5}5p (^{2}D) ^{3}F
359642	359622	20	2	37.7 4d^{5}5p (^{2}D) ^{3}D + 12.5 4d^{5}5p (^{2}D) ^{3}P + 10 4d^{5}5p (^{2}D) ^{3}F
361475.5	361356	119.5	3	53.5 4d^{5}5p (^{2}D) ^{3}D + 13.1 4d^{5}5p (^{2}D) ^{3}D + 12.9 4d^{5}5p (^{2}D) ^{3}F
363436	363364	72	3	59.1 4d^{5}5p (^{2}D) ^{1}F + 15.5 4d^{5}5p (^{2}D) ^{1}F + 8.9 4d^{5}5p (^{2}D) ^{3}F

a:a: From Kleef [43] and Joshi [44]
b: This work
c: Only the component $\geq$ 5% are given

Transitions

Table A41: Computed oscillator strengths and transition probabilities Ag VI.

Wavelength Å	Lower Level[a] cm^{-1}	J_{Low}	Upper level[a] cm^{-1}	J_{Up}	log gf	gA s^{-1}	CF
319.044	21513	6	334949	5	-0.79	1.07E+10	0.17
325.219	53991	4	361476	3	-0.57	1.68E+10	0.147
326.966	27959	5	333801	4	-0.67	1.35E+10	-0.359
327.916	56519	2	361476	3	-0.92	7.46E+09	0.251
329.316	55982	3	359642	2	-0.75	1.10E+10	0.191
329.451	29660	4	333195	3	-0.75	1.09E+10	-0.162
330.132	30361	3	333270	2	-0.83	9.14E+09	-0.164
330.213	34195	6	337029	5	-0.19	3.91E+10	-0.305
331.444	61726	4	363436	3	-0.24	3.47E+10	0.265
336.698	44725	3	341727	2	-0.84	8.44E+09	-0.166
336.762	2693	3	299639	4	-1	5.84E+09	0.13
340.6	21812	5	315412	4	-0.61	1.41E+10	-0.145
340.922	34195	6	327517	5	-0.83	8.46E+09	-0.196
340.967	53991	4	347274	3	-0.13	4.23E+10	0.5
341.88	0	4	292500	4	-1	5.65E+09	-0.152
342.043	21812	5	314173	4	-0.92	6.89E+09	-0.059
342.63	55982	3	347842	2	-0.43	2.12E+10	0.456
343.272	29660	4	320974	3	-0.97	6.02E+09	0.065
344.294	21513	6	311962	5	-0.33	2.61E+10	-0.206
344.427	25145	4	315482	3	-0.93	6.61E+09	0.083
344.55	41372	2	331606	2	-0.9	7.09E+09	-0.09
345.057	2693	3	292500	4	-0.83	8.37E+09	0.284
345.217	21513	6	311186	7	-0.73	1.05E+10	-0.348
345.544	27959	5	317357	4	-0.93	6.51E+09	0.076
346.13	25145	4	314054	3	-0.4	2.25E+10	-0.251
346.233	21513	6	310336	6	-0.71	1.08E+10	-0.162
346.259	0	4	288802	5	-0.75	9.81E+09	-0.277
346.431	21812	5	310470	4	-0.96	6.13E+09	-0.059
346.436	3953	2	292607	1	-0.91	6.88E+09	-0.263
346.866	54223	2	342519	1	-0.49	1.80E+10	0.561
347.207	2693	3	290705	3	-0.59	1.41E+10	0.324
347.372	21513	6	309389	5	-0.23	3.27E+10	0.631
347.718	0	4	287590	4	-0.06	4.84E+10	-0.721
347.734	21812	5	309389	5	-0.6	1.39E+10	-0.225
348.049	27959	5	315274	6	-0.46	1.93E+10	-0.451
348.365	0	4	287056	3	-0.77	9.44E+09	-0.265
348.437	30361	3	317357	4	-0.89	7.16E+09	-0.134
348.577	44725	3	331606	2	-0.23	3.23E+10	-0.541
348.732	21513	6	308266	5	-0.75	9.76E+09	-0.082
348.948	0	4	286576	4	-0.89	7.08E+09	-0.118
349.096	21812	5	308266	5	-0.7	1.10E+10	0.14
349.187	21513	6	307892	6	-1	5.43E+09	-0.202
349.675	20495	4	306474	3	-0.82	8.31E+09	-0.063
349.781	51665	1	337558	2	-0.78	9.04E+09	0.433
349.962	55982	3	341727	2	-0.92	6.58E+09	0.123
350	0	4	285714	4	-0.78	9.05E+09	0.304
350.477	25145	4	310470	4	-0.91	6.73E+09	0.067
351.004	2693	3	287590	4	-0.98	5.70E+09	0.27
351.082	32651	2	317485	2	-0.5	1.71E+10	-0.157
351.149	29660	4	314439	5	-0.79	8.75E+09	0.185
351.327	21513	6	306148	5	0.02	5.60E+10	-0.677
351.478	29660	4	314173	4	-0.52	1.64E+10	0.116
351.62	21812	5	306210	4	-0.72	1.03E+10	-0.106
351.64	25145	4	309527	4	-0.95	6.04E+09	-0.084
351.663	2693	3	287056	3	-0.86	7.47E+09	-0.153
351.875	53991	4	338183	3	-0.82	8.22E+09	-0.401
352.047	0	4	284053	3	-0.37	2.30E+10	-0.492
352.108	27959	5	311962	5	-0.7	1.08E+10	0.132
352.204	33558	1	317485	2	-0.99	5.55E+09	0.116
352.324	21812	5	305642	6	-0.68	1.12E+10	0.417
352.548	20495	4	304144	4	-0.86	7.33E+09	-0.05
352.807	21513	6	304954	5	-0.79	8.71E+09	0.177
353.18	21812	5	304954	5	-0.27	2.89E+10	-0.317
353.229	3953	2	287056	3	-0.45	1.88E+10	0.52
353.33	2693	3	285714	4	-0.79	8.69E+09	-0.479
353.346	27959	5	310968	4	-0.16	3.73E+10	0.473
353.568	32651	2	315482	3	-0.95	6.02E+09	-0.084
353.794	41372	2	324022	3	-0.85	7.42E+09	0.103
353.968	27959	5	310470	4	-0.29	2.72E+10	0.267
354.096	24441	3	306850	2	-0.86	7.38E+09	-0.1
354.23	29660	4	311962	5	-0.54	1.54E+10	-0.295
354.408	34195	6	316356	5	-0.23	3.13E+10	-0.186
354.568	24441	3	306474	3	-0.3	2.67E+10	-0.17
354.645	33509	3	315482	3	-0.41	2.08E+10	0.189
354.733	33509	3	315412	4	-0.92	6.40E+09	-0.108
354.753	2693	3	284579	3	-0.86	7.38E+09	0.296
354.852	30361	3	312169	3	-0.56	1.47E+10	-0.183
354.971	2693	3	284406	2	-0.23	3.13E+10	-0.647
354.994	4941	1	286636	2	-0.56	1.47E+10	-0.404
355.105	0	4	281607	5	-0.53	1.57E+10	-0.523
355.131	20495	4	302081	4	-0.8	8.43E+09	0.073
355.15	25145	4	306716	3	-0.87	7.06E+09	-0.103
355.154	27959	5	309527	4	-0.81	8.20E+09	-0.112
355.328	27959	5	309389	5	-0.67	1.13E+10	-0.144
355.416	2693	3	284053	3	-0.91	6.54E+09	-0.109
355.789	25145	4	306210	4	-1	5.30E+09	-0.06
355.805	41372	2	322425	1	-0.55	1.47E+10	0.467
355.823	56519	2	337558	2	-0.52	1.61E+10	-0.345
355.925	53991	4	334949	5	-0.42	2.01E+10	0.431
356.042	2693	3	283559	4	0	5.23E+10	-0.547
356.061	28232	1	309083	2	-0.62	1.26E+10	0.224
356.112	29660	4	310470	4	-0.88	6.87E+09	0.06
356.123	33558	1	314360	1	-0.78	8.84E+09	0.199
356.149	37481	4	318263	5	-0.98	5.57E+09	0.174
356.299	33509	3	314173	4	-0.75	9.44E+09	-0.244

Table A41: Continued

Wavelength	Lower Level	J_{Low}	Upper level	J_{Up}	log gf	gA	CF
356.371	30361	3	310968	4	-0.96	5.76E+09	-0.165
356.387	29660	4	310253	3	-0.34	2.42E+10	0.207
356.423	21042	2	301607	3	-0.51	1.61E+10	-0.247
356.450	33509	3	314054	3	-0.85	7.37E+09	-0.111
356.531	20495	4	300975	3	-0.08	4.41E+10	-0.399
356.539	33509	3	313984	2	-0.27	2.80E+10	-0.425
356.619	5380	0	285791	1	-0.43	1.95E+10	-0.613
356.645	21513	6	301904	5	-0.76	9.21E+09	0.175
356.663	0	4	280377	3	-0.14	3.81E+10	-0.387
356.751	27959	5	308266	5	-0.34	2.41E+10	0.292
356.783	3953	2	284236	2	-0.26	2.87E+10	0.574
356.788	21042	2	301320	3	-0.78	8.67E+09	-0.197
356.801	21812	5	302081	4	-0.41	2.05E+10	-0.337
356.831	34195	6	314439	5	0.44	1.43E+11	0.765
356.983	21042	2	301167	2	-1	5.27E+09	-0.096
357.015	3953	2	284053	3	-0.66	1.16E+10	-0.196
357.046	20495	4	300571	4	-0.9	6.68E+09	0.044
357.079	25307	2	305357	2	-0.73	9.82E+09	-0.135
357.08	4941	1	284990	1	-0.3	2.65E+10	-0.66
357.131	24441	3	304451	4	-0.92	6.27E+09	-0.078
357.187	20495	4	300460	3	-0.7	1.04E+10	-0.103
357.281	30361	3	310253	3	-0.43	1.96E+10	0.187
357.313	29660	4	309527	4	-0.52	1.57E+10	-0.177
357.385	53991	4	333801	4	-0.49	1.68E+10	0.477
357.422	32651	2	312432	2	-0.99	5.36E+09	-0.078
357.654	37481	4	317081	3	-0.2	3.29E+10	-0.418
357.758	32651	2	312169	3	-0.93	6.17E+09	0.185
357.827	4941	1	284406	2	-0.56	1.44E+10	-0.357
357.937	27959	5	307338	4	-0.72	1.00E+10	0.104
358.03	25145	4	304451	4	-0.2	3.31E+10	0.396
358.041	44725	3	324022	3	-0.87	7.00E+09	-0.066
358.238	20495	4	299639	4	-0.79	8.47E+09	0.085
358.26	33509	3	312636	3	-0.76	9.14E+09	-0.104
358.3	0	4	279096	4	-0.87	7.07E+09	-0.232
358.363	54223	2	333270	2	-0.17	3.48E+10	0.453
358.424	25145	4	304144	4	-0.2	3.30E+10	0.36
358.523	33509	3	312432	2	-0.58	1.38E+10	0.25
358.584	37481	4	316356	5	-0.67	1.12E+10	0.153
358.733	21812	5	300571	4	-0.08	4.35E+10	0.491
358.78	30361	3	309083	2	-0.6	1.31E+10	0.261
358.86	33509	3	312169	3	-0.98	5.50E+09	0.149
358.914	28232	1	306850	2	-0.74	9.42E+09	-0.157
359.058	24441	3	302948	2	-0.33	2.45E+10	-0.379
359.064	25145	4	303647	5	-0.36	2.28E+10	-0.393
359.201	3953	2	282349	3	-0.38	2.18E+10	-0.323
359.227	20495	4	298870	5	-0.88	6.82E+09	0.084
359.387	27959	5	306210	4	-0.53	1.52E+10	-0.146
359.41	3953	2	282187	1	-0.67	1.11E+10	-0.523
359.468	27959	5	306148	5	-0.61	1.27E+10	-0.253
359.54	25307	2	303440	1	-0.65	1.15E+10	0.29
359.712	37481	4	315482	3	-0.81	8.01E+09	-0.108
359.802	37481	4	315412	4	-0.39	2.09E+10	0.268
359.947	55982	3	333801	4	-0.63	1.21E+10	0.264
360.013	34195	6	311962	5	-0.04	4.71E+10	0.669
360.12	0	4	277686	5	0.18	7.85E+10	-0.656
360.122	2693	3	280377	3	-0.24	2.93E+10	0.486
360.162	32651	2	310303	2	-0.68	1.09E+10	0.127
360.164	21513	6	299164	7	-0.31	2.50E+10	-0.354
360.546	21513	6	298870	5	-0.87	6.88E+09	-0.136
360.636	55982	3	333270	2	-0.73	9.65E+09	0.324
360.663	20495	4	297762	4	-0.01	5.02E+10	-0.317
360.689	21042	2	298289	3	-0.76	8.94E+09	0.29
360.734	55982	3	333195	3	-0.06	4.51E+10	0.474
360.758	37481	4	314675	3	0.05	5.80E+10	-0.443
360.849	28232	1	305357	2	-0.55	1.45E+10	0.332
360.935	21812	5	298870	5	-0.1	4.05E+10	-0.371
360.938	29660	4	306716	3	-0.96	5.62E+09	0.1
360.975	21042	2	298069	1	-0.78	8.51E+09	-0.133
361.017	27959	5	304954	5	-0.39	2.10E+10	0.299
361.023	34195	6	311186	7	-0.9	6.39E+09	0.622
361.063	0	4	276960	4	-0.44	1.86E+10	-0.429
361.124	28232	1	305146	1	-0.37	2.17E+10	0.416
361.157	21042	2	297930	2	-0.83	7.61E+09	0.254
361.169	24441	3	301320	3	-0.37	2.16E+10	0.259
361.189	21513	6	298376	7	-0.66	1.13E+10	0.644
361.325	25145	4	301904	5	-0.79	8.23E+09	0.197
361.345	33509	3	310253	3	-0.89	6.61E+09	0.142
361.413	37481	4	314173	4	0.05	5.68E+10	-0.476
361.505	21513	6	298134	6	0.28	9.70E+10	-0.757
361.554	32651	2	309234	1	-0.24	2.97E+10	0.472
361.598	29660	4	306210	4	-0.6	1.30E+10	0.112
361.678	30361	3	306850	2	-0.89	6.56E+09	-0.159
361.713	25145	4	301607	3	-0.86	7.07E+09	0.143
361.721	61726	4	338183	3	0.1	6.47E+10	0.482
361.854	30361	3	306716	3	-0.86	7.11E+09	-0.122
361.992	44725	3	320974	3	-0.27	2.75E+10	0.211
362.075	27959	5	304144	4	-0.56	1.39E+10	-0.197
362.089	25145	4	301320	3	-0.49	1.64E+10	-0.233
362.134	34195	6	310336	6	0.14	6.98E+10	0.736
362.149	24441	3	300571	4	-0.78	8.42E+09	0.123
362.171	30361	3	306474	3	-0.33	2.39E+10	-0.216
362.171	41372	2	317485	2	-0.58	1.33E+10	0.204
362.301	25307	2	301320	3	-0.69	1.04E+10	-0.237
362.502	25307	2	301167	2	-0.77	8.55E+09	-0.227
362.554	25145	4	300966	5	-0.8	7.99E+09	-0.231
362.701	53991	4	329700	3	-0.86	7.06E+09	-0.238
362.729	27959	5	303647	5	-0.41	1.97E+10	-0.257
362.818	20495	4	296115	5	-0.45	1.81E+10	-0.279
362.845	27959	5	303559	6	-0.35	2.28E+10	0.558
362.892	21513	6	297077	5	-0.62	1.22E+10	-0.156
363.007	54223	2	329700	3	-0.54	1.47E+10	0.412
363.141	21042	2	296417	3	-0.49	1.65E+10	0.261
363.222	44725	3	320038	4	-0.53	1.48E+10	0.168
363.236	61726	4	337029	5	-0.47	1.70E+10	0.39
363.287	21812	5	297077	5	-0.21	3.11E+10	-0.389

Table A41: Continued

Wavelength	Lower Level	J_{Low}	Upper level	J_{Up}	log gf	gA	CF
363.375	24441	3	299639	4	-0.96	5.57E+09	0.169
363.432	37481	4	312636	3	-0.5	1.61E+10	-0.246
363.5	61726	4	336829	4	0.23	8.62E+10	0.554
363.539	0	4	275074	3	-0.6	1.27E+10	0.362
363.642	30361	3	305357	2	-0.54	1.44E+10	-0.178
363.775	33509	3	308405	2	-0.84	7.33E+09	-0.277
363.913	29660	4	304451	4	-0.36	2.20E+10	-0.183
364.307	25145	4	299639	4	-0.59	1.29E+10	0.172
364.319	29660	4	304144	4	-0.48	1.66E+10	0.161
364.324	37481	4	311962	5	-0.87	6.87E+09	0.204
364.445	21042	2	295431	1	-0.43	1.88E+10	0.267
364.561	21812	5	296115	5	-0.8	7.98E+09	0.125
364.608	2693	3	276960	4	-0.5	1.58E+10	-0.241
364.844	30361	3	304451	4	-0.69	1.02E+10	-0.14
364.868	34195	6	308266	5	-0.61	1.23E+10	-0.287
364.988	21042	2	295023	2	-0.48	1.65E+10	-0.303
364.989	53991	4	327972	4	-0.64	1.16E+10	-0.345
365.037	27959	5	301904	5	-0.07	4.21E+10	0.481
365.235	24441	3	298238	4	-0.61	1.22E+10	-0.208
365.328	24441	3	298168	4	-0.74	9.18E+09	0.235
365.34	55982	3	329700	3	-0.64	1.14E+10	-0.133
365.367	34195	6	307892	6	-0.95	5.56E+09	-0.103
365.551	21812	5	295372	4	-0.44	1.83E+10	-0.231
365.595	53991	4	327517	5	-0.63	1.18E+10	-0.427
365.646	24441	3	297930	2	-0.95	5.60E+09	0.147
365.909	33558	1	306850	2	-0.82	7.59E+09	0.2
366.093	53991	4	327145	4	0.06	5.75E+10	0.368
366.107	25145	4	298289	3	-0.75	8.85E+09	0.153
366.282	53991	4	327004	3	-0.72	9.46E+09	0.128
366.316	41372	2	314360	1	-0.81	7.71E+09	0.178
366.607	37481	4	310253	3	-0.59	1.27E+10	0.138
366.674	41639	0	314360	1	-0.82	7.51E+09	0.328
366.702	33509	3	306210	4	-0.58	1.32E+10	0.258
366.815	25145	4	297762	4	-0.85	6.98E+09	-0.073
367.079	29660	4	302081	4	-0.49	1.59E+10	-0.199
367.165	2693	3	275050	2	-0.94	5.63E+09	0.202
367.194	21513	6	293848	6	0.16	7.11E+10	-0.54
367.586	37481	4	309527	4	-0.98	5.17E+09	-0.081
367.598	21812	5	293848	6	-0.1	3.93E+10	0.487
367.739	25145	4	297077	5	-0.85	7.01E+09	-0.103
368.107	29660	4	301320	3	-0.86	6.79E+09	-0.117
368.367	61726	4	333195	3	-0.56	1.35E+10	0.418
368.396	34195	6	305642	6	0.37	1.16E+11	0.71
368.634	25145	4	296417	3	-0.82	7.52E+09	-0.146
368.782	55982	3	327145	4	-0.39	1.99E+10	-0.373
368.923	41372	2	312432	2	-0.78	8.09E+09	-0.15
369.124	27959	5	298870	5	-0.8	7.72E+09	0.098
369.28	41372	2	312169	3	-0.41	1.88E+10	0.34
369.429	21812	5	292500	4	-0.55	1.40E+10	-0.225
369.543	21513	6	292117	5	0.22	8.17E+10	0.534
369.574	24441	3	295023	2	-0.49	1.58E+10	0.215
369.706	56519	2	327004	3	-0.52	1.47E+10	-0.324
369.952	21812	5	292117	5	-0.98	5.09E+09	0.063
370.083	30361	3	300571	4	-0.94	5.58E+09	-0.097
370.084	27959	5	298168	4	-0.74	8.94E+09	0.129
370.13	27959	5	298134	6	-0.64	1.11E+10	0.123
370.438	44725	3	314675	3	-0.53	1.43E+10	0.185
370.567	37481	4	307338	4	-0.5	1.53E+10	-0.276
370.641	27959	5	297762	4	-0.65	1.09E+10	0.157
370.833	21042	2	290705	3	-0.8	7.75E+09	0.148
370.9	21513	6	291127	7	-0.44	1.76E+10	0.555
371.245	34195	6	303559	6	-0.34	2.22E+10	0.203
371.457	29660	4	298870	5	-0.47	1.63E+10	0.19
371.756	20495	4	289489	3	-0.25	2.74E+10	0.284
371.843	41372	2	310303	2	-0.36	2.11E+10	0.271
371.977	24441	3	293275	2	-0.73	8.93E+09	-0.123
371.991	24441	3	293265	3	-0.85	6.79E+09	-0.065
372.34	33509	3	302081	4	-0.82	7.34E+09	0.381
372.707	20495	4	288802	5	-0.22	2.88E+10	0.377
372.843	20495	4	288704	3	-0.5	1.52E+10	0.184
372.967	25145	4	293265	3	-0.67	1.03E+10	0.137
373.192	25307	2	293265	3	-0.87	6.43E+09	-0.166
373.258	44725	3	312636	3	-0.42	1.84E+10	-0.229
373.4	32651	2	300460	3	-0.8	7.52E+09	0.238
373.476	21812	5	289567	4	-0.26	2.61E+10	0.177
373.537	41372	2	309083	2	-0.71	9.38E+09	0.22
373.568	20495	4	288184	5	-0.78	8.00E+09	-0.164
373.828	56519	2	324022	3	-0.91	5.92E+09	0.306
373.953	27959	5	295372	4	-0.82	7.26E+09	0.135
374.068	21812	5	289143	6	-0.68	9.94E+09	0.296
374.555	53991	4	320974	3	-0.75	8.43E+09	-0.155
374.57	25145	4	292117	5	-0.49	1.55E+10	-0.31
374.59	44725	3	311683	4	-0.52	1.43E+10	0.327
374.994	21513	6	288184	5	-1	4.72E+09	-0.096
375.149	20495	4	287056	3	-0.99	4.86E+09	-0.072
375.593	61726	4	327972	4	-0.58	1.25E+10	0.296
375.757	33509	3	299639	4	-0.99	4.85E+09	-0.243
375.975	24441	3	290416	2	-0.99	4.79E+09	0.076
376.514	21042	2	286636	2	-0.82	7.08E+09	-0.268
376.537	44725	3	310303	2	-0.5	1.49E+10	-0.345
376.607	44725	3	310253	3	-0.48	1.56E+10	-0.195
376.977	30361	3	295629	2	-0.9	5.86E+09	-0.109
377.046	20495	4	285714	4	-0.44	1.71E+10	0.183
377.179	24441	3	289567	4	-0.84	6.75E+09	-0.115
377.343	30361	3	295372	4	-0.66	1.02E+10	0.158
377.37	55982	3	320974	3	-0.42	1.77E+10	0.181
377.402	34195	6	299164	7	-0.56	1.28E+10	0.617
377.484	33509	3	298421	2	-0.71	9.24E+09	0.119
378.056	33558	1	298069	1	-0.93	5.55E+09	-0.145
378.136	56519	2	320974	3	-0.83	6.96E+09	0.213
378.183	25145	4	289567	4	-0.85	6.59E+09	-0.139
378.256	33558	1	297930	2	-0.99	4.77E+09	0.255
378.295	25145	4	289489	3	-0.9	5.82E+09	0.07
378.398	53991	4	318263	5	-0.41	1.80E+10	0.218
378.527	25307	2	289489	3	-0.66	1.03E+10	-0.325

Table A41: Continued

Wavelength	Lower Level	J_{Low}	Upper level	J_{Up}	log gf	gA	CF
378.528	34195	6	298376	7	-0.57	1.25E+10	0.398
378.561	27959	5	292117	5	-0.69	9.55E+09	0.103
378.564	21812	5	285968	5	-0.49	1.50E+10	0.18
378.667	20495	4	284579	3	-0.82	6.98E+09	0.124
378.708	55982	3	320038	4	-0.8	7.35E+09	0.138
378.713	21513	6	285565	6	-0.47	1.59E+10	0.158
380.434	54223	2	317081	3	-0.55	1.30E+10	0.22
380.449	21812	5	284660	4	-0.65	1.05E+10	0.263
380.669	51665	1	314360	1	-0.96	5.06E+09	-0.181
381.014	29660	4	292117	5	-0.79	7.49E+09	-0.178
381.215	51665	1	313984	2	-0.93	5.36E+09	0.141
381.249	61726	4	324022	3	-0.64	1.05E+10	-0.102
381.809	25145	4	287056	3	-0.97	4.93E+09	0.111
382.251	27959	5	289567	4	-0.95	5.18E+09	-0.057
382.406	55982	3	317485	2	-0.92	5.50E+09	-0.118
382.422	53991	4	315482	3	-0.74	8.21E+09	0.092
382.43	44725	3	306210	4	-0.82	6.98E+09	-0.218
382.572	37481	4	298870	5	-0.49	1.48E+10	0.293
382.592	55982	3	317357	4	-0.72	8.60E+09	0.121
383.192	56519	2	317485	2	-0.4	1.79E+10	0.301
383.484	51665	1	312432	2	-0.51	1.42E+10	-0.439
383.694	32651	2	293275	2	-0.9	5.74E+09	0.141
384.127	54223	2	314554	2	-0.89	5.84E+09	0.101
384.346	53991	4	314173	4	-0.99	4.61E+09	-0.042
385.021	44725	3	304451	4	-0.82	6.78E+09	-0.226
385.215	37481	4	297077	5	-0.78	7.43E+09	-0.151
385.334	25145	4	284660	4	-0.74	8.21E+09	-0.107
385.731	61726	4	320974	3	-0.6	1.12E+10	0.147
386.087	51665	1	310674	1	-0.99	4.61E+09	-0.155
386.156	56519	2	315482	3	-0.26	2.44E+10	-0.237
386.559	55982	3	314675	3	-0.77	7.56E+09	0.13
386.63	53991	4	312636	3	-0.86	6.20E+09	0.092
386.71	24441	3	283033	2	-1	4.46E+09	-0.145
386.768	0	4	258553	3	-0.05	3.99E+10	-0.454
387.129	61726	4	320038	4	-0.11	3.45E+10	-0.278
388.19	27959	5	285565	6	-0.58	1.17E+10	0.418
388.809	33509	3	290705	3	-0.56	1.22E+10	0.187
388.996	2693	3	259765	2	-0.37	1.90E+10	-0.352
389.14	53991	4	310968	4	-0.64	1.02E+10	0.167
389.508	3953	2	260687	1	-0.81	6.88E+09	-0.297
389.558	27959	5	284660	4	-0.65	9.92E+09	0.157
389.895	53991	4	310470	4	-0.27	2.34E+10	0.286
389.939	54223	2	310674	1	-0.5	1.39E+10	0.31
389.94	55982	3	312432	2	-0.77	7.39E+09	0.131
390.155	29660	4	285968	5	-0.82	6.69E+09	0.256
390.34	55982	3	312169	3	-0.75	7.74E+09	0.091
390.44	21042	2	277163	2	-0.94	4.99E+09	-0.113
390.838	2693	3	258553	3	-0.64	9.91E+09	0.425
390.913	3953	2	259765	2	-0.55	1.25E+10	0.363
391.013	4941	1	260687	1	-0.67	9.37E+09	0.342
391.615	30361	3	285714	4	-1	4.32E+09	0.223
392.281	29660	4	284579	3	-0.96	4.81E+09	0.082
392.727	61726	4	316356	5	-0.29	2.22E+10	-0.329
393.281	55982	3	310253	3	-0.89	5.50E+09	0.064
395.706	61726	4	314439	5	-0.73	7.95E+09	0.224
398.168	33509	3	284660	4	-0.87	5.72E+09	-0.12
419.945	53991	4	292117	5	-0.93	4.42E+09	-0.298

a: Energy Levels from [43]

Ag VII

Energy Levels

Table A42: Comparison between available experimental data and calculated even energy levels (in cm^{-1}) in Ag VII

E^a_{exp}	E^b_{calc}	Δ E	J	Leading components (in %) in LS Coupling[c]
0	-65	65	2.5	97.5 $4d^5$ (^{6}S) ^{6}S
29390	29381	9	2.5	79.5 $4d^5$ (^{4}G) ^{4}G + 8 $4d^5$ (^{2}F) ^{2}F
30378	30381	-3	3.5	93.1 $4d^5$ (^{4}G) ^{4}G
30662	30668	-6	5.5	96.5 $4d^5$ (^{4}G) ^{4}G
30907	30901	6	4.5	97.4 $4d^5$ (^{4}G) ^{4}G
32005	32063	-58	2.5	44.9 $4d^5$ (^{4}P) ^{4}P + 35 $4d^5$ (^{4}D) ^{4}D + 12.3 $4d^5$ (^{4}G) ^{4}G
32994	33032	-38	1.5	53.6 $4d^5$ (^{4}P) ^{4}P + 43.6 $4d^5$ (^{4}D) ^{4}D
34605	34634	-29	0.5	66.7 $4d^5$ (^{4}P) ^{4}P + 31.9 $4d^5$ (^{4}D) ^{4}D
36485	36493	-8	3.5	91.8 $4d^5$ (^{4}D) ^{4}D
38685	38683	2	0.5	67.8 $4d^5$ (^{4}D) ^{4}D + 31.3 $4d^5$ (^{4}P) ^{4}P
39299	39243	56	2.5	54.3 $4d^5$ (^{4}D) ^{4}D + 31.8 $4d^5$ (^{4}P) ^{4}P + 6.9 $4d^5$ (^{2}D) ^{2}D
39788	39757	31	1.5	53 $4d^5$ (^{4}D) ^{4}D + 43.6 $4d^5$ (^{4}P) ^{4}P
44011	44016	-5	5.5	88.4 $4d^5$ (^{2}I) ^{2}I + 10.4 $4d^5$ (^{2}H) ^{2}H
45546	45543	3	6.5	99.9 $4d^5$ (^{2}I) ^{2}I
47119	47030	89	2.5	31.9 $4d^5$ (^{2}F) ^{2}F + 30.1 $4d^5$ (^{2}D) ^{2}D + 12 $4d^5$ (^{4}P) ^{4}P
48086	48109	-23	1.5	40.8 $4d^5$ (^{2}D) ^{2}D + 43.5 $4d^5$ (^{4}F) ^{4}F + 13.2 $4d^5$ (^{2}D) ^{2}D
48712	48950	-238	3.5	48.8 $4d^5$ (^{4}F) ^{4}F + 23.2 $4d^5$ (^{2}F) ^{2}F + 15.1 $4d^5$ (^{2}G) ^{2}G
49104	49101	3	4.5	59.8 $4d^5$ (^{4}F) ^{4}F + 32.8 $4d^5$ (^{2}G) ^{2}G + 5.3 $4d^5$ (^{2}H) ^{2}H
51049	51141	-92	2.5	75.2 $4d^5$ (^{4}F) ^{4}F + 11.7 $4d^5$ (^{2}F) ^{2}F + 6.8 $4d^5$ (^{2}F) ^{2}F
53353	53174	179	3.5	50 $4d^5$ (^{2}F) ^{2}F + 29.4 $4d^5$ (^{4}F) ^{4}F + 8.8 $4d^5$ (^{2}G) ^{2}G
53796	53836	-40	1.5	53.7 $4d^5$ (^{4}F) ^{4}F + 37.3 $4d^5$ (^{2}D) ^{2}D + 6.2 $4d^5$ (^{2}D) ^{2}D
53797	53768	29	4.5	52.3 $4d^5$ (^{2}H) ^{2}H + 29 $4d^5$ (^{4}F) ^{4}F + 18.5 $4d^5$ (^{2}G) ^{2}G
55773	55969	-196	3.5	73.3 $4d^5$ (^{2}G) ^{2}G + 19.4 $4d^5$ (^{2}F) ^{2}F + 5.6 $4d^5$ (^{2}F) ^{2}F
57413	56937	476	2.5	48.9 $4d^5$ (^{2}F) ^{2}F + 20 $4d^5$ (^{2}D) ^{2}D + 19 $4d^5$ (^{2}F) ^{2}F
57962	57884	78	5.5	86.3 $4d^5$ (^{2}H) ^{2}H + 11.3 $4d^5$ (^{2}I) ^{2}I
59223	59186	37	4.5	47.7 $4d^5$ (^{2}G) ^{2}G + 41.4 $4d^5$ (^{2}H) ^{2}H + 9.6 $4d^5$ (^{4}F) ^{4}F
59792	59608	184	3.5	77.3 $4d^5$ (^{2}F) ^{2}F + 15.8 $4d^5$ (^{4}F) ^{4}F
59954	60469	-515	2.5	17.1 $4d^5$ (^{2}D) ^{2}D + 34.3 $4d^5$ (^{2}F) ^{2}F + 28.7 $4d^5$ (^{2}F) ^{2}F
71517	71544	-27	1.5	97.3 $4d^5$ (^{2}D) ^{2}D
72934	72951	-17	2.5	90.8 $4d^5$ (^{2}D) ^{2}D + 6.5 $4d^5$ (^{2}F) ^{2}F
79131	79127	4	4.5	98.8 $4d^5$ (^{2}G) ^{2}G
79705	79729	-24	3.5	96.1 $4d^5$ (^{2}G) ^{2}G
103996	103917	79	2.5	79.5 $4d^5$ (^{2}D) ^{2}D + 19.2 $4d^5$ (^{2}D) ^{2}D
104821	104832	-11	1.5	74 $4d^5$ (^{2}D) ^{2}D + 18.1 $4d^5$ (^{2}D) ^{2}D

a: From Ryabtsev [45]
b: This work
c: Only the component ≥ 5% are given

Table A43: Comparison between available experimental data and calculated odd energy levels (in cm^{-1}) in Ag VII

E^a_{exp}	E^b_{calc}	Δ E	J	Leading components (in %) in LS Coupling^c
331200	331234	-34	1.5	39.8 4d^{4}5p (^{5}D) ^{4}P + 29.8 4d^{4}5p (^{5}D) ^{6}D + 24.8 4d^{4}5p (^{5}D) ^{6}P
333327	333186	141	2.5	62.5 4d^{4}5p (^{5}D) ^{6}P + 16.9 4d^{4}5p (^{5}D) ^{4}P + 15.9 4d^{4}5p (^{5}D) ^{6}D
334906	334682	224	3.5	85.5 4d^{4}5p (^{5}D) ^{6}P + 5.9 4d^{4}5p (^{5}D) ^{6}D
336333	336133	200	1.5	69.4 4d^{4}5p (^{5}D) ^{6}P + 17 4d^{4}5p (^{5}D) ^{6}D + 6.7 4d^{4}5p (^{5}D) ^{4}P
339172	339057	115	2.5	51.3 4d^{4}5p (^{5}D) ^{6}D + 28.1 4d^{4}5p (^{5}D) ^{6}P + 8.8 4d^{4}5p (^{5}D) ^{4}P
341227	341268	-41	0.5	64.6 4d^{4}5p (^{5}D) ^{6}D + 29.8 4d^{4}5p (^{5}D) ^{4}P + 1.5 4d^{4}5p (^{1}P) ^{1}S
341458	341405	53	3.5	61.6 4d^{4}5p (^{5}D) ^{6}D + 17.1 4d^{4}5p (^{5}D) ^{4}F + 11 4d^{4}5p (^{5}D) ^{6}F
341983	342086	-103	1.5	30.5 4d^{4}5p (^{5}D) ^{4}P + 29.7 4d^{4}5p (^{5}D) ^{6}D +
342289	342228	61	4.5	42.6 4d^{4}5p (^{5}D) ^{6}D + 24.8 4d^{4}5p (^{5}D) ^{6}F + 24.7 4d^{4}5p (^{5}D) ^{4}F
343336	343453	-117	2.5	38.7 4d^{4}5p (^{5}D) ^{4}F + 35.8 4d^{4}5p (^{5}D) ^{4}P + 5.3 4d^{4}5p (^{5}D) ^{6}P
344695	344814	-119	2.5	27.5 4d^{4}5p (^{5}D) ^{4}P + 35.7 4d^{4}5p (^{5}D) ^{4}F + 25.4 4d^{4}5p (^{5}D) ^{6}D
346061	346197	-136	3.5	55.9 4d^{4}5p (^{5}D) ^{4}F + 26.2 4d^{4}5p (^{5}D) ^{6}D
348377	348494	-117	4.5	28.8 4d^{4}5p (^{5}D) ^{4}F + 41.1 4d^{4}5p (^{5}D) ^{6}D + 5.5 4d^{4}5p (^{3}H) ^{4}I
349047	349139	-92	3.5	47.5 4d^{4}5p (^{3}H) ^{4}H + 22.5 4d^{4}5p (^{3}G) ^{4}H + 9.2 4d^{4}5p (^{3}H) ^{2}G
349721	349800	-79	4.5	0.7 4d^{4}5p (^{1}G) ^{2}H + 27.4 4d^{4}5p (^{3}H) ^{4}I + 25.6 4d^{4}5p (^{3}H) ^{4}H
352082	352117	-35	5.5	38.6 4d^{4}5p (^{3}H) ^{4}H + 31.4 4d^{4}5p (^{3}H) ^{4}I + 17.1 4d^{4}5p (^{3}G) ^{4}H
352270	352276	-6	0.5	75.9 4d^{4}5p (^{5}D) ^{4}D + 9.6 4d^{4}5p (^{1}P) ^{4}D
352685	352838	-153	2.5	25.4 4d^{4}5p (^{3}G) ^{4}G + 22.7 4d^{4}5p (^{3}F) ^{4}G + 14 4d^{4}5p (^{3}F) ^{4}G
353454	353591	-137	3.5	17.3 4d^{4}5p (^{3}H) ^{2}G + 20 4d^{4}5p (^{3}G) ^{4}H + 9 4d^{4}5p (^{3}F) ^{4}G
353549	353519	30	1.5	44.8 4d^{4}5p (^{5}D) ^{4}D + 21.2 4d^{4}5p (^{1}P) ^{4}D + 7.5 4d^{4}5p (^{1}P) ^{4}D
354122	354127	-5	4.5	12.3 4d^{4}5p (^{3}H) ^{2}G + 29.7 4d^{4}5p (^{3}H) ^{4}H + 15.7 4d^{4}5p (^{3}H) ^{4}I
354235	354195	40	2.5	76 4d^{4}5p (^{5}D) ^{4}D + 3.9 4d^{4}5p (^{3}D) ^{4}D + 2.5 4d^{4}5p (^{3}F) ^{4}F
354719	354727	-8	6.5	47.6 4d^{4}5p (^{3}H) ^{4}H + 25.3 4d^{4}5p (^{3}H) ^{4}I + 12.8 4d^{4}5p (^{3}H) ^{2}I
354869	354843	26	3.5	66.2 4d^{4}5p (^{5}D) ^{4}D + 6.1 4d^{4}5p (^{3}F) ^{4}F + 5.2 4d^{4}5p (^{3}D) ^{4}D
355790	355539	251	0.5	32.4 4d^{4}5p (^{1}P) ^{4}P + 14.8 4d^{4}5p (^{1}P) ^{4}P + 12.7 4d^{4}5p (^{1}P) ^{1}S
356233	356215	18	2.5	14.2 4d^{4}5p (^{3}F) ^{4}D + 13.4 4d^{4}5p (^{1}P) ^{4}D + 13.1 4d^{4}5p (^{3}F) ^{4}G
356416	356440	-24	4.5	31.7 4d^{4}5p (^{3}H) ^{4}I + 11.2 4d^{4}5p (^{3}G) ^{4}H + 10.7 4d^{4}5p (^{3}G) ^{4}G
356493	356663	-170	3.5	16.5 4d^{4}5p (^{3}F) ^{4}D + 11.8 4d^{4}5p (^{5}D) ^{4}D + 11.1 4d^{4}5p (^{3}G) ^{4}G
356993	356957	36	1.5	19.9 4d^{4}5p (^{3}F) ^{2}D + 19.1 4d^{4}5p (^{3}F) ^{4}F + 8.9 4d^{4}5p (^{3}F) ^{2}D
357689	357575	114	5.5	45 4d^{4}5p (^{3}H) ^{4}G + 12.8 4d^{4}5p (^{3}H) ^{2}H + 12.2 4d^{4}5p (^{3}H) ^{4}H
358392	358321	71	2.5	21.4 4d^{4}5p (^{3}F) ^{4}G + 11.5 4d^{4}5p (^{3}G) ^{2}F + 9.5 4d^{4}5p (^{1}P) ^{4}D
359687	359756	-69	3.5	6.3 4d^{4}5p (^{3}F) ^{2}G + 17.7 4d^{4}5p (^{3}G) ^{4}G + 13.2 4d^{4}5p (^{3}H) ^{4}G
360092	360121	-29	1.5	37.9 4d^{4}5p (^{1}P) ^{4}P + 14.3 4d^{4}5p (^{1}P) ^{4}P + 10.3 4d^{4}5p (^{3}D) ^{4}D
360481	360323	158	5.5	50.6 4d^{4}5p (^{3}H) ^{4}I + 14.8 4d^{4}5p (^{3}G) ^{4}G + 14 4d^{4}5p (^{3}H) ^{4}H
360482	360532	-50	4.5	17.6 4d^{4}5p (^{3}F) ^{4}G + 13.5 4d^{4}5p (^{3}G) ^{4}F + 12.3 4d^{4}5p (^{3}F) ^{4}F
361173	361035	138	3.5	40.2 4d^{4}5p (^{3}F) ^{4}G + 13.6 4d^{4}5p (^{3}H) ^{4}G + 10.1 4d^{4}5p (^{3}G) ^{4}H
361296	361402	-106	2.5	27.1 4d^{4}5p (^{3}F) ^{4}F + 10 4d^{4}5p (^{3}F) ^{2}D + 9.5 4d^{4}5p (^{3}G) ^{4}F
361593	361784	-191	3.5	25.4 4d^{4}5p (^{3}G) ^{4}F + 19.1 4d^{4}5p (^{3}D) ^{4}F + 8.9 4d^{4}5p (^{5}D) ^{4}F
361650	361610	40	4.5	32.1 4d^{4}5p (^{3}H) ^{4}G + 23.1 4d^{4}5p (^{3}G) ^{4}G + 11.2 4d^{4}5p (^{3}F) ^{2}G
362381	362524	-143	2.5	4.5 4d^{4}5p (^{1}D) ^{2}F + 18.1 4d^{4}5p (^{3}H) ^{4}G + 12.2 4d^{4}5p (^{3}D) ^{2}F
362447	362541	-94	4.5	22.3 4d^{4}5p (^{3}H) ^{4}H + 27.4 4d^{4}5p (^{3}G) ^{4}F + 7.8 4d^{4}5p (^{3}G) ^{4}H
362535	362582	-47	5.5	34.8 4d^{4}5p (^{3}H) ^{2}I + 16.3 4d^{4}5p (^{3}F) ^{4}G + 10.8 4d^{4}5p (^{3}G) ^{2}H
362942	363039	-97	3.5	25.2 4d^{4}5p (^{3}G) ^{4}H + 24.4 4d^{4}5p (^{3}H) ^{4}H + 9.5 4d^{4}5p (^{3}H) ^{2}G
362975	362853	122	2.5	23.8 4d^{4}5p (^{1}P) ^{4}D + 18.6 4d^{4}5p (^{3}G) ^{4}F + 12.1 4d^{4}5p (^{1}P) ^{4}D
363454	363574	-120	1.5	32.2 4d^{4}5p (^{3}D) ^{4}F + 31.4 4d^{4}5p (^{3}G) ^{4}F + 10.8 4d^{4}5p (^{1}P) ^{4}P
363614	363422	192	6.5	53.1 4d^{4}5p (^{3}H) ^{4}I + 37.1 4d^{4}5p (^{3}H) ^{4}H
364025	364158	-133	2.5	15.1 4d^{4}5p (^{3}D) ^{4}P + 17.6 4d^{4}5p (^{3}D) ^{2}D + 8 4d^{4}5p (^{3}F) ^{2}D
364518	364445	73	6.5	35.8 4d^{4}5p (^{3}H) ^{2}I + 23.6 4d^{4}5p (^{3}G) ^{4}H + 14.7 4d^{4}5p (^{3}H) ^{4}I
364772	364791	-19	4.5	18.9 4d^{4}5p (^{3}G) ^{4}F + 16.9 4d^{4}5p (^{3}F) ^{4}G + 12.7 4d^{4}5p (^{3}H) ^{2}G
364877	364893	-16	2.5	0.2 4d^{4}5p (^{3}F) ^{2}D + 19.2 4d^{4}5p (^{1}P) ^{4}P + 13 4d^{4}5p (^{1}P) ^{4}P
365017	365102	-85	5.5	21.5 4d^{4}5p (^{3}G) ^{4}H + 28.1 4d^{4}5p (^{3}H) ^{4}H + 17.5 4d^{4}5p (^{3}G) ^{2}H
365569	365533	36	4.5	43.6 4d^{4}5p (^{3}F) ^{4}F + 9.3 4d^{4}5p (^{3}G) ^{2}H + 7.7 4d^{4}5p (^{3}H) ^{2}H
365842	366094	-252	3.5	19.8 4d^{4}5p (^{3}F) ^{4}F + 14 4d^{4}5p (^{3}F) ^{2}G + 13.6 4d^{4}5p (^{3}D) ^{2}F
366078	365947	131	1.5	16.7 4d^{4}5p (^{1}P) ^{4}S + 15.1 4d^{4}5p (^{1}P) ^{4}S + 14.2 4d^{4}5p (^{3}F) ^{4}F
366573	366477	96	1.5	27.2 4d^{4}5p (^{3}F) ^{4}F + 13.5 4d^{4}5p (^{3}F) ^{4}D + 10.7 4d^{4}5p (^{3}F) ^{2}D
366693	366575	118	2.5	9.1 4d^{4}5p (^{3}G) ^{4}F + 13.5 4d^{4}5p (^{3}F) ^{4}D + 12 4d^{4}5p (^{3}D) ^{4}D
366806	366568	238	3.5	9.7 4d^{4}5p (^{3}H) ^{4}G + 21.2 4d^{4}5p (^{3}F) ^{4}F + 13.2 4d^{4}5p (^{3}G) ^{4}F
367483	367392	91	5.5	40.3 4d^{4}5p (^{3}F) ^{4}G + 21 4d^{4}5p (^{3}H) ^{2}I + 9.7 4d^{4}5p (^{3}G) ^{4}H
367919	367657	262	2.5	19.9 4d^{4}5p (^{1}P) ^{4}P + 25.6 4d^{4}5p (^{3}D) ^{4}P + 9.4 4d^{4}5p (^{3}G) ^{4}G
368429	368357	72	4.5	26 4d^{4}5p (^{3}G) ^{4}H + 15.6 4d^{4}5p (^{3}F) ^{4}G + 13.6 4d^{4}5p (^{3}H) ^{2}H
368569	368583	-14	1.5	23 4d^{4}5p (^{3}F) ^{4}D + 9.3 4d^{4}5p (^{3}D) ^{4}F + 7.2 4d^{4}5p (^{3}D) ^{4}D
368968	368955	13	3.5	7.1 4d^{4}5p (^{3}F) ^{2}F + 20.7 4d^{4}5p (^{1}P) ^{4}D + 12.1 4d^{4}5p (^{1}P) ^{4}D
369448	369389	59	1.5	0.2 4d^{4}5p (^{1}D) ^{2}D + 29.2 4d^{4}5p (^{3}D) ^{4}P + 20.9 4d^{4}5p (^{3}D) ^{4}D
369578	369476	102	2.5	20 4d^{4}5p (^{3}F) ^{2}F + 14 4d^{4}5p (^{3}D) ^{4}P + 13.4 4d^{4}5p (^{3}H) ^{4}G
369654	369608	46	6.5	39.3 4d^{4}5p (^{1}I) ^{2}K + 22.9 4d^{4}5p (^{1}I) ^{2}I + 18.4 4d^{4}5p (^{3}H) ^{2}I
369661	369528	133	5.5	33.7 4d^{4}5p (^{1}I) ^{2}I + 19.9 4d^{4}5p (^{3}H) ^{2}I + 15.9 4d^{4}5p (^{3}H) ^{2}H
369879	369757	122	3.5	23.4 4d^{4}5p (^{1}P) ^{4}D + 12.7 4d^{4}5p (^{3}D) ^{4}F + 9.2 4d^{4}5p (^{3}H) ^{4}G
370488	370544	-56	5.5	17.4 4d^{4}5p (^{3}G) ^{2}H + 21.1 4d^{4}5p (^{3}G) ^{4}H + 19 4d^{4}5p (^{3}G) ^{4}G
370501	370601	-100	4.5	12.6 4d^{4}5p (^{3}H) ^{2}H + 11.1 4d^{4}5p (^{3}G) ^{2}G + 9.6 4d^{4}5p (^{3}F) ^{2}G
370993	371099	-106	3.5	25.3 4d^{4}5p (^{3}G) ^{2}F + 30 4d^{4}5p (^{3}F) ^{2}F + 10 4d^{4}5p (^{3}G) ^{4}G
371061	371084	-23	4.5	23.8 4d^{4}5p (^{3}G) ^{2}H + 17 4d^{4}5p (^{3}H) ^{2}H + 11.3 4d^{4}5p (^{3}H) ^{4}G
371408.6	371168	240.6	1.5	25.4 4d^{4}5p (^{1}P) ^{2}D + 14.7 4d^{4}5p (^{1}P) ^{2}P + 12.7 4d^{4}5p (^{1}P) ^{2}D
371673	371750	-77	3.5	21.4 4d^{4}5p (^{3}G) ^{4}G + 20.9 4d^{4}5p (^{1}G) ^{2}F + 8 4d^{4}5p (^{3}F) ^{2}G
372051	372060	-9	2.5	21.6 4d^{4}5p (^{3}H) ^{4}G + 18.5 4d^{4}5p (^{3}F) ^{2}F + 17.6 4d^{4}5p (^{3}G) ^{4}G
372676	372533	143	5.5	46.4 4d^{4}5p (^{3}H) ^{2}H + 16.1 4d^{4}5p (^{1}I) ^{2}H + 12.4 4d^{4}5p (^{1}I) ^{2}I
372822	372804	18	6.5	51.1 4d^{4}5p (^{3}G) ^{4}H + 29.2 4d^{4}5p (^{3}H) ^{2}I + 7.9 4d^{4}5p (^{3}H) ^{4}H
373120	373163	-43	4.5	21 4d^{4}5p (^{3}G) ^{4}G + 14.2 4d^{4}5p (^{3}H) ^{2}H + 11.1 4d^{4}5p (^{3}G) ^{2}H
373577	373728	-151	3.5	4.1 4d^{4}5p (^{1}F) ^{2}G + 13.2 4d^{4}5p (^{3}F) ^{4}D + 12.6 4d^{4}5p (^{3}D) ^{4}D
374236	374163	73	1.5	28.8 4d^{4}5p (^{3}D) ^{4}P + 14.4 4d^{4}5p (^{3}G) ^{4}F + 6.2 4d^{4}5p (^{3}D) ^{4}F
374426	374536	-110	2.5	10.7 4d^{4}5p (^{1}P) ^{2}D + 14.3 4d^{4}5p (^{3}G) ^{4}F + 10.5 4d^{4}5p (^{1}G) ^{2}F
374810	374945	-135	0.5	13.5 4d^{4}5p (^{1}S) ^{2}P + 24.9 4d^{4}5p (^{3}D) ^{4}P + 21.7 4d^{4}5p (^{1}P) ^{2}P
374839	374990	-151	3.5	16.1 4d^{4}5p (^{1}G) ^{2}F + 12.2 4d^{4}5p (^{3}H) ^{4}G + 11.3 4d^{4}5p (^{3}G) ^{2}G
374938	375158	-220	1.5	13.1 4d^{4}5p (^{3}G) ^{4}F + 23.2 4d^{4}5p (^{3}D) ^{2}P + 13.6 4d^{4}5p (^{3}D) ^{4}F
375365	375452	-87	3.5	34.1 4d^{4}5p (^{3}G) ^{2}G + 9.6 4d^{4}5p (^{3}D) ^{4}D + 8.5 4d^{4}5p (^{3}D) ^{2}F
375489	375543	-54	0.5	46.2 4d^{4}5p (^{3}D) ^{4}P + 12.3 4d^{4}5p (^{1}P) ^{2}P + 11.4 4d^{4}5p (^{3}D) ^{4}D
375593	375771	-178	4.5	53.1 4d^{4}5p (^{3}D) ^{4}F + 15.6 4d^{4}5p (^{3}G) ^{2}G + 8.7 4d^{4}5p (^{3}H) ^{2}G
375706	375782	-76	1.5	30.9 4d^{4}5p (^{3}D) ^{4}D + 11.3 4d^{4}5p (^{3}D) ^{4}F + 10.5 4d^{4}5p (^{1}D) ^{2}D
376414	376391	23	5.5	30.7 4d^{4}5p (^{3}G) ^{4}G + 23.3 4d^{4}5p (^{3}G) ^{2}H + 17.8 4d^{4}5p (^{3}H) ^{4}G
376419	376319	100	6.5	54.5 4d^{4}5p (^{1}I) ^{2}I + 38.4 4d^{4}5p (^{1}I) ^{2}K
376543	376660	-117	2.5	21.9 4d^{4}5p (^{3}D) ^{4}F + 16.6 4d^{4}5p (^{3}D) ^{4}D + 10 4d^{4}5p (^{1}F) ^{2}F
377163	377194	-31	3.5	27.6 4d^{4}5p (^{3}D) ^{4}F + 17.9 4d^{4}5p (^{3}D) ^{4}D + 17.1 4d^{4}5p (^{3}G) ^{4}F
377393	377538	-145	4.5	22 4d^{4}5p (^{3}F) ^{2}G + 13.2 4d^{4}5p (^{3}H) ^{2}G + 10.5 4d^{4}5p (^{1}G) ^{2}H

Table A43: Continued

E^a_{exp}	E^b_{calc}	Δ E	J	Leading components (in %) in LS Coupling^c
377717	377724	-7	5.5	24.6 $4d^45p$ (^{1}I) ^{2}H + 36.1 $4d^45p$ (^{1}G) ^{2}H + 15.4 $4d^45p$ (^{3}G) ^{2}H
377910	377954	-44	1.5	20.6 $4d^45p$ (^{3}D) ^{2}P + 18.8 $4d^45p$ (^{1}S) ^{2}P + 16 $4d^45p$ (^{1}D) ^{2}P
378355	378275	80	7.5	93.7 $4d^45p$ (^{1}I) ^{2}K + 6.1 $4d^45p$ (^{3}H) ^{4}I
379061	379296	-235	3.5	0.1 $4d^45p$ (^{3}D) ^{4}D + 21.8 $4d^45p$ (^{1}F) ^{2}F + 18 $4d^45p$ (^{1}G) ^{2}G
379077	378813	264	2.5	15.4 $4d^45p$ (^{1}F) ^{2}F + 23.8 $4d^45p$ (^{1}P) ^{2}D + 13.7 $4d^45p$ (^{1}D) ^{2}D
379226	379363	-137	4.5	21.8 $4d^45p$ (^{3}G) ^{2}G + 12.2 $4d^45p$ (^{3}G) ^{4}F + 11 $4d^45p$ (^{1}G) ^{2}H
379478	379137	341	2.5	26.1 $4d^45p$ (^{3}G) ^{2}F + 22.2 $4d^45p$ (^{1}D) ^{2}F + 17.7 $4d^45p$ (^{1}F) ^{2}F
380468	380499	-31	3.5	12.4 $4d^45p$ (^{3}D) ^{2}F + 18.6 $4d^45p$ (^{3}G) ^{2}G + 15.5 $4d^45p$ (^{1}F) ^{2}F
380891	381139	-248	2.5	31.3 $4d^45p$ (^{1}G) ^{2}F + 21 $4d^45p$ (^{3}D) ^{2}D + 8.2 $4d^45p$ (^{3}F) ^{2}F
382377	382360	17	4.5	53.2 $4d^45p$ (^{1}I) ^{2}H + 11.5 $4d^45p$ (^{3}G) ^{2}H + 9.1 $4d^45p$ (^{1}G) ^{2}H
382720	383056	-336	4.5	34.1 $4d^45p$ (^{1}G) ^{2}G + 20.8 $4d^45p$ (^{1}G) ^{2}G + 12.2 $4d^45p$ (^{3}G) ^{2}G
383109	383073	36	2.5	24.2 $4d^45p$ (^{3}D) ^{2}F + 9 $4d^45p$ (^{1}F) ^{2}F + 7.2 $4d^45p$ (^{1}D) ^{2}F
383280	383295	-15	1.5	42.7 $4d^45p$ (^{3}D) ^{2}D + 18.1 $4d^45p$ (^{3}F) ^{2}D + 10.8 $4d^45p$ (^{1}D) ^{2}D
383539	383678	-139	5.5	23.5 $4d^45p$ (^{1}G) ^{2}H + 22.3 $4d^45p$ (^{1}I) ^{2}H + 17.3 $4d^45p$ (^{1}G) ^{2}H
384772	384719	53	3.5	27.9 $4d^45p$ (^{1}D) ^{2}F + 17.2 $4d^45p$ (^{1}G) ^{2}G + 8.8 $4d^45p$ (^{3}F) ^{2}F
385962	385733	229	2.5	19.3 $4d^45p$ (^{1}D) ^{2}D + 14.3 $4d^45p$ (^{3}D) ^{2}F + 9.8 $4d^45p$ (^{1}D) ^{2}F
386268	386031	237	2.5	16.6 $4d^45p$ (^{3}D) ^{2}D + 14.1 $4d^45p$ (^{3}F) ^{2}D + 10.7 $4d^45p$ (^{3}D) ^{2}F
386582	386882	-300	1.5	4.7 $4d^45p$ (^{1}P) ^{4}P + 19 $4d^45p$ (^{1}S) ^{2}P + 9.9 $4d^45p$ (^{3}F) ^{4}F
386615	386397	218	3.5	23.4 $4d^45p$ (^{1}F) ^{2}F + 23.7 $4d^45p$ (^{1}F) ^{2}G + 5.6 $4d^45p$ (^{3}F) ^{4}F
388163	387921	242	3.5	9.8 $4d^45p$ (^{1}G) ^{2}G + 25.4 $4d^45p$ (^{1}F) ^{2}G + 16.5 $4d^45p$ (^{3}D) ^{2}F
389293	389304	-11	1.5	46.9 $4d^45p$ (^{3}F) ^{4}F + 7.9 $4d^45p$ (^{1}P) ^{4}D + 6.3 $4d^45p$ (^{3}F) ^{4}D
390060	390159	-99	2.5	37.1 $4d^45p$ (^{3}F) ^{4}F + 12.3 $4d^45p$ (^{1}P) ^{4}D + 6.5 $4d^45p$ (^{3}F) ^{4}D
390759	390631	128	4.5	46.5 $4d^45p$ (^{1}F) ^{2}G + 29.4 $4d^45p$ (^{3}F) ^{4}F + 5 $4d^45p$ (^{3}F) ^{2}G
391338	391254	84	3.5	45.5 $4d^45p$ (^{3}F) ^{4}F + 11 $4d^45p$ (^{1}D) ^{2}F + 10.2 $4d^45p$ (^{3}F) ^{4}G
391396	391582	-186	2.5	31.1 $4d^45p$ (^{3}F) ^{4}G + 11.7 $4d^45p$ (^{3}F) ^{4}G + 10.9 $4d^45p$ (^{3}F) ^{2}F
391553	391584	-31	1.5	19.8 $4d^45p$ (^{1}P) ^{4}D + 13.8 $4d^45p$ (^{1}P) ^{4}D + 12.7 $4d^45p$ (^{3}F) ^{2}D
392424	392447	-23	0.5	38.1 $4d^45p$ (^{1}P) ^{4}D + 20.9 $4d^45p$ (^{1}P) ^{4}D + 10.2 $4d^45p$ (^{1}P) ^{4}P
392486	392444	42	4.5	28.3 $4d^45p$ (^{3}F) ^{4}G + 19.8 $4d^45p$ (^{1}F) ^{2}G + 18.5 $4d^45p$ (^{3}F) ^{4}F
393295	393268	27	3.5	15.9 $4d^45p$ (^{3}F) ^{4}D + 22.8 $4d^45p$ (^{3}F) ^{4}G + 12.2 $4d^45p$ (^{3}F) ^{2}F
393610	393485	125	1.5	19.9 $4d^45p$ (^{1}D) ^{2}P + 15.1 $4d^45p$ (^{1}P) ^{4}P + 9.1 $4d^45p$ (^{1}S) ^{2}P
394049	393914	135	2.5	11.9 $4d^45p$ (^{1}P) ^{4}D + 29 $4d^45p$ (^{3}F) ^{4}F + 20.8 $4d^45p$ (^{1}F) ^{2}D
396241	396260	-19	3.5	31.4 $4d^45p$ (^{1}P) ^{4}D + 20.5 $4d^45p$ (^{3}F) ^{2}F + 13.8 $4d^45p$ (^{1}P) ^{4}D
397858	397829	29	3.5	25.5 $4d^45p$ (^{3}F) ^{4}G + 22.3 $4d^45p$ (^{3}F) ^{4}F + 9.1 $4d^45p$ (^{3}F) ^{4}G
398431	398374	57	4.5	37.2 $4d^45p$ (^{3}F) ^{4}F + 24.8 $4d^45p$ (^{3}F) ^{4}G + 7.8 $4d^45p$ (^{1}G) ^{2}H
398662	398784	-122	2.5	28.6 $4d^45p$ (^{3}F) ^{2}F + 20.5 $4d^45p$ (^{3}F) ^{4}G + 7.1 $4d^45p$ (^{3}F) ^{4}G
399022	399065	-43	5.5	77.6 $4d^45p$ (^{3}F) ^{4}G + 14.1 $4d^45p$ (^{3}F) ^{4}G
399850	399834	16	1.5	9.4 $4d^45p$ (^{1}P) ^{2}D + 40.4 $4d^45p$ (^{1}F) ^{2}D + 13.7 $4d^45p$ (^{3}F) ^{2}D
400637	400577	60	2.5	24.2 $4d^45p$ (^{1}F) ^{2}D + 14.3 $4d^45p$ (^{3}F) ^{2}F + 9.5 $4d^45p$ (^{1}P) ^{4}D
401561	401542	19	4.5	33 $4d^45p$ (^{1}G) ^{2}H + 13.7 $4d^45p$ (^{1}G) ^{2}G + 13.6 $4d^45p$ (^{1}G) ^{2}H
403133	402978	155	3.5	19.7 $4d^45p$ (^{1}G) ^{2}G + 20.8 $4d^45p$ (^{3}F) ^{4}D + 9.6 $4d^45p$ (^{1}P) ^{4}D
403942	404038	-96	4.5	50.5 $4d^45p$ (^{3}F) ^{2}G + 11.7 $4d^45p$ (^{3}F) ^{2}G + 10.3 $4d^45p$ (^{3}F) ^{4}G
404117	404172	-55	3.5	27.5 $4d^45p$ (^{3}F) ^{2}F + 22.3 $4d^45p$ (^{3}F) ^{4}D + 6.8 $4d^45p$ (^{1}G) ^{2}G
406495	406657	-162	3.5	46.4 $4d^45p$ (^{3}F) ^{2}G + 17 $4d^45p$ (^{3}F) ^{2}G + 12.3 $4d^45p$ (^{1}G) ^{2}G
406673	406743	-70	0.5	35.7 $4d^45p$ (^{3}F) ^{4}D + 18.4 $4d^45p$ (^{3}F) ^{4}D + 14.8 $4d^45p$ (^{1}P) ^{2}P
409186	409360	-174	2.5	51.4 $4d^45p$ (^{1}G) ^{2}F + 19.4 $4d^45p$ (^{1}D) ^{2}F + 7.6 $4d^45p$ (^{3}F) ^{2}F
409441	409324	117	5.5	64.4 $4d^45p$ (^{1}G) ^{2}H + 25.2 $4d^45p$ (^{1}G) ^{2}H + 5.3 $4d^45p$ (^{1}I) ^{2}H
409779	409465	314	4.5	34 $4d^45p$ (^{1}G) ^{2}G + 16.7 $4d^45p$ (^{1}G) ^{2}G + 16.5 $4d^45p$ (^{1}G) ^{2}H
409889	409800	89	3.5	40.4 $4d^45p$ (^{1}G) ^{2}F + 12.6 $4d^45p$ (^{1}G) ^{2}G + 9.3 $4d^45p$ (^{3}F) ^{2}G
414230	414194	36	2.5	47 $4d^45p$ (^{3}F) ^{2}D + 16.5 $4d^45p$ (^{3}F) ^{2}D + 13 $4d^45p$ (^{1}P) ^{2}D
422985	422971	14	2.5	43.8 $4d^45p$ (^{1}D) ^{2}F + 16.1 $4d^45p$ (^{1}G) ^{2}F + 12.6 $4d^45p$ (^{1}G) ^{2}F
428522	428612	-90	3.5	70.1 $4d^45p$ (^{1}D) ^{2}F + 15.5 $4d^45p$ (^{1}D) ^{2}F + 6.7 $4d^45p$ (^{1}G) ^{2}F

From Ryabtsev [45]
b: This work
c: Only the component ≥ 5% are given

Transitions

Table A44: Computed oscillator strengths and transition probabilities Ag VII.

Wavelength Å	Lower Level[a] cm^{-1}	J_{Low}	Upper level[a] cm^{-1}	J_{Up}	log gf	gA s^{-1}	CF
284.239	57962	5.5	409779	4.5	-0.17	5.60E+10	-0.218
284.512	57962	5.5	409441	5.5	-0.93	9.72E+09	-0.088
285.172	59223	4.5	409889	3.5	-0.44	2.96E+10	0.251
285.725	59792	3.5	409779	4.5	-0.75	1.47E+10	-0.287
286.212	79131	4.5	428522	3.5	-0.3	4.12E+10	0.281
286.257	53797	4.5	403133	3.5	-0.65	1.82E+10	-0.101
286.265	49104	4.5	398431	4.5	-1	8.12E+09	-0.059
286.735	49104	4.5	397858	3.5	-0.79	1.32E+10	-0.171
287.949	53353	3.5	400637	2.5	-0.92	9.73E+09	0.063
288.071	49104	4.5	396241	3.5	-0.91	9.80E+09	0.076
289.034	57962	5.5	403942	4.5	-0.96	8.71E+09	0.031
289.572	48712	3.5	394049	2.5	-0.86	1.10E+10	-0.096
289.913	30662	5.5	375593	4.5	-0.87	1.08E+10	-0.112
289.944	59223	4.5	404117	3.5	-0.88	1.06E+10	-0.086
290.163	53797	4.5	398431	4.5	-0.37	3.41E+10	-0.313
290.536	49104	4.5	393295	3.5	-0.76	1.37E+10	0.111
291.307	79705	3.5	422985	2.5	-0.78	1.30E+10	0.112
291.814	48712	3.5	391396	2.5	-0.95	8.83E+09	0.101
291.863	48712	3.5	391338	3.5	-0.65	1.77E+10	-0.117
291.919	51049	2.5	393610	1.5	-0.77	1.34E+10	0.275
292.019	53797	4.5	396241	3.5	-0.3	3.89E+10	0.354
292.261	30662	5.5	372822	6.5	-0.52	2.36E+10	0.45
292.693	49104	4.5	390759	4.5	-0.22	4.69E+10	-0.332
293.077	48086	1.5	389293	1.5	-0.88	1.02E+10	-0.135
293.388	59792	3.5	400637	2.5	-0.56	2.11E+10	0.162
293.517	53353	3.5	394049	2.5	-0.6	1.96E+10	-0.192
293.682	51049	2.5	391553	1.5	-0.72	1.47E+10	0.178
293.712	57962	5.5	398431	4.5	-0.6	1.94E+10	0.351
293.868	51049	2.5	391338	3.5	-0.85	1.08E+10	0.194
294.208	59954	2.5	399850	1.5	-0.73	1.45E+10	0.102
294.553	53797	4.5	393295	3.5	-0.71	1.50E+10	0.181
294.804	59223	4.5	398431	4.5	-0.81	1.19E+10	-0.141
294.836	0	2.5	339172	2.5	-0.37	3.25E+10	-0.71
294.87	53353	3.5	392486	4.5	-0.55	2.15E+10	-0.259
294.934	49104	4.5	388163	3.5	-0.94	8.85E+09	-0.067
294.976	51049	2.5	390060	2.5	-0.52	2.30E+10	-0.169
294.986	30662	5.5	369661	5.5	-0.75	1.37E+10	0.191
295.303	59223	4.5	397858	3.5	-0.56	2.11E+10	-0.303
295.309	53796	1.5	392424	0.5	-0.65	1.72E+10	0.486
295.538	44011	5.5	382377	4.5	-0.06	6.61E+10	0.331
295.977	39299	2.5	377163	3.5	-0.99	7.75E+09	-0.074
296.575	29390	2.5	366573	1.5	-0.88	9.99E+09	0.135
296.72	59223	4.5	396241	3.5	-0.84	1.09E+10	0.107
296.776	72934	2.5	409889	3.5	-0.79	1.23E+10	0.153
296.894	30662	5.5	367483	5.5	-0.71	1.49E+10	0.344
296.952	39788	1.5	376543	2.5	-0.89	9.78E+09	-0.13
297.217	32994	1.5	369448	1.5	-0.62	1.82E+10	-0.265
297.324	0	2.5	336333	1.5	-0.14	5.53E+10	-0.807
297.508	38685	0.5	374810	0.5	-0.92	9.14E+09	-0.454
297.695	32005	2.5	367919	2.5	-0.83	1.10E+10	-0.094
297.884	39788	1.5	375489	0.5	-0.75	1.35E+10	0.313
297.913	49104	4.5	384772	3.5	-0.4	2.99E+10	0.21
297.953	55773	3.5	391396	2.5	-0.78	1.26E+10	-0.132
298.065	53796	1.5	389293	1.5	-0.4	2.99E+10	-0.394
298.316	44011	5.5	379226	4.5	-0.22	4.51E+10	-0.288
298.394	39299	2.5	374426	2.5	-0.79	1.22E+10	-0.099
298.488	39788	1.5	374810	0.5	-0.91	9.27E+09	0.263
298.564	39299	2.5	374236	1.5	-0.4	2.98E+10	0.337
298.565	30907	4.5	365842	3.5	-0.48	2.46E+10	0.419
298.59	30662	5.5	365569	4.5	-0.04	6.91E+10	0.641
298.591	0	2.5	334906	3.5	0.28	1.43E+11	-0.899
298.647	34605	0.5	369448	1.5	-0.91	9.16E+09	0.202
298.931	79705	3.5	414230	2.5	-0.88	9.83E+09	0.42
299.046	48712	3.5	383109	2.5	-0.46	2.61E+10	0.139
299.083	30662	5.5	365017	5.5	-0.6	1.88E+10	-0.293
299.303	30907	4.5	365017	5.5	-0.51	2.32E+10	-0.29
299.303	30662	5.5	364772	4.5	-0.81	1.14E+10	0.153
299.331	48086	1.5	382164	0.5	-0.76	1.27E+10	0.393
299.336	32005	2.5	366078	1.5	-0.72	1.43E+10	-0.187
299.344	29390	2.5	363454	1.5	-0.66	1.64E+10	-0.19
299.394	48712	3.5	382720	4.5	-0.84	1.08E+10	0.122
299.433	34605	0.5	368569	1.5	-0.74	1.37E+10	-0.239
299.522	30907	4.5	364772	4.5	-0.23	4.43E+10	-0.551
299.718	30378	3.5	364025	2.5	-0.28	3.89E+10	-0.538
299.746	49104	4.5	382720	4.5	-0.55	2.10E+10	-0.175
299.774	29390	2.5	362975	2.5	-0.96	8.12E+09	-0.099
299.803	29390	2.5	362942	3.5	-0.97	7.89E+09	0.094
299.847	59792	3.5	393295	3.5	-0.91	9.14E+09	-0.161
299.945	36485	3.5	369879	3.5	-0.65	1.68E+10	-0.241
299.986	47119	2.5	380468	3.5	-0.94	8.48E+09	-0.076
300.006	0	2.5	333327	2.5	0.04	8.18E+10	-0.882
300.063	59223	4.5	392486	4.5	-0.56	2.02E+10	0.214
300.064	53353	3.5	386615	3.5	-0.76	1.29E+10	-0.071
300.216	36485	3.5	369578	2.5	-0.69	1.50E+10	0.267
300.225	32994	1.5	366078	1.5	-0.78	1.22E+10	0.169
300.308	29390	2.5	362381	2.5	-0.5	2.37E+10	-0.197
300.344	30662	5.5	363614	6.5	-0.41	2.86E+10	-0.538
300.473	45546	6.5	378355	7.5	-0.43	2.73E+10	0.678
300.483	57962	5.5	390759	4.5	-0.04	6.76E+10	-0.555
300.694	30378	3.5	362942	3.5	-0.66	1.62E+10	0.234
300.767	36485	3.5	368968	3.5	-0.46	2.57E+10	-0.344
300.851	55773	3.5	388163	3.5	-0.76	1.28E+10	0.089
300.995	51049	2.5	383280	1.5	-0.95	8.31E+09	0.128
301.05	45546	6.5	377717	5.5	0.45	2.07E+11	0.93
301.054	53796	1.5	385962	2.5	-0.93	8.61E+09	0.193

Table A44: Continued

Wavelength	Lower Level	J_{Low}	Upper level	J_{Up}	log gf	gA	CF
301.101	59223	4.5	391338	3.5	-0.83	1.09E+10	0.126
301.142	30378	3.5	362447	4.5	-0.67	1.59E+10	0.23
301.173	30907	4.5	362942	3.5	-0.68	1.52E+10	0.37
301.187	32005	2.5	364025	2.5	-0.58	1.92E+10	0.151
301.243	47119	2.5	379077	2.5	-0.7	1.47E+10	-0.098
301.256	36485	3.5	368429	4.5	-0.75	1.31E+10	-0.473
301.29	29390	2.5	361296	2.5	-0.63	1.72E+10	-0.198
301.32	30662	5.5	362535	5.5	-0.1	5.88E+10	0.712
301.4	30662	5.5	362447	4.5	-0.02	6.97E+10	0.624
301.402	29390	2.5	361173	3.5	-0.91	9.03E+09	-0.231
301.549	39788	1.5	371409	1.5	-0.89	9.41E+09	0.196
301.585	44011	5.5	375593	4.5	-0.69	1.51E+10	0.302
301.617	59792	3.5	391338	3.5	-0.21	4.56E+10	-0.505
301.706	32005	2.5	363454	1.5	-0.51	2.26E+10	0.302
301.719	36485	3.5	367919	2.5	-0.33	3.46E+10	0.359
301.919	30378	3.5	361593	3.5	-0.51	2.24E+10	-0.32
301.932	0	2.5	331200	1.5	-0.49	2.35E+10	0.836
302.19	30378	3.5	361296	2.5	0	7.24E+10	0.519
302.231	45546	6.5	376419	6.5	0.03	7.88E+10	0.56
302.235	45546	6.5	376414	5.5	-0.24	4.19E+10	-0.371
302.302	30378	3.5	361173	3.5	-0.08	6.03E+10	0.594
302.306	47119	2.5	377910	1.5	-0.6	1.83E+10	-0.198
302.329	48712	3.5	379478	2.5	-0.49	2.34E+10	-0.176
302.336	79131	4.5	409889	3.5	-0.04	6.72E+10	-0.545
302.343	57413	2.5	388163	3.5	-0.81	1.14E+10	0.097
302.35	30907	4.5	361650	4.5	0.19	1.13E+11	-0.687
302.402	30907	4.5	361593	3.5	0.14	1.01E+11	0.63
302.436	79131	4.5	409779	4.5	-0.63	1.70E+10	-0.113
302.576	55773	3.5	386268	2.5	-0.37	3.11E+10	0.204
302.685	32005	2.5	362381	2.5	-0.86	1.01E+10	0.145
302.736	36485	3.5	366806	3.5	-0.63	1.70E+10	0.17
302.746	79131	4.5	409441	5.5	-0.52	2.20E+10	-0.495
302.784	59792	3.5	390060	2.5	-0.83	1.07E+10	0.127
302.839	36485	3.5	366693	2.5	-0.28	3.80E+10	0.455
302.857	55773	3.5	385962	2.5	-0.9	9.14E+09	0.057
302.933	59954	2.5	390060	2.5	-0.44	2.64E+10	-0.211
302.935	30378	3.5	360482	4.5	-0.68	1.51E+10	-0.518
303.048	32994	1.5	362975	2.5	-0.37	3.10E+10	0.395
303.07	49104	4.5	379061	3.5	-0.2	4.62E+10	-0.529
303.192	48086	1.5	377910	1.5	-0.89	9.31E+09	0.24
303.197	30662	5.5	360481	5.5	-0.28	3.83E+10	-0.543
303.255	53353	3.5	383109	2.5	-0.99	7.49E+09	-0.045
303.343	39788	1.5	369448	1.5	-0.67	1.54E+10	-0.22
303.421	30907	4.5	360482	4.5	-0.36	3.14E+10	0.388
303.508	79705	3.5	409186	2.5	0.1	9.10E+10	-0.642
303.56	47119	2.5	376543	2.5	-0.99	7.50E+09	0.081
303.622	36485	3.5	365842	3.5	-0.97	7.85E+09	-0.157
303.666	30378	3.5	359687	3.5	-0.21	4.42E+10	0.416
303.683	32005	2.5	361296	2.5	-0.94	8.37E+09	0.09
303.795	57413	2.5	386582	1.5	-0.33	3.37E+10	-0.218
303.841	71517	1.5	400637	2.5	-0.97	7.76E+09	0.208
303.851	44011	5.5	373120	4.5	-0.36	3.13E+10	0.143
303.95	29390	2.5	358392	2.5	-0.25	4.02E+10	0.341
303.952	55773	3.5	384772	3.5	-0.29	3.73E+10	0.267
304.155	30907	4.5	359687	3.5	-0.82	1.10E+10	0.189
304.261	44011	5.5	372676	5.5	-0.29	3.71E+10	0.239
304.303	39299	2.5	367919	2.5	-0.49	2.32E+10	-0.22
304.34	53797	4.5	382377	4.5	-0.26	3.95E+10	-0.263
304.369	57413	2.5	385962	2.5	-0.47	2.44E+10	0.122
304.514	36485	3.5	364877	2.5	-0.79	1.17E+10	-0.125
304.536	53796	1.5	382164	0.5	-0.76	1.24E+10	-0.447
304.569	71517	1.5	399850	1.5	-0.49	2.34E+10	-0.33
304.612	36485	3.5	364772	4.5	-0.56	1.99E+10	-0.314
304.684	59954	2.5	388163	3.5	-0.76	1.24E+10	-0.111
304.797	32005	2.5	360092	1.5	-0.38	3.01E+10	-0.305
304.865	30378	3.5	358392	2.5	-0.79	1.17E+10	0.232
305.035	48712	3.5	376543	2.5	-0.83	1.07E+10	0.123
305.046	47119	2.5	374938	1.5	-0.69	1.47E+10	0.154
305.154	72934	2.5	400637	2.5	-0.47	2.41E+10	-0.283
305.174	32005	2.5	359687	3.5	-0.55	2.02E+10	-0.259
305.248	29390	2.5	356993	1.5	-0.23	4.25E+10	0.534
305.337	39299	2.5	366806	3.5	-0.25	3.99E+10	0.38
305.434	48086	1.5	375489	0.5	-0.94	8.23E+09	0.35
305.442	39299	2.5	366693	2.5	-0.55	2.04E+10	0.151
305.443	38685	0.5	366078	1.5	-0.82	1.09E+10	0.271
305.444	59223	4.5	386615	3.5	-0.1	5.69E+10	0.329
305.47	79131	4.5	406495	3.5	-0.79	1.17E+10	-0.3
305.521	49104	4.5	376414	5.5	-0.69	1.47E+10	0.137
305.524	47119	2.5	374426	2.5	-0.78	1.19E+10	-0.089
305.553	45546	6.5	372822	6.5	0.11	9.30E+10	0.891
305.554	39299	2.5	366573	1.5	-0.83	1.07E+10	0.261
305.689	45546	6.5	372676	5.5	0.39	1.76E+11	-0.732
305.701	47119	2.5	374236	1.5	-0.79	1.15E+10	0.167
305.785	30662	5.5	357689	5.5	0.17	1.06E+11	-0.581
305.889	72934	2.5	399850	1.5	-0.68	1.48E+10	-0.389
305.899	39788	1.5	366693	2.5	-0.69	1.45E+10	0.144
305.957	29390	2.5	356233	2.5	-0.69	1.44E+10	-0.249
305.976	59792	3.5	386615	3.5	-0.36	3.12E+10	0.192
306.007	79705	3.5	406495	3.5	0.15	1.00E+11	-0.572
306.012	39788	1.5	366573	1.5	-0.47	2.39E+10	0.4
306.014	30907	4.5	357689	5.5	-0.24	4.08E+10	0.686
306.069	48086	1.5	374810	0.5	-0.86	9.77E+09	-0.354
306.159	59954	2.5	386582	1.5	-0.3	3.58E+10	0.23
306.181	55773	3.5	382377	4.5	-0.9	8.98E+09	0.078
306.288	44011	5.5	370501	4.5	0.36	1.61E+11	-0.732
306.289	49104	4.5	375593	4.5	-0.55	2.00E+10	0.231
306.301	59792	3.5	386268	2.5	-0.33	3.30E+10	-0.18
306.318	47119	2.5	373577	3.5	-0.85	1.01E+10	0.097
306.453	59954	2.5	386268	2.5	-0.34	3.20E+10	0.143
306.476	39788	1.5	366078	1.5	-0.7	1.41E+10	-0.207
306.589	59792	3.5	385962	2.5	-0.67	1.52E+10	0.171
306.631	53353	3.5	379478	2.5	-0.87	9.55E+09	0.086
306.784	36485	3.5	362447	4.5	-0.33	3.30E+10	-0.363
306.846	36485	3.5	362381	2.5	-0.99	7.25E+09	0.234
306.868	53353	3.5	379226	4.5	-0.87	9.61E+09	0.11
306.874	57413	2.5	383280	1.5	-0.18	4.72E+10	-0.259

Table A44: Continued

Wavelength	Lower Level	J_{Low}	Upper level	J_{Up}	log gf	gA	CF
306.98	30662	5.5	356416	4.5	-0.19	4.56E+10	-0.577
307.005	72934	2.5	398662	2.5	-0.66	1.54E+10	-0.364
307.008	53353	3.5	379077	2.5	-0.01	6.96E+10	0.411
307.023	53353	3.5	379061	3.5	-0.69	1.44E+10	-0.12
307.035	57413	2.5	383109	2.5	-0.98	7.48E+09	0.032
307.078	44011	5.5	369661	5.5	0.42	1.84E+11	0.71
307.085	44011	5.5	369654	6.5	-0.52	2.14E+10	0.448
307.146	39299	2.5	364877	2.5	-0.58	1.87E+10	0.159
307.147	57962	5.5	383539	5.5	0.39	1.73E+11	0.76
307.173	59223	4.5	384772	3.5	-0.07	6.09E+10	-0.358
307.232	34605	0.5	360092	1.5	-0.57	1.89E+10	0.366
307.287	53797	4.5	379226	4.5	-0.62	1.71E+10	0.113
307.316	32994	1.5	358392	2.5	-0.97	7.60E+09	-0.225
307.443	53797	4.5	379061	3.5	-0.06	6.21E+10	0.509
307.581	55773	3.5	380891	2.5	-0.1	5.66E+10	0.494
307.608	39788	1.5	364877	2.5	-0.95	7.99E+09	-0.155
307.706	79131	4.5	404117	3.5	-0.14	5.10E+10	-0.52
307.865	59954	2.5	384772	3.5	-0.78	1.18E+10	-0.125
307.871	79131	4.5	403942	4.5	0.19	1.09E+11	-0.717
307.911	38685	0.5	363454	1.5	-0.53	2.07E+10	0.38
307.922	57962	5.5	382720	4.5	0.09	8.66E+10	0.606
307.981	55773	3.5	380468	3.5	-0.26	3.89E+10	0.166
308.017	51049	2.5	375706	1.5	-0.82	1.06E+10	0.206
308.115	47119	2.5	371673	3.5	-0.93	8.33E+09	0.085
308.142	103996	2.5	428522	3.5	-0.72	1.34E+10	0.438
308.178	32005	2.5	356493	3.5	-0.2	4.42E+10	-0.355
308.192	49104	4.5	373577	3.5	-0.92	8.45E+09	-0.058
308.244	44011	5.5	368429	4.5	-0.51	2.16E+10	0.228
308.254	48712	3.5	373120	4.5	-0.67	1.50E+10	0.165
308.366	47119	2.5	371409	1.5	-0.64	1.62E+10	0.123
308.532	45546	6.5	369661	5.5	-0.68	1.47E+10	0.122
308.539	45546	6.5	369654	6.5	0.22	1.16E+11	-0.791
308.581	29390	2.5	353454	3.5	-0.55	1.97E+10	0.358
308.588	30662	5.5	354719	6.5	-0.24	4.03E+10	-0.545
308.64	79131	4.5	403133	3.5	-0.84	1.01E+10	0.275
308.645	36485	3.5	360482	4.5	-0.34	3.19E+10	-0.535
308.823	53353	3.5	377163	3.5	-0.63	1.66E+10	0.16
308.842	51049	2.5	374839	3.5	-0.78	1.17E+10	-0.139
308.886	30378	3.5	354122	4.5	-0.42	2.68E+10	-0.437
308.923	55773	3.5	379478	2.5	-0.24	4.02E+10	0.202
309.027	53797	4.5	377393	4.5	-0.67	1.49E+10	0.1
309.122	59223	4.5	382720	4.5	-0.9	8.77E+09	0.05
309.157	30662	5.5	354122	4.5	-0.36	3.06E+10	0.581
309.188	79705	3.5	403133	3.5	-0.83	1.03E+10	-0.146
309.237	51049	2.5	374426	2.5	-0.47	2.36E+10	0.261
309.247	53797	4.5	377163	3.5	-0.66	1.52E+10	0.29
309.285	59954	2.5	383280	1.5	-0.5	2.22E+10	-0.127
309.304	72934	2.5	396241	3.5	-0.85	9.86E+09	0.224
309.369	32994	1.5	356233	2.5	-0.52	2.10E+10	-0.322
309.418	39788	1.5	362975	2.5	-0.56	1.93E+10	0.243
309.45	59223	4.5	382377	4.5	0.01	7.20E+10	0.443
309.635	48712	3.5	371673	3.5	-0.08	5.75E+10	0.43
309.728	32005	2.5	354869	3.5	-0.69	1.43E+10	0.198
309.793	32994	1.5	355790	0.5	-0.55	1.94E+10	-0.412
309.965	53797	4.5	376414	5.5	-0.66	1.52E+10	0.212
310.032	30907	4.5	353454	3.5	-0.65	1.57E+10	-0.375
310.117	47119	2.5	369578	2.5	-0.6	1.76E+10	0.133
310.145	79131	4.5	401561	4.5	-0.38	2.87E+10	0.45
310.223	48712	3.5	371061	4.5	-0.8	1.09E+10	-0.137
310.242	47119	2.5	369448	1.5	-0.73	1.30E+10	-0.23
310.263	30378	3.5	352685	2.5	-0.83	1.02E+10	0.228
310.276	39299	2.5	361593	3.5	-0.61	1.70E+10	-0.174
310.337	32005	2.5	354235	2.5	-0.93	8.07E+09	0.089
310.547	53353	3.5	375365	3.5	-0.94	7.93E+09	-0.057
310.6	49104	4.5	371061	4.5	-0.37	2.93E+10	-0.369
310.666	49104	4.5	370993	3.5	-0.27	3.71E+10	0.306
310.698	79705	3.5	401561	4.5	-0.54	2.00E+10	-0.428
310.705	47119	2.5	368968	3.5	-0.85	9.88E+09	0.119
310.763	48712	3.5	370501	4.5	-0.85	9.83E+09	0.099
310.883	57413	2.5	379077	2.5	-0.41	2.66E+10	0.164
310.926	55773	3.5	377393	4.5	-0.95	7.80E+09	-0.092
310.976	53797	4.5	375365	3.5	-0.5	2.19E+10	0.184
310.986	44011	5.5	365569	4.5	-0.43	2.55E+10	0.2
311.05	48086	1.5	369578	2.5	-0.79	1.13E+10	0.191
311.056	53353	3.5	374839	3.5	-0.03	6.41E+10	-0.37
311.154	49104	4.5	370488	5.5	-0.43	2.57E+10	0.3
311.27	57962	5.5	379226	4.5	-0.08	5.68E+10	0.386
311.347	34605	0.5	355790	0.5	-0.85	9.82E+09	0.367
311.357	30907	4.5	352082	5.5	-0.58	1.82E+10	-0.285
311.389	53796	1.5	374938	1.5	-0.79	1.11E+10	0.25
311.415	72934	2.5	394049	2.5	-0.51	2.14E+10	-0.388
311.43	59792	3.5	380891	2.5	-0.93	8.06E+09	-0.093
311.456	53353	3.5	374426	2.5	-0.83	1.01E+10	-0.084
311.486	53797	4.5	374839	3.5	-0.74	1.27E+10	-0.115
311.525	51049	2.5	372051	2.5	-0.28	3.60E+10	0.443
311.588	59954	2.5	380891	2.5	-0.14	5.02E+10	-0.265
311.592	79705	3.5	400637	2.5	-0.53	2.01E+10	0.32
311.841	72934	2.5	393610	1.5	-0.61	1.68E+10	0.364
311.886	53796	1.5	374426	2.5	-0.72	1.30E+10	-0.333
311.959	32994	1.5	353549	1.5	-0.6	1.74E+10	0.274
311.999	59954	2.5	380468	3.5	-0.94	7.86E+09	0.059
312.006	44011	5.5	364518	6.5	-0.91	8.45E+09	-0.304
312.029	48086	1.5	368569	1.5	-0.77	1.17E+10	0.247
312.148	72934	2.5	393295	3.5	-0.96	7.49E+09	-0.18
312.465	71517	1.5	391553	1.5	-0.63	1.59E+10	0.366
312.497	59223	4.5	379226	4.5	-0.19	4.44E+10	0.261
312.663	48086	1.5	367919	2.5	-0.76	1.18E+10	-0.301
312.676	55773	3.5	375593	4.5	-0.86	9.46E+09	0.196
312.715	53797	4.5	373577	3.5	-0.77	1.17E+10	-0.08
312.739	57962	5.5	377717	5.5	-0.52	2.06E+10	-0.177
312.807	59792	3.5	379478	2.5	-0.67	1.47E+10	0.173
312.835	29390	2.5	349047	3.5	-0.42	2.59E+10	-0.32
312.899	55773	3.5	375365	3.5	-0.28	3.61E+10	0.198
313.017	45546	6.5	365017	5.5	-0.42	2.62E+10	0.186
313.034	47119	2.5	366573	1.5	-0.97	7.26E+09	-0.094
313.057	57962	5.5	377393	4.5	-0.1	5.37E+10	-0.256

Table A44: Continued

Wavelength	Lower Level	J_{Low}	Upper level	J_{Up}	log gf	gA	CF
313.143	30378	3.5	349721	4.5	-0.77	1.16E+10	0.23
313.163	53797	4.5	373120	4.5	-0.47	2.28E+10	0.196
313.2	59792	3.5	379077	2.5	-0.49	2.18E+10	-0.188
313.209	32994	1.5	352270	0.5	-0.87	9.16E+09	0.325
313.276	48712	3.5	367919	2.5	-0.88	8.86E+09	-0.153
313.359	59954	2.5	379077	2.5	-0.93	7.89E+09	-0.049
313.375	59954	2.5	379061	3.5	-0.5	2.15E+10	-0.197
313.422	30662	5.5	349721	4.5	-0.56	1.88E+10	0.359
313.507	45546	6.5	364518	6.5	-0.9	8.50E+09	-0.061
313.522	79705	3.5	398662	2.5	-0.73	1.27E+10	-0.16
313.599	53797	4.5	372676	5.5	-0.97	7.30E+09	-0.123
313.647	51049	2.5	369879	3.5	-0.81	1.04E+10	0.186
313.948	44011	5.5	362535	5.5	-0.82	1.03E+10	-0.067
313.978	59223	4.5	377717	5.5	-0.7	1.36E+10	0.177
313.985	48086	1.5	366573	1.5	-0.58	1.77E+10	-0.286
314.014	57962	5.5	376419	6.5	-0.31	3.34E+10	-0.597
314.035	44011	5.5	362447	4.5	-0.74	1.24E+10	-0.172
314.086	36485	3.5	354869	3.5	-0.63	1.57E+10	0.13
314.213	53796	1.5	372051	2.5	-0.51	2.09E+10	0.342
314.297	59223	4.5	377393	4.5	-0.49	2.21E+10	-0.12
314.303	104821	1.5	422985	2.5	-0.48	2.23E+10	0.413
314.372	48712	3.5	366806	3.5	-0.79	1.09E+10	-0.126
314.546	51049	2.5	368968	3.5	-0.6	1.70E+10	-0.287
314.659	55773	3.5	373577	3.5	-1	6.81E+09	-0.065
314.713	36485	3.5	354235	2.5	-0.88	8.84E+09	0.134
314.747	30662	5.5	348377	4.5	-0.4	2.66E+10	0.251
314.754	53353	3.5	371061	4.5	-0.81	1.05E+10	-0.145
314.797	34605	0.5	352270	0.5	-0.76	1.17E+10	0.411
314.823	44011	5.5	361650	4.5	-0.98	7.04E+09	0.078
314.849	53796	1.5	371409	1.5	-0.67	1.44E+10	-0.394
314.86	59792	3.5	377393	4.5	-0.6	1.70E+10	0.187
315.112	55773	3.5	373120	4.5	-0.63	1.57E+10	0.266
315.262	53797	4.5	370993	3.5	-0.55	1.91E+10	-0.212
315.267	59223	4.5	376414	5.5	-0.29	3.44E+10	0.561
315.328	48712	3.5	365842	3.5	-0.45	2.41E+10	0.206
315.332	72934	2.5	390060	2.5	-0.68	1.39E+10	0.357
315.348	79131	4.5	396241	3.5	-0.8	1.06E+10	0.119
315.551	47119	2.5	364025	2.5	-0.68	1.40E+10	0.115
315.752	53797	4.5	370501	4.5	-0.67	1.44E+10	-0.097
315.765	53797	4.5	370488	5.5	-0.85	9.45E+09	0.14
316.292	57413	2.5	373577	3.5	-0.62	1.60E+10	0.155
316.374	53797	4.5	369879	3.5	-0.74	1.21E+10	-0.119
316.543	49104	4.5	365017	5.5	-0.42	2.51E+10	0.504
316.592	53797	4.5	369661	5.5	-0.78	1.11E+10	-0.145
316.655	59792	3.5	375593	4.5	-0.69	1.37E+10	-0.298
316.789	49104	4.5	364772	4.5	-0.66	1.44E+10	0.175
316.841	59223	4.5	374839	3.5	-0.37	2.82E+10	0.255
316.887	39299	2.5	354869	3.5	-0.61	1.65E+10	-0.255
317.305	30907	4.5	346061	3.5	-0.2	4.17E+10	0.301
317.413	59792	3.5	374839	3.5	-0.47	2.27E+10	-0.223
317.597	38685	0.5	353549	1.5	-0.98	6.93E+09	-0.175
317.735	55773	3.5	370501	4.5	-0.87	8.89E+09	0.13
317.749	57962	5.5	372676	5.5	-0.43	2.47E+10	-0.108
317.832	53797	4.5	368429	4.5	-0.66	1.45E+10	0.237
318.019	39788	1.5	354235	2.5	-0.6	1.66E+10	-0.287
318.113	59223	4.5	373577	3.5	-0.82	1.00E+10	0.066
318.15	30378	3.5	344695	2.5	-0.68	1.39E+10	0.169
318.172	48086	1.5	362381	2.5	-0.72	1.25E+10	0.232
318.205	48712	3.5	362975	2.5	-0.79	1.07E+10	-0.128
318.305	79131	4.5	393295	3.5	-0.48	2.17E+10	-0.255
318.476	57413	2.5	371409	1.5	-0.66	1.46E+10	-0.117
318.69	59792	3.5	373577	3.5	-0.85	9.36E+09	0.101
318.795	72934	2.5	386615	3.5	-0.54	1.90E+10	-0.335
319.127	79131	4.5	392486	4.5	-0.6	1.66E+10	-0.296
319.139	49104	4.5	362447	4.5	-0.61	1.62E+10	0.182
319.148	72934	2.5	386268	2.5	-0.64	1.52E+10	-0.125
319.532	30378	3.5	343336	2.5	-0.39	2.69E+10	0.305
319.552	48712	3.5	361650	4.5	-0.61	1.60E+10	0.154
319.61	48712	3.5	361593	3.5	-0.78	1.09E+10	0.08
319.905	29390	2.5	341983	1.5	-0.53	1.91E+10	0.333
319.96	57962	5.5	370501	4.5	-0.67	1.41E+10	-0.063
320.343	57413	2.5	369578	2.5	-0.78	1.08E+10	0.093
320.624	36485	3.5	348377	4.5	-0.87	8.80E+09	0.372
320.635	59792	3.5	371673	3.5	-0.86	8.93E+09	-0.092
320.756	71517	1.5	383280	1.5	-0.41	2.55E+10	-0.35
320.82	32994	1.5	344695	2.5	-0.92	7.73E+09	0.276
320.822	57962	5.5	369661	5.5	-0.82	9.88E+09	0.062
320.831	79705	3.5	391396	2.5	-0.47	2.21E+10	-0.288
320.896	30662	5.5	342289	4.5	-0.54	1.88E+10	-0.23
321.111	53353	3.5	364772	4.5	-0.95	7.34E+09	0.099
321.202	32005	2.5	343336	2.5	-0.65	1.47E+10	0.178
321.336	59792	3.5	370993	3.5	-0.9	8.10E+09	0.107
321.845	59792	3.5	370501	4.5	-0.83	9.58E+09	0.143
321.909	71517	1.5	382164	0.5	-0.58	1.67E+10	-0.437
322.008	30907	4.5	341458	3.5	-0.81	9.91E+09	-0.222
322.337	103996	2.5	414230	2.5	-0.01	6.32E+10	0.505
322.604	32005	2.5	341983	1.5	-0.92	7.72E+09	0.14
322.793	55773	3.5	365569	4.5	-0.93	7.56E+09	-0.309
322.846	59223	4.5	368968	3.5	-0.96	7.04E+09	-0.051
323.022	36485	3.5	346061	3.5	-0.88	8.48E+09	0.362
323.197	104821	1.5	414230	2.5	-0.55	1.81E+10	-0.427
323.591	79131	4.5	388163	3.5	-0.64	1.47E+10	-0.144
323.722	48086	1.5	356993	1.5	-0.85	9.05E+09	0.139
323.899	53797	4.5	362535	5.5	-0.51	1.96E+10	-0.347
324.06	49104	4.5	357689	5.5	-0.5	2.02E+10	0.223
324.224	57413	2.5	365842	3.5	-0.76	1.10E+10	-0.135
324.401	59223	4.5	367483	5.5	-0.9	7.89E+09	-0.314
324.43	32994	1.5	341227	0.5	-1	6.27E+09	-0.421
324.454	36485	3.5	344695	2.5	-0.86	8.77E+09	-0.194
324.716	71517	1.5	379478	2.5	-0.36	2.78E+10	-0.531
325.167	72934	2.5	380468	3.5	-0.94	7.27E+09	0.117
325.321	49104	4.5	356493	3.5	-0.51	1.93E+10	0.203
325.891	36485	3.5	343336	2.5	-0.68	1.30E+10	0.196
326.205	57962	5.5	364518	6.5	-0.67	1.33E+10	-0.339
326.44	47119	2.5	353454	3.5	-0.67	1.33E+10	0.175
326.523	79705	3.5	385962	2.5	-0.8	9.98E+09	0.118

Table A44: Continued

Wavelength	Lower Level	J_{Low}	Upper level	J_{Up}	log gf	gA	CF
326.63	48712	3.5	354869	3.5	-0.76	1.09E+10	-0.23
326.912	103996	2.5	409889	3.5	-0.26	3.46E+10	0.466
327.049	49104	4.5	354869	3.5	-0.4	2.50E+10	0.231
327.181	79131	4.5	384772	3.5	-0.8	9.93E+09	-0.102
327.308	48712	3.5	354235	2.5	-0.64	1.43E+10	0.167
327.444	39299	2.5	344695	2.5	-0.64	1.44E+10	0.301
327.665	103996	2.5	409186	2.5	-0.61	1.53E+10	0.515
327.89	59792	3.5	364772	4.5	-0.94	7.17E+09	-0.146
328.506	79131	4.5	383539	5.5	-0.98	6.51E+09	-0.089
328.553	104821	1.5	409186	2.5	-0.45	2.21E+10	0.263
329.393	79131	4.5	382720	4.5	-0.97	6.61E+09	-0.055
329.831	51049	2.5	354235	2.5	-0.77	1.04E+10	-0.169
329.964	53353	3.5	356416	4.5	-0.88	8.13E+09	0.16
330.017	79705	3.5	382720	4.5	-0.97	6.64E+09	-0.174
330.391	79705	3.5	382377	4.5	-0.52	1.86E+10	0.235
332.146	53797	4.5	354869	3.5	-0.97	6.55E+09	0.109
332.356	53353	3.5	354235	2.5	-0.96	6.61E+09	0.084
332.481	53353	3.5	354122	4.5	-0.88	7.91E+09	-0.158
332.488	79705	3.5	380468	3.5	-0.63	1.40E+10	-0.142
333.199	103996	2.5	404117	3.5	-0.38	2.50E+10	0.593
333.228	79131	4.5	379226	4.5	-0.82	9.06E+09	-0.132
334.23	32005	2.5	331200	1.5	-0.84	8.58E+09	0.251
335.276	79131	4.5	377393	4.5	-0.85	8.46E+09	-0.077
335.504	72934	2.5	370993	3.5	-0.74	1.07E+10	0.244
337.311	79131	4.5	375593	4.5	-0.72	1.11E+10	0.198
338.048	104821	1.5	400637	2.5	-1	5.80E+09	-0.153
338.226	79705	3.5	375365	3.5	-0.8	9.24E+09	-0.132
340.663	79131	4.5	372676	5.5	-0.36	2.53E+10	-0.472

a: Energy Levels from [44, 45]